



28TH Annual Conference Proceedings

Lithium-Battery Technology-Rare Earths

Co-Sponsored by



ALTA Metallurgical Services, Melbourne, Australia

www.altamet.com.au

**PROCEEDINGS OF
ALTA 2024 Lithium-Battery Technology-Rare-Earths SESSIONS**

**30 May 2024
Perth, Australia**

978-0-6458390-1-2

**ALTA Metallurgical Services Publications
All Rights Reserved**

Publications may be printed for single use only. Additional electronic or hardcopy distribution without the express permission of ALTA Metallurgical Services is strictly prohibited.

Publications may not be reproduced in whole or in part without the express written permission of ALTA Metallurgical Services.

The content of conference papers and presentations are the sole responsibility of the authors



The Future Battery Industries Cooperative Research Centre is Australia's largest partnership of industry, government and researchers focused on the battery industry.

We are proud to work at the heart of the energy transition and contribute to the development of local capability.

Thursday 30 May 2024

	Page
Keynote Presentation: Moving up The Value Chain from Mines to Batteries Celina Mikolajczak, Chief Battery Technology Officer, Lyten (Virtual) Andrew Nissan, Senior Director of Battery Strategic Sourcing, Lyten	1
Australian Leverage to Global Carbon Neutrality Adrian Griffin, Principal, Future Technology Trust, Australia	21
Piloting the Neometals ELI Process Mike Tamlin, Head of Lithium, Neometals, Australia	49
Process Modelling and Life Cycle Assessment: Conventional and Novel Processing of Spodumene Mike Dry, Owner, Arithmetek, Canada Phoebe Whatoff, Director, Minviro, Australia	58
The Production of High-Purity Battery-Grade Lithium Carbonate Product from Lithium Brine Sources Nipen Shah, Head of Sales, JordProxa, Australia	73
Membrane-Assisted Direct Lithium Extraction Amir Razmjou, Associate Professor, Edith Cowan University, Australia	86
Kinetics of Spodumene Recrystallisation Bogdan Długogórski, Distinguished Research Professor, Charles Darwin University, Australia	99
Phosphate Removal from Wastewater Using Calcium Silicate By-Products Derived from the LieNA Process Shilpi Ray Biswas, Researcher, Murdoch University, Australia	115
Clariant New-Generation Collectors for Flotation of Lithium Ores Matthew Pupazzoni, Business Development Metallurgist, Clariant Mining Solutions, Australia	128
Rethinking Powder Handling in Critical Minerals Processing: Designing for Robustness and Value Retention Tristan Bower, Head of Global Sales, Floveyor, Australia	134
Processing and Disposal of Residues Comprising Naturally-Occurring Radioactive Material (NORM) Hagen Gunther Jung, Executive Director, GeoEnergy Consult, Germany	148
Process Selection Considerations for Recovery of Rare Earths from Mineral Sands Concentrates Gavin Beer, Head Metallurgical Projects, Met-Chem Consulting, Australia	159
Lessons Learned from Ionic Clay Testwork Matthew Nicholls, Senior Process Engineer, METS Engineering, Australia	171
Optimising Reagent Use in Clay Hosted Rare Earth Extraction Jess Page, Manager, Data Analytics, WGA, Australia	189
Rare Earth Extraction with Ionquest 801 Chiara Francesca Carrozza, Technical Development Specialist, Italmatch Chemicals, Italy	198

Friday 31 May 2024

	Page
Thermodynamic Modelling of Rare Earth Solvent Extraction Brett Schug, Senior Simulation Consultant, SysCAD, Canada	208
Precipitation of Rare Earth Element Salts of High Purity Kerstin Forsberg, Professor, KTH Royal Institute of Technology, Sweden	224
Australia's Only Rare Earths Project With In Situ Recovery Potential Robert Blythman, Exploration Manager, Cobra Resources, Australia	249
Lithium-ion Battery Shredding Challenges Andreas Mönch, Principal Research Consultant, CSIRO, Australia	260
Impact of Organic Impurities on Acid Leaching of Valuable Metals from Used Li-ion Batteries Mooki Bae, Researcher, Korea Institute of Geoscience and Mineral Resources (KIGAM), South Korea	271
Lewatit Ion Exchange Resins for the Recycling of Lithium-ion Batteries Dirk Steinhilber, Manager, Technical Marketing, LANXESS, Germany	286
Low-Carbon Footprint Bio-Diluents for Solvent Extraction in Lithium-ion Battery Recycling Zubin Arora, Global Market Manager, TotalEnergies Fluids, France	300
Hydrometallurgical Process to Extract Metals from LFP-NMC Blackmass in Spent Lithium-Ion Batteries Alexandre Chagnes, Professor, Université de Lorraine, France	309
Recent Technological Progress in Metals' Recovery from Spent NCM Battery Promoted by New Separation Reagents Shengxi Wu, Lecturer, Central South University, China	319
Optimised Nickel and Cobalt Recovery from Battery Waste Using Solvent Extraction Leslie Miller, Senior Application Engineer, OLI Systems, USA	347
Integrated Technologies for Efficient Recycling of Lithium-Ion Batteries Leonel Yew, Process Engineer, Neometals, Australia	358
Development of Aurubis' Hydrometallurgical Li-ion Battery Recycling Process Andrew Harris, Senior Research & Development Metallurgist, Aurubis AG, Germany	366
Matte Smelting and Purification Process for Recycling of EoL-LiB Joon Sung Choi, Researcher, Research Institute of Industrial Science and Technology (RIST), South Korea	380

Keynote Address

MOVING UP THE VALUE CHAIN FROM MINES TO BATTERIES

By

Celina Mikolajczak (joining virtually)

Andrew Nissan,

Celina.mikolajczak@lyten.com | andrew.nissan@lyten.com

Lyten, USA

SUMMARY

The presentation explores the critical role of innovation, sustainability, and strategic partnerships with mining companies into the production of battery raw materials. The need for the mining industry to adopt advanced technologies and sustainable practices to meet the growing demand for battery materials driven by the expansion of global demand for electrification. This talk highlights successful case studies and industry best practices that demonstrate the potential for value creation along the entire supply chain. Overall, the presentation underscores the opportunities and challenges faced by the mining sector in moving up the value chain in partnership with the global battery industry.

BIOS



Education

B.S., Engineering & Applied Science California Institute of Technology (Caltech, USA)
MA, Mechanical Engineering Princeton University, USA

Current Position

Celina Mikolajczak is the Chief Battery Technology Officer at Lyten, USA.

Previous Experience

Celina was the Chief Manufacturing Officer at QuantumScape, responsible for bringing QuantumScape's technology to mass production. Previously, Celina was a member of the board of directors at QuantumScape and the Vice President of Engineering and Battery Technology at Panasonic Energy of North America (PENA), which produces Li-ion cells for Tesla at the Gigafactory near Reno, NV. Celina has 20 years of experience in the battery industry which includes filling a variety of roles ranging from developing safety tests and failure analysis techniques, leading cell quality activities, conducting cell materials development, developing battery regulatory frameworks, and leading design of li-ion battery packs at Exponent, Tesla, and Uber.



Education

Ph.D. in Metallurgical and Materials Engineering, Colorado School of Mines, USA
Bachelor of Science in Material Science and Engineering, University of California, USA

Current Position

Andrew Nissan is the Senior Director of Battery Strategic Sourcing at Lyten, USA

Previous Experience

Director of materials engineering at Panasonic Energy of North America (PENA). In this role he led a team of dedicated scientists and engineers to conduct material and supplier development for the largest cylindrical lithium-ion battery manufacturer in the world. PENA produces around 66 batteries per second or about 2-billion cells per year for Tesla at the Gigafactory in Sparks, Nevada. Andrew specialized in material characterization, fracture mechanics, metallurgical engineering, and physical metallurgy. Prior to joining Panasonic, he was a staff metallurgical engineer at Tesla and worked to help drive the mission of accelerating the world's transition to sustainable energy. Andrew had previously held positions at Chevron and Exponent.

Moving up the Value Chain: From Mines to Batteries

ALTA 2024 Conference

Perth, Australia
May 30, 2024



LYTEN OVERVIEW

LYTEN

2

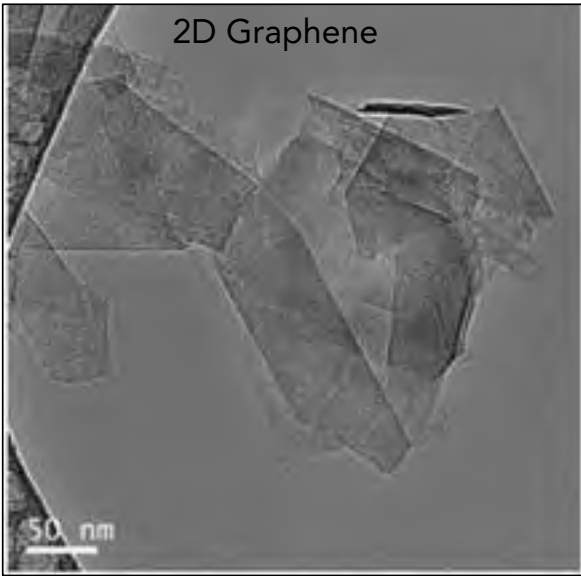


- Founded 2015 – Produce Lyten 3D Graphene™
- Leader in 3D Graphene Patents (>415 patent matters)
- >\$410M Raised; finishing Series B
- Initial Applications of Lyten 3D Graphene™
 - Lithium-Sulfur Batteries
 - Composites
 - Sensors
 - US Government Applications
- 145k ft² Facilities in Silicon Valley
 - 3D Graphene Fab (2022)
 - Pilot Cell Production Line (2023)
- > 280 employees; >70% advanced degree

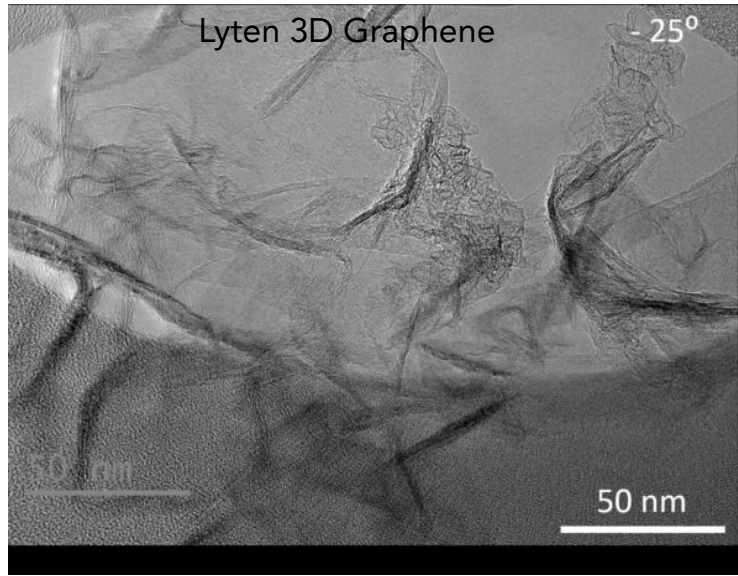
2

3D GRAPHENE: AN ENABLING BREAKTHROUGH

Proprietary manufacturing method; proprietary application tuning

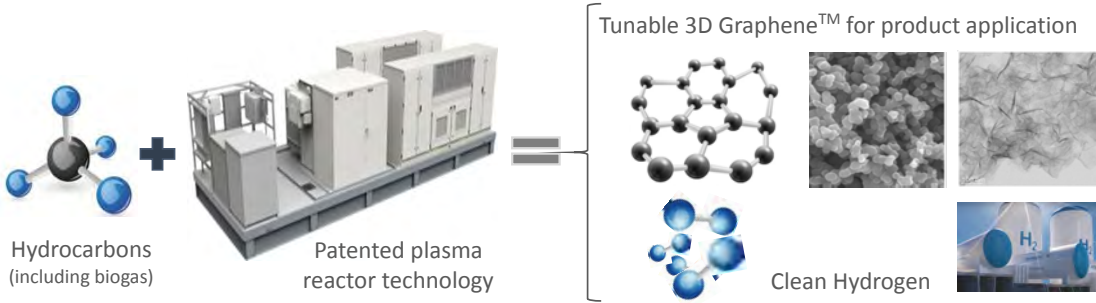


Conventional graphene: expensive with limited functionality



3D graphene: complex structure with high functionality, readily manufacturable

LYTEN 3D GRAPHENE™ PROCESSING

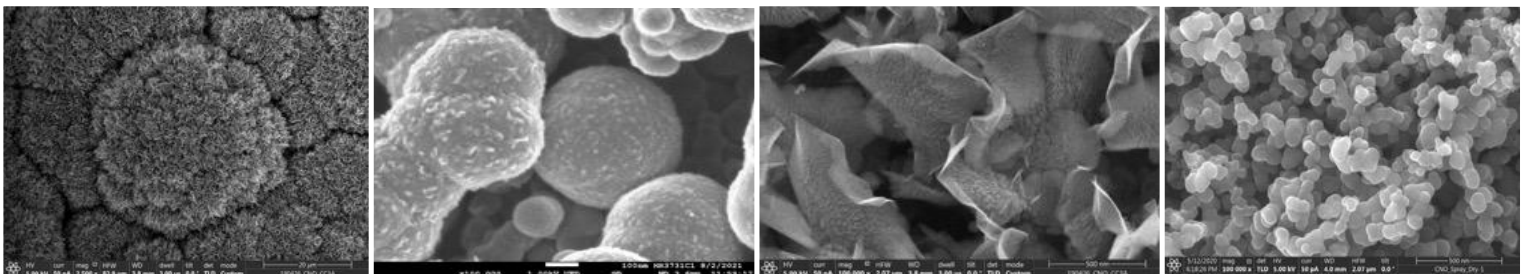


GHG Emissions Target

-2.5

KG CO₂eq / KG 3D Graphene

Lyten 3D Graphene™ targets to be a carbon negative material at scale.*



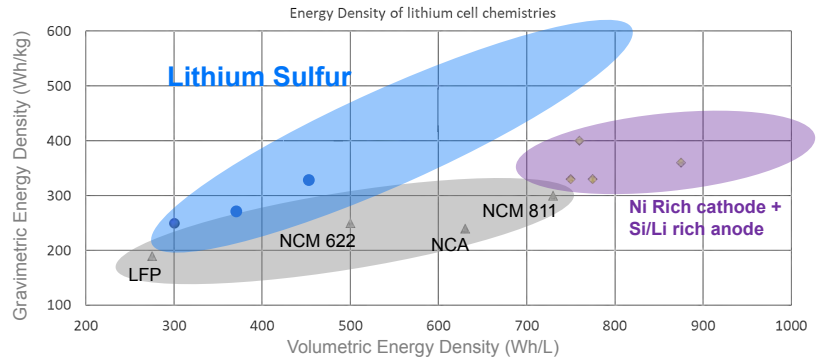
LITHIUM SULFUR CELL CHEMISTRY

Key Advantages of Lithium Sulfur

- Nickel/cobalt/graphite - free □ fully domestic supply chain
- Abundant, low-cost materials: sulfur, carbon, solvents
- Inherently safer due to unique conversion chemistry
- At maturity, 600 Wh/kg and 800 Wh/L possible

Key Challenges for Traditional LIBs

- Predominantly foreign-sourced active materials
- Cell performance reaching its fundamental limits
- Nickel shortfall in coming years



Class 1 refined production by country, % of global production, 2019

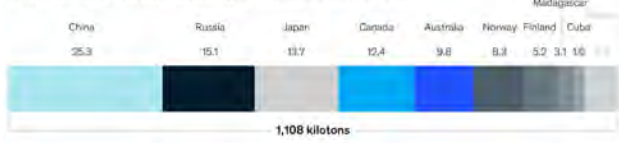
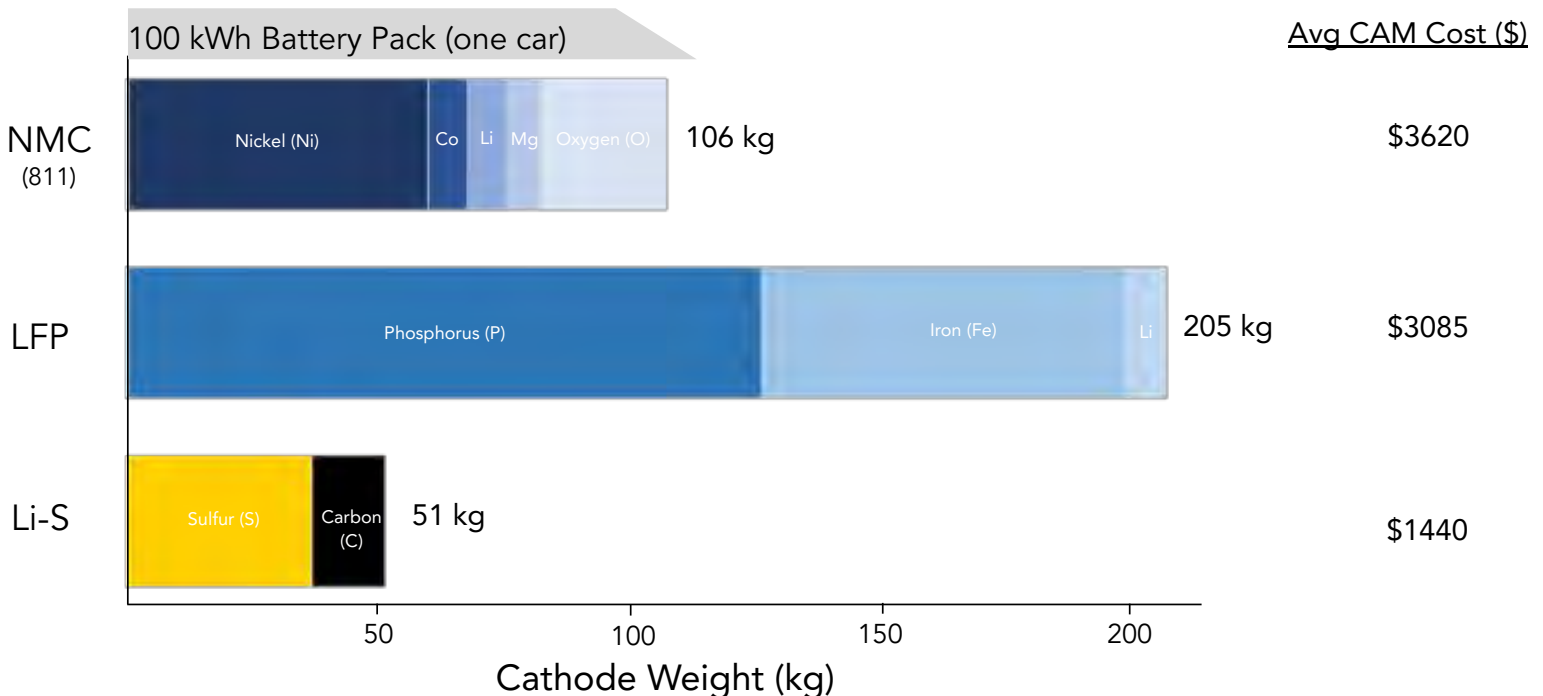


Exhibit 4 Class 1 nickel supply-demand balance Kt



CATHODE RAW MATERIAL WEIGHT & COST (2030)



LIFE CYCLE ANALYSIS (CARBON FOOTPRINT)

- Lyten Li-S LCA estimates a carbon footprint of 24.5 kg CO₂eq / kWh at scale.
- Result is 50% lower than any other battery in comparison group of 28 batteries from 10 peer reviewed LCAs. Lyten result is 80% lower than the mean of all batteries.
- Lyten working on a pathway to drive the carbon footprint Li-S towards or past carbon neutral.

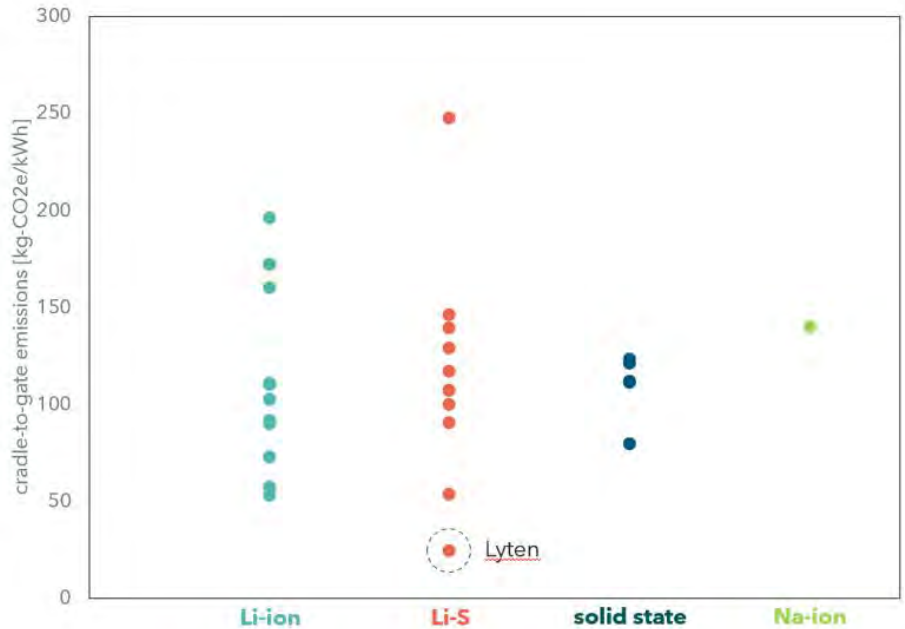


Figure. Cradle-to-gate emissions from 28 battery chemistries analyzed by 10 peer reviewed LCAs (details provided) compare to LCA for Lyten Li-S battery. LCA and comparison study completed by EcoEngineers.



Li-S Value Proposition



Lowest \$/Wh



Replacing Ni-based cathodes with Sulfur is projected to lower raw material BOM cost by >50%

High Specific Energy (Wh/kg)



>2x practical specific energy compared to existing technologies

Abundant and Accessible Raw Materials



Sulfur is abundant in high quantities as a byproduct of minerals and petrochemical production – eliminates world reliance on scarce Ni resources

Reliable North America Raw Material Supply



Target 100% sourced and manufactured in NA: Lyten could help OEMs meet 2025 USMCA mandates

Decarbonization Material Platform



Target: 60%+ lower cell material emissions – eliminate conventional cathode active material production, eliminate conventional graphite processing, generate graphene and H₂ from light hydrocarbons

Safety



Strong resistance to overcharge, metal contamination, and puncture failure modes

Minimal Technology Switching Costs



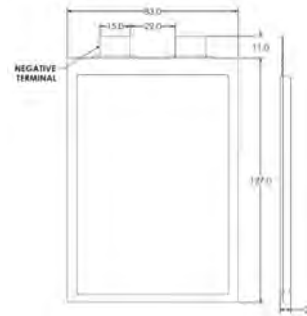
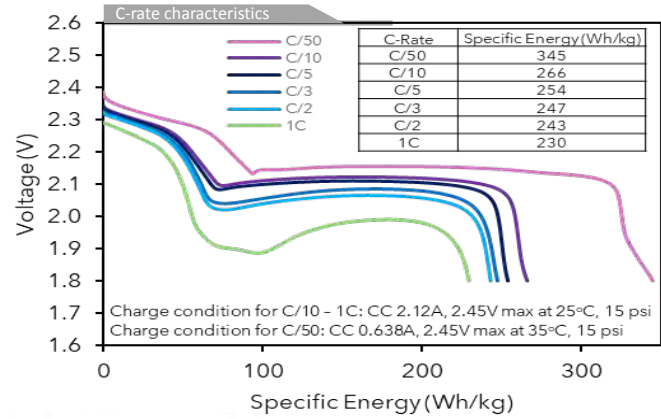
Lower greenfield capex and minimal incremental brownfield conversion capex due to a simpler manufacturing process and Li-ion B facility compatibility

SHIPPING COMMERCIAL LI-S A-SAMPLES

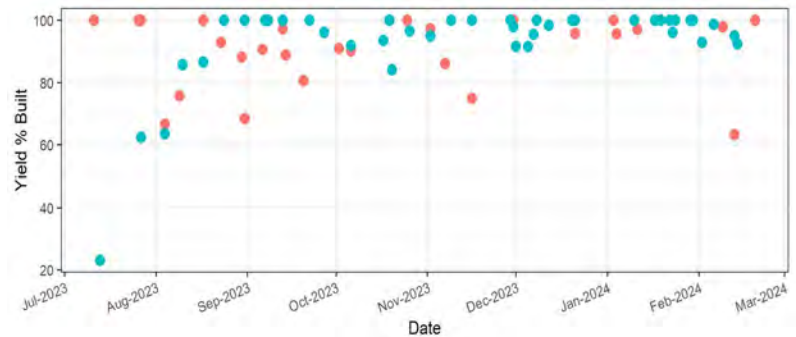
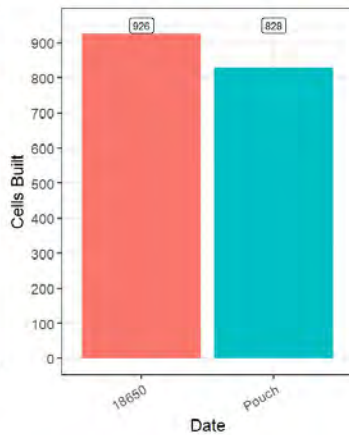
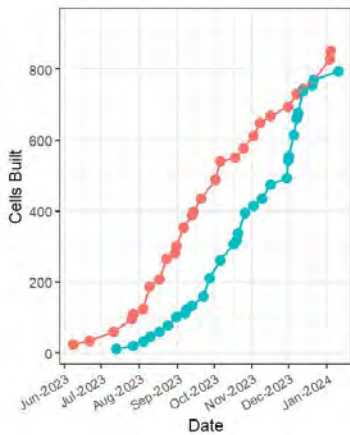
- Capable of up to 345 Wh/kg at C/50, 35°C
- 93% Available energy at 1C relative to C/3

Specifications	
Nominal Capacity	6.55 Ah
Specific Energy	248 Wh/kg
Energy Density	300 Wh/L
Nominal Voltage	2.1 V
Mass	57.2 g
Cycle Life (100% DOD)	230 min. @ 60% Capacity
Max Continuous Discharge	6A @ 1C
Peak Discharge 10s	24A @ 4C (0 - 100% SOC)
DCIR @ 100% SOC, 1C, 10s	1.8 mΩ
Operating Temperature	Charge: 10°C to TBD Discharge: -35°C to 45°C Storage: -35°C to 45°C
Cell Breathing	3 - 5% typical, TBD

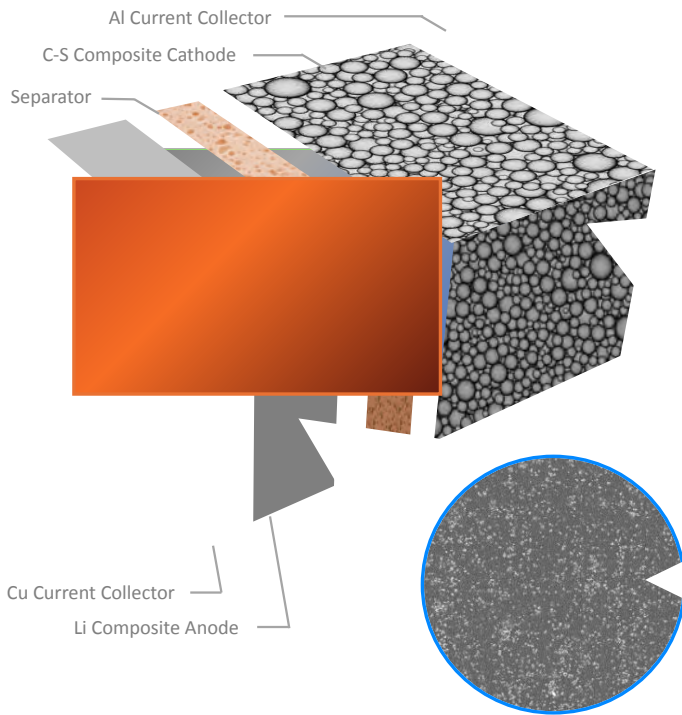
*All values are typical and determined at 25°C, C/D @ C/3 (2.12A), 15 psi



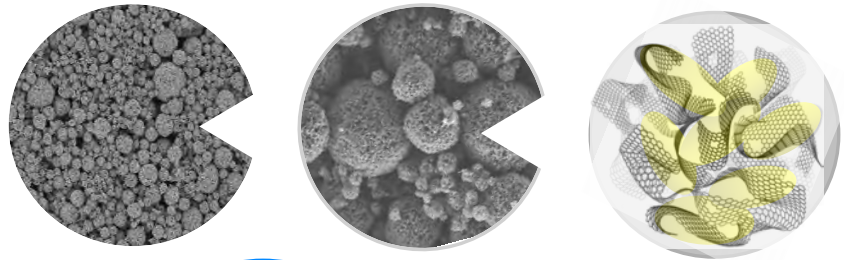
PILOT LINE YIELD AND PRODUCTION NUMBERS



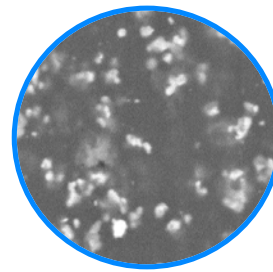
LYTEN Li-S CELL ARCHITECTURE



Nanostructured 3D Graphene™ mitigates polysulfide shuttle
 High conductivity of 3D Graphene™ for high charge/discharge rates



Lithium metal composite anode mitigates anode degradation



LITHIUM SALTS AND METAL PRODUCTION SUMMARY



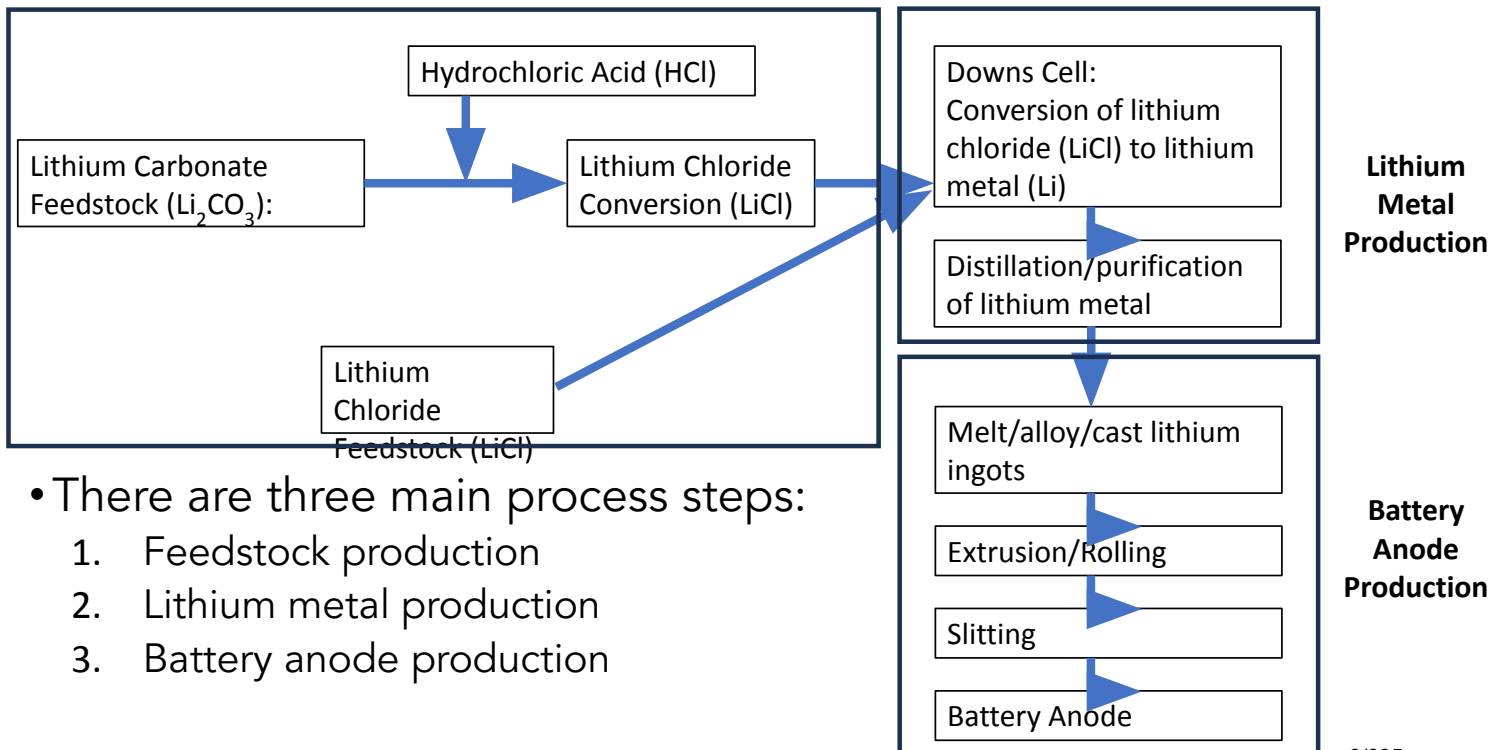
- To achieve energy densities required by customers Lyten utilizes lithium metal in the anode of our batteries
- >90% of all lithium metal is produced in China with ~4.5% of worldwide lithium metal produced in the United States
- The most common lithium metal conversion process is using a modified Downs cell to convert lithium chloride to lithium metal
- The inflation reduction act (IRA) changed the dynamic and sourcing strategies for battery manufacturing in the USA
- Lyten is developing lithium metal production and anode processing in-house but is also looking for partners to work on creating a new lithium metal ecosystem based on safety, efficiency, and cost reduction

INFLATION REDUCTION ACT (IRA)

- Inflation reduction act was signed by President Biden on August 16, 2022 and became law
- The inflation reduction act provides subsidies for USA domestic battery manufacturing
- Foreign entities of concern (FEOC) were defined and sourcing products/components from them are not allowed if the manufacturing subsidy is to be received
- The legislation also resulted in defining fifty critical minerals strategically needed by the USA though only lithium is mentioned and not any specific form (e.g. Li_2CO_3 , LiOH , LiCl , Li metal, etc.)
- Lyten is developing strategic partnerships to create a non-FEOC lithium ecosystem as we begin building our first Giga-Factory with production expected in late 2026 – lithium metal is the end-goal of this ecosystem

LITHIUM ANODE PRODUCTION

Lithium Salt - Feedstock Production



- There are three main process steps:
 1. Feedstock production
 2. Lithium metal production
 3. Battery anode production

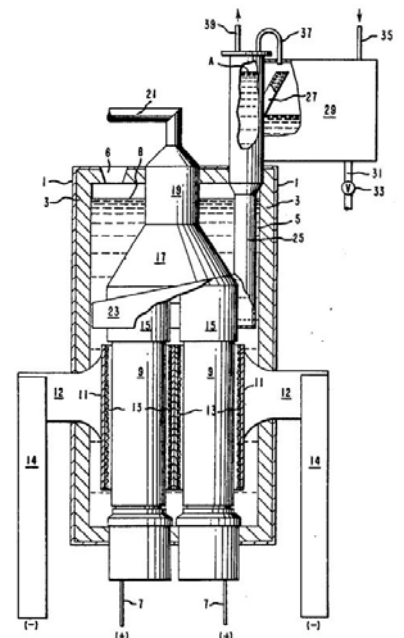
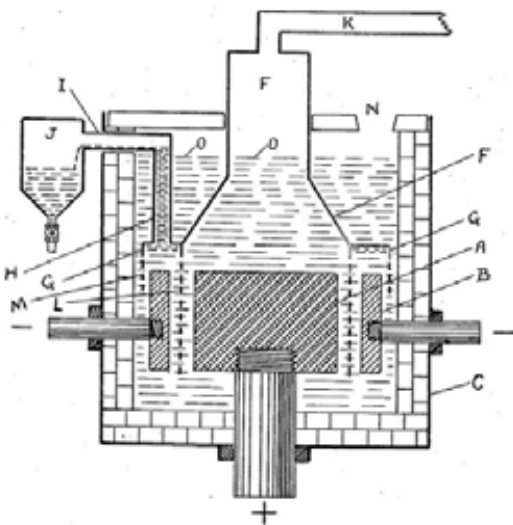


- The main processing routes for lithium salts are:
 - Brine
 - Hardrock
 - Direct Lithium Extraction (DLE)
 - Lithium from recycled batteries
- From all the processing routes there are two main grades of lithium salts that are available for purchase:
 - Technical and Battery Grade
- In the future, to improve sustainability and minimize processing steps Lyten would like to work directly with mining operators to break free of these standard grades and determine what levels of impurities are acceptable:
 - Lithium sulfur batteries can accept significantly higher and different levels of impurities in the feedstock as compared to traditional battery chemistries (NMC, NCA, and LFP)
 - Because the lithium salts will be converted into a distilled lithium metal product the balance between purity and final processing needs to be established

LITHIUM SALT PRODUCTION

- Lyten is actively working with suppliers of lithium salts to identify what impurities can be allowed and at what levels
 - Allowance of impurities and minimizing processing is critical to creating a cost-competitive lithium metal product
- Many producers that we talk to mention that they will make >99% pure lithium salts...this is most likely not needed and will result in over-processing of the mineral
- The end user and the mineral producer need to have constructive dialogs to minimize processing to be cost competitive across the entire value chain

LITHIUM METAL PRODUCTION



LITHIUM METAL PRODUCTION (DOWNS CELL)

- Lithium metal is produced primarily from the conversion of lithium chloride to lithium metal
- A modified Downs cell is used for the conversion (originally used for conversion of sodium chloride to sodium metal)
- Though there have been advancements in cell operation the basic design of the cell has not changed significantly since it was patented in 1924

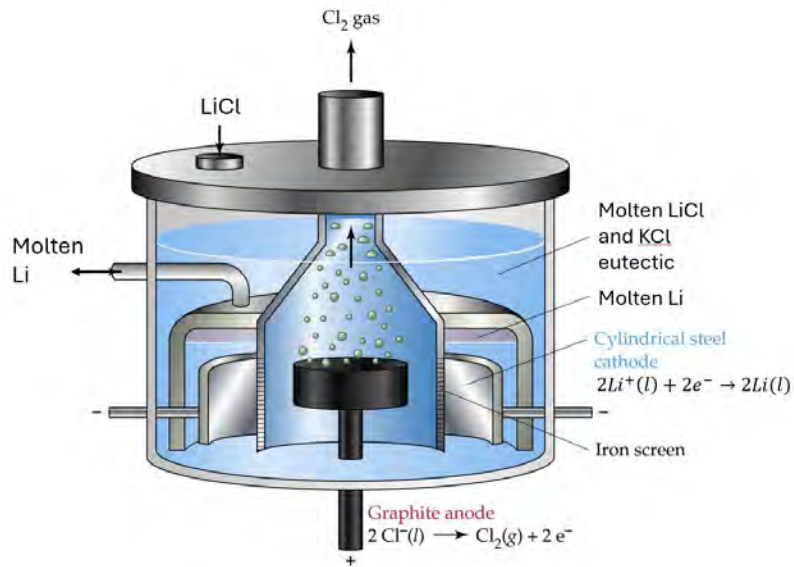


Figure modified from: [CHEM 1180: November 2010](#)

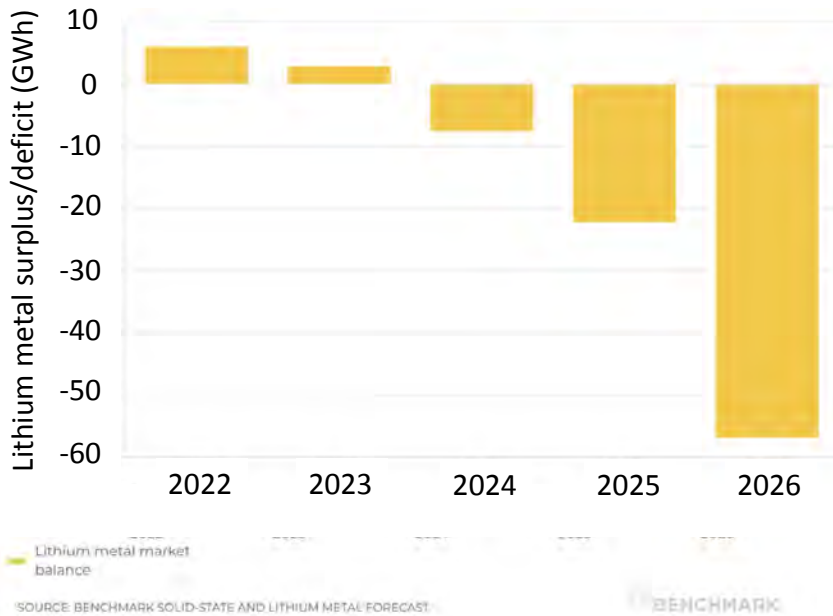
LITHIUM METAL PRODUCTION



- China produces >90% of all lithium metal worldwide
- The USA produces ~4.5% of worldwide lithium metal
- Russia capacity is no longer catalogued

There is not enough available lithium metal for Lyten's growth plans!

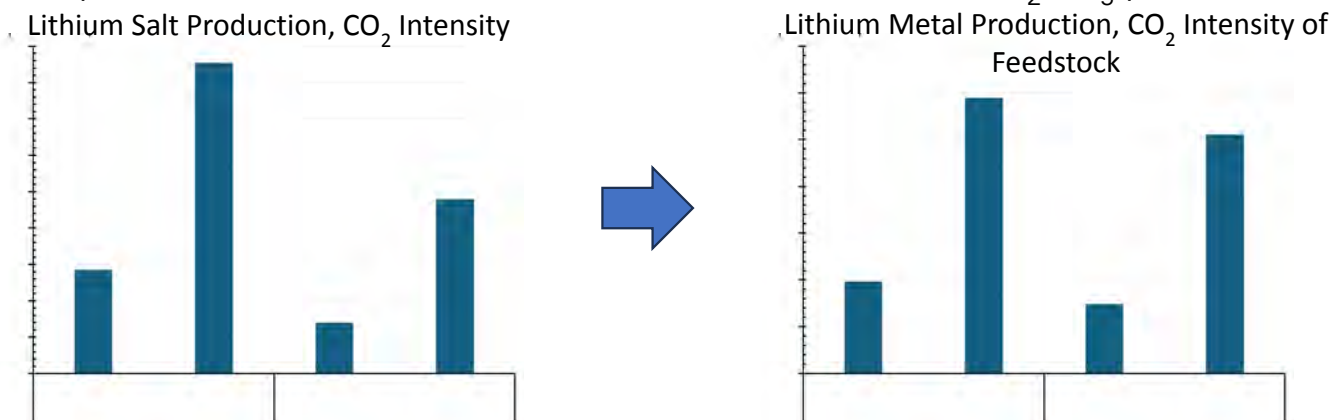
LITHIUM METAL PRODUCTION



- A lithium metal deficit has been predicted and we are seeing this play out with the development of solid state and lightweighting with lithium metal anodes
- To not use Chinese produced lithium in our supply chain we will need to begin building and innovating on production of lithium metal in anticipation of mass production in 2026

LITHIUM METAL PRODUCTION – CO2 INTENSITY

- Hardrock lithium production results in more CO₂ emissions than Brine production however other metrics such as production location, water use, and energy mix will be considered as we move towards mass production of lithium metal
- Using a theoretical conversion of 3.45 for LiOH and 5.32 for Li₂CO₃, the CO₂ intensity for the lithium metal feedstock can be calculated
- Coupled with a low carbon Lyten battery net negative or close to zero total carbon intensity per battery cell can be achieved through the LiOH or Li₂CO₃ processing routes



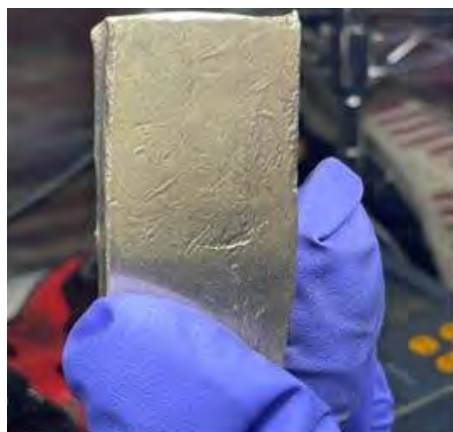
LITHIUM METAL PRODUCTION

- Using the current SMM spot price for Li_2CO_3 and LiOH the input material costs for lithium metal can be calculated
- Processing costs for lithium metal include conversion of feedstock to LiCl and final conversion to metal
- Because the Downs cell is powered only by electricity (as opposed to natural gas) it lends itself well to being powered entirely by renewable energy

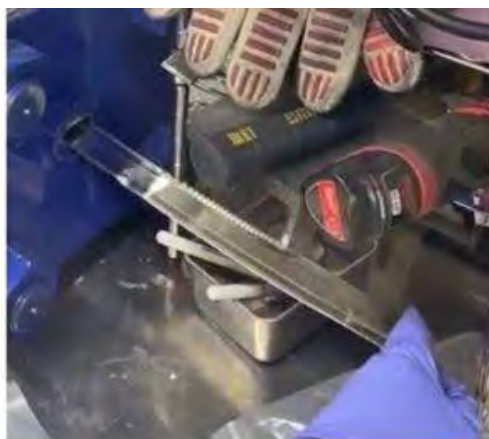
	Product Grade	Cost/kg[1]	Theoretical Conversion	Input Material Cost
Li_2CO_3	Battery (>99.5%)	\$14.63	5.32	\$77.83
	Industrial (>99.2%)	\$14.07		\$74.85
LiOH (>56.5%)	Battery	\$13.83	3.45	\$68.48
	Industrial	\$11.98		\$59.30
Li Metal	Battery	\$124-225		

[1] Spot prices accessed from Shanghai Metal Markets (SMM) on 5/28/2024

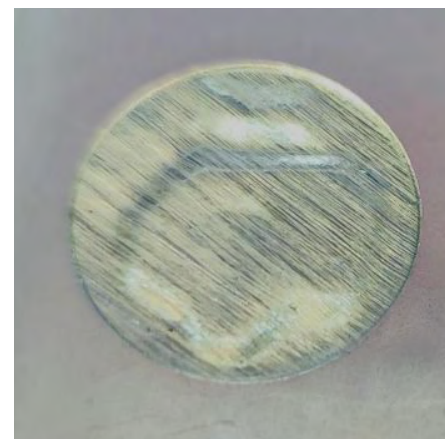
BATTERY ANODE PRODUCTION



Ingot Cut for Extrusion



Extruded (300um)



Cut Li-sample for Coin Cell Testing

BATTERY ANODE PRODUCTION



- Lyten is developing or commissioning the following systems for anode production:
 - On order: Lithium melting/alloying/casting system to produce lithium ingots and the gen2 system is being designed
 - Lyten commissioned a lithium extrusion/rolling system to produce anodes for pouch and cylindrical cells
 - Slitting system for lithium metal has been designed and ordered



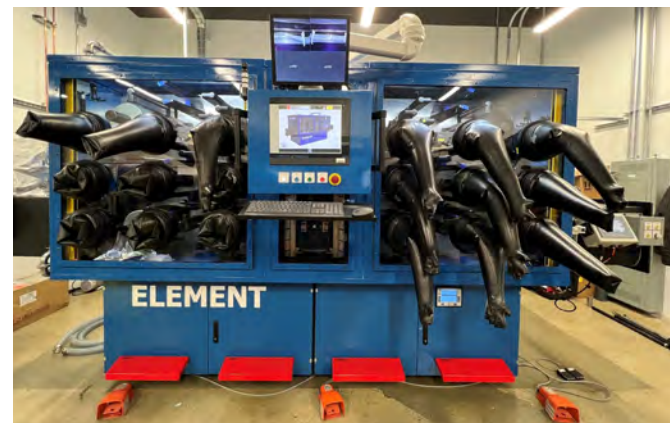
BATTERY ANODE PRODUCTION

Lithium Extrusion Unit

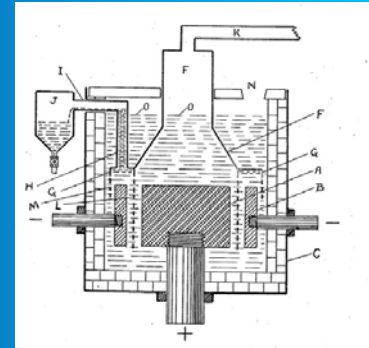


With the commissioning of the extrusion and rolling mill at Lyten's HQ in San Jose we believe that we have one of the largest lithium processing capacities in North America

Lithium Rolling Mill



Lithium: What is Next?



27

LITHIUM METAL INNOVATION



- Learn from other metal chloride to metal processes (e.g. magnesium, aluminum, and titanium) to determine efficiencies and optimization for future lithium metal cells
- Develop in-house expertise and capability to vertically integrate the lithium value chain from mine to anode.
- Engage directly with mines to source “non-standard” lithium salts
- We believe that with innovation and engagement from mineral processors we can develop the next generation of lithium metal production that is safer, more efficient, and are cost competitive with lithium metal made in China
- Bottom line: there is room for innovation

CONCLUSIONS

- The production of lithium salts falls into commodity “bins” but we are looking to find partners that want to sell a specialty mineral that minimizes processing and CO₂ intensity to create a cost-competitive feedstock for metal production
- Leveraging all the innovation over the last century since Downs original patent, other metal chloride processes, and using modern control systems we are confident that we can create a lithium metal conversion process that is safe, efficient, and cost competitive
- Lithium sulfur batteries can be produced from domestically sourced minerals in any country that has lithium metal, elemental sulfur, and natural gas



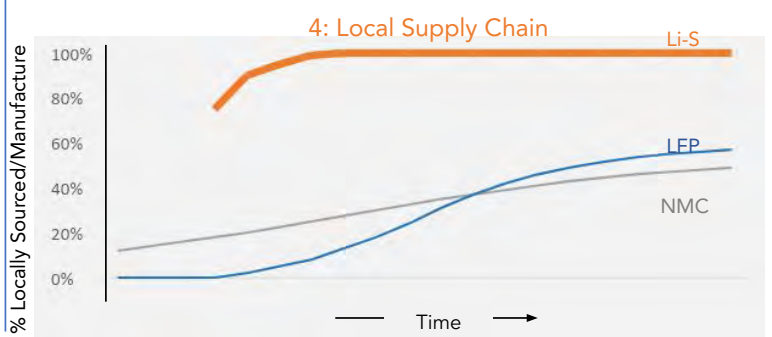
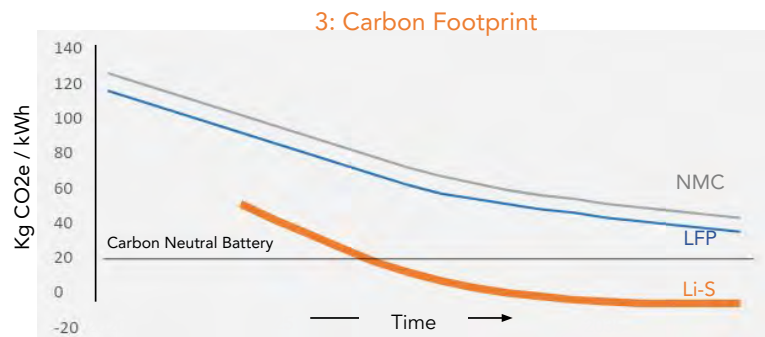
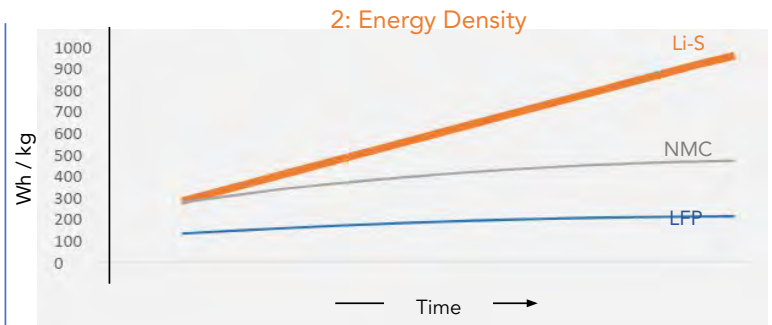
LYTEN BATTERY TEAM

Approximately 80 members: ~ 50 engaged in R&D, ~30 in cell manufacturing

- 20 Technicians, 60 engineers and scientists
- 23% Female
- 30% Caucasian, 20% Asian, 34%South Asian, 12% Latino, 4% African
- Backgrounds in industrial cell development and manufacturing, Cell R&D, and EV, Solar, and Semi-Conductor Industries: Panasonic, Tesla, Rivian, Quantumscope, A123, NexTech, ZAF, Sakuu, AB Systems, Apple, Applied Materials, NOHMs, Paraclete, JPL, PNNL, Sandia National Labs, Joby Aviation, Equity Solar, Lam Research, Micron, 3DXPoint, Intel



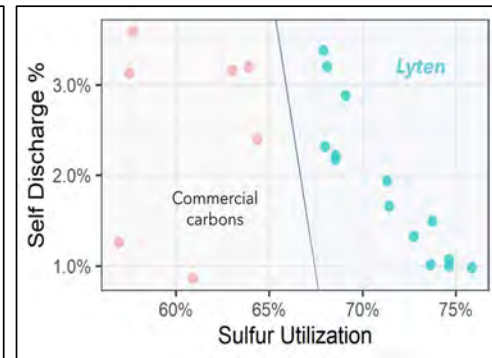
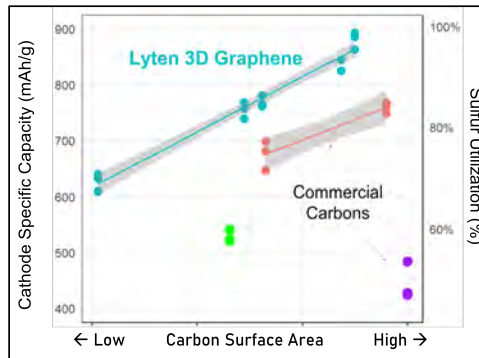
Li-S VS NMC (SOLID STATE, Si ANODE) AND LFP



LYTEN 3DG EXHIBITS SUPERIOR PERFORMANCE

Lyten 3D Graphene forms the primary structure of the cathode

- Chemical environment of 3D graphene may be tuned with aliovalent doping and functionalization to enhance sulfur affinity and kinetics
- Outperforms high surface area commercial carbons. Unique core-shell structure, coupled with high surface-area, results in excellent utilization and low self-discharge.
- Cathodes fabricated with spray-dried active materials with aqueous binder using standard coaters



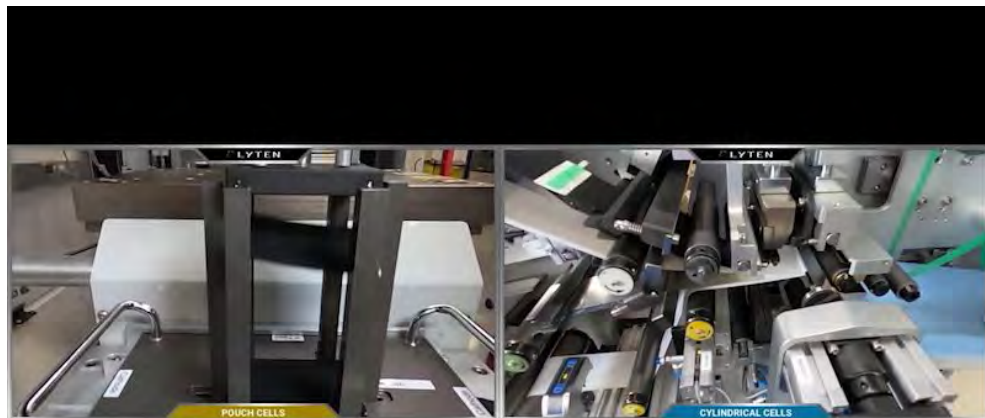
Li-S PRODUCT AND INDUSTRY ROADMAP

Sectors	Qualification Timeline	Cell Form Factor	2024	2025	2026	2027	2028	2029
Automotive	2.5 - 3 Years	Pouch 21700	TRL4	TRL5	TRL6	TRL7	TRL8	
Last Mile Delivery	2 - 2.5 Years	21700	TRL4/5	TRL6	TRL7	TRL8		
Defense - General	1.5 - 2 Years	18650	TRL5/6	TRL7	TRL8			
Defense/Commercial - Drone	1 - 1.5 Years	Pouch	TRL 7	TRL8				
Defense/Commercial - Satellite	1 - 1.5 Years	Pouch 18650	TRL5/6	TRL 7	TRL8			
EVTOL	2.5 - 3 Years	21700	TRL5	TRL6	TRL6/7	TRL7/8	TRL8	
Non-Auto (e-bike, Motorcycle, Marine)	2 - 2.5 Years	TBD	TRL4/5	TRL6	TRL7	TRL8		
Other (e.g. Heavy Trucking, Earth Moving)	2 - 2.5 Years	TBD	TRL4/5	TRL6	TRL7	TRL8		

TRL4/5 Sampling
 TRL6 Fleet Testing
 TRL7 Field Piloting
 TRL8 Full Production

▲ First gigafactory start





Ramping to 200,000+ cells per year
2MWh nameplate capacity

Commercial LIB production line
With only minor modifications



AUSTRALIAN LEVERAGE TO GLOBAL CARBON NEUTRALITY

By

Adrian Griffin

Future Technology Trust, Australia

Presenter and Corresponding Author

Adrian Griffin
ag@esg-energy.com.au

ABSTRACT

The global ESG compliance push is affecting almost all businesses, with supply-chain emissions doing the front-running. Emission reductions inherent in the renewable energy sector are perceived as a climate-change saviour; however, that sector relies on the minerals industry, which not only supplies it with raw-material inputs but also leads the way in recycling end-of-life materials to maintain sustainability and minimise carbon footprints. Indeed, a vast range of critical minerals is required to maintain the very existence of renewable energy, not to mention the battery back-up necessary for power storage and grid levelling. The battery industry, an insatiable consumer of minerals, is thus an integral element of the drive towards carbon neutrality and greening of the planet.

Australia occupies a unique position in the supply chain being developed to achieve carbon neutrality, since it is a significant source of many of the resources required, including nickel, cobalt, manganese, lithium and rare earths. That supply chain starts with exploration and mining to feed the downstream processing and manufacture of the materials being created to electrify the world, including domestic, industrial and transport applications. But that's not the end of the materials lifecycle; the fate of spent materials at the end of each product's life must also be considered.

Reducing carbon footprints involves more than examining ways of shipping the nickel, cobalt, lithium, iron and phosphorous to battery producers for fashioning into storage devices, as indeed it takes more than the mining of rare earths to produce high-performance magnets or the production of copper to expand power grids. Lifecycle optimisation must also extend into high-technology manufacturing areas.

As the source of a large proportion of the world's critical minerals, Australia has the greatest potential of any country to reduce carbon footprints by downstreaming its mineral products into things like refined metals, magnets, motors, wind turbines, battery chemicals, precursors, anode and cathode active materials, cells and batteries. But if such downstream production is necessary, Australia cannot simply rest on its laurels, producing the same minerals as it always did (including nickel for the production of ternary cells). Shouldn't Australia instead backward-integrate from a product with superior lifecycle attributes and mine that product accordingly? As the country strives to adopt the best available technologies to supply precursors, cathode powders and, ultimately, batteries for renewable-energy storage, the lithium chemical lithium ferro phosphate ('LFP') is a case in point. For original equipment manufacturers ('OEMs'), advanced materials like LFP offer previously unrecognised advantages in relation to the reduction of carbon emissions.

Advanced metallurgical techniques currently in development by Australian companies as part of 'urban mining' – the rebirthing of the critical materials contained in end-of-life products – provide further environmental benefits.

One could say, then, that Australia has the ultimate leverage in terms of global decarbonisation.

Keywords: ESG, legislation, sustainability, lithium, battery, critical materials, emission reduction, Australia, carbon neutrality.

INTRODUCTION

The global push towards carbon neutrality has lit legislative fires around the globe and influenced policy on resource development. Indeed, that push is impacting all aspects of daily life, none more so than the way energy is generated and used. Together, transport, electricity and heating account for nearly 50% of greenhouse gas ('GHG') emissions. Displacing coal-fired power generation and removing the use of fossil fuels in transport applications are the most obvious methods of re-engineering for the benefit of Earth's fragile atmosphere and the dire consequences of accumulating further GHGs.

Today, the supply chains that provide the critical materials required to reduce GHG emissions are as fragile as the atmosphere itself; hence, most developed nations have a target list of what is referred to as 'critical minerals', 'critical materials', 'strategic commodities' or similar. Put simply, these are substances that may be subject to supply disruption, which impacts economies, national security and/or the delivery of advanced technologies.

In 2023, the Australian federal government published its Critical Minerals Strategy[1], citing the nation's wealth of mineral resources, mining and processing expertise and reliability of supply as fundamental factors in developing the nation as a renewable-energy superpower. Although the government failed to define what a 'superpower' actually is, it is probably fair to assume that it relates to sovereign control of a significant portion of the renewable-energy supply chain. That being the case, the strategy is heavily oriented towards battery materials and the metals required for e-mobility and power generation, with a focus on Australian control of the renewable-energy supply chain.

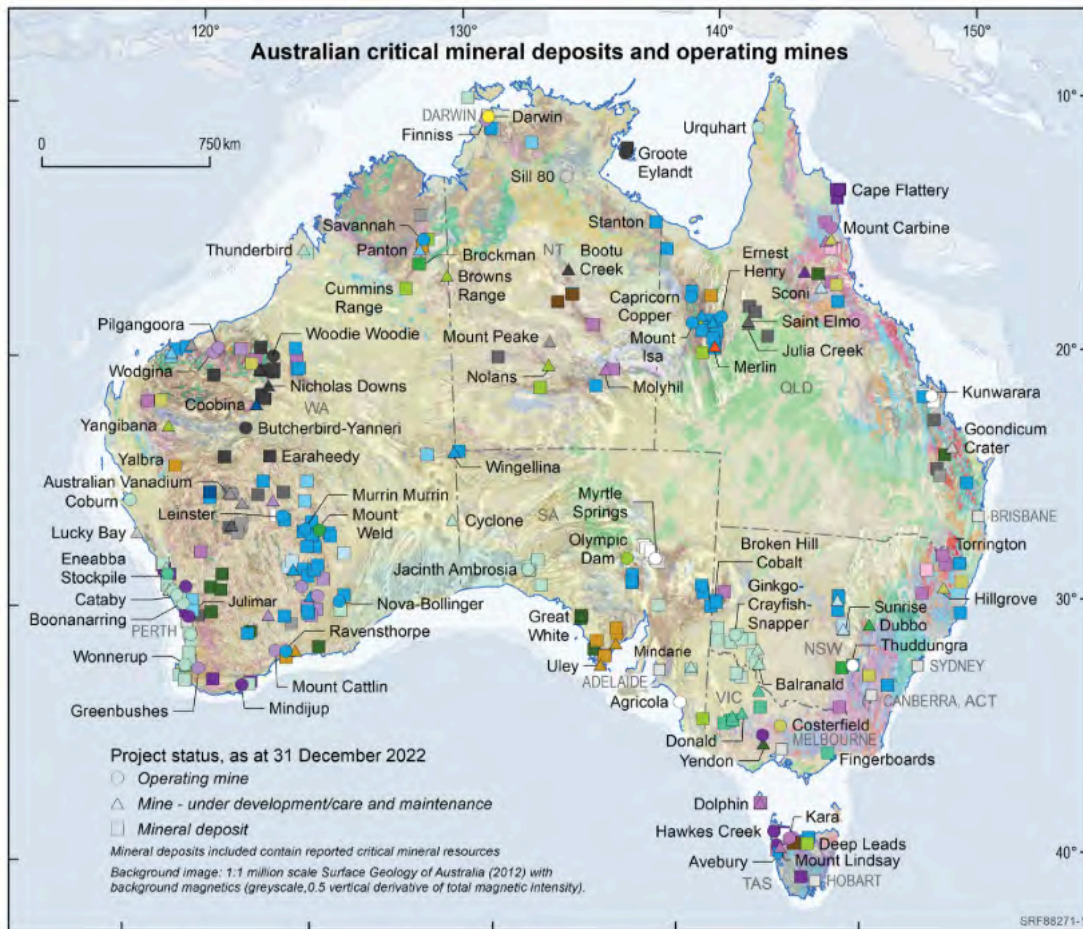
More recently (in May 2024), when the Australian federal government handed down its annual budget, it was noted that:

"This net zero transformation presents opportunities for Australia's economy, regions, industries, and communities. Achieving Australia's emissions reduction commitments and realising the opportunities that accompany the transition will require significant investment by governments and the private sector."

Australia is the world's largest producer of lithium, primarily in the form of spodumene concentrates, but downstream processing is also positioning the nation as a supplier of lithium chemicals. Historically, Australia has been a major producer of nickel and cobalt and this too has morphed into the supply of battery-grade chemicals, albeit threatened by expanded production out of Indonesia that is fuelled by that country's government policy and international investment, mainly from China. The graphite used in battery anodes is also produced in Australia and advancement towards downstream products such as spherical graphite is well underway.

The rare-earths industry outside China is dominated by Lynas Rare Earths Ltd, with ore sourced from the Mt Weld carbonatite in Western Australia and downstream processing occurring in Malaysia. However, some of the latter capacity is being repatriated to Kalgoorlie. Iluka Resources Ltd, a late entry into the rare-earths market, has received substantial Australian federal government funding to build downstream refining capacity based on monazite feed from its West Australian mineral-sands operations. The refinery is located at Eneabba, on the Western Australian coast. There, separated rare-earth oxides will be produced not only from Iluka feed stock but also from concentrates supplied by Northern Minerals Ltd's hydrothermal quartz/xenotime breccias at Browns Range in Western Australia.

The above examples illustrate Australia's potential/future lead in the supply of raw materials, as was clearly acknowledged in *Australia's Critical Minerals Strategy 2023-2030'* and summarised geographically in Figure 1.



- Commodity type**
- Aluminium (HPA)
 - Antimony
 - Bismuth, +/- Cobalt, +/- Indium
 - Chromium, +/- Cobalt, +/- PGE
 - Cobalt
 - Platinum Group Elements (PGE), +/- Cobalt
 - Scandium, +/- Cobalt, +/- PGE
 - Graphite
 - Helium
 - Indium
 - Lithium, +/- Tantalum, +/- Niobium
 - Magnesium
 - Manganese ore
 - Heavy Mineral Sands (HMS) - Titanium, Zirconium
 - HMS - Titanium, Zirconium, REE
 - Rare Earth Elements (REE)
 - REE, Zirconium, Niobium, +/- Hafnium, Lithium, Tantalum, Gallium
 - Rhenium
 - Silicon
 - Tungsten
 - Titanium
 - Titanium, Vanadium
 - Vanadium

© Commonwealth of Australia (Geoscience Australia) 2022

Figure 1 shows Australia's critical minerals endowment.

While it is clear that Australia's mineral endowment forms the first link of the critical minerals supply chain, the control required for the nation to become a 'superpower' is clearly lacking. Downstream processing has never been a great national attribute, whereas operating as one of the world's largest quarries has. While that is changing, planning for the future involves gaining a competitive advantage via further development of new technologies that increase the sustainability of Australia's resources, expanding downstream processing capabilities and investing in the high-tech applications of the products produced.

The political powerhouses of the world – the European Union ('EU') and the United States ('US') in particular – have developed inward-looking policies to protect their supply chains; however, the Australian market is too small for such policy drivers to be effective. Australia MUST look outwards and focus on becoming the preferred and reliable supplier of critical materials and value-added products for the global development of carbon-reduction technologies.

This paper examines some of the global drivers of change and how Australian technologies and products can become indispensable to the supply chains necessary for achieving carbon neutrality. Much more than a technical challenge, there is an opportunity for Australia to use the global push for carbon neutrality to expand its economy.

LEGISLATIVE DRIVERS

Global trends

The legislative and policy drivers towards carbon neutrality are many and varied, with the most visible being the Kyoto Protocol (effective 2005) and the 'Paris Agreement'. The latter is an internationally binding treaty, effective as of November 2016 and adopted by 196 parties, to hold *“the increase in the global average temperature to well below 2°C above pre-industrial levels”* and pursue efforts *“to limit the temperature increase to 1.5°C above pre-industrial levels.”* Backed by analysis on the part of the Intergovernmental Panel on Climate Change (IPCC) of GHG emissions on climate change, the parties agreed protocols to reduce emissions on a nation-by-nation basis.

To achieve emission reduction targets, new technologies must be developed and implemented. From a practical point of view this has required the development of targets that affect the phase-out of old technologies such as internal combustion engines and coal fired power plants and the phase-in of alternatives. In the transport sector the alternatives are limited; hydrogen, ammonia and biodiesel are the most advanced zero-carbon fuels but the most advanced propulsion systems remain battery-powered.

The rate at which legislation is driving ambitions is demonstrated by the introduction of policies in the US and EU, as depicted in Figure 2 below.

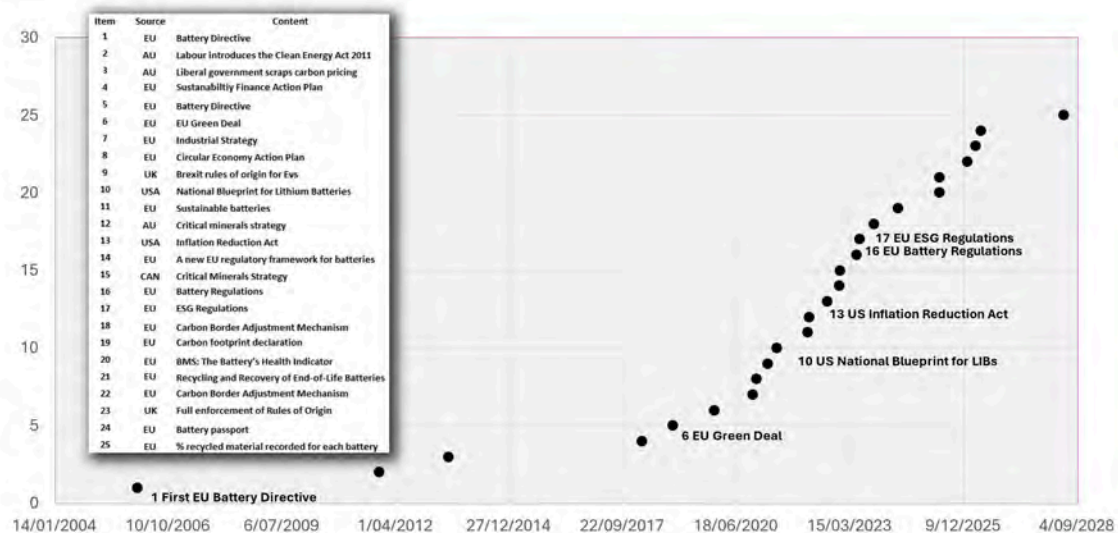


Figure 2 shows major policy implementation in the EU and US, commencing with the first EU battery directive in 2005 and extending to sustainability compliance in 2028.

The EU

To aid sustainability, the EU has set targets for battery recycling that include collection rates, total material yield and lithium recovery, as shown in Figure 3.

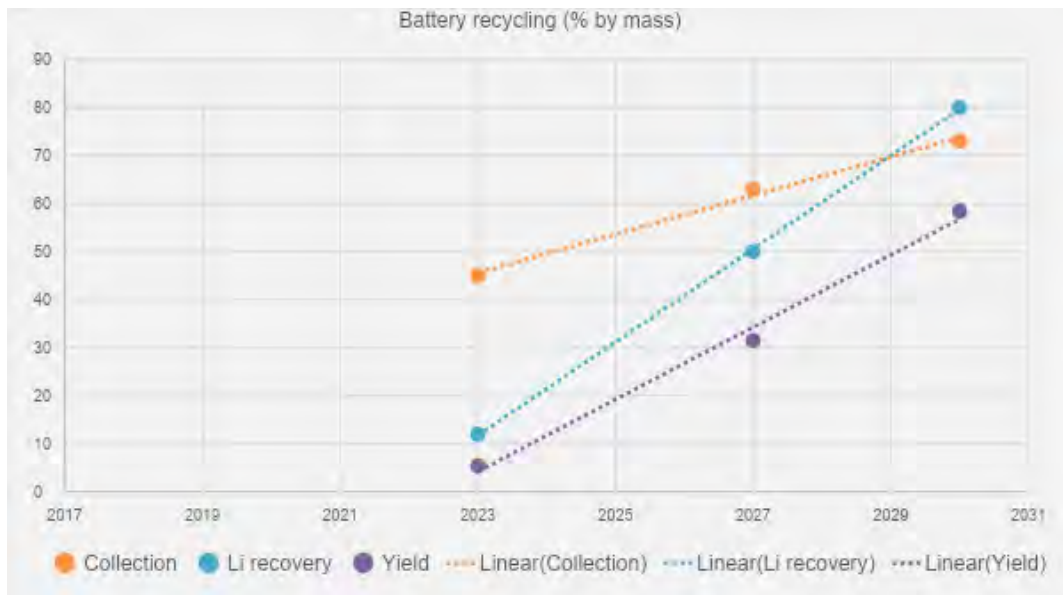


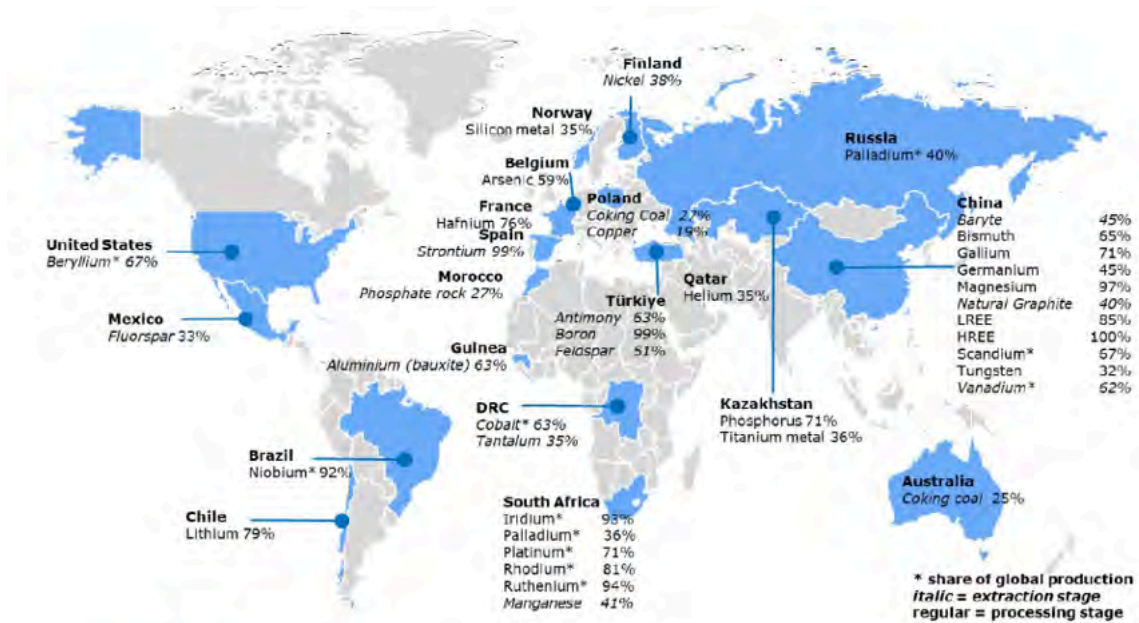
Figure 3 shows EU Battery Regulations, May 2023 that provide the framework for battery sustainability by setting targets for recycling.

In addition to the sustainability requirements, the EU protects supply chains by mandating that OEMs have minimum content by mass of batteries and that the electric vehicles ('EVs') into which these batteries are installed are domestically sourced. Further protection is afforded by the EU Carbon Border Adjustment Mechanism (CBAM), a tariff that protects European industry from imports free of carbon tax, and by the *European Critical Raw Materials Act*, which provides for inclusion of the following provisions in the critical minerals supply chain by 2030.

- No less than 10% domestic supply input.
- At least 40% domestic downstream processing.
- At least 15% of annual consumption recycled.
- No more than 65% of each strategic raw material, regardless of the extent of downstream processing, to be sourced from a single country outside the EU.

The *European Critical Raw Materials Act* clearly reveals Europe's supply-chain vulnerabilities in terms of decarbonising the economy and some of the opportunities for Australia, as illustrated in Figure 4. The European Commission has listed 20 minerals as 'critical'. While that list is updated periodically, until recently it didn't include lithium. Why? Because there were no cathode producers in the EU, so lithium was not considered a vulnerable supply. It is worth noting that lithium, phosphorus, graphite and cobalt are currently on the list, with nickel conspicuous by its absence. Turmoil in the nickel industry, and the strong association of Indonesia and China in the production of that metal, may result in other changes to the list in the future, particularly as EU lithium-ion cell production expands and the London Metal Exchange ('LME') applies sanctions to Russian metal production as a consequence of the war in the Ukraine.

In July 2022, the government of the United Kingdom ('UK') imposed a 35% additional duty on imports of Russian nickel and shortly thereafter the LME suspended Russian nickel brands on warrant in LME-listed UK warehouses.



Source: [European Commission](#), 2023.

Figure 4 shows the source of EU critical raw materials in 2023, demonstrating potential future lack of supply compliance (no more than 65% from one country) for lithium, cobalt, phosphorus, beryllium, niobium, hafnium, bauxite, platinum group metals, antimony, boron, bismuth, gallium, magnesium, rare earths and scandium.

The EU is seeking reciprocal arrangements with the US on strategic raw material supply BUT the reality is that neither the EU nor the US is capable of securing significant supply within their state boundaries. Supply-chain security must include agreements with the nations that supply the raw materials.

The US

The US has implemented the *Inflation Reduction Act* ('IRA') which, although a very broad piece of legislation, provides supply-chain protection for the battery industry by way of subsidies, loans, grants and tax incentives. It is an adjunct to the *US National Battery Blueprint*, which provides for the following.

1. Secure access to raw and refined materials for commercial and defence applications.
2. Support for processing industries to meet domestic battery demand.
3. Stimulation of domestic production of active materials, cells and battery packs.
4. Development of end-of-life recycling for critical materials.
5. Advances in battery technology through research and development, science, technology, engineering and mathematics (STEM) education and workforce training.

The IRA focuses strongly on internal supply and domestic production but treats nations with free-trade agreements as complying with the act and able to supply commodities without the end-users of those commodities losing the benefits that may otherwise accrue through domestic supply. The IRA further requires that, by 2024, US EV manufacturers source 40% of critical battery minerals domestically or through free-trade partners, increasing to 80% in 2026. This strongly favours the use of Australian-sourced lithium and other battery metals.

Moreover, the IRA defines Foreign Entities of Concern ('FEOC'), which can be sovereign states or companies with more than 25% Chinese equity. FEOC include China, Russia, North Korea and Iran. While these defined states may seem remote in terms of Australian commerce, much of Australia's mining and mineral processing industry includes a considerable proportion of Chinese equity. Australian public companies need to manage their share registers to avoid being labelled an FEOC or quarantined producer through the judicious use of joint ventures.

Most of the IRA provisions will become effective in the near future, with full implementation by 2025. This has prompted an appeal by China to the World Trade Organisation regarding restrictive trade practices that prejudice the Chinese economy. In April 2024, as a consequence of pressure from OEMs, the US Biden administration extended the IRA compliance timeframe for graphite – 90% of which is sourced in China – by a further two years, to 2027.

Adding to the above complexities, the European Commission is currently investigating whether Chinese manufacturers benefit from unfair state subsidies. This brings to the fore China's similar allegations with respect to the Australian wine industry, whereby China countered by applying an up to 200% tariff on Australian wine to decimating effect! The critical minerals industry is currently in a three-way trade war (the EU, the US and China) that is causing collateral damage to Australia and other jurisdictions.

The US has only 20 free-trade agreements in place, these being critical if foreign supply is to comply with the IRA. Significantly, few of the counterparties are potential suppliers of critical raw materials to the US or involved in the supply of materials to the green-energy sector. The exceptions are:

- Australia;
- Canada;
- Chile;
- South Korea;
- Mexico, and
- Morocco,

which collectively have supply capability for lithium, nickel, cobalt, graphite, rare earths and phosphorus. South Korea can also provide a range of value-added products to service the US battery industry.

Notably, the IRA imposes penalties on product imported from China, currently the biggest supplier to the US battery industry. The US government has put the relationship between General Motors ('GM') and China's CATL (the latter the world's largest battery manufacturer) under the microscope, seeking documentation of the CATL/GM partnership and the plan to build a \$3.5 billion battery manufacturing plant in Michigan using Chinese technology. It seems GM has been reluctant to supply the requested documents and construction is in hibernation.

In the US, 2023/24 saw a slowing in demand for EVs and the continued dominance of Chinese supply as the US domestic industry builds capacity. It seems too that the contractual/corporate relationships between US OEMs and the Chinese battery superpowers are changing to accommodate the advantages available through the IRA. Regardless of corporate strategies, the fact that Australia has a free-trade agreement with the US provides a path of least resistance for the supply of raw and/or processed materials.

Australia

The federal budget 2024

On Tuesday 14 May 2024, the Australian federal treasurer handed down the 2024 budget on behalf of the federal Labor government. The budget, which is part of the mechanism for implementing policy, acknowledged that critical minerals are a key input into many clean-energy technologies.

The budget papers further noted that:

“Scaling the supply of critical minerals will be essential to support the global transition to net zero by 2050. Australia can improve the resilience of supply chains and add more value to our resources by processing and refining critical minerals.

“Critical minerals are a key input to many clean-energy technologies. Scaling the supply of critical minerals will be essential to support the global transition to net zero by 2050. By adding more value to our resources by processing and refining critical minerals, Australia can improve the resilience of

global supply chains. This Budget establishes a Critical Minerals Production Tax Incentive for eligible processing and refining costs from 2027-28 to 2039-40 to incentivise investment in refining and processing of the 31 critical minerals currently identified on the Government's Critical Minerals List, at an estimated cost of \$7.0 billion over the decade.

"The Government is also partnering with states and territories to complete pre-feasibility studies for critical minerals common-use infrastructure through the Critical Minerals National Productivity Initiative and supporting up to \$1.2 billion in priority critical minerals projects through the Critical Minerals Facility and Northern Australia Infrastructure Facility. This includes the Alpha HPA alumina project in Queensland and Arafura Rare Earth's Nolans rare earth project in the Northern Territory.

"The Government is investing \$556.1 million over ten years to progressively map Australia's potential for critical minerals, alternative energy, groundwater and other resources, providing scientific information to guide future investment."

The budget provides for a 10% tax rebate on eligible production expenditure or an equivalent refund if there is no taxable revenue. The estimated cost is a total of A\$17.6 billion up to 2041. It all seems like a positive move, but the program will not commence until 2027 and runs the political risk of being overturned with an intervening change of government. Moreover, this budget decision, rather than being positive, may force the closure of further ailing Australian nickel operations that are an integral part of the battery-materials supply chain. Clearly, such an outcome was not contemplated by Resources Minister Madeleine King, who commented the budget was "... the most significant resources budget that any government has ever released."

In the traditional budget reply speech delivered by Peter Dutton, leader of the federal opposition on 16 May 2024, Australia's critical minerals policy became a political football, in that he pledged the removal of the A\$17.6 billion in tax incentives to the critical minerals and renewable hydrogen sectors if his party gained power at the next election, which must be held before 27 September 2025.

The Australian Critical Minerals Facility

Export Finance Australia manages the A\$2 billion Critical Minerals Facility established in 2021. So far, A\$1.5 billion has been committed to Iluka Resources Ltd, Renascor Ltd Resources and EcoGraf Ltd (see **THE INNOVATORS** below).

RENEWABLE ENERGY STORAGE

Hydroelectricity is likely to remain the world's largest energy-storage mechanism for many years to come and 'pumped hydro' a practical means of optimising capacity utilisation. Grid-scale power storage via batteries is flourishing in areas with plenty of wind and/or sunshine, making Australia a prime candidate for large-scale battery storage. On a smaller scale, Australia could be considered the Mecca of rooftop solar, given that more than one in four houses has solar-generated power capacity. Indeed, per capita, Australia's rooftop solar installations far exceed those of other jurisdictions considered leaders in green energy, including Japan, California and Germany. Conventional lithium-ion batteries, including LFP and ternary batteries such as nickel cobalt manganese ('NCM'), dominate current storage and backup solutions for rooftop solar power generation.

Other battery storage candidates include sodium-ion and various types of 'flow' batteries. The latter include zinc bromine (patented in 1879) and the vanadium flow battery patented by the University of New South Wales ('UNSW') in 1986. UNSW leads the way in flow-battery commercialisation, with the largest example installed in the Chinese city of Dalian; it has a capacity of 400 megawatt hours ('MWh') and output of 100 megawatts ('MW'), enough supply up to 200,000 residents daily.

Australia's first commercial installation of a vanadium flow battery, completed in South Australia in mid-2023, is modest by comparison, taking power from nearby photovoltaic panels and storing up to 8 MWh.

The choice of battery for renewable-energy storage must consider many factors, including lifecycle, cost, footprint and recyclability. In fact, the latter will be a major driver in future as material supply and

sustainability become paramount. The vanadium flow battery, for instance, boasts great longevity, is close to 100% recyclable and operates well at high temperatures. The most competitive lithium-ion counterpart, and the fastest growing sector of the battery industry, is LFP, a chemistry that is ideally suited to stationary energy storage and significantly cheaper than its ternary counterparts. In fact, LFP now accounts for more than 50% of the lithium-ion battery market.

While LFP batteries seem a great candidate for energy storage, being able to recycle their active materials on a commercial basis is proving a challenge ... and, while that challenge remains unresolved, vanadium flow batteries may be the most sustainable choice for large-scale stationary energy-storage applications. That said, LFP recycling solutions could be an area in which Australian expertise provides a leading edge for the LFP market on a global basis.

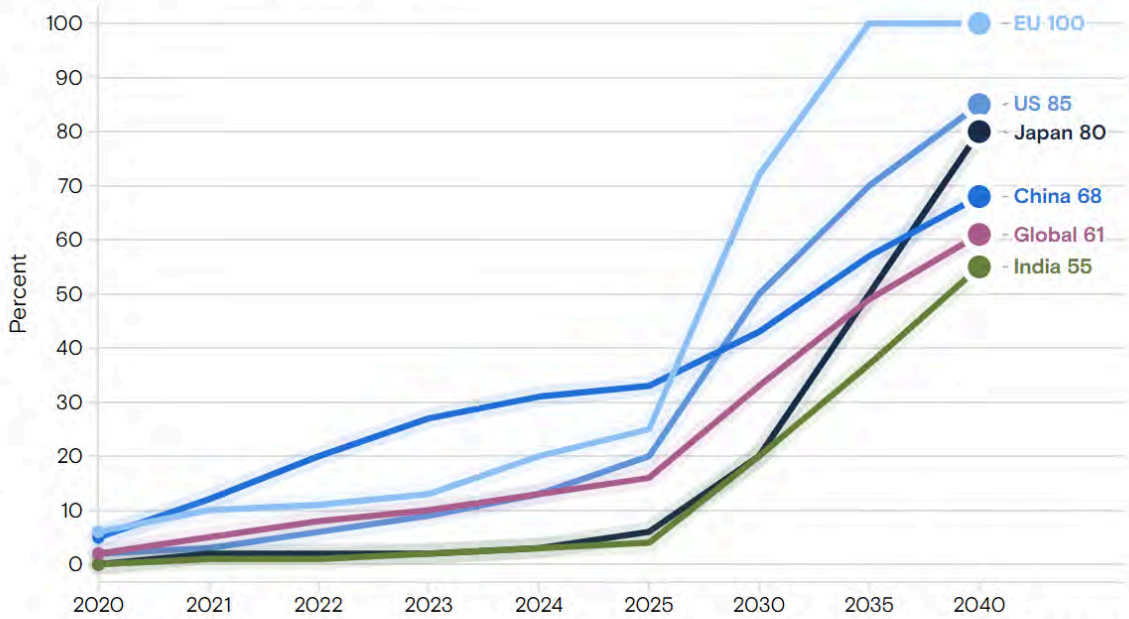
ELECTRIC VEHICLE SUPPLY PROJECTIONS

China currently commands about 45% of the global EV market, with about 10 million sales predicted for 2024. Worldwide, sales of electric vehicles ('EVs') rose by 14% in 2022 compared with the previous year and were up a further 18% in 2023. Markets are sensitive to subsidies, tariffs and purchase prices and, with recent lithium price peaks, OEMs were searching for ways to reduce the cost of their vehicles, passing on those savings to consumers to maintain demand. Not only did the high price of lithium affect demand but it also accelerated development of high-energy-density LFP technologies to cut costs. Not only does LFP use less lithium per unit of energy stored than comparable ternary cells but the other elements in the cathode active material – iron and phosphorus – are cheap in comparison with the costs of the nickel and cobalt used in ternary cells.

China, which introduced the first tax exemptions for EVs 10 years ago, has announced several extensions since and recently extended the tax breaks offered until 2027. Presently, each vehicle, be it EV, plugin hybrid or hydrogen fuel cell, commands a sales-tax exemption of up to 30,000 yuan (about US\$4,175), sliding back to zero in 2027. Previously, the threat of removal of tax exemptions slowed EV demand in China, with subsequent demand-driven impacts on the price of battery commodities. The biggest impact was on the prices of lithium chemicals, which tumbled from late 2022 in parallel with that of cobalt. Potentially, this rings warning bells for 2027, when China once again plans to remove EV subsidies.

Goldman Sachs, meanwhile, suggests that the global EV market will expand to 73 million units per annum, up from a mere 2 million in 2020. The company predicts a change in demographics over that period, with the EU eclipsing China in terms of proportion of the vehicle market dominated by EVs (Figure 5).

Electric vehicle sales ratio (%)



Source: IHS Global Insight, Goldman Sachs Research • 2022-2040 are forecasts

Goldman Sachs

Figure 5 shows EV sales expressed as a percentage of total vehicle sales.

QUANTUM OF CRITICAL MINERALS REQUIRED

Defining demand for critical minerals on a global basis is a daunting task, as the materials defined as critical vary from jurisdiction to jurisdiction. Suffice to say, the largest tonnage commodities involved in the energy transition are a little easier to quantify, as has been done by United Nations Trade and Development ('UNCTAD') (Figure 6). While this information represents only a small proportion of the critical minerals by number, it does constitute the bulk of the critical metals required to produce cathode-active materials for lithium-ion batteries. UNCTAD's projections demonstrate a consensus that critical minerals will be in short supply as the world strives to achieve zero carbon. Many projections predict much greater supply gaps, but none foresee oversupply in the medium to long term.

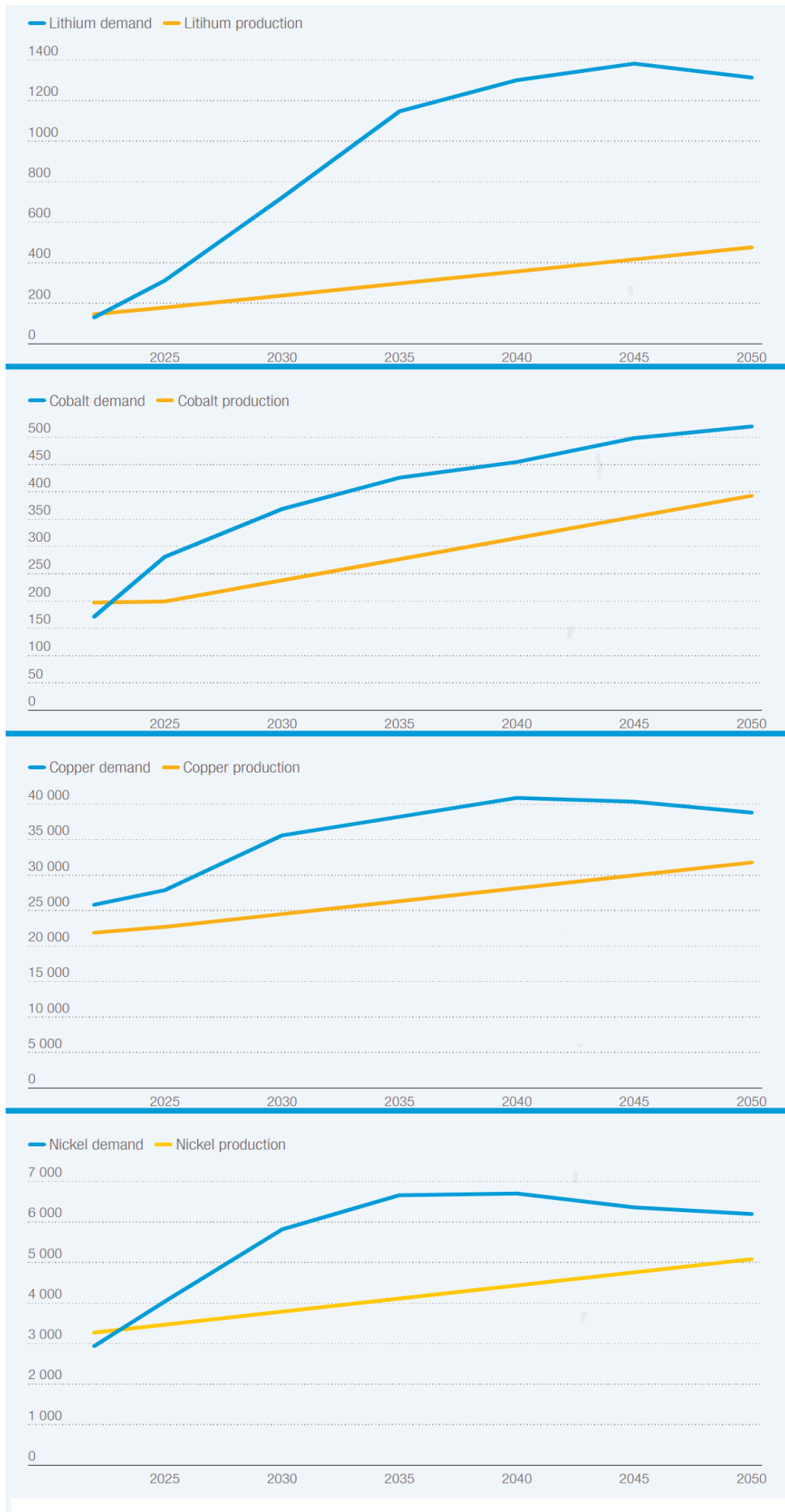


Figure 6 shows world mine production and demand for lithium, cobalt, nickel and copper in metric tons.

Australia is a significant producer of battery metals; indeed, it is the largest producer of lithium and the eighth largest producer of copper internationally, being home to the world's second-largest copper-producing company, BHP. Groote Eylandt, operated by South 32, produces 12% of the world's manganese ore.

As for cobalt, Australia is the fourth largest producer behind the Democratic Republic of Congo ('DRC'), Russia and Indonesia. Globally, 98% of cobalt is produced as a byproduct, mainly from nickel and copper production. Australia is no exception, with Glencore's Murrin Murrin lateritic nickel operation the largest cobalt producer in the country. As previously noted, however, changing dynamics in the nickel market have seen a rapid rise in Indonesian production of both nickel and cobalt. Nickel production in Indonesia has risen tenfold since 2015, making it the world's largest producer at around 1.8 million tonnes in 2023^[2]. That stratospheric rise in production resulted from the banning of nickel-ore exports and subsequent Chinese investment in Indonesia's domestic nickel production.

Currently, consumer pressure and voluntary constraints on the use of cobalt originating from the DRC have not only affected market dynamics but also influenced the chemistry of choice in lithium-ion battery production, resulting in a reduction in the use of cobalt and an increase in nickel in NCM (lithium nickel cobalt manganese) cells and a shift towards LFP cells.

Being a prolific producer of battery metals, Australia is well-positioned to engineer a more beneficial role in the supply chain by developing the expertise to produce value-added products from these metals rather than exporting ore or concentrates.

CAN AUSTRALIA BRIDGE THE SUPPLY GAPS?

The impact of supply and demand on battery materials is not synchronous due to the varied provenance of materials, legislative constraints, consumer pressure and changing battery chemistries. This makes it imperative to evaluate the impacts of future changes and maximise the benefits Australia can reap by filling the gaps, not only at a natural resource level, but also by short-circuiting some of the supply chain through downstream value-adding, as well as the application of advanced technologies to improve sustainability, from mining through to battery production and beyond into recycling. Some of the trends evident are presented below and these must be considered as Australia seeks to maximise its leverage to global carbon neutrality. Opportunities abound but pre-empting supply-chain changes will amplify the benefits.

Nickel

Using nickel as an example and analysing the effects of a rapid increase in supply from Indonesia supported by Chinese capital, it is evident that there has been severe impact on the nickel price. Nickel prices have remained relatively low since Indonesia introduced its nickel-ore export bans about 10 years ago and subsequently ramped up Australian nickel production.

With nickel production currently coming offline in Australia due to competitive pressures, it would seem logical that supply gaps be filled by further expanding production from Indonesia. However, the Indonesian industry, dominated as it is by the high-pressure acid-leaching ('HPAL') of laterites and the smelting of laterites to produce nickel pig iron (NPI). The Indonesian nickel industry has a very high carbon footprint^[4] and produces considerable environmental pollution. In fact, HPAL plants have about twice the carbon footprint of nickel produced from sulphides, while the NPI plants, fuelled by coal, have about six times the carbon footprint. There is now enormous pressure from consumers, OEMs, the World Trade Organisation ('WTO') and governments for Indonesia to clean up its nickel industry and remove trade restrictions imposed by the banning of nickel ore exports.^[5] In 2021 the EU lobbied the WTO to establish a panel to seek the elimination of unlawful export restrictions imposed by Indonesia. Meanwhile, deforestation, carbon emissions, tailings disposal and coal-ash disposal issues continue to plague the Indonesian nickel industry.

So it is that the world's largest nickel producer may itself become a supply chain vulnerability, exacerbating the projected gap between future supply and demand. Further supply concerns arose in May 2024, with Philippine trade officials announcing that country's intention to expand from its current

two refineries by adding a further three HPAL plants. Potential investment from China, Australia, America, Japan and Korea has been cited as the source of capital. Other news reports suggest the US is negotiating directly with the Philippines government to prevent Chinese dominance. It is thought that these negotiations include a trilateral arrangement by which the Philippines would supply ore, the US would provide financing and a third country such as Japan, South Korea or Australia would provide processing expertise^[6].

Lithium

Softening of EV demand in 2023 has been widely credited for the reduction of record 2022 inventory levels held by lithium chemical companies and battery producers. Destocking reduced demand, with a subsequent catastrophic fall in the price of both lithium chemicals and concentrates (Figure 7). Lower government incentives and inadequate charging infrastructure are expected to curtail EV sales in 2024. According to Wood Mackenzie, the rise of LFP cathode chemistries that require lower lithium content is outpacing the growth of high-nickel cathode chemistries^[7]. This trend exerts further downward pressure on the growth in lithium demand but does provide an opportunity for Australian companies involved in the development of LFP cathode-active materials.

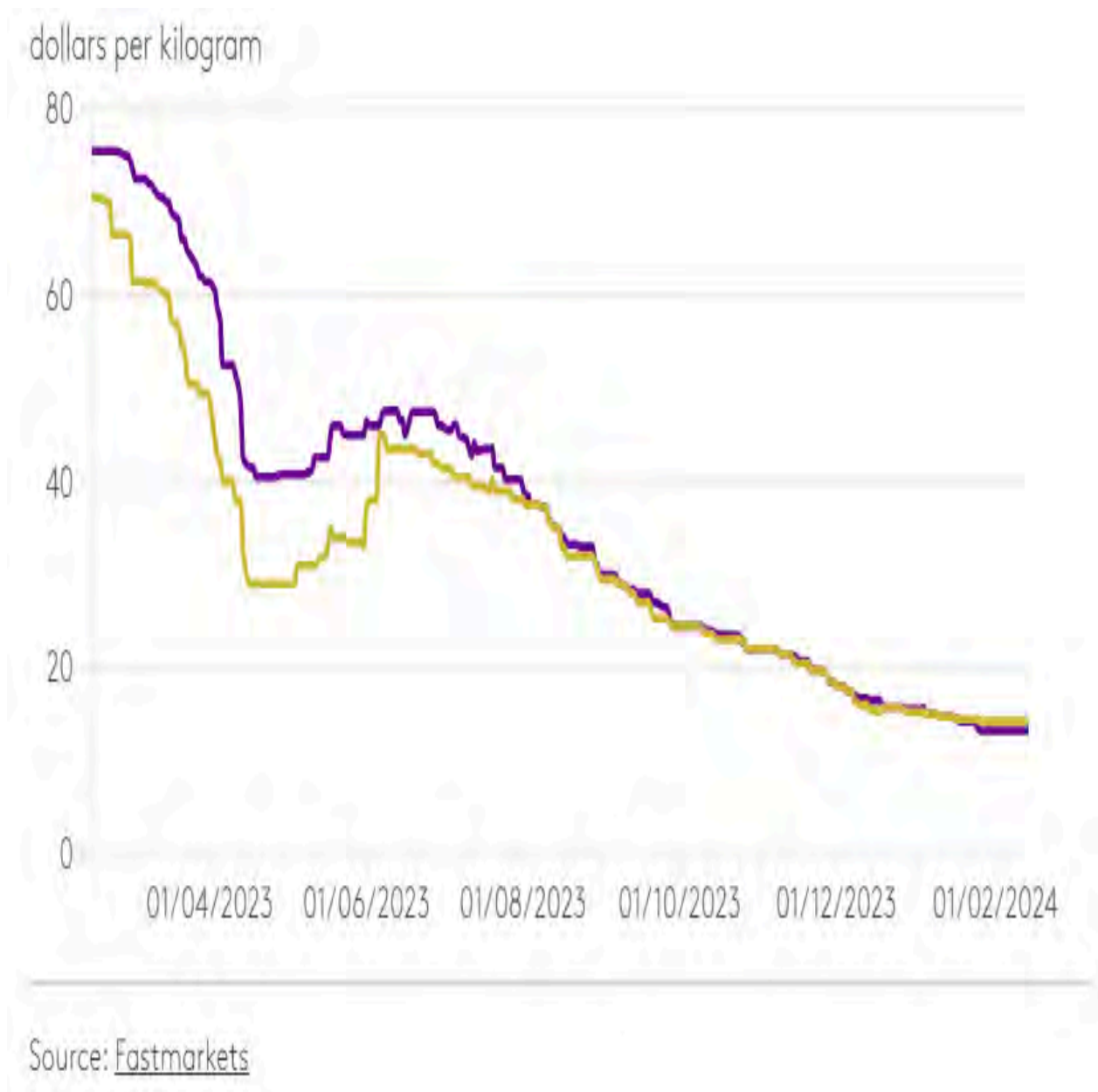


Figure 7 shows recent pressure on lithium prices.

This year lithium carbonate prices plummeted from spot highs of around US\$90,000/tonne to current levels (May 2024) of around US\$15,000. Reduced demand has led to major producers curtailing production; however, demand is likely to rise as restocking becomes a necessity and improved EV charging infrastructure boosts consumer confidence.

While the opinions of financial analysts differ with respect to timing on lithium’s future rise from over-supply to deficit, most agree that deficit will occur, bolstering commodity prices and creating greater opportunities to utilise latent capacity and expand operations. That aside, the Australian lithium industry needs to critically evaluate its own performance and strive to optimise its use of resources. The Australian lithium industry is based on the recovery of spodumene from pegmatites and it is that recovery which is preventing optimal utilisation of resources. At best, producers of spodumene concentrate achieve a yield of around 75%, with some far below that level.

If the recovery dilemma can be resolved, perhaps the pending supply gap can be filled from Australian spodumene production without even expanding planned mining output; that is, simply recovering more lithium units from the materials mined. Australia has a great opportunity to develop technologies that improve yield, reduce operating costs, reduce carbon footprints and extend resource life.

Cobalt

Cobalt is a byproduct metal, with 60% of global production emanating from copper mining and 38% from nickel production; only 2% is from primary production in Morocco and Canada. The forecast supply gap is exacerbated by this lack of primary production, as most output is tied to copper and nickel production. As such, there is little flexibility in controlling output to meet demand.

Recent publicity relating to human rights abuse and the child labour employed in operations in the DRC evoked outcry around the globe, particularly with products such as mobile phones^[8]. Consumer pressure has led to companies such as Tesla increasing the nickel content of their batteries at the expense of cobalt or even transitioning to cobalt-free batteries such as LFP or LMFP (lithium manganese ferro phosphate), albeit the latter examples are probably driven more by issues of cost and safety than ethical concerns. Be that as it may, the cobalt supply gap is likely to be with us for some time, as the rate of increase in demand (Figure 8) is predicted to rise in the short term, reducing to a constant rate from about 2030 (see Figure 6).

As the rate of increase in demand for copper and nickel diminishes, the ability to supply the necessary amounts of cobalt may be jeopardised unless more primary – as opposed to byproduct – cobalt production is brought onstream. Potentially, production of primary cobalt is one solution that could benefit Australia as a potential supplier.

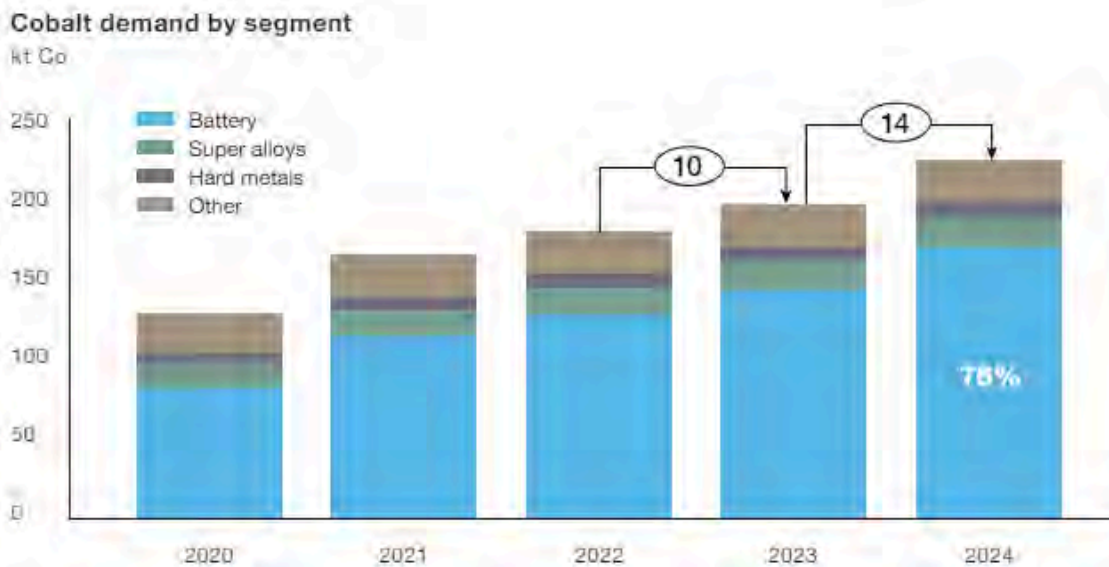


Figure 9 shows the increasing rate of demand for cobalt rising from 10% in 2023 to 14% in 2024 (source – the Cobalt Institute)

Copper

Copper has more diversity of applications than other battery material, with 60% consumed in the production of electrical wire and cables alone, as well as 20% in roofing and plumbing. In 2020, about 24% of copper was consumed in clean-energy technologies, with that usage anticipated to grow to 45% by 2040^[9].

The diverse use of copper results in much more complex demand dynamics than the critical metals supplying clean-energy technologies as the bulk of their market. Regardless, the move away from fossil fuels, particularly in the transport sector, will require substantial upgrades to power grids. The fossil fuel energy displaced by renewables will require copper cabling to deliver the equivalent amount of energy in the form of electrical power to consumers and it is unlikely that existing grid infrastructures will have the necessary capacity.

More than half of Western Australia's electrical power is delivered outside the state-controlled grid. Most of that is thanks to microgrids, with many unfortunately serviced by diesel generators on remote mine sites. Regardless, miners are leading the energy transition, with some of the world's largest non-government renewable energy projects currently being installed by them. Australian expertise in the establishment and utilisation of microgrids is a potential export opportunity.

Graphite

Graphite is the most commonly used active material in lithium-ion anodes. While probably not ideal, in terms of a trade-off of cost versus performance it is very hard to beat. Natural or synthetic, graphite comes in a wide range of product forms and quality; however, for battery applications natural graphite is superior. That said, natural graphite does need substantial downstream processing, often entailing very significant production losses and the cost and performance of synthetic graphite does pose a threat to conventional production.

China produces around two-thirds of the world's natural graphite and dominates the global market in downstream graphite products, meaning an already constrained graphite supply chain is now subject to Chinese export controls (imposed in October 2023 to preserve graphite for the Chinese domestic market). This creates a great opportunity for other graphite-producing jurisdictions, including Australia, where a number of projects are preparing for production, some vertically integrated with downstream processing.

RECYCLING – THE SUPPLY-GAP DISABLER?

We live in a world characterised by prolific waste and poor resource utilisation. Society needs to ditch its single-use mentality and focus on sustainability instead. There are of course exceptions to the rule, the lead-acid battery industry being one. Lead-acid batteries have been in service since 1859 as the principal means of electrical storage; today, though, they are being replaced by lithium-ion batteries. Recycling of lead-acid batteries began in 1920 and today 95% are recycled on a global basis, a great success story.

Unfortunately, lithium-ion batteries pose far greater recycling challenges than their lead-acid counterparts. Recycling of the latter requires little more than breaking, separation, sulphur removal, smelting and refining – the components are few and the chemistry constant. By contrast, lithium-ion batteries contain copper and aluminium in the current collectors, a vast range of compositions in both the anodes and cathodes and a variety of binders and electrolytes. Their casings too are complex (a combination of metals and polymers) and solder, wiring and battery management systems must also be dealt with during the recycling process. To date, the development of recycling technologies for lithium-ion batteries has focused on ternary cells containing lithium, nickel, manganese and cobalt. The lithium is relatively easy to recover as it remains soluble even at a very high pH. The other metals can be recovered using a range of common hydrometallurgical or pyrometallurgical techniques.

The focus on recycling of ternary cells has been driven by the value of the nickel and cobalt they contain. With LFP chemistry, however, the iron and phosphorus can be expensive to remove, so the cost of recycling such batteries must be covered by lithium revenue or tolling fees. This has led the South Korean government to remove subsidies for imported LFP-based EVs and battery packs due to the low yield of commercial commodities recovered during the recycling process^[10].

Unlike lead-acid batteries, the longevity of lithium-ion batteries (in the order of 10 years for ternary cells and 20 years for LFP) creates a substantial interval from the time a battery is placed into service until its availability for recycling. In EV applications, it is generally considered that the batteries will be retired when their charge reaches 80% of new battery capacity, at which point they may be repurposed for stationary storage applications, resulting in a similar second lifespan. In China, lead-acid batteries have been phased out of telecommunication applications, with repurposed, second-life EV batteries, principally LFP, being used instead.

If recycling is to significantly impact supply, two things must be achieved:

- recycling rates for lithium-ion batteries must be commensurate with those of lead-acid batteries, and
- a practical commercial solution to recycling LFP needs to be developed and implemented.

Indeed, a commercial solution for the recycling of LFP is imperative, given its rapidly increasing market share and likely future dominance of the lithium-ion battery market.

CARBON REDUCTION AT THE SOURCE OF RAW MATERIALS

New or used equipment?

The carbon footprint of today's mineral production is heavily weighted towards the energy used in the mining, processing and metallurgical recovery. The switch from fossil fuels to renewables will have an enormous impact on the critical minerals sector's push towards zero carbon. That said, there are other factors that might be considered; for example, the carbon footprint associated with the initial manufacture of mining fleets and equipment, and the benefits of refurbishment rather than making new purchases. It is worth noting that one major miner, Freeport McMoran, in an effort to reduce the carbon footprint associated with the supply of newly manufactured dump trucks, procures used trucks and refurbishes them. As a result, Freeport McMoran has not bought a new dump truck since 2006.

Australia could well benefit by establishing remanufacturing facilities in area where there are very large fleets of mining equipment such as the Pilbara, Kalgoorlie, Mount Isa, Broken Hill and the New South Wales and Queensland coalfields.

Fleet electrification

Fleet electrification is a primary factor in phasing out fossil fuel and achieving a subsequent reduction in carbon emissions, provided the electrical power required for recharging comes from renewable, or perhaps nuclear, sources.

Fortescue Metals Group ('FMG') has led the charge in this respect, with the aim of being zero-carbon by 2030. This resulted in the testing of the first, and at the time largest, electric dump truck in 2021 and has progressed to the use of hydrogen-powered blast-hole rigs and hydrogen-fuel-cell dump trucks. The benefits are clearly shown in FMG's Scope 1 emissions, 26% of which emanated from haul trucks and 36% from drill rigs and excavators prior to the commencement of decarbonisation. Rail haulage of iron ore from the various mining hubs to Port Hedland for export is also a heavy contributor to Scope 1 emissions. The FMG solution is the 'Infinity Train', a system that relies on electricity being generated on the downhill, loaded sections that comprise most of the line^[12]. That electricity is stored in batteries that fuel the locomotives for the return, unloaded journey. The system is designed to remove the need for the installation of renewable energy generation and recharging infrastructure, making it a capital-efficient solution for eliminating diesel emissions.

Not surprisingly, Rio Tinto is also making a push into electrification by partnering with OEMs for the development of zero-emissions autonomous haul trucks for use in its Pilbara iron-ore mining operations. BHP and Freeport McMoRan have similar programs underway.

Autonomous haulage (see also THE AUSTRALIAN INNOVATORS below)

While autonomous haulage certainly reduces labour cost, it is also a way of achieving greater utilisation and availability for a given fleet, thereby reducing both costs and emissions. The iron-ore miners of Western Australia's Pilbara region are world leaders in autonomous haulage, which involves not just trucks but also rail transport.

Rio Tinto's autonomous truck haulage has operated for some time, with the first unit developed and tested in partnership with Komatsu in 2017 using automation software developed by Rio Tinto. By 2018, 20% of Rio's truck fleet was autonomous as a result of the retrofit of its existing Komatsu units. Today, only 20% of Rio Tinto's fleet requires drivers. Meanwhile, Rio Tinto has been using autonomous rail haulage since 2019, although this has not been without its challenges, including three derailments in the first five months of 2024. In 2018, BHP suffered a derailment of one of its driverless trains (not to be confused with an autonomous train). In that case the train, hauling 268 wagons of iron ore, escaped without its driver and travelled at high speed until intentionally derailed ... with disastrous consequences.

Mineral Resources operates autonomous triple-trailer road trains to carry 330 tonnes of iron ore approximately 150 kilometres on a private, sealed haul road from the Ken's Bore mine site to the port of Ashburton. Autonomous road trains are being added to the fleet at the rate of 10 per month, with target commissioning of 120 units by the end of 2024.

Green fuels

Green fuels include biodiesel, hydrogen, ammonia, bioethanol and biochar. Research and development are key to the commercialisation of alternative fuels that can be used to displace fossil fuels. Government bodies within Australia are making significant investment in this field. Australia's Clean Energy Finance Corporation ('CEFC'), with access to around A\$30 billion of Australian government funding, leads decarbonisation investment in clean energy and co-funds projects with the commercial sector.

The Australian Renewable Energy Agency ('ARENA') funds renewable energy and sustainable transport projects, including biofuels and sustainable aviation fuel.

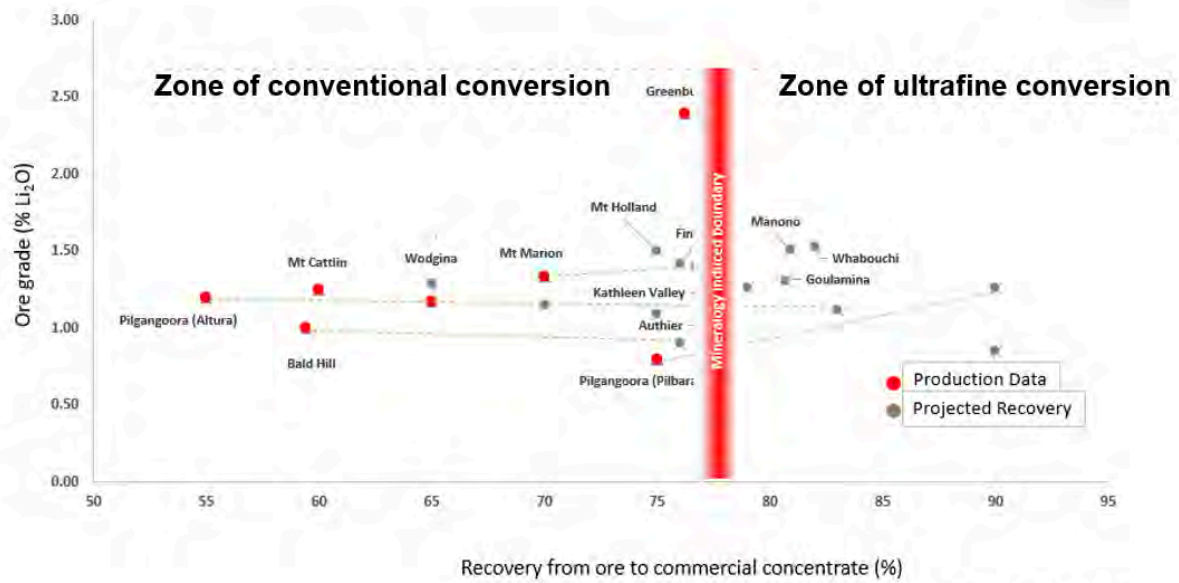
Meanwhile, significant corporate funding is being devoted to green hydrogen and green ammonia production and commercial supplies of these are imminent albeit potentially threatened by a change in government.

Improved mineral processing

Most battery metals are recovered by proven mineral processing techniques that have evolved over decades or more; hence, their acceptable efficiencies have developed as a result of economic necessity. Lithium is an exception; given the meteoric rise in its production to meet the demands of the battery industry, there has been insufficient time for processing techniques to fully evolve. Until recently, with a lack of vertical integration from mine through to chemical producer, the Chinese lithium converters dictated product specifications to both miners and concentrators. This created an environment in which concentrate specifications benefited converters but were suboptimal for the concentrators. Particle size in particular has been a major constraint, with conventional conversion commencing in rotary kilns unsuitable for fine concentrate feed.

Spodumene is a problematic mineral. It has two perfect cleavages, resulting in greater attrition during comminution than the associated quartz and feldspar contained within the pegmatites from which it is extracted. The resulting tendency is that a large proportion of spodumene fines are generated in the comminution process that precedes concentration. This is particularly evident in scale-up from laboratory and pilot testing through to commercial production. The trend has created a large

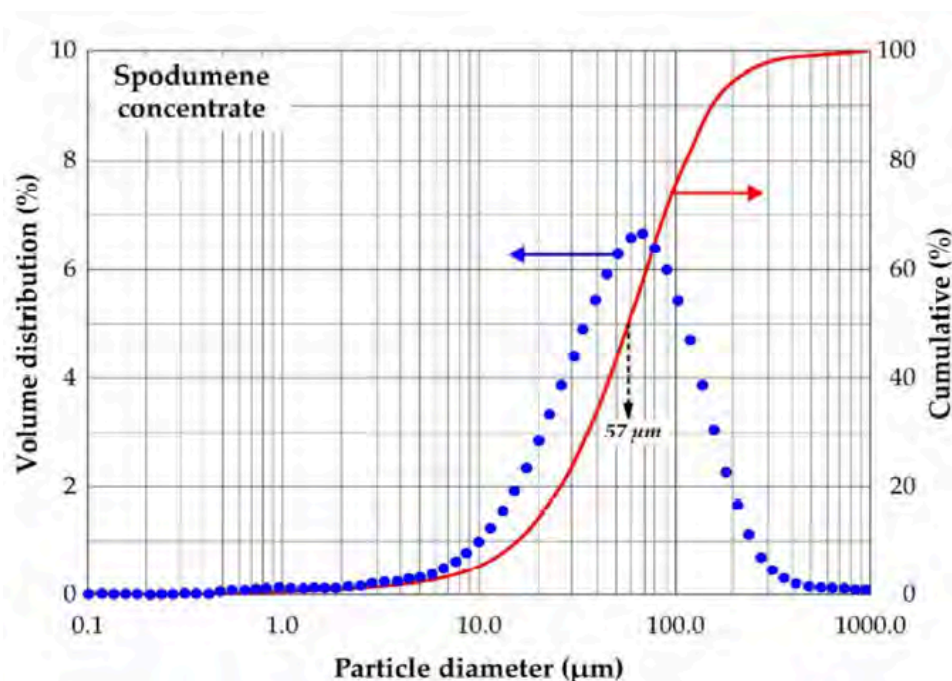
discrepancy between recoveries used in feasibility studies and the recoveries achieved to commercial concentrate where particle size is a principal specification (Figure 10).



Source: historic data c 2018

Figure 10 shows the comparison of feasibility study spodumene recovery rates to those achieved in commercial production.

The reason for this poor performance is illustrated in Figure 11, which reflects the properties of a spodumene concentrate from the Pilbara region of Western Australia.



Source: Fosu, A.Y. et al. Physico-Chemical Characteristics of Spodumene Concentrate and Its Thermal Transformations. *Materials* 2021, 14, 7423. <https://doi.org/10.3390/ma14237423>

Figure 11 shows the particle size distribution of a spodumene concentrate produced from pegmatite mined in the Pilbara region of Western Australia.

It should be noted that the yield from ore to concentrate of the material depicted in Figure 11 was 85%, with only 40% of the concentrate exceeding 75 µm. At the time this analysis was undertaken it

was not uncommon for the converter to specify 75 µm as the bottom size cut hence imposing a heavy penalty on the yield from ore to commercial spodumene concentrate. It is important to note that the ultimate recovery to concentrate is not metallurgical constraint but rather a commercial specification imposed by the end user as a consequence of the limitations of suboptimal equipment.

The carbon footprint associated with spodumene production can be reduced proportionally with an increase in recovery to commercial concentrate. The key then becomes the ability to convert fine or low-purity spodumene to viable lithium chemicals. Several processes under trial aim to achieve that outcome, which involves changes to the conversion process to enable fine or contaminated material to be processed. In particular, Pilbara Minerals Ltd and Calix Ltd have chosen a pyrometallurgical solution, while Lithium Australia Ltd ('Lithium Australia') and Mineral Resources Ltd ('Mineral Resources') have developed an innovative hydrometallurgical technique (see **THE INNOVATORS** below).

Carbon capture and storage ('CCS')

CCS has long been mooted as a solution for carbon dioxide emissions. The concept is simple – capture the carbon dioxide, compress it and pump it into subterranean reservoirs. Clearly, the success of CCS relies on accessing suitable geological formations with the permeability to receive the carbon dioxide, as well as cap rocks to seal the system and avoid leakage. Under some circumstances the carbon dioxide will react with other components in the reservoir, forming stable carbonates that pose little future risk. Exhausted gas fields are a prime target for CCS, as the geological conditions have proved suitable for gas containment over eons. These reservoirs simply need to be repurposed for CCS containment.

Today around 40 CCS projects operate around the globe. One of the world's largest is located at Barrow Island off the Western Australian coast. Fortunately, Australia's geological endowment hosts numerous potential CCS reservoirs, with one being developed in South Australia by Santos and another being considered in the Timor Sea. Other prospective locations include Queensland and New South Wales.

With most developed nations putting a price on carbon, Australia's ability to sequester carbon dioxide provides it with the opportunity to generate an enormous amount of revenue simply by repurposing the gas fields from which the carbon originated. The financial trade-offs are obvious: substituting a carbon tax at the point of the pollution with a sequestration fee for subsequent carbon storage in Australia. This could prove very attractive for nations that import Australian gas but lack geological formations suitable for CCS.

THE AUSTRALIAN INNOVATORS

The history of development of new technologies is littered with corporate carcasses, as the journey to successful commercialisation can be long, tortuous and difficult to fund, let alone turn into a profitable business. The fortitude required to embark on developing new technologies is summed up well in a quote from US president Theodore Roosevelt:

"Far better to dare mighty things, to win glorious triumphs, even though checkered by failure, than to take rank with those poor spirits who neither enjoy much nor suffer much, because they live in the grey twilight that knows not victory nor defeat."

Fortunately, the Australian government is providing some support for the development of new technologies, and that support is widely used in the mining and mineral processing industries, in addition to downstream processing. Government support is often used by innovators likely to positively impact the nation's path to decarbonisation. Some of it is provided through the likes of CEFC, ARENA, Austrade and the Australian Taxation Office Research and Development Tax Incentive. The latter provides a rebate for eligible expenditure at a premium to corporate tax rates for annual expenditure of up to A\$150 million and is rebated at the corporate tax rate beyond A\$150 million.

Many Australian innovators have targeted a reduction in carbon emissions during the development of commercial technologies, not always successfully. Other companies provide unique leverage to decarbonisation by being an integral part of the supply chain, or alternatives to existing threatened supply. Outlined below are some examples. However, the list is far from exhaustive and not ranked in any particular order.

Future Battery Industry Cooperative Research Centre ('FBICRC') – battery research and development

The Future Battery Industry Cooperative Research Centre was established in 2019, through the Australian government's cooperative research program, which amalgamates government, research institutions and industry. One such enterprise is the FBICRC, which covers 15 research projects (<https://fbicrc.com.au/projects/>). Collectively, the projects – which are valued at \$120 million, with funding provided by industry and topped up by government – span the entire battery value chain from mining through to processing, manufacture, service provision and the recycling and reuse of batteries. This provides the opportunity for participants to gain commercial opportunities through application of the knowledge base developed by the FBICRC.

Lithium Australia /Mineral Resources joint venture – improving spodumene utilisation

Lithium Australia, a first mover in the field of lithium processing, identified a number of supply problems and developed processing solutions to mitigate their impact and capitalise on underutilised lithium resources.

That company developed the SiLeach[®] process for the recovery of lithium from micas and the LieNA[®] process for the hydrometallurgical recovery of lithium from spodumene.

The LieNA[®] process is a caustic conversion at elevated temperature and pressure. Spodumene is converted to synthetic lithium sodalite, which is subsequently leached and the lithium precipitated in a choice of forms – hydroxide, carbonate or phosphate.

At present, LieNA[®] is focused on fine spodumene otherwise unsuitable for conventional processing. Such feed is available at marginal operating cost, as the mining and much of the separation costs have been covered in producing the coarser commercial concentrate used as the feed for conventional converters. The fine spodumene may comprise 50% or more of all the lithium units mined or not recovered. Even with efficient concentrators, the fine material usually comprised more than 25%.

Commercialisation of the LieNA[®] process, which is being undertaken in conjunction with Mineral Resources Ltd, will provide licensing opportunities that have the potential to return revenue to the Australian owners of the process while optimising the carbon footprint of those who use it.

Pilbara Minerals/Calix – utilisation of fine spodumene

Pilbara Minerals Ltd was one of the first companies involved in the production of spodumene concentrates to address the poor recovery inherent in the industry. Their solution was to form a joint venture with Calix in developing an innovative 'mid-stream' refining process for sustainable lithium production. The process utilises fine spodumene generated during the concentration process that cannot otherwise be fed to conventional converters (that is, the processing plants converting spodumene to lithium chemicals) because of its particle size. The project is advancing towards construction of an onsite demonstration plant, located in the northwest of Western Australia, that will harness Calix's patented electric calcination technology fuelled by renewable energy. It is supported by A\$20 million in Australian government funding, announced under the Modern Manufacturing Initiative.

VSPC – cathode-powder production and LFP recycling

VSPC Pty Ltd ('VSPC'), which has operated for more than 20 years, has developed patented technology to produce nano powders, LFP in particular. The VSPC process is a single-pass operation

with relatively low energy consumption and little waste. The synthesis techniques are covered by a number of international patents however in the simplest form powders are manufactured by combining surfactant and soluble metals in the stoichiometric proportions required in the final product. This produces particles that can be spray dried and calcined to create the final product: cathode powder. The process, which is composition-agnostic, is capable of producing ternary cathode powders, LFP and catalysts.

In 2020, VSPC, together with Australia's Commonwealth Scientific and Industrial Organisation ('CSIRO'), the University of Queensland and others, was awarded government support in a \$5 million CRC-P program to develop fast-charge lithium-ion batteries for use in new-generation battery-powered trams. Such trams eliminate the need for overhead power lines, which are expensive, visually polluting and potentially hazardous.

Samples of VSPC-produced LFP and LMFP are currently being evaluated by battery producers and the company plans to build a demonstration plant for material qualification.

The ability to effectively set and forget the composition of the powder produced by the VSPC process has significant advantages in terms of quality control compared with competing processes. It also provides the potential to recover lithium, iron and phosphorus from spent LFP batteries by dissolving the powder, polishing the solution and reprecipitating the cathode powder. This may be the answer to one of the battery industry's greatest challenges – finding a commercial method of recycling LFP.

Envirostream – lithium-ion battery recycling

Envirostream Pty Ltd ('Envirostream'), a wholly owned subsidiary of Lithium Australia, has operated commercially since 2017. As Australia's premier lithium-ion battery recycler, it has established an extensive-battery collection network. At its two processing plants in Melbourne, Australia where batteries are shredded and their components separated. Metal from the current collectors, primarily copper and aluminium, is sold into the metal recycling market, while 'mixed metal dust', otherwise known as 'black mass', is sold to specialist refiners.

The sophistication of Envirostream's operations and the safety standards built into its handling of hazardous materials, including mitigation of fire risk, are second to none. Its systems have been developed in-house and have export and partnering potential on a global basis.

Neometals

Neometals was a first mover in the Australian lithium industry, once owning the Mt Marrison spodumene mine near Kalgoorlie in Western Australia. In later years, Neometals has focused on downstream processing and recycling and now has four divisions:

- lithium-ion battery recycling – commercial;
- lithium chemicals – pre-commercial;
- vanadium recovery – pre-commercial, and
- precious metal recovery – in research and development.

Neometals' battery recycling is EU-based through a joint venture (Primobius GmbH) with German company SMS Group. It focuses on processing ternary batteries, finishing with the separation of the metal salts for return to the regeneration of cathode material.

Pilbara iron-ore producers – electrification and autonomous haulage

As previously discussed, Australia's iron-ore producers lead the way in mine electrification and the use of autonomous equipment. Today, the latter extends beyond haulage to include drilling and loading. These miners are also leaders in the field of microgrids; most operations are self-sufficient in power and now are now transitioning from hydrocarbons as an energy source to renewables on a large scale, supported by wind and solar power generation.

Fortescue Future Industries ('FFI') – green hydrogen and ammonia

FFI is part of the Fortescue Metals Group ('Fortescue'). The latter was on schedule to burn 100 billion litres of diesel annually by 2030 but now, with radical innovation, plans to drop that projected consumption to zero.

Fortescue, which boasts Australia's largest gas and liquid hydrogen refuelling plant, has developed the world's first ammonia-**powered** ship, is developing ammonia-powered rail locomotives and has the 'Infinity Train' under design^[12]. As previously discussed, the Infinity Train is an iron-ore haulage set the concept of which embraces the concept of perpetual motion; that is, all the train set's power requirements are met by the batteries being charged from the downhill run from Fortescue's Pilbara iron-ore mining operations to the port loading facilities at Port Hedland. The return journey, with the train set unladen, is completely powered by the energy harnessed from that downhill run. This is carbon neutrality at its most sophisticated and a system worthy of duplication wherever loaded transport legs are followed by an empty return journey.

FFI is involved in the production of green hydrogen and ammonia and recently acquired the Phoenix Hydrogen Hub in the US. FFI commenced construction of the world's largest electrolyser facility in 2022 as the first stage of its Green Energy Manufacturing Centre ('GEM') in Gladstone Queensland. GEM will be powered by green energy and is set to become a major new pollution-free green manufacturing hub. Planned growth includes the development of green manufacturing technology such as batteries, wind turbines and solar panels. This has huge potential for domestic and export markets.

Iluka Resources Ltd– separated rare earths

The Australian Critical Mineral Facility has provided a loan of A\$1.25 billion to Iluka Resources Ltd ('Iluka') to develop its Eneabba rare earths refinery, located 280 kilometres north of Perth in Western Australia. The refinery will produce separated rare-earth oxide products, including praseodymium, dysprosium, neodymium and terbium, which are used in permanent magnets, EVs and clean wind turbines, as well as in the telecommunications, medical and defence sectors. Initially, feed will come from existing monazite stockpiles generated during the separation of mineral sands from Iluka's own mineral sands mining and separation operations. The refinery will also take third-party feed, including xenotime concentrates from the Browns Range deposit of Northern Minerals Ltd.

Renascor Resources Ltd– vertically-integrated graphite production

Renascor Resources Ltd received an A\$185 million loan from the Australian Critical Mineral Facility for development of its Siviour graphite project, located on South Australia's Eyre Peninsula. Siviour hosts the world's second-largest Proven Reserve of graphite. The project will establish a vertically-integrated graphite and processing facility to produce purified spherical graphite for lithium-ion batteries. This project provides an alternative source to that currently dominated by China the supply of which is being progressively tightened by Chinese export restrictions.

Thorion Energy Ltd– sedimentary vanadium to flow batteries

Thorion Energy Ltd, Australia's first vanadium redox flow-battery manufacturer, also owns the Richmond vanadium project. Located 400 kilometres east of Mt Isa in Queensland, it boasts the largest known sedimentary vanadium deposit on Earth. Definitive feasibility has commenced, with the aim of producing around 13,000 tonnes per annum of battery-grade vanadium pentoxide flake. The company is well-placed to service its own supply requirements, as well as those of other domestic consumers of vanadium based electrolytes, one of which may be the Queensland government. In 2021, the latter announced it would build and own a new vanadium common-user facility in Townsville that will be used for downstream refining of vanadium concentrate to vanadium pentoxide suitable for battery use. This is part of the state's plan to make Queensland a leading producer and exporter of new-economy minerals.

The infrastructure, natural resources and technology provide leverage for Australia in the quest for decarbonisation.

Avenira Ltd– from mining to LFP production

Avenira Ltd ('Avenira') is proprietor of the Wonarah phosphate project, located on the Barklay Highway east of Tennant Creek in Australia's Northern Territory. At start-up, the project has a direct shipping rock phosphate component. Beyond that, production of yellow phosphorus is planned and, ultimately, thermal phosphoric acid for LFP production and other uses.

In 2023, Avenira and Aleees (the latter being the largest producer of LFP outside of China, albeit not far outside – it's in Taiwan!) executed a binding Licence and Technology Transfer Agreement granting Avenira the right to use Aleees' intellectual property for the manufacture and global distribution of LFP cathode-active material from Avenira's proposed LFP battery-cathode manufacturing plant in Darwin. Production of LFP in Darwin may provide an avenue into the US market, complete with the financial benefits provided by the US *Inflation Reduction Act*.

LFP production out of Darwin, using technology with end-user acceptance, offers Australia a potential first-mover advantage into LFP-hungry markets that are yet to establish domestic production.

Hazer Group Limited – carbon-negative methane cracking

The University of Western Australia developed and patented a methane catalytic cracking process that is now being commercialised by the Perth-based Hazer Group Limited ('Hazer'). As part of that commercialisation process, ARENA has provided part of the funding to construct a groundbreaking hydrogen production facility in Munster in Western Australia. Feed to the plant is biogas, produced from the treatment of sewage. The Hazer process, which converts bio-methane to renewable hydrogen and graphite via an iron-ore catalyst to create a hydrogen pathway, is an alternative to the traditional approaches of steam methane reforming and electrolysis.

Achieving first production in January 2024, the demonstration plant heralds Australia's involvement in the global hydrogen market. It has the potential to produce graphite for battery production and other applications.

Utilisation of this technology provides Australia with an international opening into carbon-negative clean energy and other benefits, both through the production of green hydrogen and global application of the Hazer process. The opportunity has not gone unnoticed, with Hazer announcing a deal with POSCO Steel of South Korea, on 31 May 2024. The parties will collaborate on the production of green hydrogen and decarbonising carbon intensive steel production.

Cobalt Blue Holdings Ltd– primary cobalt production

Cobalt Blue Holdings Ltd ('Cobalt Blue') occupies an uncommon position in the market, given that its Broken Hill cobalt project, located 25 kilometres west of Broken Hill, is cobaltiferous pyrite with very low levels of other base metals. Cobalt Blue has patented processes that produce elemental sulphur, iron oxide and a mixed metal hydroxide from the ore. The hydroxide will be transported to Perth. There it will be refined in a Cobalt Blue facility (based in Kwinana) engineered to produce cobalt sulphate for the battery industry. Commissioning of the Kwinana facility on third-party feed is planned for 2025 and processing of the mixed hydroxide from Cobalt Blue's Broken Hill facility in 2027.

Being a primary cobalt producer, Cobalt Blue can potentially contribute to filling the cobalt supply deficit without affecting the supply balance of other battery metals such as copper and nickel. This offers great potential, as there is little competition in the field of primary cobalt production.

International Graphite Ltd – vertical integration from mining to micronised graphite

Perth-based International Graphite Ltd ('International Graphite') owns the Springdale graphite project near Hopetoun on the south coast of Western Australia. Springdale will be the feed source for micronised graphite to be produced at International Graphite's plant in Collie, about 400 kilometres east of the planned mining operation. The Collie plant will form part of the Western Australian government's planned Collie Battery and Hydrogen Industrial Hub.

International Graphite has successfully wet-commissioned its new 200 tonnes-per-annum graphite micronising plant. Ultimately, the qualification-scale microniser, the largest in Australia, is planned for scale-up to a commercial capacity of 4,000 tonnes per annum at an estimated capital cost of \$12.5

million. International Graphite will mitigate risk by servicing markets beyond those associated with the battery industry, including markets for polymers, lubricants, conductors and alkaline battery-cell producers.

In a climate of tough capital markets, International Graphite has excelled in attracting government support in the form of grants that now total A\$13.2 million. This mitigates the impact on shareholders of raising research and development funding in the equity markets and provides an alternative to Chinese dominated supply of micronized graphite.

While not unique, the production of downstream products for the battery industry offers potential leverage for both the company and the Australian economy.

Reedy Lagoon – green pig iron

Reedy Lagoon Corporation, a Melbourne-based explorer with interests in gold, lithium and iron ore, is proprietor of the Burracoppin iron project, located on the transcontinental railway line 260 kilometres east of Perth. There, the iron occurs as magnetite within a metamorphose banded-iron formation that can be liberated by coarse grinding (P_{80} 150 μm), resulting in concentrates of 67-70% iron. The concentrates are of around 3% SiO_2 , 0.5% Al_2O_3 , with very low phosphorous (around 0.005%).

The company, which has a HIs melt licence, is evaluating the use of biochar as a reductant to generate green pig iron for feed to domestic and/or offshore green-steel producers. HIs melt is Australian technology sold to and commercialised in China. Its application, under licence, in Australia could provide an entry into the green-steel market. In fact, the use of such processes is an imperative in the steel industry, which currently accounts for about 8% of global carbon dioxide emissions.

Sunrise CSP – mirrors to produce high-temperature heat

The 'Big Dish' technology of Sunrise CSP – developed by researchers at the Australian National University – was commercialised in 2018. It generates electrical power by using mirrors to concentrate energy from the sun and convert it into high-temperature heat.

This technology has created an instant export opportunity, with its first application involving the provision of heating in an Indian hospital. Since then, Sunrise CSP has partnered with Indian Engineers Limited to roll out the technology in other Indian applications.

Australian Strategic Metals Ltd – polymetallic critical mineral production

Australian Strategic Metals Ltd ('ASM') is developing the Dubbo Project located about 400 kilometres northwest of Sydney, Australia. Mineralisation is within a trachyte intrusive which hosts a globally significant resource of rare earths, zirconium, niobium and hafnium. ASM has diversified downstream, establishing a processing plant in South Korea initially for the production of neodymium and neodymium iron boron alloys used in the permanent magnets of EVs and wind turbines. Other products contemplated for future production include high-purity titanium, zirconium, hafnium and niobium.

ASM provides a strategic alternative supply for much needed decarbonising commodities and will be a valuable store of processing knowledge in the production of rare earths, a market currently dominated by China.

THE OPPORTUNITIES

All the opportunities discussed above provide Australia with leverage as the world advances towards carbon neutrality. Commencing at the mine site, they advance through mineral processing, the development of high-end products from the processed minerals, the manufacture of final products for consumers and industry and, finally, the recycling of those products. Significant commercial leverage and environmental advantages can be derived by the **THE INNOVATORS** (above) commercialising the processes that are currently under development.

Historically, Australian innovations in the mining and processing sectors have been prolific, among them the following:

- recovery of gold from leach liquors using carbon, which began in the 1890s and led to the development of contemporary carbon-in-pulp (CIP) and carbon-in-leach (CIL);
- perfection (not necessarily invention) of froth flotation to gain greater value from the sulphide ores at Broken Hill in the early 1900s and now adapted globally as a preferred method of separating sulphide;
- commercialisation of pyrite smelting by Robert Sticht at Mt Lyell in the 1890s;
- development of IsaSmelt, an energy efficient smelting process, by Mt Isa Mines Ltd (MIM) and the CSIRO during the 1970s, 80s and 90s;
- development of HIs melt – direct reduction of iron ore – by Rio Tinto in the 1980s and sold to Chinese interests in 2017;
- development of the atomic absorption spectrometer in 1952 (it is still one of the most widely used chemical analytical instruments), and
- development of the wine cask by Thomas Angove in 1962, facilitating comfort, relaxation and enjoyment among many in society, including in the minerals industry, by providing easy access to anaerobically stored alcoholic beverages.

It is interesting to note that, in addition to being drivers of development, each of the above probably reduced carbon emissions when compared with other competing processes at the time. Even the wine cask eliminated the carbon footprint associated with producing glass for the bottles more commonly used in the beverage industry.

Electrification and autonomy

Examples provided in the preceding section (**THE INNOVATORS**) clearly show that Australia leads the way in mining efficiency through electrification and autonomy, with much of the technology developed by Australian companies in their own backyards. There is a great opportunity to introduce this technology and know-how to the rest of the mining world and develop supporting systems for a global industry. Furthermore, these technologies can be extended to transport applications beyond the mining sector.

Improvements in processing technology

New processing technologies can improve the sustainability of existing orebodies, while their licensing can provide advantages for the environment via a reduction in carbon emissions, as well as a revenue stream back to Australian companies through licensing fees, royalties or equity interests in the projects in which they are employed. These technologies may even turn Resources into Reserves by reducing the operating costs of the metal units produced.

Remanufacturing

The Australian mining industry is one of the world's largest consumers of drilling, blasting, loading and haulage equipment. The units involved are usually large and heavy and have a high carbon footprint at the time of delivery. Following the Freeport McMoRan example (see **New or Used Equipment?** above), refurbishment rather than replacement of such equipment could have a significant impact on carbon emissions, not to mention improved capital utilisation. Because of the high concentration of equipment in specific mining jurisdictions such as the Pilbara in Western Australia, the New South Wales and Queensland coal fields and Western Australia's goldfields region, regional refurbishment centres could be established to service these localities with long-term environmental benefits.

Training

Westrac, the Western Australian Caterpillar dealer, has been supplying services to the mining industry in Western Australia, New South Wales and the Australian Capital Territory since the 1990s. It

operates training institutes, primarily for apprentices, in Western Australia and New South Wales and recently opened the Westrac Technology Training Centre in Collie, about 220 kilometres south of Perth. The centre, the first of its kind in the southern hemisphere, delivers training courses to technicians of autonomous equipment like the haul trucks used in the mining industry. Parent company Caterpillar operates a similar facility in the US but there is clearly an opportunity for the industry to develop more extensive training courses for not only for domestic personnel but also other participants in the global mining industry.

Value-added products

Australia can leverage its position in the critical minerals supply chain and reduce the carbon footprint associated with product transport by producing a range of products downstream from mining and concentration. This can take many forms. In the case of rare earths, Iluka is proceeding to the production of separated rare-earth oxides, greatly enhancing product value and enabling an alternative supply chain to that of the dominant route through China. And, with separated rare-earth oxides available domestically, there is the potential for Australia to develop magnet alloys and service the EV industry, as well as the power generation, electronics, defence and communications sectors.

Turmoil in the nickel industry has put significant pressure on Australian producers. While BHP awaits a decision on the future of its subsidiary NickelWest (anticipated August 2024), In the meantime BHP has at least capitalised on some of the value-add by producing nickel sulphate from a large proportion of the nickel it refines in Kwinana, Western Australia. This is used as a feed stock in the lithium-ion battery industry. BHP is involved, with others through the FBICRC, in developing mixed nickel/cobalt precursors for cathode production. Longer-term, the availability of these precursors could lead to an Australian NCM cathode-powder industry.

Meanwhile, two companies aspire to produce LFP cathode powders locally – Lithium Australia, through its wholly owned subsidiary VSPC, and Avenir. The former employs home-grown technology, while the latter has a licensing agreement with Aleees, the world's largest LFP producer outside of China. At present, more than 98% of LFP is produced within China and the success of Lithium Australia and/or Avenir would provide alternative supply chains for battery producers, as well as greater competition. The commercial competitiveness of these products could, however, be somewhat problematic, as Chinese production does have a low cost base. That said, the global paranoia surrounding supply-chain security and diversity may well overshadow the issue of cost.

CONCLUSION

Australia's commercial leverage in terms of decarbonisation in the critical minerals sector involves not simply availability but also the development of downstream industries that provide secure supply chains for Australia's trading partners. Australia is abundant in critical minerals, the development of which must be controlled to improve supply-chain security and reduce carbon footprints. Downstream processing is a positive step in removing unnecessary energy consumption in the transport of low-grade or low-yield products to other jurisdictions. Ideally, the concentrating and refining of critical minerals should be accomplished as close to the sources of the raw materials as possible, to reduce the carbon footprint associated with transporting waste associated with manufacturing. This has been exemplified in the Australian lithium industry, which has seen a rapid transition from the direct shipping of ore to production of concentrates and, further downstream, to the creation of lithium chemicals. The leveraging of such opportunities can add more value via the production of other battery precursors or even the cathode powders themselves. It could make Australia an indispensable link in the battery supply chain.

Constrained markets in graphite also present a high-leverage opportunity if Australian graphite production became vertically integrated, adding enormous value. This is already being achieved in a number of locations.

Australia is at the forefront of developing technologies aimed at more effective production of raw materials. This is evident in the growing use of automation and electrification of mining operations to improve efficiency, reduce costs and minimise environmental impacts. Harnessing Australian expertise in these fields represents a great commercial opportunity, one that has the potential to streamline mining operations on a global basis.

Utilisation of Australia's mineral resources can be further improved through the use of advanced processing technologies that create greater yield for marginal additional cost and contribute to sustainability while reducing the carbon footprint required to deliver value-added products. Indeed, the Australian technologies being developed in mineral processing are likely to lead the world, as has been the case in the past.

Now too, Australia is showing its ability to provide advanced solar technologies for the production of renewable energy, with green hydrogen and green ammonia no longer visions for the future – they are here now and have been developed with Australian knowhow.

Australia has demonstrated the viability of carbon capture and storage and should look to provide its trade partners with access to the nation's abundant and eminently suitable geological formations to sequester carbon dioxide ... particularly if Australia has already provided the gas that generated the carbon emissions in the first place.

As can be seen, there are many areas in which Australia can leverage its commercial and environmental outcomes as it aims for carbon neutrality. While there does seem to be some political impetus to support that leverage, alas, the Australian government's contribution to date remains modest in comparison with those of the EU and US, and its programs extend for periods that are far too long. That said, changes of government remain a risk in Australian jurisdictions, so it is up to industry to prove its points and gain the support it requires.

Political policy remains a concern in terms of maximising the leverage Australia has with regard to decarbonisation. The domestic market is too small to enable self-sufficiency with respect to many of the necessary developments, and government policy would do well focus on export outcomes to reap the benefits of abundant opportunities. Such 'export' should involve not only hard goods but intellectual property, knowledge and education. The clean-energy lobby, including the critical minerals sector, needs to maintain pressure on the government and demonstrate that additional tax revenue can be created by stimulating the industry.

In conclusion, Australia has a lot to offer as an integral participant in the global push for decarbonisation and will gain enormous leverage by providing the materials required to meet climate-change targets.

REFERENCES

1. Australian Government, 2023. Critical Minerals 2024 Strategy 2023-2030. 64pp
2. Madhumitha Jaganmohan, Global nickel mine production 2023, by country. <https://www.statista.com/statistics/264642/nickel-mine-production-by-country/#:~:text=In%202023%2C%20Indonesia%27s%20mines%20produced%20an%20estimated%201.8,nickel%20from%20mines%20worldwide%20by%20a%20large%20margin.> (accessed May 2024)
3. International Energy Agency, 2023. Prohibition of the export of nickel ore. <https://www.iea.org/policies/16084-prohibition-of-the-export-of-nickel-ore> (accessed May 2024)
4. International Energy Agency, 2021. GHG emissions intensity for class 1 nickel by resource type and processing route – Charts – Data & Statistics - IEA (accessed May 2023)
5. Climate Rights International, 2023. Nickel Unearthed - The Human and Climate Costs of Indonesia's Nickel Industry. 138pp
6. Bloomberg News, May 1, 2024. US, Philippines eye agreement to cut China nickel dominance. US, Philippines eye agreement to cut China nickel dominance - MINING.COM (accessed May 2024)
7. Wood Mackenzie, 2024. Lithium market faces a transition as demand growth slows. <https://www.woodmac.com/press-releases/lithium-five-things/> (accessed May 2024)
8. Amnesty International, 2016. Is My Phone Powered by Child Labour? <https://www.amnesty.org/en/latest/campaigns/2016/06/drc-cobalt-child-labour/> (accessed May 2024)
9. International Energy Agency, 2021. Total copper demand by sector and scenario, 2020-2040. <https://www.iea.org/data-and-statistics/charts/total-copper-demand-by-sector-and-scenario-2020-2040> (accessed May 2024)
10. The South Korean Times, Feb 2024. Tesla, Chinese battery firms hit by Korea's new EV subsidy rules. https://www.koreatimes.co.kr/www/tech/2024/02/419_368375.html (accessed May 2024)
11. More, P. 2021. International Mining: Fortescue Future Industries begins testing of hydrogen powered mining truck & blasthole drill rig. <https://im-mining.com/2021/08/30/fortescue-future-industries-begins-testing-hydrogen-powered-mining-truck-blasthole-drill-rig/> (accessed May 2024)
12. Blain, L, March 2022. New Atlas: Battery-electric "Infinity Train" will charge itself using gravity. <https://newatlas.com/transport/fortescue-wae-infinity-train-electric/> (accessed May 2024)

PILOTING THE NEOMETALS ELI PROCESS

By

Michael Tamlin, Kausar Shah, David Robinson

Neometals Ltd, Australia

Presenter and Corresponding Author

Mike Tamlin

mtamlin@neometals.com.au

ABSTRACT

Considering the rapidly growing demand for lithium and the activity in the sector, the development of a lower cost direct route to battery grade lithium hydroxide monohydrate from a purified lithium chloride solution is long overdue. Over the past 7 years Neometals has been developing the patented ELi process to achieve exactly this goal.

Most recently Neometals has been working with commercial laboratories and technology vendors to develop and demonstrate a flexible flowsheet for both spodumene and lithium chloride brine feeds, that can effectively reduce key impurity levels enabling direct electrolysis to produce a lithium hydroxide solution (avoiding much of the costs and inefficiencies of conventional routes).

In support of an engineering cost study, Neometals has now completed bench and pilot scale demonstration of the critical unit processes needed for purification of several lithium chloride brines and a lithium chloride solution derived from a Western Australia spodumene sample. The purification flowsheet involves sequential i) bulk impurity removal steps and ii) impurity rejection / polishing steps to achieve levels of impurities, including the divalent cations (Mg^{2+} , Ca^{2+} , Sr^{2+}), boron, silicon and sulphate to sub-mg/L levels.

Results from the purification and electrolysis steps will be presented in this paper and used to support the claimed relative economic advantages of this flowsheet compared to more conventional processing options.

Keywords: Lithium, Spodumene, Brine, Purification, Hydrometallurgy.

The ELi™ Process – Greener Lithium for Battery Materials

By

Mike Tamlin
mtamlin@neometals.com.au

Disclaimer

Summary information:

This document has been prepared by Neometals Ltd ("Neometals" or "the Company") to provide summary information about the Company and its associated entities and their activities current as at the date of this document. The information contained in this document is of general background and does not purport to be complete. It should be read in conjunction with Neometals' other periodic and continuous disclosure announcements lodged with the Australian Securities Exchange, which are available at www.asx.com.au.

Forward-looking information:

This document contains, opinions, projections, forecasts and other statements which are inherently subject to significant uncertainties and contingencies. Many known and unknown factors could cause actual events or results to differ materially from the estimated or anticipated events or results included in this document. Recipients of this document are cautioned that forward-looking statements are not guarantees of future performance.

Any opinions, projections, forecasts and other forward-looking statements contained in this document do not constitute any commitments, representations or warranties by Neometals and its associated entities, directors, agents and employees, including any undertaking to update any such information. Except as required by law, and only to the extent so required, directors, agents and employees of Neometals shall in no way be liable to any person or body for any loss, claim, demand, damages, costs or expenses of whatever nature arising in any way out of, or in connection with, the information contained in this document.

Financial data:

All figures in this document are in Australian dollars (AUD) unless stated otherwise.

Not financial product advice:

This document is for information purposes only and is not financial product or investment advice, nor a recommendation to acquire securities in Neometals. It has been prepared without taking into account the objectives, financial situation or needs of individuals. Before making any investment decision, prospective investors should consider the appropriateness of the information having regard to their own objectives, financial situation and needs and seek legal and taxation advice appropriate to their jurisdiction.

Investment risk:

An investment in securities in Neometals is subject to investment and other known and unknown risks, some of which are beyond the control of Neometals. The Company does not guarantee any particular rate of return or the performance of Neometals. Investors should have regard to the risk factors outlined in this document.

Compliance Statement:

The Company confirms that it is not aware of any new information or data that materially affects the information included in the original market announcements and that all material assumptions and technical parameters underpinning the estimates in the market announcements continue to apply and have not materially changed. The Company confirms that the form and context in which the Competent Persons' findings are presented have not been materially modified from the original market announcements.

Lithium Hydroxide for the EV Era

The old days – A Niche Material:

- Small volume production, limited installed capacity
- Limited quantities of product suitable for battery cathode
- Use of bulk industrial chemical reagents for two step chemical conversion via lithium carbonate
 - Long distance haulage of bulk materials was relatively insignificant
- The relatively high carbon footprint was not a factor
- Relatively high cost through “double conversion”

The EV Era Needs:

- Large volume production
- Consistent and high purity
- Small carbon footprint
- Lower cost production
 - Protection for producers during lower price phases
 - Lower cost for cathode and battery producers under pressure to reduce battery cost
- Production from both brines and hard rock sources to meet demand growth

Lithium Hydroxide Production

The old days – Chemical Conversion:

Hard Rock

- $\text{Li}_2\text{SO}_4 + \text{Na}_2\text{CO}_3 = \text{Li}_2\text{CO}_3 + \text{Na}_2\text{SO}_4$ Low market value by-product with energy-intensive production
- $\text{Li}_2\text{CO}_3 + \text{Ca}(\text{OH})_2 = 2 \text{LiOH} + \text{CaCO}_3$ Bulk residue, disposal cost

Brine

- $2\text{LiCl} + \text{Na}_2\text{CO}_3 = \text{Li}_2\text{CO}_3 + 2\text{NaCl}$
- $\text{Li}_2\text{CO}_3 + \text{Ca}(\text{OH})_2 = 2 \text{LiOH} + \text{CaCO}_3$ Bulk residue, disposal cost

The modernized old days:

Hard rock

- $\text{Li}_2\text{SO}_4 + 2\text{NaOH} = 2 \text{LiOH} + \text{Na}_2\text{SO}_4$ Low market value by-product with energy-intensive production

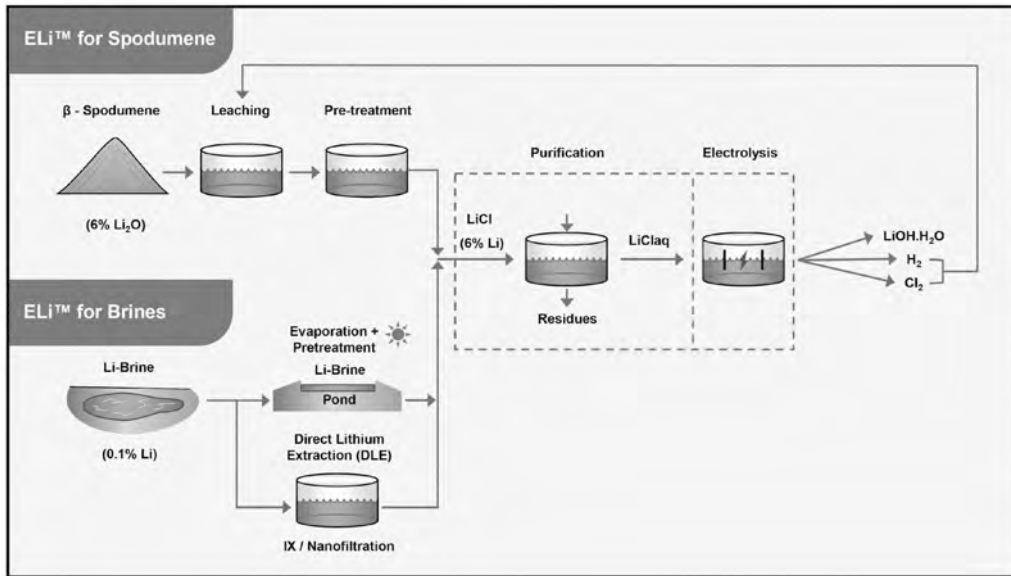
The Modern ELi™ Process:

$2\text{LiCl} + 2\text{H}_2\text{O} + e = 2\text{LiOH} + \text{Cl}_2 + \text{H}_2$ (synthesised into 32% HCl)

- **Suitable to convert spodumene concentrates and sub-surface lithium brines**
- **Low carbon electricity**
 - Has increasing availability
 - Further reduction of carbon footprint
- **No bulk industrial chemical reagents**
 - Minimises heavy transport costs
 - Reduces carbon footprint associated with production of reagents and transport of reagents
 - Reduced pressure on the reagent supply chains
- **Minimised waste materials and disposal**

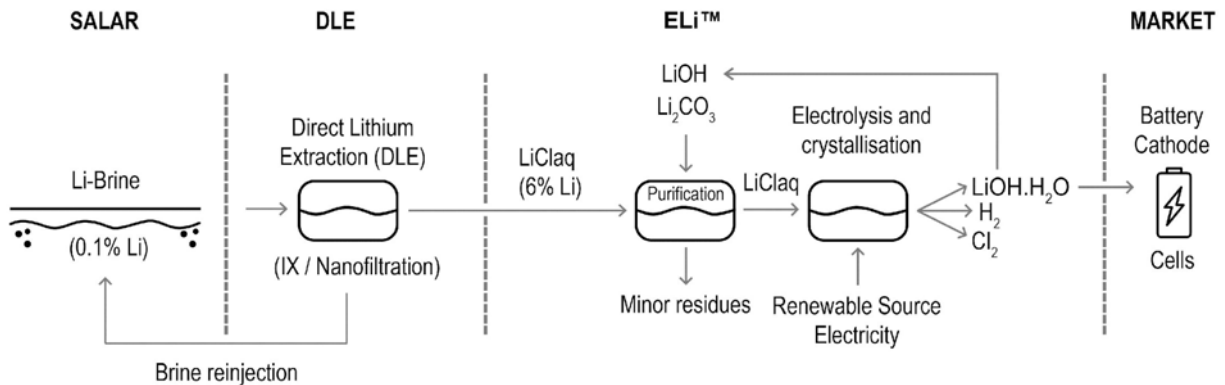
ELi™ – A New Technology Solution to an Old Problem

Flowsheets for processing spodumene and for processing sub-surface brines



Where ELi™ fits into the Lithium Brine Production Chain

Combined DLE and ELi™ Process for Lithium Production



The Starting Point

- Brine compositions are highly variable
 - Typical impurity concentrations and ratios vary salar to salar
 - Vary between brine and spodumene sources
- Purify to a higher degree than conventional lithium processes
- Minimise lithium losses associated with impurity removal

Typical Sub-surface Brine after pre-treatments

(mg/L)	Li	Ca	Mg	B	Sr	Si
Before	33,000-49,000	3,400-6,500	8,600-13,000	3,500-5,400	30-40	20-40

The “Aha” Moment

Membrane electrolysis directly converts lithium chloride to hydroxide and eliminates transport & use of bulk reagents

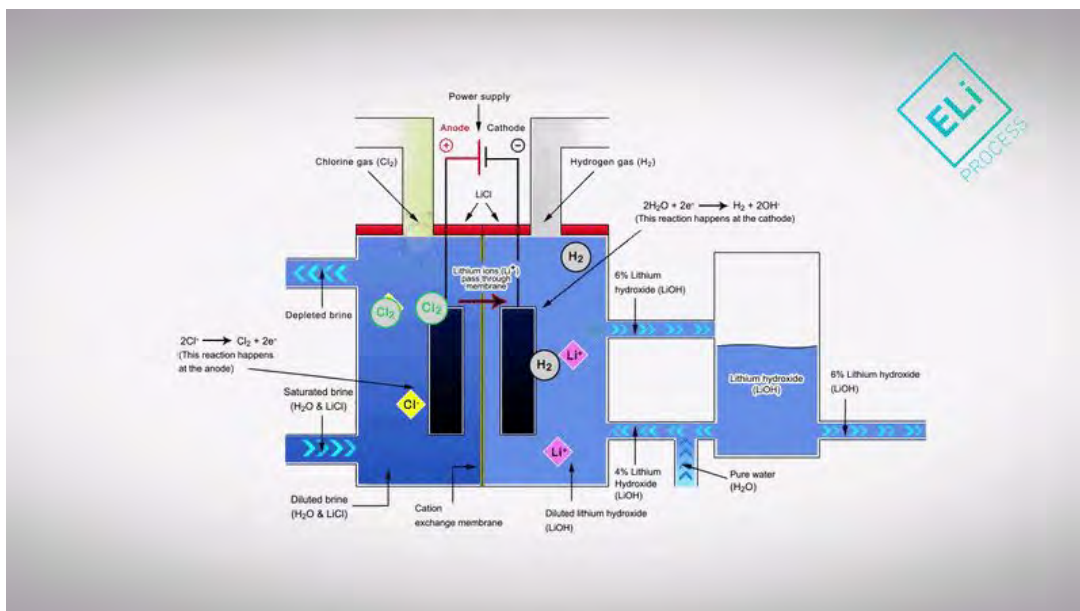
Process	ELi™	Conventional Processes
Bulk Lime	No	Yes
Bulk Soda Ash	Minimal	Yes
Power	Yes (renewable)	Yes
Gas/oil	Yes	Yes

The Enabler – Ultrapure LiCl Feed to Electrolysis

- Successful brine purification pilot enables efficient electrolysis
 - The higher purity the solution, the higher the product purity and the lower the power cost
 - Flowsheet successfully piloted
 - Previous electrolysis tests were successful on less pure feed
- Next piloting phases are long duration electrolysis tests and LHM crystallisation
 - Electrolysis tests are evaluating membrane durability and cell hydrodynamics

(mg/L)	Li	Ca	Mg	B	Sr	Si
Before	62,654	6,260	15,792	7,141	71	52
After (ave)	45,100	< 0.9	< 0.09	< 0.4	< 0.002	1
% removed*	n/a	> 99.98	> 99.99	> 99.99	> 99.99	> 97

ELi™ Membrane Electrolysis



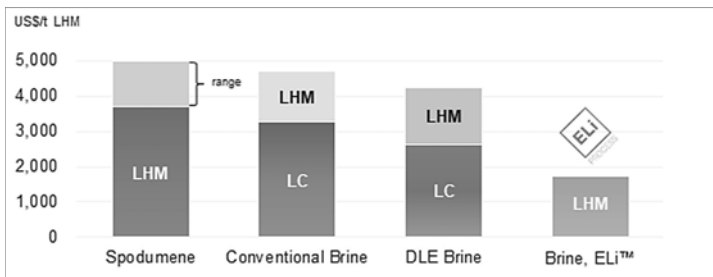
ELi™ Membrane Electrolysis Equipment



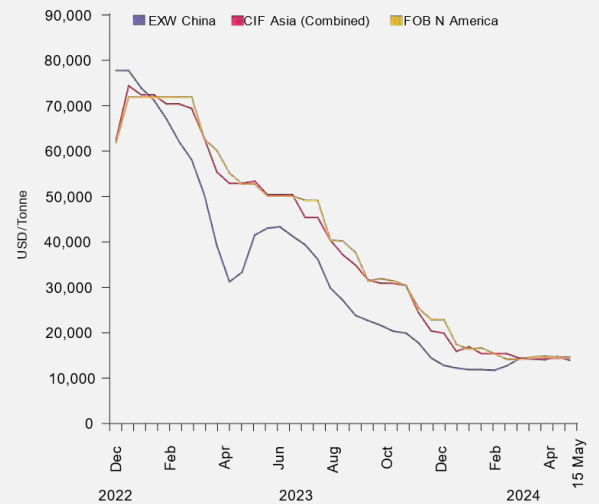
Source: Denora

Low Opex is Compatible with Periods of Low Market Prices

Estimated Opex Comparison (Conversion to LHM)



Source: ALB, E3 Li, PLL, Livent, Management estimated, Class 3 ECS, Benchmark Mineral Intelligence.



Source: Benchmark

Commercialisation – Further Piloting and Scale-Up

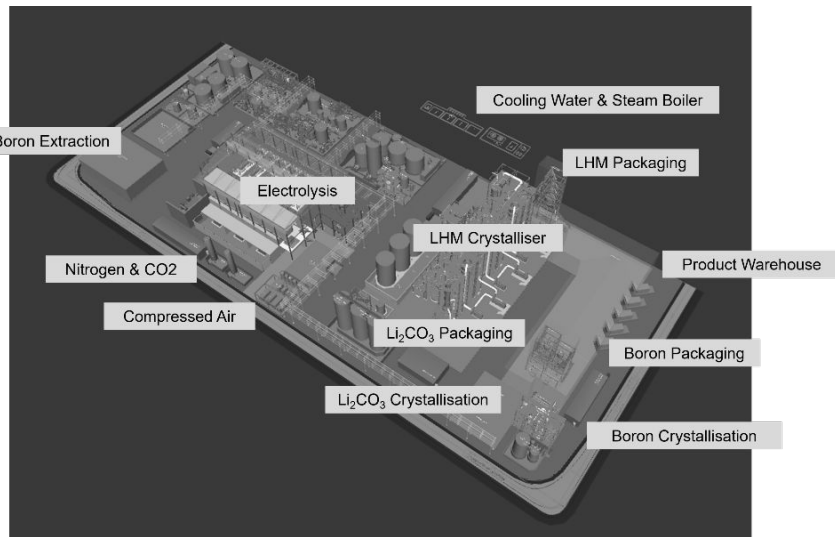
Disciplined, gated approach to reaching commercial operations

Process batch pilot evaluation:

- Performed on a Sth American brine eluate
- Pre-concentration completed and characterized
- Purification completed
- Long-duration electrolysis commencing
- Product crystallisation from catholyte to follow
- Next step is sub-commercial scale continuous pilot

Plant design and estimation:

- Vendor packages were integrated into Engineering Cost Study to AACE Class 3 (+/- 15% accuracy)
- Plant layouts and PFDs completed, brownfields site
- Partial completion of P+IDs
- Capex and Opex estimates completed
- Process LCA on gate-to-gate basis completed, in peer review

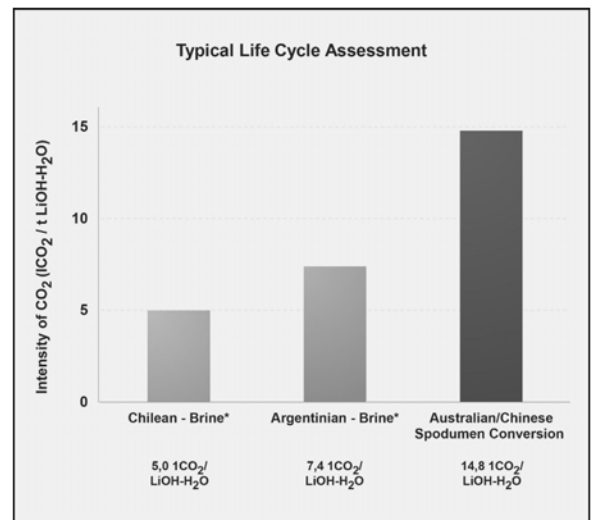
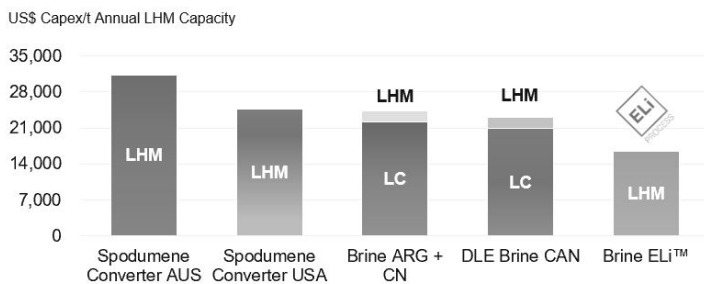


Result – Lowest Opex Conversion & Potentially Lowest CO₂

Estimated Opex Comparison (Conversion to LHM)



Estimated Capital Intensity (Conversion to LHM)



Source: ALB, E3 Li, PLL, Livent, Management estimated, Class 3 ECS, Benchmark Mineral Intelligence.

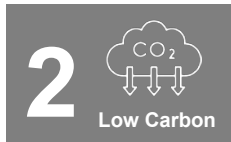
Source: SQM 2024

Sustainable Competitive Advantages for Plant Operators

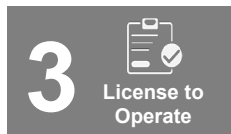
Commercial operating licence for highly efficient, lithium hydroxide plant utilising our patented processing flowsheet



No bulk reagents ensures essential lithium produced at substantial discount to conventional process



Replacement of carbon-heavy traditional bulk reagents



Reduces the lithium carbon footprint for EV batteries

- **Commercial deployment of ELi™**
 - Licensing business model, to producers, for royalty payments
 - Partnership model with producers
- **RAM holds 17 granted patents and 14 pending patents worldwide**
 - 4 families of patents covering brine and hard rock processing
- **Major lithium resource production regions**
 - Incl USA, Argentina, Chile, Australia

PROCESS MODELLING AND LIFE CYCLE ASSESSMENT: CONVENTIONAL AND NOVALITH PROCESSING OF SPODUMENE

By

Steven Vassiloudis, Cheng Zhou¹, ²Mike Dr, ²Maricha Bornman, ³Rachel Harris and ³Phoebe Whattoff

Novalith Technology, Australia

²Arithmetek, Canada

³Minviro, Australia

Corresponding Author

Mike Dry

mike.dry@arithmetek.com

ABSTRACT

Lithium is critical to the transition from a fossil-fueled to an electric economy. It is estimated that lithium demand will grow by up to 500% by 2050, compared to 2018 production. However, the cost of production will remain important, and it is critical that the increased production required for moving to an electric economy is not offset by an increase in adverse environmental impacts arising from increased production.

In this study, process modelling is combined with prospective life cycle assessment (LCA). This enables earlier and much better-informed decisions about economic and environmental sustainability. The production of lithium carbonate from spodumene is considered. The conventional route is thermal decrepitation, sulphuric acid bake, water leach, purification, and recovery of lithium. The novel (Novalith) approach is thermal decrepitation, pressure leaching with CO₂, precipitation and purification of lithium carbonate.

To ensure holistic decision-making it is important that costs, revenue, carbon footprint, water scarcity footprint and other environmental impact categories are all considered throughout the iterative design phase. Process modelling can be used to evaluate the technical and economic feasibility of a project design, whilst life cycle assessment (LCA) can be used to quantify the environmental impacts of a production route or processing technology. LCA is a methodology to quantify environmental impacts associated with all stages of a product, process, or activity. An integrated approach is presented that enables the early consideration of economic and environmental factors when evaluating alternative technologies.

Keywords: Lithium, CO₂, water, environment, LCA, economics

INTRODUCTION

Lithium is critical to the transition from a fossil-fueled to an electric economy. It is estimated that lithium demand will grow by a few hundred percent, for electric vehicles alone, by 2050 compared to 2018 production levels¹. However, the cost of production remains important, and the required increase in production cannot come at the expense of increased adverse environmental impacts.

Process modelling combined with prospective life cycle assessment (LCA) enables earlier and much better-informed economic and environmental decision-making. In this paper, two routes producing lithium carbonate from spodumene are examined to showcase the combination of process/economic modelling and LCA. One route is the conventional thermal decrepitation, sulphuric acid bake, water leach, purification, and precipitation of lithium carbonate. The other is a novel approach being developed by Novalith Australia, entailing thermal decrepitation, pressure leaching with CO₂, precipitation and purification of lithium carbonate.

The purpose of process/cost modelling is to enable rational evaluation of the process or processes concerned, specifically including preliminary estimates of capital and operating costs, well before substantial costs have been incurred in the development of the process or processes concerned. The purpose of early-stage LCA is to quantify environmental impacts before irreversible decisions are made about the process.

METHODOLOGY

The two circuits chosen for this exercise were modelled using commercially available software known as Aspen Plus to generate detailed mass-energy balances that were used to calculate operating costs and exported to cost estimation software commercially known as Aspen Process Economic Analyzer, and used there to generate preliminary estimates of the capital costs of the process equipment for each circuit. This methodology has been presented before¹.

LCA is a scientific methodology to assess global environmental impacts associated with a product or process life cycle. LCA is a comprehensive and reliable tool that enables environmentally informed decision-making throughout all stages of a project's or product's life. LCA makes it possible to evaluate indirect impacts arising from a product or processing system over its entire life cycle, providing information that otherwise may not be considered. A wide range of environmental impacts can be captured scientifically and quantitatively. This holistic approach generates information on how decisions made at one stage of the life cycle might have consequences elsewhere, enabling informed decisions and avoiding the mere shifting of an environmental burden². It must be noted that LCA is a powerful tool to determine impacts at a global scale, however, it is less suitable for determining local impacts that are commonly investigated using environmental (and social) impact assessment studies.

LCA can use process data to quantify the various environmental impacts. One source of this data, which is not available when the operations under consideration do not yet exist, is actual operating plants. When the plant is yet to be built, process modelling³ can be used to generate plausible preliminary data. An important caveat here is that, while process modelling is a very useful tool for project evaluation, it is beyond risky to use it in isolation. The assumptions used (for example recoveries, reagent consumptions, solid-liquid separation efficiencies) must be verified experimentally before major expenditure such as detailed engineering design is undertaken, and certainly before a decision is made to construct the actual plant. The exercise presented here uses process modelling to generate preliminary data for the two processing options examined.

Principles as outlined under ISO 14040⁴ and ISO 14044⁵ standards series were applied in this study. These outline a four-step process, as shown in Figure 1.

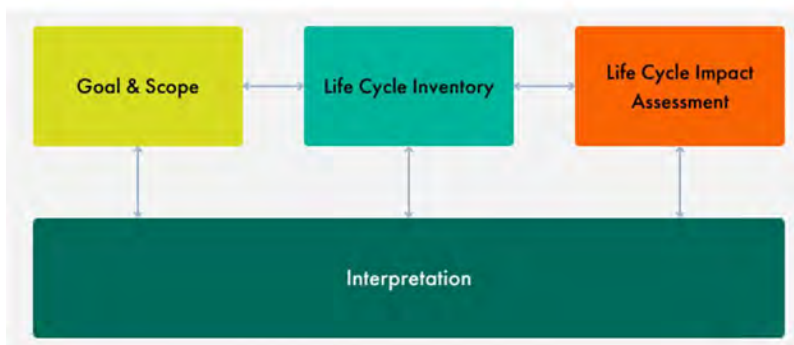


Figure 1 – Life Cycle Assessment Stages

The scope of a life cycle assessment study in the resource sector can be either:

- Cradle-to-gate: a partial life cycle assessment study of a product life cycle, from resource extraction to a defined end gate (e.g. lithium chemical delivered to the market).
- Gate-to-gate: a partial life cycle assessment study of a product life cycle, from factory entry gate to a defined end gate (e.g. lithium chemical delivered to the market).
- Cradle-to-grave or cradle-to-cradle: complete life cycle assessment study on the product life cycle, from resource extraction throughout the use phase and evaluating end-of-life impacts (grave) or recycling pathways (cradle).

The LCA presented here takes a cradle-to-gate and gate-to-gate approach. For the cradle-to-gate scenario, the impacts are accounted for from the point of extraction and production of spodumene concentrate to the final product, being battery-grade lithium carbonate produced and ready for shipment to customers. For the gate-to-gate scenario, the impacts of the spodumene concentrate have been excluded. Two scenarios are modelled:

(1) the production of lithium carbonate via the conventional sulphation route, with sodium sulphate as a co-product, and

(2) the production of lithium carbonate via the Novalith process.

The system boundaries used in this study are presented in Figure 2. The results of this LCA study are considered to be relevant input for rational decision-making and ranking processing options. The results of the study are not intended to communicate comparative assertions to the public.

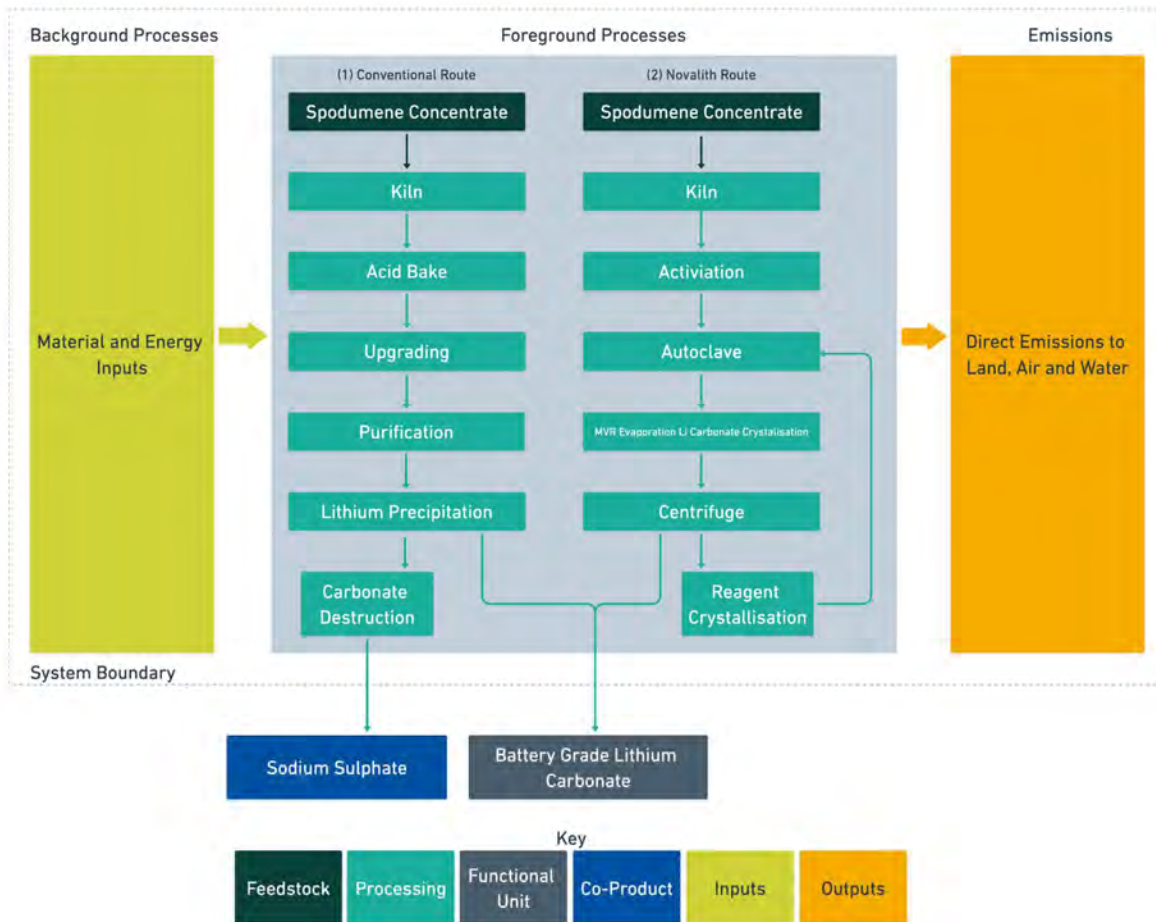


Figure 2 – System Boundary Applied in this Lithium Carbonate Life Cycle Assessment Study

LIFE CYCLE IMPACT ASSESSMENT

The life cycle impact assessment categories evaluated in this study are climate change and water use.

Climate change

Climate change is the term generally used to mean an increasing global temperature arising from the effect of “greenhouse gases” (GHG) released by human activity. There is now scientific consensus that the increase in these emissions is having a noticeable effect on climate. Climate change is one of the major environmental effects on economic activity, and one of the most difficult to control because of its global scale⁶. The environmental profiles characterisation model is based on factors developed by the UN’s Intergovernmental Panel on Climate Change. Factors are expressed as GWP (Global Warming Potential) over various time horizons, the most common historically being 100 years, measured in the reference unit, **kg CO₂ eq.**

The GHG Protocol identifies three “scopes” of GHG emissions which have been included in this study, however, it should be noted that scopes of emissions are not a framework inherent to LCA. The GHG Protocol defines scopes of emissions as:

Scope 1: Direct GHG emissions (e.g. furnace off-gas, combustion of fuels).

Scope 2: Indirect GHG emissions from consumption of purchased electricity, heat, or steam (e.g. emissions embodied in grid power or embodied in steam at an industrial park).

Scope 3: Other indirect emissions such as the extraction and production of purchased materials and fuels, transport-related activities in vehicles not owned or controlled by the reporting entity, electricity-related activities (e.g. transmission and distribution losses) not covered in scope 2, outsourced activities, and waste disposal. Scope 3 emissions can be either “upstream” or “downstream”. In a cradle-to-gate LCA, “upstream” scope 3 must be included.

Water use

The AWARE method is applied to quantify the environmental performance of products and operations regarding fresh water. This method was developed by Water Use in Life Cycle Assessment (WULCA), a working group of the United Nations Environment Programme (UNEP) and the Society for Environmental Toxicology and Chemistry (SETAC) Life Cycle Initiative, on a water scarcity midpoint method for use in LCA and for water scarcity footprint assessments. This approach is based on the available water remaining per unit of surface area in a given watershed after human and ecosystem demands have been met, relative to the world average. The resulting characterisation factor ranges between 0.1 and 100 and can be used to calculate water scarcity footprints⁷. A value close to 0.1 means that plenty of water is available in that region, whilst a water scarcity of 100 means that water in that region is extremely scarce. Units of the characterisation factor are dimensionless, expressed in **m³ world eq. per m³**. It is important to note that this impact relates to the potential for water deprivation to humans or ecosystems, rather than direct water use by the project. Another way to think about this is that it is a life cycle impact assessment value, not an inventory flow. The water stress index for the project in development is assumed to be **2.4 m³ world eq. per m³**.

Allocation

If a system produces multiple products, it is required to divide the impacts between those products that represent the distribution of the impacts between those products and the benefits of those products in a fair way. This is defined as allocation and should follow a stepwise approach⁸. For the scenario assessing the impact of lithium carbonate produced via the conventional sulphation circuit, sodium sulphate is produced. One scenario has assumed the sodium sulphate is sold. The impacts of this scenario have been distributed via system expansion. For the Novalith circuit, no co-products are produced, meaning no allocation is required.

SPODUMENE

Rationally comparing two process options for processing spodumene requires them to use the same feed. The spodumene selected as feed for the study is shown in Table 1.

Table 1 – Spodumene composition, mass %.

α -LiAlSi ₂ O ₆	70.84	Mg ₅ Al ₄ Si ₃ O ₁₈ H ₈	2.09
Fe ₂ O ₃	1.93	CaCO ₃	1.74
SiO ₂	7.44	KAl ₃ Si ₃ O ₁₂ H ₂	7.54
NaAlSi ₃ O ₈	6.43	Al ₂ Si ₄ O ₁₂ H ₂	1.99

CONVENTIONAL CIRCUIT

Figure 2 illustrates the conventional circuit, which has been described in the literature^{9,10}. Incoming spodumene concentrate is first heated to 1050°C in a rotary kiln, converting the α -spodumene to β -spodumene. The requisite energy is supplied by burning fuel (natural gas, represented by methane) in air.

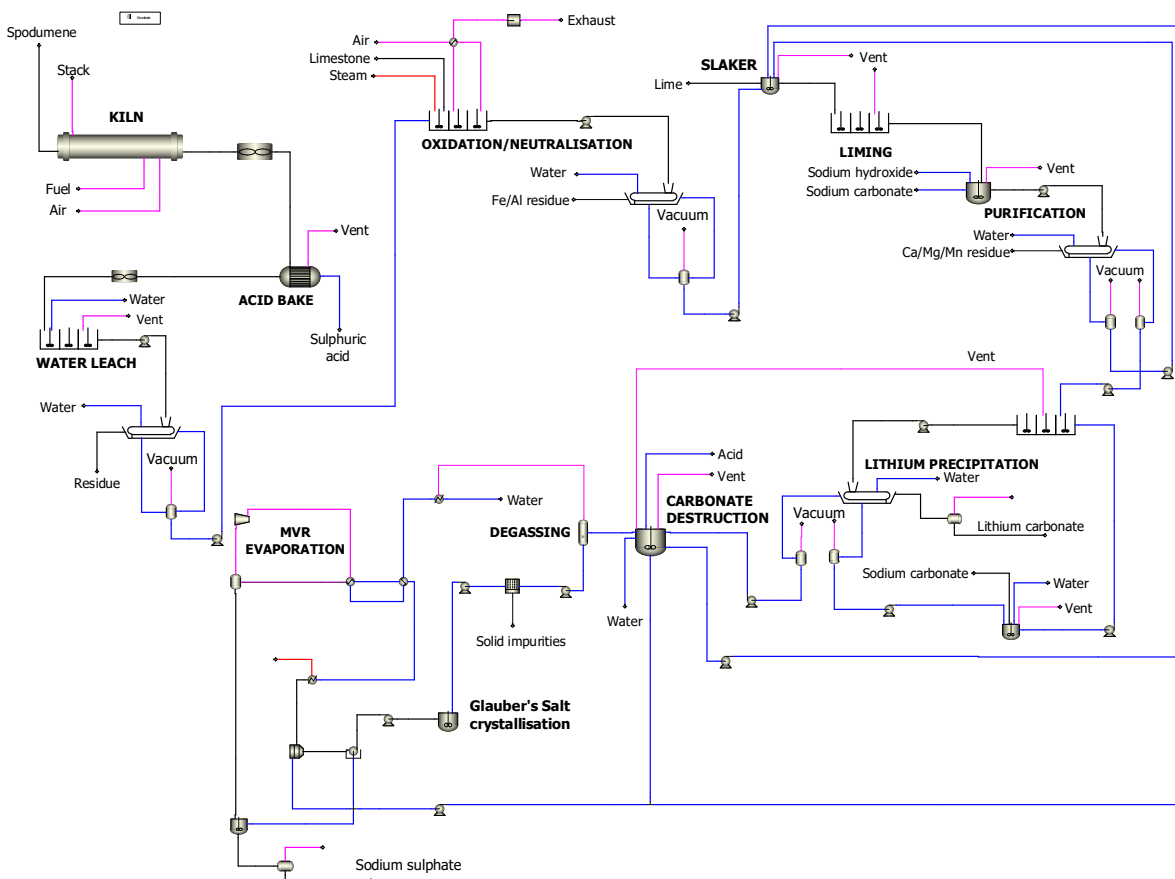
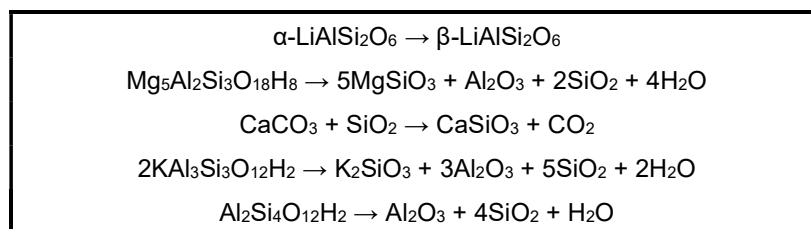


Figure 2 – Conventional Circuit.

The flows of solids and gas are counter-current, allowing for some pre-heating of the incoming air and cooling of the hot calcine. Table 2 shows the stoichiometry used to represent the calcination.

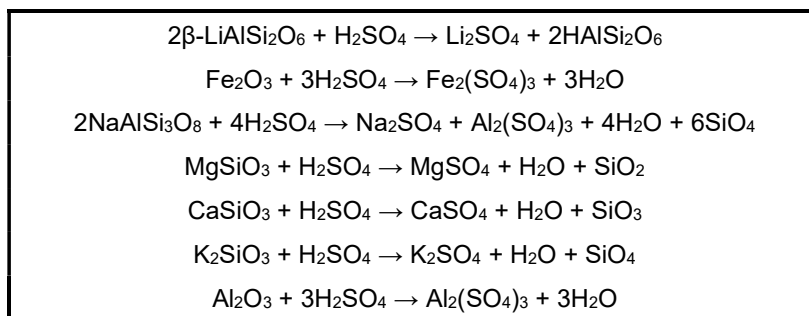
Table 2 – Calcination Chemistry.



The hot calcine is cooled, mixed with concentrated sulphuric acid and baked at about 200°C, then cooled and leached with water. The sulphate salts formed in the acid bake dissolve fully, except for calcium sulphate, which dissolves to the extent dictated by its limited solubility in water. The water-leached slurry is filtered, and the filter cake is washed with water and discarded. Table 3 shows the acid-bake chemistry.

The filtrate from the water leach is oxidised with air and neutralised with calcium carbonate to oxidise any ferrous iron to ferric iron and precipitate the iron and aluminium as hydroxides. The resulting slurry is filtered, the filter cake is washed with water and discarded, and the filtrate is neutralised further with slaked lime to precipitate magnesium hydroxide. The resulting slurry is dosed with sodium hydroxide and sodium carbonate, raising the pH beyond what is achievable with lime and precipitating the residual magnesium as magnesium hydroxide and the residual calcium as calcium carbonate. The precipitated solids are filtered off, rinsed with water and discarded. The wash filtrate is recycled to the upstream lime slaking step.

Table 3 – Acid-Bake Chemistry.

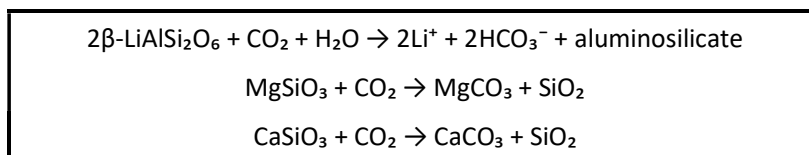


The primary filtrate from the purification sequence is dosed with sodium carbonate to precipitate lithium carbonate that is recovered by filtration, washed with water and collected as the required product. The wash filtrate is used to dissolve the incoming sodium carbonate, the dissolved sodium carbonate returning to the precipitation of lithium carbonate. The primary filtrate is dosed with sulphuric acid to decompose carbonates to carbon dioxide that is removed in a vacuum degassing step, then cooled to crystallise sodium sulphate decahydrate (Glauber's Salt). The remaining solution is recycled. The Glauber's Salt is remelted and the melt is further evaporated, crystallising sodium sulphate that is captured, dried and removed from the circuit.

NOVALITH CIRCUIT

The Novalith circuit is illustrated in Figure 3. The chemistry of the dissolution step is shown in Table 4. The incoming spodumene concentrate is calcined as in the conventional circuit, converting the α -spodumene to β -spodumene. After cooling, calcine is mixed with make-up and recycled reagents, milled, and activated, making the β -spodumene more reactive towards aqueous carbon dioxide. The details of the activation step remain, for the present, proprietary to Novalith.

Table 4 – Novalith chemistry



The activated solids are mixed with water and pumped, via feed-product heat exchange and a pre-heater, into a leaching reactor and reacted with carbon dioxide and water at high pressure and moderate temperature, dissolving the lithium carbonate into aqueous lithium bicarbonate. Mineral carbonation occurs in this reactor mainly for the lithium, and to a small extent for the impurities in the spodumene feed, e.g. a very small amount of calcium silicate is converted to calcium carbonate. The exit slurry is cooled and filtered, the filter cake is washed with water, and the washed filter cake is discarded.

The filtrate is purified through ion exchange, removing any residual divalent cations (primarily calcium) then concentrated by reverse osmosis. The concentrated solution is evaporated to release CO_2 and precipitate lithium carbonate which is recovered by filtration. The vapour is re-compressed and partially condensed in the hot side of the evaporator. The condensate is recycled as process water. The remaining vapour is cooled, condensing out more water that is also recycled as process water, and the remaining vapour (now mainly CO_2) is recompressed and recycled to the autoclave.

The filter cake is centrifuged, washed with water and dried, exiting as the lithium carbonate product. The filtrate and concentrate solutions are combined, evaporatively concentrated to manage the overall water balance, and recycled. The condensate from this evaporation step is recycled as process water

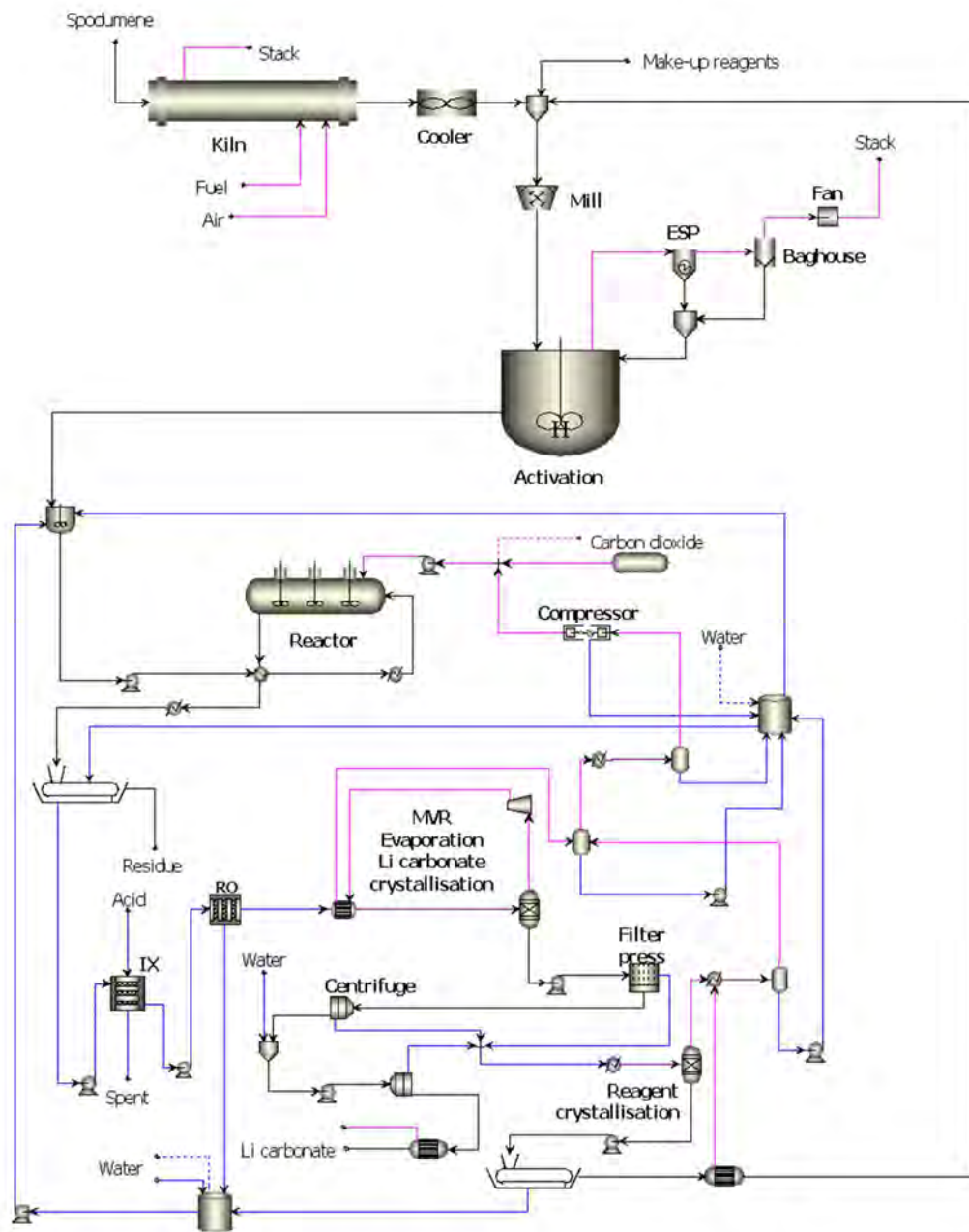


Figure 3 – Novalith Circuit.

COMPARISON

The amounts of the various reagents and utilities consumed in each circuit were extracted from the mass-energy balances emanating from the two process models. These quantities, the unit costs used and the resulting operating costs are summarised in Table 5 and Table 6. The conventional circuit consumes a little more spodumene than the Novalith circuit because there is a little lithium in the sodium sulphate by-product. The Novalith circuit does not generate sodium sulphate.

Table 5 – Feed, Reagents and Utilities, Conventional Circuit.

Item	Amount	\$/t Li ₂ CO ₃
Spodumene (\$500/t)	7540 kg	3770
Fuel, approximated as CH ₄ (\$350/t)	274 kg	96
Sulphuric acid, as 100% H ₂ SO ₄ (\$180/t)	3994 kg	719
Limestone, as 100% CaCO ₃ (\$60/t)	1193 kg	72
Lime, as 100% CaO (\$180/t)	17 kg	3
Sodium hydroxide, as 100% NaOH (\$500/t)	43 kg	21
Sodium carbonate, as 100% Na ₂ CO ₃ (\$300/t)	2879 kg	864
Steam (\$10/t)	33485 kg	325
Water (\$5/t)	46956 kg	235
Electricity (\$0.06/kWh)	2416 kWh	152
Feed, reagent & utility cost, \$/t LCE		6257

Table 6 – Feed, Reagents and Utilities, Novalith Circuit.

Item	Amount	\$/t Li ₂ CO ₃
Spodumene concentrate (\$500/t)	7122 kg	3561
Fuel, approximated as CH ₄ (\$350/t)	295 kg	103
Carbon dioxide, as 100% CO ₂ (\$34/t)	3 kg	0.1
Activation reagent (\$350/t)	1208 kg	423
Process water (\$5/t)	2060 kg	10
Cooling water make-up (\$5/t)	35033 kg	175
Utility steam (\$10/t)	13346 kg	129
Electricity to compression (\$0.06/kWh)	2864 kWh	181
Electricity to pumping (\$0.06/kWh)	922 kWh	58
Feed, reagent & utility cost, \$/t LCE		4641

Techno-economics

The capital costs listed in Table 7 are based on a production capacity of 20 thousand tonnes per year of lithium carbonate. The capital and operating costs lead to the cash flow analyses shown in Figure 4. Granted, the conventional circuit is commercially proven, and the Novalith circuit is not yet proven. However, there would appear to be more than enough potential economic benefit to justify further development of the Novalith circuit.

Table 7 – Preliminary capital cost estimates for 20 kt/y LCE, US\$ million

Item	Conventional	Novalith
Purchased Equipment	32	59
Equipment Setting	0.5	1
Piping	15	24
Civil	2	3
Steel	0.4	0
Instrumentation	7	7
Electrical	6	6
Insulation	1	1
Other	29	36
G and A Overheads	3	4
Contract Fee	43	4
Contingencies	18	26
Total estimated capital	117	170

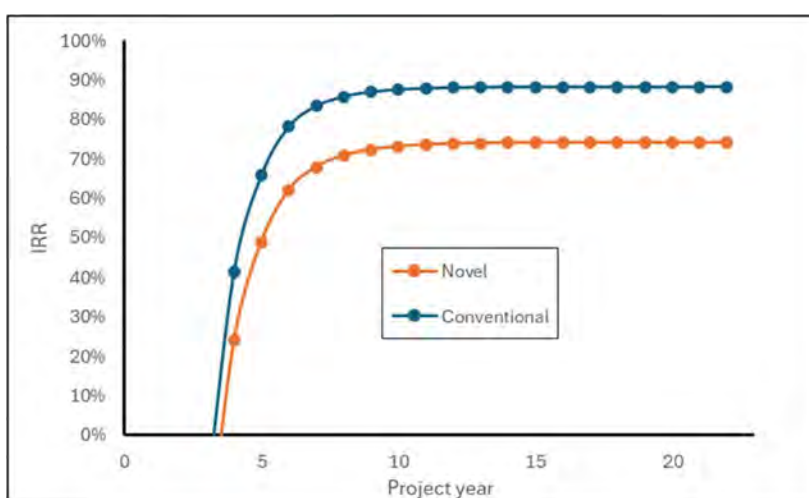


Figure 4 – Internal Rate of Return Versus Project Year.

LCA

Table 8 and Table 9 list the flows exiting each circuit.

Table 8 – Exit Flows, Conventional Circuit, kg/tonne Li_2CO_3 .

Description	Vapour		Liquid		Solids
	CO_2	Total	H_2O	Total	
Flue gas ex calciner	810	7205			
Vent ex acid bake	0	15			
Vent ex Fe oxidation	522	1740			
Vent ex lime slaking	0	0			
Vent ex purification	0	0			
Vent ex decarbonation	546	1686			
Vent ex Na_2SO_4 drier	0	633			
Vent ex Li_2CO_3 drier	1	245			
Water leach residue			801	804	7234
Fe/Al residue			206	207	1859
Ca/Mg/Mn residue			5	5	44
Li carbonate			0	0	1002
Na sulphate			3	3	3877

Table 9 – Exit Flows, Novalith Circuit, kg/tonne Li_2CO_3 .

Description	Vapour		Liquid		Solids
	CO_2	Total	H_2O	Total	
Flue gas ex calcination	765	6809			
Vent ex activation	0	585			
Bicarbonation leach residue	-	-	1822	1822	7319
Waste solutions ex IX	-	-	0.06	0.07	-
Vent ex Li_2CO_3 drier	1	245	-	-	0

Climate Change

Figure 5 shows the climate change impact for producing battery-grade lithium carbonate via the conventional circuit, where sodium sulphate is assumed to be a product. The total climate change impact is then calculated to be 14.9 kg CO_2 eq. per kg Li_2CO_3 . Contribution analysis figures aggregate contributors making up less than 1% of the impact category total as 'other'.

- The main contributor to climate change impact is the spodumene concentrate.
 - 3.8 kg CO_2 eq. per kg Li_2CO_3 which equates to 20.5% of the climate change impact.
 - The primary impact of spodumene concentrate in Australia is the use of diesel in the mining fleet and electricity generation.
- The total contribution of energy used in the process is 6.2 kg CO_2 eq. per kg Li_2CO_3 .
 - Utility steam contributes 4.5 kg CO_2 eq. per kg Li_2CO_3 , which equates to 24.3% of the total climate change impact.
 - Electricity to pumping contributes to <0.1 kg CO_2 eq. per kg Li_2CO_3 , and is incorporated in "Other".
 - Electricity to compression contributes to 0.3 kg CO_2 eq. per kg Li_2CO_3 .
 - Electricity to run refrigeration contributes to 1.3 kg CO_2 eq. per kg Li_2CO_3 which equates to 7.0% of the total climate change impact.
- The use of reagents in the process, which in total contribute 8.4 kg CO_2 eq. per kg Li_2CO_3 , of which the main contributors are as follows:
 - Sodium carbonate (Li purification) contributes 3.6 kg CO_2 eq. per kg Li_2CO_3 .
 - Sulphuric acid contributes 0.7 kg CO_2 eq. per kg Li_2CO_3 .

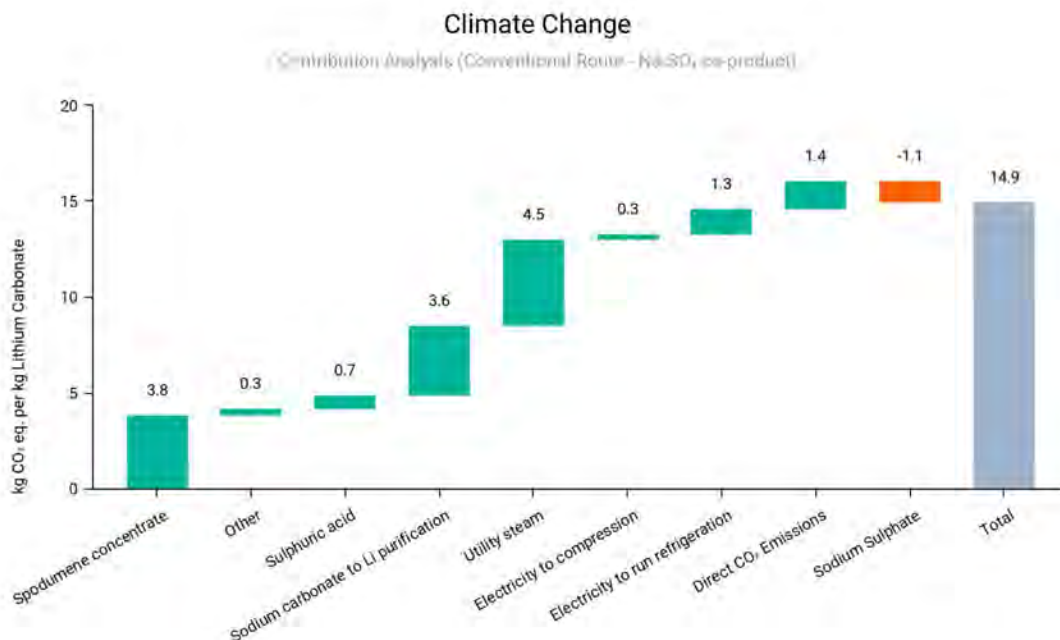


Figure 5 – Climate Change Contribution Analysis for Lithium Carbonate Produced from Spodumene Concentrate via the Conventional Circuit (Sodium Sulphate as Co-Product).

Figure 6 presents the climate change impact of lithium carbonate produced via the Novalith circuit. This production route's total climate change impact is 10.5 kg CO₂ eq. per kg Li₂CO₃. The climate change impact is made up of the following factors:

- Spodumene concentrate equates to 34.7% of the climate change impact, at 3.6 kg CO₂ eq. per kg Li₂CO₃.
- Electricity accumulates to 25.0% of climate change impacts, at 2.6 kg CO₂ eq. per kg Li₂CO₃.
- Utility steam contributes to 17.3% of climate change impacts, at 1.8 kg CO₂ eq. per kg Li₂CO₃.

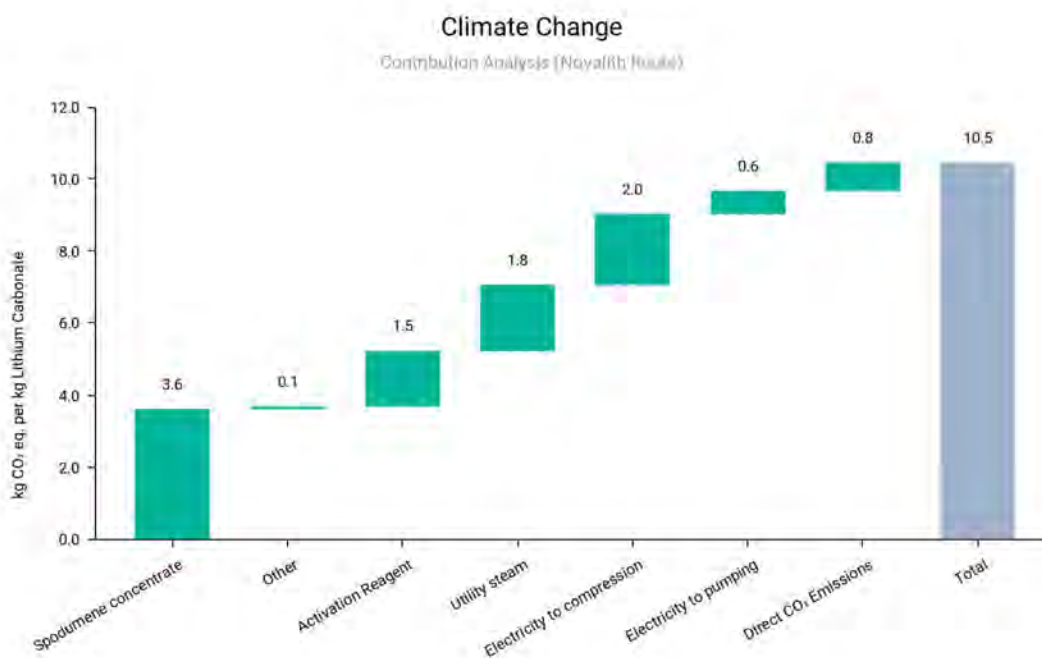


Figure 6 – Climate Change Contribution Analysis for Lithium Carbonate Produced from Spodumene Concentrate via the Novalith Circuit.

Comparing the results presented in Figures 5 and 6 shows that, overall, the conventional route has a higher total climate change than that of the Novalith route. The major differences between the conventional route and the Novalith route are the direct emissions, energy requirements, and reagents used. The conventional route has a higher impact due to the exhaust gases produced during the calcination and purification stages, which vent CO₂ into the atmosphere.

The Novalith circuit is an electrified process totalling 3.8 kWh per kg Li₂CO₃, with the greatest electricity demand required for the compression of recycled carbon dioxide. As a result, the composition of the electricity source (e.g. renewable electricity vs. fossil-fuel sources) for the Novalith process can have a large influence on the total climate change impact. In comparison, the conventional sulphation route sources energy from steam, generated by a natural gas boiler, and electricity from the Western Australian grid.

As for the reagents, the conventional route requires more reagent input than the Novalith route, due to the neutralisation and purification stages of the process. As seen in Figure 5, sodium carbonate is one of the main reagents contributing to the climate change impact for the conventional route, compared to Figure 6, where the activation reagent has the largest contribution. This is due to the amount of sodium carbonate used in the process; a total of 2.2 kg of sodium carbonate per kg Li₂CO₃ for the conventional route. The embodied impact of producing sodium carbonate is driven by its manufacturing process, which entails the dissolving of ammonia and carbon dioxide followed by calcination (Solvay process), which requires a large amount of thermal energy.

A key difference between the conventional route and the Novalith route is that the conventional route has the co-product of sodium sulphate. The conventional route where sodium sulphate is considered an economically viable co-product and has the climate change impact of 14.9 kg CO₂ eq. per kg Li₂CO₃. The Novalith route, however, has a lower climate change impact of 10.5 kg CO₂ eq. per kg Li₂CO₃, which is approximately 30% lower than the conventional sulphation process.

Figure 7 shows the climate change impact results for the conventional circuit and the Novalith circuit classified into scope 1, 2 and upstream scope 3 emissions. Scope 3 emissions make up the majority of the impact for both routes. This highlights the value of using a LCA approach, rather than just a GHG inventory analysis. For the conventional route, the upstream scope 3 emissions make up 56% of the total climate change impact. For the Novalith route, the scope 3 emissions account for 54% of the total climate change impact. A notable

difference is the relative difference between the emissions of scope 2 and particularly scope 1. For the conventional route, the scope 1 emissions make up 32.9%, compared to the scope 1 emissions of the Novalith route, which contribute 21% of the total emissions. For the conventional route, scope 2 emissions make up 11.2% of the total emissions, and with Novalith the scope 2 emissions make up 25%.

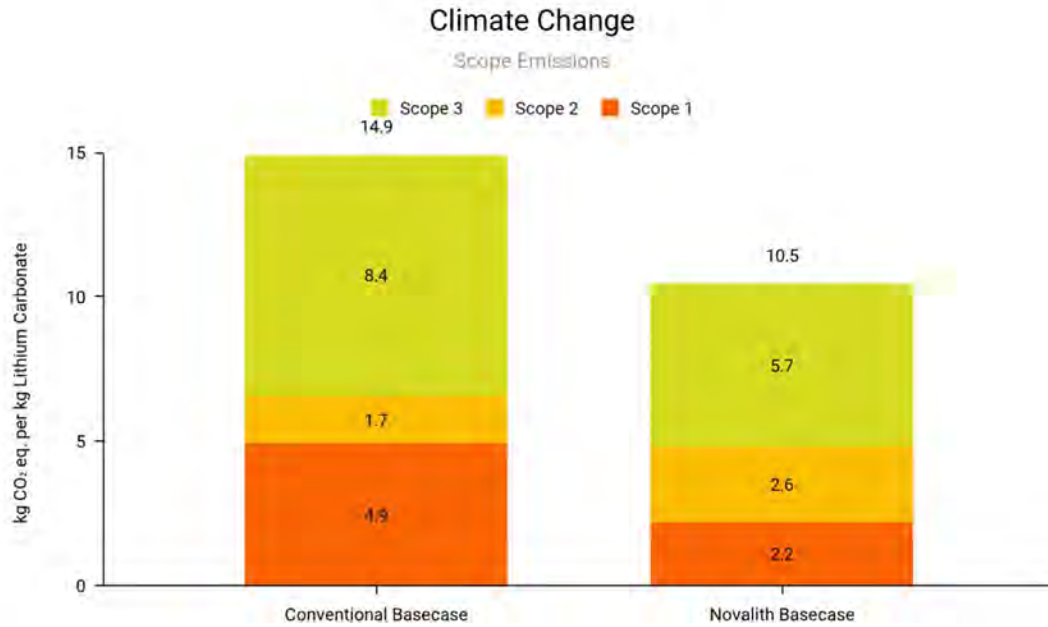


Figure 7 – Climate Change Impact for Lithium Carbonate Produced via the Different Pathways Broken Down into Scope Emissions.

Water Use

Figure 8 presents the water use calculated for lithium carbonate via the conventional route, totalling 19.4 m³ world eq. per kg Li₂CO₃. This total water use calculation accounts for direct freshwater use on-site and embodied water impacts of consumables used.

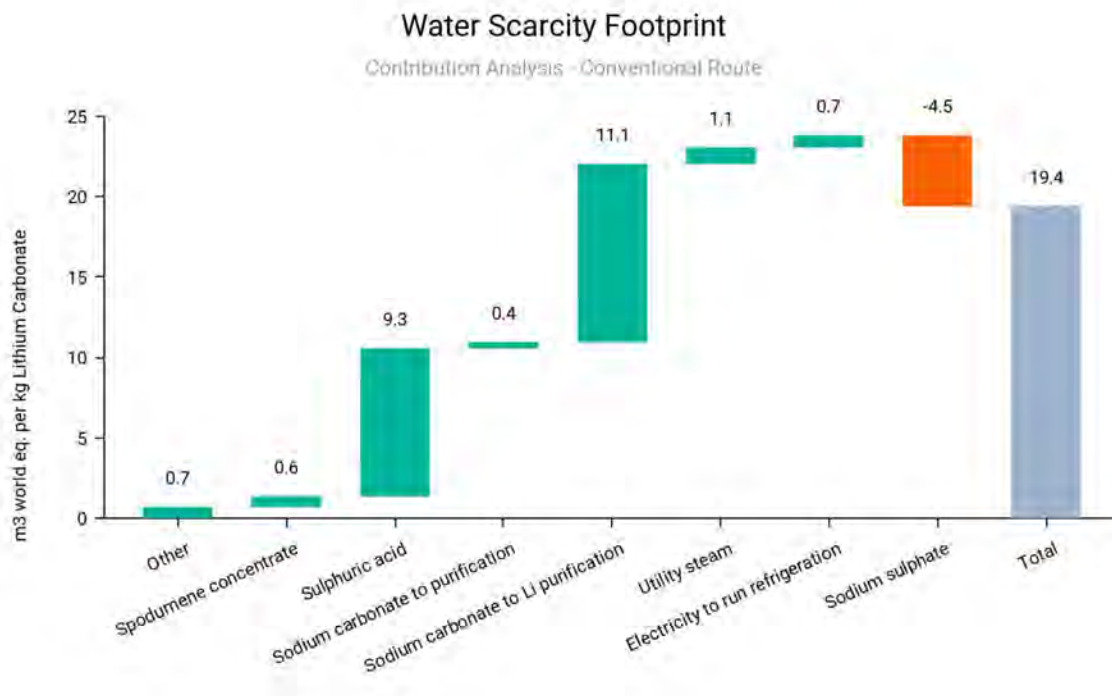


Figure 8 – Water Contribution Analysis for Lithium Carbonate Produced from Spodumene Concentrate via the Conventional Route.

In this case, water captured from recycled condensate is taken into account. Of the total water out, 87% exits as water vapour to the atmosphere, and the rest in residue to be disposed of. The non-agricultural water scarcity footprint of the study area is 2.4 m³ world eq. per m³. This indicates that the region where the project is has 2.4 times less available water remaining per area than the world average.

The main contribution to the water impact is from sodium carbonate for Li purification, totalling 11.1 m³ world eq. per kg Li₂CO₃. This is due to the embodied impacts of sulphuric acid production. Furthermore, -4.5 m³ world eq. per kg Li₂CO₃ has been removed, as this is the impact associated with sodium sulphate which has been removed from the system via system expansion.

Figure 9 presents the water use calculated for lithium carbonate via the Novalith route, totalling 7.4 m³ world eq. per kg Li₂CO₃. The activation reagent is the main contributing factor in this case, with 4.8 m³ world eq. per kg Li₂CO₃. This is due to the embodied impact of producing the activation reagent being a water-intensive process. For the Novalith route, 60% of the water leaving the circuit exits as vapour to the atmosphere, the rest in discarded residue.

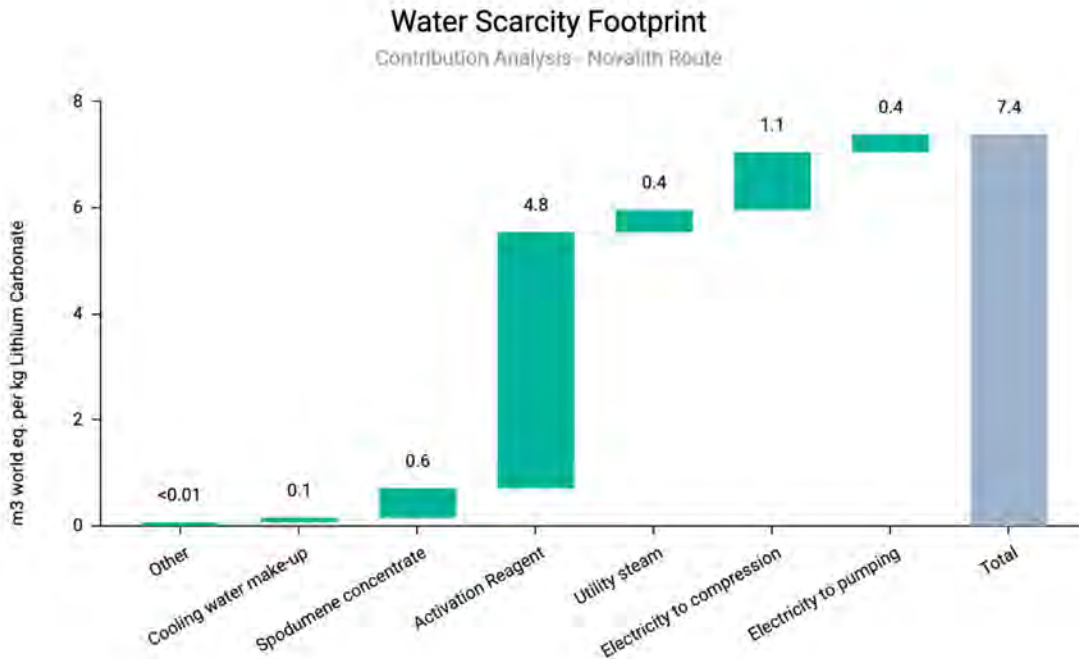


Figure 9 – Water Contribution Analysis for Lithium Carbonate Produced from Spodumene Concentrate via the Novalith Route.

Sensitivity Analysis

Three sensitivity analyses were performed on the primary assumptions. The scenarios include:

1. Sodium sulphate as a waste - this analysis looks at the scenario where lithium becomes so abundant that the sodium sulphate co-product is no longer economically viable and therefore becomes a waste product.
2. Novalith renewable energy - this scenario examines the current Western Australian grid mix versus a more renewable energy mix, in this case; a 70% renewable grid mix.
3. Gate-to-Gate - this sensitivity scenario looks at the base case conventional route and the base case Novalith route, where the system boundary has removed the cradle and hence the impacts of spodumene concentrate. Therefore, only the impacts of processing the lithium carbonate are considered.

Figure 10 depicts the base case scenarios, plus sensitivity analyses 1-2 as described above. The Novalith circuit has a 30% lower impact than the conventional base case circuit with 10.5 kg CO₂ eq. per kg Li₂CO₃ and 14.9 kg CO₂ eq. per kg Li₂CO₃, respectively. However, having a clean electrical grid (at least 70% renewables) for Novalith has a significant decrease of 23.7% of the climate change impact. This graph also shows that the conventional route can have a 12.9% increase in the climate change impact where sodium sulphate is considered a waste product compared to the conventional base case scenario.

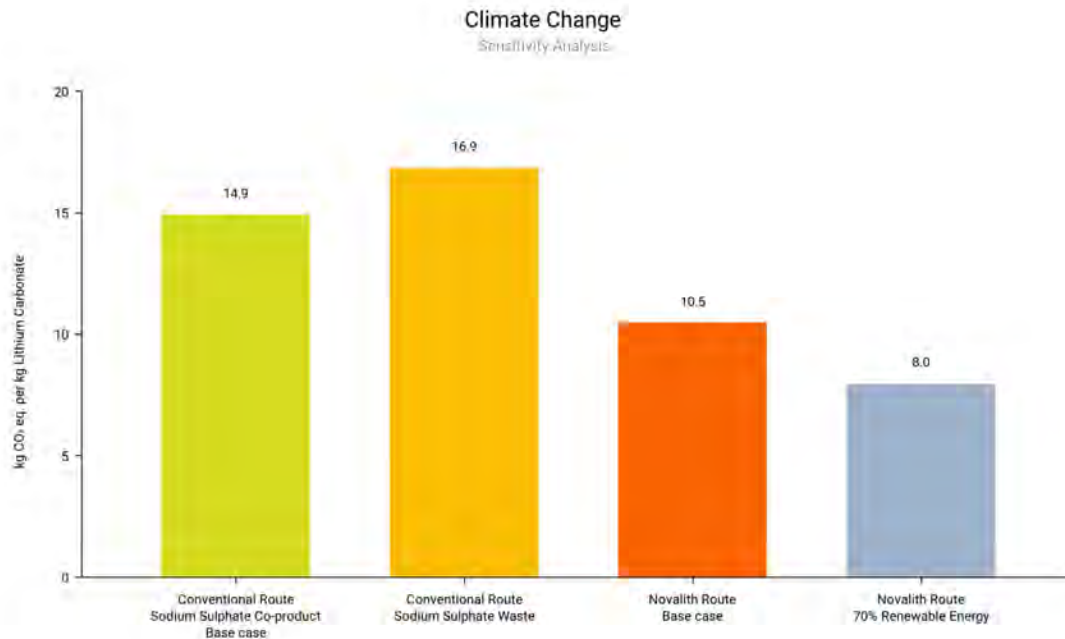


Figure 10 – Climate Change Contribution Sensitivity Analysis for Lithium Carbonate Produced.

Figure 11 presents the climate change impact of the base case scenarios when the impact of spodumene concentrate is excluded. The conventional route processing has a larger processing impact than the Novalith route.

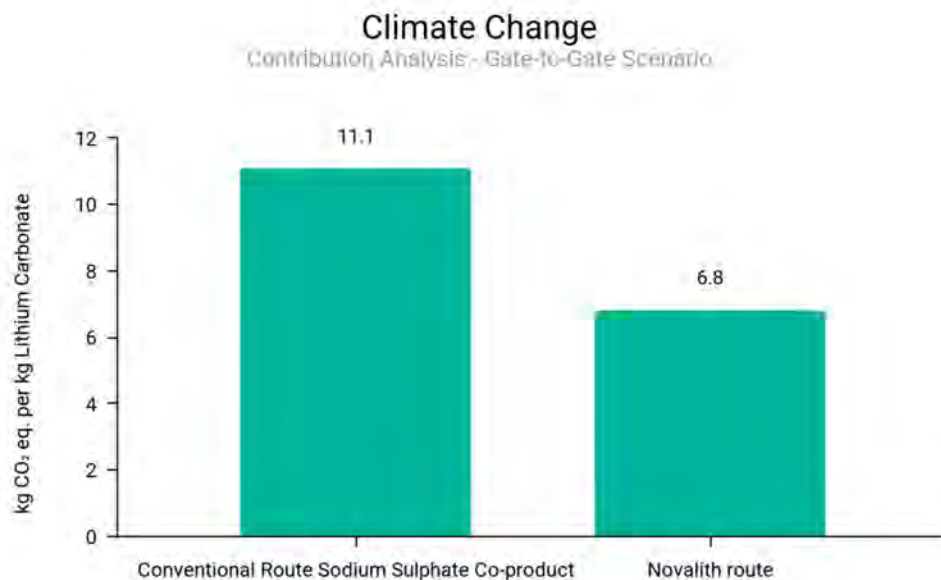


Figure 11 – Climate Change Contribution Gate-to-Gate Analysis for Lithium Carbonate Produced.

CONCLUSIONS

This paper shows how a combination of life cycle assessment based on process modelling and techno-economic evaluation allows early quantification and investigation of the relationship between mineral resource project economics and environmental impacts before substantial development expenditure has been incurred. The example used is the production of lithium carbonate from spodumene concentrate in a conventional circuit and in the novel Novalith circuit.

The techno-economic analysis indicates that the Novalith route offers distinctly better economics than the conventional route, making its ongoing development a rational decision.

Depending on the production pathways, the climate change impact can range from 8.0-16.9 kg CO₂ eq. per kg Li₂CO₃ produced. The water use impact of the two circuits is shown to range between 7.4-19.4 m³ world eq. per kg Li₂CO₃. For climate change impact, the Novalith circuit has the lowest climate change impact, particularly if the energy can be sourced from at least 70% renewable energy, highlighting the benefits of a more electrified process and a clean electricity mix. For the water use impact, the Novalith circuit has a lower water use impact of 7.4 m³ world eq. per kg Li₂CO₃. The conventional circuit has an impact of 19.4 m³ world eq. per kg Li₂CO₃. This impact would further increase if impacts of sodium sulphate are included in the conventional route, rather than excluded through system expansion. This increase is due to the electricity and energy requirements for the crystallisation and waste treatment of sodium sulphate. It must be noted that the impact values of the two circuits can change depending on the process location, energy sources, material consumption and process route.

This study shows the value of using and integrating life cycle assessment methods into the early development phase of a project phase, particularly capturing the upstream scope 3 emissions. This enables environmentally informed decisions that can be used to understand and mitigate environmental impacts while the development phase of the project is still flexible.

REFERENCES

1. Dry, M., Harris, B. A Metallurgical Evaluation of the Transition to Electric Vehicles. Alta 2020, May 2020.
2. Horne, R. E., Grant, T. & Verghese, K. Life Cycle Assessment: Principles, Practice and Prospects. (CSIRO Publishing, 2009).
3. Dry, M. J. Early evaluation of metal extraction projects. Alta 2013, Perth, May 2013.
4. International Organization for Standardization. ISO14040: 2006 Environmental Management. Life Cycle Assessment. Principles and Framework. 2006
5. International Organization for Standardization. ISO14044: 2006 Environmental Management. Life Cycle Assessment. Requirements and Guidelines. 2006
6. Intergovernmental Panel on Climate Change (IPCC). *Climate Change 2021 - The Physical Science Basis: Working Group I Contribution to the Sixth Assessment Report of the Intergovernmental Panel on Climate Change*. (Cambridge University Press, 2023).
7. Boulay, A. M., Bare, J., Benini, L., Berger, M., Lathuilière, M. J., Manzardo, A., ... & Pfister, S. (2018). The WULCA consensus characterization model for water scarcity footprints: assessing impacts of water consumption based on available water remaining (AWARE). *The International Journal of Life Cycle Assessment*, 23(2), 368-378.
8. International Organization for Standardization. ISO14044: 2006 Environmental Management. Life Cycle Assessment. Requirements and Guidelines. 2006
9. Granata, G., Da Gama, R., Petrides, D. Lithium Extraction from Spodumene Ore: Modelling and Evaluation with SuperPro Designer. https://www.researchgate.net/publication/340593032_Lithium_Extraction_from_Spodumene_Ore_-_Techno-Economic_Assessment_with_SuperPro_Designer (accessed 2024-03-07)
10. Desemond, C., Lajoie-Ieroux, F., Soucy, G., Laroche, N., Mangan, J. Spodumene: The Lithium Market, Resources and Processes. *Minerals* 2019, 9,334. <https://www.mdpi.com/2075-163X/9/6/334>

THE PRODUCTION OF HIGH PURITY BATTERY GRADE LITHIUM CARBONATE PRODUCT FROM LITHIUM BRINE SOURCES

By

Nipen Shah, ²Dave Rogans, ²Theresa McBride, ²Katherine Lombard

JordProxa, Australia
²JordProxa, South Africa

Presenter and Corresponding Author

Nipen Shah
nshah@jordproxa.com

ABSTRACT

The rise in demand for low-cost, high-energy density, safe and reliable batteries for the EV market is driving process and flowsheet development to produce high-quality low-cost precursor materials.

Lithium is extracted from various feed sources around the world and is available for refining into a battery-grade product as lithium carbonate or lithium hydroxide. Differing geologies and upstream chemistry in particular present a broad range of “impurity fingerprints” in the feed solutions that will determine the number of processing steps we need to incorporate in the flow sheet to achieve the desired product purity. These challenging feeds require careful examination and testing to prepare optimal flowsheets for each application with primary focus on meeting the stringent purity requirements, whilst seeking a balance between capital and operating costs.

The lithium brines have a variable lithium content depending on each salt flat, and various impurities that are not desirable in the final product (such as calcium, magnesium, boron, sulphate, among others). The brine goes through a number of processing steps such as lithium extraction, concentration, refining and conversion to lithium carbonate to produce battery grade lithium carbonate.

With the use of sophisticated simulation software, test work and extensive technical know-how, robust flowsheets have been developed to produce battery grade lithium carbonate from a variety of brine feed sources. This paper briefly outlines the typical feed chemistries and corresponding flow sheet options, and the balance between purity, capital and operating expenditures during flowsheet development.

Keywords: *Lithium carbonate, crystallisation, product purity, brine*

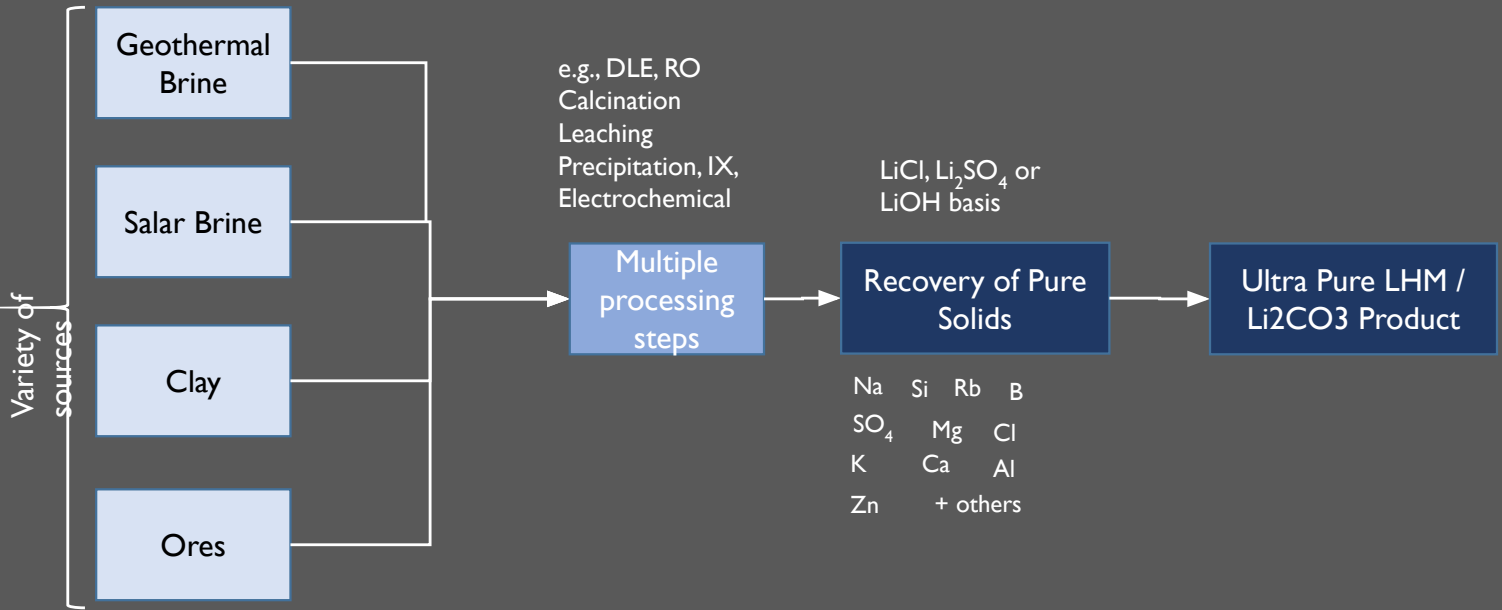


**THE PRODUCTION OF HIGH PURITY BATTERY GRADE LITHIUM CARBONATE PRODUCT
FROM LITHIUM BRINE SOURCES**

Nipen Shah – Head of Sales

+61 472 847 484 | nshah@jordproxa.com | jordproxa.com

Li Sources



Design Approach

2



- PURITY - Free from impurities



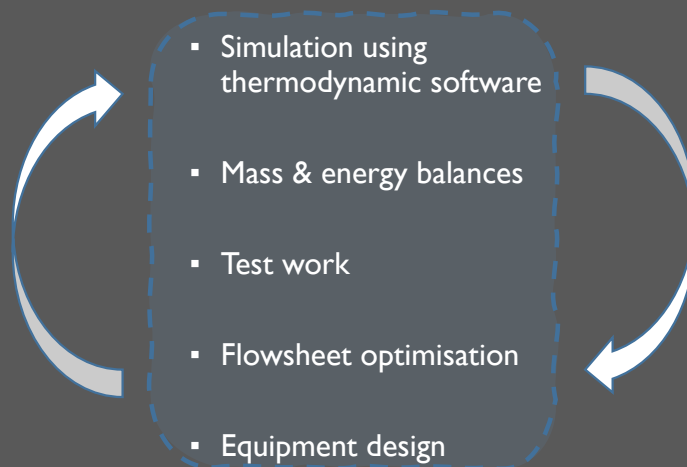
- SUSTAINABILITY – Heat integration and water recovery



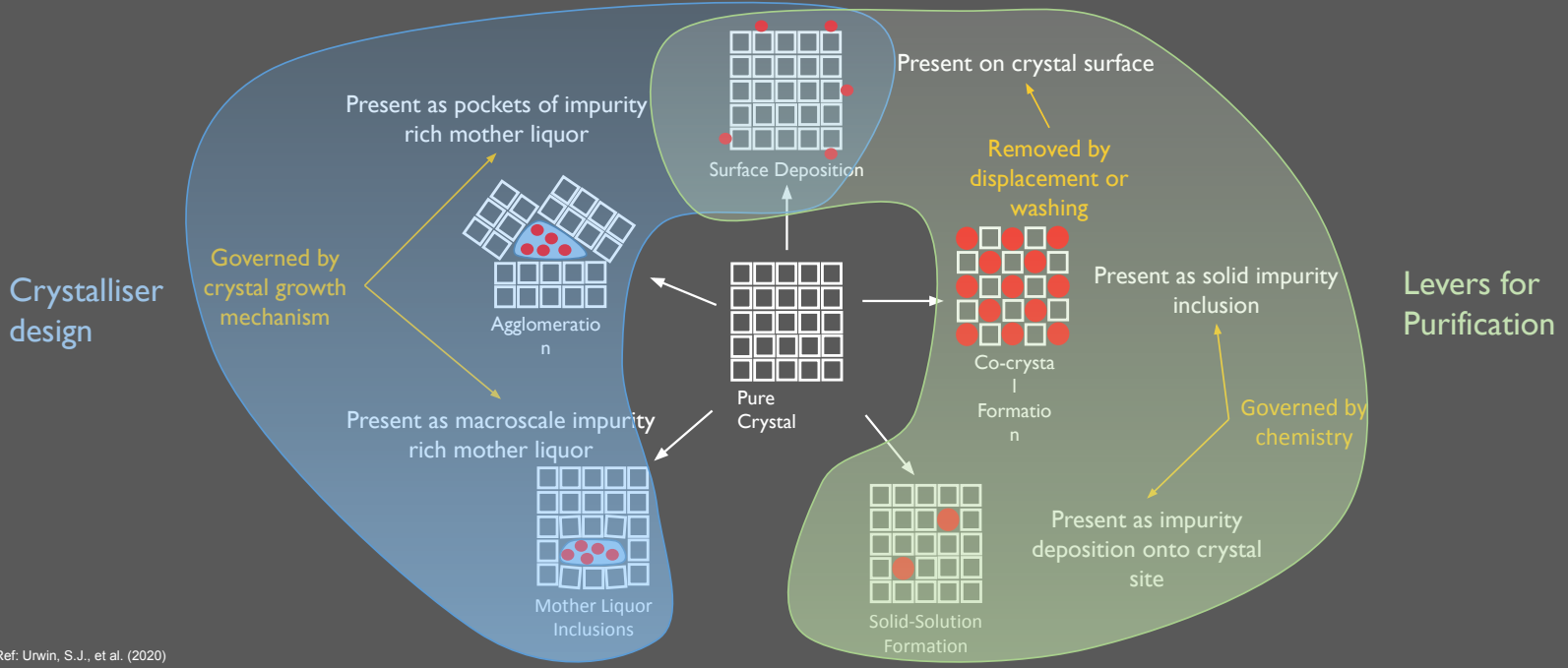
- VALUE – Delivery, schedule, costs

Design Objectives

- Maximise purity
- Maximise yield
- Minimise CAPEX and OPEX costs
- Ease of operation with robust design

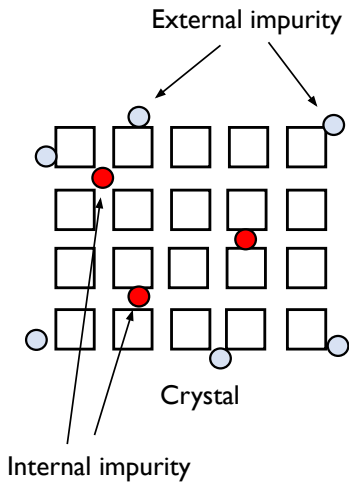


Impurity Entrainment

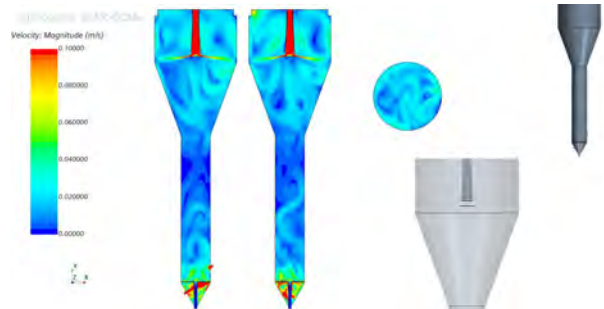


Ref: Urwin, S.J., et al. (2020)

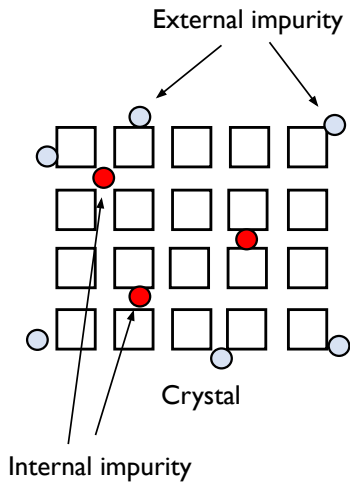
Levers for Purification



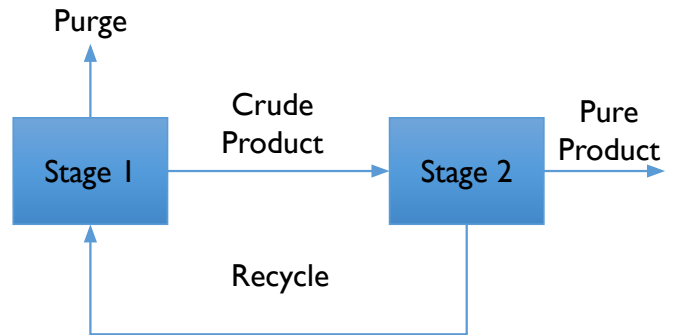
- **Centrifugation** displaces surface depositions by washing and ML removal.
- **Wash legs** reduce surface depositions by partly displacing high impurity ML with feed. (LHM only)



Levers for Purification

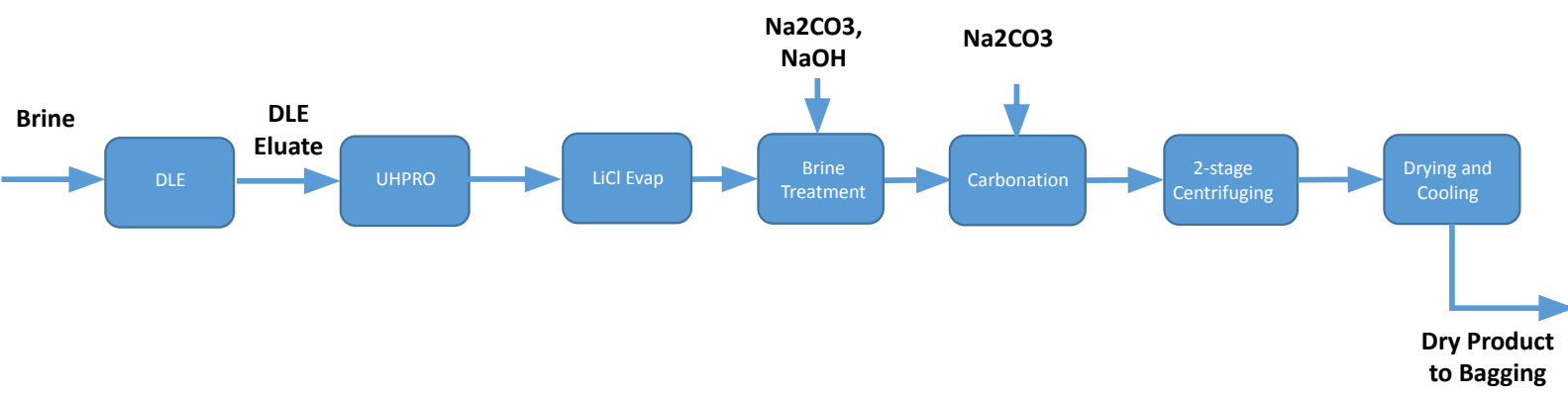


- **Staged crystallisation** reduces ML impurity fingerprint profile.
- **Purge/Recycle rates** reduce ML impurity fingerprint profile.

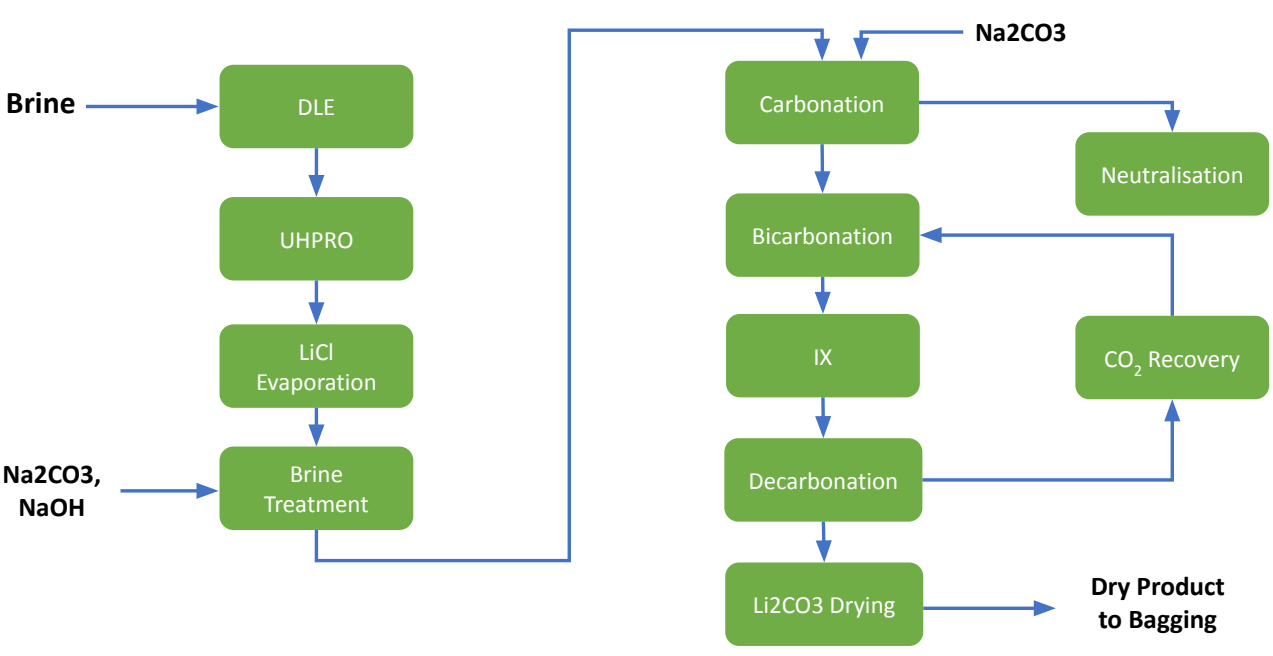


Flow sheet and Design Considerations

3



Confidential



Confidential



Lithium Chloride Evaporation

- Falling film evaporator to pre-concentrate LiCl brine before the carbonation step
- 2 or 3 stage MVR fans required depending upon the BPE
- Concentration up to 25 g/L Li or 40 g/L depending upon the process requirements

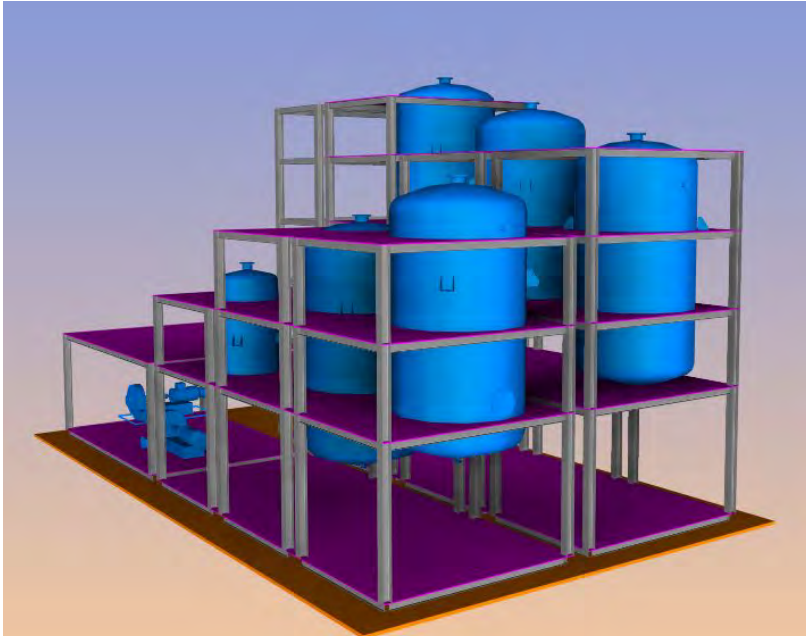
Confidential



Lithium Chloride Carbonation Reactor



- Intense mixing zone of lithium chloride with bulk solution
- Separate sodium carbonation inlet to provide a slight excess
- Agitator provides homogenous mixing in reactor zone for dissipation of supersaturation and growth of crystals
- Gentle mixing to minimise crystal breakage



Lithium Carbonate Dissolution (Bicarbonation)



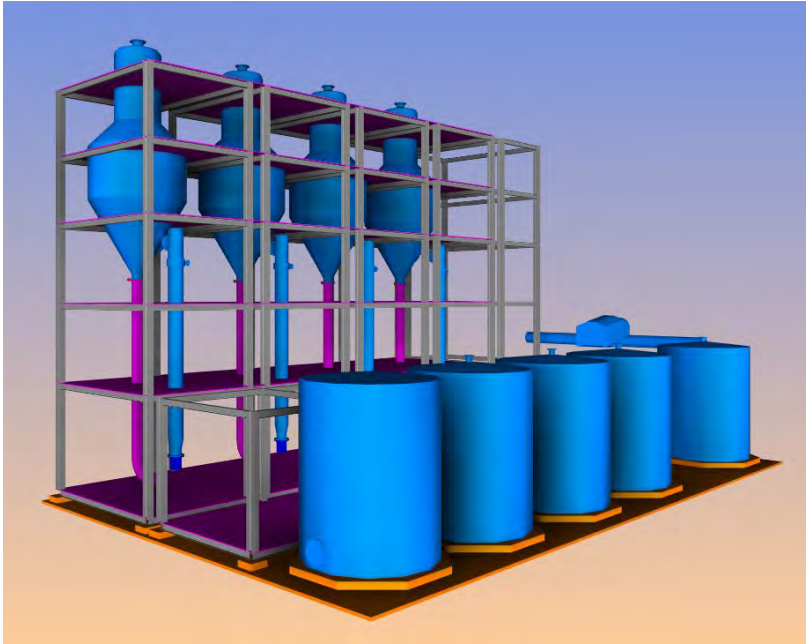
- Bicarbonation reactors used for re-dissolution of the crude lithium carbonate into lithium bicarbonate in a series of reactors
- Intense mixing to disperse CO_2 and encourage mass transfer and dissolution of carbonate

Confidential

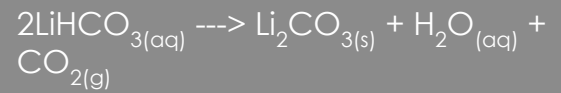


Impurity Removal

- Divalent IX system to remove Ca and Mg impurities before recrystallising Li_2CO_3
- Regeneration with HCl and NaOH
- Merry-go-round configuration (lead-lag)



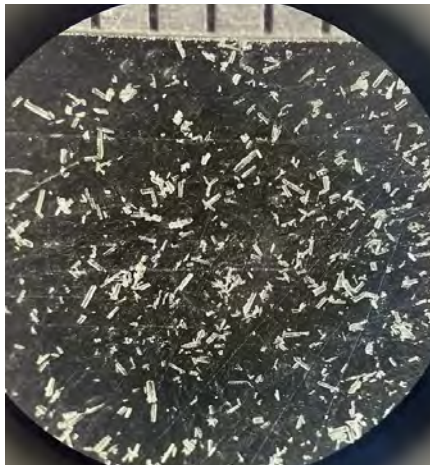
Lithium Carbonate Recrystallisation (Decarbonation)



- FC crystalliser design with vertical heater for heat input (Steam)
- Homogenous mixing with slow speed axial flow pump
- Dispersion of bicarbonate feed with high dilution in slurry to reduce the effect of supersaturation on crystal growth.

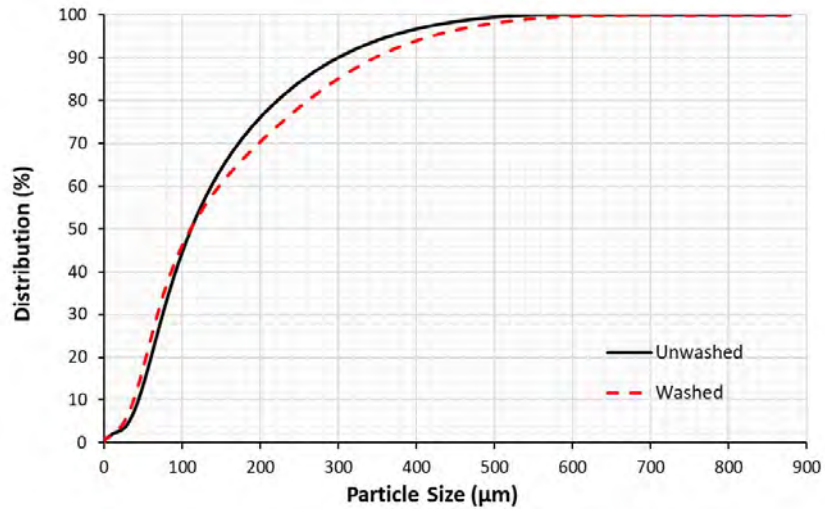
Confidential

Crystals of Lithium Carbonate produced by JordProxa



Scale divisions =
1mm

Crystal size distribution for Lithium Carbonate

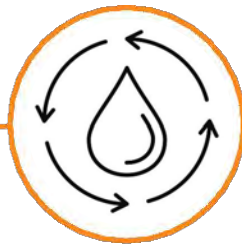


Confidential

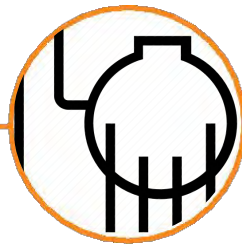
Flowsheet Optimisation



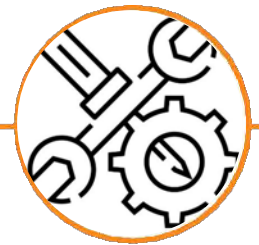
Heat Recovery & Integration



Water Recovery & Management



Utilities & Reagent



Maintenance & Cleaning

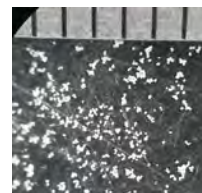
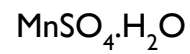
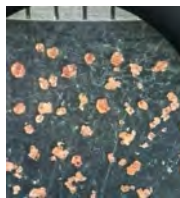
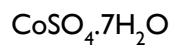
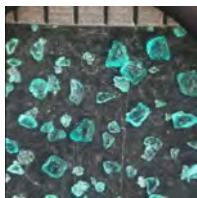
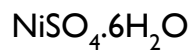
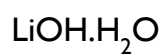
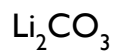
Conclusions

4

CONCLUSIONS

- Crystallisation is a key step in the processing of battery materials such as lithium carbonate to achieve the desired product purity.
- A carefully designed crystalliser can produce crystals large enough for effective dewatering and washing.
- Battery grade lithium carbonate can be produced by either repulping and centrifuging crude Li_2CO_3 , or through bicarbonation and decarbonation steps, depending upon the brine chemistry.
- Impurity removal steps are critical to produce the battery grade product.

Expertise in Battery Chemicals



Nipen Shah

+61 472 847 484 | nshah@jordproxa.com | jordproxa.com

MEMBRANE-ASSISTED DIRECT LITHIUM EXTRACTION

by

^{1,2,3} Amir Razmjou, ^{1,3} Yasaman Boroumand

¹Mineral Recovery Research Center (MRRC), Edith Cowan University, Australia.

²UNESCO Centre for Membrane Science and Technology, University of New South Wales. Australia

³School of Engineering, Edith Cowan University, Australia

Presenter and Corresponding Author

Amir Razmjou
amir.razmjou@ecu.edu.au

ABSTRACT

Direct lithium extraction (DLE) has led to the development of numerous technologies with the potential to recover up to 90% of lithium from various brines through laboratory studies. Nevertheless, establishing a sustainable DLE process that supports a lithium-dependent low-carbon economy still faces challenges. In recent times, there has been a continuous quest for DLE technologies that require fewer pre-treatments, use fewer materials, and employ simplified extraction procedures while ensuring high selectivity for lithium.

This abstract introduces DLE technologies, exploring the different methods used to extract lithium directly from various sources. It discusses the principles, benefits, and challenges associated with these technologies. Moreover, it emphasizes the environmental advantages, sustainability considerations, and potential reduction in carbon footprint achievable through DLE processes, highlighting their capacity to minimize environmental impacts compared to conventional extraction methods.

The economic aspects of DLE, including cost-effectiveness, scalability, and market potential are also explained. Moreover, membrane technology is explored as a disruptive method that could significantly enhance the large-scale implementation of DLE. Dr. Razmjou's team has used several types of building blocks, such as nano-clay, metal/covalent organic frameworks, graphene/oxide, and MXene, to make significant progress in this field by experimentally fabricating membranes. This overview summarizes their findings and outlines the strategies for designing materials to develop lithium-selective membranes incorporating nanochannels and nanopores.

Keywords: Lithium Recovery, Direct Lithium Extraction (DLE), Membrane Technology, Lithium Selective Membranes

MEMBRANE-ASSISTED DIRECT LITHIUM EXTRACTION

By

Amir Razmjou

Mineral Recovery Research Centre (MRRC)

Edith Cowan University, Australia



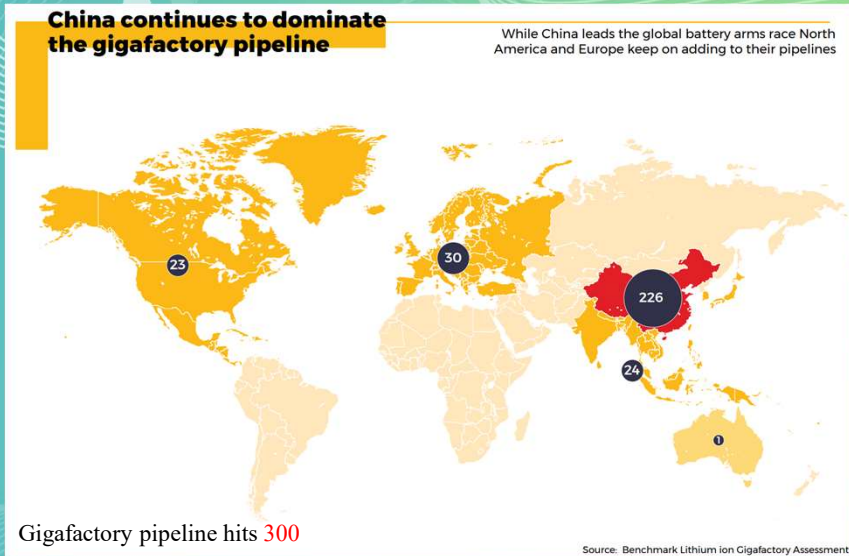
Introduction

Lithium Demand



Source: Benchmark Mineral Intelligence

Lithium Demand



Source: Benchmark Mineral Intelligence

Lithium Demand

HOW MANY MINES DO WE NEED?

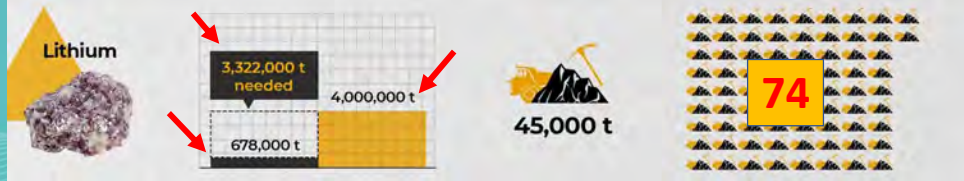
As the lithium ion battery revolution gains momentum, **Benchmark** forecasts just how many mines need to be built to keep up with the exceptional volumes of demand for key raw materials expected by 2035.



2022 Supply vs 2035 Demand

Average Mine/Plant Size

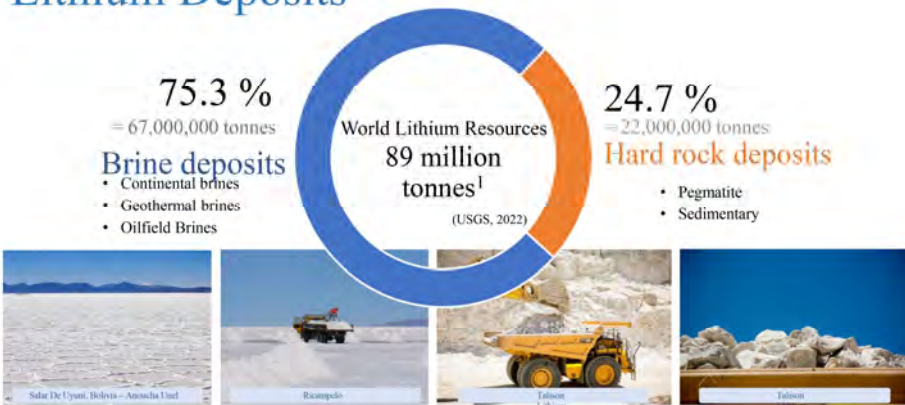
No. of Mines/Plants Needed



Source: Benchmark Mineral Intelligence

Lithium Resources

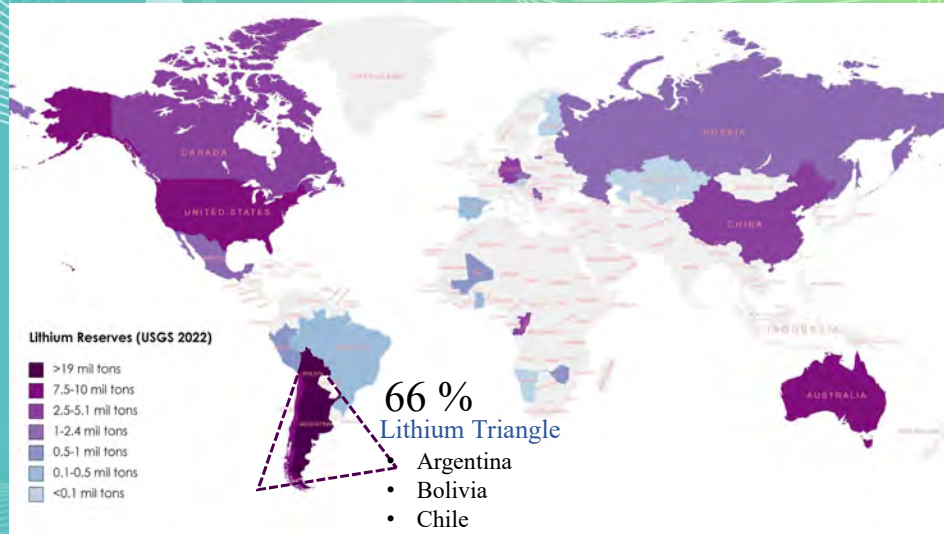
Lithium Deposits



¹ U.S. Geological Survey, Mineral Commodity Summaries, January 2022

Source: U.S. Geological Survey, Mineral Commodity Summaries, January 2022

Lithium Resources



Source: U.S. Geological Survey, Mineral Commodity Summaries, January 2022

Lithium Extraction Methods

GLOBAL LITHIUM SUPPLY TODAY

60%
global
lithium
production



Hard rock mining

Sourcing lithium hydroxide from hard rock mines for lithium currently has a high CO₂ footprint. Once you mine it, the rock must be roasted with fossil fuels and using large volume of sulphuric acid to produce lithium hydroxide.

30%
global
lithium
production



Brines: Reagent and evaporation pond usage

Use reagents to remove impurities from the brine

Lithium extraction from brines evaporates large quantities of water in some of the driest places on earth. It also has a significant CO₂ footprint, through large use of chemical reagents.

10%
global
lithium
production



Brines: Adsorption-type Direct Lithium Extraction (A-DLE)

Extract only the lithium from the brine, leave everything else in it

Low or net zero CO₂ footprint, depending on how the brine is heated. Very low reagent usage in A-DLE process. Low water usage if recycling systems are built into process.

Source: Vulcan energy, BRIDGING ENGINEERING STUDY RESULTS, PHASE ONE FINANCING LAUNCH EDITION, 04 2023.

Direct Lithium Extraction (DLE)

Introduction

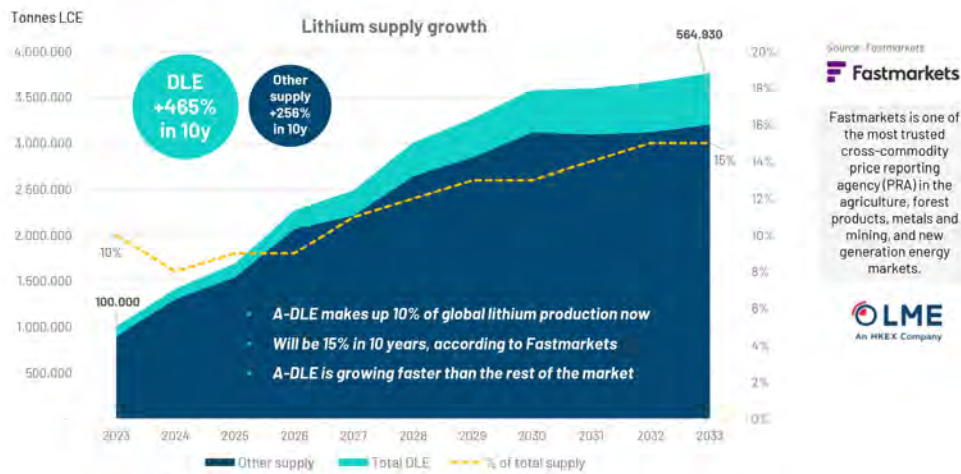
Direct Lithium Extraction

Membrane

Pilot facility (ECU DLE line)

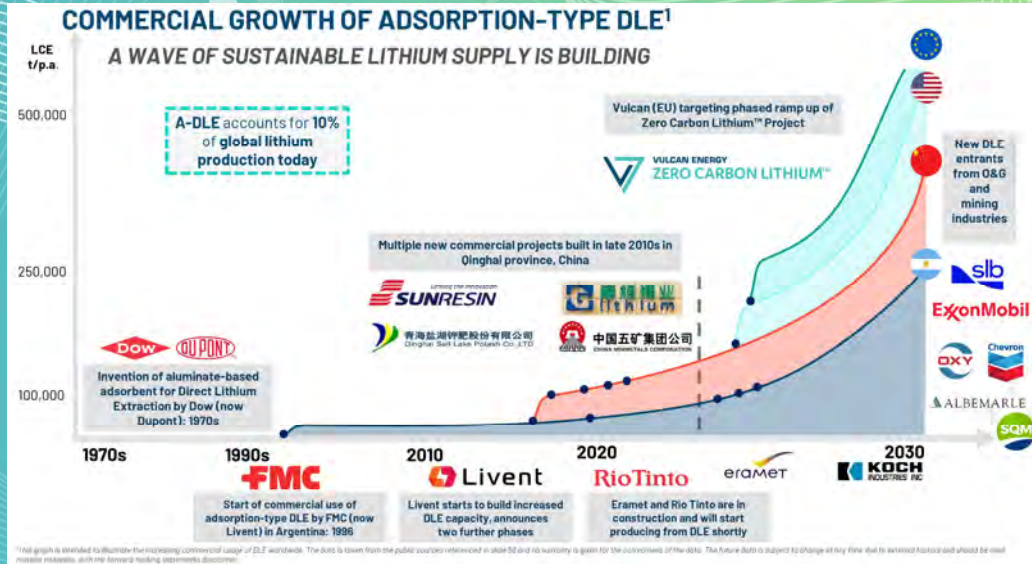
Introduction to DLE

COMMERCIAL GROWTH OF DLE



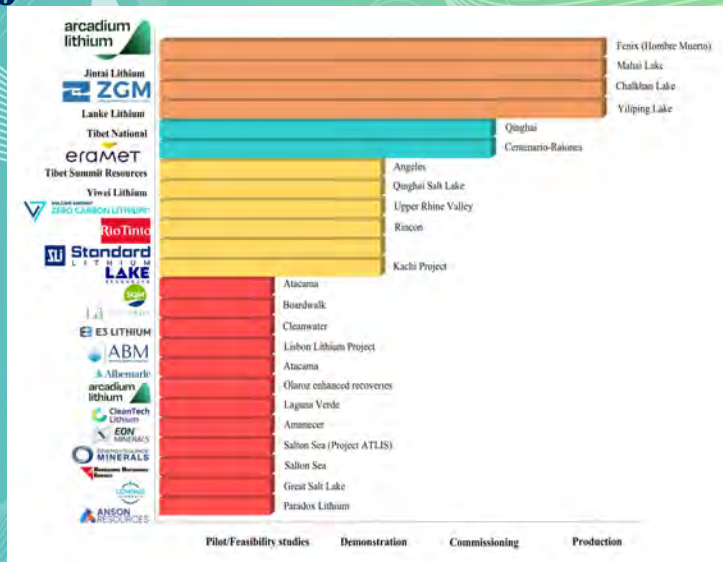
Source: Vulcan energy, BRIDGING ENGINEERING STUDY RESULTS, PHASE ONE FINANCING LAUNCH EDITION, 04 2023.

Commercial Growth



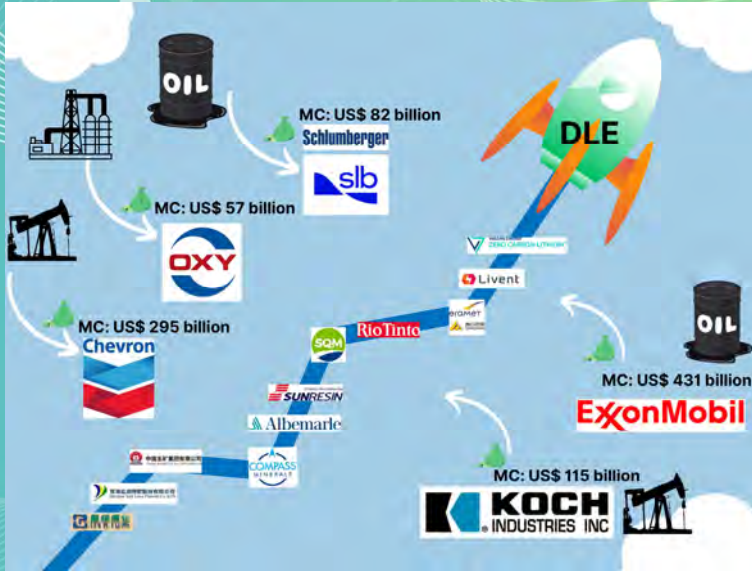
Source: Vulcan energy, BRIDGING ENGINEERING STUDY RESULTS, PHASE ONE FINANCING LAUNCH EDITION, 04 2023.

DLE Projects Status



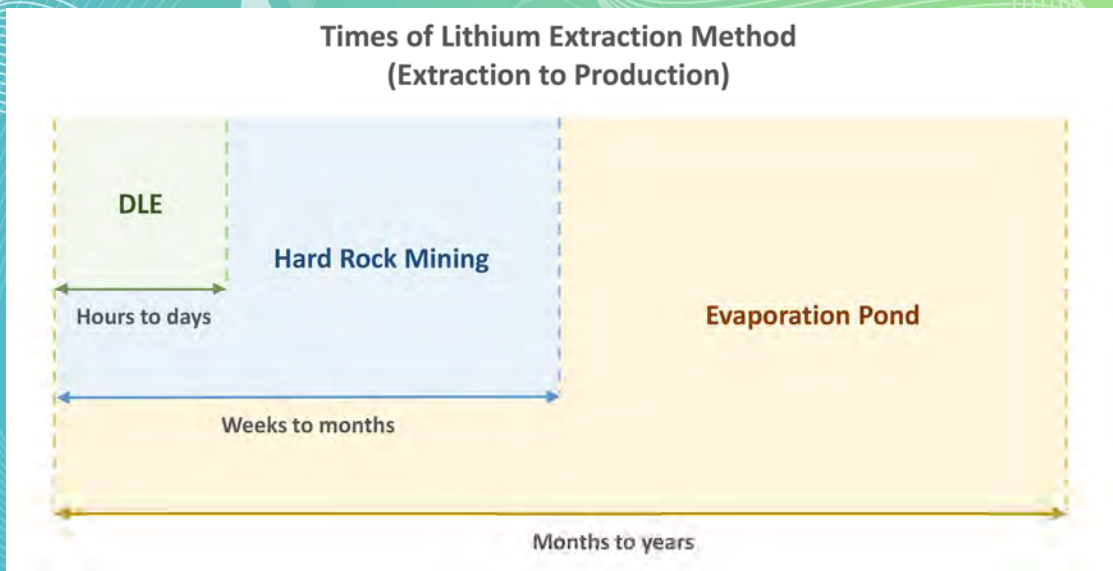
Source: DLE 101 – A New Report from ILiA & Rockwell Automation - International Lithium Association, n.d.)

DLE Upcoming Companies

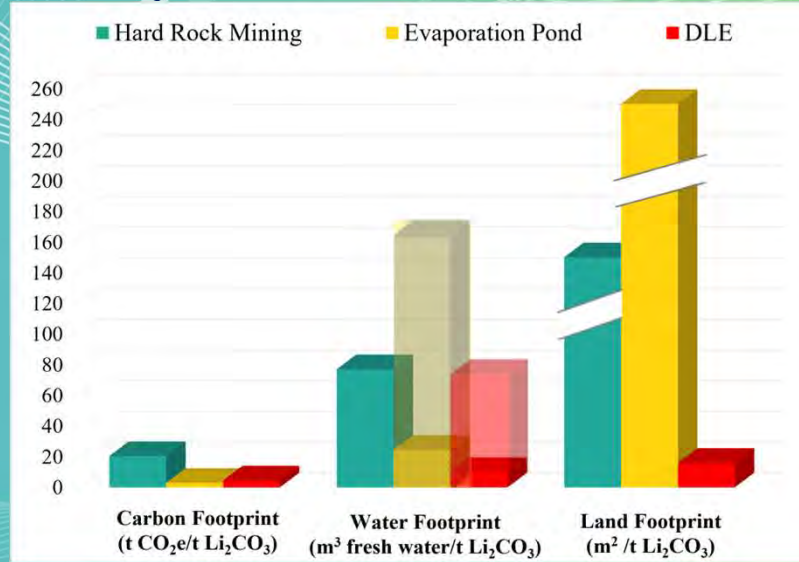


Data from: Vulcan energy. BRIDGING ENGINEERING STUDY RESULTS. PHASE ONE FINANCING LAUNCH EDITION. 04 2023.

Lithium Extraction Methods



Sustainability of DLE Methods



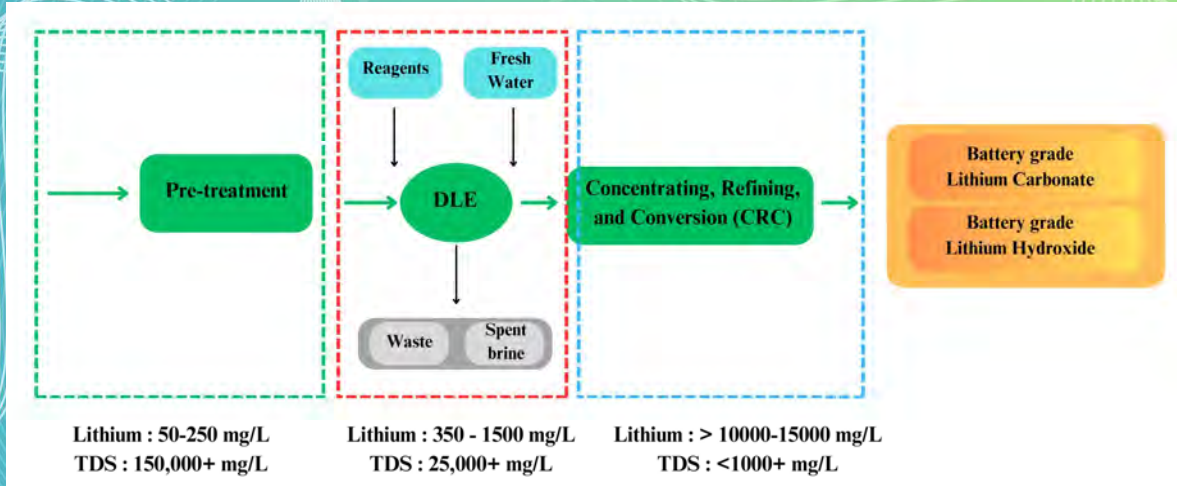
Source: DLE 101 – A New Report from ILiA & Rockwell Automation - International Lithium Association, n.d.)

DLE Methods

	Adsorption	Ion exchange	Solvent extraction	Membrane
Advantages	<ul style="list-style-type: none"> High selectivity Adaptability Global commercialization Easy operation Not require chemical reagents Can achieve >90% efficiency Low waste Low energy usage Low environmental impact 	<ul style="list-style-type: none"> High selectivity Lower initial investment High separation efficiency High theoretical lithium-uptake capacity Relatively low energy and water usage More adaptable for low-grade quality brines 	<ul style="list-style-type: none"> High efficiency High selectivity Adaptability Simple and continuous operation Low operating cost Less dependent on post-treatment to achieve high LICI concentration 	<ul style="list-style-type: none"> Simple and continuous operation High recovery rate High efficiency Low levels of impurities Relatively low energy usage No contact between the extractant and brine Environmental friendliness No need for additional purification for industrial purposes
Disadvantages	<ul style="list-style-type: none"> Dissolution loss Complex regeneration of adsorbents Temperature dependent process (> 50 °C) Need for post-treatment and purification steps Brine contamination issue High upfront capital costs 	<ul style="list-style-type: none"> Large acid and base inputs Environmental hazards production Post-treatment and purification steps may be necessary Acid supply safety risk Adsorbent degradation risk at low pH in the long term High operating cost 	<ul style="list-style-type: none"> Complicated preparation Corrosive additives and solvents Environmental concerns Organic contamination of product High waste production Potentially larger capital cost Intensive pretreatment is required for brines with a high $\text{Ca}^{2+}/\text{Li}^+$ and $\text{Mg}^{2+}/\text{Li}^+$ mass ratio 	<ul style="list-style-type: none"> Fouling issues Require pre-treatment Instability for geothermal brines High costs High initial investment and operating costs for fabricating and regenerating different membranes

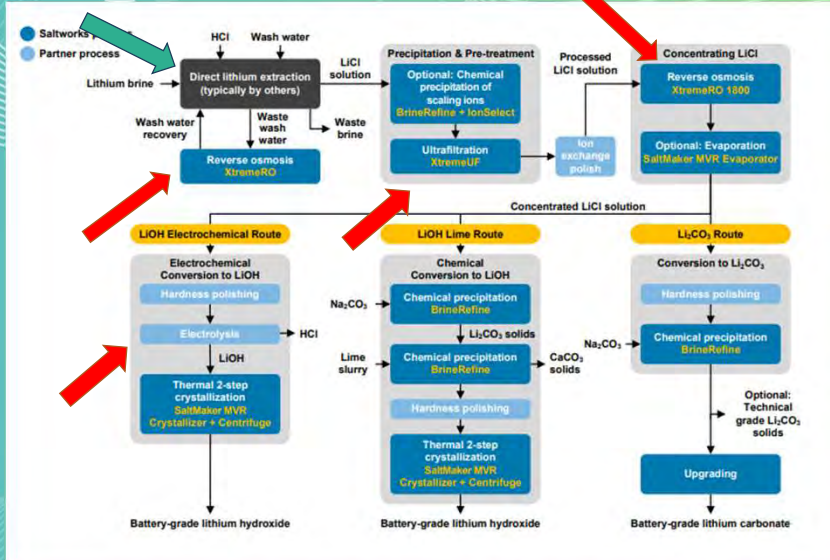
Source: DLE 101 – A New Report from ILiA & Rockwell Automation - International Lithium Association, n.d.)

DLE Processing



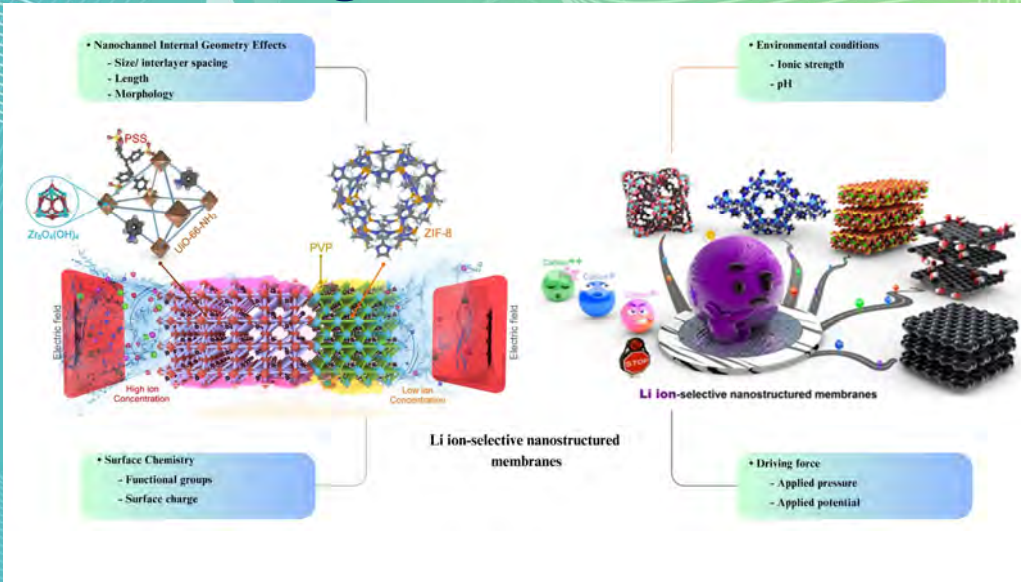
Membranes

DLE Processing

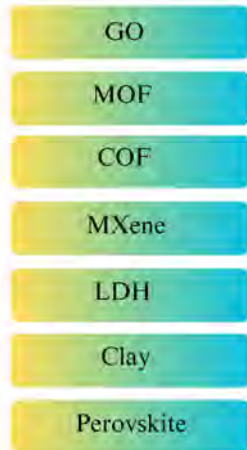


Source: Saltworks Technologies, Inc.

Membranes Design

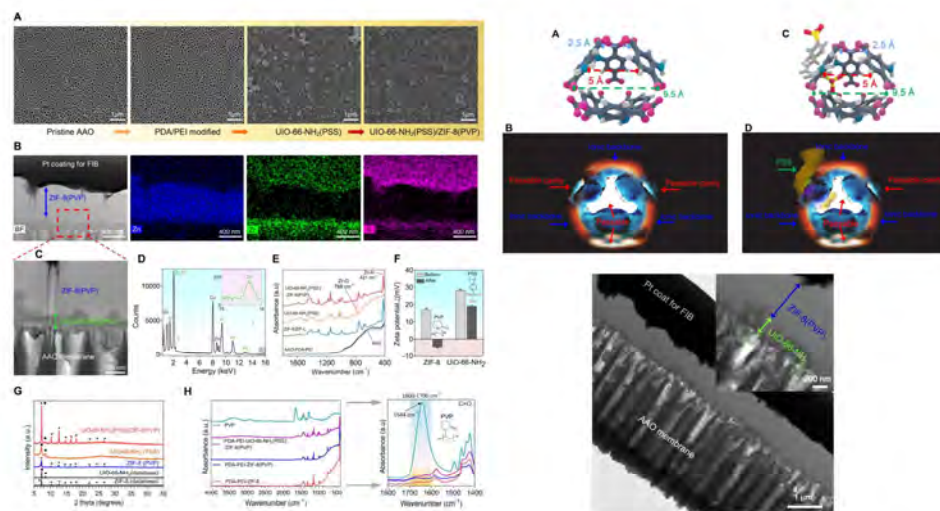


Li-selective Membranes

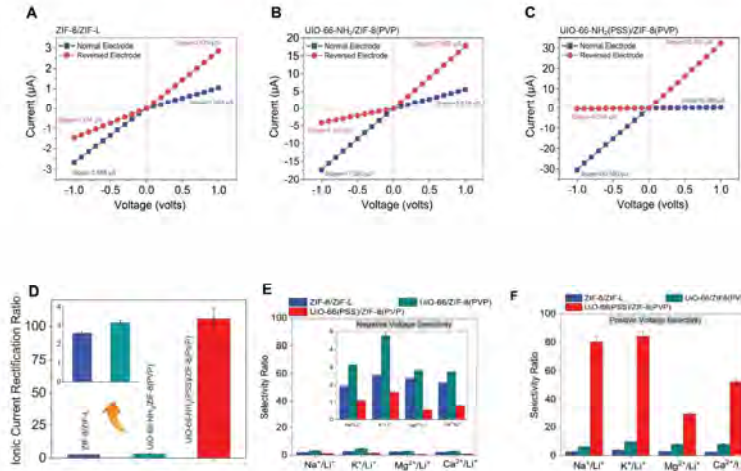


- Desalination 575, 117249 (2024).
- Desalination 577, 117406 (2024).
- Chemosphere 142401 (2024)
- Adv Compos Hybrid Mater 7, 1–14 (2024).
- A. Polymeric materials for membrane formation, 321–343 (2024)
- Ind Eng Chem Res 62, 18612–18620 (2023).
- Separation and Purification Technology 307, 2023, 122628
- Desalination Volume 538, 15 Septembre 2022, 115888
- Desalination, 2022, 532, 115733.
- Desalination, 2022, 532, 115733.
- Desalination 538, 2022, 115935
- Journal of Membrane Science, 639, 2021, 119752
- Journal of Membrane Science, Volume 639, 1 December 2021, 119752
- Applied Materials Today 21 (2020) 100884
- Journal of Membrane Science Volume 598, 15 March 2020, 117687
- Desalination 496, 2020, 114729
- Journal of Membrane Science, 588,2019, 117210
- Advanced Materials 34 (9), 2107878
- Journal of Membrane Science 670, 121312
- Advanced Materials 34 (9), 2107878
- Journal of Membrane Science 624, 118974
- Water Research 159, 313-323
- Membranes 12 (11), 1042

Li-selective Membranes

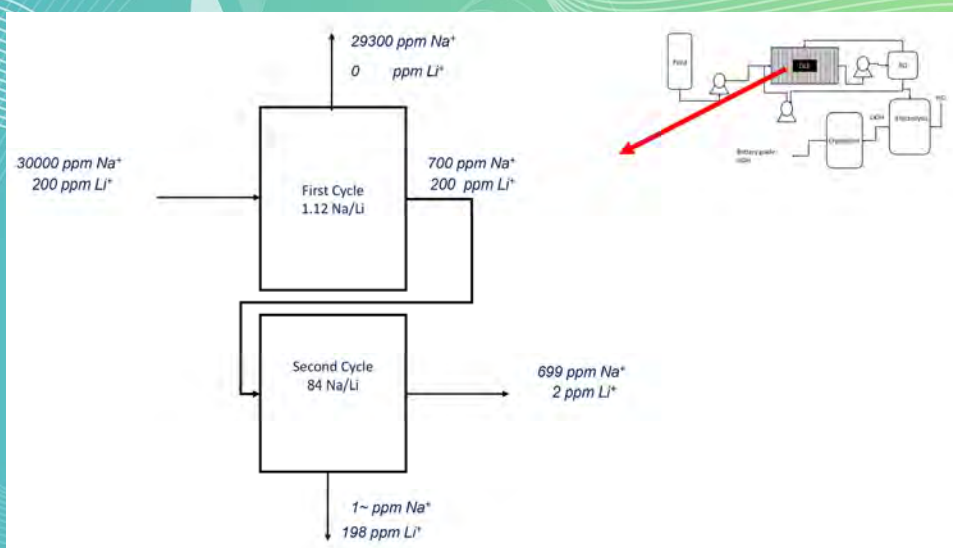


Li-selective Membranes



Source: Abdollahzadeh, M. et al. Designing Angstrom-Scale Asymmetric MOF-on-MOF Cavities for High Monovalent Ion Selectivity. *Advanced Materials* 34, 2107878 (2022).

Li-selective Membranes



KINETICS OF SPODUMENE RECRYSTALLISATION

Bogdan Z. Dlugogorski, ^bArif A. Abdullah, ^cHans Oskierski, and ^dGamini Senanayake

Energy and Resources Institute, Charles Darwin University, Casuarina Campus, Australia

^bDepartment of Chemical Engineering, Oil Projects Company (SCOP), Ministry of Oil, Iraq

^cSustainable Geochemistry and Mineral Science, Harry Butler Institute, Murdoch University, Australia

^dCollege of Science, Technology, Engineering and Mathematics (STEM), Murdoch University, Australia

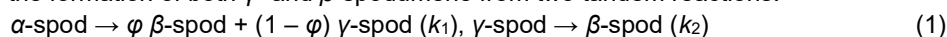
Presenter and Corresponding Author

Bogdan Dlugogorski

bogdan.dlugogorski@cdu.edu.au

ABSTRACT

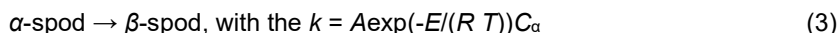
In this presentation, we will review the kinetic models that cast the decrepitation of α -spodumene to β -spodumene [1-4] in terms of simple, and easy to apply, mathematical equations. We will also provide the predictions from the models, as shown in Fig. 1, for typical operating conditions of the kilns in lithium refineries. Such predictions could serve to optimise the kilns, and therefore to assist in the decarbonisation of spodumene processing. Two of the models [2,3] derive from the X-ray diffraction (XRD) measurements, allowing predictions of the formation of both γ - and β -spodumene from two tandem reactions:



where, φ is the selectivity parameter that typically falls between 0.3 and 0.5. The kinetic rates (k_1 and k_2) correspond to the products of the Arrhenius formula and the first order reaction model:

$$k_1 = A_1 \exp(-E_1/(R T)) C_\alpha \quad \text{and} \quad k_2 = A_2 \exp(-E_2/(R T)) C_\gamma \quad (2)$$

where, E and A have their traditional meaning of the activation energy and the frequency factor, respectively, and C_α , C_γ and R reflect the mass fraction of α -spodumene and γ -spodumene and the ideal gas constant, in that order. Typical values of the Arrhenius constants are 780 kJ mol^{-1} and 75 for $E_{1,2}$ and $\ln(A_{1,2}/\text{min}^{-1})$, respectively [2]. The more recent work of Fosú et al. quotes E_1 and E_2 as 655 kJ mol^{-1} and 730 kJ mol^{-1} , correspondingly, as well as $\ln(A_1/\text{min}^{-1}) = 59.3$ and $\ln(A_2/\text{min}^{-1}) = 63.7$. In contrast, the models based on the heat measurements in the DTA (differential thermal analyser) [1] and DSC (differential scanning calorimeter) [4] consider the spodumene recrystallisation process to proceed in an idealised one-step unimolecular reaction, which, for the model of Botto et al. [1], comprises $E = 275 \text{ kJ mol}^{-1}$ and $\ln(A/\text{min}^{-1}) = 25.3$:



The model of Abdullah et al. makes fA and E to be functions of conversion, where f is the reaction model [4].

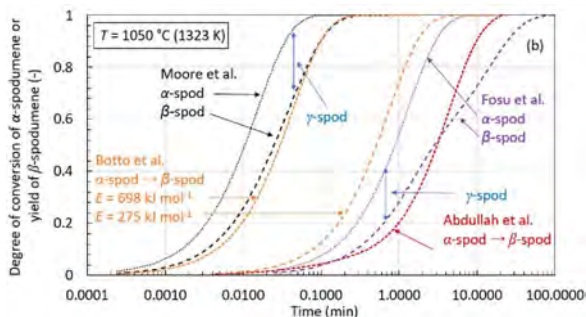


Fig. 1. Calcination of α -spodumene at $1050 \text{ }^\circ\text{C}$.

As evident in Fig. 1, the models of Fosú et al. [3] and Abdullah et al. [4] yield pragmatic predictions of the decrepitation time required for the complete recrystallisation of α -spodumene to β -spodumene. They also comprise physically meaningful values of the rate parameters. Evidently, it takes substantially longer to convert γ - to β -spodumene than just to convert α -spodumene to its products [2,3]. The model of Moore et al. [2], developed for particle sizes of around $5 \text{ }\mu\text{m}$, leads to predictions of unrealistically short heating time for industrially-relevant spodumene particles.

Keywords: Lithium refining; Reconstructive transformation; Phase change; Lithium chemicals

- [1] I. Botto, S. Cohen Arazi, T.G. Krenkel, Bol. Soc. Esp. Cerám. Vidr. 14 (1975) 433-40 (in Spanish).
- [2] R.L. Moore, J.P. Mann, A. Montoya, B.S. Haynes, Phys. Chem. Chem. Phys. 20 (2018) 10753-10761.
- [3] A.Y. Fosú, N. Kanari, D. Bartier, H. Hodge, J. Vaughan, A. Chagnes, Materials 14 (2021) 7423.
- [4] A.A. Abdullah, B. Z Dlugogorski, H.C. Oskierski, G. Senanayake, In preparation

Kinetics of spodumene recrystallisation

Bogdan Z Dlugogorski¹, Arif A Abdullah², Hans C Oskierski³ and Gamini Senanayake⁴

¹ Charles Darwin University, Energy and Resources Institute, Casuarina Campus, Purple 12.01.08, Darwin, NT 0909

Contact: Bogdan.Dlugogorski@cdu.edu.au, +61 408 965 978

² Department of Chemical Engineering, Oil Projects Company (SCOP), Ministry of Oil, Baghdad 10001, Iraq

³ Sustainable Geochemistry and Mineral Science, Harry Butler Institute, Murdoch University, Murdoch, WA 6150, Australia

⁴ College of Science, Technology, Engineering and Mathematics (STEM), Murdoch University, Murdoch, WA 6150, Australia

This presentation reviews kinetic models that cast the decrepitation of α -spodumene to β -spodumene in terms of simple, and easy to apply, mathematical equations. This presentation also reveals the predictions from the models and their limitations, for typical operating conditions of the kilns in lithium refineries.

ALTA 2024, Perth, Australia (30 May 2024)

Presentation outline

1. Introduction

- Energy requirements and decarbonisation
- Spodumene polymorphs
- Mechanism of calcination (Abdullah et al., 2019)
- XRD models
- DTA/DSC-based models

2a. Kinetic models

- Model of Fosu, Kanari, Bartier, Hodge, Vaughan and Chagnes (Fosu et al., 2021)
- Model of Moore, Mann, Montoya and Haynes (Moore et al., 2018)
- Model of Botto, Cohen Arazi and Frenkel (Botto et al., 1975)

2b. Crucial information

- Experimental measurements
- Mechanism and kinetic parameters
- Predictions and fit to own data
- Comparison with experiments (Peltosaari et al., 2015)

3. Summary remarks

- Lack of particle size dependence; amorphous vs crystalline pathways
- Diffusion limitation
- Importance of recrystallisation of β -spodumene
- Effect of additives

Abdullah, A.A., Oskierski, H.C., Altarawneh, M., Senanayake, G., Lumpkin, G., Dlugogorski, B.Z., Phase transformation mechanism of spodumene during its calcination. *Minerals Engineering*, 2019, **140**, 105883.

Botto, I.L., Cohen Arazi, S., Krenkel, T.G., Kinetic study of polymorphic transformation of spodumene I into spodumene II (in Spanish). *Boletín de la Sociedad Española de Cerámica y Vidrio*, 1975, **14**, 433-440.

Dessemond, C., Soucy, G., Harvey, J.-P., Ouzilleau, P., Phase transitions in the α - γ - β spodumene thermodynamic system and impact of γ -spodumene on the efficiency of lithium extraction by acid leaching. *Minerals*, 2020, **10**, 519.

Fosu, A.Y., Kanari, N., Bartier, D., Hodge, H., Vaughan, J., Chagnes, A., Physico-chemical characteristics of spodumene concentrate and its thermal transformations. *Materials*, 2021, **14**, 7423.

Moore, R.L., Mann, J.P., Montoya, A., Haynes, B.S., *In situ* synchrotron XRD analysis of the kinetics of spodumene phase transitions. *Physical Chemistry Chemical Physics*, 2018, **20**, 10753-10761.

Peltosaari, O., Tanskanen, P., Heikkinen, E.-P., Fabritius, T., $\alpha \rightarrow \gamma \rightarrow \beta$ -phase transformation of spodumene with hybrid microwave and conventional furnaces. *Minerals Engineering*, 2015, **82**, 54-60.

Salakjani, N.K., Singh, P., Nikoloski, A.N., Mineralogical transformations of spodumene concentrate from Greenbushes, Western Australia. Part 1: Conventional heating. *Minerals Engineering*, 2016, **98**, 71-79.

Dlugogorski, Abdullah, Oskierski and Senanayake, Kinetics of spodumene recrystallisation, ALTA 2024, Perth, Australia

1. Introduction

- Energy requirements and decarbonisation

Table 4
Material, energy, and water inputs per tonne concentrated spodumene produced.

Per tonne concentrated spodumene	Quantity	Units
Materials input		
Spodumene ore (0.8-0.9% conc.)	4.5	tonne
Other ^a	0.015	tonne
Fresh water	3	m ³
Energy input		
Diesel	4500	MJ

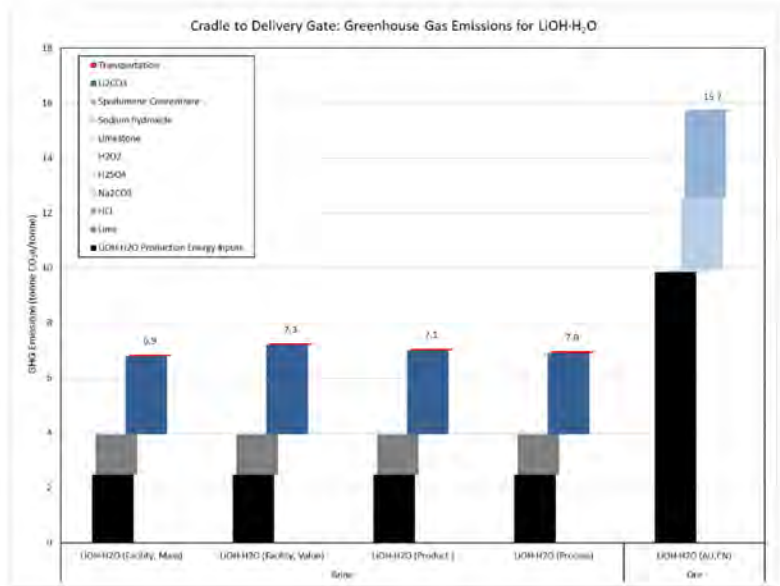
^a Includes sodium carbonate and a dispersant.

Table 5
Material and energy flow summary per tonne of LiOH•H₂O and Li₂CO₃ produced in China from Australian spodumene concentrate.

	Input Per tonne LiOH•H ₂ O	Input Per tonne Li ₂ CO ₃	Unit
Materials input			
Spodumene concentrate (6% Li ₂ O)	6.42	7.3	tonne
H ₂ SO ₄ (98% conc.)	1.52	1.71	tonne
Na ₂ CO ₃ (98.8% conc.)	0.025	2.05	tonne
NaOH (96% conc.)	1.18	0.05	tonne
CaCO ₃ (> 98% conc.)	0.6	0.7	tonne
Fresh water	11.24	40	m ³
Energy input			
Electricity (China grid)	12,600	6480	MJ
Coal (for LiOH•H ₂ O) ^b	71,243	-	MJ
Coal (for Li ₂ CO ₃) ^b	-	135,890	MJ
By-product output			
Na ₂ SO ₄	1.72	1.92	tonne

^a 54% for steam and 46% for kiln.

^b 39% for steam and 61% for kiln.



Kelly, J.C., Wang, M., Dai, Q., Winjobi, O., Energy, greenhouse gas, and water life cycle analysis of lithium carbonate and lithium hydroxide monohydrate from brine and ore resources and their use in lithium ion battery cathodes and lithium ion batteries. Resources, Conservation & Recycling, 2021, **174**, 105762.

Dlugogorski, Abdullah, Oskierski and Senanayake, Kinetics of spodumene recrystallisation, ALTA 2024, Perth, Australia

1. Introduction

- Spodumene polymorphs

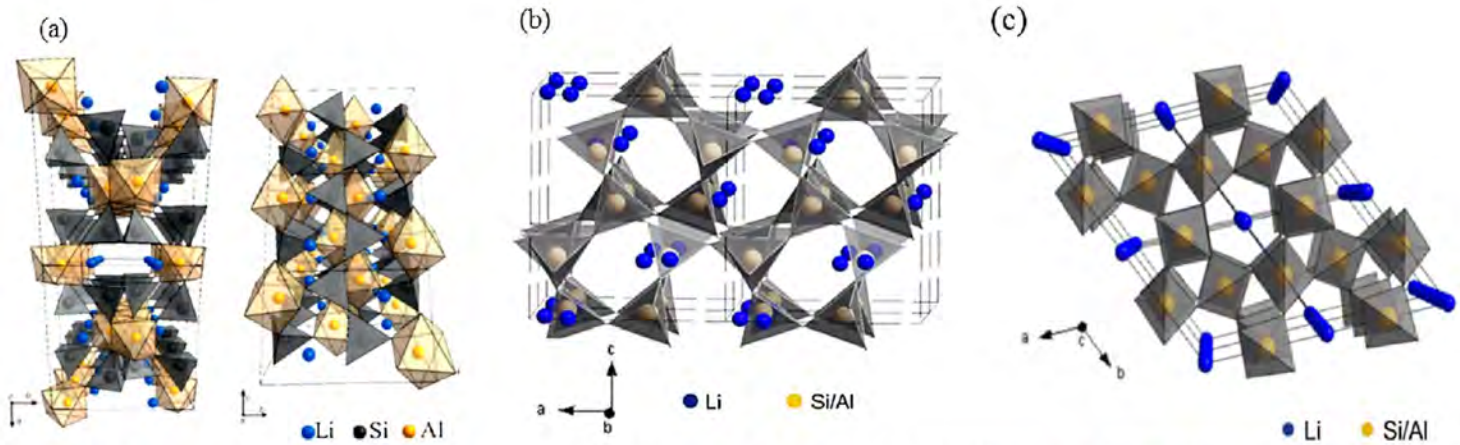


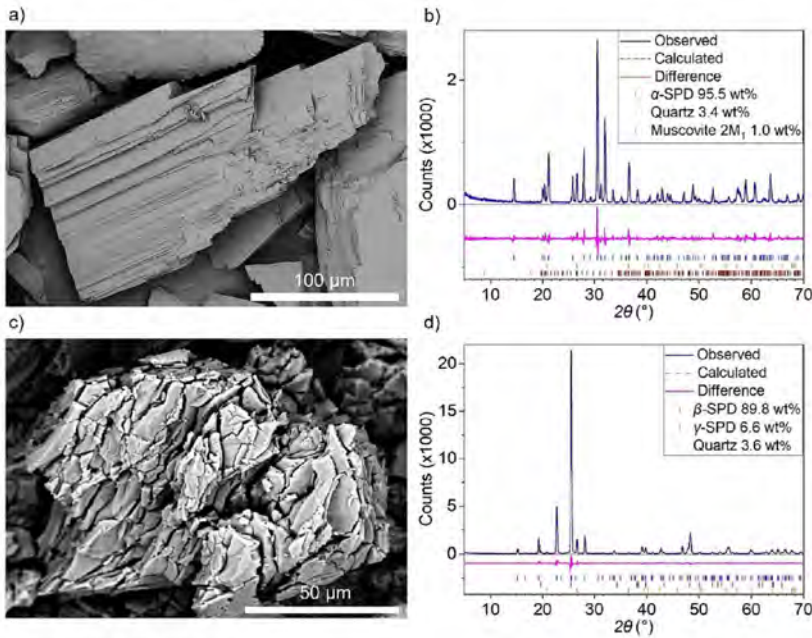
Fig. 1. Graphical representation of the structures of (a) α -spodumene of $V = 389.15 \text{ \AA}^3$ and $\rho = 3.160 \text{ g cm}^{-3}$ (Clark et al., 1969), (b) β -spodumene of $V = 520.67 \text{ \AA}^3$ and $\rho = 2.365 \text{ g cm}^{-3}$ (Li and Peacor, 1968), and (c) γ -spodumene of $V = 128.79 \text{ \AA}^3$ and $\rho = 2.395 \text{ g cm}^{-3}$ (Li, 1968). (after Welsch et al., 2015).

Abdullah, A.A., Oskierski, H.C., Altarawneh, M., Senanayake, G., Lumpkin, G., Dlugogorski, B.Z., Phase transformation mechanism of spodumene during its calcination. Minerals Engineering, 2019, **140**, 105883.
 Clarke, P.T., Spink, J.M., The crystal structure of β spodumene, LiAlSi₂O₆-II. Zeitschrift für Kristallographie, 1969, **130**, 420-426.
 Li, C.-T., The crystal structure of LiAlSi₂O₆ III (high-quartz solid solution). Zeitschrift für Kristallographie 1968, **127**, 327-348.
 Li, C.-T., Peacor, D.R., The crystal structure of LiAlSi₂O₆-II (" β spodumene"). Zeitschrift für Kristallographie, 1968, **126**, 46-65.
 Welsch, A.-M., Murawski, D., Prekajski, M., Vulic, P., Kremenovic, A., Ionic conductivity in single-crystal LiAlSi₂O₆: influence of structure on lithium mobility. Physics and Chemistry of Minerals, 2015, **42**, 413-420.

Dlugogorski, Abdullah, Oskierski and Senanayake, Kinetics of spodumene recrystallisation, ALTA 2024, Perth, Australia

1. Introduction

- Spodumene polymorphs (2)



Before calcination

Morphology and mineralogy of concentrates of α and β -spodumene: a) BSE-SEM image of dense α -spodumene with typical cleavage planes; b) XRD and Rietveld refinement of α -spodumene; c) BSE-SEM image of β -spodumene with cracks due to the thermal treatment at 1100 °C for 2 h; d) XRD and Rietveld refinement of β -spodumene

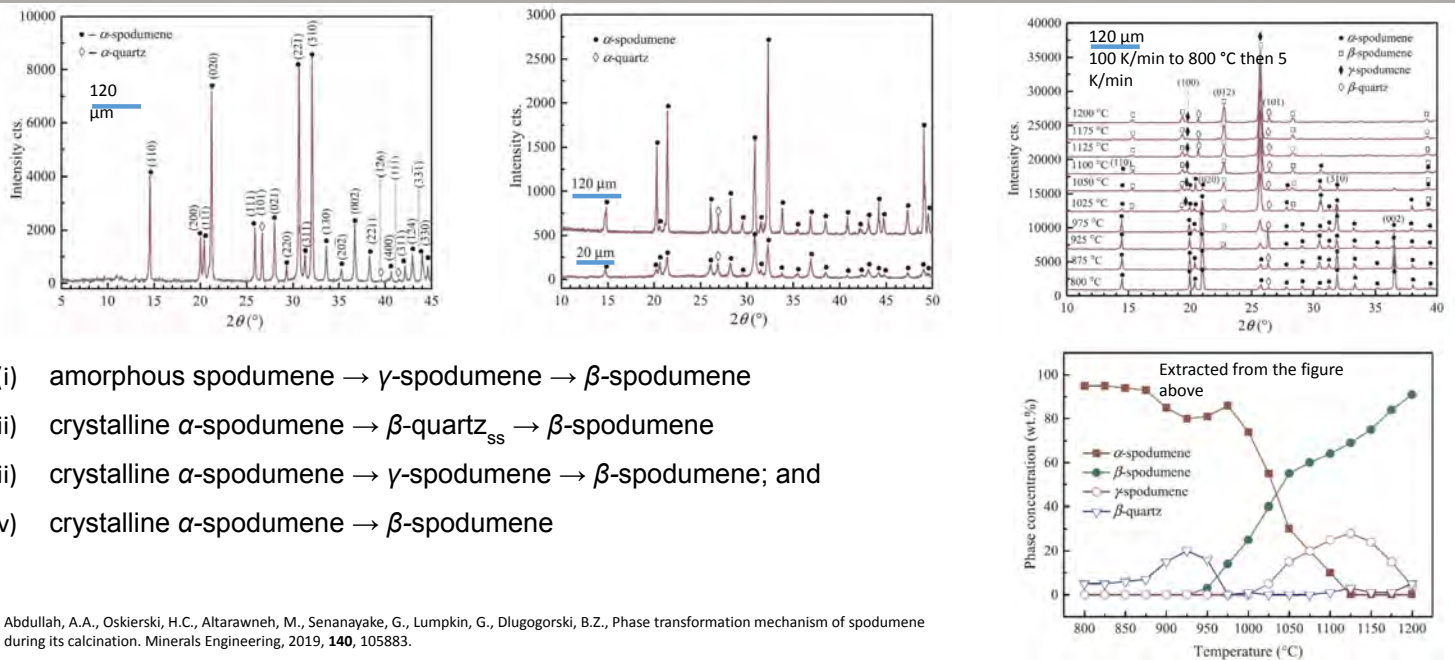
After calcination (1100 °C, 2 h)

Alhadad, M.F., Oskierski, H.C., Chishi, J., Senanayake, G., Dlugogorski, B.Z., Lithium extraction from β -spodumene: A comparison of keatite and analcime processes. Hydrometallurgy, 2023, 215, 105985. Salakjani, N.K., Singh, P., Nikoloski, A.N., Mineralogical transformations of spodumene concentrate from Greenbushes, Western Australia. Part 1: Conventional heating. Minerals Engineering, 2016, 98, 71-79.

Dlugogorski, Abdullah, Oskierski and Senanayake, Kinetics of spodumene recrystallisation, ALTA 2024, Perth, Australia

1. Introduction

- Mechanism of calcination (Abdullah et al., 2019)



- (i) amorphous spodumene \rightarrow γ -spodumene \rightarrow β -spodumene
- (ii) crystalline α -spodumene \rightarrow β -quartz_{ss} \rightarrow β -spodumene
- (iii) crystalline α -spodumene \rightarrow γ -spodumene \rightarrow β -spodumene; and
- (iv) crystalline α -spodumene \rightarrow β -spodumene

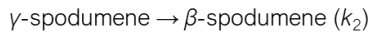
Abdullah, A.A., Oskierski, H.C., Altarawneh, M., Senanayake, G., Lumpkin, G., Dlugogorski, B.Z., Phase transformation mechanism of spodumene during its calcination. Minerals Engineering, 2019, 140, 105883.

Dlugogorski, Abdullah, Oskierski and Senanayake, Kinetics of spodumene recrystallisation, ALTA 2024, Perth, Australia

1. Introduction

- XRD-based models (Moore et al., 2018; Fosu et al., 2021)

- Based on quantitative (Rietveld) or semiquantitative analysis of X-ray diffraction spectra
- Include conversion of α -spodumene and formation of γ -spodumene and β -spodumene
- Assume homogeneous first order reaction models (no particle size dependence)
- Reaction mechanism (cf. Abdullah et al. for the initial $k_{III} \approx k_{IV}$)



- Equations

$$\frac{dx_\alpha}{dt} = -k_1 x_\alpha$$

$$k_1 = A_1 \exp\left(-\frac{E_1}{RT}\right)$$

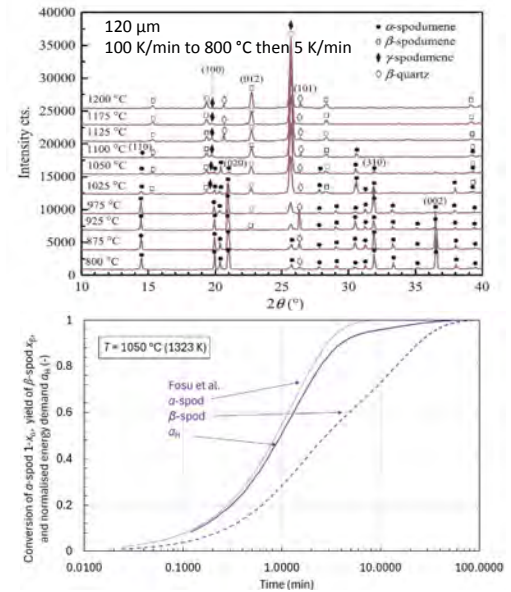
$$\frac{dx_\beta}{dt} = \varphi k_1 x_\alpha + k_2 x_\gamma$$

$$k_2 = A_2 \exp\left(-\frac{E_2}{RT}\right)$$

$$\frac{dx_\gamma}{dt} = (1 - \varphi) k_1 x_\alpha - k_2 x_\gamma$$

$$\frac{d\alpha_H}{dt} = \frac{\varphi k_1 x_\alpha \Delta H_{\alpha \rightarrow \beta} + (1 - \varphi) k_1 x_\alpha \Delta H_{\alpha \rightarrow \gamma} + k_2 x_\gamma \Delta H_{\gamma \rightarrow \beta}}{\Delta H_{\alpha \rightarrow \beta}}$$

Abdullah, A.A., Oskierski, H.C., Altarawneh, M., Senanayake, G., Lumpkin, G., Dlugogorski, B.Z., Minerals Engineering, 2019, 140, 105883.
 Fosu, A.Y., Kanari, N., Bartier, D., Hodge, H., Vaughan, J., Chagnes, A., Materials, 2021, 14, 7423.
 Moore, R.L., Mann, J.P., Montoya, A., Haynes, B.S., Physical Chemistry Chemical Physics, 2018, 20, 10753-10761.



Dlugogorski, Abdullah, Oskierski and Senanayake, Kinetics of spodumene recrystallisation, ALTA 2024, Perth, Australia

1. Introduction

- Heat demand models (Botto et al. 1975, Abdullah et al. 2024)

- Based on the endothermic heat demand measured by differential thermal analysis DTA (Botto et al., 1975) or differential scanning calorimetry DSC (Abdullah et al., 2024)
- Botto et al.



$$\frac{dx_H}{dt} = -k x_H \quad k = A \exp\left(-\frac{E}{RT}\right)$$

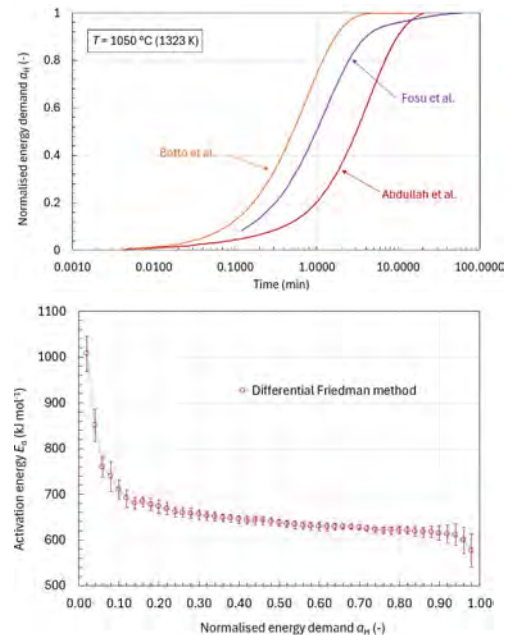
Simple and approximate; covered in this presentation

- Abdullah et al.

Isoconversional approach that produces $E(\alpha_H)$, $A(\alpha_H)$ and $f(\alpha_H)$, where $f(\alpha_H)$ is the reaction model

$$\frac{d\alpha_H}{dt} = A(\alpha_H) \exp\left(-\frac{E(\alpha_H)}{RT(t)}\right) f(\alpha_H)$$

Very accurate, can be applied to an arbitrary heating program, provides significant mechanistic insights; Not covered in this presentation



Abdullah et al., in review, 2024.
 Botto, I.L., Cohen Arazi, S., Krenkel, T.G., Kinetic study of polymorphic transformation of spodumene I into spodumene II (in Spanish). Boletín de la Sociedad Española de Cerámica y Vidrio, 1975, 14, 433-440.
 Fosu, A.Y., Kanari, N., Bartier, D., Hodge, H., Vaughan, J., Chagnes, A., Physico-chemical characteristics of spodumene concentrate and its thermal transformations. Materials, 2021, 14, 7423.

Dlugogorski, Abdullah, Oskierski and Senanayake, Kinetics of spodumene recrystallisation, ALTA 2024, Perth, Australia

Presentation outline

1. Introduction

- Energy requirements and decarbonisation
- Spodumene polymorphs
- Mechanism of calcination (Abdullah et al., 2019)
- XRD models
- DTA/DSC-based models

2a. Kinetic models

- Model of Fosu, Kanari, Bartier, Hodge, Vaughan and Chagnes (Fosu et al., 2021)
- Model of Moore, Mann, Montoya and Haynes (Moore et al., 2018)
- Model of Botto, Cohen Arazi and Frenkel (Botto et al., 1975)

2b. Crucial information

- Experimental measurements
- Mechanism and kinetic parameters
- Predictions and fit to own data
- Comparison with experiments (Peltosaari et al., 2015)

3. Summary remarks

- Lack of particle size dependence; amorphous vs crystalline pathways
- Diffusion limitation
- Importance of recrystallisation of β -spodumene
- Effect of additives

Abdullah, A.A., Oskierski, H.C., Altarawneh, M., Senanayake, G., Lumpkin, G., Dlugogorski, B.Z., Phase transformation mechanism of spodumene during its calcination. Minerals Engineering, 2019, **140**, 105883.
 Botto, I.L., Cohen Arazi, S., Krenkel, T.G., Kinetic study of polymorphic transformation of spodumene I into spodumene II (in Spanish). Boletín de la Sociedad Española de Cerámica y Vidrio, 1975, **14**, 433-440.
 Fosu, A.Y., Kanari, N., Bartier, D., Hodge, H., Vaughan, J., Chagnes, A., Physico-chemical characteristics of spodumene concentrate and its thermal transformations. Materials, 2021, **14**, 7423.
 Moore, R.L., Mann, J.P., Montoya, A., Haynes, B.S., *In situ* synchrotron XRD analysis of the kinetics of spodumene phase transitions. Physical Chemistry Chemical Physics, 2018, **20**, 10753-10761.
 Peltosaari, O., Tanskanen, P., Heikkinen, E.-P., Fabritius, T., $\alpha \rightarrow \gamma \rightarrow \beta$ -phase transformation of spodumene with hybrid microwave and conventional furnaces. Minerals Engineering, 2015, **82**, 54-60.

Dlugogorski, Abdullah, Oskierski and Senanayake, Kinetics of spodumene recrystallisation, ALTA 2024, Perth, Australia

2. Kinetic models and their crucial information

- Model of Fosu et al. [Experimental measurements]

- Spodumene provenance, particle size and purity

- Pilbara, Western Australia
- $d_{80} = 113 \mu\text{m}$
- 4.6 wt% Li_2O ; 57.4 wt% purity

- Experimental

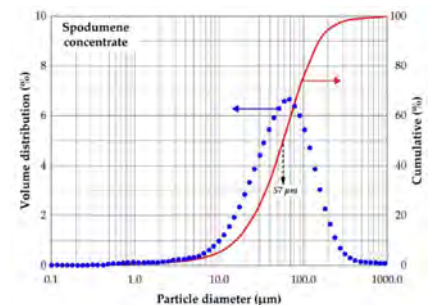
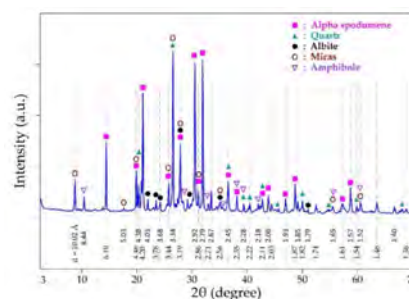
Ex-situ X-ray diffraction (XRD)

- Experimental methodology

- Roasted isothermally in carbolite furnace at 1173, 1198, 1223, 1248, 1273, 1298, 1323
- Residence time 7.5, 15, 60, 240 and 480 min
- Residence time includes heating to the target temperature
- Furnace preheated for 60 min

- Modal concentrations

- Semi-quantitative relative abundances of phases from EVA software coupled to PDF2 data base
- Peak relative heights, assuming that all crystalline phases add up to 100 %



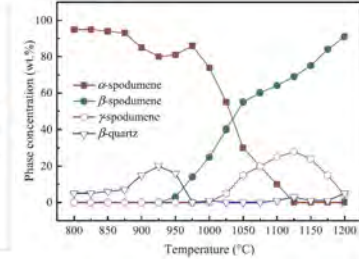
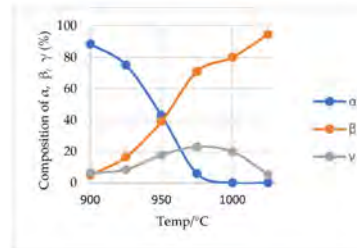
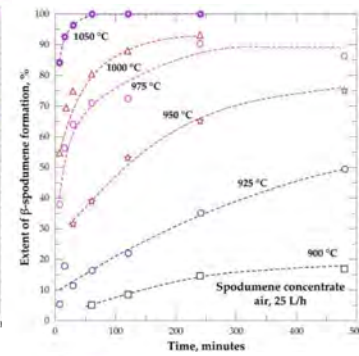
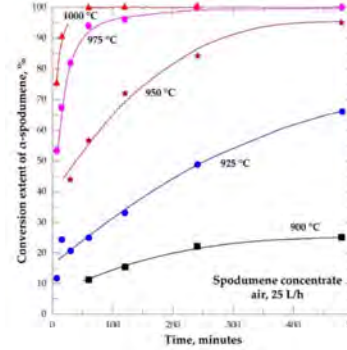
Fosu, A.Y., Kanari, N., Bartier, D., Hodge, H., Vaughan, J., Chagnes, A., Physico-chemical characteristics of spodumene concentrate and its thermal transformations. Materials, 2021, **14**, 7423

Dlugogorski, Abdullah, Oskierski and Senanayake, Kinetics of spodumene recrystallisation, ALTA 2024, Perth, Australia

2. Kinetic models and their crucial information

- Model of Fosu et al. [Mechanism and kinetic parameters]

- Reaction mechanism
 - α -spodumene $\rightarrow \varphi \beta$ -spodumene + $(1 - \varphi) \gamma$ -spodumene (k_1)
 - γ -spodumene $\rightarrow \beta$ -spodumene (k_2)
- Parameters
 - k_1 : $E_1 = 655 (\pm 20) \text{ kJ mol}^{-1}$; $\ln(A_1/\text{min}^{-1}) = 59.3 (\pm 2.0)$
 - k_2 : $E_2 = 730 (\pm 19) \text{ kJ mol}^{-1}$; $\ln(A_2/\text{min}^{-1}) = 63.7 (\pm 1.7)$
 - Selectivity: $\varphi = 0.5$
 - $\ln(A_{1,2}/\text{min}^{-1})$ and errors from Tables S23 & S24 of Fosu et al.
- Reaction model
 - First order in mass fraction of α -spodumene and γ -spodumene



Fosu et al.

Abdullah et al.

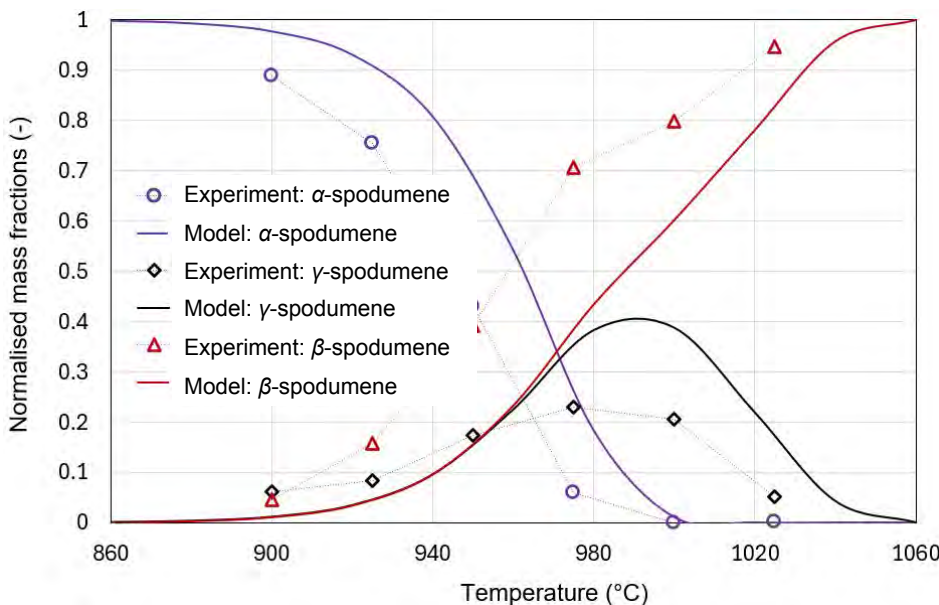
Abdullah, A.A., Oskierski, H.C., Altarawneh, M., Senanayake, G., Lumpkin, G., Dlugogorski, B.Z., Phase transformation mechanism of spodumene during its calcination. Minerals Engineering, 2019, 140, 105883.

Fosu, A.Y., Kanari, N., Bartier, D., Hodge, H., Vaughan, J., Chagnes, A., Physico-chemical characteristics of spodumene concentrate and its thermal transformations. Materials, 2021, 14, 7423

Dlugogorski, Abdullah, Oskierski and Senanayake, Kinetics of spodumene recrystallisation, ALTA 2024, Perth, Australia

2. Kinetic models and their crucial information

- Model of Fosu et al. [Predictions and fit to own data]



Predictions and fit to Fosu's et al. own measurements (Figure 11):

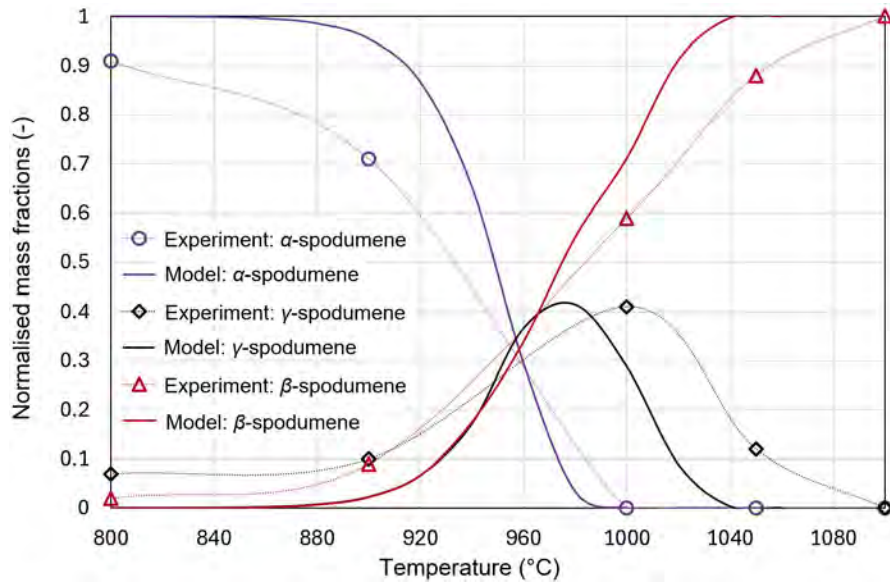
- polymorph distribution after 1 h of thermal treatment
- solid lines denote the modelling predictions and points are experimental measurement
- dotted line plotted as a guide to an eye

Fosu, A.Y., Kanari, N., Bartier, D., Hodge, H., Vaughan, J., Chagnes, A., Physico-chemical characteristics of spodumene concentrate and its thermal transformations. Materials, 2021, 14, 7423

Dlugogorski, Abdullah, Oskierski and Senanayake, Kinetics of spodumene recrystallisation, ALTA 2024, Perth, Australia

2. Kinetic models and their crucial information

- Model of Fosu et al. [Comparison with Peltosaari's et al. data]



Comparison of Fosu's et al. model with Peltosaari's et al. measurements:

- polymorph distribution after 2 h of thermal treatment
- solid lines denote the modelling predictions and points are experimental measurement
- dotted line plotted as a guide to an eye for the data of Peltosaari et al.

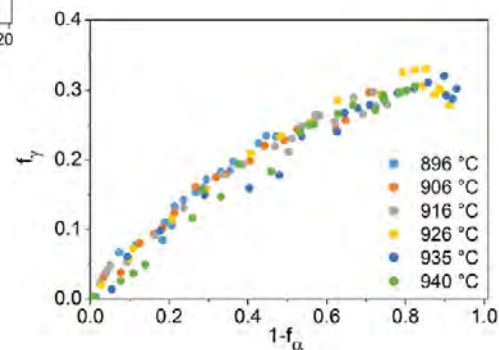
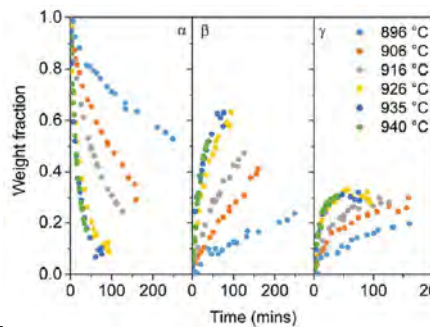
Fosu, A.Y., Kanari, N., Bartier, D., Hodge, H., Vaughan, J., Chagnes, A., Physico-chemical characteristics of spodumene concentrate and its thermal transformations. *Materials*, 2021, **14**, 7423
 Peltosaari, O., Tanskanen, P., Heikkinen, E.-P., Fabritius, T., $\alpha \rightarrow \gamma \rightarrow \beta$ -phase transformation of spodumene with hybrid microwave and conventional furnaces. *Minerals Engineering*, 2015, **82**, 54-60.

Dlugogorski, Abdullah, Oskierski and Senanayake, Kinetics of spodumene recrystallisation, ALTA 2024, Perth, Australia

2. Kinetic models and their crucial information

- Model of Moore et al. [Experimental measurements]

- Spodumene provenance, particle size and purity
 - Mt Cattlin mine, Western Australia
 - $d_{\text{Sauter}} = 4.67 \mu\text{m}$
 - 7.2 wt% Li_2O ; 90 wt% purity
- Experimental
 - In-situ synchrotron X-ray diffraction (XRD)
- Experimental methodology
 - Calcined isothermally in capillaries at 1163, 1179, 1189, 1199, 1208, 1213 K
 - Residence time up to 300 min
 - Air-gun heating, preheating time negligible
- Modal concentrations
 - Rietveld refining



Moore, R.L., Mann, J.P., Montoya, A., Haynes, B.S., *In situ* synchrotron XRD analysis of the kinetics of spodumene phase transitions. *Physical Chemistry Chemical Physics*, 2018, **20**, 10753-10761.

Dlugogorski, Abdullah, Oskierski and Senanayake, Kinetics of spodumene recrystallisation, ALTA 2024, Perth, Australia

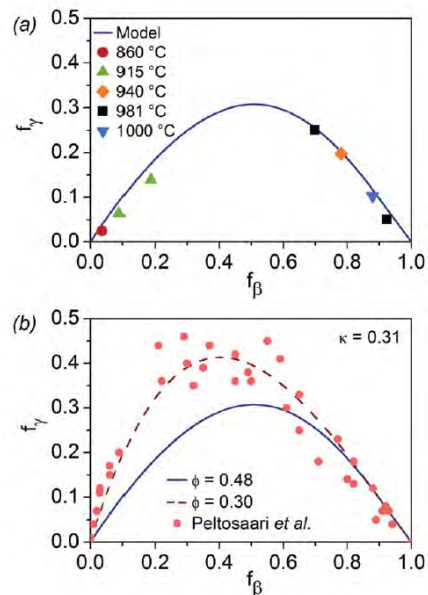
2. Kinetic models and their crucial information

- Model of Fosu et al. [Mechanism and kinetic parameters]

- Reaction mechanism
 - α -spodumene $\rightarrow \phi$ β -spodumene + $(1 - \phi)$ γ -spodumene (k_1)
 - γ -spodumene $\rightarrow \beta$ -spodumene (κk_1)
- Parameters
 - k_1 : $E_1 = 780 (\pm 170)$ kJ mol⁻¹; $\ln(A_1/\text{min}^{-1}) = 75 (\pm 7)$
 - Selectivity: $\phi = 0.48 \pm 0.01$ ($\phi = 0.30$ for Peltosaari et al.)
 - Parameter κ : $\kappa = 0.31 \pm 0.03$
- Reaction model
 - First order in mass fraction of α -spodumene and γ -spodumene

Moore, R.L., Mann, J.P., Montoya, A., Haynes, B.S., *In situ* synchrotron XRD analysis of the kinetics of spodumene phase transitions. *Physical Chemistry Chemical Physics*, 2018, **20**, 10753-10761.

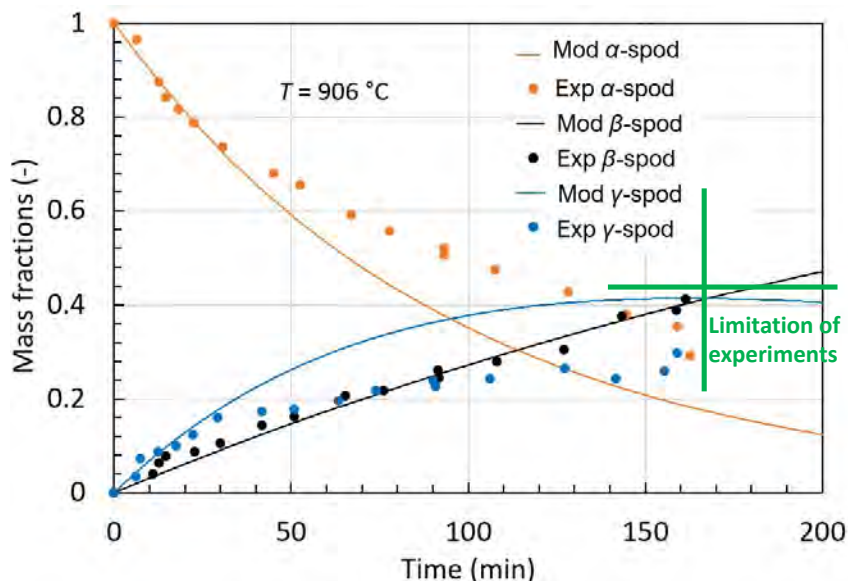
Peltosaari, O., Tanskanen, P., Heikkinen, E.-P., Fabritius, T., $\alpha \rightarrow \gamma \rightarrow \beta$ -phase transformation of spodumene with hybrid microwave and conventional furnaces. *Minerals Engineering*, 2015, **82**, 54-60.



Dlugogorski, Abdullah, Oskierski and Senanayake, Kinetics of spodumene recrystallisation, ALTA 2024, Perth, Australia

2. Kinetic models and their crucial information

- Model of Moore et al. [Predictions and fit to own data]



Moore, R.L., Mann, J.P., Montoya, A., Haynes, B.S., *In situ* synchrotron XRD analysis of the kinetics of spodumene phase transitions. *Physical Chemistry Chemical Physics*, 2018, **20**, 10753-10761.

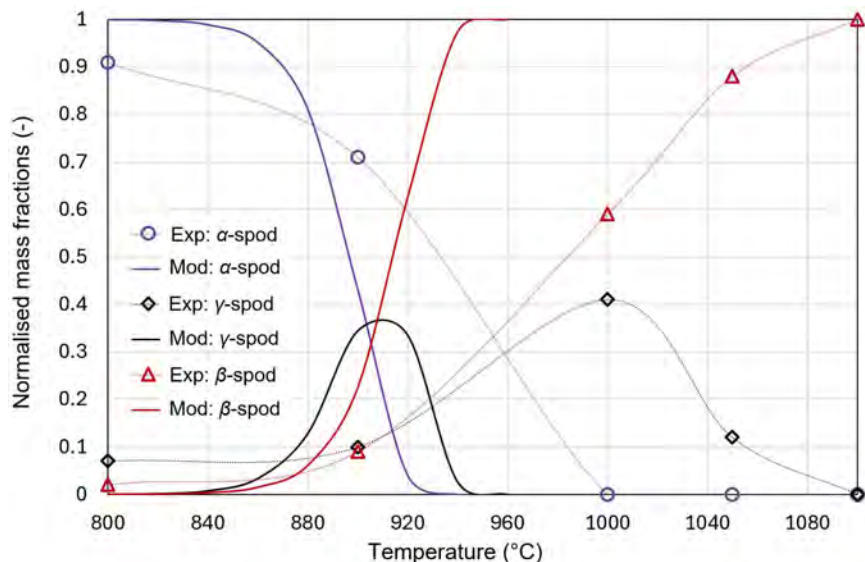
Dlugogorski, Abdullah, Oskierski and Senanayake, Kinetics of spodumene recrystallisation, ALTA 2024, Perth, Australia

Predictions and fit to Moore's et al. own measurements (Figure 3, $T = 906$ °C):

- Recall large error in the activation energy
- Note good match for β -spodumene, but not for α - and γ -spodumene
- Note lack of measurements for large conversion, which are important for practical applications

2. Kinetic models and their crucial information

- Model of Moore et al. [Comparison with Peltosaari's et al. data]



Moore, R.L., Mann, J.P., Montoya, A., Haynes, B.S., *In situ* synchrotron XRD analysis of the kinetics of spodumene phase transitions. *Physical Chemistry Chemical Physics*, 2018, **20**, 10753-10761.
 Peltosaari, O., Tanskanen, P., Heikkinen, E.-P., Fabritius, T., $\alpha \rightarrow \gamma \rightarrow \beta$ -phase transformation of spodumene with hybrid microwave and conventional furnaces. *Minerals Engineering*, 2015, **82**, 54-60.

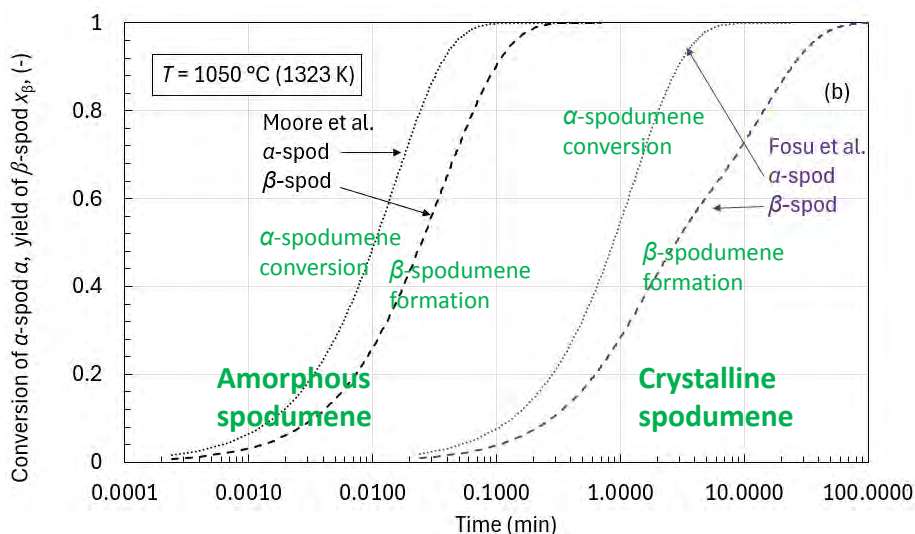
Dlugogorski, Abdullah, Oskierski and Senanayake, Kinetics of spodumene recrystallisation, ALTA 2024, Perth, Australia

Comparison of Moore's et al. model with Peltosaari's et al. measurements:

- polymorph distribution after 2 h of thermal treatment
- solid lines denote the modelling predictions and points are experimental measurement
- dotted line plotted as a guide to an eye for the data of Peltosaari et al.
- Very fast, due to amorphisation & defects introduced during grinding

2. Kinetic models and their crucial information

- Model of Moore et al. [Comparison with Fosu's et al. model]



Comparison of Moore's et al. model with the model of Fosu et al. measurements:

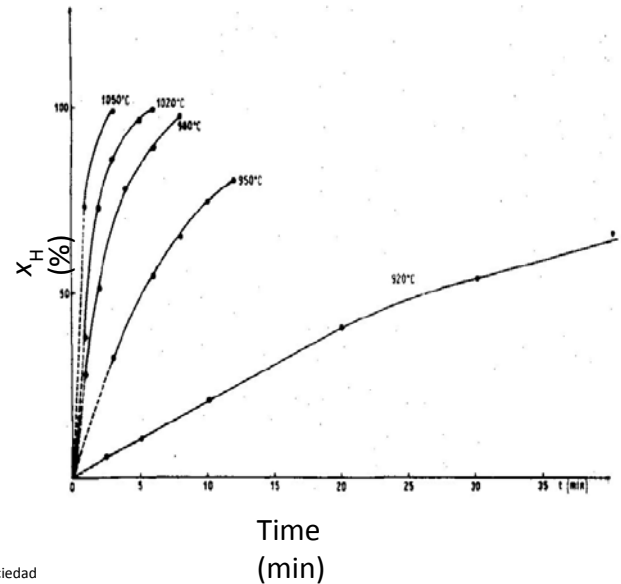
- Moore's et al. model is fast, due to amorphisation and defects introduced during grinding
- The model follows different kinetics, i.e., pathway (i) of Abdullah et al.
- Apparent* size dependence, because of the switch in the mechanism

Abdullah, A.A., Oskierski, H.C., Altarawneh, M., Senanayake, G., Lumpkin, G., Dlugogorski, B.Z., Phase transformation mechanism of spodumene during its calcination. *Minerals Engineering*, 2019, **140**, 105883.
 Fosu, A.Y., Kanari, N., Bartier, D., Hodge, H., Vaughan, J., Chagnes, A., Physico-chemical characteristics of spodumene concentrate and its thermal transformations. *Materials*, 2021, **14**, 7423.
 Moore, R.L., Mann, J.P., Montoya, A., Haynes, B.S., *In situ* synchrotron XRD analysis of the kinetics of spodumene phase transitions. *Physical Chemistry Chemical Physics*, 2018, **20**, 10753-10761.

Dlugogorski, Abdullah, Oskierski and Senanayake, Kinetics of spodumene recrystallisation, ALTA 2024, Perth, Australia

2. Kinetic models and their crucial information

- Model of Botto et al. [Experimental measurements]
- Spodumene provenance, particle size and purity
 - San Luis Province, Argentina
 - < 74 μm
 - 5.5 wt% Li_2O ; 68.5 wt% purity and 7.95 wt% Li_2O ; 99 wt% purity
- Experimental: Differential thermal analysis
- Experimental methodology
 - Roasted isothermally in furnace at 1163, 1193, 1223, 1293, 1323 K
 - Heated at 10 K min^{-1} to target temperature then isothermal
 - Conversion factor, $26.4 (\pm 0.5)\text{ kJ mol}^{-1}$
 - Assume JMAK (Avrami-Erofeev) nucleation, obtain $u = 1$, then kinetic analysis
- Derivation of kinetic rates
 - Obtain k at different heating times at constant T
 - Apply Arrhenius equation to extract Arrhenius parameters



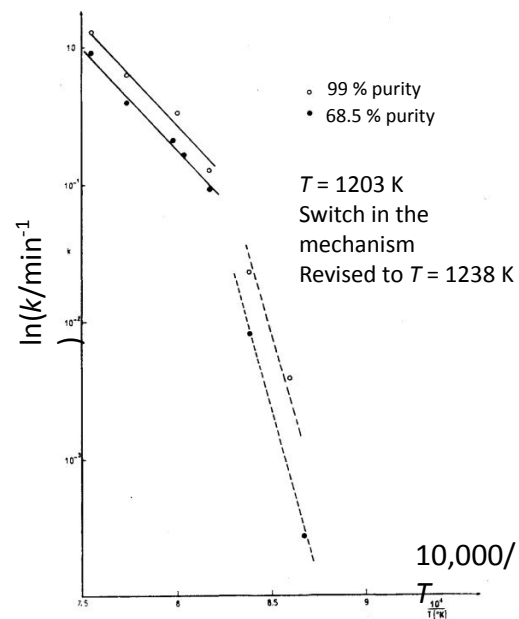
Botto, I.L., Cohen Arazi, S., Krenkel, T.G., Kinetic study of polymorphic transformation of spodumene I into spodumene II (in Spanish). Boletín de la Sociedad Española de Cerámica y Vidrio, 1975, 14, 433-440.

Długogorski, Abdullah, Oskierski and Senanayake, Kinetics of spodumene recrystallisation, ALTA 2024, Perth, Australia

2. Kinetic models and their crucial information

- Model of Botto et al. [Mechanism and kinetic parameters]

- Reaction mechanism
 - Normalised heat demand
 - α -spodumene \rightarrow β -spodumene
- Parameters
 - $T \leq 965\text{ }^\circ\text{C}$
 - $E = 698 (\pm 21)\text{ kJ mol}^{-1}$; $\ln(A/\text{min}^{-1}) = 66.6 (\pm 2.1)$
 - $T \geq 965\text{ }^\circ\text{C}$
 - $E = 275 (\pm 19)\text{ kJ mol}^{-1}$; $\ln(A/\text{min}^{-1}) = 25.3 (\pm 1.7)$
- Reaction model
 - First order in normalised energy demand

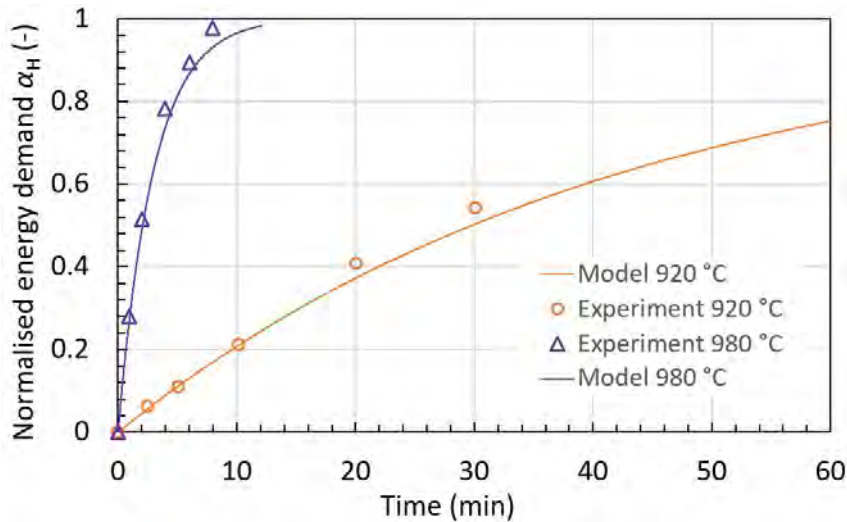


Botto, I.L., Cohen Arazi, S., Krenkel, T.G., Kinetic study of polymorphic transformation of spodumene I into spodumene II (in Spanish). Boletín de la Sociedad Española de Cerámica y Vidrio, 1975, 14, 433-440.

Długogorski, Abdullah, Oskierski and Senanayake, Kinetics of spodumene recrystallisation, ALTA 2024, Perth, Australia

2. Kinetic models and their crucial information

- Model of Botto et al. [Predictions and fit to own data]



Predictions and fit to Botto's et al. own measurements (Figure 2c&d):

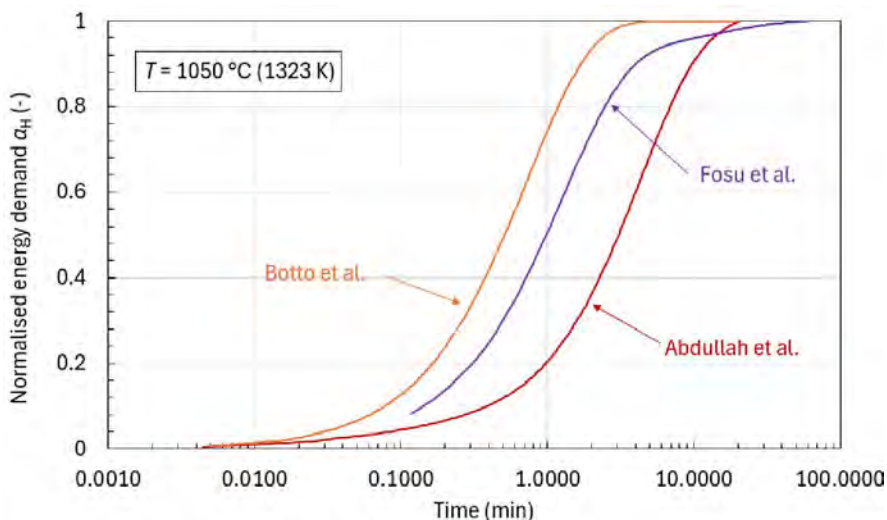
- Normalised energy demand (α_H)
- solid lines denote the modelling predictions and points are experimental measurement

Botto, I.L., Cohen Arazi, S., Krenkel, T.G., Kinetic study of polymorphic transformation of spodumene I into spodumene II (in Spanish). Boletín de la Sociedad Española de Cerámica y Vidrio, 1975, 14, 433-440.

Dlugogorski, Abdullah, Oskierski and Senanayake, Kinetics of spodumene recrystallisation, ALTA 2024, Perth, Australia

2. Kinetic models and their crucial information

- Model of Botto et al. [Comparisons with other models]



Comparison of Botto's et al. model with models of Fosu et al. and Abdullah et al.:

- there are no isothermal measurements in the literature for the normalised energy demand
- Fosu's et al. predicts modal distribution of polymorphs and, with an additional energy equation, yields the normalised energy demand
- Abdullah's et al. model predicts the normalised energy demand directly

Abdullah et al., in review (2024)

Botto, I.L., Cohen Arazi, S., Krenkel, T.G., Kinetic study of polymorphic transformation of spodumene I into spodumene II (in Spanish). Boletín de la Sociedad Española de Cerámica y Vidrio, 1975, 14, 433-440.

Fosu, A.Y., Kanari, N., Bartier, D., Hodge, H., Vaughan, J., Chagnes, A., Physico-chemical characteristics of spodumene concentrate and its thermal transformations. Materials, 2021, 14, 7423

Dlugogorski, Abdullah, Oskierski and Senanayake, Kinetics of spodumene recrystallisation, ALTA 2024, Perth, Australia

Presentation outline

1. Introduction

- Energy requirements and decarbonisation
- Spodumene polymorphs
- Mechanism of calcination (Abdullah et al., 2019)
- XRD models
- DTA/DSC-based models

2a. Kinetic models

- Model of Fosu, Kanari, Bartier, Hodge, Vaughan and Chagnes (Fosu et al., 2021)
- Model of Moore, Mann, Montoya and Haynes (Moore et al., 2018)
- Model of Botto, Cohen Arazi and Frenkel (Botto et al., 1975)

2b. Crucial information

- Experimental measurements
- Mechanism and kinetic parameters
- Predictions and fit to own data
- Comparison with experiments (Peltosaari et al., 2015)

3. Summary remarks

- Lack of particle size dependence; amorphous vs crystalline pathways
- Diffusion limitation
- Importance of recrystallisation of β -spodumene
- Effect of additives

Abdullah, A.A., Oskierski, H.C., Altarawneh, M., Senanayake, G., Lumpkin, G., Dlugogorski, B.Z., Phase transformation mechanism of spodumene during its calcination. *Minerals Engineering*, 2019, **140**, 105883.
Botto, I.L., Cohen Arazi, S., Krenkel, T.G., Kinetic study of polymorphic transformation of spodumene I into spodumene II (in Spanish). *Boletín de la Sociedad Española de Cerámica y Vidrio*, 1975, **14**, 433-440.
Fosu, A.Y., Kanari, N., Bartier, D., Hodge, H., Vaughan, J., Chagnes, A., Physico-chemical characteristics of spodumene concentrate and its thermal transformations. *Materials*, 2021, **14**, 7423.
Moore, R.L., Mann, J.P., Montoya, A., Haynes, B.S., *In situ* synchrotron XRD analysis of the kinetics of spodumene phase transitions. *Physical Chemistry Chemical Physics*, 2018, **20**, 10753-10761.
Peltosaari, O., Tanskanen, P., Heikkinen, E.-P., Fabritius, T., $\alpha \rightarrow \gamma \rightarrow \beta$ -phase transformation of spodumene with hybrid microwave and conventional furnaces. *Minerals Engineering*, 2015, **82**, 54-60.

Dlugogorski, Abdullah, Oskierski and Senanayake, Kinetics of spodumene recrystallisation, ALTA 2024, Perth, Australia

3. Summary remarks

- What have we learned?

1. Recrystallisation of amorphous (defect-laden) and crystalline spodumene proceeds along different pathways; pathway (i) vs pathways (iii) and (iv), in the mechanism of Abdullah et al. (2019); cf. (Fosu et al., 2021; Moore et al., 2018). No dependence on particle size.
2. Impurities, such as SiO_2 , induce the appearance of additional pathways; pathway (ii) in the mechanism of Abdullah et al. (2019).
3. Diffusion is the limiting mechanism for the calcination of α -spodumene to β -spodumene; it is not nucleation nor crystallisation
4. The final recrystallisation of β -spodumene from γ -spodumene governs the temperature and the residence time of the calcination process (Abdullah et al., 2018; Dessemond et al., 2020; Fosu et al., 2021; Peltosaari et al., 2015; Salakjani et al., 2016).
5. Kinetic parameters in the Arrhenius relationship are correlated! Good predictions are possible for unphysical values of E and $\ln(A)$, as errors in E are offset by errors in $\ln(A)$.

Abdullah, A.A., Oskierski, H.C., Altarawneh, M., Senanayake, G., Lumpkin, G., Dlugogorski, B.Z., Phase transformation mechanism of spodumene during its calcination. *Minerals Engineering*, 2019, **140**, 105883.
Dessemond, C., Soucy, G., Harvey, J.-P., Ouzilleau, P., Phase transitions in the α - γ - β spodumene thermodynamic system and impact of γ -spodumene on the efficiency of lithium extraction by acid leaching. *Minerals*, 2020, **10**, 519.
Fosu, A.Y., Kanari, N., Bartier, D., Hodge, H., Vaughan, J., Chagnes, A., Physico-chemical characteristics of spodumene concentrate and its thermal transformations. *Materials*, 2021, **14**, 7423.
Moore, R.L., Mann, J.P., Montoya, A., Haynes, B.S., *In situ* synchrotron XRD analysis of the kinetics of spodumene phase transitions. *Physical Chemistry Chemical Physics*, 2018, **20**, 10753-10761.
Peltosaari, O., Tanskanen, P., Heikkinen, E.-P., Fabritius, T., $\alpha \rightarrow \gamma \rightarrow \beta$ -phase transformation of spodumene with hybrid microwave and conventional furnaces. *Minerals Engineering*, 2015, **82**, 54-60.
Salakjani, N.K., Singh, P., Nikoloski, A.N., Mineralogical transformations of spodumene concentrate from Greenbushes, Western Australia. Part 1: Conventional heating. *Minerals Engineering*, 2016, **98**, 71-79. 111/395

3. Summary remarks

3.1 Lack of particle size dependence; amorphous vs crystalline pathways

- (i) **amorphous** spodumene $\rightarrow \gamma$ -spodumene $\rightarrow \beta$ -spodumene
 - (ii) *crystalline* α -spodumene $\rightarrow \beta$ -quartz_{ss} $\rightarrow \beta$ -spodumene
 - (iii) **crystalline** α -spodumene $\rightarrow \gamma$ -spodumene $\rightarrow \beta$ -spodumene; and
 - (iv) **crystalline** α -spodumene $\rightarrow \beta$ -spodumene
- XRD models are very specific and, at present, cannot differentiate between pathways (i) and (iii – iv) and do not include (ii).
 - The mechanistic pathways switch for concentrates dominated by amorphous and crystalline materials. This manifests itself in the apparent dependence on particle size. There is minor size-dependence due to heating of the particles.
 - Pathway (ii) is naturally included in the isoconversional DSC-based models (not presented today) but is yet to be included in the XRD-based models.
 - We estimate the particles of $d_{80} = 20 \mu\text{m}$ to be 75 % amorphous and only 30 % amorphous if characterised by $d_{80} = 50 \mu\text{m}$; based on Abdullah et al. (2019).
 - Isoconversional DSC models must be developed for each concentrate. At present, this is also true for the XRD models. It should be possible to incorporate pathways (i) and (ii) as separate corridors in future XRD models.

Abdullah, A.A., Oskierski, H.C., Altarawneh, M., Senanayake, G., Lumpkin, G., Dlugogorski, B.Z., Phase transformation mechanism of spodumene during its calcination. Minerals Engineering, 2019, **140**, 105883.

Dlugogorski, Abdullah, Oskierski and Senanayake, Kinetics of spodumene recrystallisation, ALTA 2024, Perth, Australia

3. Summary remarks

3.2 Additional pathways due to impurities

- (ii) *crystalline* α -spodumene $\rightarrow \beta$ -quartz_{ss} $\rightarrow \beta$ -spodumene (Abdullah et al., 2019; Urazov et al., 1957)

The composition of the samples of α -spodumene in weight % (Urazov et al., 1957).

Sample	SiO ₂	Al ₂ O ₃	Fe ₂ O ₃	CaO	MgO	Na ₂ O	K ₂ O	Li ₂ O	Σ
1	64.04	31.18	Trace	0.22	Trace	0.01	Trace	5.12	100.57
2	65.34	30.10	Trace	0.20	Trace	0.01	0.14	4.70	100.49
3	66.34	27.58	Trace	0.22	Trace	0.12	0.12	6.05	100.43

Range of transformation of $\alpha \rightarrow \beta$ spodumene (Urazov et al. 1957).

Sample	Rate of heating, °C/min	Range of spodumene transformation, °C
1	11	995-1050
1	21	1005-1070
2	10	1025-1070
2	22	1026-1100
3	11	990-1035
3	22	995-1070

The effect of SiO₂ and K₂SO₄ additives on the temperature and $\alpha \rightarrow \beta$ conversion of spodumene; at a constant heating rate of ≈ 11 °C/min (Urazov et al. 1957).

Sample	Additive to spodumene, mass %	Range of transformation, °C
1	5 (SiO ₂)	995-1050
1	20 (SiO ₂)	915-1000
1	5 (K ₂ SO ₄)	1005-1035
1	50 (K ₂ SO ₄)	965-990
2	5 (SiO ₂)	990-1035
2	20 (SiO ₂)	925-1020
2	5 (K ₂ SO ₄)	1005-1035
2	50 (K ₂ SO ₄)	975-1010
3	5 (SiO ₂)	960-1005
3	20 (SiO ₂)	905-1000
3	5 (K ₂ SO ₄)	965-995
3	50 (K ₂ SO ₄)	950-980

Abdullah, A.A., Oskierski, H.C., Altarawneh, M., Senanayake, G., Lumpkin, G., Dlugogorski, B.Z., Phase transformation mechanism of spodumene during its calcination. Minerals Engineering, 2019, **140**, 105883.
 Urazov, G.G., Plyushchev, V.E., Shakhno, I.V., On monotropic transformation of spodumene (in Russian). Doklady Akademii Nauk SSSR, 1957, **113**, 361-363.

Dlugogorski, Abdullah, Oskierski and Senanayake, Kinetics of spodumene recrystallisation, ALTA 2024, Perth, Australia

3. Summary remarks

3.3 Diffusion is the limiting mechanism of calcination

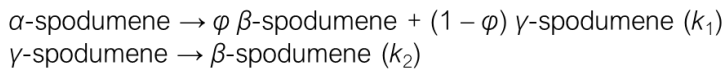
Diffusion is the limiting mechanism for the calcination of α -spodumene to β -spodumene; it is not nucleation or crystallisation

Compare $k = A \exp(-\frac{E}{RT})$ and $D = D_0 \exp(-\frac{\Delta H}{RT})$

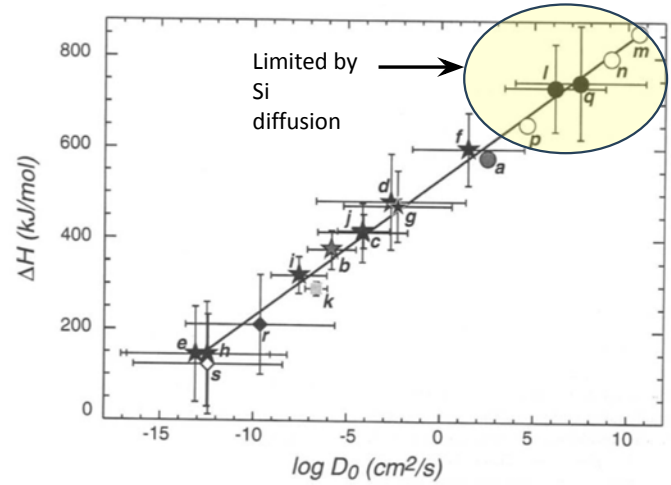
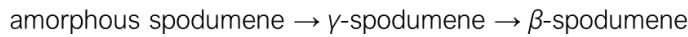
ΔH is the activation enthalpy for diffusion

This also the reason for the mechanism of Moore et al. (2018) and Fosu et al. (2021) to be equivalent to pathways (iii) and (iv) of Abdullah et al. (2018).

Moore et al. and Fosu et al.



Abdullah et al.



Compensation relationship for diffusion (Béjina and Jaoul, 1997)

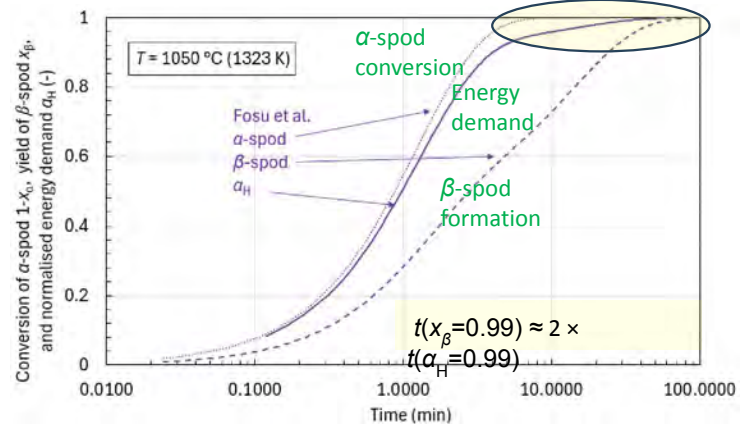
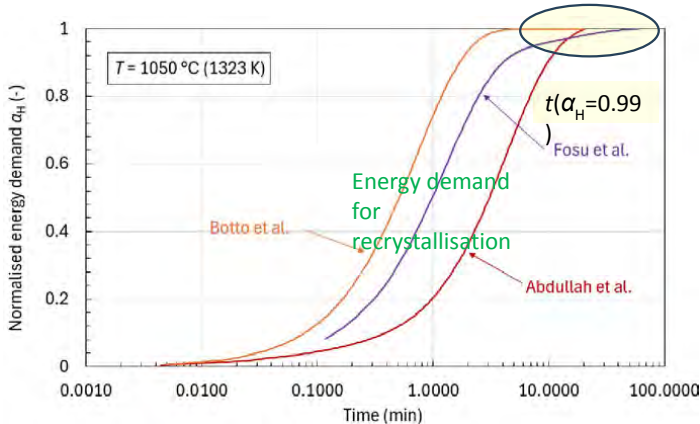
Abdullah, A.A., Oskierski, H.C., Altarawneh, M., Senanayake, G., Lumpkin, G., Dlugogorski, B.Z., Phase transformation mechanism of spodumene during its calcination. Minerals Engineering, 2019, 140, 105883.
 Béjina, F., Jaoul, O., Silicon diffusion in silicate minerals. Earth and Planetary Science Letters, 1997, 153, 229-238.
 Fosu, A.Y., Kanari, N., Bartier, D., Hodge, H., Vaughan, J., Chagnes, A., Physico-chemical characteristics of spodumene concentrate and its thermal transformations. Materials, 2021, 14, 7423.
 Moore, R.L., Mann, J.P., Montoya, A., Haynes, B.S., In situ synchrotron XRD analysis of the kinetics of spodumene phase transitions. Physical Chemistry Chemical Physics, 2018, 20, 10753-10761.

Dlugogorski, Abdullah, Oskierski and Senanayake, Kinetics of spodumene recrystallisation, ALTA 2024, Perth, Australia

3. Summary remarks

3.4 Recrystallisation of β -spodumene from γ -spodumene

The final recrystallisation of β -spodumene from γ -spodumene governs the temperature and the residence time of the calcination process (Dessemond et al., 2020; Fosu et al., 2021; Peltosaari et al., 2015).



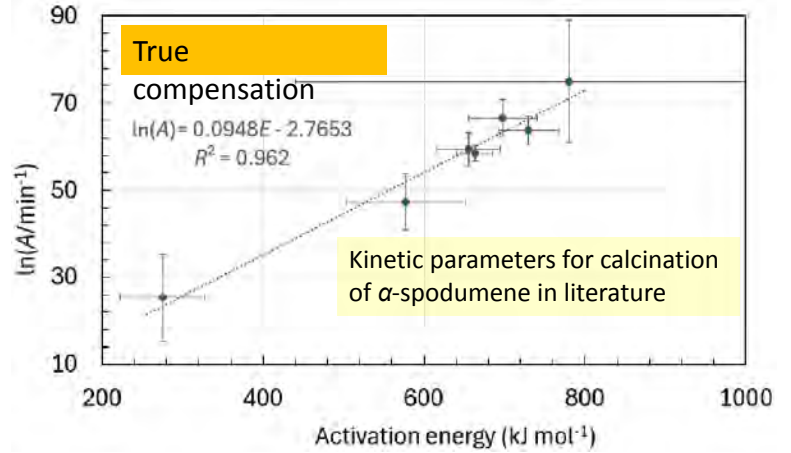
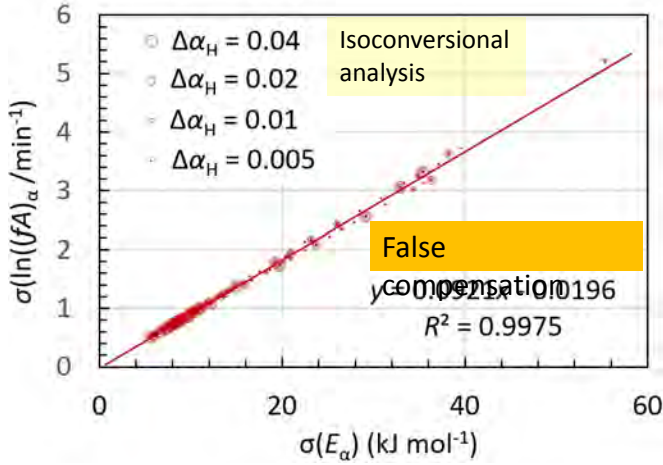
Abdullah et al., in review (2024)
 Botto, I.L., Cohen Arazi, S., Krenkel, T.G., Kinetic study of polymorphic transformation of spodumene I into spodumene II (in Spanish). Boletín de la Sociedad Española de Cerámica y Vidrio, 1975, 14, 433-440.
 Dessemond, C., Soucy, G., Harvey, J.-P., Ouzilleau, P., Phase transitions in the α - γ - β spodumene thermodynamic system and impact of γ -spodumene on the efficiency of lithium extraction by acid leaching. Minerals, 2020, 10, 519.
 Fosu, A.Y., Kanari, N., Bartier, D., Hodge, H., Vaughan, J., Chagnes, A., Physico-chemical characteristics of spodumene concentrate and its thermal transformations. Materials, 2021, 14, 7423.
 Peltosaari, O., Tanskanen, P., Heikkinen, E.-P., Fabritius, T., $\alpha \rightarrow \gamma \rightarrow \beta$ -phase transformation of spodumene with hybrid microwave and conventional furnaces. Minerals Engineering, 2015, 82, 54-60.

Dlugogorski, Abdullah, Oskierski and Senanayake, Kinetics of spodumene recrystallisation, ALTA 2024, Perth, Australia

3. Summary remarks

3.5 Compensations

Fitting Arrhenius relationship to experimental data “invites” compensations. E and $\ln(A)$ are independent, but their statistical estimators are “falsely” compensated. This is because errors in $\sigma(E)$ and $\sigma(\ln(A))$ are correlated.



Abdullah et al., in review (2024)

Botto, I.L., Cohen Arazi, S., Krenkel, T.G., Kinetic study of polymorphic transformation of spodumene I into spodumene II (in Spanish). Boletín de la Sociedad Española de Cerámica y Vidrio, 1975, **14**, 433-440.

Fosu, A.Y., Kanari, N., Bartier, D., Hodge, H., Vaughan, J., Chagnes, A., Physico-chemical characteristics of spodumene concentrate and its thermal transformations. Materials, 2021, **14**, 7423.

Moore, R.L., Mann, J.P., Montoya, A., Haynes, B.S., *In situ* synchrotron XRD analysis of the kinetics of spodumene phase transitions. Physical Chemistry Chemical Physics, 2018, **20**, 10753-10761.

Długogorski, Abdullah, Oskierski and Senanayake, Kinetics of spodumene recrystallisation, ALTA 2024, Perth, Australia

PHOSPHATE REMOVAL FROM WASTEWATER USING CALCIUM SILICATE BY-PRODUCTS DERIVED FROM THE LIENA[®] PROCESS

Shilpi R. Biswas, Shane Wilson, Lyndon Jee, Aleksandar N. Nikoloski*

Harry Butler Institute (Centre for Water Energy and Waste), College of Science, Health, Engineering and Education, Murdoch University, Australia

Presenter: Shilpi R. Biswas

Shilpi.RayBiswas@Murdoch.edu.au

* Corresponding author:

A.Nikoloski@murdoch.edu.au

ABSTRACT

Phosphorus is present in soils, sediment, and water in various chemical forms, most commonly as the phosphate (PO_4^{3-}) species. High phosphorus concentrations in aquatic environments may result from agricultural and urban runoff, leaking septic systems, or discharges from sewage treatment plants. Phosphorus abundance can cause eutrophication of water bodies and may lead to algal blooming, which can be toxic to humans and animals. On the other hand, phosphorus is an important nutrient for living cells, but it is a finite resource. Consequently, the recovery and recycling of phosphorus from wastewater for applications such as fertiliser manufacture would be beneficial. This study evaluates the use of calcium silicate by-product (CSB) residue derived from the LieNA[®] process to remove phosphate from wastewater systems. LieNA[®] is a novel technology developed by Lithium Australia Limited to extract lithium directly from α -spodumene without the requirement for high-temperature conversion to β -spodumene. XRF, SEM, and TIMA analysis reveal that the CSB residue mostly comprises calcium, sodium, silicon, and oxygen. Phosphate removal experiments using CSB were conducted under a variety of conditions. The CSB showed good adsorption properties for the removal of phosphate from simulated phosphate-containing wastewater. Phosphate removal efficiency was strongly controlled by the dosage of CSB, the initial pH of the solution, and the adsorption time. Phosphate removal efficiency reached 99% after 24 hours adsorption time, at a temperature of 25°C, an adsorbent dose of 20 g L⁻¹, an initial pH of 12, and a 100-rpm stirring speed. The phosphate adsorption had reached equilibrium after 24 hours and the adsorption capacity under these conditions was 4.93 mg PO_4^{3-} per gram of CSB. The data from adsorption kinetic measurements were well fitted by a Lagergren pseudo-first-order model. The phosphate removal efficiency of CSB was compared to that of other calcium compounds, specifically laboratory-grade calcium hydroxide and calcium metasilicate, both of which have been shown to be effective for phosphate removal in previous research studies. The removal efficiency of CSB was only slightly less than that of calcium metasilicate, possibly due to impurities in the CSB, but was ~20% lower than the removal efficiency of calcium hydroxide. The removal of toxic metals was also studied. CSB exhibited 57% removal efficiency for Hg, and the removal efficiency of selected toxic metals (Zn, Cu, Cd, Pb and As) was observed to vary between 10-20% after 24 hours of adsorption time at 25°C, with an adsorbent dose of 5 g L⁻¹, an initial pH of 5, and a stirring speed of 100-rpm. This investigation has demonstrated the potential for using CSB to reduce the concentration of phosphate and toxic elements in wastewater.

Keywords: LieNA[®] process; Residue; By-product; Adsorption; Wastewater treatment.

INTRODUCTION

Phosphorus is an important mineral nutrient ^[1] for all living things and plays a vital role in the transfer of energy within living cells. It is a major component of nucleic acids (DNA and RNA), teeth and bones and is crucial for cell membranes ^[2,3]. The most common form of phosphorus is phosphate (PO_4) ^[4], and it occurs naturally in the earth's crust, typically in sedimentary rocks and ocean sediments. It can also be found in soil and different types of foods, such as dairy products, meats and poultry, fish, eggs, nuts, vegetables, and grains ^[3,5,6]. Phosphate contributes to the agricultural and industrial sectors, for example, in the production of steel, detergents, rust removers, corrosion preventers, animal feeds, and fertilisers to enhance soil quality for crop growth ^[5,7].

External phosphate inflow into surface water bodies may be a result of agricultural and urban runoff, leaking septic systems, discharges from sewage treatment plants or mobilisation of legacy phosphate ^[8]. Phosphate abundance can cause eutrophication of water bodies and may lead to algal blooming and the growth of invasive aquatic plants, which can be toxic to humans and animals ^[4,9]. It has been reported that eutrophication in an aquatic environment can result in a phosphate concentration between $25 \mu\text{g L}^{-1}$ and 0.03mg L^{-1} ^[4]. Consequently, abatement of phosphate inflow into surface water systems is a necessary measure to mitigate and control water eutrophication ^[4,10].

Several investigations have been conducted for the removal and recovery of phosphate from water, including adsorption process, chemical precipitation, advanced biological treatment, electrochemical process, membrane technologies and crystallisation ^[9,11]. Biological treatments such as the conventional activated sludge method can remove 75–100 % of phosphate but are less effective at low phosphate content and require large land areas. A large amount of sludge and waste is produced during phosphate removal by chemical precipitation. Other technologies, such as electro dialysis and reverse osmosis processes are expensive for phosphate removal ^[11].

Adsorption technology is not commonly used on an industrial scale to remove phosphate from wastewater, but it continues to be studied for this purpose due to its simplicity in operation, lower waste generation, significant removal efficiency, environmental friendliness, and low cost ^[11,12].

A number of studies have established that calcium compounds such as $\text{Ca}(\text{OH})_2$ (calcium hydroxide), CSH (calcium silicate hydrate) and CaSiO_3 (wollastonite) are effective adsorbents for the removal and recovery of phosphate from wastewater streams ^[4,10,13,14,15]. Calcium hydroxide reacts immediately with dissolved phosphate in wastewater and produces calcium phosphate, which then precipitates out of the water ^[13,16].

Wollastonite is a calcium metasilicate (CaSiO_3) material primarily composed of calcium (Ca), silicon (Si) and oxygen (O_2), though a small percentage of impurities (e.g., iron, magnesium, manganese, aluminium, potassium, sodium etc.) can be present ^[16,17]. About 48.3% of the calcium metasilicate is calcium oxide, and this component plays a vital part in the adsorption of phosphate from wastewater systems ^[18].

To date, numerous studies have reported that CSH is a promising adsorbent for phosphate removal and recovery from phosphate-bearing wastewater ^[4,9,10,15,19]. CSH is a semi-crystalline material and chemically represented as $\text{CaO}_3\text{Si}\cdot n\text{H}_2\text{O}$. The composition of CSH is 25% CaO and 30% SiO_2 with a Ca/Si ratio of approximately 1 ^[10]. CSH acts as a seed crystal and the calcium ion donor during the phosphate adsorption process. Simultaneously, CSH also adjusts the pH of the solution which removes the need to add extra chemicals for pH adjustment, thereby increasing the ease of removal of phosphate in the adsorption process ^[9]. Therefore, CSH can be considered a feasible and low-cost adsorbent for phosphate removal from wastewater ^[20]. CSH has been synthesised from various waste products such as alum factory solid waste residue ^[9], carbide residue ^[21], waste glass and shells ^[22], and blast furnace slag ^[23]. Studies ^[9,24,25] have shown that CSH has an ability to adsorb phosphate ions from wastewater systems due to CSH's strong affinity with phosphate ions which produces insoluble calcium phosphate species.

Water contamination by toxic metals is also a serious environmental concern due to the rapid growth of industries and other anthropogenic activities that use or produce these metals ^[26,27,28]. The presence of toxic elements such as copper (Cu), lead (Pb), zinc (Zn), mercury (Hg), cadmium (Cd), arsenic (As), chromium (Cr) and nickel (Ni) in water bodies can threaten both aquatic ecosystems and human health ^[27]. Research ^[29,30,31] has reported that CSH can be utilised as an adsorbent to remove toxic metal ions (including Cu^{2+} , Cd^{2+} , Pb^{2+} , As^{5+} , Zn^{2+} , Ni^{2+} etc.) from water.

Inspired by previous research studies, this investigation aimed to investigate the use of the calcium silicate by-product (CSB) residue produced from the LieNA[®] process to remove phosphate from wastewater systems. LieNA[®] is a novel technology developed by Lithium Australia Limited (LIT) to

extract lithium directly from α -spodumene. As per LIT's estimation, about 40% of total waste is generated as calcium silicate by-products (CSB) during the extraction of lithium from α -spodumene using the LieNA[®] process. Therefore, the reuse of this CSB waste residue for phosphate removal from wastewater, without the requirement of additional chemicals could provide significant economic value add.

This work explored the effect of the phosphate initial concentration, adsorbent dosage, initial solution pH, and contact time on phosphate removal efficiency and adsorption capacity. The phosphate removal efficiencies using each of the calcium compounds $\text{Ca}(\text{OH})_2$, CaSiO_3 and CSB were quantified and compared. Chemical kinetics were investigated in order to obtain the adsorption process mechanism, and the most likely adsorption kinetic model was fitted to the experimental data.

MATERIALS AND METHODS

LieNA[®] Residue Sample

The CSB used in this study was a LieNA[®] residue provided by Lithium Australia Limited, Australia. The LieNA[®] process was developed by Lithium Australia Limited to extract lithium from naturally occurring α -spodumene. This is a less energy-intensive process for extracting lithium from fine spodumene tailings compared to the conventional sulfuric acid method. LieNA[®] is an environmentally friendly process and has the potential to improve sustainability. However, a significant amount of waste residue is produced during this lithium extraction process. **Figure 1** illustrates the flow diagram of the LieNA[®] process and the CSB generating point.

The elemental composition of CSB was analysed using X-ray fluorescence (Bureau Veritas, Australia) and is given below in **Table 1**.

Table 1: Elemental composition of calcium silicate by-product (CSB)

Elements	Ca	Si	Na	Al	Fe	Mg	K	P	LOI
%	21.11	14.14	15.6	0.15	0.06	0.1	0.125	0.034	17.93

Note: The sum of elemental composition does not equal 100 due to the presence of oxygen in the CSB. SEM and TIMA were also used to characterise the elemental and mineralogical composition of the CSB.

CHEMICALS

All chemicals involved in this study were of analytical grade without further purification. The simulated phosphate-containing wastewater samples were prepared from AR grade KH_2PO_4 (potassium dihydrogen phosphate, ChemSupply, Australia). The acid and base solutions used to adjust the initial pH were prepared from AR grade HCl (hydrochloric acid, Rowe Scientific, Australia) and NaOH (sodium hydroxide, ChemSupply, Australia) pellets, respectively. Laboratory grade $\text{Ca}(\text{OH})_2$ (calcium hydroxide, Ajax Fine-chem, Australia) and calcium metasilicate (CaSiO_3 , Choice Analytical Pty Ltd, Australia) were chosen for comparison with the phosphate adsorption capacity by CSB. CaSiO_3 was chosen instead of pure CSH due to its restricted supply from chemical providers. High-purity Zn, Cu, Cd, Pb, As and Hg ICP-OES standard solutions (Choice Analytical Pty Ltd, Australia) were used as simulated toxic metals in the wastewater.

PHOSPHATE REMOVAL EXPERIMENTS

A stock solution of phosphate (100 mg L^{-1}) was prepared by dissolving the appropriate quantity of KH_2PO_4 in deionised water. A water bath rotary shaker was used to maintain the temperature during phosphate removal experiments. All phosphate adsorption tests were performed with a continuous stirring speed of 100-rpm.

The effect of the initial pH on phosphate adsorption was investigated for pH values of 3,7,9 and 12 in a 100 mL Erlenmeyer flask at 25°C for 24 hours. The supernatants were filtered, and the residual phosphate concentration in the solutions were measured. The initial pH of the phosphate solution was adjusted using NaOH (0.1 mol L^{-1} & 1 mol L^{-1}) and HCl (0.1 mol L^{-1} & 1 mol L^{-1}). The pH was measured by a pH meter (WP-80 handheld pH/mV Meter, TPS, Australia). A dosage of CSB was chosen as 5 g L^{-1} since the CSB sample quantity was limited, but in addition, Fang et al ^[21] achieved the optimum phosphate removal efficiency with a dosage of 5 g L^{-1} to 7 g L^{-1} in 100 mL of simulated wastewater.

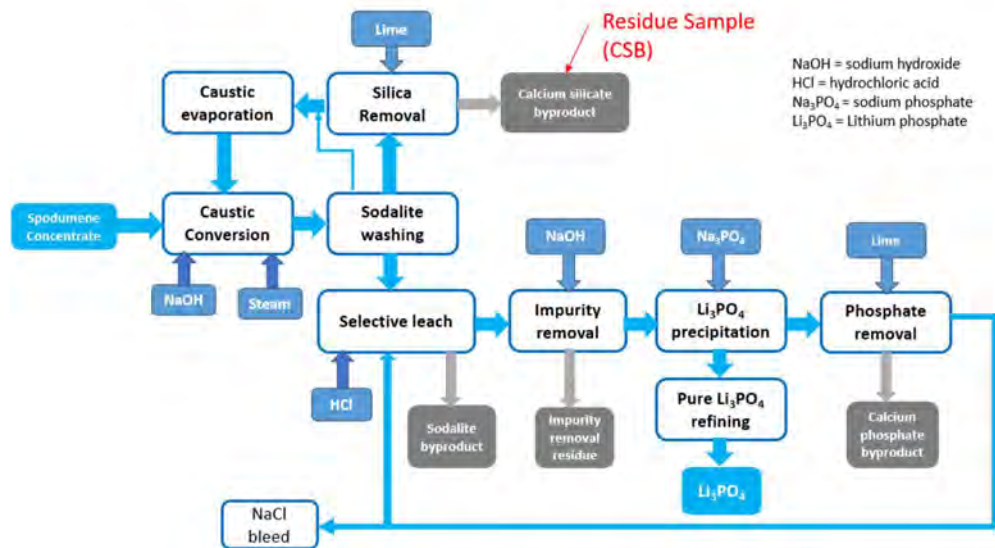


Figure 1: Flow diagram of LieNA® process showing the CSB generating point (adopted from Lithium Australia Limited).

The effect of each of the calcium compounds Ca(OH)₂, CaSiO₃, and CSB on phosphate removal was investigated for doses of 1, 5, 10, 15, 20 or 25 g L⁻¹ of each compound. Each dose was mixed with 100 mL of phosphate solution (100 mg L⁻¹) for 24 hours at a temperature of 25 °C. Initially, the pH of the phosphate solution was 4.83 without any adjustment of pH. The separated suspension was filtered. The phosphate concentration in the resulting suspension was determined, and concentration results from all experiments were compared.

After optimisation of CSB dosage and initial pH, the impact of adsorption time on phosphate removal efficiency by CSB was investigated. The parameters for this experiment were 20 g L⁻¹ of CSB in a 100 mL phosphate solution with an initial pH of 12 and a temperature of 25 °C, and the experiment was stopped after 168 hours. Supernatant was collected from the solution at selected times during the experiment, with the first collection occurring at 0.5 hours. The specimen was filtered through a 0.2 µm filtration membrane, and the residual phosphate and toxic metals concentration in the solution were measured by an inductively coupled plasma-optical emission spectrometer (ICP-OES, Agilent Technologies, Australia).

The phosphate removal efficiency (R_e) and phosphate adsorption capacity of CSB (Q_t) were calculated by the following equations [15,19,30].

$$R_e = \{(C_0 - C_t)/C_0\} * 100\% \quad 1$$

R_e = Removal efficiency (%) of phosphate

C_0 = Initial phosphate concentration (mg L⁻¹) at time t = 0

C_t = Phosphate concentration (mg L⁻¹) at time t

$$Q_t = \{(C_0 - C_t) V\}/m \quad 2$$

Q_t = Adsorption capacity (mg g⁻¹)

V = Volume (L)

M = Adsorbent mass (g)

Phosphate adsorption model

Lagergren pseudo-first-order and second-order kinetic models [32, 33, 34] were investigated to determine if one of these models closely matched the data from the phosphate adsorption experiments, which would indicate the mechanism for phosphate adsorption on CSB. The Lagergren pseudo-first-order model is expressed in equation (3)

$$dQ_t/dt = k_1 (Q_e - Q_t) \quad 3$$

Equation (3) can be integrated for the boundary conditions t = 0, $Q_t = 0$ and t = t, $Q_t = Q_t$ to get equation (4):

$$\ln(Q_e - Q_t) = \ln Q_e - k_1 t$$

4

where, Q_e and Q_t are the amounts of phosphate adsorbed when the system has reached equilibrium (min) and at time t (min), respectively, and k_1 is the pseudo-first-order adsorption rate coefficient (min^{-1}), which can be obtained from the slope of the linear plot between $\ln(Q_e - Q_t)$ and t .

The pseudo-second-order model may be investigated using equation (5)

$$dQ_t/dt = k_2 (Q_e - Q_t)^2$$

5

Equation (5) can be integrated for the boundary conditions $t = 0, Q_t = 0$ and $t = t, Q_t = Q_t$ to get equation (6):

$$t/Q_t = 1/(k_2 Q_e^2) + (1/Q_e) * t$$

6

where, k_2 is the second-order kinetic rate constant (min^{-1}), which can be obtained from the inverse of the slope of the linear plot between t/Q_t and $1/Q_e^2$.

TOXIC METAL REMOVAL EXPERIMENTS

The adsorption experiments for selected toxic metals were performed at a temperature of 25 °C with continuous stirring at 100-rpm in a 100 mL (10 mg L^{-1}) conical flask that contained 0.5 g of CSB adsorbent. The toxic metal removal experiment lasted for 24 hours. After this time, a supernatant sample was collected and filtered ($0.2 \mu\text{m}$), and the residual concentration of the toxic metals in the sample was then determined using ICP-OES. The removal efficiency (R_e) and the adsorption capacity of CSB (Q_t) were determined using equations 1 and 2.

RESULTS AND DISCUSSION

CSB Characterisation

TIMA (Tescan Integrated Mineral Analyser, Australia) analysis of the CSB revealed that the primary phases were natrite, an O-Na-Ca-Si system and oyelite. A small amount of calcite and wollastonite were also present in the CSB sample. **Figure 2** is the mineral composition map of the CSB for the $+500 \mu\text{m}$ fractions. 85% of particles in the CSB had a size of $<10 \mu\text{m}$.

A CSB sample was prepared and mounted on aluminium stubs and evaluated using SEM to identify the surface morphology (

Figure 3). The energy dispersive spectra (EDS) of the CSB was also observed (**Figure 4**). The CSB was predominantly composed of sodium, calcium, silicon, and oxygen. Potassium was also detected by SEM-EDS analysis.

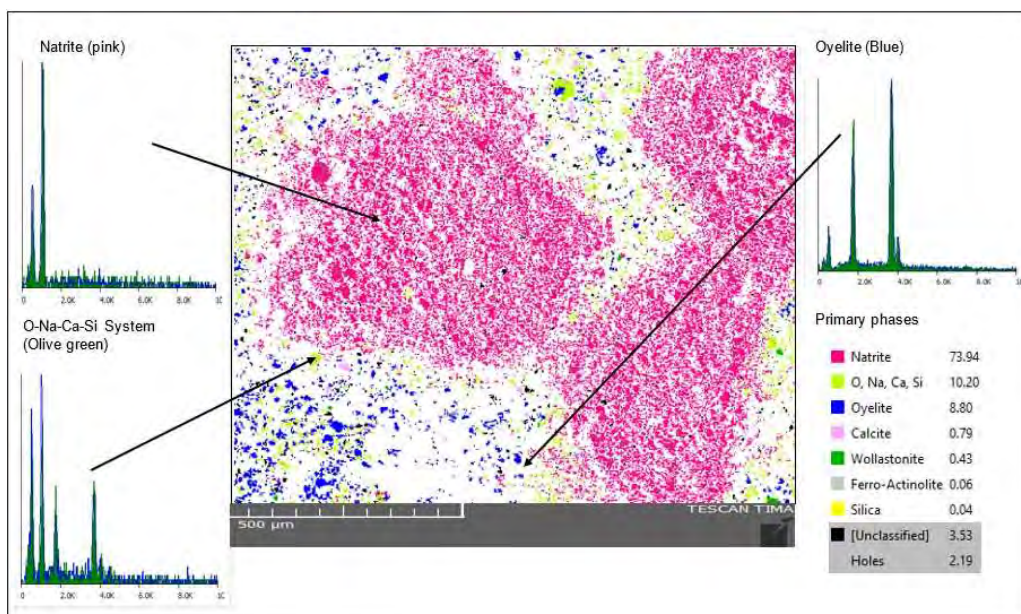


Figure 2: TIMA mineral composition map of a CSB cross section showing primary phases present in the sample.

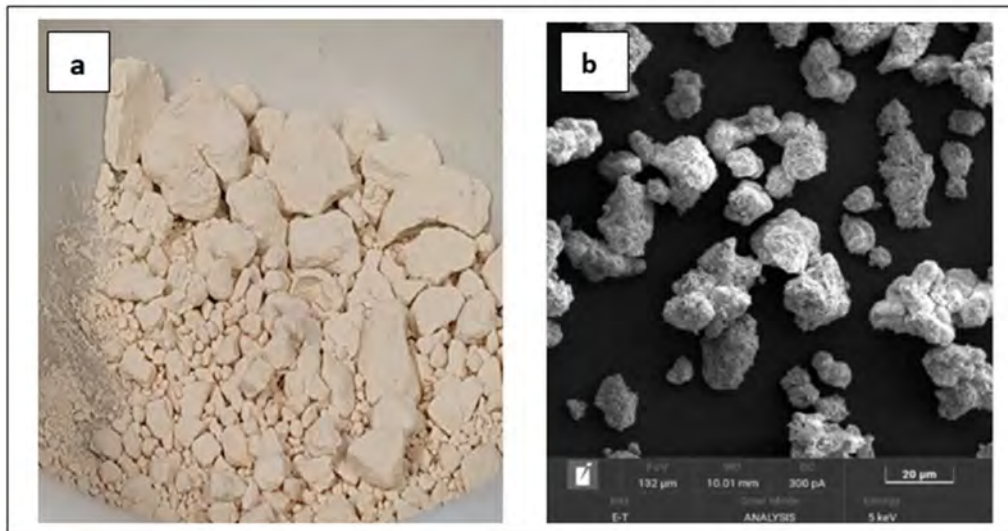


Figure 3: Optical (a) and SEM (b) images of the CSB sample.

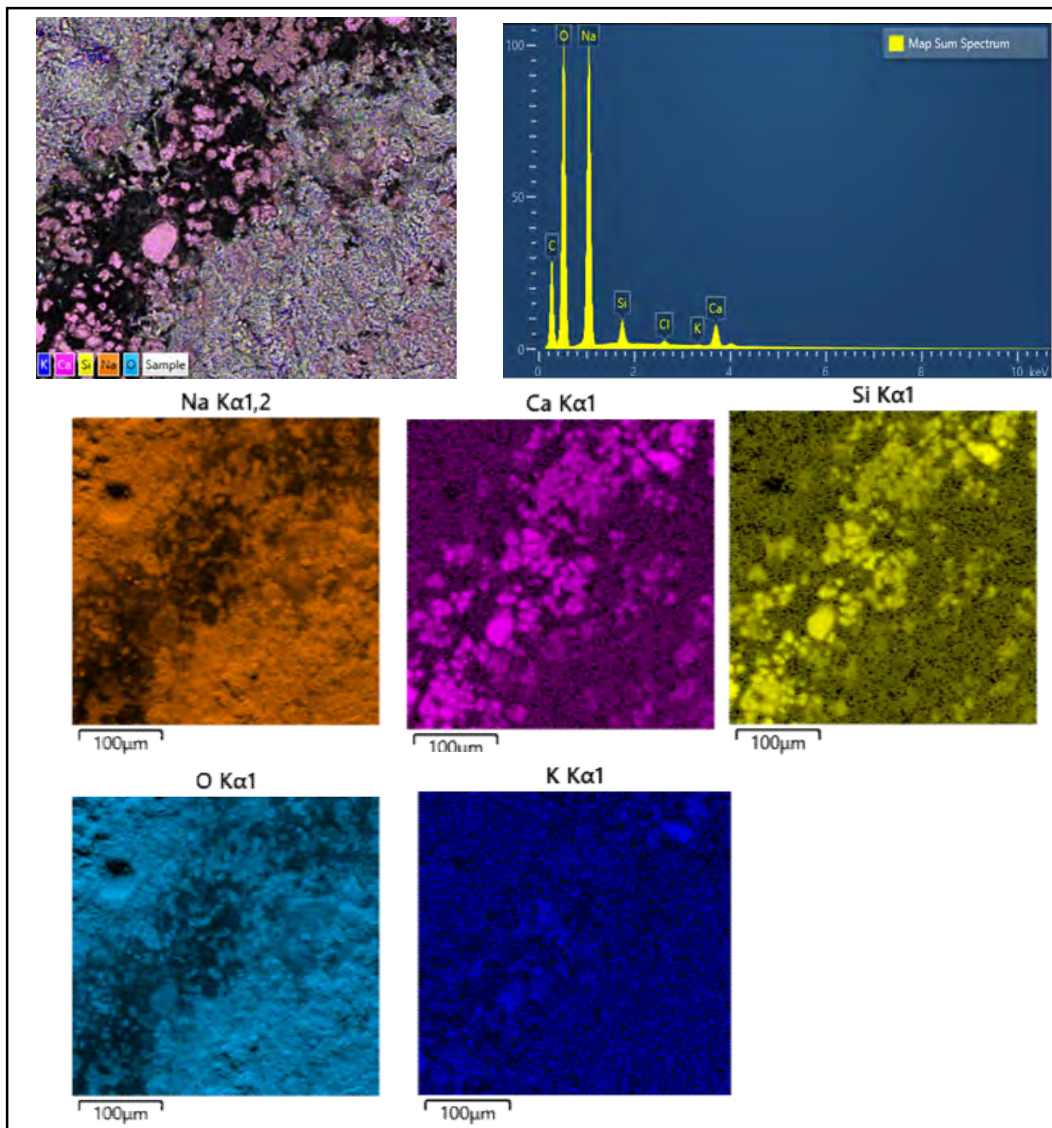


Figure 4 : EDS elemental distribution maps showing the distribution of Na, Ca, Si and K in various grains in the CSB sample.

Phosphate adsorption

Phosphate adsorption at different initial pH values

Typically, the pH value of a solution is an important factor that influences the adsorption of phosphate by a calcium silicate material, as it directly impacts the existence of different species of phosphate such as H_3PO_4 , H_2PO_4^- , HPO_4^{2-} [9,35,36]. Therefore, it is vital to assess adsorption behaviour of phosphate on CSB in solution with different pH values.

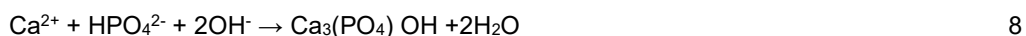
Initial pH values in the range from 3 to 12 were investigated with an adsorbent dosage of 5 g L⁻¹. Phosphate removal efficiency (R_e) and phosphate adsorption capacity (Q_t) calculated from the experimental data are presented in **Figure 5**.

The removal of phosphate from the wastewater system increased as the initial pH value was increased. The highest adsorption occurred in an alkaline condition with a pH value of 12, while the phosphate intake was lowest in an acidic condition (pH = 3). No significant variation in phosphate removal efficiency was observed in a pH range of 7–9. This trend is similar to results from a previous study [31] using EMR–CSH as an adsorbent. Other research has also shown that pH is an important factor that determines phosphate adsorption using calcium silicate compounds [24,35,37,38,39,40].

The results are potentially due to the existence of different phosphate species in different pH conditions. Phosphate usually occurs as hydrogen phosphate (HPO_4^{2-}) in an alkaline condition, while it exists as dihydrogen phosphate (H_2PO_4^-) and phosphoric (H_3PO_4) in acidic conditions [24,41]. The distribution of various phosphate species at different pH values is shown in Error! Reference source not found. [24].

A significant amount of Ca^{2+} ions were released during the adsorption process throughout the entire pH (3–12) range [42]. An increase in solution pH (>9) indicates an elution of Ca^{2+} due to the dissolution of calcium silicate material and a simultaneous release of OH^- ion [42]. As a result, Ca^{2+} , OH^- and HPO_4^{2-} developed a supersaturated condition and calcium phosphate species [43, 44] were precipitated. The solution was unsaturated at low pH (<5) to form potential calcium phosphate species [44].

The adsorption reaction can be described by the following equations [9]



Therefore, the adsorption process may occur at the interface between aqueous phosphate and CSB. The phosphate species replaced the hydroxyl ions on the surface of the adsorbent to create stable, distributed calcium phosphate species.

Phosphorous removal with different calcium compounds and the effect of their dosages

The adsorption process is most economically viable when the highest removal efficiency is achieved at the minimum dosage [9]. The effect of dosage on phosphate adsorption removal efficiency was assessed for the commonly used calcium containing materials $\text{Ca}(\text{OH})_2$ [10] and CaSiO_3 [18] in addition to CSB.

The adsorbent dosages were increased from 1 g L⁻¹ to 25 g L⁻¹ and the relationships between the dosage of calcium compounds and the removal efficiency of phosphate are shown in **Figure 7**. The results for CSB and CaSiO_3 showed similar trends. The removal efficiency increased as the dosage increased, and the maximum removal efficiency obtained using either CSB or CaSiO_3 was at a dosage of 20 g L⁻¹. However, the removal efficiency for each of these adsorbents at a dosage 25 g L⁻¹ declined slightly. The removal efficiency of CSB was lower than CaSiO_3 , possibly due to impurities present in the CSB residue sample. Excellent removal efficiency (99%) was obtained using even a low $\text{Ca}(\text{OH})_2$ dosage of 1 g L⁻¹, and this was maintained for all doses. **Figure 8** shows the adsorption capacity of the CSB in addition to removal efficiency. This decreased significantly for dosages of 10 g L⁻¹ or more, indicating that the full adsorption capacity of CSB is not being used at higher dosages. Based on these results, the dosage of CSB selected for further experiments was 20 g L⁻¹.

Effect of adsorption time

Adsorption time strongly affects the process of adsorption. Therefore, it is essential to evaluate the effect of time on the phosphate adsorption performance using CSB [9,21,36,25]. To study the impact of adsorption time on the phosphate removal efficiency of CSB, an adsorption experiment was run with an initial pH of 12, a temperature of 25°C, a CSB dose of 20g L⁻¹, and a 100-rpm stirring speed.

Supernatants were collected at adsorption times between 0.5 and 168 hours, and the residual concentrations of phosphate were determined. Figure 9 illustrates phosphate removal efficiency as a function of adsorption time. The phosphate removal progressed slowly at the beginning of the reaction (0.5 to 2 hours). As a result, the residual concentration of phosphate did not decrease significantly. The removal efficiency rapidly increased from 2 to 24 hours and the maximum removal efficiency of 99.9% was achieved after 24 hours of adsorption. After that, the removal efficiency did not vary until the end of the experiment at 168 hours since the adsorption process had reached an equilibrium. The adsorption capacity of CSB in this experiment was 4.93 mg g^{-1} .

Phosphate adsorption mechanism

Figure 10 and Figure 11 show equations 4 and 6 for the Lagergren pseudo-first-order model and the Lagergren pseudo-second-order model, respectively, for the adsorption of phosphate on CSB for 30-1440 min at 25°C . The equilibrium rate constant of the pseudo-first-order model (k_1) was estimated to be 0.0088 min^{-1} and the equilibrium rate constant of the pseudo-second-order model (k_2) was 0.1641 min^{-1} . The pseudo-first-order equation fitted the experimental data better with a correlation coefficient $R^2 = 0.9608$ compared with $R^2 = 0.9286$ for the second-order equation.

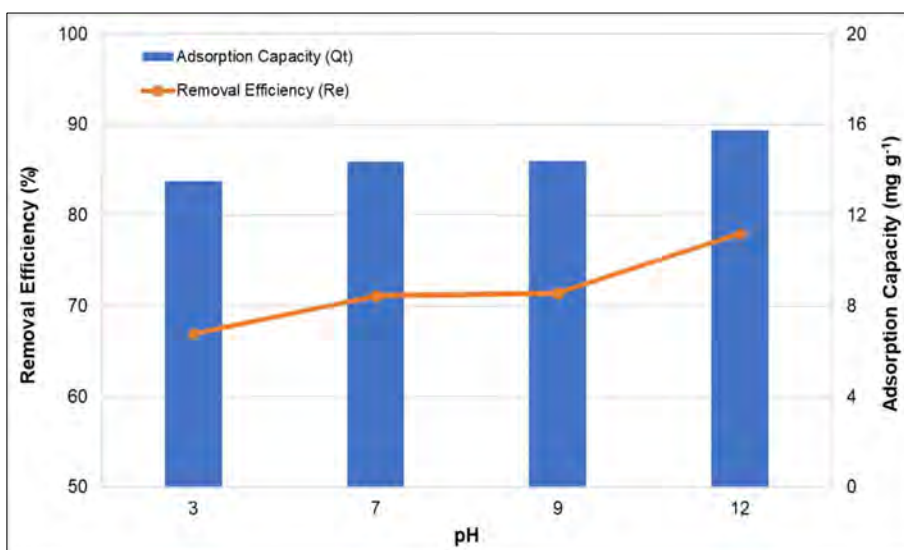


Figure 5: Effect of pH value on phosphate adsorption (initial phosphate concentration - 100 mg L^{-1} ; adsorbent dose - 5 g L^{-1} ; adsorption time - 24 hours; temperature - 25°C ; and stirring speed - 100 rpm)

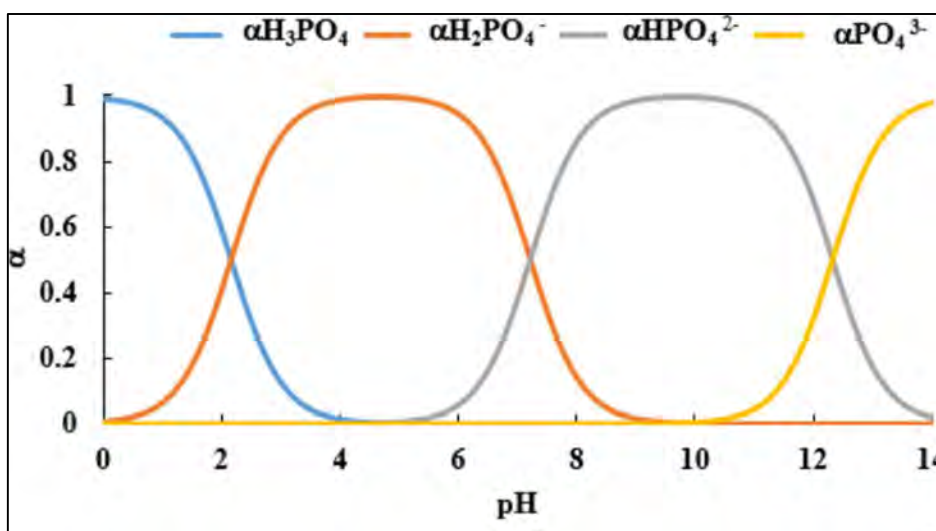


Figure 6: Existence of phosphate species as a function of pH in natural environment ^[24] (α is the distribution co-efficient)

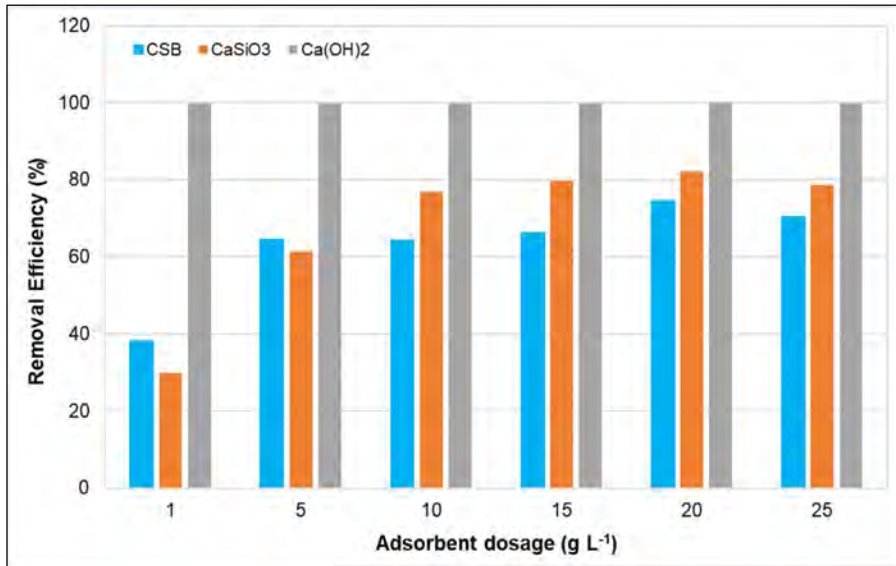


Figure 7 : Effect of different calcium compound's dosage on phosphate removal (initial phosphate concentration -100 mg L⁻¹; initial pH – 4.83; adsorption time - 24 hours; temperature at 25 °C; and stirring speed -100 rpm)

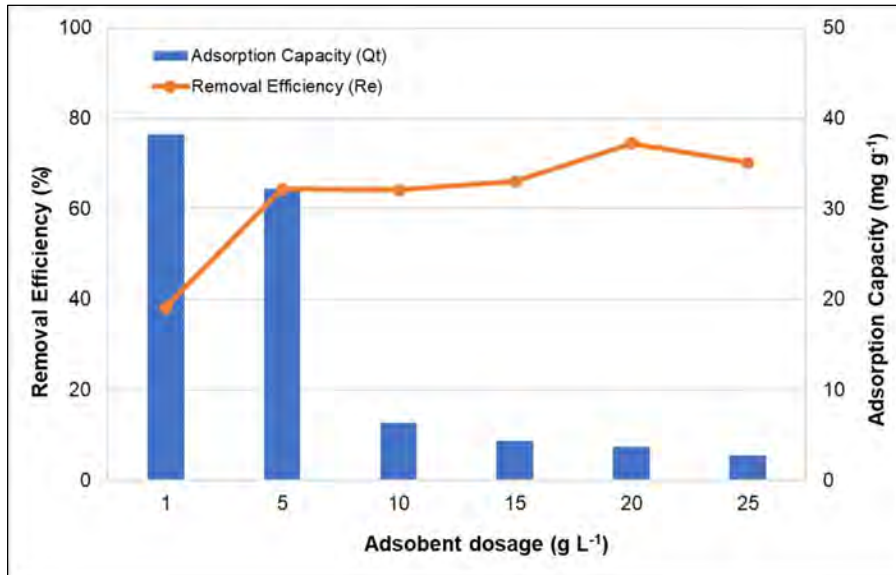


Figure 8: Effect of CSB dosage on phosphate removal efficiency and its adsorption capacity (initial phosphate concentration -100 mg L⁻¹; initial pH – 4.83; adsorption time - 24 hours; temperature at 25 °C; and stirring speed -100 rpm)

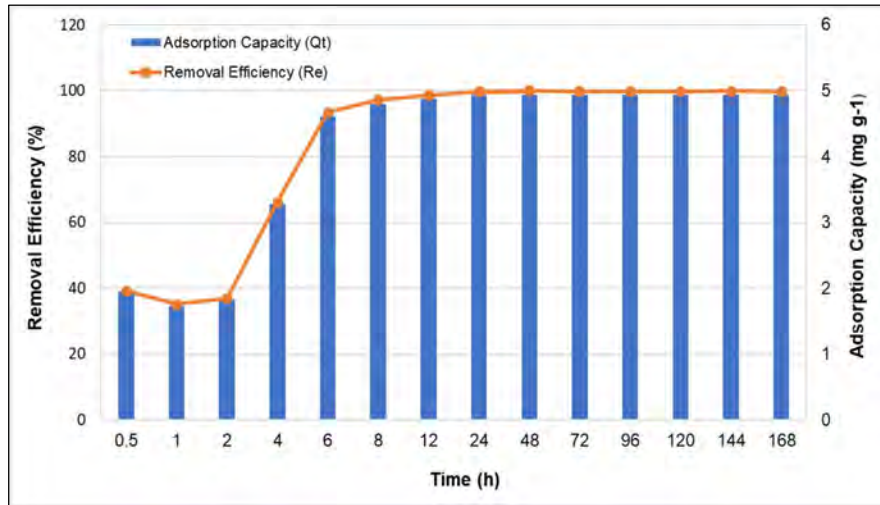


Figure 9: Effect of adsorption time on phosphate removal efficiency and its adsorption capacity (initial phosphate concentration -100 mg L⁻¹; initial pH – 12; adsorption time - 24 hours; temperature at 25 °C; adsorbent dose - 20 g L⁻¹; pH - 12).

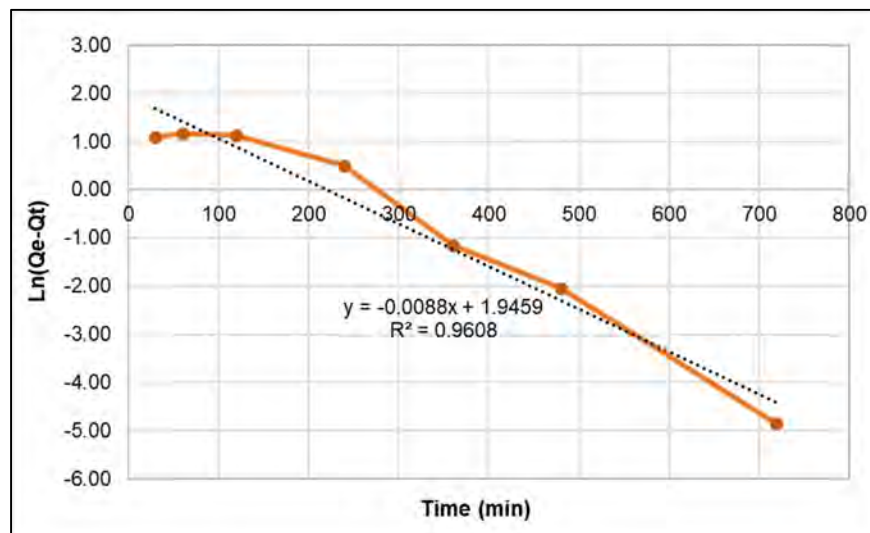


Figure 10: Lagergren pseudo-first-order kinetics adsorption for phosphorus by CSB.

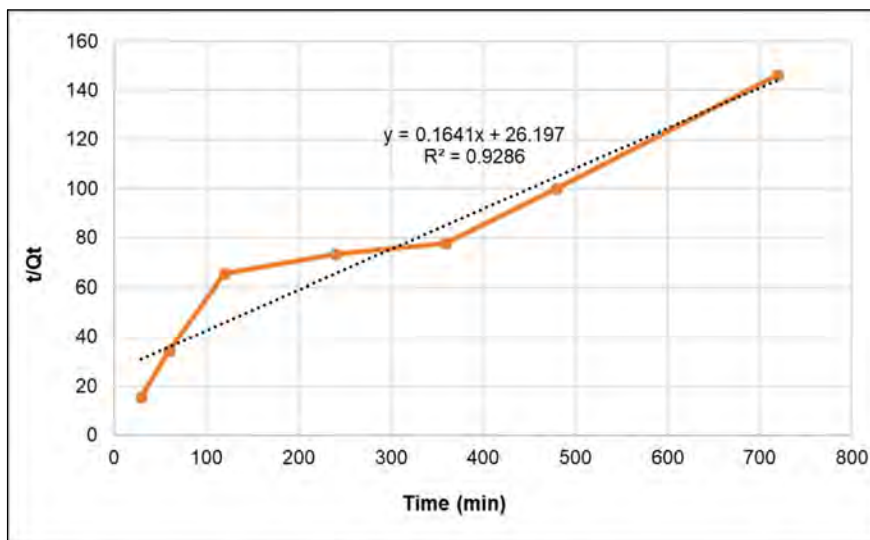


Figure 11: Lagergren pseudo-second-order kinetics adsorption for phosphorus by CSB.

Toxic metals adsorption

An investigation was carried out to observe toxic element adsorption utilising CSB from simulated toxic metal-contaminated water, as adsorption is one of the most effective ways to remove different kinds of pollutants, including toxic metals, from water [45].

The removal efficiency of the selected toxic materials using CSB is shown in **Figure 12** for 24 hours adsorption time, at 25°C. This figure shows the results obtained for Cu, As, Cd, Hg, Pb and Zn. For mercury (Hg), a removal efficiency of ≈ 60% was obtained and the removal efficiencies for other toxic metals (Cu, As, Cd, Pb, Zn) were in the range 10 to 20%.

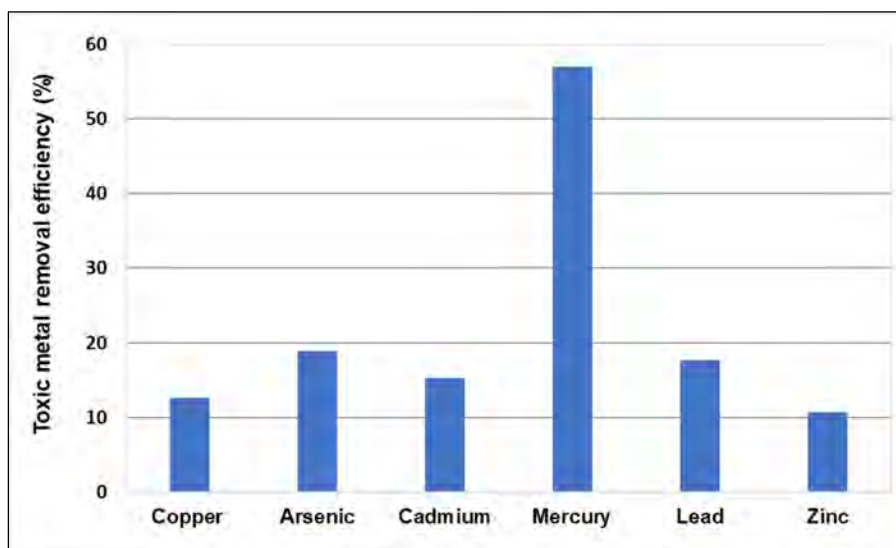


Figure 12: Removal efficiency of toxic elements using LieNA[®] derived CSB (adsorption time of 24 hours, temperature at 25°C; adsorbent dose of 5 g L⁻¹; and stirring speed -100 rpm)

CONCLUSIONS

This study investigated the adsorptive removal of phosphate from simulated wastewater by CSB, a metallurgical residue generated by the LieNA[®] process. CSB primarily consists of Na, Ca, and Si. It was shown to remove phosphate from wastewater with a high removal efficiency of 99% using an initial phosphate concentration of 100 mg L⁻¹, an adsorption time of 24 hours, a temperature of 25 °C, an adsorbent dose of 20 g L⁻¹ and an initial pH of 12. CSB also showed removal efficiencies of ≈ 60% for Hg and 10-20% for Cu, As, Cd, Pb and Zn for simulated toxic wastewater.

This investigation has therefore developed the foundation for an environmentally friendly use of solid LieNA[®] CSB residue as an adsorbent for wastewater treatment.

REFERENCES

1. Manschadi, M. A., Kaul H-P., Vollmann, J., Eitzinger J., Walter, W., 2014. Developing phosphate-efficient crop varieties—An interdisciplinary research framework. *Field Crops Research* 162, 87-98.
2. Simpson, R., 2019. Phosphate: a finite resource essential for life, critical for agriculture and food security. Web Page. <https://www.csiro.au/en/news/all/articles/2019/june/phosphorous>.
3. Chan, T.H., 2023. Phosphate: The Nutrition Source. Web Page. <https://www.hsph.harvard.edu/nutritionsource/phosphate>.
4. Taweekarn, T., Wongniramaikul, W., Choodum, A., 2022. Removal and recovery of phosphate using a novel calcium silicate hydrate composite starch cryogel. *Journal of Environmental Management* 301, 113923.
5. MS Calvo, KL Tucker., 2013. Is phosphate intake that exceeds dietary requirements a risk factor in bone health? *Annals of the New York Academy of Sciences* 1301(1), 29-35.
6. Vorland, C.J., Stremke, E.R., Moorthi, R.N., Hill Gallant, K.M., 2017. Effects of excessive dietary phosphate intake on bone health. *Current osteoporosis reports* 15(5), 473-82.
7. Guan, W., Ji, F., Chen, Q., Yan, P., Pei, L., 2013. Synthesis and Enhanced Phosphate Recovery Property of Porous Calcium Silicate Hydrate Using Polyethylene glycol as Pore-generation Agent. *Materials (Basel)* 6(7), 2846–2861.

8. Stackpoole, S. M., Stets, E. G., Sprague, L. A., 2019. Variable impacts of contemporary versus legacy agricultural phosphate on US river water quality. *Proceedings of the National Academy of Sciences* 116 (41), 20562-20567.
9. Gizaw, A., Zewgec, F., Chebudec, Y., Tesfayeb, M., Mekonnen, A., 2022. Phosphate abatement using calcium silicate hydrate synthesized from alum factory solid waste residue. *Separation Science and Technology* 57 (11), 1669-1687.
10. Lee, C.-G., Alvarez, P. J., Kim, H.-G., Jeong, S., Lee, S., Lee, K.B., 2018. Phosphorous recovery from sewage sludge using calcium silicate hydrates. *Chemosphere* 193, 1087-1093.
11. Almanassra, I. W., Kochkodan, V., Subeh, M., McKay, G., Atieh, M., Al-Ansari, T., 2020. Phosphate removal from synthetic and treated sewage effluent by carbide derive carbon. *Journal of Water Process Engineering* 36 ,101323.
12. Almanassra, I. W., Kochkodan, V., McKay, G., Atieh, M. A., Al-Ansar, T., 2021. Review of phosphate removal from water by carbonaceous sorbents. *Journal of Environmental Management* 287 ,112245.
13. Chen, Zhi-Gang., Li, Su-Mei., Chen, J., Wan, Hui-Yun., Lin, Wan-Xia., Wang M., Du, Jian-De. ,2023. The effects of phosphate concentration on the recovery of phosphate from alkaline solution by hydrated lime and calcined oyster shell: recovery efficiency, capacity, and hydroxyapatite purity. *Environmental Advances* 12 ,100363.
14. Hedstrom, A., 2006. Wollastonite as reactive filter medium for sorption of wastewater ammonium and phosphate. *Environmental Technology* 27 (7), 801-809.
15. Zhang, Z., Wang, X., J. Zhao, J., 2019. Phosphate recovery from wastewater using calcium silicate hydrate (CSH): sonochemical synthesis and properties. *Environmental Science: Water Research & Technology* 5 (1),131-139.
16. Sheffield, R.E., Moreira, V.R., LeBlanc, Brian D., Davis, T., 2010. Lime Precipitation and Phosphate Removal from Dairy Wastewater. Webpage.
17. Virta R.L., Van Gosen B.S., 2001. Wollastonite—A Versatile Industrial Mineral. Unite States Geological Survey Factsheet.
18. Brooks, A. S., Rozenwald M. N., Geohring, L. D., Lion, L. W., Steenhuis, T. S., 2000. Phosphate removal by wollastonite: A constructed wetland substrate. *Ecological Engineering* 15 (1), 121-132.
19. Zhao, Y., Chen, H., Q. Yan, 2017. Enhanced phosphate removal during the simultaneous adsorption of phosphate and Ni²⁺ from electroless nickel wastewater by calcium silicate hydrate (CSH). *Environmental Technology & Innovation* 8, 141-149.
20. Peng, L., Dai, H., Wu, Y., Peng, Y., Lu, X., 2018. A Comprehensive Review of the Available Media and Approaches for Phosphate Recovery from Wastewater. *Water, Air & Soil Pollution* 229, 1-28.
21. Fang, D., Huang, L., Fang, Z., Zhang, Q., Shen, Q., Li, Y., Xu, X., Ji, F., 2018. Evaluation of porous calcium silicate hydrate derived from carbide slag for removing phosphate from wastewater. *Chemical Engineering Journal* 354 ,1-11.
22. Jiang, D., Amano, Y., Machida, M., 2017. Removal and recovery of phosphate from water by calcium-silicate composites-novel adsorbents made from waste glass and shells. *Environmental Science and Pollution Research* 24 (9), 8210-8218.
23. Kuwahara, Y., Yamashita, H., 2017. Phosphate removal from aqueous solutions using calcium silicate hydrate prepared from blast furnace slag. *Isij International* 57 (9),1657-1664.
24. Azam, H. M., Alam, S. M., Hasan, M., Yameogo, D. D. S., Kannan, A. D., Rahman. A., Kwon, M.J., 2019. Phosphorous in the environment: characteristics with distribution and effects, removal mechanisms, treatment technologies, and factors affecting recovery as minerals in natural and engineered systems. *Environmental Science and Pollution Research*.
25. Zhao, Y., Wang, J., Luan, Z. K., et al., 2009. Removal of phosphate from aqueous solution by red mud using a factorial design. *Journal of Hazardous Materials* 165 (1–3), 1193–1199.
26. Aziz, K. H. Hama., Mustafa, F. S., Omer, K. M., Hama, S., Hamaraw, R. F., Rahman, K. O., 2023. Heavy metal pollution in the aquatic environment: efficient and low-cost removal approaches to eliminate their toxicity: a review. *RSC Adv* 13 (26), 17595-17610.
27. Qasem, N. A. A., Mohammed, R. H., Lawal, D. U., 2021. Removal of heavy metal ions from wastewater: a comprehensive and critical review. *NPJ Clean Water* 4(1), 36.
28. Shao, N., Lia, S., Yana, F., Sua, Y., Fei Liua, F., Zhanga, Z., 2020. An all-in-one strategy for the adsorption of heavy metal ions and photodegradation of organic pollutants using steel slag-derived calcium silicate hydrate. *Journal of Hazardous Materials* 382 ,121120.
29. Shao, N., Tang, S., Liu, Z., Li, L., Yan, F., Liu, Li, S., Zhang, Z., 2018. Hierarchically structured calcium silicate hydrate-based nanocomposites derived from steel slag for highly efficient heavy metal removal from wastewater, *ACS Sustain. Chem. Eng.* 6, 14926–14935.
30. Valenzuela, F., Quintana, G., Briso, A., Ide, V., Basualto, C., Gaete, A., Montes, G.,2021. Cu (II), Cd (II), Pb (II) and As (V) adsorption from aqueous solutions using magnetic iron-modified calcium silicate hydrate: Adsorption. *Journal of Water Process Engineering* 40 ,101951.

31. Le, Q. T., Vivas E. L., Cho, K., 2021. Calcium oxalate/calcium silicate hydrate (Ca-Ox/C-S-H) from blast furnace slag for the highly efficient removal of Pb⁺² and Cd⁺² from water. *Journal of Environmental Chemical Engineering* 9, 106287.
32. Gupta, S.S., Bhattacharyya, K.G., 2011. Kinetics of adsorption of metal ions on inorganic materials: a review. *Advances in colloid and interface science* 162 (1-2), 39-58.
33. Kowanga, K. D., Gatebe, E., Mauti, G. O., Mauti E. M., 2016. Kinetic, sorption isotherms, pseudo-first-order model and pseudo-second-order model studies of Cu (II) and Pb (II) using defatted *Moringa oleifera* seed powder. *The journal of phytopharmacology* 5 (2), 71-78.
34. Taweekarn, T., Wongniramaikul, W., Choodum, A., 2022. Removal and recovery of phosphate using a novel calcium silicate hydrate composite starch cryogel. *Journal of Environmental Management* 301, 113923.
35. Chen, M., Huo, C., Li, Y., Wang, J., 2016. Selective adsorption and efficient removal of phosphate from aqueous medium with Graphene-Lanthanum composite. *ACS Sustainable Chemistry & Engineering* 4, 1296-1302.
36. Li, C., Yu, Y., Li, Q., 2019. Kinetics and equilibrium studies of phosphate removal from aqueous solution by calcium silicate hydrate synthesized from electrolytic manganese residue. *Adsorption Science & Technology* 37, 547-565.
37. Choi, J. W., Choi, Y. S., Hong, S. W., Kim, D. J., Lee, S. H. 2012. Effect of pH and coexisting anions on removal of phosphate from aqueous solutions by inorganic-based mesostructures. *Water Environment Resource* 84 (7), 596-604.
38. Bian, Y., Chen, X., Ren, Z.J., 2020. pH dependence of phosphate speciation and transport in flow-electrode capacitive deionization. *Environmental Science & Technology* 54 (14), 9116-9123.
39. Vilela, H.S., Rodrigues M.C., Fronza, B.M., Teinca, R.B., Vichi, F. M., Braga, R.R., 2021. Effect of temperature and pH on calcium phosphate precipitation. *Crystal Research and Technology* 2021 56 (12), 2100094 (1-9).
40. Ferguson, J.F., Jenkins, D., Eastman, J., 1973. Calcium phosphate precipitation at slightly alkaline pH values. *Water Pollution Control Federation* 45 (4), 620-631.
41. Zhang, Z., Yan, L., Yu, H., Yan, T. Li, X., 2019. Adsorption of phosphate from aqueous solution by vegetable biochar/layered double oxides: Fast removal and mechanistic studies. *Bioresource Technology* 284, 65-71.
42. Guan, W., Ji, F., Chen, Q., Yan, P., Zhang, Q., 2013. Preparation and phosphorus recovery performance of porous calcium-silicate-hydrate. *Ceramics International* 39, Issue 2, 1385-1391.
43. Kuwahara, Y., Yamashita, H., 2017. Phosphate removal from aqueous solutions using calcium silicate hydrate prepared from blast furnace slag. *ISIJ International* 57, Issue 9, 1657-1664.
44. Lei, Y., Song, B., Weijden, R. D. van der., Saakes, M., Buisman, C. J. 2017. Electrochemical induced calcium phosphate precipitation: importance of local pH. *Environmental science & technology* 51, Issue 19, 11156-11164.
45. Zamora-Ledezma, C., Negrete-Bolagay, D., Figueroa, F., Zamora-Ledezma, E., Ming, Ni., Alexis, F., 2021. Heavy metal water pollution: A fresh look about hazards, novel and conventional remediation methods. *Environmental Technology & Innovation* 22, 01504.

CLARIANT NEW GENERATION COLLECTORS FOR FLOTATION OF LITHIUM ORES

By

¹Matthew Pupazzoni, ²Wagner Silva, ³Suresh Raju Mudnuru

¹Clariant Mining Solutions, Australia

²Clariant Mining Solutions, USA

³Clariant Mining Solutions, UAE

Presenter and Corresponding Author

Matthew Pupazzoni

matthew.pupazzoni@clariant.com

ABSTRACT

Global demand for lithium has increased significantly in recent years due to a dramatic increase in the use of rechargeable lithium-ion batteries in a multitude of applications, including electric vehicles, electric power storage and electronic devices. Hard rock mining of pegmatites has emerged as a major source of lithium to meet this growing demand. The key minerals include spodumene, lepidolite and petalite, and they are often beneficiated via complex flowsheets using multiple techniques including dense media separation, magnetic separation, and froth flotation.

In the flow sheets for processing lithium ores, flotation is often used for processing fine particle size feed, for complex ore deposits, and where high-grade concentrates are required. Clariant Mining Solutions is focused on helping the mining industry deliver the minerals needed to enable the decarbonization megatrend in a sustainable way, and to this effect, Clariant has been working to develop a range of new collectors for more efficient flotation of spodumene and other challenging lithium ores. This paper presents some of the most recent developments.

Fatty acids are often used for lithium flotation; however, the grade and recovery achieved with these collectors is often below the desired level. Also, high dosages of fatty acids are often required, and residual fatty acids in the concentrates can impart a fatty odour to the lithium concentrate which is undesired during further processing into lithium carbonate or hydroxide. Fatty acid collectors can also cause formation of calcium soaps which give rise to filtration problems and the need for acid washing.

Clariant is using two strategies to develop improved lithium collectors. The first is to formulate collectors containing fatty acids but minimizing the negative effects of fatty acids, and the second strategy is to completely replace the fatty acids with alternative chemicals.

Modified fatty acid formulations can improve the metallurgical performance and significantly lower dosages, thereby minimizing the issues associated with residual fatty odour and soap formation while achieving lithium recoveries greater than those achieved with conventional fatty acid collectors at an improved grade.

Furthermore, Clariant's novel collectors that are free of fatty acids have been found to produce superior grade concentrates and improved recovery at less than half the dosage of fatty acid collectors. These collectors completely eliminate the residual fatty odour and have also shown improvements in the filtration efficiency of the final concentrate.

Keywords: Lithium, Flotation, Beneficiation, Fatty Odour

INTRODUCTION

Lithium is an important element in the world economy, with applications as diverse as glass and ceramics, lubricating greases and polymer synthesis⁽¹⁾. Recently, the development of rechargeable lithium-ion batteries, coupled with the global trend towards electrification of the transportation fleet, has led to a dramatic increase in the demand for lithium⁽²⁾. In addition to the production of lithium from brines, the production of lithium from hard rock ores is increasing, and flotation has proved to be an effective means for the beneficiation of many pegmatitic lithium ores⁽³⁾.

Fatty acids are often used for lithium flotation⁽⁴⁾; however, the grade and recovery achieved with these collectors is often below the desired level⁽⁵⁾. Also, high dosages of fatty acids are often required, and residual fatty acids in the concentrates can impart a fatty odour to the lithium concentrate which is undesired during further processing into lithium carbonate or hydroxide. Fatty acid collectors can also cause formation of calcium soaps which give rise to filtration problems and the need for acid washing.

Clariant is using two strategies to develop improved lithium collectors. The first is to formulate collectors containing fatty acids but minimizing the negative effects of fatty acids, and the second strategy is to completely replace the fatty acids with alternative chemicals.

In previous work, Clariant's collectors containing fatty acids but formulated to minimize the negative effects of fatty acids were described⁽⁶⁾. In those tests, spodumene rougher flotation tests were performed to compare a standard fatty acid to FLOTINOR™ 10339 (Figure 1 and Figure 2). The results showed that FLOTINOR™ 10339 was able to achieve the same grade at half the dose of the standard fatty acid (Figure 1). For example, with fatty acid dosed at 2000 g/ton, the grade achieved was 3.9% lithium oxide, and FLOTINOR™ 10339, was able to achieve the same grade at only 1000 g/ton.

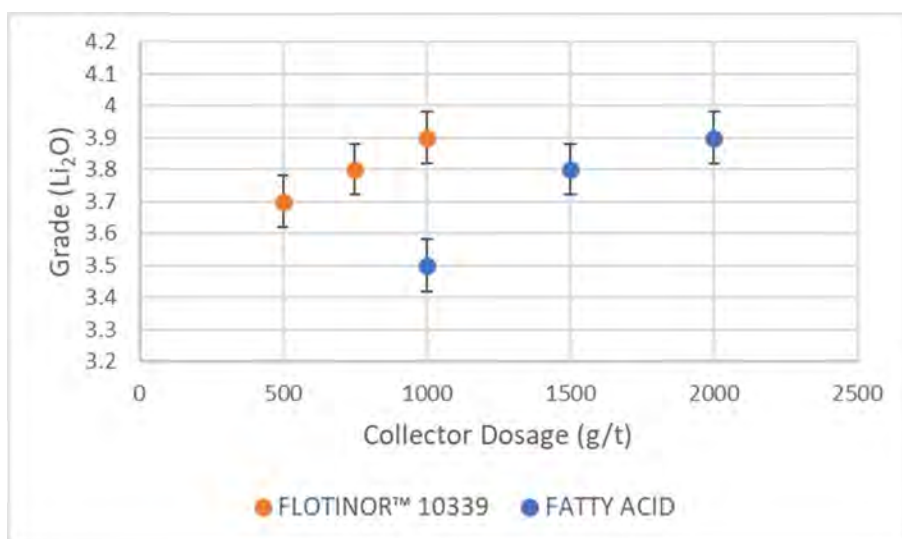


Figure 1: Grade vs Collector Dosage for Rougher Flotation Tests

The lithium rougher recovery results also showed that FLOTINOR™ 10339 was also able to achieve a higher recovery than a standard fatty acid at half the dosage (Figure 2). For example, at a 1500 g/ton fatty acid dosage, the lithium recovery was 90%, and FLOTINOR™ 10339, delivered a recovery of 92% at just 750 g/ton.

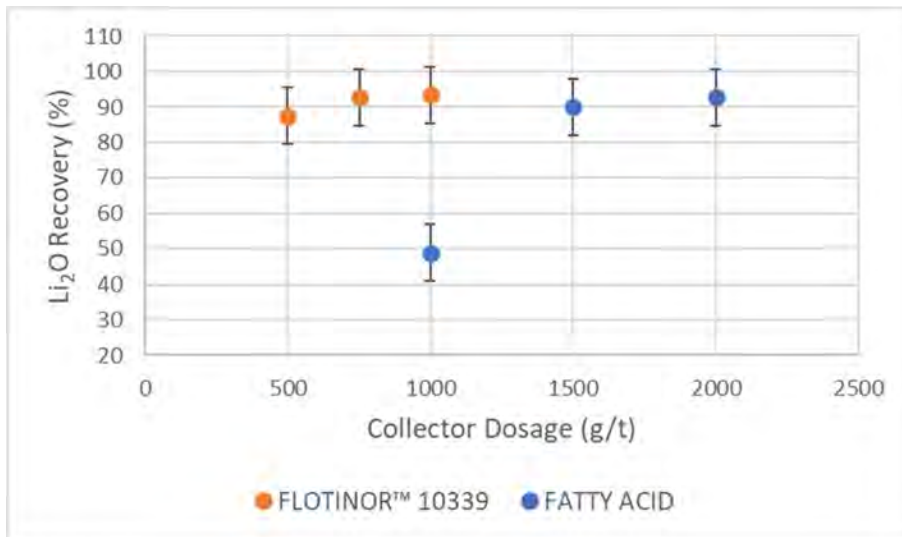


Figure 2: Recovery vs Collector Dosage for Rougher Flotation

In the previous work⁽⁶⁾, both spodumene rougher and cleaner tests were also performed to compare a standard fatty acid with FLOTINOR™ 10381 (Figure 3 and Figure 4). Although there was some variability in the results, FLOTINOR™ 10381 could achieve a grade of approximately 6%, which is higher than the fatty 5.5% that was achieved with a standard fatty acid (Figure 3). This showed that FLOTINOR™ 10381 was more selective against gangue minerals than the standard fatty acid.

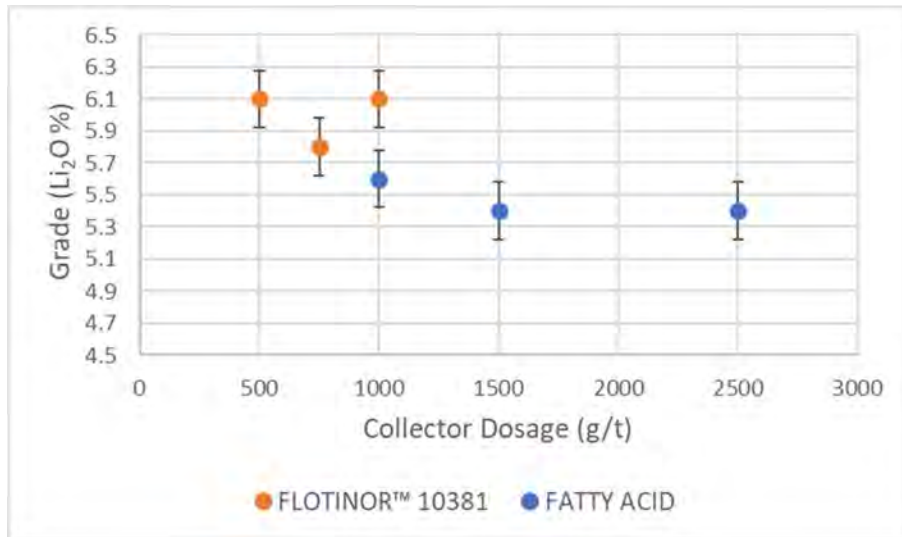


Figure 3: Grade vs Collector Dosage for Rougher and Cleaner Test

FLOTINOR™ 10381 also yielded a higher recovery than the standard fatty acid at all dosage points (Figure 4). As shown in Figure 4, FLOTINOR 10381 was dosed at 500, 750 and 100 g/ton, and the standard fatty acid was dosed at 1000, 1500, and 2500 g/ton, knowing that it would require higher dosages. At the only common dosage, 1000 g/ton, FLOTINOR™ 10381 delivered a dramatically higher recovery of 84.3% versus 65.3%. Increasing the dosage of the standard fatty acid to 2500 g/ton did increase the recovery to 78.6%, but FLOTINOR™ 10381 was able to achieve that same recovery (78.7%) at 500 g/ton, one fifth of the dosage of the standard fatty acid. Such a significant decrease in chemical consumption has multiple benefits, including reduced traffic and emissions from deliveries, requiring less packaging or smaller bulk tanks, and reducing the amount of collector that can plug filter screens.

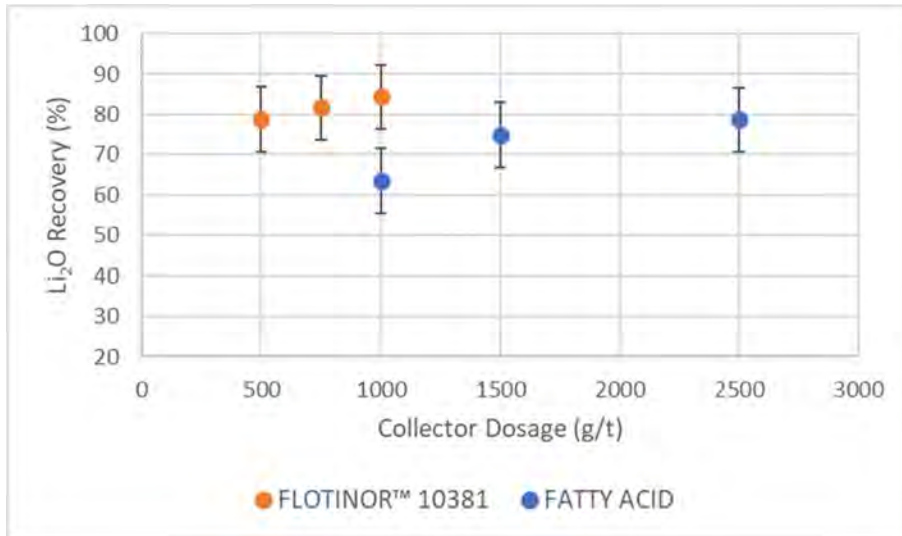


Figure 4: Recovery vs Collector Dosage for Rougher and Cleaner Test

RESULTS AND DISCUSSION

Spodumene Rougher Flotation

Spodumene rougher flotation tests were performed on a lithium ore containing spodumene to compare a standard fatty acid to Clariant's novel FLOTINOR™ 19010 spodumene collector that does not contain fatty acids. This collector is part of a range of novel collectors that are being evaluated to improve metallurgical performance as well reduce consumption of collector significantly compared to fatty acid collectors. These collectors not only achieve required metallurgical performance but also completely eliminate fatty odour in the lithium concentrate, which is undesired during further processing into lithium carbonate or hydroxide.

Spodumene rougher flotation tests were performed to compare a standard fatty acid to FLOTINOR™ 19010 (Figure 5 and Figure 6). The results show that FLOTINOR™ 19010 is able to achieve a similar grade at half the dose of the standard fatty acid (Figure 5). For example, at 1500 grams per tonne of fatty acid, the grade achieved is 4.35% lithium oxide, and FLOTINOR™ 19010, is able to achieve the same grade at only 800 g/ton. At all the dosages evaluated the novel collector could achieve similar grades at almost half dosage. Such a significant decrease in chemical consumption has multiple benefits, including reduced traffic and emissions from deliveries, requiring less packaging or smaller bulk tanks.

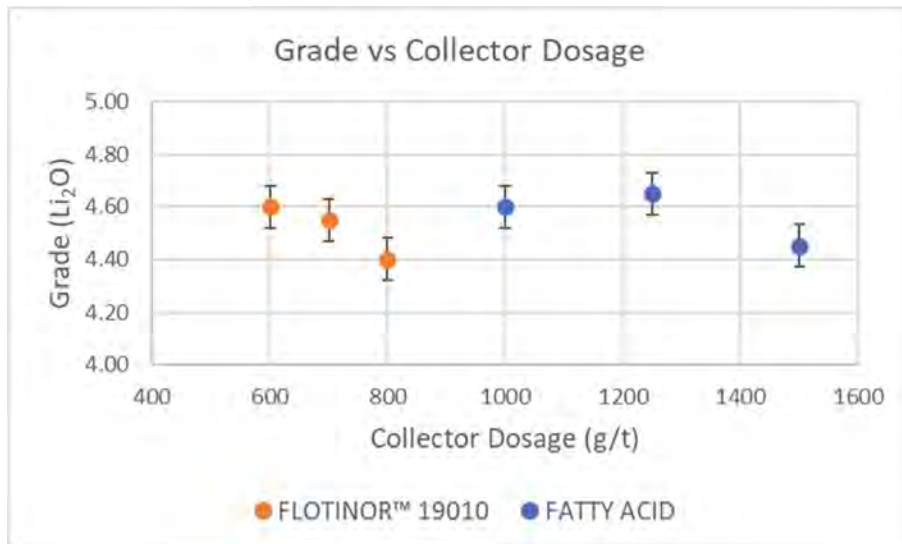


Figure 5: Grade vs Collector Dosage for Rougher Flotation Tests with Clariant's novel FLOTINOR™ 19010

The lithium rougher recovery results further shows that FLOTINOR™ 19010 is also able to achieve a higher recovery than a standard fatty acid at half the dosage (Figure 6). For example, at a dosage of 1500 g/ton of fatty acid, the lithium recovery is 62%, and FLOTINOR™ 10339, delivers a recovery of 66% at just 800 g/ton.

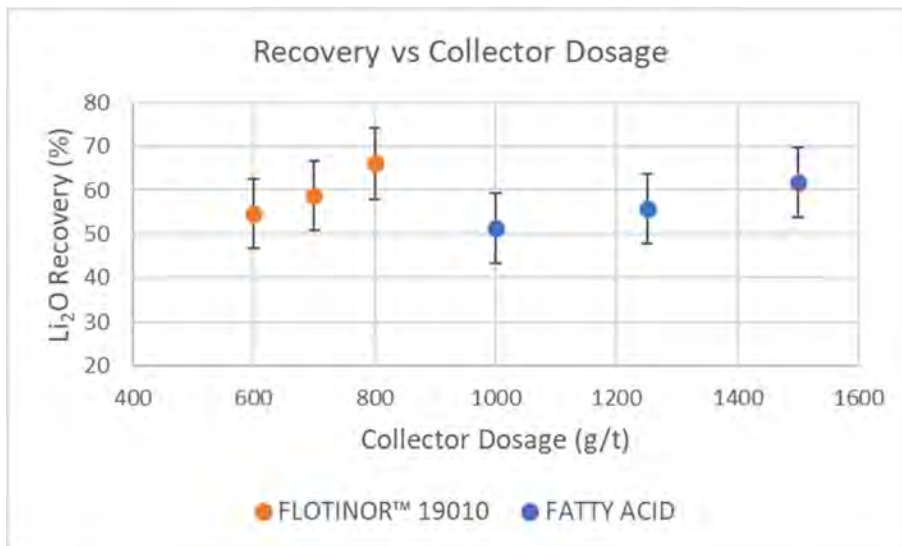


Figure 6: Recovery vs Collector Dosage for Rougher Flotation Tests with Clariant's novel FLOTINOR™ 19010

Clariant's novel FLOTINOR™ 19010 collector not only improved metallurgical performance and almost half of the standard fatty acid dosages, but also produces a lithium concentrate that is free of fatty odour, which is more desirable in further processing into lithium carbonate or hydroxide. Furthermore, FLOTINOR™ 19010 also eliminates the formation of calcium soaps which give rise to filtration problems and the need for acid washing.

METHODS

The flotation tests were conducted using the standard conditions in use at the mines where the ores were sourced. Most notably, long conditioning times were used in order to achieve effective attachment of the collectors on the spodumene surfaces.

Rougher Test

The ore was crushed to -3.35 mm and split into 1.3 kg lots. For each flotation test the sample was ground to a P80 of 150 µm and deslimed in a 600 x 140mm cylindrical column. After mixing in the column and allowing the slurry to settle for a predetermined time, the top 525 mm of slimes pulp was decanted off. The remaining coarse settled pulp was transferred to a 2 L Agitair cell. The pulp was conditioned for 10 minutes at 1000 rpm with the required amount of collector and 1.2 ml of 8% soda ash solution. Three rougher cons were collected at 30 seconds, 1-minute and 1-minute intervals. Lithium assays were performed at an external laboratory by peroxide fusion using ICP-AES.

Rougher and Cleaner Test

The ore was crushed to -3.35 mm and split into 1.3 kg lots. For each flotation test the sample was ground to a P80 of 150 µm and deslimed in a 600 x 140mm cylindrical column. After mixing in the column and allowing the slurry to settle for a pre-determined time, the top 525 mm of slimes pulp was decanted off. The remaining coarse settled pulp was transferred to a 2 L Agitair cell. The pulp was conditioned for 10 minutes at 1000 rpm with the required amount of collector and 1.2 ml of 8% soda ash solution.

The rougher flotation was conducted for 3 minutes, followed by a 3 minute cleaner flotation. Lithium assays were performed at an external laboratory by peroxide fusion using ICP-AES.

CONCLUSIONS

Several FLOTINOR™ collectors for lithium ores have been developed that deliver an equal or better grade and recovery of lithium compared to standard fatty acids at almost half the dose. In addition to the improved metallurgical performance, the lower dose of FLOTINOR™ collector could reduce or eliminate the need for downstream acid washing processes that are often required when using fatty acids and may improve filtration performance. The novel Clariant FLOTINOR™ 19010, part a new range of collectors that do not include fatty acids in the composition, not only improves metallurgical performance but also eliminates fatty odour from the lithium concentrate.

REFERENCES

1. Gunther Martin, L. R. (2017). Lithium market research - global supply, future demand and price development. *Energy Storage Materials*, 6, 171-179.
2. Laurence Kavanagh, J. K. (2018). Global Lithium Sources - Industrial Use and Future in the Electric Vehicle Industry: A Review. *Resources*, 7, 57.
3. Bogale Tadesse, F. M. (2019). The beneficiation of lithium minerals from hard rock ores: A review. *Minerals Engineering*, 131, 170-184.
4. Rui Sousa, V. R. (2019). Flotation of lithium ores to obtain high-grade concentrates. Are there any mineralogical limitations? *International Journal of Mining, Materials, and Metallurgical Engineering (IJMME)*, 5, 7-18.
5. Longhua Xu, Y. H. (2016). Surface crystal chemistry of spodumene with different size fractions and implications for flotation. *Separation and Purification Technology*, 169, 33-42.
6. Raju, M. S. (2022). The lure of lithium. *Global Mining Review*, March, 10-16.

RETHINKING POWDER HANDLING IN CRITICAL MINERALS PROCESSING: DESIGNING FOR ROBUSTNESS AND VALUE RETENTION

By

Tristan Bower, Rhys Walker

Floveyor, Australia

Presenter and Corresponding Author

Tristan Bower
Tristan.b@floveyor.com

ABSTRACT

The increasing demand for critical minerals, encompassing lithium, nickel sulphate, rare earths, graphite, and vanadium, underscores the importance of overcoming operational hurdles in mineral refineries. Effective powder handling at the end of the production stream is essential to maintaining the integrity of these valuable products and ensuring consistent plant operation.

Conveying systems play a central role in the quality of the final product. Impurities in the input materials and suboptimal conditions during mineral processing can lead to sizeable and expensive complications, including agglomeration, surface deposition, and moisture problems, potentially disrupting operations and impacting the quality of the final product.

To mitigate these risks, a shift in design philosophy is required, from anticipating optimal conditions to preparing for worst-case scenarios. Incorporating strategies in the process, such as redundancy lines, inline material conditioning, non-stick coatings, and strategic maintenance measures, can significantly enhance plant resilience. Furthermore, acknowledging powder handling as an integral part of the process, rather than an ancillary concern, is vital for ensuring robust and efficient operations.

The stakes are high, considering the commercial value of these critical minerals. Any compromise in product integrity due to structural damage, contamination, or operational disruptions can lead to major financial losses. Investing in resilient plant design and robust powder handling systems contributes to maximising returns while safeguarding both the integrity of these valuable mineral products and the continuity of refinery operations.

This presentation delves into downstream processing, highlighting the critical role of innovative, industrial powder handling systems to ensure value retention and operational reliability in the processing of critical minerals.

Keywords: *Mineral processing, Downstream processing, Powder handling, Conveying systems, Process line*



**Rethinking powder handling
in critical minerals processing:
Designing for robustness,
value retention & innovation**

Tristan Bower, Floveyor Pty Ltd
tristan.b@floveyor.com

**Exploring how to advance powder
handling in critical minerals processing.**

**The importance of proactive
collaboration and adapting to operational
challenges from the start.**

Bulk materials handling experience

1958

Operating since 1958

WA 7,000+

Headquartered in Perth

7,000+

Installations

52

Countries

40

Regional partners

Our materials handling industries



Food and Beverage



Agriculture



Critical Minerals



Manufacturing



Mining and Resources



Chemical Processing

Our critical minerals experience



Nickel sulphate



Cobalt sulphate



Lithium hydroxide monohydrate



Rare earths



Graphite



Sodium sulphate

Impact analysis on key issues of process design



HSE & Plant Reliability



Product Yield



Throughput



1. HSE & Plant Reliability



Process conditions impact product



Impact

- Decrease in equipment availability
- Overall Equipment Effectiveness (OEE) and ROI
- OPEX creep



Remedy

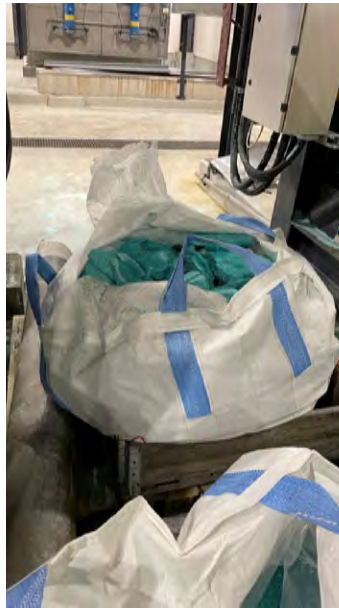
- Test, test, test
- Benchmark against plants in other industries using materials with similar characteristics
- Bring in experts with experience of similar challenges



Lean on vendors' experiences of similar conditions

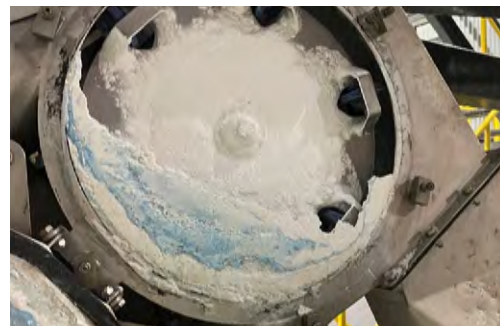
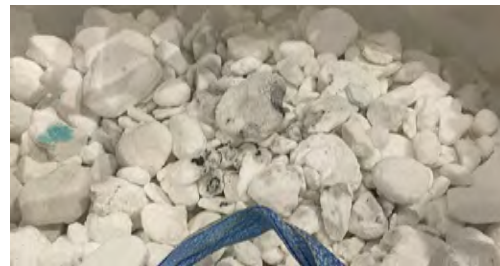
Example 1: Decrease in equipment availability

Tender specifications	
Bulk density	1,350 kg/m ³
Crystal size distribution	D10: 600 µm D50: 900 µm D90: 1,200 µm
Physical appearance	Free flowing
Moisture	<0,2 % (free)



Example 2: Decrease in equipment availability

Tender specifications	
Bulk density	1,050 kg/m ³
Crystal size distribution	D10: 600 µm D50: 1,500-1,800 µm D90: 2,400 µm
Physical appearance	Free flowing
Moisture	<0,2 % (free)





Refined materials are more toxic, reactive - and valuable



Impact

- Injuries, downtime, and labour shortages
- Product contamination



Remedy

- Select equipment that isolates operators from materials
- Keep on top of process innovations



OEMs have insights on designing for safety and innovation

Example 3: Product contamination / spillage





Getting plant back online after a shutdown



Impact

- Extended unplanned downtime
- Technicians and parts not readily available extend downtime
- Damage to upstream equipment if conveyors go offline



Remedy

- Plan for the unplanned.
- Consider equipment, parts, labour, and access for unplanned stoppage
- How long does key equipment take to bring back online?

 **Ask vendors for options to minimize start-up time**



2. Product Yield



Out of spec product



Impact

- Product yields decrease
- Product requires rework or even dumping
- Inferior materials must be removed to get plant operating at full capacity



Remedy

- Take a helicopter view of the whole process
- Determine how a marginal quality product affects downstream process



Call the OEM, chances are they already have a benchmark reference



Process design creates contamination risks



Impact

- Ferrous contamination
- CO2 exposure
- Moisture, air impurities



Remedy

- Reduce product exposure to contact surfaces
- Ensure most efficient conveying route
- Borrow design philosophies from food and life science industries



Ask OEMs about manufacturing standards in other industries



Tenders only consider perfect specifications and conditions



Impact

- Underperforming equipment
- Premature ageing of equipment



Remedy

- Include 'out of spec' conditions in design discussions
- Consider how 'out of spec' products can be reworked



Bring vendors together to make a holistic assessment of your plant



3. Throughput



Minimum, maximum and nominal rates are not accounted for



Impact

- Plant trips from material floods or trickles
- Product degradation that requires removal



Remedy

- Scenario and stress test across the process
- Add effective bi-product removal to the process design



Consult with OEMs for operational limits on equipment

Example 4: Specification vs Instantaneous rates

Material crystallization capacity

Tender Specification	24.5 tph
Conveyor specification	27.5 tph
Instantaneous rates experienced	0 - 40 tph



Key areas of equipment design are not understood



Impact

- Storage of raw materials can change flow dynamics, leading to build-up and blocking



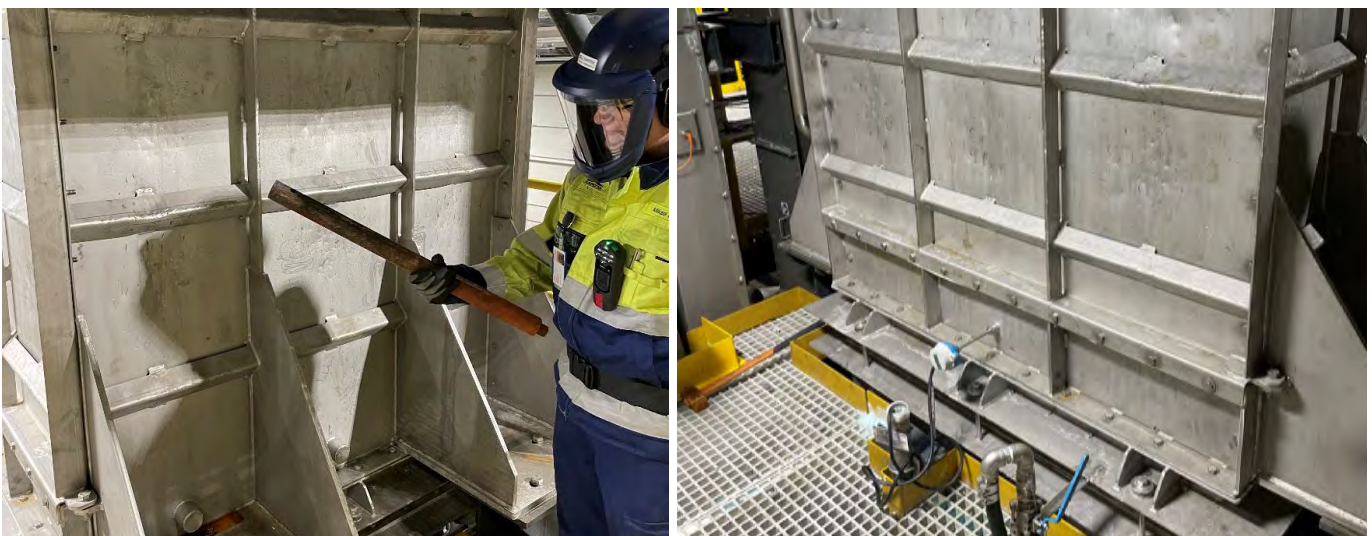
Remedy

- Get specific about material handling designs



Vendors can suggest ways to optimise equipment for the required use in the flowsheet

Example 5: Material blockage in storage



Example 6: Material blocks in storage



Design lacks process redundancies



Impact

- Throughput cannot be diverted in event of unplanned downtime or maintenance



Remedy

- Integrate process redundancies



Explore the benefits of redundancies during process design

No one has all the answers.

EPCs, vendors, OEMs, and resource companies must work together.

For each project ask:

1. How well are the materials, products and bi-products understood?
2. What levels of redundancy need to be factored in?
3. How can we leverage powder handling experience early in the design?

PROCESSING AND DISPOSAL OF RESIDUES COMPRISING NATURALLY OCCURRING RADIOACTIVE MATERIAL (NORM)

By

Dr Hagen Gunther Jung

GeoEnergy Consult, Germany

Presenter and Corresponding Author

Dr Hagen Gunther Jung

hagen.jung@geoenergyconsult.com

ABSTRACT

Through mining/processing of Rare-Earths and further commodities like Uranium, Tantalum etc. NORM residues accumulate, posing radiological hazards and affecting the operational efficiency.

If all possibilities for minimization are exhausted, managing those requires a well-considered sequence of safe processing. NORM residues need to be (radiologically) characterised, optionally decontaminated and treated/conditioned, and finally disposed of in licensed facilities.

Regulators require well-planned measures as precondition for permitting. Moreover, a good management of NORM residues helps to avoid liability risks.

Removal of radionuclides from equipment and facilities (e.g. pipework for in-situ-leaching, other processing installations etc.) through decontamination leads to dose reduction for staff and public and prevents from any contamination spreading. In a technical view the huge advantage of removing radioactive contamination is:

- 1) Waste volume reduction, essential e.g. in the course of decommissioning: by decontamination only a residual fraction, then containing the separated radionuclides, requires further treatment as NORM waste while the largest part becomes eligible for disposal as cheaper conventional waste
- 2) Re-usability of spent equipment (which otherwise would have to be disposed of), thus minimizing the equipment consumption

Manual preparation and water-jetting are relatively mild and usually allow re-use of decontaminated equipment. By contrast, as chemical decontamination can employ reagents like phosphoric acid the opportunity for equipment re-use here needs to be verified specifically. Abrasive blasting with sand does usually not allow re-use due to the caused loss in material thickness. In general, all decontamination technologies can be conducted manually or are automated for higher throughput.

Important objectives of optional treatment, if indicated, are volume reduction and foremost fixation/immobilisation of radionuclides to prevent from spreading. For various residue types, different treatment or sequence of treatment options apply like radionuclide extraction, purification (of waste water), incineration or high-force compaction etc.

In the case this becomes necessary NORM residues are ready for final disposal, if treatment is accomplished. Often the state is assumed to be responsible for actual disposal, i.e. operations only deliver (treated) residues to licensed disposal facilities. However, e.g. in case of high volume it can be justified that operations have an own onsite disposal facility. Anyway, several disposal options are given, like backfill in mined-out underground voids or open pits, reinjection into original deposit (of flowable residues), surface/near-surface disposal (e.g. landfill) or underground disposal (e.g. co-disposal with radioactive waste).

Which option will be realized depends both on technical/radiological properties and on country-specific regulatory requirements.

Keywords: Naturally Occurring Radioactive Material NORM, Waste, Residues, Permitting, Decontamination, Purification, Immobilisation, Re-usability, Conditioning, Disposal

GeoEnergy Consult

Processing and Disposal of Residues comprising Naturally Occurring Radioactive Material (NORM)

Dr Hagen Gunther Jung, GeoEnergy Consult, Germany,
hagen.jung@geoenergyconsult.com



GeoEnergy Consult

Challenges caused by NORM

Monazite (Ce, La, Nd, Th) [PO₄]

- Compliance with [specific] regulatory requirements
- Radiological health/safety of workers and public
- Operational and long-term safe management of NORM waste

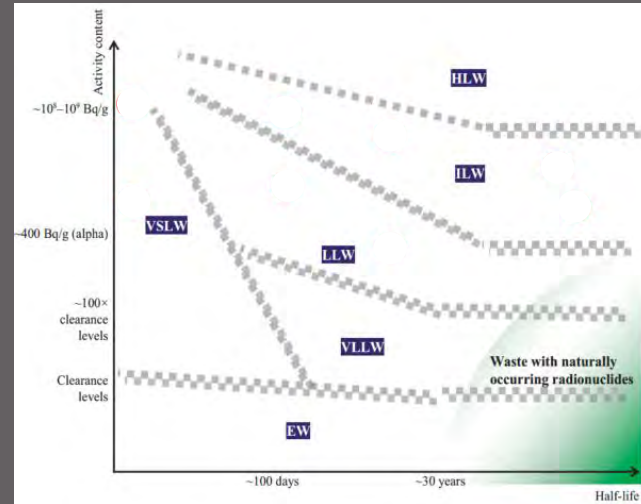


- Prevention of radionuclide spreading
- Avoiding contamination of site and facilities
- Prevention of undue environmental impact
- Avoidance of liability risks

GeoEnergy Consult

Radiological characteristics of NORM

- Usually long half-life
- Modest activity
 - > 1 Bq/g Disposal as NORM waste
 - [or restricted re-use/recycling if dose < 1 mSv/a]
 - < 1 Bq/g Disposal as conventional waste
 - [or unrestricted re-use/recycling]
- Internal Exposure (dominated by α -/ β -radiators)
 - Inhalation of dust
 - Ingestion of contamination



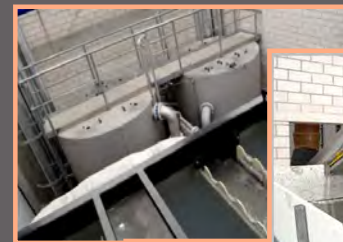
www.geoenergyconsult.com

GeoEnergy Consult

Generated NORM waste types:

- Waste rock below cut-off grade
- Scales
- Sediments from settling pond
- Inorganic process solutions
- Process residues
- Spent resins
- Spent organic solvents
- Tailings
- Mixed waste
- Contaminated components/facilities
- Contaminated bulk material (soil etc.)

- Below/above exemption limits ?
- Disposable after which treatment ?



www.geoenergyconsult.com

150/395

GeoEnergy Consult

NORM-affected Mining phases



www.geoenergyconsult.com

GeoEnergy Consult

Overcoming refusal of getting permitted

- Convince the *regulators* to be capable of safely managing NORM:
 - (1) *Radiation Protection Plan* to ensure occupational/public safety
 - (2) *Waste Management Plan* enables safe management of NORM
 - (3) *Preliminary Closure Plan* to prevent generation of future legacies

...



- Convince the *stakeholders* including the public, demonstrating sustainable safety



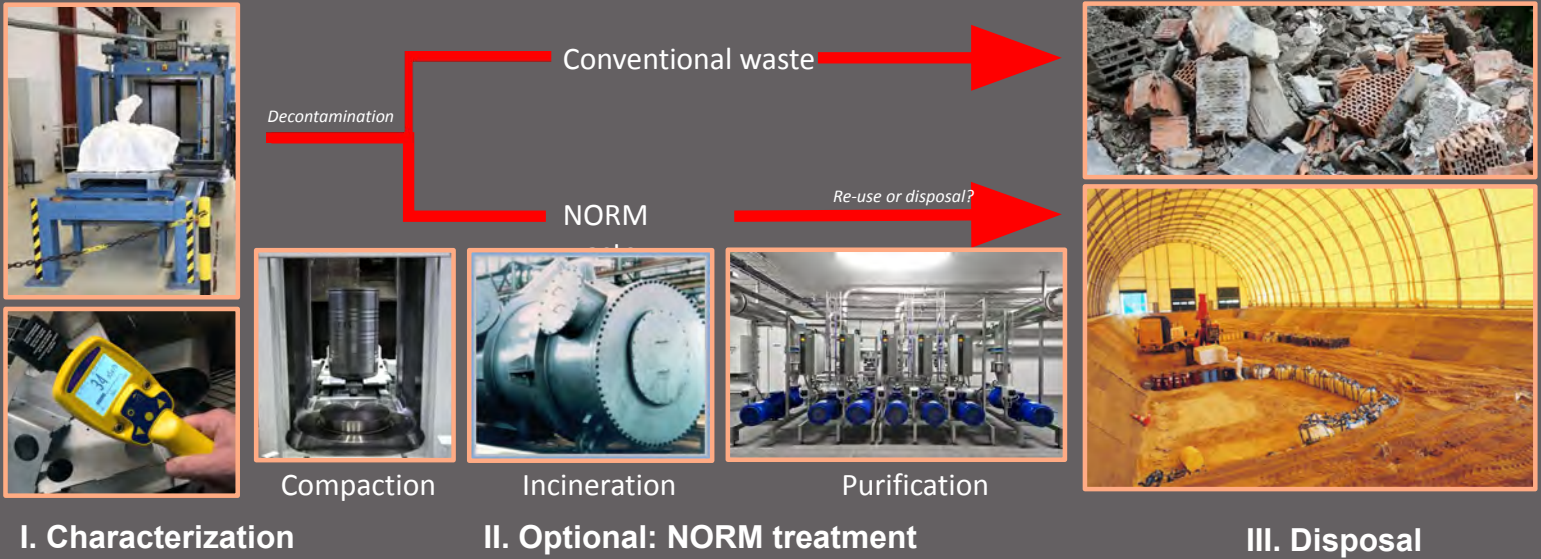
www.geoenergyconsult.com

151/395

GeoEnergy Consult

Management of NORM waste

Radiological characterization separates in *NORM waste* – *conventional waste*



www.geoenergyconsult.com

GeoEnergy Consult

I. Radiological characterisation of generated waste

- Systematic determination of
 - Activity/specific dose
 - Kind of radionuclides etc.
- NORM *inventory*



www.geoenergyconsult.com

152/395

GeoEnergy Consult

II a. Decontamination of contaminated waste/equipment

- Decontaminated waste might be exempted
- Only a small part of waste requires management as NORM
- Re-usability can minimize equipment consumption
- Technologies (from mild to aggressive):
Manual Brushing □ *Water-Jetting* □ *(Electro-) Chemical Bathing* □ *Abrasive Blasting*



www.geoenergyconsult.com

GeoEnergy Consult

II b. Treatment technologies for NORM

Optional treatment reduces mobility of radionuclides and reduces the volume



Treatment technology \ Waste type	Scales	Sediments from settling pond	Tailings	Spent resins	Spent organic solvents	Spent inorganic solutions	Processing residues	Mixed waste	Contaminated equipment	Contaminated bulk material
Radionuclide Extraction			X				X			X
Purification					X	X				
Dehydration	X	X		X			X			
Incineration				X	X			X		
Decontamination	X					X			X	
High-force compaction				X				X	X	
Cementation						X			X	
Radionuclide separation		X						X		X

www.geoenergyconsult.com

153/395

GeoEnergy Consult

II c. Conditioning/Packaging

As the hazard potential of NORM waste is mostly not remarkably high just packaging in big-bags or steel drums can become necessary



www.geoenergyconsult.com

GeoEnergy Consult

III. Disposal

- Safely isolates from the biosphere through geological + multiple technical barriers
 - The higher the activity/half-life the more capable barriers need to be
- How disposal is realized depends on
 - Technical/radiological properties
 - Country-specific requirements
- Can be required over some thousands to hundreds of thousands of years
 - Depends on the radiological properties
 - On the isolation capability
 - On country-specific requirements

www.geoenergyconsult.com

154/395

GeoEnergy Consult

III a. Tailings Impoundments

Disposal in tailings impoundments – appropriate solution ?

Advantages:

- Reasonable operational costs
- Available temporary solution

Disadvantages:

- Drainage generation possible
- Risk of dam failure / erosion
- Maintenance and monitoring needs
- Long-term integrity problematic
- Long-term safety not satisfying

Need for future remediation likely

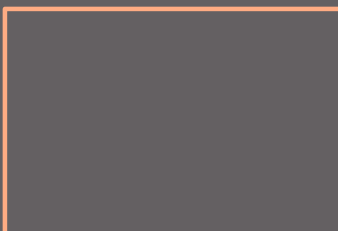
Better: backfill in mined-out underground voids/
open pits or disposal at landfills for NORM waste



GeoEnergy Consult

III b. Landfill / Near-Surface-Disposal

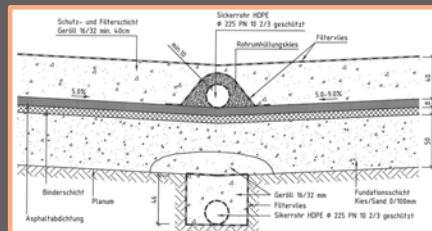
- Sufficient for usual NORM activities, but volume limited
- Takes advantage ideally of naturally impermeable clay and/or of a constructed base seal, optionally with drainage of potentially leaking solutions
- After waste placement a soil cover is constructed, whose layers have low permeability and thus prevent from rainwater ingress



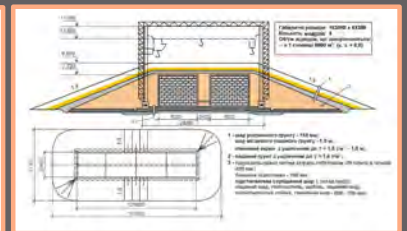
Landfill Disposal



Near-Surface-Disposal



Base seal



Soil cover

GeoEnergy Consult

Case study

Torngat Metals' REE Project (Canada)

Transport/disposal of concentrates and residues from pilot processing

www.geoenergyconsult.com

GeoEnergy Consult

Case study

Developing the Processing Flowsheet

□ Requires Class 7 Transport of Concentrates and Disposal of Residues



- Transport of the Ore
- Transport of
- Sending of Samples
- Disposal of Residues

www.geoenergyconsult.com

156/395

GeoEnergy Consult

Case study

Class 7 Transport of Concentrates

- The IAEA transport requirements are generally accepted as an international standard; national regulations usually adopt those
- To chemically/thermally processed materials stricter criteria e.g. for the allowed activity apply than if only physically processed
- Dose rate for an *Excepted Package* < 5 $\mu\text{Sv/h}$
If dose rate is higher, shielding by filling of the space between an inner basket and an outer drum e.g. with sand can reduce the dose
- Import-/export licenses can be required, e.g. from 500 ppm uranium or thorium on



Photos by Metso

www.geoenergyconsult.com

GeoEnergy Consult

Case study

Disposal of Residues

- Due to their limited volume, instead of any re-use disposal of the pilot processing residues at designated NORM waste landfills is indicated
- Seeking disposal in Finland would be very demanding with an uncertain result:
 - Finland: - no specific NORM facilities, case-by-case decision
 - environmental permit required, based on leaching test etc.
 - safety assessment for operation and post-closure required (estimates of staff and public dose)
 - Canada: - selected disposal facilities are already licensed to accept NORM
 - only requirement: radionuclides < 300 Bq/g

www.geoenergyconsult.com

157/395

GeoEnergy Consult

Conclusions

- To get permitted projects need to demonstrate to safely encounter any impact through capable radiation protection, waste management and closure planning.
- NORM is managed through (I) radiological characterisation, optional decontamination/treatment and (III) re-use or disposal. (II)
- As activities of NORM are mostly modest usually landfill disposal is sufficient, though more sophisticated facilities can become necessary.
- Pilot processing can also serve as a pilot for transport and disposal for the full-scale operation.

PROCESS SELECTION CONSIDERATIONS FOR RECOVERY OF RARE EARTHS FROM MINERAL SANDS CONCENTRATES

By

Gavin Beer

Met-Chem Consulting, Australia

Presenter and Corresponding Author

Gavin Beer

gavin@metchemconsult.com.au

ABSTRACT

Mineral sand deposits contain a concentrated amount of economically important minerals known as “heavy minerals”. The minerals of economic interest typically comprise of zircon (a zirconium source) and rutile, leucoxene and/or ilmenite (titanium sources). These deposits also contain rare earth minerals such as monazite and xenotime. With the increased demand for rare earths, and specifically “magnet rare earths” of praseodymium, neodymium, terbium and dysprosium, there is an increased focus to recover the rare earths from these deposits.

As both monazite and xenotime are only sparingly soluble in acid solutions, a pretreatment (“cracking”) stage is required. There are presently two commercial methods used in industry for the cracking this type of concentrate. The most widely used method, known as sulphuric acid baking, mixes the concentrate with concentrated sulphuric acid followed by thermally heating to produce solid rare earth sulphates. The other method, known as caustic conversion, involves the mixing of the concentrate with a strong sodium hydroxide solution and heating to near boiling point to produce solid rare earth hydroxides. Both methods then can dissolve the soluble rare earths followed by purification prior to separation either on site or at a remote facility via solvent extraction.

This paper discusses the metrics such as cost, recovery, operability, waste management and radionuclide department that need to be considered when selecting a process route for these rare earth concentrates.

Keywords: Rare earth recovery, monazite, xenotime, mineral sands, radionuclides

PROCESS SELECTION CONSIDERATIONS FOR RECOVERY OF RARE EARTHS FROM MINERAL SANDS CONCENTRATES

Gavin Beer

Met-Chem Consulting Pty Ltd

Caveats and Context

Public Domain Information:

The content presented is based on publicly available information. For further details, refer to original sources where applicable.

Estimates and Guides:

All values provided are approximate and should be used as general guides only. Values presented are project and location specific and have been prepared by third parties based on specific flowsheets and required outcomes.

Personal Opinion:

The insights and interpretations shared are based on the author's personal perspective. It is advised to consider multiple viewpoints and expert sources for a particular application.

No Professional Advice:

The information provided does not constitute professional advice. For expert advice, consult relevant professionals or authoritative sources.

Dynamic Field:

The field is continuously evolving; newer findings and data may supersede the information presented.

Rare Earth Sources

The world production of rare earths are derived from 3 deposits styles:

- Hard rock - 85 to 90% of world supply:
 - Mainly from China and Australia.
 - Bastnaesite and monazite are the main host minerals.

- Ionic clays – 5 to 10% of world supply:
 - Mainly Southern China and Myanmar.
 - This is the main contributor to the “heavy rare earths” (HRE) Sm to Lu.
 - See my paper from ALTA 2023.

- Mineral sands – 3 to 5% of world supply:
 - Mined in Australia, South Africa, China and India.
 - Main host minerals are monazite and (to a lesser extent) xenotime.

3

Mineral Sands Processing

Minerals sands have seen an increased focus as a viable and sustainable source of rare earths (REs).

- Economic deposits typically contain up to ~5% by weight of saleable products comprising of:
 - Titanium minerals (rutile, leucoxene, ilmenite).
 - Zirconium minerals (zircon).
 - RE minerals (monazite and xenotime).

- As the minerals are already liberated, comminution (crushing and grinding) isn't required. Flowsheets typically include gravity (spirals), magnetic, electrostatic and flotation separation processes.

- RE mineral concentrates can contain grades up to 60% rare earth oxide (REO) depending on the mineralogy.

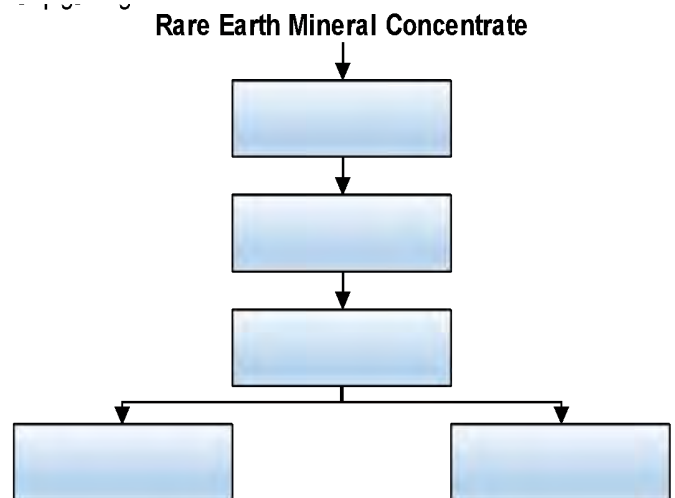
Mineral Sands Rare Earth Mineral Concentrates

- The most common RE mineral found in these deposits is monazite (Ce, La, Th, Nd, Y)PO₄.
 - Main source of praseodymium (Pr) and neodymium (Nd) essential to RE magnets in EV drivetrains, wind turbines, micro motors etc.
 - Contains significant thorium (Th) – typically 5 to 12% by weight.
 - It is “refractory” and resistant to dissolution in most acids at ambient temperature.
- The mineral xenotime (HRE, Y)PO₄ is often (but not always) present.
 - A significant source of high value terbium (Tb) and Dysprosium (Dy) after ionic clays. These elements when added to RE magnets provide high temperature stability.
 - This mineral is considered more refractory than monazite – particularly with respect to caustic cracking.

5

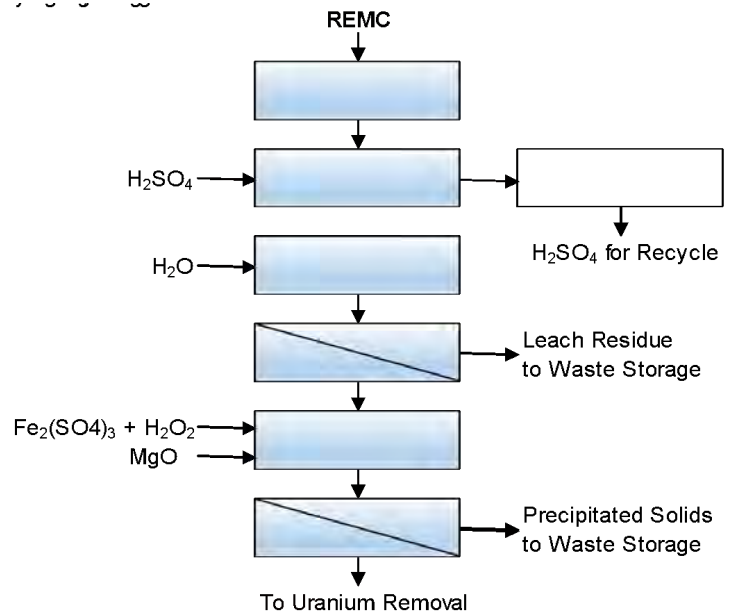
General Flowsheet

- RE mineral concentrates require “cracking”.
- Cracking is via concentrated acid or alkali conditions at elevated temperatures.
- Cracked solids are acid leached via added acid or residual acid from cracking.
- Impurities are removed from the solution.
- Purified solution is sent to separation or a mixed RE product is precipitated.



Acid Bake Flowsheet (1)

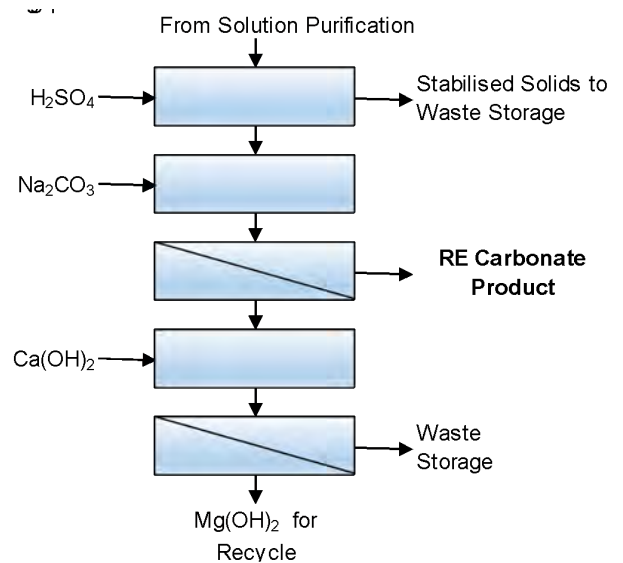
- Rare earth mineral concentrate (REMC) dried via rotary drier.
- Concentrated sulphuric acid mixed with dry REMC @ 1.2 to 1.5 tonnes per tonne of REMC.
- Acid baking undertaken in rotary kilns at 250°C to 350°C but may be as high as 700°C.
- Water leaching in rubber lined or fiberglass reinforced polymer (FRP) stirred tank reactors.



7

Acid Bake Flowsheet (2)

- Purified solution treated via ion exchange (IX) to remove uranium. Uranium is generally precipitated to form stable sodium diuranate.
- RE carbonate product is usually formed by adding soda ash.
- Alternatively, the RE sulphate solution can be sent directly to an onsite solvent extraction (SX).
- Magnesium hydroxide can be regenerated from the RE depleted solution using cheaper slaked lime.



8

Acid Bake Features (1)

- Very robust process and widely employed. Used in Australia, Malaysia and China.
- High extraction rates (~95% or better) of REs from monazite with similar extractions for xenotime.
- Risks are more around equipment selection, engineering and installation.
- The REMC must be dried before mixing with acid (i.e. CAPEX and energy cost considerations).
- Significant quantities of sulphuric acid required – more than the feed mass.
- Energy (generally natural gas) for acid bake kiln is considerable.
- Gas scrubbing circuit is substantial both in footprint and CAPEX.

9

Acid Bake Features (2)

- Significant ferric sulphate (more than half the feed mass) may be required in purification at significant cost.
- Uranium can be easily recovered as a saleable minor by-product if required.
- ANSTO Minerals has developed and piloted the magnesia recycle process using cheap lime. This generates a significant (but not radioactive) waste stream of calcium sulphate.
- Large water requirement/disposal (>20 times dry feed mass) or significant additional CAPEX to recycle (i.e. nano filtration and evaporators).
- Large solid waste volumes (circa 4 times feed mass).

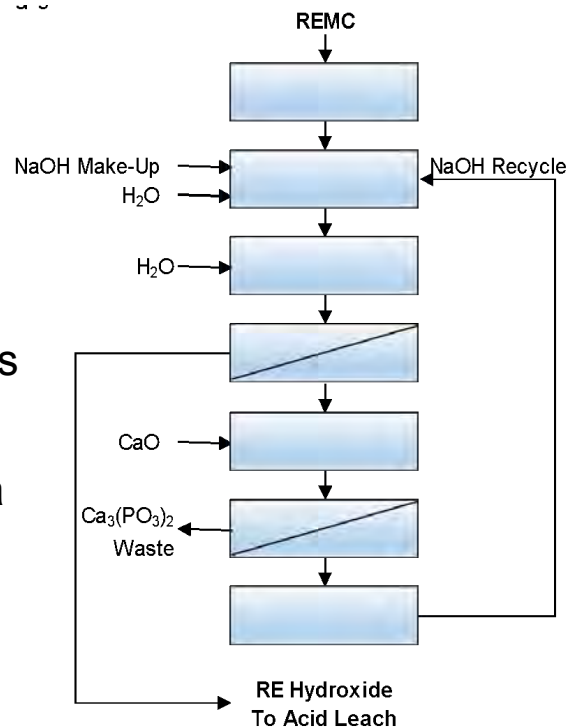
Acid Bake Features – Water, Waste and Radioactivity

- Large water requirement & disposal (>20 times dry feed mass) or significant additional CAPEX/OPEX to recycle (i.e. nano filtration and evaporators).
- Large solid waste volumes - circa 4 times feed mass.
- Radionuclides are spread across multiple waste streams:
 - Leach residue is often higher in radioactivity than the feed due to mass loss and un-leached thorium. This will be categorised as Dangerous Goods (Class 7).
 - Purification precipitate contains thorium but is diluted with (mainly) iron phosphate. Potentially can be combined with gypsum waste from magnesia regeneration.
 - Uranium recovered from IX can be stabilised during waste-water treatment stage where overall solids streams radioactivity will be low.
- Actinium (specifically Ac-227) follows the rare earths and reports to the RE carbonate rendering it radioactive (or even potentially DG Class 7). It can be removed during subsequent solvent extraction (SX).

11

Caustic Crack – Front End

- REMC generally needs grinding (~53um) but not drying.
- Cracking is done in high nickel reactors in concentrated caustic solution (>50% w/w) at elevated temperatures (>140°C).
- Phosphates from monazite/xenotime minerals are solubilised.
- Lime can be used to regenerate caustic soda and form calcium phosphate waste solids.
- REs converted to hydroxides and remain in solid phase. These go to acid leach.



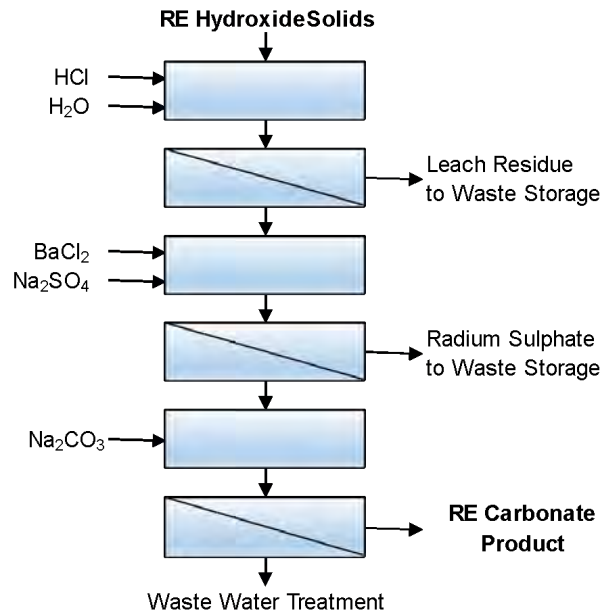
Caustic Crack Features

- REMC requires grinding to maximise the cracking process extractions.
- Undertaken on wet feed which reduces risk of radioactive dust exposure.
- The energy requirements for the heated reactors are lower than acid baking.
- High nickel content reactors are required due to very corrosive environment.
- Gas scrubbing is significantly smaller than acid bake process. Overall footprint also much smaller reducing civil/structural costs.
- RE conversion is generally very high (>95%) for monazite. Conversion of the heavy REs in xenotime can be significantly lower affecting Tb/Dy revenue.
- Thorium extractions similar to RE. U extractions typically 50 to 80%.
- Caustic soda recycle is very high (>90%) using cheap slaked lime.

13

Caustic Crack Chloride Route

- Selective leach using weak hydrochloric acid (pH 3 to 4) is undertaken in stirred reactors (rubber lined or FRP).
- As radium chloride is soluble, this radioactive element is removed by co-precipitating with barium as a sulphate.
- The purified RE solution from radium removal can be sent to an adjacent SX separation plant or precipitated as a RE carbonate as per the Acid Bake route.



Chloride Route Features, Waste and Radiation (1)

- No longer widely practiced but been well demonstrated commercially in India (IREL since 1950's). USA (Energy Fuels) and Canada (SRC) are constructing large scale demonstration plants.
- The selective leach is designed to target mainly RE dissolution but does result in a large volume radioactive waste stream.
- Cerium dissolution can be controlled by hot air drying the caustic cracked solids if required.
- HCl requirement is significant with slightly more than 1 tonne of 32% HCl required per tonne of REMC feed. Proximity to HCl supply is important.

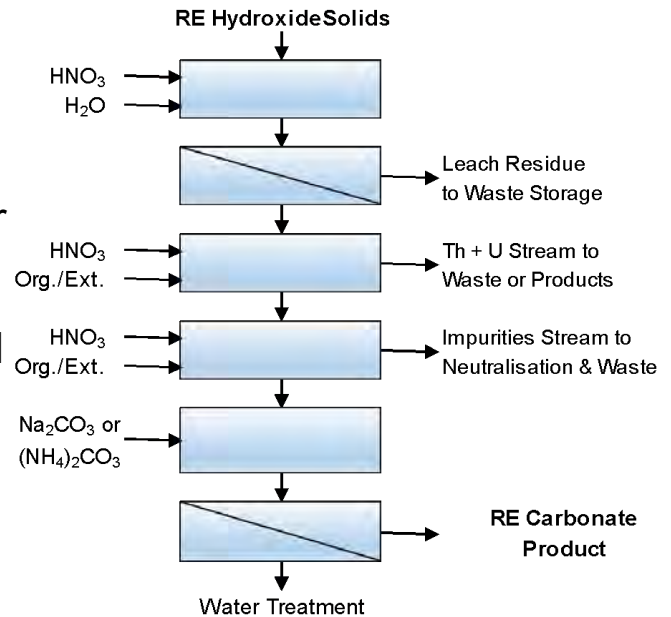
15

Chloride Route Features, Waste and Radiation (2)

- Radium/barium sulphate precipitate waste stream is low volume but categorised as DG Class 7.
- Overall solid waste stream low mass – just over the REMC feed mass.
- Waste-water stream is ~ 75% of Acid Bake and is mainly dilute NaCl solution.
- Overall OPEX is ~20% less than Acid Bake depending on HCl cost.
- Overall CAPEX is expected to be higher than the Acid Bake mainly due to the NaOH recycle circuit which includes an evaporator.

Caustic Crack Nitrate Route

- “Hard” leach (1 to 5% nitric acid) typically in stainless steel stirred reactors.
- First SX stage targets Th and U which can be subsequently separated to product(s) or stabilised for waste disposal.
- Second SX loads all REs and rejects metal impurities including radium.
- Strip solution can go to adjacent SX plant or precipitate RE carbonate. Precipitant choice based on water disposal strategy and if SX separation plant is installed adjacent.



17

Nitrate Route Features, Waste and Radiation (1)

- Main commercial application was at La Rochelle in France (Rhodia 1950's to 1990's).
- The hard leach using nitric acid solubilises Th and U almost completely with increased solubilisation (compared to chloride route) of other impurities.
- HNO₃ requirement is similar to HCl (for the chloride route) by volume but at a higher strength (60%).
- SX uses commercially available extractant (TBP) which is widely employed for uranium processing. This is presently used for RE processing in Estonia (Silmet) and France (Solvay). Western Australia will also use TBP in nitric acid for separating REs at Iluka's Eneabba facility which is under construction.

Nitrate Route Features, Waste and Radiation (2)

- SX uses diluted nitrate solution for stripping which is then concentrated using evaporators. This has a significant saving in reagent (OPEX) costs but at a positive CAPEX differential. Note power for evaporators will offset some savings.
- Radiation is concentrated into Th/U SX strip solution. This precipitated as a low volume (but high radioactivity) solids for disposal. It can also be further separated via SX into Th and U nitrate “products”.
- Radium in principle could be removed by barium sulphate co-precipitation, however SX with TBP is effective and very similar to the preceding Th/U SX.
- Overall solid waste stream volumes are the lowest of all three routes.
- Waste water stream volumes are low and can engineered to be net zero via nano filtration and evaporator use.

19

General Selection Matrix

METRIC	COMMENT	SULPHATION BAKE	CAUSTIC CONVERSION - CHLORIDE	CAUSTIC CONVERSION - NITRATE
CAPEX	Assumes caustic soda and magnesia recycle.	Lowest - however complex gas scrubbing with acid recycle may elevate costs.	Mid	Highest
OPEX	Highly dependent on reagent and power cost.	Highest	Mid	Lowest
LIGHT RE (Nd/Pt) RECOVERY	Recovery to RE carbonate.	High	High	High
HEAVY RE (Tb/Dy) RECOVERY	Recovery to RE carbonate.	High	Lower - especially if xenotime is present.	Lower - especially if xenotime is present.
FLWSHEET OPERABILITY and TECHNOLOGY SUPPORT	How easy is the circuit to commission, operate and maintain.	Considered a "standard" process in China and Australia. Tolerant to multiple concentrate mineralogies.	Only commonly now used in India but plants under construction in USA and Canada. Chemistry and know how well known, however.	Previously practiced in France but ceased in 1993. Know how available via Carister. SX technology well known from uranium industry.
RADIONUCLIDE DEPARTMENT	With regards to operations and waste streams.	Dust inhalation (during drying, baking and gas scrubbing) most likely source for exposure. Leach residue & purification residue classified radioactive.	Selective leach results in large volume radioactive leach residue stream. Also radioactive radium/barium precipitate waste stream.	Th/U concentrated to a high purity small volume waste stream. Same for radium.
SOLID WASTE GENERATION	Focus on volume which requires onsite storage or 3rd party disposal.	Largest volume of waste solids.	Significantly lower volume of waste solids volume.	Lowest volume of solid waste.
REAGENTS	Quantity and cost contribution of reagents to OPEX.	A lot of sulphuric acid ferric sulphate required. These reagents are a significant proportion of overall OPEX along with kiln fuel requirements.	Main reagent costs are hydrochloric acid and soda ash. Proximity to cheap acid is important.	Main reagent costs are nitric acid and soda ash. Proximity to cheap acid is important. No requirement for barium salt for radium removal.
WATER REQUIREMENTS	Water requirements dictate both cost of supply and cost of recycle or disposal.	Highest	Low	Lowest or net zero.

Note green shading indicates preferred route for the specific metric

Summary

Choice of flowsheet is quite a complex exercise and must be undertaken once the following metrics are locked down:

- Feed mineralogy and sources tested through the flowsheet options.
- Expected life of facility – i.e. long term lower OPEX versus higher CAPEX.
- Location:
 - Proximity to reagents and cost.
 - Power costs.
 - Water availability.
 - Waste disposal options for solids, solutions and radioactive streams.
 - Access to technical resources for construction, commissioning and operation.
- Whether a separation plant will be included at the same location.

21

Acknowledgements

Sincere appreciation is extended for the technical review of this presentation extends to:

- ANSTO Minerals (<https://www.ansto.gov.au/services/resources-sector/minerals>)
- Carester (<https://www.carester.fr/en>)

I also extend my gratitude to the following companies who have engaged me on managing testwork and piloting programs:

- VHM Ltd (<https://www.vhmltd.com.au/>)
- Base Resources Ltd (<https://baseresources.com.au/>)

LESSONS LEARNED FROM IONIC CLAY TESTWORK

By

Damian Connelly

METS Engineering Group, Australia

Presenter

Matthew Nicholls

Matthew.Nicholls@METSEngineering.com

ABSTRACT

There exists a third class of rare earth (RE) ores, which are called ionic clays. They are typically found in southern China and other subtropical areas. They are formed by the chemical weathering of rare earth elements (REE)-containing parent rocks, resulting in the formation and mobilization of REE ions, which are then adsorbed onto the clay particles and hence, the class name.

The Caralue Prospect in South Australia was initially established as a high purity kaolin prospect following identification of thick intervals of bright white kaolin—close to surface—in several historical drill holes. A 2022 drilling program undertaken by iTech identified significant REEs, in the kaolin rich intervals, over a large area. The Caralue Bluff Prospect has an exploration target of 110-220 Mt @ 635-832 ppm TREO and 19-22% Al₂O₃. This exploration target is based on 80 drill holes, from a total program of 260 holes, across an area of approximately 12km x 12km, as reported by iTech on 18 August 2022, "Exploration Target Defined at Caralue Bluff". Significantly, it remains open in multiple directions allowing for possible expansion. The REE mineralisation is rich in key magnet REEs namely neodymium, praseodymium, dysprosium and thulium (Nd-Pr-Dy-Tb) averaging 25% of the REE basket.

Initial testwork organised by Itech Minerals at a commercial laboratory achieved zero recovery. Itech contacted METS and a metallurgical testwork program was developed and executed resulting in eighty seven percent (87%) leaching recovery of the REEs. In addition, process optimisation resulted in a reduced OPEX and CAPEX. At the same time a kaolin product was produced as a by-product.

Keywords: Caralue Bluff Prospect, ionic clays, leaching, process optimisation, rare earth elements, total rare earth oxides (TREO).

Lessons Learned From Ionic Clay

Author: Damian Connelly
Principal Consulting Engineer, METS Engineering Group
Presenter: Matthew Nicholls
Senior Process Engineer, METS Engineering Group
Trusted Specialists for 30+ Years

METS Engineering

PO Box 1699

West Perth WA 6872

P: (+61 8) 9421 9000

ABN: 92 625 467 674

W: www.metsengineering.com

DISCLAIMER

With respect to all the information contained herein, neither METS Engineering Group Pty Ltd, nor any officer, servant, employee, agent or consultant thereof make any representations or give any warranties, expressed or implied, as to the accuracy, reliability or completeness of the information contained herein, including but not limited to opinions, information or advice which may be provided to users of the document. No responsibility is accepted to users of this document for any consequence of relying on the contents hereof.

COPYRIGHT ©

Passing of this document to a third party, duplication or re-use of this document, in whole or part, electronically or otherwise, is not permitted without the expressed written consent of METS Engineering Group Pty Ltd.

ACKNOWLEDGEMENTS

This document is a dynamic record of the knowledge and experience of personnel at METS Engineering Group. As such it has been built upon over the years and is a collaborative effort by all those involved. We are thankful for the material supplied by and referenced from various equipment manufacturers, vendors, industry research and project partners.

About METS Engineering

OUR

EXPERTISE

Mineral Processing
Hydrometallurgy
Pyrometallurgy
Testwork & Management
Plans
Engineering Studies
Optimisation
Project Capital Reduction
Product Innovation
Specialist Services

+ More

GLOBAL INDEPENDENT CONSULTANT

Since 1988
Australasia
Asia
Europe
Americas
Africa

ALL COMMODITIES

Alumina
Copper
Garnet
Gold/Silver
Graphite
Iron Ore
Kaolin
Lead/Zinc
Lithium
Mineral Sands

+ More

30+ YEARS EXPERIENCE

Domestic and
International Projects
All Industries
Investigation, Studying,
Execution and Verification
of Projects
Locally owned & operated
40+ Training Courses
We share our knowledge
with the industry

Key Attributes

- ✓ **Global.** Since 1985 we have worked with clients in Perth, Australia, to as remote as Guyana, South America.
- ✓ **Experienced.** Have worked on 10,000+ mineral jobs over the last 35 years.
- ✓ **Innovators.** Unique solution finders. We are not scared to challenge conventional wisdom to overcome project issues.
- ✓ **Specialists.** We are experts in mineral processing, smelting and hydrometallurgy across the life cycle of a project.
- ✓ **Service Delivery.** We engage our clients at each stage through weekly progress status reports.
- ✓ **Continuous Improvement.** We are committed to the advancement of technology and processing within the resource of energy.

Introduction

Ionic Clays

- The global demand for rare earth elements is on the rise due to the increasing adoption of modern and environmentally sustainable technologies, including wind turbines, electric vehicles, fuel cells, and advanced materials.
- REE-bearing ores are typically found in the form of carbonates or phosphates.
- Extraction from these ores involves processing with concentrated sulfuric acid, hydrochloric acid, or sodium hydroxide at elevated temperatures.
- Ionic clays, found in areas like southern China, represent a unique class of REE-ores.
- These clays are formed through the chemical weathering of REE-containing parent rocks, resulting in the mobilization and enrichment of REE ions onto the clay surface through ion adsorption.

Introduction

- No clay REE deposit exists purely as 'ionic'. They are formed as nature and time weather a REE-rich hard rock source, like granite, into three distinct phases.
- The adsorbed (ionic) phase is easily, quickly and cheaply desorbed with a salt solution at pH4, for instance.
- Then you have a secondary mineral phase. Here, as the minerals release the rare earths as they break down, which then form a secondary mineralisation.
- These rare earths can be extracted with a modest pH solution, which is more expensive, but possible.
- Finally, there is a resistive phase. That's the mineral containing rare earths which hasn't been broken down. This stuff is uneconomic to extract at the low-grade characteristic of IAC deposits.

Ionic Clays

- Ionic clays are a special type of clay formed through the chemical weathering of rocks containing rare earth elements (REEs).
- REEs, such as lanthanum, cerium, and neodymium, are mobilized and adsorbed onto the surface of the resulting clay particles.
- Chemical breakdown of parent rocks containing these rare earth elements.
- The ions of rare earth elements are mobilized and adsorbed onto the surface of the resulting clays.
- Ionic adsorption is a phenomenon where ions adhere to the surface of a solid, in this case, clay particles.



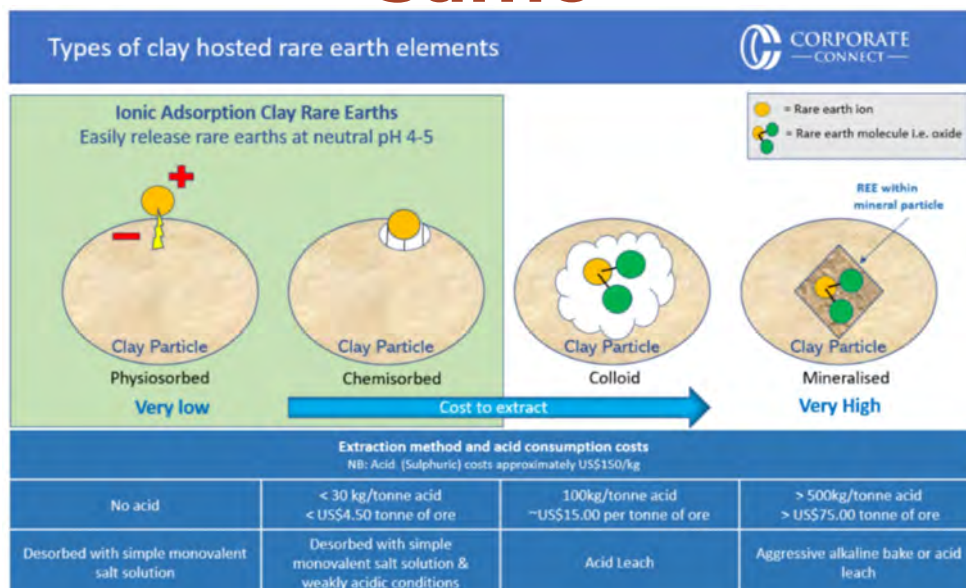
Ionic Clays

- A distinctive feature of Ionic Clays is that rare earth elements are primarily found on the surface of clay particles, rather than being encapsulated within larger mineral phases. This makes rare earth elements more accessible and, consequently, easier to extract compared to other types of rare earth minerals.
- Ionic Clays, especially those found in subtropical regions like southern China, often allow for the leaching of rare earth elements under relatively mild conditions. This can be achieved through heap leaching or in-situ leaching with mild leaching solutions, resulting in the collection of a stream rich in rare earth elements.
- These resources have become of significant interest in the pursuit of more sustainable and economically viable alternatives for the production of rare earth elements.
- Driven by the growing global demand and the challenges associated with conventional production methods.

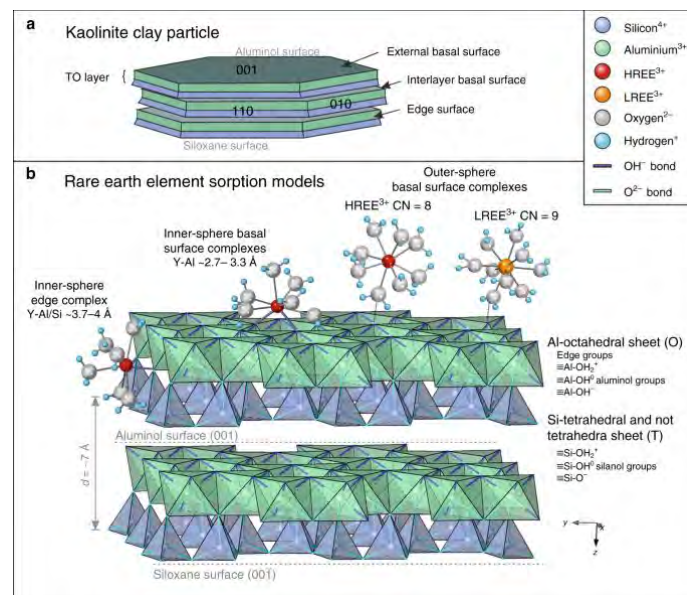
Properties and Characteristics of Ionic Clays

Surface Adsorption	<ul style="list-style-type: none"> • One of the key features is the surface adsorption of rare earth elements (REEs) onto clay particles. • REE ions are concentrated on the surface, making them more accessible for extraction.
Accessibility of REEs	<ul style="list-style-type: none"> • Unlike some rare earth minerals encapsulated within larger mineral phases, REEs in Ionic Clays are predominantly found on the clay surface. • This surface location enhances the ease of extraction, contributing to the economic viability of these clays.
Ionic Adsorption Phenomenon	<ul style="list-style-type: none"> • The adsorption of REE ions onto clay particles is an ionic adsorption phenomenon. • This phenomenon involves the adherence of ions to the surface of the solid clay particles.
High Cation Exchange Capacity	<ul style="list-style-type: none"> • Ionic Clays exhibit a high cation exchange capacity, allowing them to readily absorb and release ions. • This property contributes to their versatility and applicability in various industries.
Formation Flexibility	<ul style="list-style-type: none"> • The formation of Ionic Clays occurs through the chemical weathering of rocks containing rare earth elements. • This natural process allows for the formation of clays in diverse environments, contributing to their global distribution.

Not All Ionic Clays Are The Same

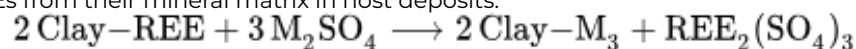


Occurrence characteristics of rare earth elements on the surface of kaolinite



Extraction techniques

- Chemical leaching plays a crucial role in the extraction of Rare Earth Elements (REEs) from regolith-hosted deposits.
- This process involves using a leaching solution, or lixiviant, to initiating an ion-exchange reaction with clay minerals of the ore. As the lixiviant interacts with the REE-adhered clay minerals, displacement occurs, causing the REEs to dissolve into the leaching solution.
- An illustrative example involves the use of a metal sulphate lixiviant, where the ion-exchange reaction transforms REEs adhered to clay minerals into dissolved REEs in the leaching solution.
- This chemical leaching method serves as a key mechanism for liberating and recovering REEs from their mineral matrix in host deposits.



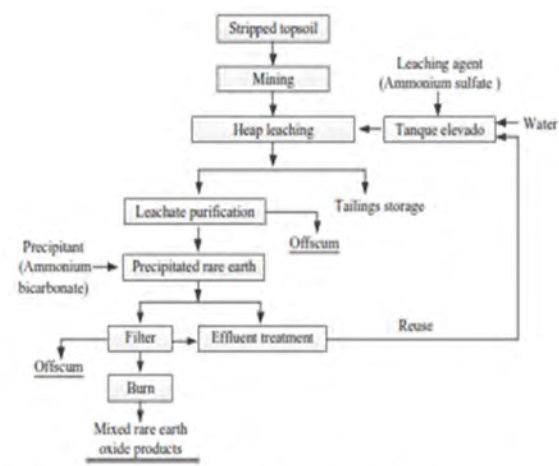
Overview of Leaching Technologies for Ion-Adsorption Clays

- Ion-adsorption clays are characterized by containing 0.05 to 0.3 wt.% rare earth elements (REE)
- With over 60% typically existing as physically adsorbed species recoverable through simple ion-exchange leaching. The leaching process involves the use of concentrated inorganic salt solutions with monovalent cations.
- During leaching, physically adsorbed REE are easily and selectively desorbed, substituting on the substrate with monovalent ions and transferring into solution as soluble sulfates or chlorides, following a theoretical 3:1 stoichiometry.
- However, the actual lixiviant usage often exceeds stoichiometric requirements due to competing desorption of other cations (e.g., Al) also adsorbed on clays.

Variety of Leaching Methods

Leaching methods for extracting REEs from IACs include:

- **Heap leaching:** Excavating minerals, placing them in a mound, and spraying with solutions.
- **Tank/VAT leaching:** Placing minerals into a tank/VAT and immersing them with solutions.
- **In-situ leaching/ recovery (ISL/ISR):** Dominating technology due to less topsoil removal, on-site processing, and reduced environmental impacts.



Lixiviants

Ammonium Sulphate $(\text{NH}_4)_2\text{SO}_4$

- A traditional lixiviant used for REE extraction, particularly from ionic adsorption clays.
- Weakly acidic ammonium sulfate is often used to leach REEs from the ore matrix.

Hydrochloric Acid HCl

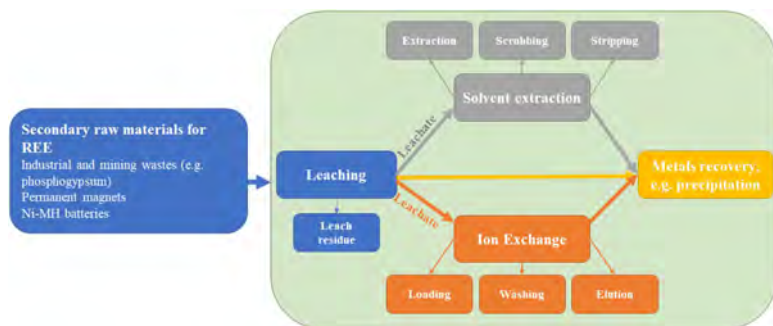
- A strong acid commonly employed in laboratory and industrial settings for REE extraction.
- Hydrochloric acid, particularly at $\text{pH} < 5$ and elevated temperatures (e.g. 80°C), has shown effectiveness in dissolving REEs.

Sulphuric Acid H_2SO_4

- A strong acid commonly employed in industrial settings for REE extraction at elevated temperatures commonly seen in the sulfuric acid baking process.
- Has shown effectiveness in dissolving REEs.

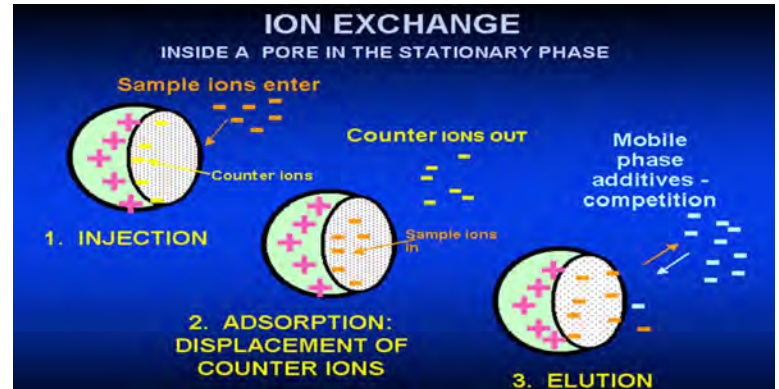
Recovery Techniques-Adsorption

- Adsorption techniques play a crucial role in the recovery and concentration of Rare Earth Elements (REEs) from leach solutions.
- These techniques involve the selective adherence of REEs to certain surfaces or materials, facilitating their separation from the solution.
- Selection of specific adsorption agents or ion exchange resins to selectively capture and concentrate the dissolved REEs from the leach solution.



Ion exchange

- Ion exchange (IX) is the separation of ions from a solution using solid inorganic oxides or organic ion exchange resins with negative or positive charges.
- Ion exchange resins can selectively capture and concentrate specific REEs from a leach solution.



Adsorption techniques

Chelating Agents:

- Chelating agents are organic compounds that form stable complexes with metal ions. In the context of REE extraction, chelating agents can surround and capture individual REEs, forming soluble complexes.

Clays and Minerals:

- Clays and minerals have high surface areas and specific chemical properties that enable adsorption through surface interactions. The minerals' surfaces attract and bind with REEs present in the solution.
- Some clay minerals can act as natural adsorbents for REEs, and the selection of the appropriate clay or mineral depends on the specific characteristics of the ore and solution.

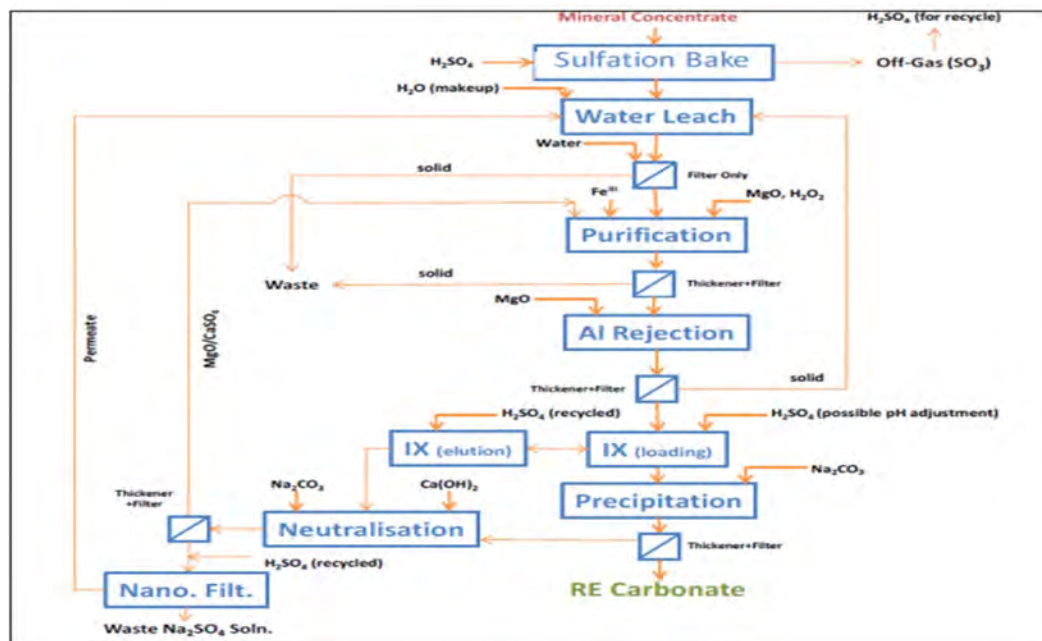
Activated Carbon:

- Activated carbon has a highly porous structure with a large surface area. It adsorbs substances through physical interactions, such as van der Waals forces and pi-pi interactions.
- In REE extraction, activated carbon can be employed as an adsorbent to capture REEs from solution, offering versatility in different extraction processes.

Silica Gel:

- Silica gel, composed of porous silicon dioxide, can adsorb substances through physical adsorption and capillary condensation within its pores.
- Silica gel can be utilized as an adsorbent for REEs under specific conditions, providing a selective capture method.

Plant Flowsheet



Current and Future Demand

- Rare earths play a key role in modern society featuring use in a variety of applications.
- Many current applications include being used for catalytic converters in cars and are used as magnetics for components in wind turbines.
- They are also used in the production of smart phones where they are used for producing the colours of a phone display.
- In the future demand is expected to continue due to the growing industry for electric vehicles (EVs) where they are required for rechargeable batteries and traction motors.

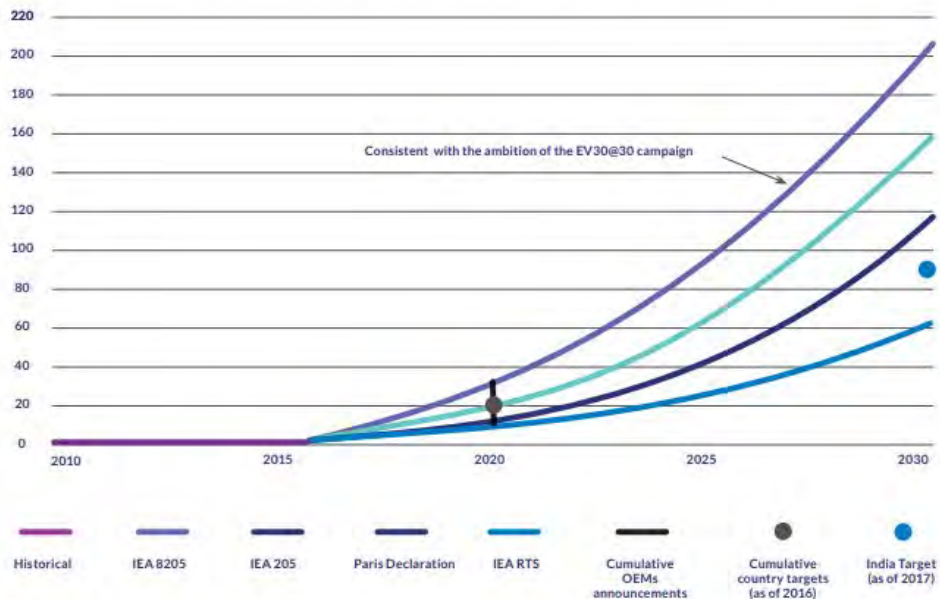
General Uses of Rare Earths

- Globally, most REEs are used for catalysts and magnets
- In USA, more than half of REEs are used for catalysts, ceramics, glass and polishing
- Other important uses of REEs include the production of high performance alloys, glasses, and electronics
- REE has also been used in agriculture as REE-enriched fertilizers



Electric Vehicles

Figure 12-2 Deployment scenarios for the stock of electric cars to 2030



Ionic Adsorbent Clay (IAC) Testwork

- Testwork approach in ionic adsorbent clay (IAC) need to be a systematic and technical examination conducted in a laboratory setting to understand and optimize the process of extracting rare earth elements (REE) from these clay deposits.
- This intricate process involves conducting experiments using various methodologies and leaching agents to assess the feasibility and efficiency of liberating and adsorbing REE from IAC.
- Key objectives include identifying effective leaching agents, maximizing REE recovery, overcoming initial challenges observed in the results, and continually optimizing the process to achieve economic and sustainable performance.

Ionic Adsorbent Clay (IAC) Testwork

- Collaboration with metallurgical experts to ensure a comprehensive understanding of the material's behavior. This technical approach plays a pivotal role in enhancing operational efficiency and reducing costs, while potentially yielding valuable by-products such as kaolin.
- By providing a solid foundation, the insights gained from testwork contribute to informed decision-making for the scale-up implementation of REE extraction processes from IAC. This technical focus sets the groundwork for potential expansions and future research in this specialized field.

Study Cases - Caralue Bluff, Australia

1. Discovery:

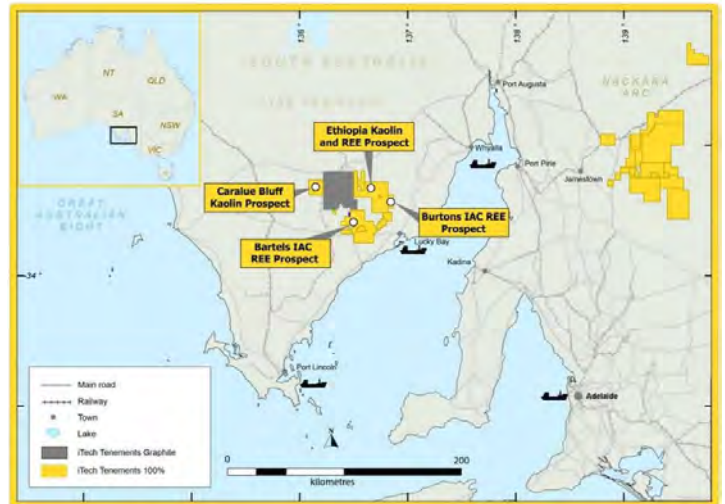
- Originally identified as a high-purity kaolin prospect.
- 2022 drilling by iTech revealed significant REEs in kaolin-rich intervals.

2. Exploration Target:

- Caralue Bluff Prospect's exploration target: 110-220 Mt @ 635-832 ppm TREO, 19-22% Al₂O₃.
- Based on 80 drill holes from a total program of 260 holes across a 12km x 12km area.

3. Mineralization Characteristics:

- REE mineralization rich in key magnet REEs (Nd-Pr-Dy-Tb), averaging 25% of the REE basket.



iTech Minerals Testwork

The Situation

- iTech Minerals' initial testwork at a commercial lab.
- Initial testwork failure achieved near zero recovery.

The Challenge

- The challenge was to identify the cause of the zero recovery.
- Overcome the difficulties in extracting REEs from the iTech sample.

Methodology

Metallurgical Testwork Program

1. Leaching Testwork:

- iTech Minerals sought assistance from METS.
- A metallurgical testwork program was developed and executed.
- Improved leaching recovery of REEs.

2. Lixiviants Investigation:

- Various lixiviants, including ammonium sulfate and hydrochloric acid, were tested.
- Laboratory results favored hydrochloric acid at pH<5 and 80°C for >87% REE extraction.

3. Beneficiation Testing:

- Beneficiation through screening doubled the REE grade for processing.
- Process optimization led to reduced OPEX and CAPEX.

5. Variability in IAC Deposits:

- Tests on an Australian IAC revealed differences in deposits.

Leaching Testwork

Recoveries:

- 86% TREO achieved in leaching tests.
- 88% MREOs (Nd, Pr, Dy, Tb) recovered.

High Chloride Environment:

- Hydrochloric acid was used to create a high chloride environment.
- High chloride environment is required to liberate REEs from the clay solution.

IAC Characterisation:

- Bulk of the REEs not bound to within the lattice structure of the clay particles or in resistive minerals such as zircon or monazite.

	REE Extractions (%)		
	Test 1 (10% HCl)	Test 2 (20% HCl)	Test 3 (32% HCl)
La	70.66%	84.22%	82.50%
Ce	73.36%	85.32%	81.68%
Pr	78.21%	87.60%	84.44%
Nd	81.84%	90.22%	85.78%
Sm	83.23%	91.60%	85.78%
Eu	74.40%	88.37%	79.56%
Gd	83.36%	88.32%	88.28%
Tb	80.96%	92.41%	86.64%
Dy	76.14%	82.06%	77.58%
Ho	68.06%	82.01%	72.17%
Er	70.01%	75.20%	75.98%
Tm	0.00%	0.00%	0.00%
Yb	56.05%	54.91%	50.97%
Lu	0.00%	0.00%	0.00%
Y	73.21%	81.10%	77.82%
Total	75.34%	86.31%	82.95%

Beneficiation Testwork

Concentration of REEs:

- Through simple screening at 20 µm.
- Concentration in the -20 µm fraction of just over half sample mass (51%).

Recoveries:

- 74.5% total REEs deport to fine fraction.
- >75% Magnet REEs (Nd + Pr).

Reduction Leach Feed Volume:

- Lower acid consumption.
- Smaller clay volumes to leaching.
- OPEX and CAPEX reductions

Valuable By Product:

- This fraction contains the potentially valuable kaolin by-product.

Size (µm)	TREE+ Y Mass (mg)	TREE+Y Dist. (%)	Nd Dist. (%)	Pr Dist. (%)
+150	57.08	10.13	9.46	9.32
+106	15.63	2.77	2.74	2.70
+75	15.39	2.73	2.64	2.58
+45	23.65	4.20	3.96	4.00
+38	4.10	0.73	0.68	0.69
+20	27.99	4.97	4.96	4.87
-20	419.78	74.48	75.57	75.84
Head Assay	563.62	100	100	100

Notes:

TREE: Total Rare Earth Elements

HREE: Heavy Rare Earth Elements

LREE: Light Rare Earth Elements

Testwork Outcomes

Initial Testwork Challenges:

- iTech Minerals faced zero recovery in initial commercial lab testwork.

METS Collaboration:

- Collaboration with METS led to an 87% leaching recovery of REEs.
- Process optimization to reduced operational and capital expenditures.
- Simultaneously produced a kaolin product as a by-product during the process.

Conclusion

- The existence of ionic clays highlights the diverse nature of rare earth ores, particularly in subtropical regions like southern China, expanding the scope for resource exploration.
- The success of the Caralue Bluff Prospect's drilling program suggests significant potential for rare earth extraction, with an open-ended exploration target and rich magnet REE mineralization.
- iTech Minerals' metallurgical achievements, including an 86% leaching recovery and process optimization, not only enhance resource extraction efficiency but also yield a valuable kaolin by-product, demonstrating sustainable resource utilization.

Conclusion

- iTech Minerals' collaboration with METS showcased resilience in overcoming challenges, transforming zero recovery in initial testwork to an impressive 87% leaching recovery for REEs through process optimization.
- The success in China using weakly acidic ammonium sulphate underlines the economic efficiency of processing IAC, aligning with very low overall costs.
- Varied outcomes in Australian IAC testwork emphasize the need for tailored beneficiation strategies, with screening doubling REE grades, showcasing the diversity within IAC deposits.



Acknowledgement

The authors would like to thank METS Engineering for permission to publish this presentation and all colleagues and engineers at various sites, METS staff and other consultants for their contribution and the management of METS for their permission and constructive criticism of various drafts of this presentation.

OPTIMISING REAGENT USE IN CLAY HOSTED RARE EARTH EXTRACTION

By

Jess Page, Chantelle Bardadyn, ²Rick Pobjoy

WGA, Australia

²AR3, Australia

Presenter and Corresponding Author

Jess Page

jpage@wga.com.au

ABSTRACT

Understanding what makes a project profitable in the design phase is crucial. We usually rely on existing data for benchmarking, but in this case, due to limitations on data availability, WGA supported an extensive bench and pilot test work campaign with Australian Rare Earths (AR3) to create cost estimates and designs. As a result of this approach, our focus in flowsheet development is to find ways to reduce operating costs, particularly by recycling reagents. This approach involved using a data science approach to quickly test different scenarios and pinpoint what most drives profitability.

Project Background

AR3's Koppamurra project is a large clay hosted rare earths prospect in Southeast South Australia. The mineral resource is 186 Mt at 712 ppm TREO and contains valuable magnet elements Nd, Pr, Dy, and Tb which are essential in high strength permanent magnets used in wind turbines and electric vehicles. WGA have been supporting AR3 for three years, starting with drilling data management, then metallurgical test work program management, and now through to cost estimation and preliminary engineering. To make sense of the flowsheet economics, we need to understand what drives profitability. We needed to define what are the big levers that will make a project profitable over the life of operations.

Methodology

Typically, we rely on existing plant design and operating costs to do preliminary 'back of the envelope' cost estimates. But, as most of the historical work has been done in China, a lot of that information isn't available in Australia. So given we need a flowsheet to evaluate project profitability, and we have limited or no access to benchmarking data, WGA supported AR3 in conducting a comprehensive test work campaign, with over 300 bench scale tests and pilot operations at ANSTO, SGS Lakefield, Bureau Veritas, and University of Toronto, to understand the process set points. From this a flowsheet and cost estimate were developed based on the met test work and pilot results.

There are several moving parts to the profitability calculation, but to focus our efforts to get the most impact during flowsheet design, a multi scenario analysis was developed to rapidly assess several scenarios to identify the big levers. WGA automatically ran thousands of cases to identify the most profitable scenarios with the support of the WGA data science team. Multiple scenarios were run to increase profitability using these levers, but operating costs remain the biggest lever, so the focus is on minimising and recycling leach and impurity removal reagents in flowsheet development through WGA's ongoing support of the AR3 Koppamurra project.

Outcome

Our integrated team of process engineers and data scientists were able to collaborate with AR3 to develop a comprehensive mass balance model and profitability analysis to focus flowsheet development, with the objective of reducing time to commercialisation.

Keywords: clay hosted rare earths, profitability, economic analysis, pilot operations

INTRODUCTION

Australian Rare Earths' Koppamurra project is a large clay hosted rare earths prospect in Southeast South Australia (Figure 1). The mineral resource is 186 Mt at 712 ppm TREO and contains the valuable magnet elements Nd, Pr, Dy, and Tb which are essential in high strength permanent magnets used in wind turbines and electric vehicles. Australian Rare Earths vision is to become Australia's first clay hosted rare earths producer, and to support this drive to commercialisation, we needed to identify key drivers and major factors that will influence the project's profitability throughout its operations. Typically, we rely on existing plant design and operating costs to do preliminary 'back of the envelope' cost estimates, but the availability of that information is limited. As a result, Australian Rare Earths conducted a comprehensive test work campaign, with over 300 bench scale tests and a pilot operation to understand the process set points for flowsheet and cost estimate. As a result of our approach, our focus in flowsheet development is finding ways to reduce operating costs, particularly by recycling reagents. This approach involved using a data science approach to quickly test different scenarios and pinpoint what drives profits the most.

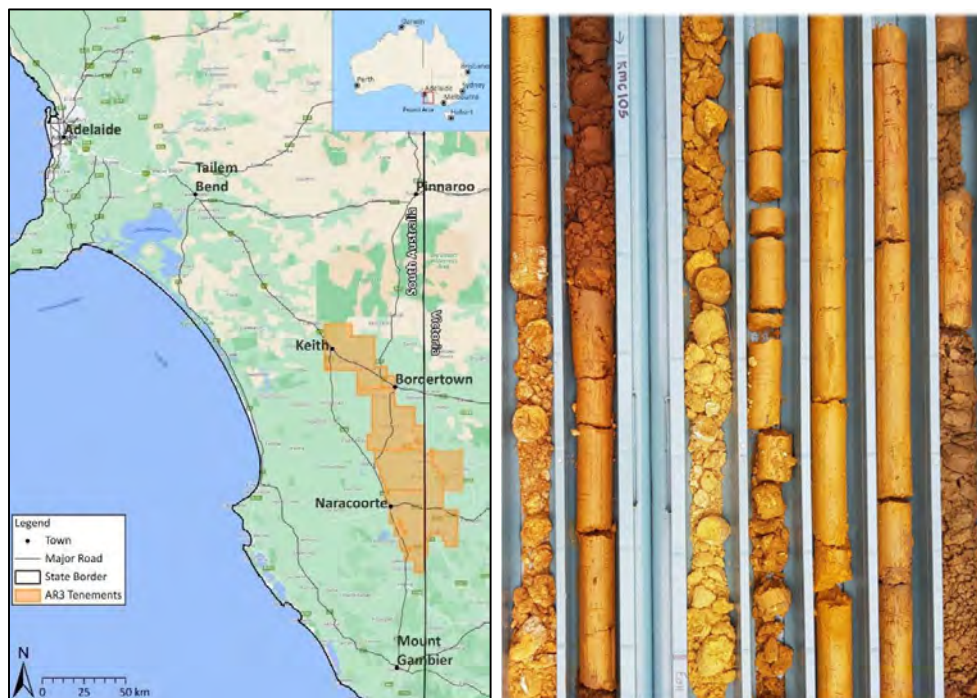


Figure 1: The Koppamurra project is located in the southeast of south Australia, around the Naracoorte region. The latest resource estimate of the deposit is a 186 Mt at 712 ppm Total rare earth oxides.

PROJECT BACKGROUND

Rare earths are essential in high strength permanent magnets, which increase the efficiency of electric motors, including those used for wind turbines, and electric vehicles. Therefore, the magnet rare earths, Nd, Pr, Dy, and Tb, have an important role to play in a sustainable future. China has historically dominated the global production and supply of rare earths, accounting for a significant share of the market. Efforts have been made in recent years to diversify the supply chain and reduce dependency on China. Australian Rare Earths Koppamurra project will play an important role in Australia's supply of these critical minerals.

The location of Koppamurra is favourable for access to utilities and local labour, and Australian Rare Earths has already engaged the community in several initiatives including open days and high school career events. The Australian Rare Earths exploration team have progressed significant drilling campaigns to derive the resource estimate and produced several representative composites and bulk samples for the metallurgical program, including a trial pit. Importantly, the Koppamurra deposit contains valuable magnet elements Nd, Pr, Dy, and Tb. These rare earths are concentrated with the fine clays and distributed to the lanthanite minerals, which means that these rare earths can be extracted 'easily' as compared to other rare earth minerals that require energy intensive cracking and roasting.

COST ESTIMATE AND PROFITABILITY APPROACH

The cost estimate was developed to guide understanding what drives profitability of the project, that is, identification of the big levers that will make a project profitable over the life of operations. Through this analysis it was identified that operating costs are driven by reagent use, while capital costs in a slurry leach flowsheet are driven by dewatering equipment size, and revenue is driven by magnet rare earth production.

envelope' cost estimates. However, a lot of that information isn't available in Australia. So given a flowsheet is required to evaluate project profitability, and there is limited or no access to whole of plant benchmarking data, AR3 conducted a comprehensive test work campaign, with over 300 bench scale tests and a pilot operation at ANSTO, SGS Lakefield, Bureau Veritas, and University of Toronto, to understand the process set points. From this work a flowsheet and a cost estimate were developed, based on the metallurgical test work and pilot results.

The following approach was used to produce a cost estimate, to assess profitability and identify levers, and then pull these levers from the earliest stages of the project to maximise potential:

- Flowsheet development for the Mixed Rare Earth Carbonate (MREC) process shown in Figure 2. Typically, existing plant design and operating costs are used to do preliminary 'back of the
- Process set points were derived from test work for input to the mass balance to estimate capital, operating costs, and revenue.
- Capital costs were built off major mechanical equipment, with factored costs, and benchmarking.
- Operating costs from consumables and utilities use.
- Revenue from rare earth production rates.

Using these costs, profitability was measured by net present value (NPV). NPV compares present value of cash inflows to cash outflows for the life of the project. There are other ways to measure profitability, but this is a widely used way that's easy to interpret, so it's been applied to this project.

The cost analysis is built on the mass balance and robust models for rare earth extraction and acid consumption. The predictive models in the mass balance are based on over 200 leach tests that have been ingested into the metallurgical database. The acid consumption model is relatively simple, driven by acidity, calcium content and leach duration. The extraction models are accurate, shown in Figure 3, and are aiding understanding what the secondary factors driving extraction might be, through a machine learning approach to identify key features of the extraction.

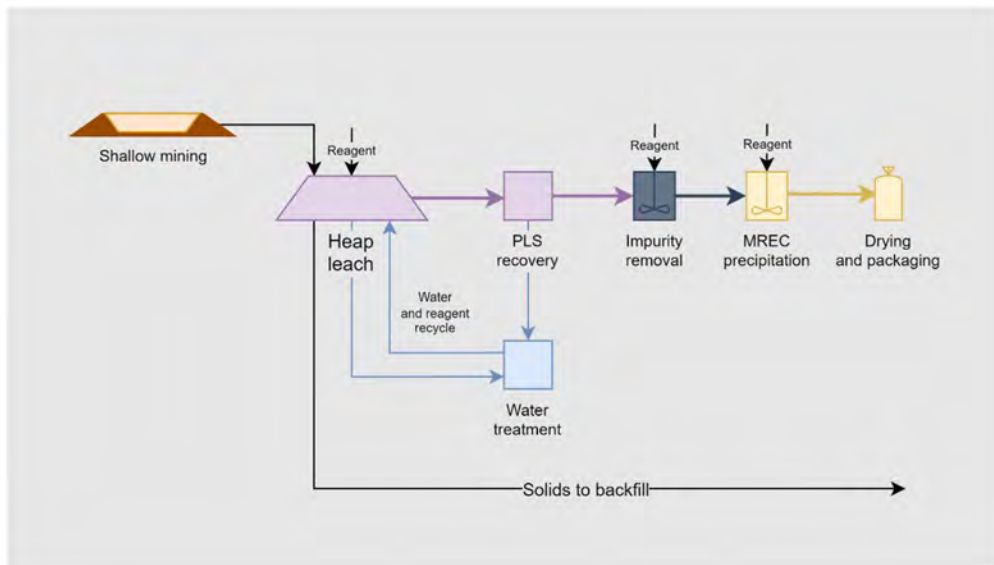


Figure 2: The cost estimate was built off the flowsheet mass balance for Mixed Rare Earth Carbonate (MREC) production

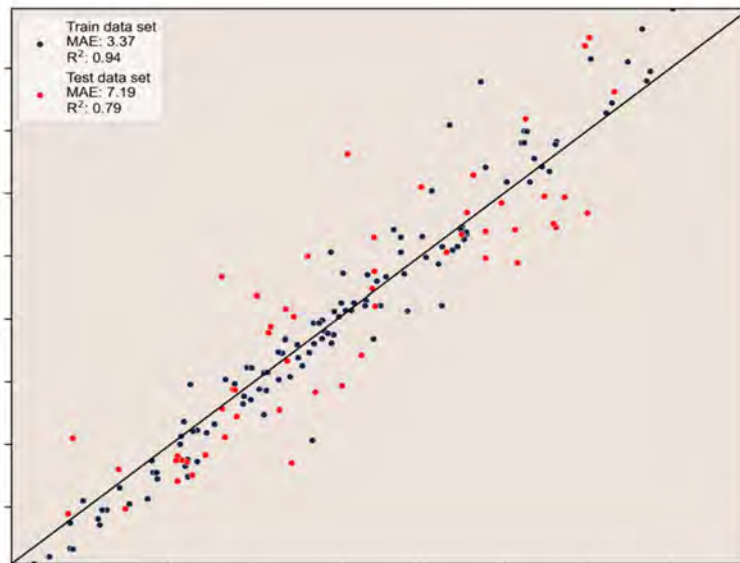


Figure 3: The models used in the mass balance for acid consumption, rare earth extraction and gangue dissolution had high accuracy as shown in this plot of actual versus predicted. These predictive models, including machine learning models, were built using over 200 Koppamurra leach tests.

CAPITAL COSTS

Since capital costs were built of major mechanical equipment benchmarking, the costly items are quickly identified. In terms of capital costs, the dewatering equipment size in a slurry leach has a large impact and was a key factor in investigating the applicability of heap leach. In the slurry leach flowsheet option, there are two key areas where clay is separated from liquor:

- After leach, the rare earth rich leach liquor is separated from the clay waste.
- After neutralising of the slurry leach residue, the neutralised clay waste is separated from water. These solids to are used as backfill, to rehabilitate and return the land to the landholders.

Filtering a clay presented challenges in practice, but evaluation of several techniques, led to either a centrifuge or screw press at a commercial scale being proposed.

Through this evaluation of slurry leach and dewatering, WGA saw an opportunity to reduce technical risk and capital costs through application of heap leach in place of slurry leach for rare earth extraction, in the Koppamurra flowsheet. Using a heap leach rather than slurry leach means that the dewatering steps are eliminated:

- Separating of the rare earth rich liquor from the clay waste is achieved through normal operation of the heap leach.
- Neutralisation of the material before backfilling could be achieved in the heap rather than in a stirred tank. This potentially means that the neutralised heaped material is ready for immediate backfill, supporting rapid rehabilitation of the land.

The heap has both capital and operating cost advantages over a slurry leach. Capital cost of a heap leach is lower than slurry leach tanks due to reduction in dewatering equipment. There are also benefits to reduction in operating cost through reduction in flocculant, water, and power consumption that were required for dewatering. Based on this evaluation, AR3 has initiated heap leach test work at ANSTO. The material has been successfully agglomerated and percolated on a small scale in column heap leach. Several column leaches have been conducted at 2-4m height with ore variability to represent the deposit. The preliminary column leach results conducted at ANSTO have shown rare earth recoveries that are comparable to slurry leach.



Figure 4: Capital cost of a heap is lower than slurry leach tanks, plus there are benefits to reduction in operating cost through reduction in flocculant and power consumption from dewatering. The material has been successfully agglomerated and percolated on a small scale at ANSTO

OPERATING COSTS

Operating costs remain the biggest lever to increase profitability, so in current test work there is a focus on minimising and recycling reagents in the flowsheet. For this project, mining costs are comparatively low due to the shallow nature of the deposit (Figure 7), and they are not explored further in this paper.

Reagent operating costs are highly connected to extraction reagent use and how it impacts downstream reagent use in the impurity removal step in the following ways:

- In REE recovery, increase in acid use increases rare earth recovery, (positive), but also increases dissolution of impurities (negative). The main impurities that impact MREC quality are Al and Fe.
- In impurity removal, any increase in impurities extracted in REE extraction step, increases the reagent use in the impurity removal step.

Therefore, there are two operating cost penalties for increasing the acidity, so the trade-off for the increased extraction and revenue needs to be positive.

The approaches being investigated to minimise operating costs are pH optimisation, leach duration, and reagent recycle:

- **pH optimisation:** By increasing the pH, we can get a 50% reduction in acid consumption, and a reduction in iron and aluminium dissolution (Figure 5). This reduces operating costs in the impurity removal step and can produce higher quality product with less effort and cost. Previous work has shown that high REE recoveries can be achieved at pH 2 at ambient conditions, with sulphuric acid and magnesium sulphate. This was recently proven for heap leach column test work at ANSTO which showed that at lower acidity, of pH 2.2, the acid consumption halved compared to pH 1.5, the ratio of REE to aluminium increased (Figure 6) The heap leach test work indicated that the heap leach Pregnant Liquor Solution (PLS) may have a lower impurity profile with higher rare earth concentration.
- **Leach duration:** Another lever to consider in operating costs is leach duration, given that for a lower acidity, a longer leach may yield similar recoveries, and potential have a positive impact on REE to impurity ratios. The trade-off between acidity and leach duration is being investigated. The trade-off is a decrease in operating costs, for an increase in plant capital costs, that is, trading acid costs for either slurry leach tank install or heap leach setup costs, which has a positive impact on NPV.
- **Reagent recycle:** There are opportunities to recycle up to 98% of reagents by regenerating chemicals onsite. The trade-off is again between operating and capital costs, that is, trading cost of purchasing reagents for cost of capital for water treatment. Recovery of water and reagents is being assessed at a desktop level and will be tested through application of nanofiltration (NF) and ultrafiltration (UF) in an upcoming test work program. Potentially acid and salt used in REE extraction can be recycled. Impurity removal precipitation reagents could also be recycled.

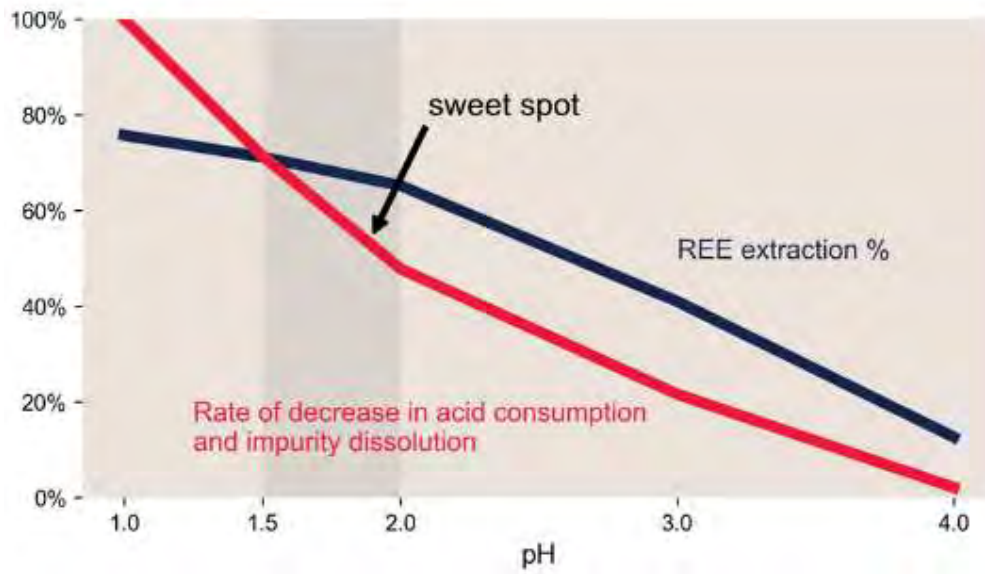


Figure 5: By increasing the pH, we can get a 50% reduction in acid consumption, and a reduction in impurity dissolution.

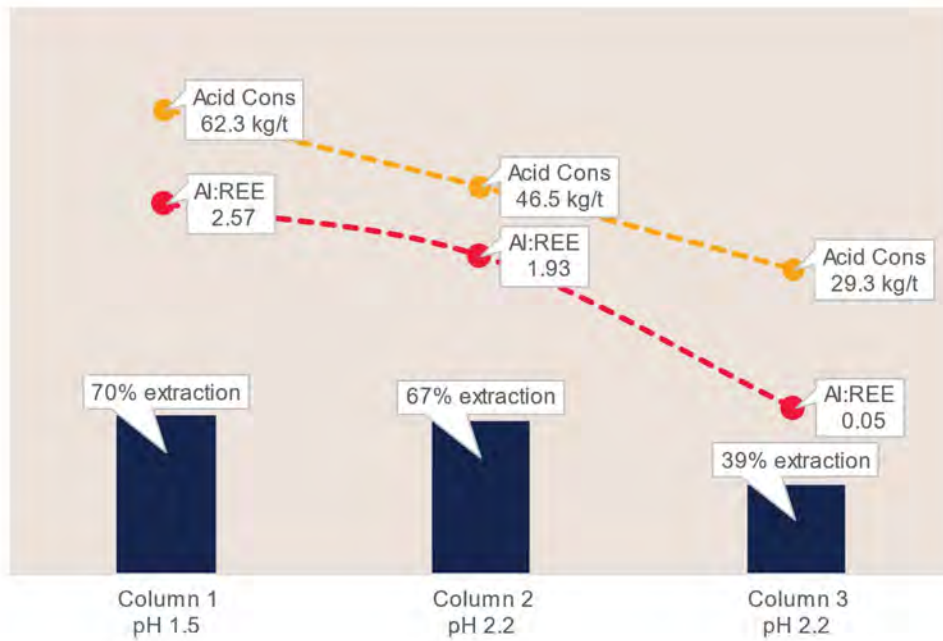


Figure 6: Heap leach column test work at ANSTO showed that at pH 2.2, the acid consumption reduced by up to 50% compared to pH 1.5, and the ratio of aluminium to REE decreased.



Figure 7: The Koppamurra deposit is within the first 10m, which means that surface mining costs are relatively low compared to other key operating costs such as reagent consumption. This image shows a trial pit excavated at Koppamurra in 2022.

REVENUE

Revenue is driven by magnet rare earth production, which in simple terms, is derived from ore grade, and recovery.

In the clay hosted ionic clays at Koppamurra, the rare earth grade of the clay is not enough to inform the recovery. Up to 77% recovery of the four magnet rare earths can be achieved from the Koppamurra ore, but the test work at varying pH, with over 200 tests at ANSTO and University of Toronto, has shown that there are likely three phases of rare earths. This understanding could not have been inferred from the rare earth grade and mineralogy alone – the metallurgical test work program was required. Those three phases, present in all clay hosted rare earths, are:

- Rare earths that are ionically adsorbed, that are removed to solution at mild acidity.
- Secondly, rare earths that are more tightly bound and require higher acidity.
- And thirdly, a small amount of mineralised rare earths that require either roasting or cracking.

Another factor to consider that impacts revenue, is the distribution of the four magnet rare earths in the ore and product. This impacts the value of the mixed rare earth carbonate product.

In the test work program, the focus is on pH to drive revenue and profitability, but there may be opportunities to target high grade areas to increase production. This especially makes sense at the beginning to pay off the project. Application of temporary or progressive heap leaching may maximise revenue in the early stages of Koppamurra. Recent resource modelling has identified high-grade rare earth subsets that would support this approach. Therefore, high grade satellite mine sites with temporary heap pads to target these high-grade areas may increase profitability. Another advantage to this progressive heap leach is rapid and progressive rehabilitation of the land. The extracted topsoils and overburden could be temporarily set aside, ready to be placed back on top of the washed clay. There is also an opportunity to expand and scale up production over time across the region.

CONCLUSIONS

WGA's integrated team of process engineers and data scientists collaborated with Australian Rare Earths to develop a comprehensive mass balance model and profitability analysis to focus flowsheet development, with the objective of reducing time to commercialisation. There are several moving parts to the profitability calculation that can be pursued, but to focus effort, and ensure efficient use of time and resources, WGA developed a multi scenario analysis to rapidly assess several scenarios to identify the big levers. Through this analysis it was identified that operating costs are driven by reagent use, capital costs are driven by dewatering equipment size, and revenue is driven by magnet rare earth production. Through this analysis we identified an opportunity to reduce technical risk and capital costs through the application of heap leach in place of slurry leach to eliminate dewatering costs. Australian Rare Earths are now focusing on reducing operating costs through water and reagent recycle, and progressive heap leach approach to target high grade areas to increase profitability.

RARE EARTH EXTRACTION WITH IONQUEST 801

By

Chiara Carrozza, Filip Dutoy, Maria Bruna Stella

Italmatch Chemicals Spa, Italy

Presenter and Corresponding Author

Chiara Francesca Carrozza

c.carrozza@italmatch.com

ABSTRACT

Rare earth elements (REEs) are indispensable components in the manufacturing of high-tech devices, renewable energy technologies, and defence applications. As global demand for these elements continues to rise, there is a pressing need to optimize extraction processes for both efficiency and environmental sustainability. This study explores approaches to rare earth extraction using IONQUEST 801® and integrates a predictive modelling to enhance process understanding and optimization.

We conducted a screening test varying process parameters such as temperature, pH, and reagent concentrations systematically to optimize extraction efficiency. Starting PLS solution was prepared in the lab with the following rare earth element, La – Ce – Gd – Dy – Y at 0.02 M. The data obtained were used to develop empirical and mechanistic models to predict rare earth extraction yields and flowsheet.

Further tests were performed mixing specific concentration of different extractant and/or phase modifier. Our experimental results demonstrate the effectiveness of the proposed extraction methods, highlighting improvements in both yield and selectivity. The developed models successfully capture the complex relationships between process parameters and extraction efficiency, providing valuable insights for process optimization.

INTRODUCTION

Rare Earth Elements (REEs) constitute a family of 15 elements crucial for various high-tech applications, including wind turbines, electric motors, catalysts, and batteries. The surge in REE prices in 2010, triggered by China's decision to reduce exports, underscored the need for countries to secure their own REE supplies. As a result, there's been a growing interest in exploiting REE resources domestically and through recycling.

The majority of REE production comes from mining ore bodies, where the elements are clustered in minerals like bastnasite and monazite. Extracting REEs from these ores requires separating and precipitating them into individual rare earths, a process typically accomplished through solvent extraction (SX) in mixer-settlers.

Unlike the more commonly used SX processes for metals like copper or uranium, REE extraction poses unique challenges due to the chemical similarities among the elements and the need for extensive separation steps. While conventional SX circuits may involve fewer than 10 units, REE separation circuits can require over 1000 mixer-settlers, making piloting and plant design exceptionally complex.

Model Construction

For a common multi-components feed, the process configuration consists of sequentially arranged units, each of them well defined by specific inputs (e.g., composition g/L, pH, mass balance between inlet and outlet). The outcomes should be able to solve the requirements of stage extraction efficiencies, considering all the experimental variables. The complexity of the system increases from bench to pilot scale and as a result, the output profile requires a large data set for obtaining an accurate representation. In addition, this challenge is directly linked to the optimization of design flowsheet, especially for the industrial applications (Figure 1.).

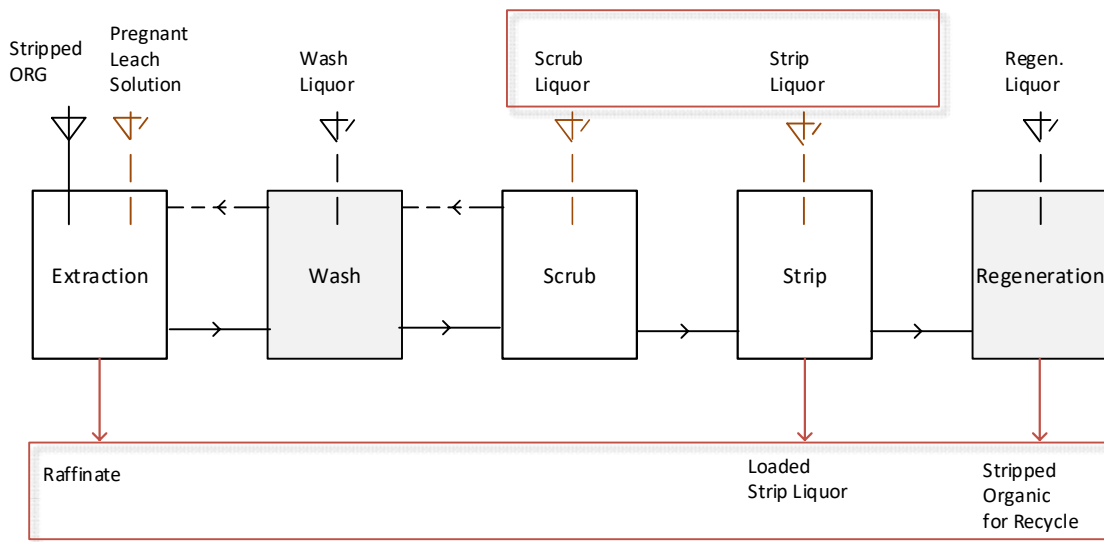


Figure 1: Global view of a typical flowsheet for metal recovery.

To improve the description of the extraction performances related to different scenarios, the experimental data need to be coupled to computing strategy. The simpler idea is starting from equilibrium parameters collected during the lab screening as input to develop a steady state model. The equilibrium concentrations of the target REE are calculated under fixed conditions of temperature and

pH. Those data are used to construct a curve fitting based on distribution ratio: this is the best choice to estimate the mass transfer between the phases and evaluate how the extraction profile is affected to pH.

The next level consists of extending this approach on counter-current separation model to include the description of multi-stage extraction. The D-ratios can be included in a set of equations which define the mass balance for each REE in the mixer unit. The goal is the calculation of metal amount in every stage by setting some known parameters such as the total number of stages, the organic and aqueous flow rate, and the selected equilibrium pH. This approach works under the assumption that the steady-state variables are reasonable for a good representation of reactions rapidly proceed, not including kinetic or interfacial phenomenon.

EXPERIMENTAL SECTION

A mid/heavy REE solution was chosen to evaluate IONQUEST® 801 performances (0.3 M in aliphatic diluent ESCAID 110 provided by Exxon Mobil). The primary purpose was to find the operating conditions in terms of pH, as REE recovery occurs at remarkable acidic range. The pregnant leach solution (PLS) was prepared in HCl media (0.02 M REE as chloride). The aqueous and organic phase were kept in contact at room temperature under magnetic stirring for 15 min. HCl 20 %wt and NaOH 13%wt were used for pH adjustment. The IONQUEST® 801 profile was compared the data obtained with commercial phosphonic acid-SX.

Table 1: REE feed composition (PLS).

REE	MW salt	molarity REE	g/L REE
La	371.4	0.02	2.78
Ce	372.6	0.02	2.80
Gd	263.6	0.02	3.15
Dy	377.0	0.02	3.25
Y	303.4	0.02	1.78

The metal ion concentration was determined by ICP-OES. The extraction efficiency can be calculated according to equation [1]:

$$\% \text{Extraction} = \frac{C_0 - C}{C_0} \times 100 \quad [1]$$

The distribution ratio and the separation factor are introduced to evaluate and quantify the performance of extractant. For the metals A and B, they are respectively expressed as equations [2] and [3]:

$$D_A = \frac{\text{Concentration of metal A (organic)}}{\text{Concentration of metal A (aqueous)}} \quad [2]$$

$$\beta_{AB} = \frac{D_A}{D_B} \quad [3]$$

RESULTS AND CONCLUSIONS

Solvent extraction results

The plots in Figure 2 exhibits a good trend of extraction for IONQUEST® 801. As expected for Dy and Y, the percentage of extraction is high already at low pH, similarly for Gd where the recovery gradually increases as pH increases. The lowest grouping La and Ce needs less acidic conditions to overcome the issue of co-extraction, but globally IONQUEST® 801 can achieve far better results when compared with those obtained from the commercial phosphonic acid in Figure 3.

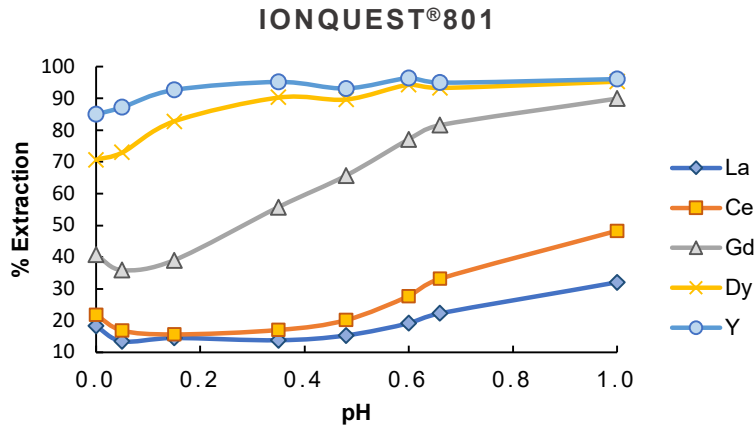


Figure 2: IONQUEST® 801 – experimental extraction curve vs pH. 1M extractant in ESCAID 110. 0.02 rare earth metals as chloride.

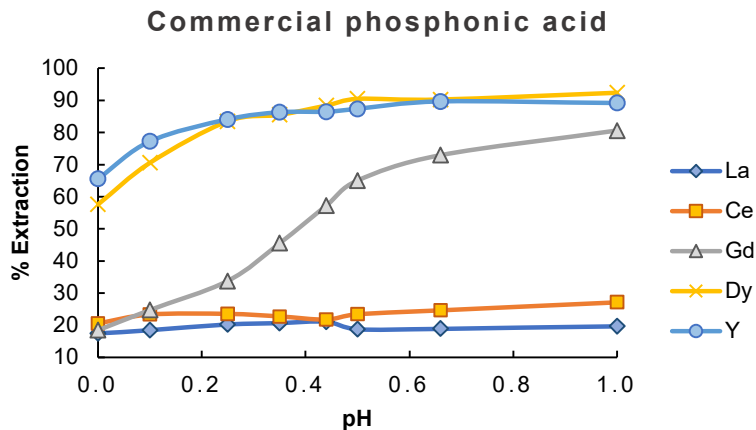


Figure 3: Commercial phosphonic acid SX – experimental extraction curve vs pH. 1M extractant in ESCAID 110. 0.02M rare earth metals as chloride.

The good trend is evidence when distribution ratios are calculated for each REE. Three values of pH are selected to achieve a description of extraction capability. As depicted in Figures 4 and 5, the IONQUEST® 801 distributions are much more efficient for Gd, Dy and Y when compared with commercial phosphonic acid ones. Typically, it implies a high extractability of metal ions from the

aqueous phase, in addition to separation factors (β) that reflect how selectively metal can be extracted. In the Table 2 separations factors are listed for IONQUEST® 801 and commercial phosphonic acid. IONQUEST® 801 shows a remarkable selectivity for the heavy REE (Gd, Dy, Y) at the investigated pH interval. For La and Ce IONQUEST® 801 offers the same separation performances as commercial extractant but increases the percentage of extraction for the same conditions.

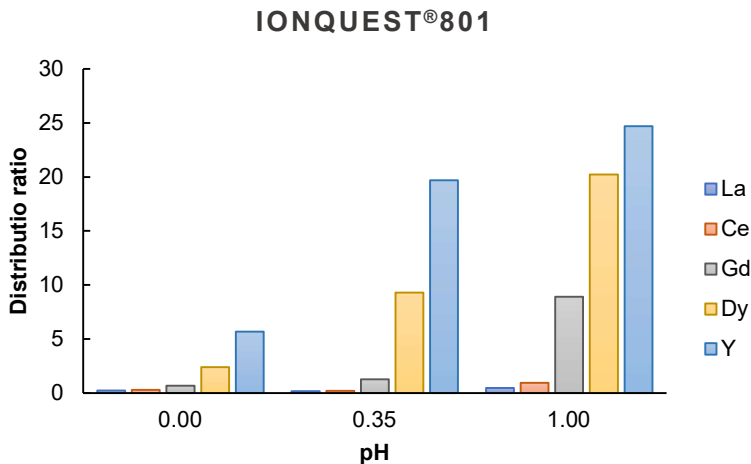


Figure 4: Distribution ratio experimentally calculated for IONQUEST® 801 at three different pH (0.00, 0.33, 1.00).

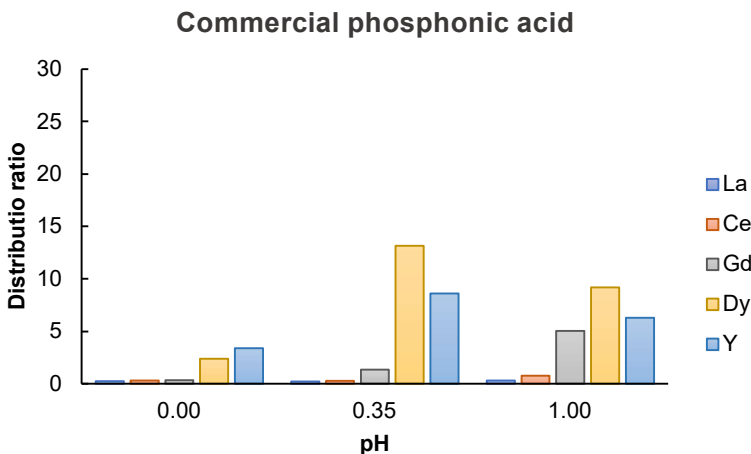


Figure 5: Distribution ratio experimentally calculated for commercial phosphonic acid SX at three different pH (0.00, 0.33, 1.00).

Table 2: Separation factors experimentally calculated for IONQUEST® 801 (left side) and commercial phosphonic acid (right side) at three different pH (0.00, 0.35, 1.00).

pH 0.00	IONQUEST® 801				Commercial phosphonic acid			
	Ce	Gd	Dy	Y	Ce	Gd	Dy	Y
La	1.25	3.08	10.77	25.37	1.20	1.30	9.40	13.33
Ce		2.47	8.63	20.33		1.08	7.82	11.08
Gd			3.50	8.24			7.25	10.28
Dy				2.36				1.42
pH 0.35	IONQUEST® 801				Commercial phosphonic acid			
	Ce	Gd	Dy	Y	Ce	Gd	Dy	Y
La	1.28	7.87	58.03	123.06	1.31	1.31	62.07	40.61
Ce		6.13	45.21	95.87		4.82	47.22	30.90
Gd			7.37	15.64			9.81	6.42
Dy				2.12				0.65
pH 1.00	IONQUEST® 801				Commercial phosphonic acid			
	Ce	Gd	Dy	Y	Ce	Gd	Dy	Y
La	1.98	18.88	42.93	52.41	2.51	16.62	30.29	20.69
Ce		9.54	21.68	26.47		6.61	12.05	8.23
Gd			2.27	2.78			1.82	1.24
Dy				1.22				0.68

Simulation of metal distribution

The distribution ratios experimentally determined were used to validate the fitting curves resulted from the simulations. The approach is to functionalize empirical correlations with parameters known to affect equilibrium distribution. An intuitive strategy is proposed in the equations [4] e [5]: D-ratios can be expressed in function of pH and then predicted from a polynomial fitting. Note that the polynomial grade is directly related at stoichiometric coefficients of proton in the equilibrium reaction and, consequently to ionic state of metal in the aqueous phase.

$$D = f(\text{pH}) \quad [4]$$

$$\text{Log } D = a_1(\text{pH})^2 + a_2 \text{pH} + a_3 \quad [5]$$

A programming tool was developed to estimate how extraction profile was affected by pH. The point was fitting the experimental D-ratio by minimizing the sum of the squares of the deviations of the data from the model (least-squares fit). The results are showed in Table 3. The correlations reveal a good agreement between two data set for the selected range of pH. The threshold for the error estimation is below 5%, but some small discrepancies can be corrected by changing the grade of polynomial fitting. In other words, the model gives back a good representation of which are the best conditions to achieve a target REE composition.

Table 3: Laboratory data and model predictions for REE distribution with IONQUEST® 801.

Distribution factor – Model results						Distribution factors – Exp results				
pH	La	Ce	Gd	Dy	Y	La	Ce	Gd	Dy	Y
0.00	0.19	0.22	0.53	2.43	6.41	0.22	0.28	0.69	2.41	5.67
0.33	0.18	0.24	1.36	7.69	14.99	0.16	0.21	1.26	9.28	19.69
1.00	0.50	1.03	9.82	19.71	23.15	0.47	0.93	8.90	20.23	24.70

Develop of graphical interface

The next challenge is successfully implementing the D-ratio model into a model for counter-current extraction flowsheet. The first step consists of including the experimental data in the species mass balance equations (Equation [6] and [7]). In according to mass transfer, as schematized in the Figure 6, the objective is determining the REE composition at the stage *n* for each unit is present in the entire flowsheet.

$$v_{Org} C_{Org,n-1}^{REE} + v_{Aq} C_{Aq,n+1}^{REE} = v_{Org} C_{Org,n}^{REE} + v_{Aq} C_{Aq,n}^{REE} \tag{6}$$

$$C_{Aq,n}^{REE} D_n = C_{Org,n}^{REE} \tag{7}$$

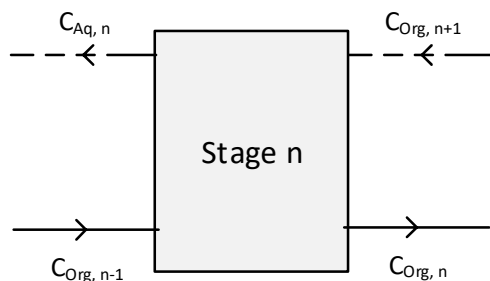


Figure 6: Mass balance diagram illustration for a single unit in a current-current extraction process.

The programming key will be solving a set of simultaneously equations to achieve the organic and aqueous metal profile in terms of percentage of extraction. Inlet and outlet flow are characterized by some input parameters, such as flow rates volumetric ratios and pH feed (See Table 4).

The future work will be centred on the develop of an application tool, with the purpose of acquiring the metal profile specifically for a selected set of operative conditions. The interface will facilitate the user ability to sort the experimental parameters which are stored in a complete database (See Fig. 7).

Table 4: Parameters set up for counter-current simulation flowsheet.

	Input	Output
Experiment	pH feed PLS composition	Distribution ratio for batch scale Efficiency for single stage
Model	$C_{Org,n-1}^{REE}, C_{Aq,n+1}^{REE}$ (Mass balance) v_{Org}, v_{Aq} (Flow rates)	Distribution ratio for flowsheet process Efficiency for n stages

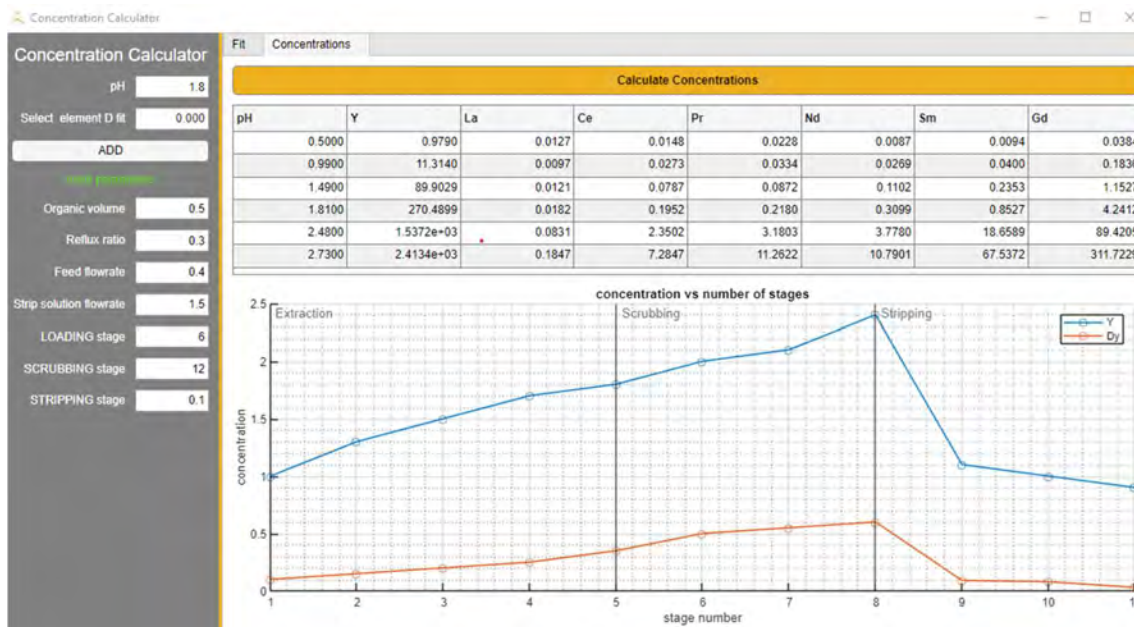


Figure 7: Application interface for D-ratio model. Example of REE calculated profile using equilibrium parameters.

ACKNOWLEDGMENTS

This work, in particular related to the modelling development, is supported by the IPCEI Eu-Batin project. We thank all people included for the hard work and collaboration.

REFERENCES

1. Aguilar, Manuel, and José Luis Cortina, eds. *Solvent extraction and liquid membranes: Fundamentals and applications in new materials*. CRC Press, 2008.
2. Iloje, Chukwunwike O. (2020). Modeling Liquid-Liquid Extraction for Critical Elements Separations: An Overview Multidisciplinary Advances in Efficient Separation Processes. *ACS Symposium Series American Chemical Society*. pp 335-365.

3. Lyon, Kevin L. Utgikar, Vivek P. Greenhalgh, Mitchell R. (2017). Dynamic Modeling for the Separation of Rare Earth Elements Using Solvent Extraction: Predicting Separation Performance Using Laboratory Equilibrium Data *Ind. Eng. Chem. Res.* 56, 4, 1048–1056 American Chemical Society.
4. Omelchuk, Kateryna, and Alexandre Chagnes. (2018). New cationic exchangers for the recovery of cobalt (II), nickel (II) and manganese (II) from acidic chloride solutions: Modelling of extraction curves. *Hydrometallurgy* 180, 96-103.

THERMODYNAMIC MODELLING OF RARE EARTH SOLVENT EXTRACTION

By

Kevin L. Heppner and ²Brett W. Schug

KWA Kenwalt Australia [SysCAD], Canada

²KWA Kenwalt Australia [SysCAD], USA

Presenter and Corresponding Author

Brett W. Schug

brett.schug@syscad.net

ABSTRACT

Rare Earth Elements (REEs) are becoming increasingly important due to their critical role in the transition to clean energy. In recent times, there has been significant activity and investment in production from mining and recycling. A key area of difficulty for metallurgical production of REEs is their separation, largely due to their similar electron structures which makes them chemically similar.

In this work, a thermodynamic model of solvent extraction (SX) is presented based solely upon experimental data in open literature. This model is embedded in SysCAD connected to PHREEQC⁽¹⁾ via the Thermodynamic Calculation Engines (TCE) interface. In previous work, Heppner⁽²⁾ calculated reaction equilibrium constants for the extraction of Nd and Pr based upon fitting to experimental data of Lyon et al.⁽³⁾. Here, that model is extended using separation factors published by Zhang et al.⁽⁴⁾ and references therein to estimate the equilibrium constants for all 15 REEs. Pitzer parameters and their temperature dependence are calculated for each cation-anion interaction in the REE chloride system from correlations published by Simoes et al.⁽⁵⁾⁽⁶⁾. It is noteworthy that aqueous/organic exchange reactions are written in terms of free acid, not hydrochloric acid, and thus, are suitable for use in any acidic medium (e.g. chloride, sulphate, nitrate).

A test of the model was performed where a solution containing REE chlorides was fed to an extraction, scrubbing, and stripping circuit with conditions typical for initial separation of light, medium, and heavy REE elements. Results of the test model showed trends that are typical of SX separation of REEs in practice, confirming the validity of the approach. This fundamental approach enables a wider range of applicability for the model compared to the use of plant isotherms.

This work focuses on the modelling methodology of the REE SX process, rather than the modelling of a specific processing plant. For this reason, the presented model requires validation against relevant plant data prior to use for plant design or optimisation.

Keywords: Rare earth elements, solvent extraction, SysCAD, PHREEQC, process simulation, process optimisation, process design, digital twin, REE, battery metals

INTRODUCTION

REE Separation Process and Challenges

The solvent extraction separation of rare earth elements involves numerous circuits and hundreds of mixer-settler units. Individual circuits consisting generally of extraction, scrubbing, and stripping are employed to separate different rare earth metals into various cuts, thereby allowing further separation downstream. The resulting process includes significant recycle loads both within individual circuits, as well as between separation areas. The result is a process that is not only complex to simulate, but also to operate. Steady-state conditions can take very long times to achieve. As noted in Turgeon et al.⁽⁷⁾, "it takes 14 days to stabilize a pilot plant for one condition". For this reason, it is important to have a mathematical model of a solvent extraction process.

Conventional approaches to solvent extraction involve the use of plant isotherms and/or distribution coefficients to understand loading behaviour of rare earth elements in different conditions. Plant isotherms, while highly useful, are limited to the chemical solution from which they are obtained. Changes in feed chemistry will affect the loading behaviour due to the competitive nature of the extraction process. Furthermore, isotherms are required for each of the circuits. Distribution coefficients are obtained at a consistent pH and extraction concentration, and thus, are indicative of the separability of adjacent rare earths. These coefficients are also limited in their application to the pH for which they are obtained. Turgeon et al.⁽⁷⁾ presented an equilibrium approach whereby equilibrium constants for individual reactions were calculated by fitting to experimental data. This approach is an improvement in that it is applicable over a wider operating range and adjustable for changing feed conditions. However, it did not consider solution non-ideality. In the work presented herein, the PHREEQC interface is used with SysCAD to model solvent extraction considering non-ideal solution behaviour. Activities of components in the aqueous solution are calculated using Pitzer's model, which accounts for short- and long-range interactions between ions and neutral species.

In earlier work, Heppner⁽²⁾ calculated the equilibrium constants for acid dissociation, neodymium extraction, and praseodymium extraction using experimental data reported by Lyon et al.⁽³⁾. Here, that original work is expanded to include all rare earth elements. Using the calculated equilibrium values from the previous work, separation factors reported by Zhang et al.⁽⁴⁾ are employed as quasi-indicators of equilibrium constant ratios, thereby allowing the calculation of extraction equilibrium constants for the rare earth elements, not including Promethium and Scandium. Together with aqueous speciation and activity calculations, a highly robust model for the calculation of rare earths separation was developed.

MATHEMATICAL MODEL

Background

Aqueous phase chemistry is modelled using the thermodynamic package PHREEQC supplemented with Pitzer's ionic interaction model. PHREEQC is embedded as one of several available thermodynamic engines within SysCAD. Other thermodynamic engine links include OLI, AQSol, ChemApp, and HSC Chemistry. The ChemApp interface allows incorporation of databases generated using FactSage and other data sources. Long-range and short-range interaction terms for Na⁺ and Cl⁻ are obtained from the Pitzer.dat database in PHREEQC. Additional Pitzer parameters for Nd⁺³, Pr⁺³ and Cl⁻ were taken from Roy et al.⁽⁸⁾ and Simoes et al.⁽⁵⁾⁽⁶⁾. Pitzer's parameters are a virial expansion of binary and ternary interactions between cations, anions, and neutral species, incorporating all important permutations and combinations. Debye-Hückel type terms in the equation account for long-range interactions, which scale according to ionic strength. These equations allow calculation of individual activity coefficients for dissolved neutral and ionic species, along with the osmotic coefficient of water.

Information on the electrolyte chemistry models used in PHREEQC are documented by Parkhurst and Appelo⁽¹⁾. In brief, chemical equilibrium and mass balance equations are combined to calculate the reactions which occur to achieve the minimum free energy state of a system. Chemical equilibrium equations are expressed as:

$$K_i = \prod_{j=1}^{N_i} a_{i,j}^{v_{i,j}} \quad (1)$$

Where $a_{i,j}$ and $v_{i,j}$ are the activity and stoichiometric coefficient of the j^{th} species involved in the i^{th} reaction. The activity is calculated from the species concentration and the activity coefficient. The activity coefficient is calculated from Pitzer's equations using temperature-dependent terms. With appropriate interaction coefficients, the Pitzer model is typically applicable up to and including the range of 2 – 6 molal concentration, depending on the solute, per Pitzer and Mayorga⁽⁹⁾, and thus is suitable for application to this model.

Cation Extraction

Liquors containing rare earths as dissolved chloride salts are typically processed using suitable cation extractants dissolved in an organic solvent. The relevant equilibria are shown below:



Here, Pc represents the cation exchanger PC88A. The mechanism of extraction involves acid form extractant dissociation, equation (2) and cation exchange, equation (3) as per Lyon et al.⁽³⁾. From previous work⁽²⁾, it was shown that solvation reactions, while reported to occur in certain situations by Sato⁽¹⁰⁾, did not occur in this system at the concentration ranges of interest. In equation (3), the REE species represents all 15 rare earth elements considered in this work. Equation (4) is the saponification of acidified organic, typically using sodium hydroxide solution.

Calculation of the Equilibrium Constants

Equilibrium constants for neodymium and praseodymium extraction were taken from previous work by Heppner⁽²⁾. To extend the database for all rare earth elements, reported separation factors of Zhang et al.⁽⁴⁾ were used. Recall that the separation factor for rare earth i from rare earth j has the following form:

$$S_{i,j} = \frac{K_{d,i}}{K_{d,j}} \quad (5)$$

Where $K_{d,i}$ is the ratio of rare earth i in the organic to that in the aqueous phase at equilibrium, i.e. the distribution coefficient:

$$K_{d,i} = \frac{a_{\text{Pc}_3\text{REE}_i}}{a_{\text{REE}_i^{+3}}} \quad (6)$$

Separation factors are evaluated at a constant final pH and extraction concentration. Now consider the form of an equilibrium constant for the i^{th} rare earth element:

$$K_i = \frac{(a_{\text{Pc}_3\text{REE}_i})(a_{\text{H}^+})^3}{(a_{\text{REE}_i^{+3}})(a_{\text{PcH}})^3} = K_{d,i} \left(\frac{a_{\text{H}^+}}{a_{\text{PcH}}} \right)^3 \quad (7)$$

As stated previously, the bench scale experiments conducted to evaluate separation factors use the same final pH and same extractant concentration. Since adjacent rare earth elements have similar chemical properties, it is assumed that, in these experiments, acid distributes in a similar manner for both rare earths. By applying this assumption, it is postulated that the separation factor can be related to the ratio of equilibrium constants of adjacent rare earths, i.e.:

$$S_{i,j} = \frac{K_i}{K_j} \quad (8)$$

Using separation factors reported by Zhang et al.⁽⁴⁾, equation (8) was applied to the previously determined equilibrium constants for neodymium and praseodymium to estimate the equilibrium constants of the other 13 rare earth elements considered in this work.

Saponification equilibrium constants were calculated such that 50% saponification of fully acidified organic (0.015 M Ionquest 801 in kerosene) was achieved when mixed in a 1:1 volumetric ratio with 2 M NaOH solution, as in Zaki et al.⁽¹¹⁾.

Verification of Approach

The approach of using separation factors as a proxy for equilibrium constant ratios was verified through a test of the Nd/Pr system. This system was chosen because both Nd and Pr equilibrium constants were obtained independent of the separation factor approach. As noted earlier, Nd and Pr were obtained by fitting to published experimental data⁽²⁾. The following steps were taken:

1. SysCAD models of the shakeout of 1% by mass solutions of both NdCl₃ and PrCl₃ in 2 molar PC088A in kerosene were built.
2. Both shakeout test models were used to simulate the experiment where sodium hydroxide was used to achieve a final aqueous solution pH of 1.5.
3. Predicted organic and aqueous concentrations from the model were used to compute the distribution coefficients for both Nd and Pr at these conditions.
4. The ratio the equilibrium constants for each of the reactions were also computed.

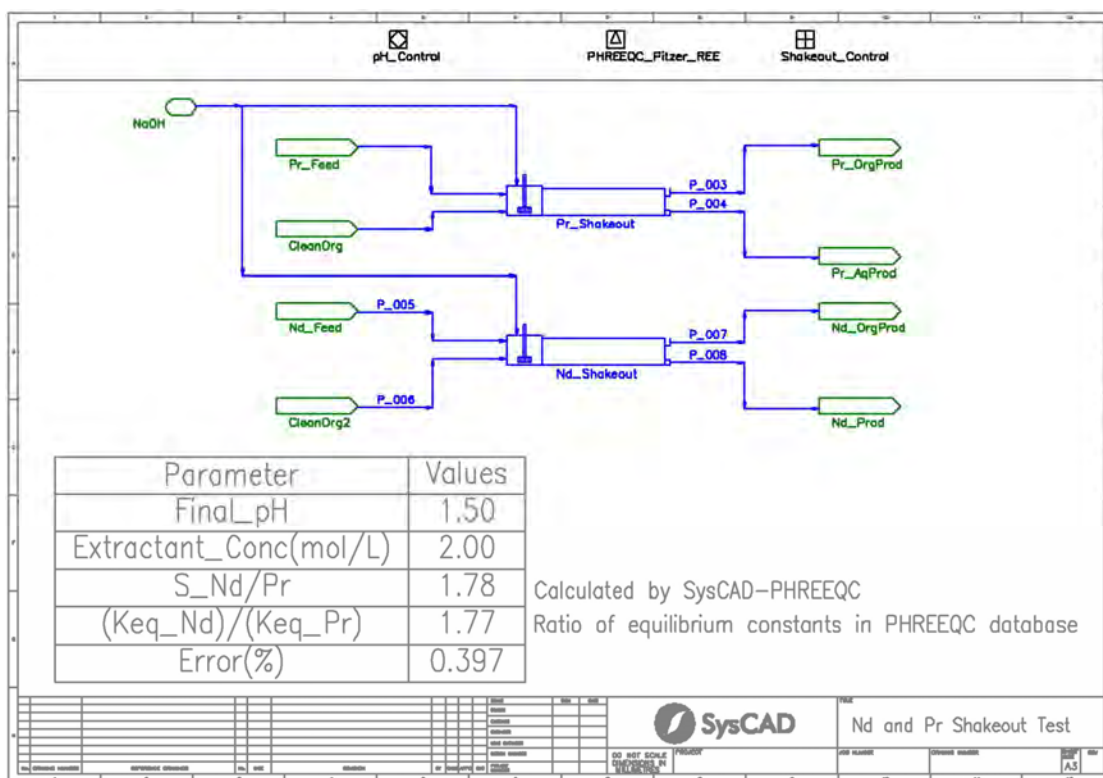


Figure 1: SysCAD Model of Shakeout Tests for Nd and Pr Extraction

It can be seen from the results shown in Figure 1 that the deviation between the ratio of the distribution coefficient and ratio of the equilibrium constant is less than 0.4%. From equation (7), this close agreement implies that the distribution coefficient for acid is equivalent for adjacent rare earths, thereby verifying the approach.

Solvent Extraction Modelling

Solvent extraction unit operations are modelled as sequential mixer-settler units. Either recovered aqueous or organic may be recycled to control the O/A ratio in the mixer. Incomplete phase separation and crud formation may also be considered. The input parameters for a solvent extraction unit include entrained organic in aqueous, entrained aqueous in organic, and other operational parameters.

In this SysCAD model, each mixer-settler has a PHREEQC thermodynamic calculation embedded, allowing for first principles calculation of the organic-aqueous interfacial reactions. Reactions are not specified in the solvent extraction unit, but rather, are determined by free energy minimisation. Although not done in this work, reaction kinetic effects can also be incorporated through the implementation of constrained free energy methods.

The model incorporates three circuits – extraction, scrubbing, and stripping. Removal of heavy rare earths is modelled using a subsequent black-box model. The organic stream resulting from heavy REE removal is saponified with sodium hydroxide solution to a target saponification extent. Saponification extent is defined as the mole fraction of extractant which is bound to sodium.

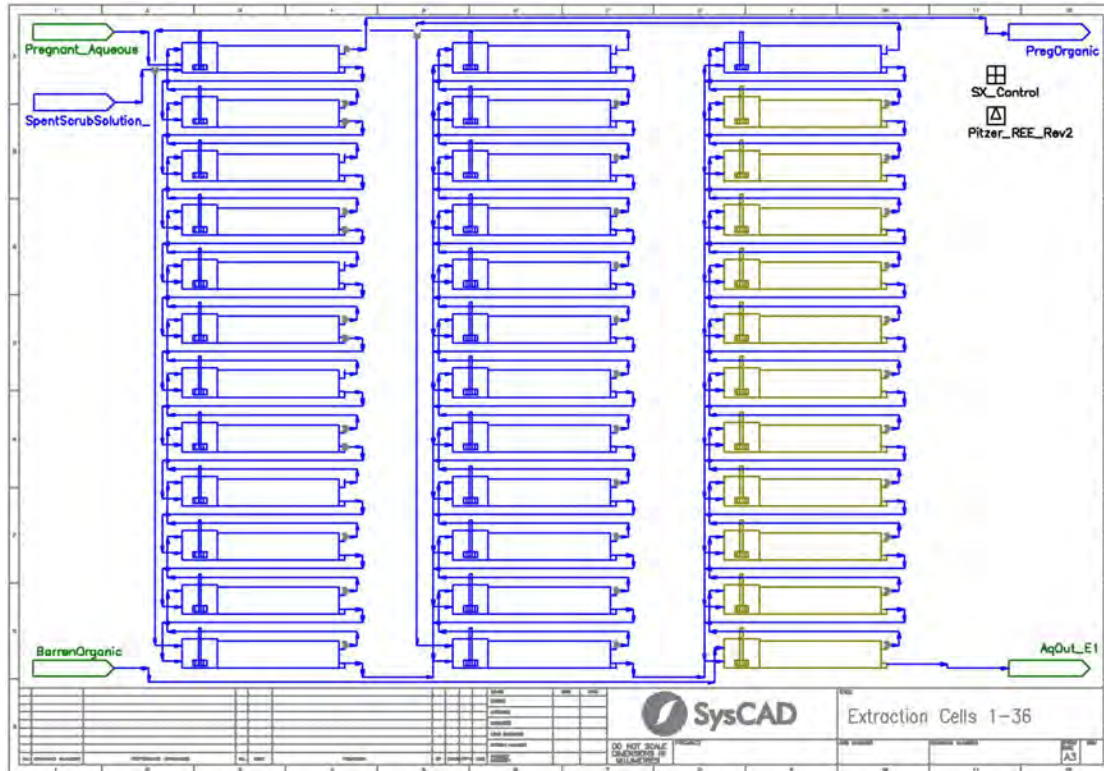


Figure 2: SysCAD Model of Extraction Area

Figure 2 shows 36 extraction area mixer-settler cells in series, although only 25 are in service (olive-coloured cells are offline). The cells can be switched on and off in the model to allow easy re-configuration for process design or operational changes. Similarly, Figure 3 shows 36 scrubbing cells in series, with 15 of them in service.

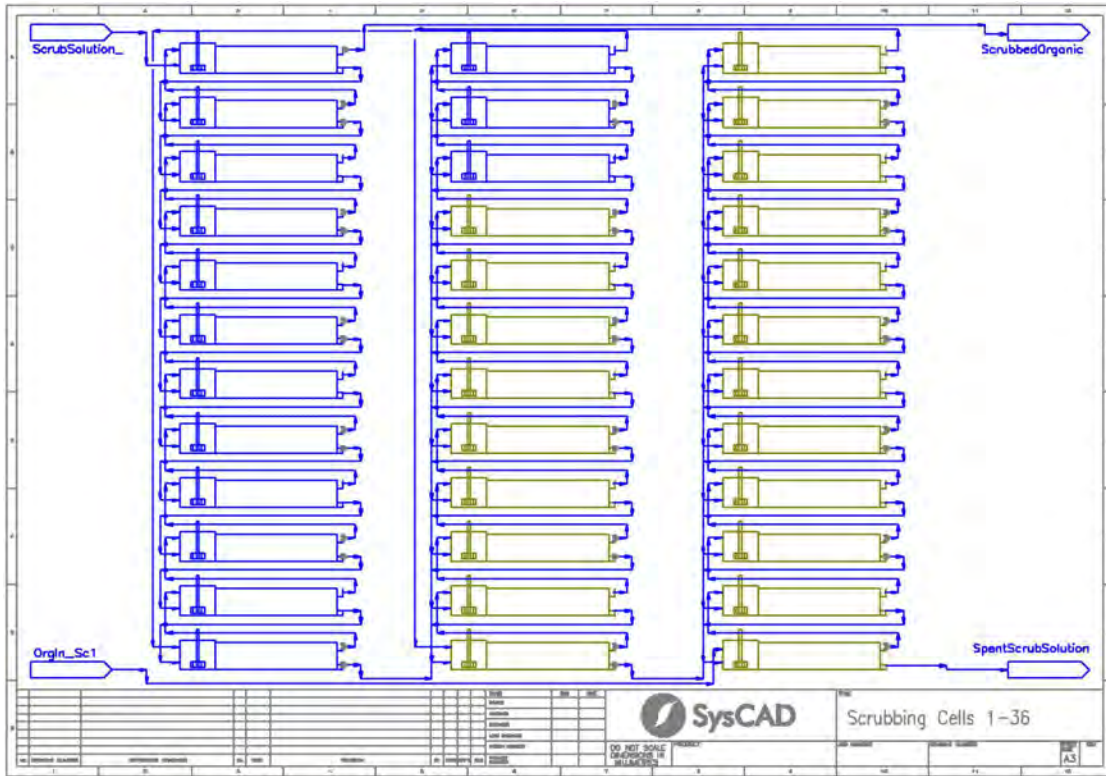


Figure 3: SysCAD Model of Scrubbing Area

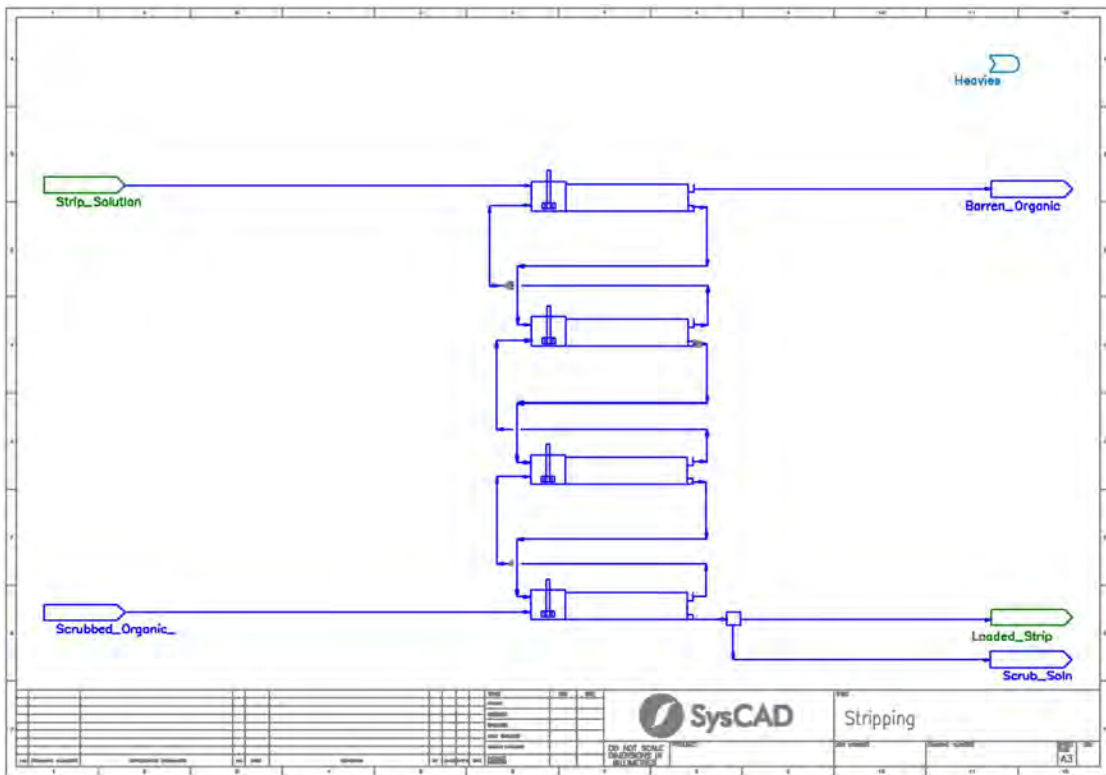


Figure 4: SysCAD Model of Stripping Area

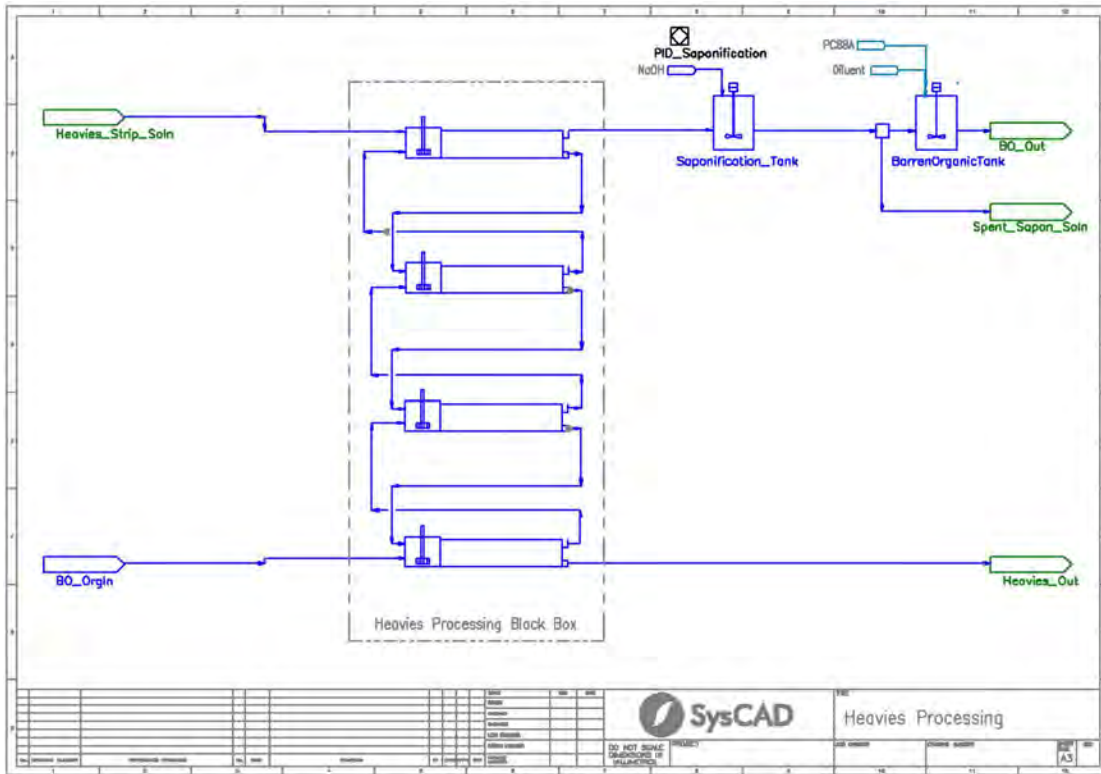


Figure 5: SysCAD Model of Heavies Processing Area

SIMULATION CASE STUDY

Base Case

Turgeon et al.⁽⁷⁾ provided a typical REE leach solution composition which was used as a basis for the pregnant leach solution feed to the model (Table 1).

Table 1: Pregnant Leach Solution Composition

Element	Concentration (g/L)
La	57.31
Ce	2.64
Pr	7.06
Nd	22.14
Sm	1.07
Eu	0.19
Gd	0.36
Tb	0.03
Dy	0.05
Ho	0.02
Er	0.03
Tm	0.003
Yb	0.01
Lu	0.002
Y	0.09

For the base case simulation, the SysCAD model calculated full stream composition data for all intermediate and final process model streams, including the three rare earths exit streams: raffinate, loaded strip, and heavies strip. The distribution of each present rare earth element to each of these three exit streams can be seen in Figure 6 as stacked columns. Notice that in this base case, all

elements distribute to one, or at most two, process area exit streams. The destinations are as expected, with Lanthanum going to raffinate, Ytterbium going to heavies strip, and a smoothly changing distribution for all elements between the two extremes. Note that given their low concentrations, Tm and Yb have been omitted.

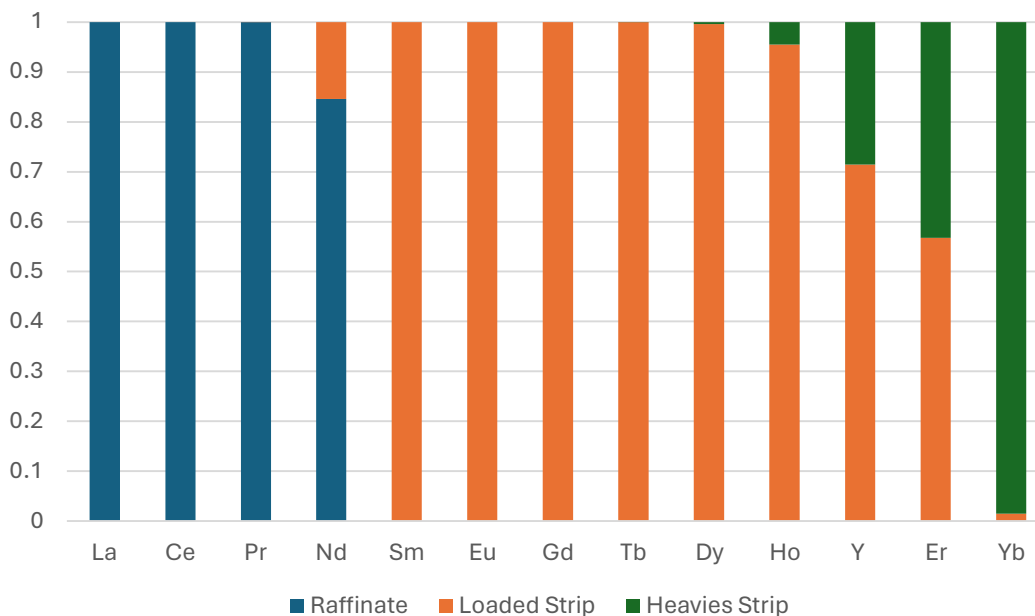


Figure 6: Base Case Elemental Distribution to Exit Streams

Sensitivity Analysis

After completing simulation of the base case conditions, the following operational parameters were varied in a sensitivity analysis:

- Organic-to-Aqueous volumetric ratio (O/A Ratio)
- Saponification Extent
- Cell Count (the number of cells in Extraction, Scrubbing, and Stripping)

The base case conditions were:

- Extraction O/A Ratio*: 2.0
- Scrubbing/Stripping Circuit O/A Ratio: 10.0 / 5.0
- Saponification Extent: 25.0%
- Cell Count (Extraction/Scrub/Strip): 25 / 15 / 4

*Organic to Pregnant Aqueous Solution Volumetric Ratio

Additional (sensitivity analysis) cases retained all base case conditions except for a single change for each sensitivity analysis case. Sequentially, the single change from the base case for the sensitivity analysis cases were:

- Scrubbing/Stripping Circuit O/A Ratio: 11.0 / 5.5
- Scrubbing/Stripping Circuit O/A Ratio: 9.0 / 4.5
- Saponification Extent: 27.5%
- Saponification Extent: 22.5%
- Cell Count (Extraction/Scrub/Strip): 15 / 15 / 4
- Cell Count (Extraction/Scrub/Strip): 25 / 10 / 4
- Cell Count (Extraction/Scrub/Strip): 25 / 15 / 2

These scenarios were selected because they represent typical parameter adjustments used in the design and operation of rare earths separation circuits. Cell count is important for optimising process design. Once in operation, O/A ratios, strip reflux, and saponification extent are some of the parameters adjusted to maintain optimal circuit performance.

Results of the sensitivity analysis are presented in Figures 7 – 15. In all cases, the results are consistent with expected design and operational trends.

Varying O/A Ratios

These scenarios (Figures 7 – 9) predict an increased distribution of elements to the later product streams when the O/A Ratios are increased. At the light elements end, Nd distribution to raffinate decreases, and Nd distribution to loaded strip increases, as the O/A Ratios increase. At the heavy end of the elements, Ho, Y, and Er distribution to loaded strip decreases, and their distribution to heavies strip increases, as the O/A Ratios increase.

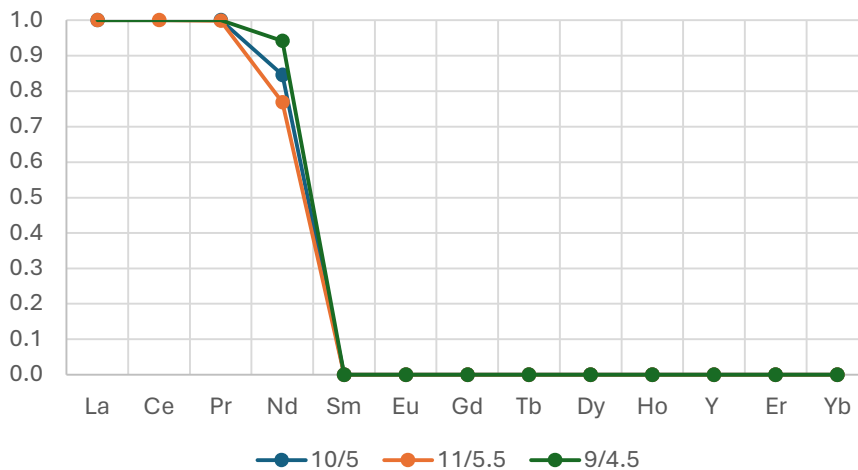


Figure 7: Elemental Distribution to Raffinate – Varying O/A Ratio

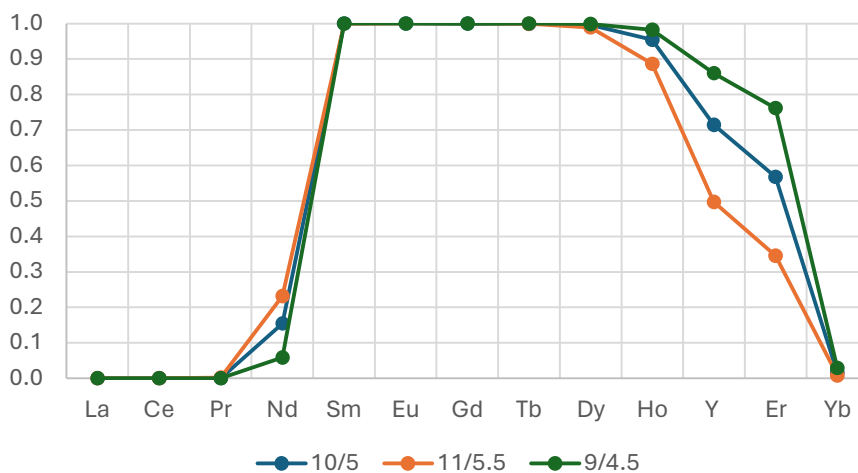


Figure 8: Elemental Distribution to Loaded Strip – Varying O/A Ratio

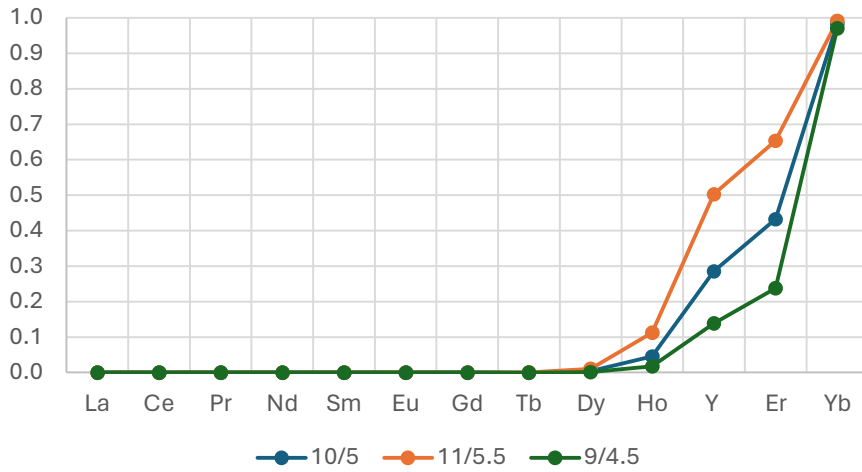


Figure 9: Elemental Distribution to Heavies Strip – Varying O/A Ratio

Varying Saponification Extent

The trends for the increasing saponification extent cases (Figures 10 – 12) mirror those for increasing O/A Ratios, with increased distribution of elements to later product streams when the saponification extent is increased. The trends are most noticeable for Nd (light end) and Ho, Y, and Er (heavy end).

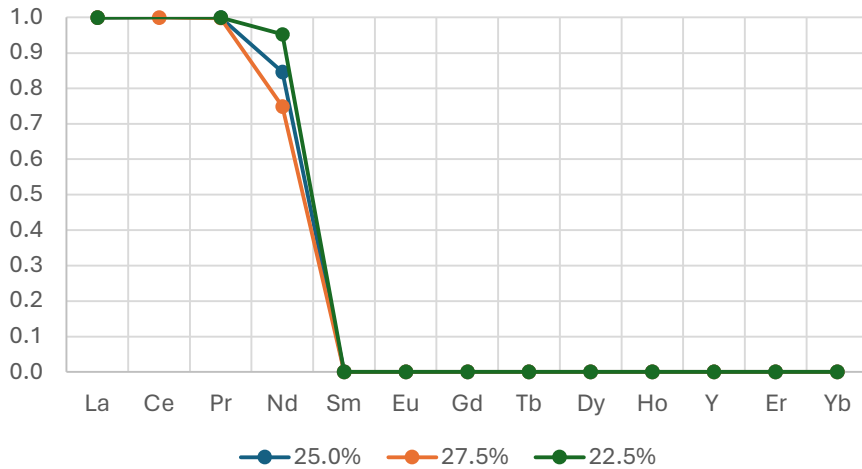


Figure 10: Elemental Distribution to Raffinate – Varying Saponification Extent

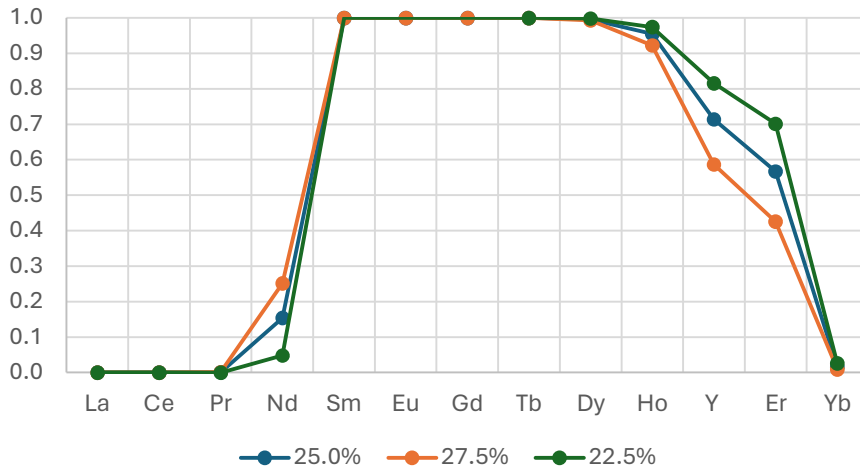


Figure 11: Elemental Distribution to Loaded Strip – Varying Saponification Extent

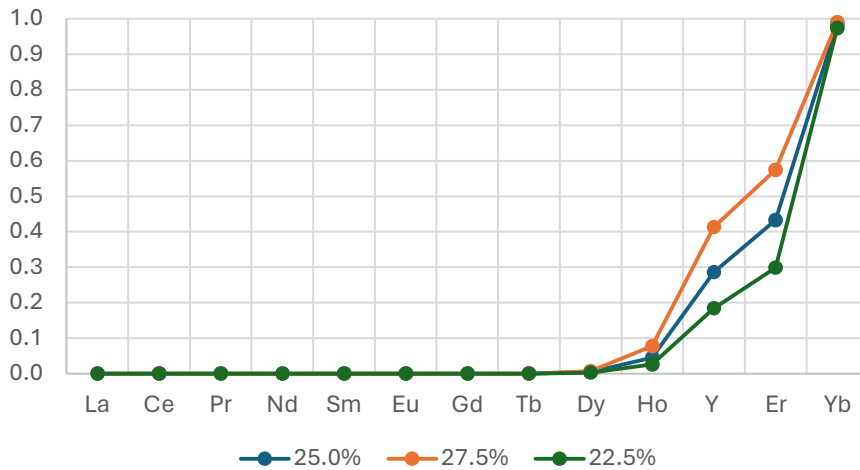


Figure 12: Elemental Distribution to Heavies Strip – Varying Saponification Extent

Varying Cell Count

Varying the cell count for this system (Figures 13 – 15) provides results which show little changes except for the case where we decrease the number of strip cells. Decreasing the number of cells by 40% in extraction from 25 to 15 cells, or by 33% for scrubbing from 15 to 10 cells creates minimal changes to the element distributions. Making a larger percentage decrease of 50%, or 4 to 2 cells, in stripping does create a noticeable change for the heavier elements Dy, Ho, Y, and Er, as their distributions decrease for loaded strip and increase for heavies strip. It appears that the extraction and scrubbing areas have more cells than are necessary for the specified conditions.

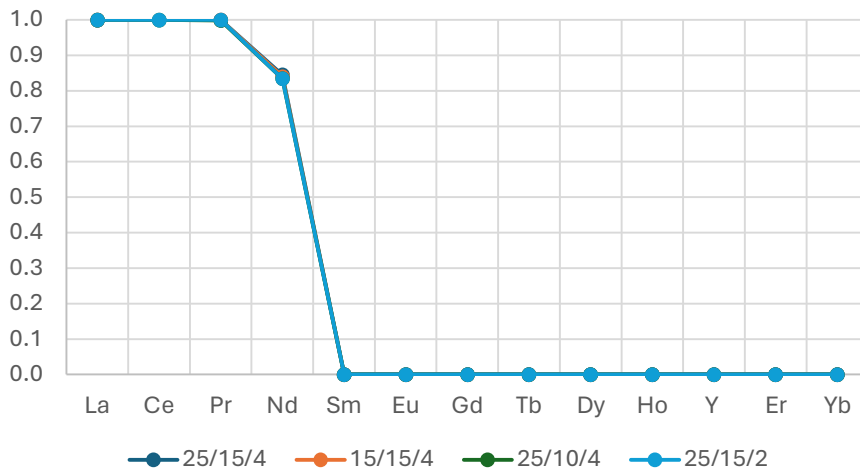


Figure 13: Elemental Distribution to Raffinate – Varying Cell Count (Extraction/Scrub/Strip)

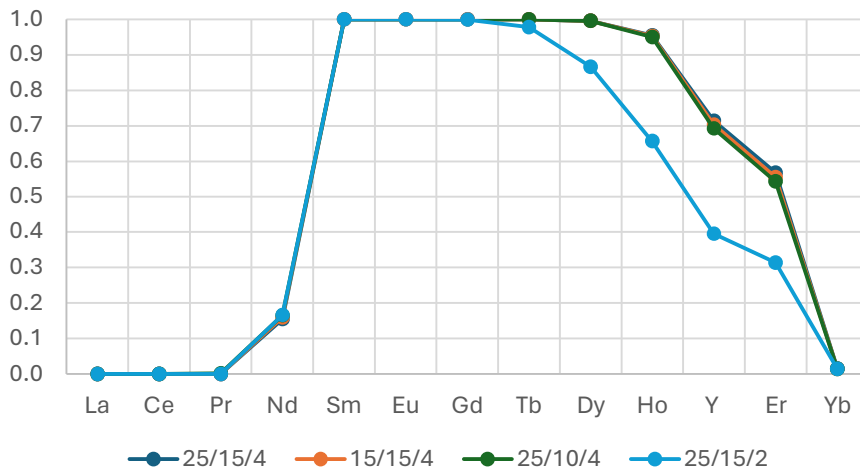


Figure 14: Elem. Distribution to Loaded Strip – Varying Cell Count (Extraction/Scrub/Strip)

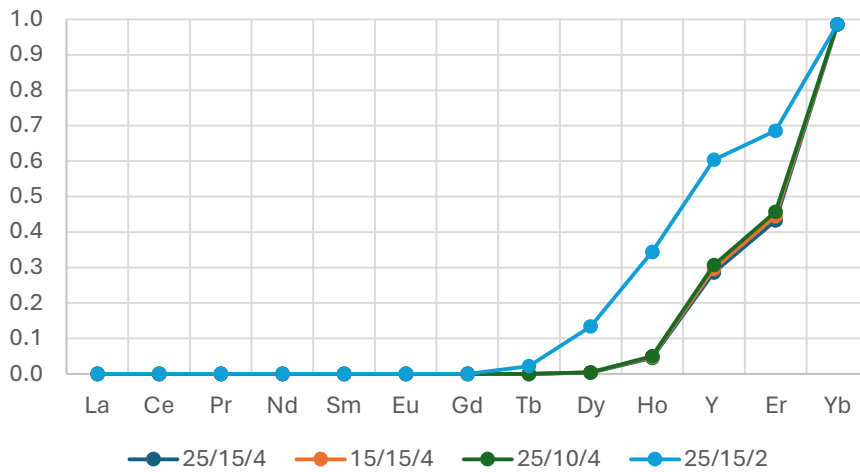


Figure 15: Elem. Distribution to Heavies Strip – Varying Cell Count (Extraction/Scrub/Strip)

Additional Cases

With the process simulation capability, additional cases may be explored in a relatively short amount of time. As one example – a single added case converged to a steady state in 475 seconds on a typical desktop computer using six cores. The TCE (Thermodynamic Calculation Engines) interface in SysCAD supports parallel computing, and in this case, up to 12 PHREEQC calculations could proceed at the same time. In addition to the changes noted above, one could expand or otherwise change the process simulated, change the process layout, feed composition, and change many other process factors, to simulate an existing process or a process being designed.

Further Saponification Sensitivity Analysis

Following the above sensitivity analysis for Scrubbing/Stripping Circuit O/A Ratio, Saponification Extent, and Cell Count, the impact of degree of saponification was further investigated. For these additional cases, the Scrubbing Circuit O/A Ratio and Cell Count were returned to the base case settings. The Saponification Extent was then varied from the base case condition of 25.0% to a maximum of 50.0% in 5.0% increments. This range was chosen because these are typical operating saponification values.

The predicted effect of greater saponification is presented in Figures 16 – 21. The same trends previously seen in Figures 10 – 12 are present at these higher saponification extent values: increased distribution of elements to later product streams when the saponification extent is increased. The trends are most noticeable for Nd (light end) and Ho, Y, and Er (heavy end). Reviewing the results further, in Figures 16 – 18, as saponification increases, the distribution curves shift more in favour of the Heavies Strip than they do against the Raffinate, yielding a narrower distribution curve to the Loaded Strip, Figure 17. Thus, at the highest saponification extents, only Nd distributes more than 50% to the Loaded Strip exit stream.

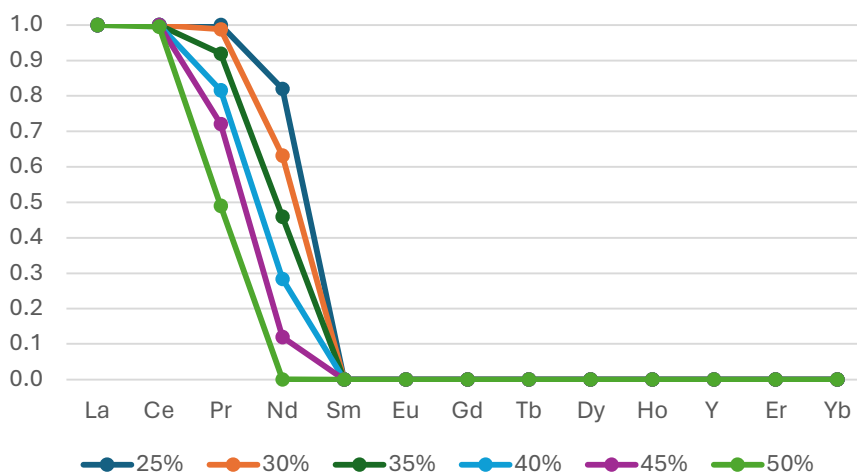


Figure 16: Elemental Distribution to Raffinate – Increasing Saponification Extent

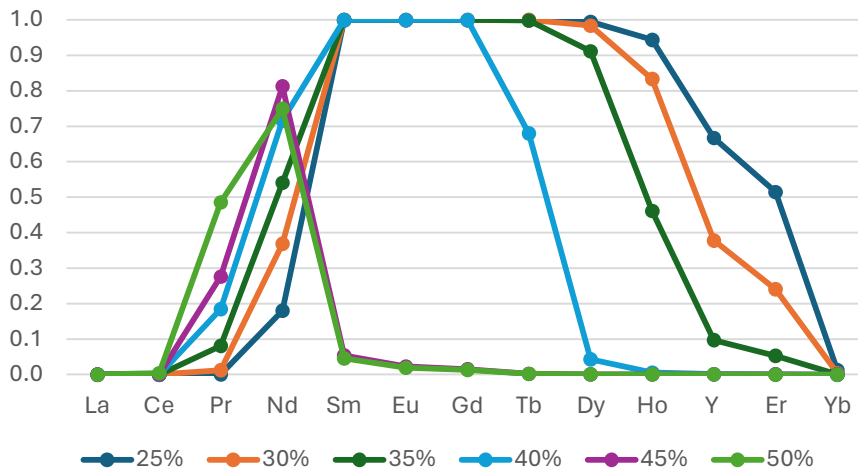


Figure 17: Elemental Distribution to Loaded Strip – Increasing Saponification Extent

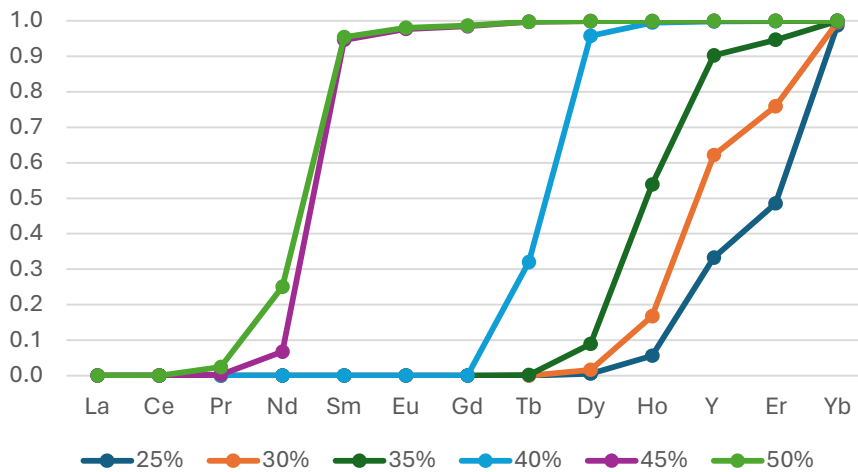


Figure 18: Elemental Distribution to Heavies Strip – Increasing Saponification Extent

Figures 19 – 21 present the data in a different manner – providing a stacked bar distribution for a single element each, across the range of saponification extent values. This visualisation is presented here for three of the elements. Nd (Figure 19) is the only element in this saponification study that ever exhibits a condition with more than 5% distribution to all three exit streams – see the 45% saponification bar, where the distribution is approximately 12 / 81 / 7 % to Raffinate / Loaded Strip / Heavies Strip. For all elements, this type of plot clearly illustrates the shift away from raffinate and towards Heavies Strip exit points. In Figure 20, Eu exhibits a sudden shift from Loaded Strip to Heavies Strip as saponification reaches 45%. And in Figure 21, Er exhibits a gradual shift from Loaded Strip to Heavies Strip as saponification increases. For other elements, not shown graphically, the shift is sometimes sudden and sometimes gradual.

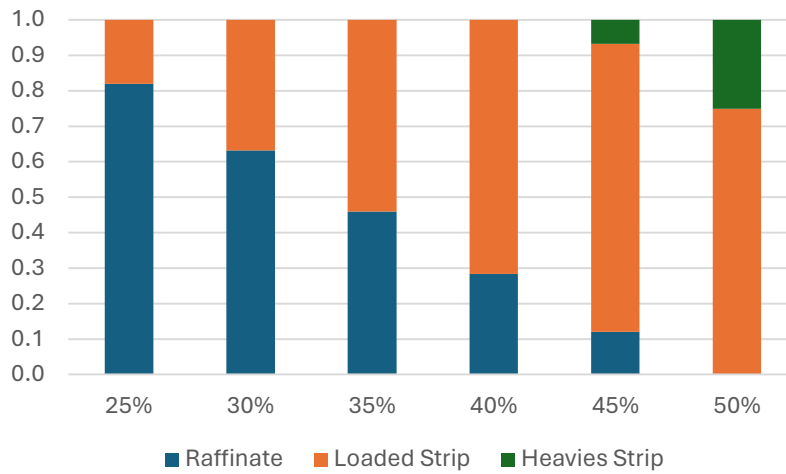


Figure 19: Neodymium Distribution – Increasing Saponification Extent

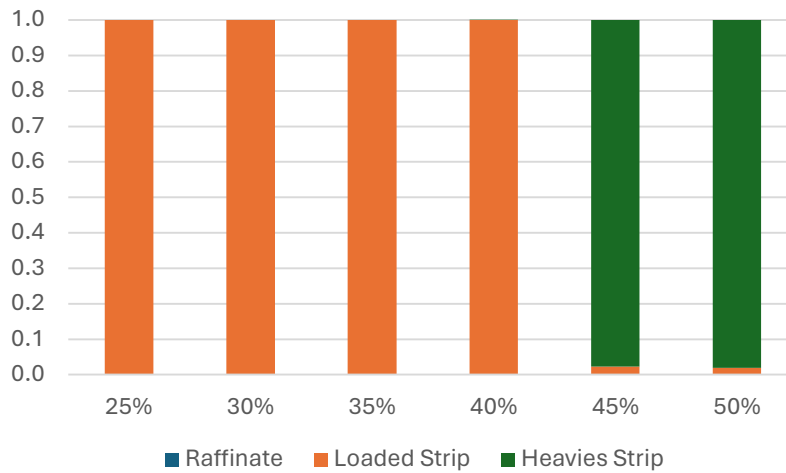


Figure 20: Europium Distribution – Increasing Saponification Extent

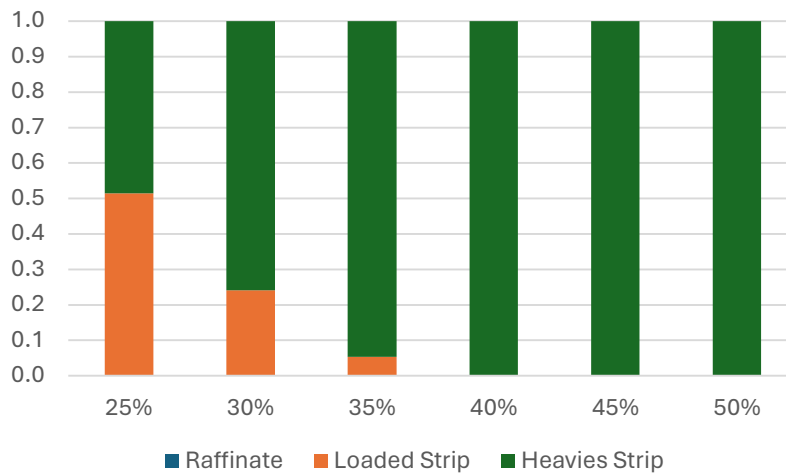


Figure 21: Erbium Distribution – Increasing Saponification Extent

CONCLUSIONS

Through this case study, the capability of a SysCAD model with embedded PHREEQC technology is presented. This technology enables the thermodynamic modelling of rare earths solvent extraction, and the simulation of many different cases in a practical time period. Within the simulation, an industry-typical feed pregnant leach solution was fed to an extraction, scrubbing, and stripping circuit. The demonstrated trends as reported by the simulation are consistent with those expected in industrial applications. Use of the model herein for actual project/operational applications would require model validation. This fundamental approach avoids the need for plant isotherms and provides a wide range of applicability in design and optimisation of rare earths solvent extraction separation processes.

Application of this methodology to a specific plant or project may require expansion of the chemical model in some cases. Such cases could include significantly different operating temperatures, a different extractant than that used in this work, additional elements in the feed, and other changes that could affect applicability of the model. However, this work provides a template for any such needed model expansion.

REFERENCES

1. Parkhurst, D.L., Appelo, C.A.J., 2013. Description of input and examples for PHREEQC version 3—A computer program for speciation, batch-reaction, one-dimensional transport, and inverse geochemical calculations. U.S. Geological Survey Techniques and Methods, book 6, chap. A43, 497 p. Available only at <http://pubs.usgs.gov/tm/06/a43/>
2. Heppner, K., 2021. Modelling the Solvent Extraction Separation of Neodymium from Praseodymium Using a First Principles Thermodynamic Model. Proceedings of the 60th Conference of Metallurgists 2021, August 17-19, 2021.
3. Lyon, K.L., Utgikar, V.P., Greenhalgh, M.R., 2017. Dynamic Modeling for the Separation of Rare Earth Elements Using Solvent Extraction: Predicting Separation Performance Using Laboratory Equilibrium Data. *Ind. Eng. Chem. Res.*, 56 (2017) pp. 1048 – 1056.
4. Zhang, Y., Gu, F., Su, Z., Liu, S., Anderson, C., Jiang, T., 2020. Hydrometallurgical Recovery of Rare Earth Elements from NdFeB Permanent Magnet Scrap: A Review. *Metals*, Vol. 10, p. 841; doi:10.3390/met10060841
5. Simoes, M.C., Hughes, K.J., Ingham, D.B., Ma, L., Pourkashanian, M., 2016. Estimation of the Pitzer Parameters for 1–1, 2–1, 3–1, 4–1, and 2–2 Single Electrolytes at 25 °C. *Journal of Chemical & Engineering Data*, Vol. 61, No. 7, pp. 2536-2554.
6. Simoes, M.C., Hughes, K.J., Ingham, D.B., Ma, L., Pourkashanian, M., 2017. Temperature Dependence of the Parameters in the Pitzer Equations. *Journal of Chemical & Engineering Data*, Vol. 62 No. 7 (2017) pp. 2000-2013.
7. Turgeon, K., Boulanger, J-F., Bazin, C., 2023. Simulation of Solvent Extraction Circuits for the Separation of Rare Earth Elements. *Minerals*, 13, 714
8. Roy, R.N., Roy, L.N., Tabor, B.J., Himes, C.A., Richards, S.J., Cummins, M.P., Christiansen, E.B., Roy, C.N., Sharma, V.K., Millero, F.J., 2005. Thermodynamics of Electrolyte Mixtures: HCl + NdCl₃ + H₂O from 5 to 55°C. *Journal of Solution Chemistry*, Vol. 34, No. 9, 1033–1044.
9. Pitzer, K.S., Mayorga, G., 1973. Thermodynamics of Electrolytes. II. Activity and Osmotic Coefficients for Strong Electrolytes with One or Both Ions Univalent. *The Journal of Physical Chemistry*. Vol. 77, No. 19, pp. 2300 – 2308.
10. Sato, T. 1989. Liquid-Liquid Extraction of Rare-Earth Elements from Aqueous Acid Solutions by Acid Organophosphorus Compounds. *Hydrometallurgy*, 22, pp. 121-140.
11. Zaki, E.E, Ismail, Z.H., Sabet, S.A., Aly, H.F., 2020. Equilibrium Studies on the Extraction of Yttrium from Chloride Medium by Mono (2-Ethylhexyl) 2-Ethylhexyl Phosphonic Acid. Report #EG0800276, Preprint, Mar 2020.

PRECIPITATION OF RARE EARTH ELEMENT SALTS OF HIGH PURITY

By

Nitin Pawar, Michael Svärd, Kerstin Forsberg

KTH Royal Institute of Technology, Sweden

Presenter and Corresponding Author

Kerstin Forsberg

kerstino@kth.se

ABSTRACT

Rare earth elements (REE) are essential in high performing permanent magnets used in e.g., wind turbines and motors. A rising demand coupled with a scarcity of supply makes some of the REE identified as critical raw materials in many parts of the world. There is a need to develop more sustainable and competitive processes for REE extraction from primary and secondary resources. Magnets can be recycled via different approaches including reuse, direct recycling, or indirect recycling. In indirect or chemical recycling, the end-of-life products are processed to extract the REE and to make the elements available for new uses. Developing techniques to do this in an economically and environmentally sustainable way is vital to create a raw-materials circular economy for these materials.

An important step is the precipitation of REE salts, which should be designed to obtain crystals of high quality in terms of crystal size, size distribution and purity. Antisolvent precipitation is a promising technique to obtain rare earth salts with high yield and of high quality. In this talk key aspects in the design of REE antisolvent precipitation processes for obtaining crystals of high quality will be presented. The focus will be on precipitation of mixed REE sulphates from impure leach liquors in the recycling of magnet waste. Different mechanisms for impurity incorporation will be discussed. Possibilities to control the precipitation process to avoid impurity incorporation will be presented. The findings can be directly applied to processes for recycling of magnet waste, but also to other hydrometallurgical processes where there is a need to recover REE salts of high quality.

Keywords: Rare earth elements, magnets, recycling, hydrometallurgy, precipitation, crystallization

Precipitation of Rare Earth Element Salts of High Quality

Kerstin Forsberg, professor

KTH Royal Institute of Technology, *Stockholm*

Dept. of Chemical Engineering

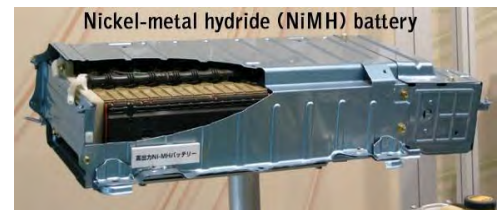
Rare Earth Elements (REE)



Sc (Al alloy)



Sc (SOFC)



La, Ce, Pr, Nd, Sm



Nd, Pr, Dy, Sm

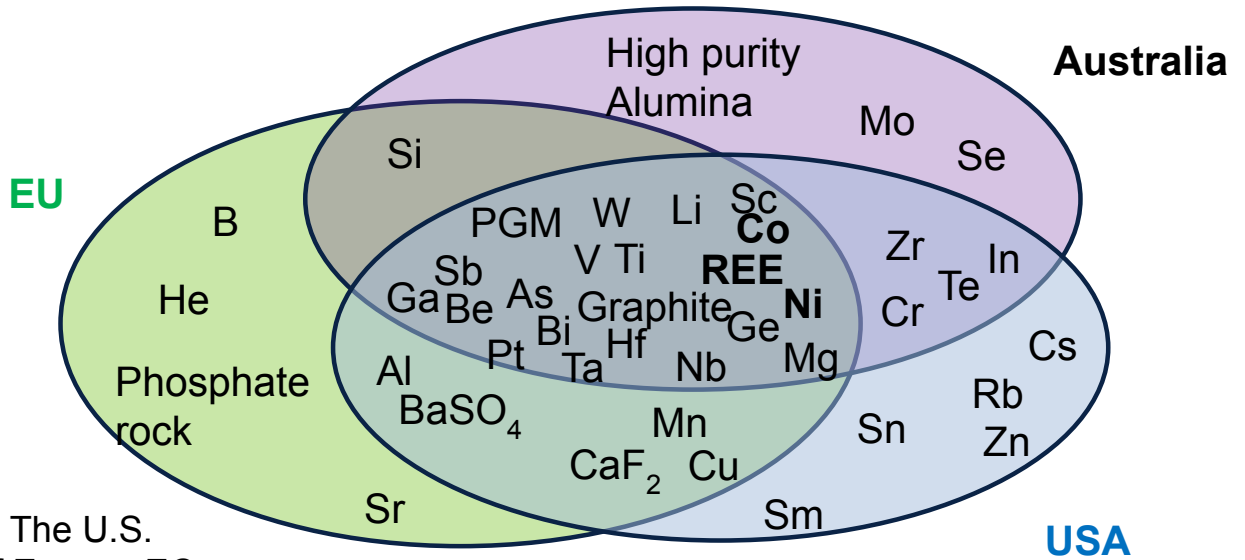


Ce, Eu, La, Y, Tb



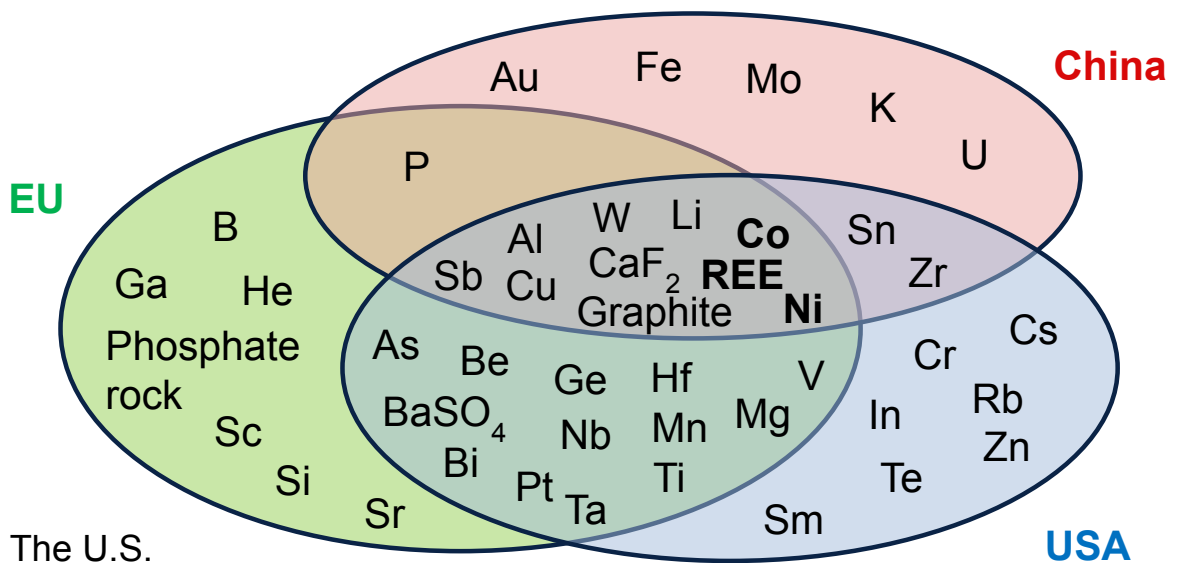
Magnets (25%), catalysts (22%), batteries (14%), polish (14%), metallurgy (9%), glass (6%), luminescence (6%)

Critical Raw Materials



Source: Irena, The U.S. Department of Energy, EC, Australian Gov.

Critical Raw Materials



Source: Irena, The U.S. Department of Energy, EC

Periodic Table of the Elements

1 H 1.01																	2 He 4.00
3 Li 6.94	4 Be 9.01											5 B 10.81	6 C 12.01	7 N 14.01	8 O 16.00	9 F 19.00	10 Ne 20.18
11 Na 22.99	12 Mg 24.30											13 Al 26.98	14 Si 28.09	15 P 30.97	16 S 32.07	17 Cl 35.45	18 Ar 39.95
19 K 39.10	20 Ca 40.08	21 Sc 44.96	22 Ti 47.88	23 V 50.94	24 Cr 52.00	25 Mn 54.94	26 Fe 55.85	27 Co 58.93	28 Ni 58.69	29 Cu 63.55	30 Zn 65.39	31 Ga 69.72	32 Ge 72.61	33 As 74.92	34 Se 78.96	35 Br 79.90	36 Kr 83.80
37 Rb 85.47	38 Sr 87.62	39 Y 88.91	40 Zr 91.22	41 Nb 92.91	42 Mo 95.94	43 Tc (97.91)	44 Ru 101.07	45 Rh 102.91	46 Pd 106.42	47 Ag 107.87	48 Cd 112.41	49 In 114.82	50 Sn 118.71	51 Sb 121.75	52 Te 127.60	53 I 126.90	54 Xe 131.29
55 Cs 132.91	56 Ba 137.33	57 La 138.91	58 Ce 140.91	59 Pr 140.91	60 Nd 144.24	61 Pm (144.91)	62 Sm 150.36	63 Eu 151.97	64 Gd 157.25	65 Tb 158.93	66 Dy 162.50	67 Ho 164.93	68 Er 167.26	69 Tm 168.93	70 Yb 173.04	71 Lu 174.97	
87 Fr (223.02)	88 Ra (226.03)	89 Ac (227.03)	90 Th 232.04	91 Pa 231.04	92 U 238.03	93 Np (237.05)	94 Pu (244.06)	95 Am (243.06)	96 Cm (247.07)	97 Bk (247.07)	98 Cf (251.08)	99 Es (252.08)	100 Fm (257.10)	101 Md (258.10)	102 No (259.10)	103 Lr (262.11)	

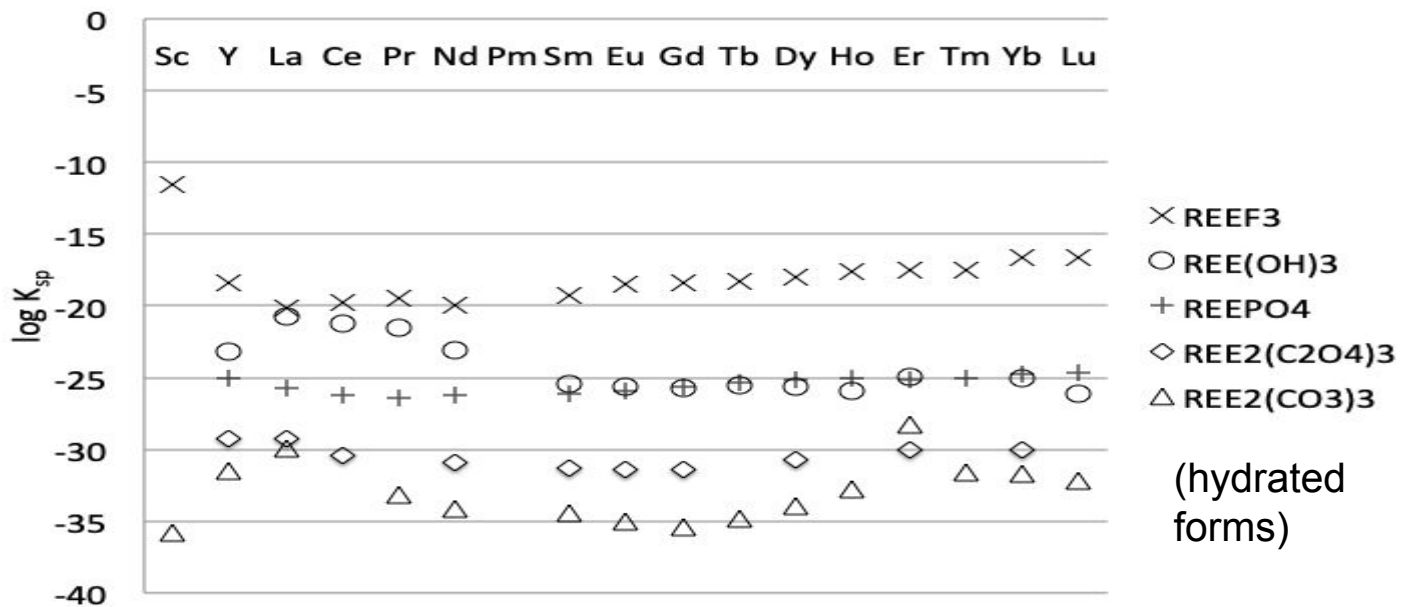
Separation of REE

Callow, 1967:

“Discussing lanthanon separation is like discussing chess. There are a limited number of opening moves, which can be analysed in detail. As the game develops, possibilities multiply enormously...”



Sparingly soluble REE salts

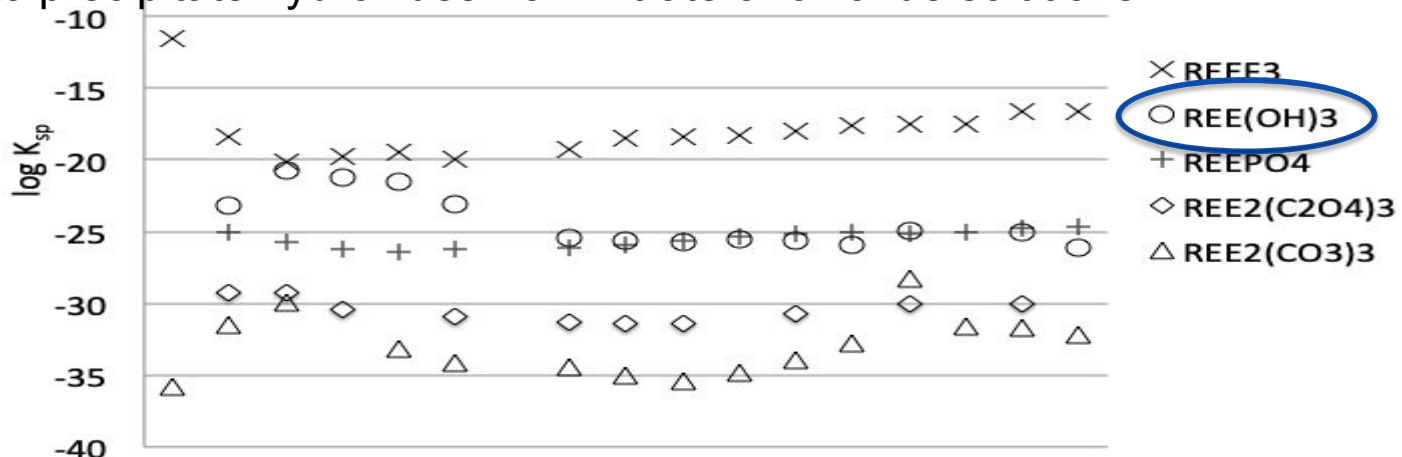


Solubility products, valid at 25°C and zero ionic strength.

7

Sparingly soluble REE salts

Basicity precipitation (e.g. using magnesia or caustic soda) is widely used in industry. Ammonia has also been used in large scale to precipitate hydroxides from nitrate or chloride solutions.

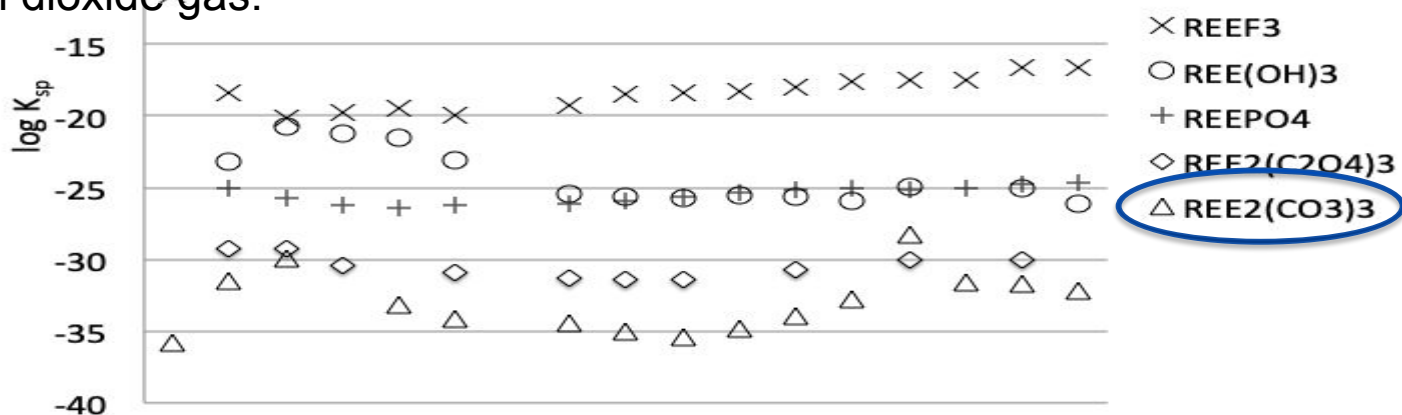


Solubility products, valid at 25°C and zero ionic strength.

8

Sparingly soluble REE salts

Carbonates are almost insoluble in water but readily soluble in dilute acids. Carbonates can be precipitated from aqueous solutions e.g. by addition of alkali carbonates, bicarbonates or carbon dioxide gas.



Solubility products, valid at 25°C and zero ionic strength.

9

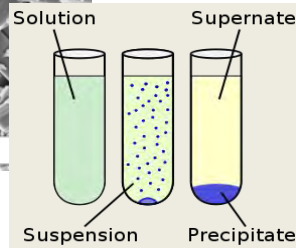
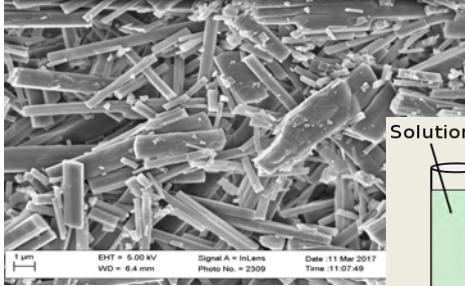
Recycling of magnets – closing the loop

- **Reuse** – Large PM can be dismantled and reused, e.g. those in generators in wind turbines and potentially those in vehicle electric motors.
- **Direct recycling** – PM are harvested and used to make new PM, like in-house recycling of materials from production.
- **Indirect recycling** – due to the complexity of the products, oxidation or other contamination and varying alloy composition the PM might need to undergo metallurgical processes to extract and recover the metals separately.

Hydrometallurgical recycling

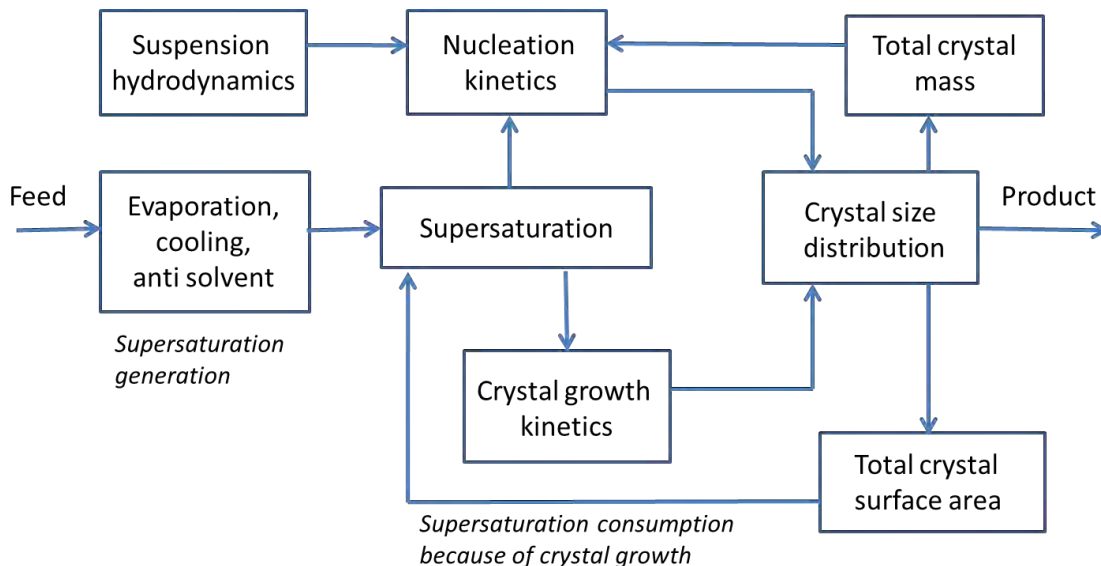
Leaching (with or without roasting) followed by separation

by solvent extraction, ion exchange, **crystallization/precipitation**

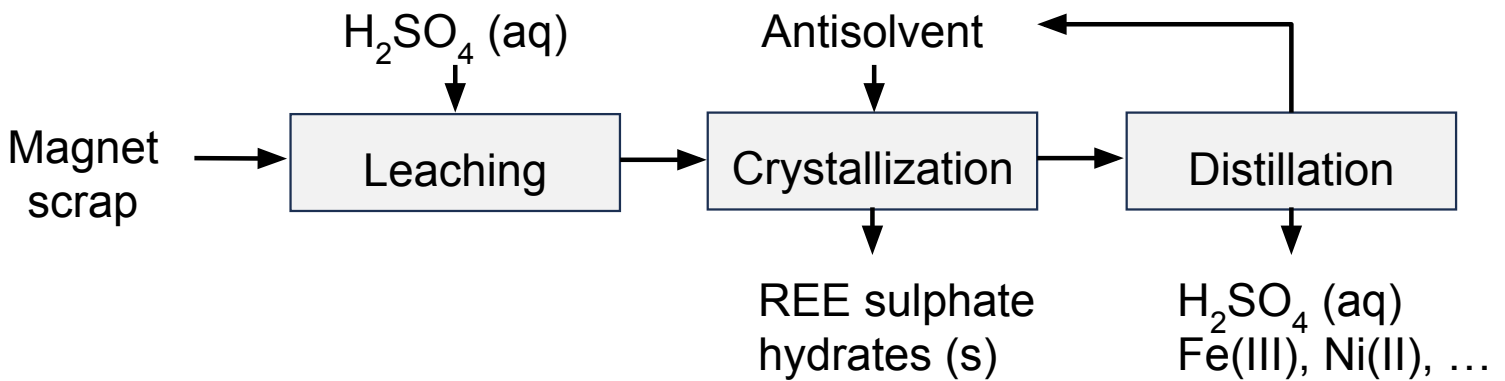


- The REE (Nd, Pr, Dy, Gd, Tb) are obtained as a mixture or as individual salts
- The final REE product is often the oxides or fluorides

Principles of Crystallization



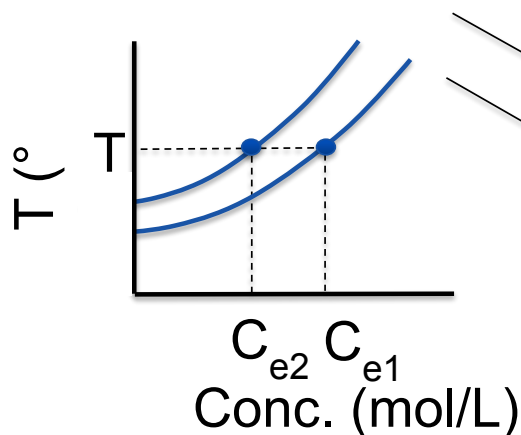
Recycling of magnets



- The REE can be selectively separated from the leach liquor
- The REE sulfate hydrates have a high solubility in water
- The solvents can be recovered by distillation
- Choice of antisolvent: economy, availability, safety, recovery

Antisolvent crystallization

- By adding an antisolvent the solubility of the salt decreases

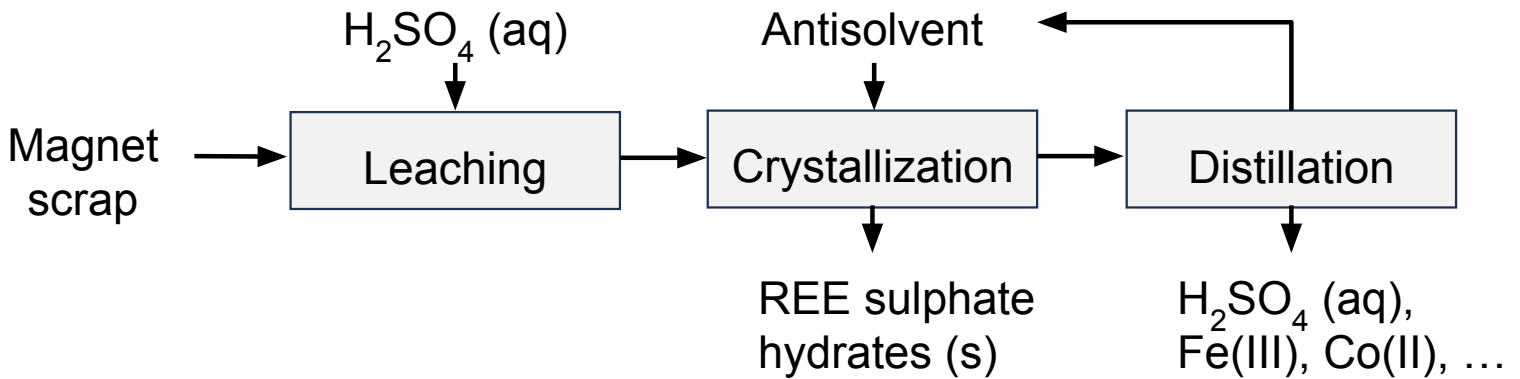


Anti-solvent added
Initial solvent

Water can attract and form layers surrounding both negatively and positively charged ions and thus keep them apart (high dielectric constant/polarizability).

Alcohols have lower dielectric constants than water, which means that they have

Recycling of magnets



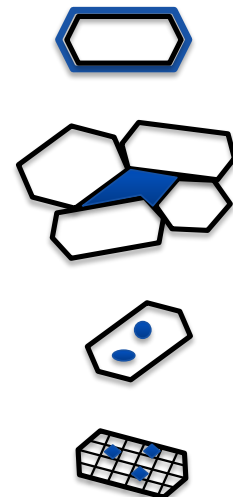
Synthetic solutions

- Nd(III) (8 g/kg) and Dy(III) (0.9 g/kg) in H_2SO_4
- Iron (25 g/kg) in the form of either Fe(II) or Fe(III)
- Crystallization of either $Nd_2(SO_4)_3 \cdot 8H_2O$ or $(Nd/Dy)_2(SO_4)_3 \cdot 8H_2O$

15

Mechanisms of impurity incorporation

- Solution adhering to the surface
"Interfacial tension and viscosity"
 Washing and centrifuge
- Macroscopic inclusion
"Surface irregularity"
 Crushing, reslurrying, and washing
- Microscopic inclusion
"Step behaviour"
 Sweating, reslurrying
- Lattice incorporation



16

Mechanisms of impurity incorporation

Kinetically controlled non-equilibrium lattice impurity incorporation and incorporation by 3D inclusion or by adhesion to mother liquor can all be influenced by modifying the crystallization conditions or downstream processes.

- Slow growth rate enhances purity (- productivity)
- Effective mixing enhances purity (> 10- 20 μm)
- Avoid agglomeration
- Suitable CSD and shape gives shorter washing and filtration times which in turn leads to improved product quality, e.g. better purity

The formation of a solid solution is a thermodynamically controlled process. Thus the purity from a single step crystallization is limited;

Antisolvent crystallization

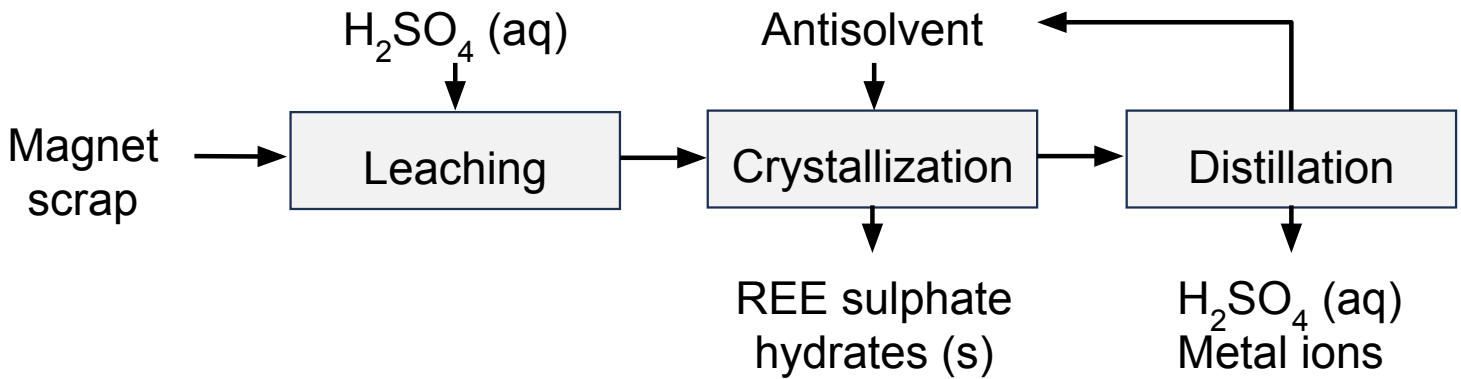
Which parameters are important?

- Choice of antisolvent (solubility of impurities, shape)
- Dosing of antisolvent (amount, concentration and rate)
- Operation and mixing techniques (micro/macro)
- Study aging and agglomeration
- **Seeding**



Thermodynamics and kinetics are important

Recycling of magnets



- 25 °C
- Nd(III) (8 g/kg) and Dy(III) (0.9 g/kg) in H₂SO₄
- Iron (25 g/kg) in the form of either **Fe(II) or Fe(III)**

□ Crystallization of either Nd₂(SO₄)₃·8H₂O or (Nd/Dy)₂(SO₄)₃·8H₂O

Recycling of magnets

Balance the generation and consumption of supersaturation

Promote growth and avoid secondary nucleation

- Antisolvent addition rate (generation of supersaturation)
- Seed loading (higher seed loading -> lower linear growth rate)

Addition rate (mL/min)	Seed loading
0.25	10%
0.1	1%
0.1	2.5%
0.1	5%
0.1	10%

Antisolvent crystallization

8 g/kg of Nd(III)

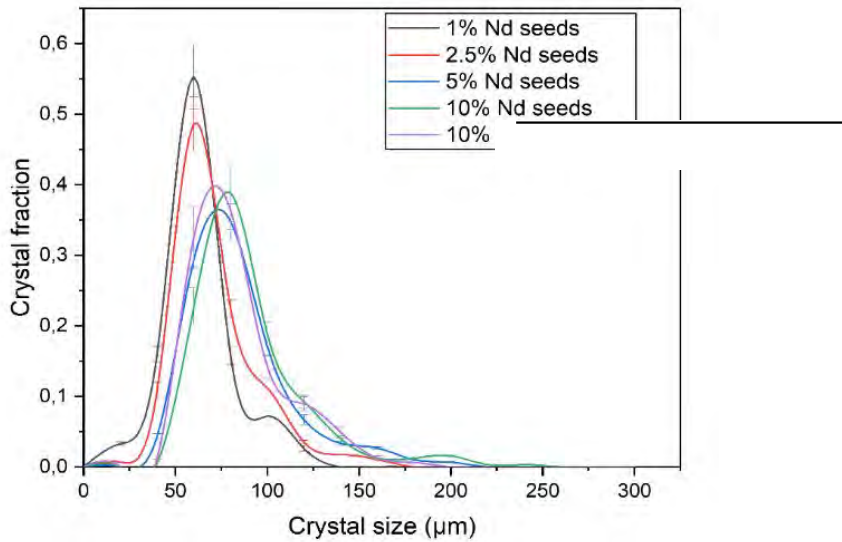
25 g/kg Fe(II)

Seeding with Nd₂(SO₄)₃·8H₂O

Antisolvent: Ethanol (100%)

25 C

Recycling of magnets



Optimal
10% seed loading

21

Recycling of magnets

Purity of $\text{Nd}_2(\text{SO}_4)_3 \cdot 8\text{H}_2\text{O}$ (c)

Addition rate (mL/min)	Seed loading	Fe (II) (g/kg)	Purity ¹ (%)
0.1	1%	9 ± 2	97.1 ± 0.6
0.1	2.5%	7 ± 2	98.3 ± 0.4
0.1	5%	4 ± 3	98.9 ± 0.5
0.1	10%	2 ± 1	99.5 ± 0.2
0.25	10%	17 ± 4	95.6 ± 0.8

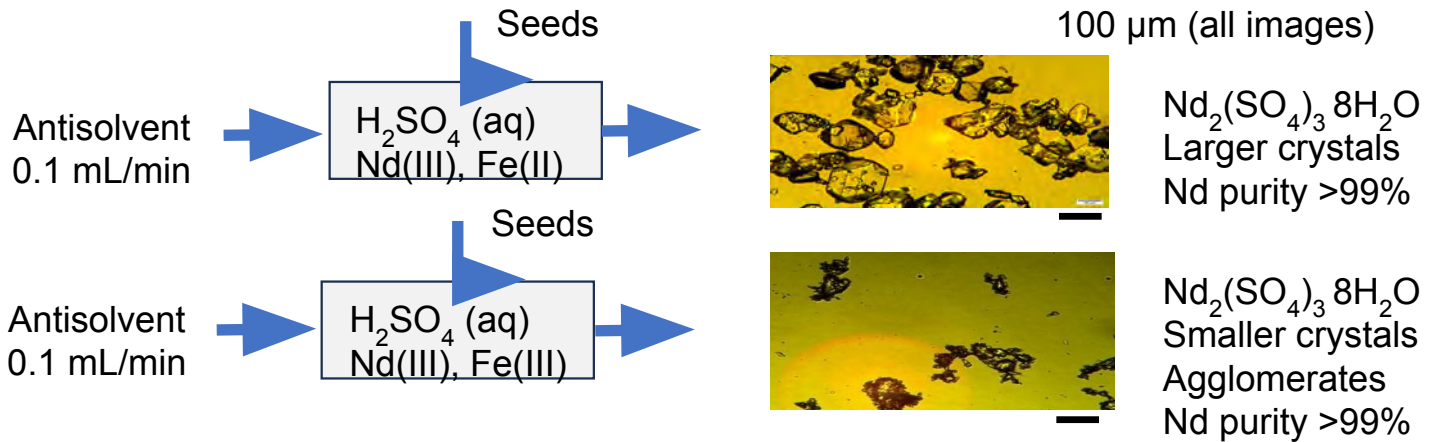
Optimal
10% seed loading
0.1 mL/min addition rate

- The systematic change in purity with seed loading and antisolvent addition rate indicate that the Fe(II) is primarily introduced into the sample during the crystallization process rather than during the washing stage.
- It is not possible to determine to which extent the iron is present as separate crystals or incorporated into the neodymium phase respectively.

22

Recycling of magnets

Antisolvent Crystallization of REE sulphates



Co-funded by the Horizon 2020 programme of the European Union

ANTISOLVO
Nd-Fe-B

23

Thank you for your attention

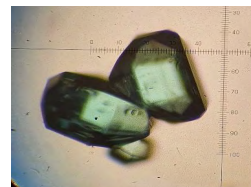
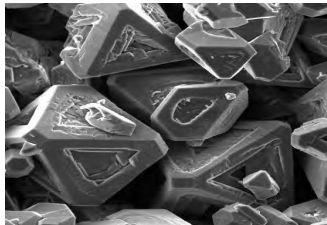


Kerstin Forsberg, *professor*

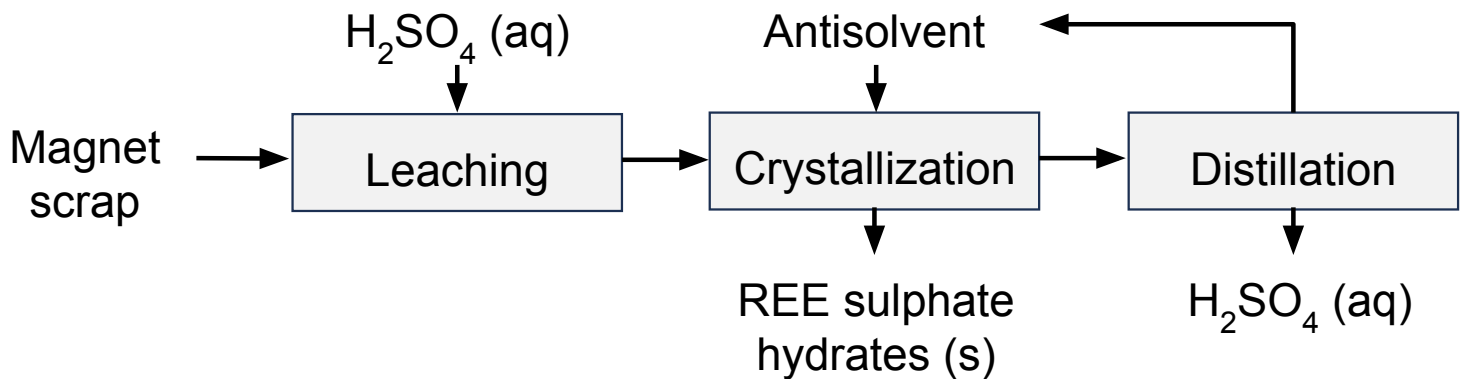
M. Svärd, N. Pawar, T. Punt, M. Geetika Sanku

KTH Royal Institute of technology, Stockholm

Dept. of Chemical Engineering

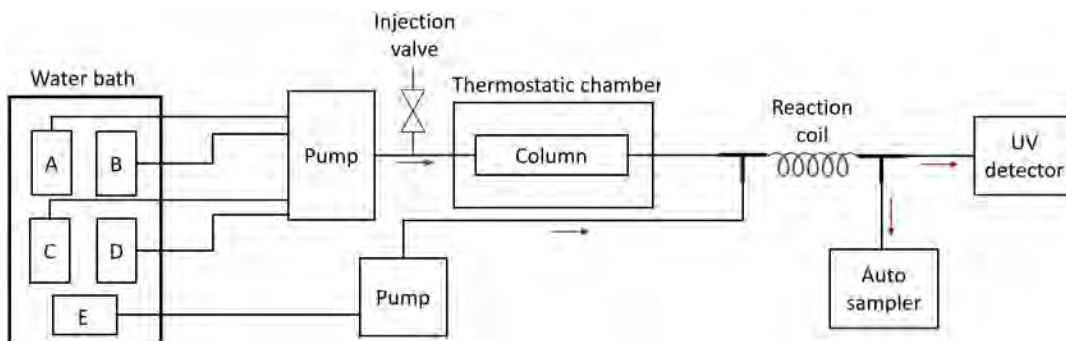


Recycling of magnets



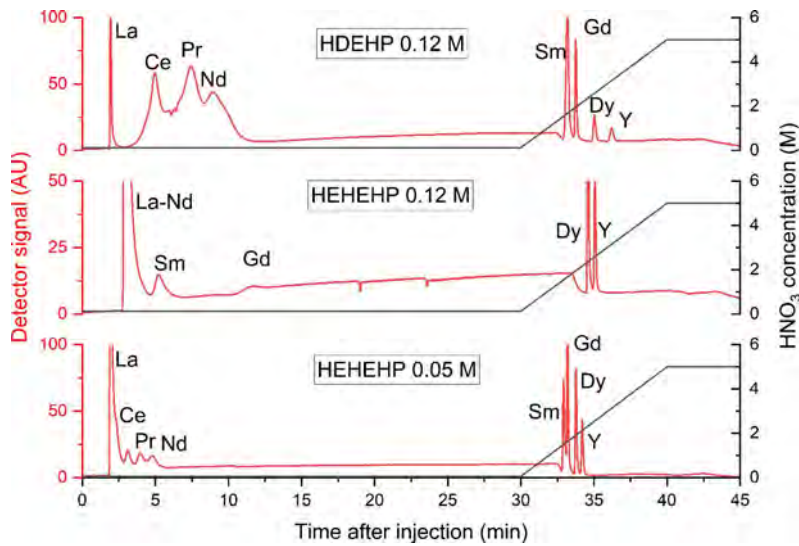
- The REE can be selectively separated from the leach liquor
- The REE sulfate hydrates have a high solubility in water
- The solvents can be recovered by distillation
- **What to do with the REE concentrate?**

Extraction Chromatography



Schematic of the HPLC setup used in this work. The solutions used at the different channels in the water bath vary with the purpose. For column preparation: A – column conditioner, B – acidic organophosphorus solution, C – ethanol, and D – Milli-Q water. For REE separation: A – Milli-Q water, B – 2 M HNO_3 , C – 5 M HNO_3 and E –

Extraction Chromatography



Chromatograms

C18 column functionalized with 0.5 mmol of HDEHP (top) and HEHEHP (middle and bottom)

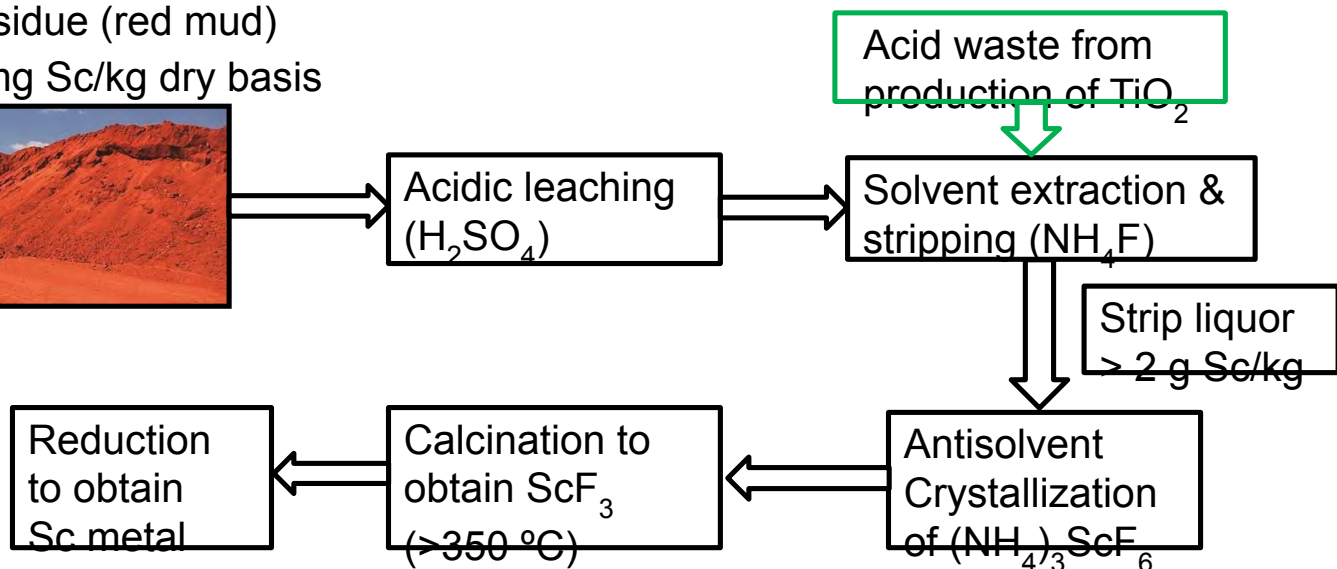
30 min isocratic elution at the concentration specified in the legend followed by 10 min gradient elution to 5 M HNO_3 (elution profiles shown as black lines on second axis).

Geetika Sanku M., Forsberg K. and Svärd M. (2022). Preparation of Extraction Chromatography Columns by Organophosphorus Acid Compounds. *Journal of Chromatography A*, vol. 1676, 463278.

27

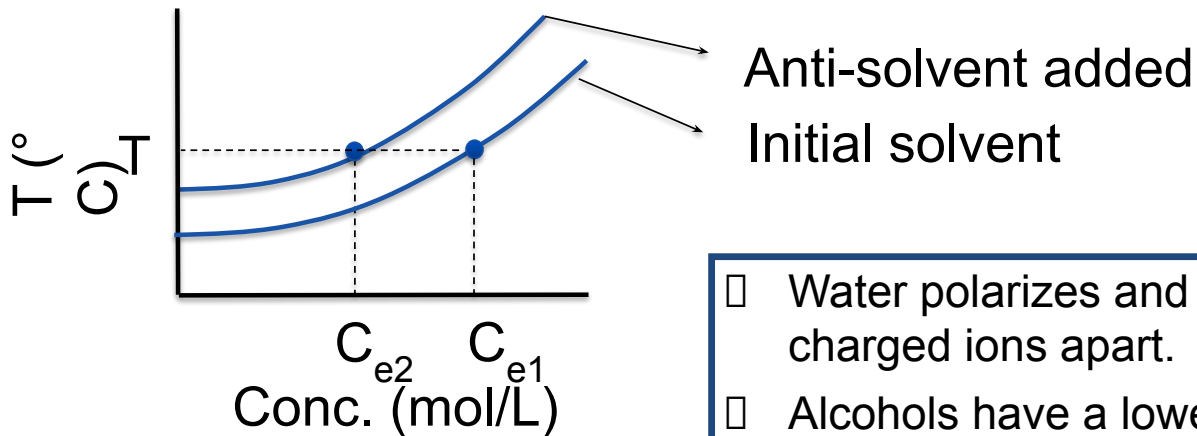
Recovery of Sc

Bauxite residue (red mud)
50 – 150 mg Sc/kg dry basis



Antisolvent precipitation

- By adding an antisolvent the solubility of the salt decreases

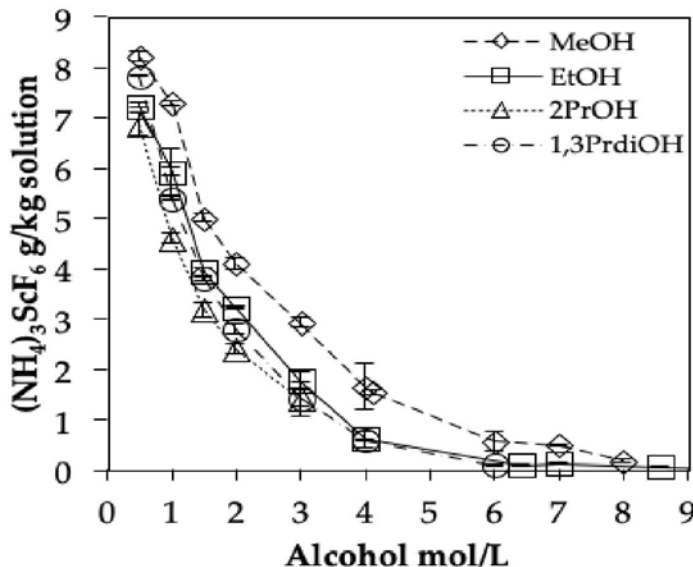


- Water polarizes and can keep charged ions apart.
- Alcohols have a lower ability to keep charged ions apart

(dielectric constant/ polarizability)

Antisolvent crystallization of $(\text{NH}_4)_3\text{ScF}_6$

Choice of antisolvent



Antisolvent crystallization

Which parameters are important?

- Choice of antisolvent (solubility of impurities, shape)
- Dosing of antisolvent (amount, concentration and rate)
- **Operation and mixing techniques** (micro/macro)
- Study aging and agglomeration
- **Seeding**

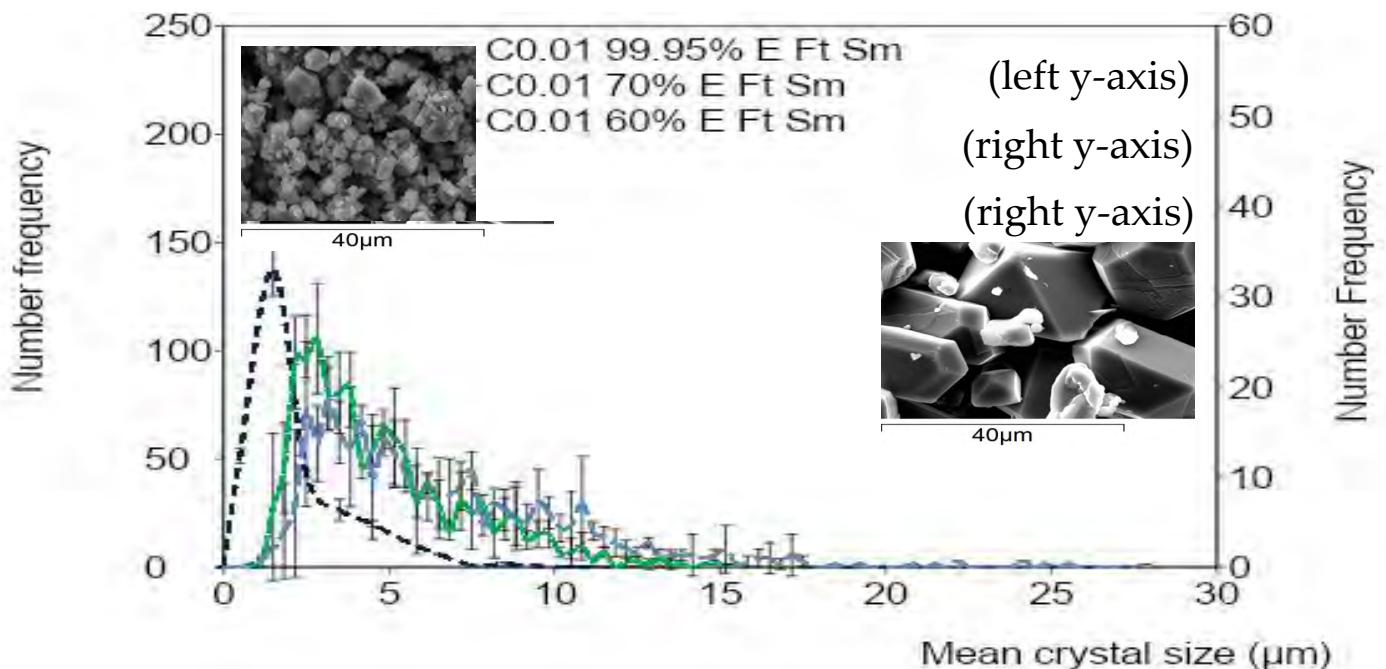


Thermodynamics and kinetics are important

31

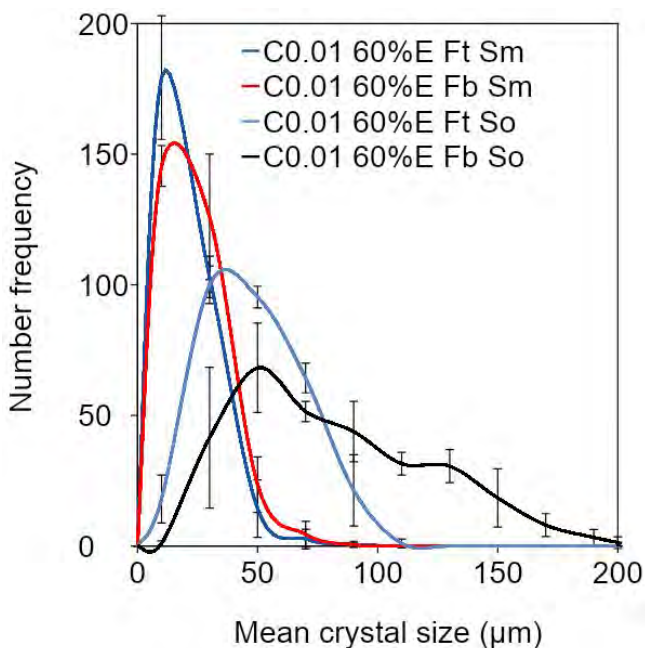
Antisolvent crystallization of (NH₄)₃ScF₆

Dosing of antisolvent (concentration)

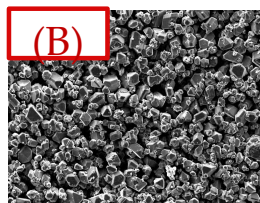


Antisolvent crystallization of $(\text{NH}_4)_3\text{ScF}_6$

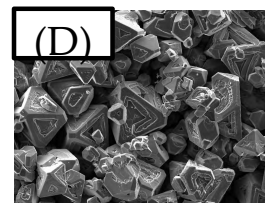
Operation and mixing techniques



(A)
(B)
(C)
(D)

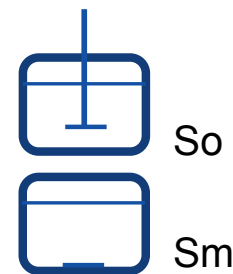


300 μm

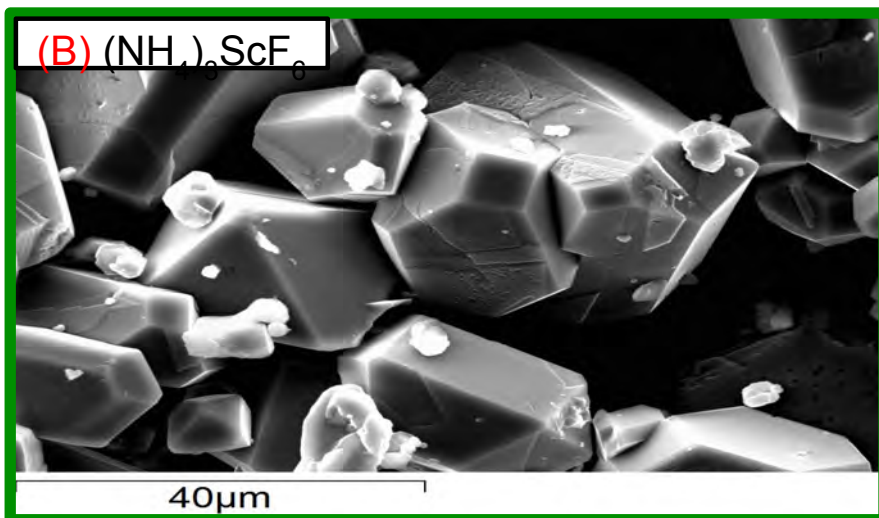


300 μm

Ft: Top feed
Fb: Bottom feed
So: Overhead stirring
Sm: Magnetic stirring



Antisolvent crystallization of $(\text{NH}_4)_3\text{ScF}_6$

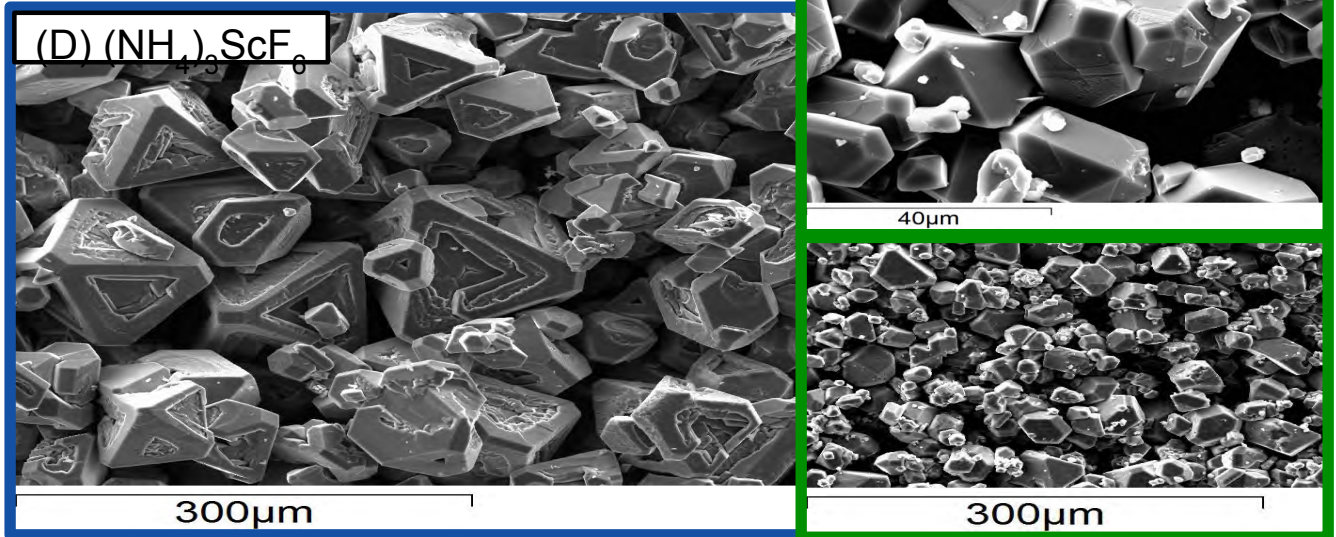


- Dosing 0.01 mL/s
- 60% EtOH
- Magnetic Stirring
- Top feed



Antisolvent crystallization of $(\text{NH}_4)_3\text{ScF}_6$

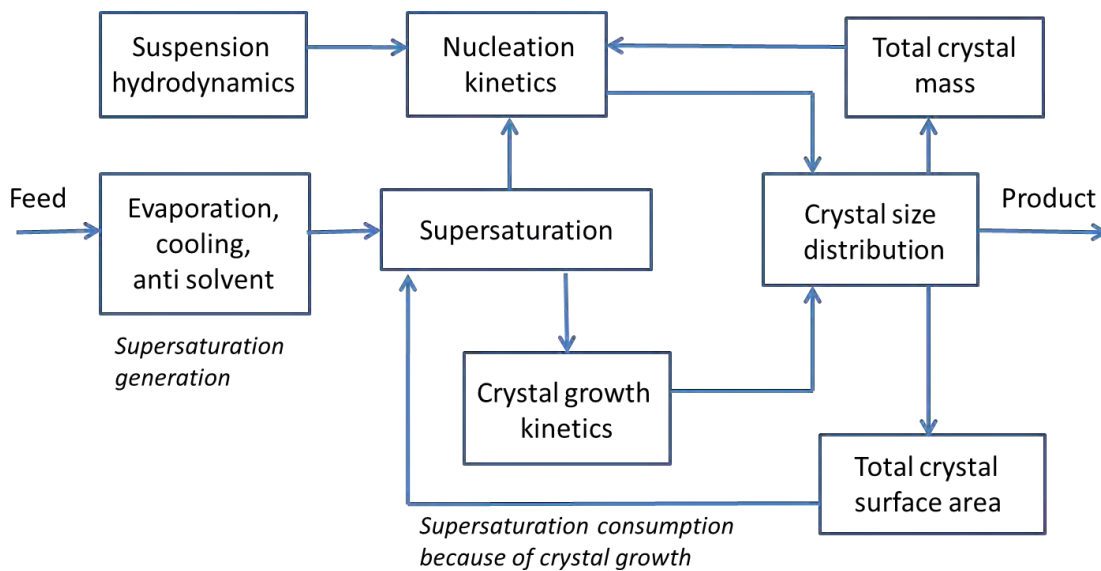
Hopper crystals



35

Peters E., Svärd M., Forsberg K. (2022). Impact of process parameters on product size and morphology in hydrometallurgical antisolvent crystallization, *CrystEngComm*, 24, 2851- 2866.

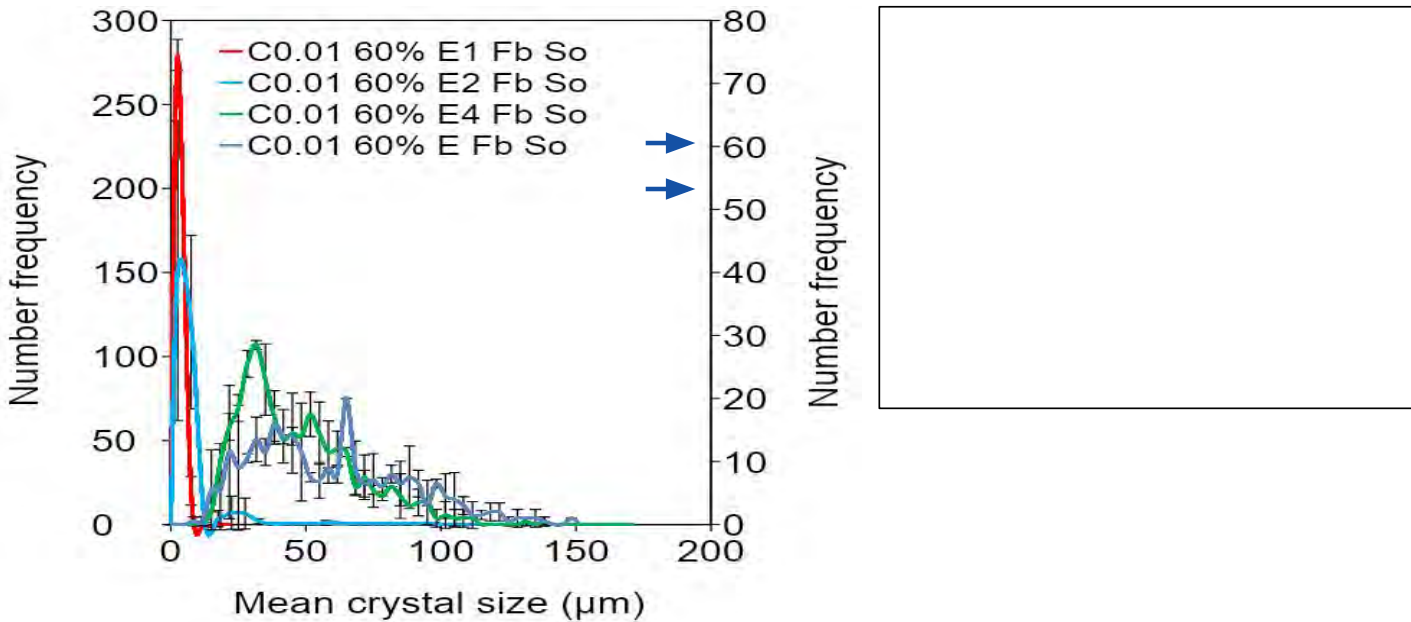
Principles of Crystallization



36

Antisolvent crystallization of $(\text{NH}_4)_3\text{ScF}_6$

Seeding (internal)



Research Activities

Hydrometallurgy, separation processes

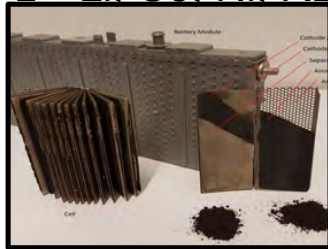
Magnet recycling

☐ REE, Co



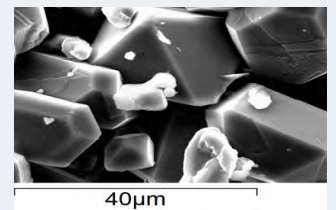
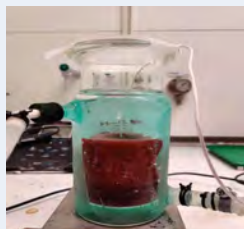
Battery recycling

☐ Li, Co, Ni, REE



Mining waste

☐ V and Sc



Critical Raw Materials

Critical and strategic Raw Materials for the EU

2023 CRMs (5th list)

Aluminium/Bauxite	Coking Coal	Lithium	Phosphorous
Antimony	Feldspar	Light REE	Scandium
Arsenic	Fluorspar	Magnesium	Silicon metal
Baryte	Gallium	Manganese	Strontium
Beryllium	Germanium	Natural Graphite	Tantalum
Bismuth	Hafnium	Niobium	Titanium metal
Boron/Borate	Helium	Platinum group metals	Tungsten
Cobalt	Heavy REE	Phosphate Rock	Vanadium
		Copper*	Nickel*

New materials added to the list in 2023 in **bold**

39

* Cu and Ni are included only as strategic raw materials (CRMs Act)

Critical and Strategic Raw Materials

Critical Raw Materials (CRMs):

Economic importance - importance for the EU economy regarding end-use applications and value added of corresponding EU manufacturing. Corrected by the substitution index related to technical and cost performance of the substitutes for individual applications.

Supply risk - reflects risk of a disruption in the EU supply. Based on primary supply from countries, considering governance performance and trade aspects. Measured at the 'bottleneck' stage of the material (extraction or processing), presenting the highest supply risk.

Substitution and recycling are considered risk-reducing measures.

Strategic Raw Materials (SRMs):

Raw materials important for technologies that support the twin green and digital transition and defence and aerospace objectives

Naturhistoriska addera...



Discovery of REE

Year	Element	Origin of Name	Discovery	Nationality
1794	Yttrium	Ytterby mine, Sweden	Johan Gadolin	Finnish
1803	Cerium	From the Swedish word for 'earthen' (cer)	Johan Gadolin	Swedish
1839	Lanthanum	From Greek lathano = concealed	Carl Gustav Mosander	Swedish
	Erbium	Derived from Ytterby mine, Sweden	Carl Gustav Mosander	Swedish
1878	Terbium	Derived from Ytterby mine, Sweden	Carl Gustav Mosander	Swedish
	Ytterbium	Derived from Ytterby mine, Sweden	Jean Charles de Marignac	French
1879	Samarium	After the mineral samarskite	Paul E. Lecoq de Boisbaudran	Swedish
1879	Scandium	After Scandinavia	Lars Fredrik Nilson	Swedish
1879	Holmium	After the Latin for Stockholm	Per Teodor Cleve	Swedish
1879	Thulium	After the name for the island of Thule	Per Teodor Cleve	Swedish



J. Gadolin



C.G. Mosander

Permanent magnets

- Green and smart technologies need magnets for use in e.g. sensors, motors and generators
- Permanent magnets (PM) are very strong allowing the magnets to be smaller and the items lighter
- PM are crucial for wind turbines, computer hard disc drives, motors in cordless tools, hybrid and electric vehicles etc.
- The strongest type (NdFeB) contain boron and the rare earth elements (REE) Nd, Pr and Dy, (Gd, Tb), (Co)
- China supplies Europe with 100% of HREE and 85% LREE

Recycling of magnets – closing the loop

- In the short term recycling of PM can only satisfy a small part of the total REE demand globally
- In the long term, by 2100, recycling is estimated to be able to satisfy almost 50% of the Nd and Dy demand

How can the magnets from EOL products be recycled and how do they age?

The magnets vary in size in different applications and small magnets are not dismantled.

Different items reach their EOL at different times

Hydrometallurgy for Resource Recovery



Bauxite residues and acid waste from TiO_2 pigment production

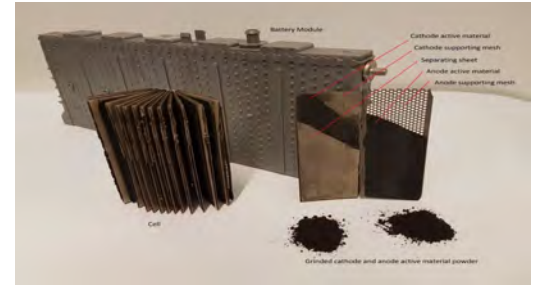
□ Recovery of Sc

**Scale-Up,
EIT Raw Materials**



Apatite concentrate
 $\text{Ca}_{10}(\text{PO}_4)_6(\text{OH},\text{F},\text{Cl})_2$

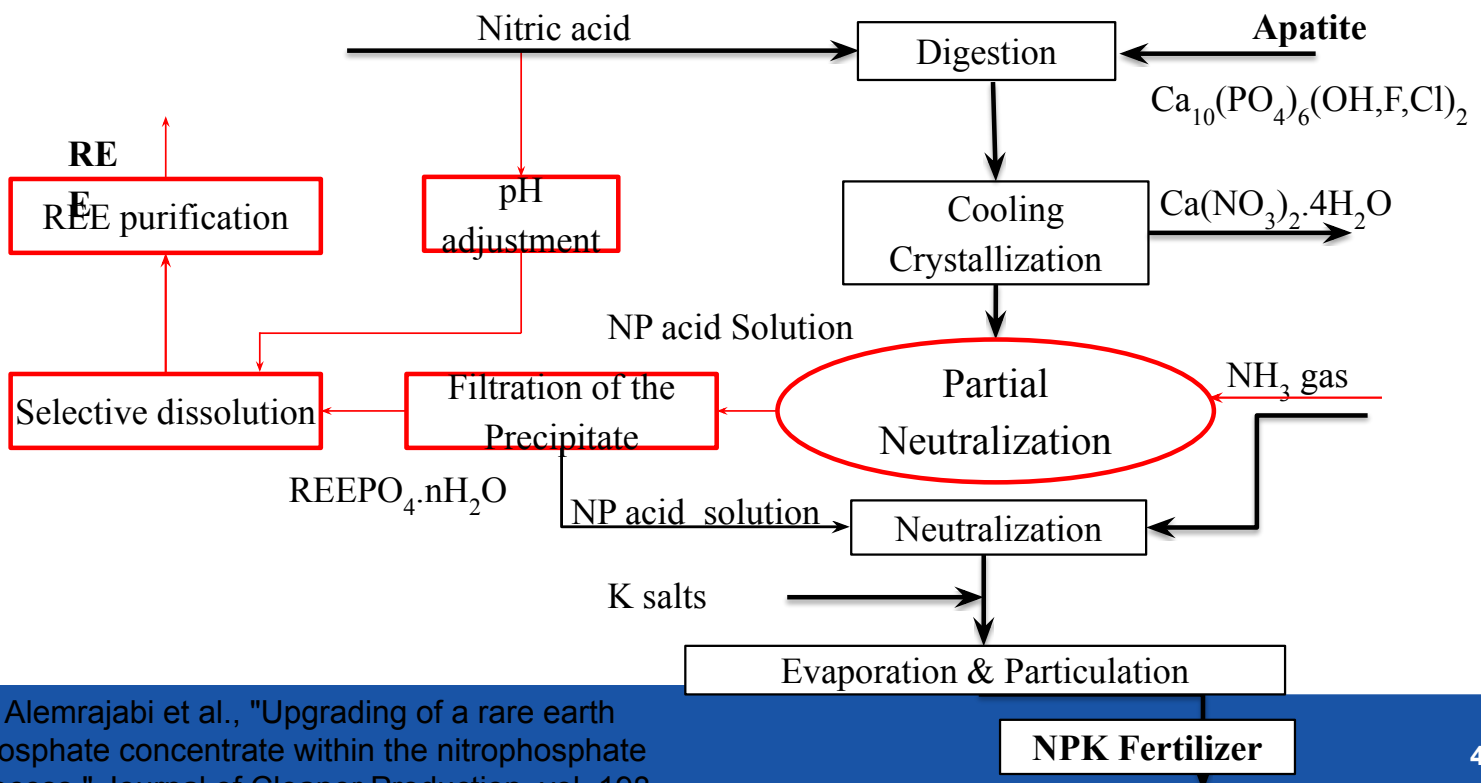
□ Recovery of P and Ce, Nd, Y, La, Pr, Dy...



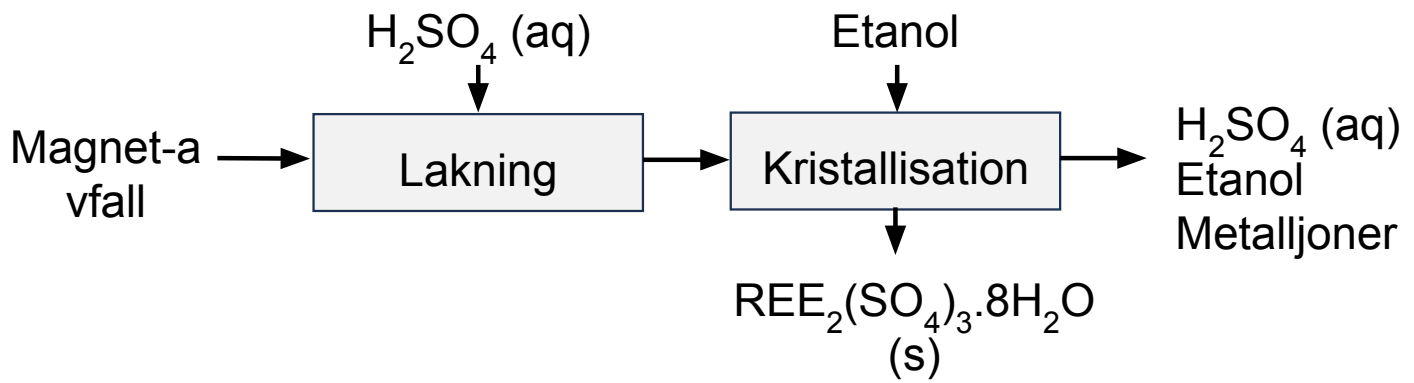
HEV NiMH batteries

□ Recovery of Ni, Co, La, Ce, Nd, Pr and Y

REE separation integrated with the NP process



Recycling of magnets



AUSTRALIA'S ONLY RARE EARTHS PROJECT WITH IN SITU RECOVERY POTENTIAL

By

Robert Blythman, Rupert Verco

Cobra Resources PLC, Australia

Presenter and Corresponding Author

Rob Blythman

ABSTRACT

The Boland Rare Earth Project is a new rare earth deposit style that is amenable to in situ recovery (ISR) mining. ISR is an established mining method for Uranium. ISR uranium mines dominate the lowest cost producers of uranium globally with CAPEX 10-15% of conventional mines and OPEX 30-40% lower than conventional mines (UXC,2023). Cobra has executed an exploration approach to identify a style of rare earth mineralisation type that allows for sustainable low-cost extraction of rare earths.

Preliminary leach results completed by ANSTO demonstrate magnet rare earth recoveries of up to 58% and heavy rare earth recoveries of up to 65% at a pH of 3-4 over 30 minutes to 6 hours at ambient temperatures and utilising an AMSUL wash. Dissolution of gangue elements (Al, Ca, Fe U, Th) are low. Cobra is in the process of undertaking low pressure column leach testwork through ANSTO to confirm amenability to in situ recovery. A wellfield test pattern was installed in early 2024 to build an aquifer baseline dataset to support a future ISR trial.

ISR circumvents challenges compared to conventional mining of clay deposits including particle size separation (beneficiation), heap or tank leaching, desliming and material management. The paleochannel geological setting is distinct from the Southern China weathered slope setting, allowing for greater reagent control in situ and post extraction aquifer remediation.

Pregnant solution from the column leach test will be used to assess membrane desorption as a low-cost method to process and deliver higher value selective rare earth carbonates.

Keywords: rare earths, ISR, low cost, ionic clay

AUSTRALIA'S ONLY RARE EARTH PROJECT WITH IN SITU RECOVERY POTENTIAL

By

Robert Blythman

Cobra Resources, Australia

rb@cobraplc.com

1

DISCLAIMER

THIS PRESENTATION AND ITS CONTENTS ARE NOT FOR RELEASE, PUBLICATION OR DISTRIBUTION, IN WHOLE OR IN PART, DIRECTLY OR INDIRECTLY, IN OR INTO OR FROM THE UNITED STATES OF AMERICA, AUSTRALIA, CANADA, JAPAN, THE REPUBLIC OF SOUTH AFRICA OR ANY JURISDICTION WHERE SUCH DISTRIBUTION IS UNLAWFUL.

This presentation has been prepared by Cobra Resources plc (the "Company") solely for your information. For the purposes of this disclaimer: (i) this "presentation" means this document, any oral presentation, any question and answer session and any written or oral material discussed or distributed during the presentation meeting; and (ii) any reference to any provision of any legislation herein shall include any amendment, modification, re-enactment or extension thereof.

This presentation may not be copied, distributed, reproduced or passed on, directly or indirectly, in whole or in part, or disclosed by any recipient, to any other person (whether within or outside such person's organisation or firm) or published in whole or in part, for any purpose or under any circumstances.

The presentation has not been independently verified and no representation or warranty, express or implied, is made or given by or on behalf of the Company, or its directors, officers, partners, employees, agents, affiliates, representatives or advisers (together, "Affiliates") or any other person, as to, and no reliance should be placed on, the accuracy, completeness or fairness of the information or opinions contained in this presentation and no responsibility or liability is assumed by any such person for any errors, omissions or inaccuracies in such information or opinions or for any loss, cost or damage suffered or incurred howsoever arising, directly or indirectly, from any use of this presentation or its contents or otherwise in connection with the subject matter of this presentation.

All information presented or contained in this presentation is provided as at the date of its publication and is subject to verification, correction, updating, amendment, revision, completion and change without notice and does not purport to contain all information that may be required to evaluate the Company or its securities. In giving this presentation, neither the Company, any of its Affiliates nor any other person, undertakes any obligation to amend, correct or update this presentation or to provide the recipient with access to any additional information that may arise in connection with it, or to advise any person of changes in the information set forth in this presentation after the date hereof.

This presentation has not been approved by an authorised person for the purposes of section 21 of the Financial Services and Markets Act 2000, or otherwise by the UK Financial Conduct Authority or London Stock Exchange plc.

This presentation does not constitute or form part of, and should not be construed as, any offer, invitation or recommendation to purchase, sell or subscribe for any securities in any jurisdiction and neither the issue of the information nor anything contained herein shall form the basis of or be relied upon in connection with, or act as an inducement to enter into, any investment activity. This presentation does not purport to contain all of the information that may be required to evaluate any investment in the Company or any of its securities and should not be relied upon to form the basis of, or be relied on in connection with, any contract or commitment or investment decision whatsoever. This presentation is intended to present background information on the Company, its business and the industry in which it operates and is not intended to provide complete disclosure upon which an investment decision could be made. The merit and suitability of an investment in the Company should be independently evaluated and any person considering such an investment in the Company is advised to obtain independent advice as to the legal, tax, accounting, financial, credit and other related advice prior to making an investment.

To the extent available, the industry, market and competitive position data contained in this presentation has come from official or third-party sources. Third-party industry publications, studies and surveys generally state that the data contained therein have been obtained from sources believed to be reliable, but that there is no guarantee of the accuracy or completeness of such data. While the Company believes that each of these publications, studies and surveys has been prepared by a reputable source, the Company has not independently verified the data contained therein. In addition, certain of the industry, market and competitive position data contained in this presentation come from the Company's own internal research and estimates based on the knowledge and experience of the Company's management in the market in which the Company operates. While the Company believes that such research and estimates are reasonable and reliable, they, and their underlying methodology and assumptions, have not been verified by any independent source for accuracy or completeness and are subject to change without notice. Accordingly, undue reliance should not be placed on any of the industry, market or competitive position data contained in this presentation.

This presentation is only being distributed and addressed to, and directed at: (i) persons in member states of the European Economic Area (each, an "EEA Member State") who are "qualified investors" within the meaning of the Prospectus Regulation (EU) 2017/1129 (the "Prospectus Regulation") ("Qualified Investors"); and (ii) persons in the UK that are "qualified investors" within the meaning of the UK version of the Prospectus Regulation, which forms part of UK domestic law pursuant to the European Union (Withdrawal) Act 2018, and are persons: (a) who have professional experience in matters relating to investments falling within Article 19(5) of the Financial Services and Markets Act 2000 (Financial Promotion) Order 2005 (the "Order"); (b) who are high net worth persons or entities falling within Article 49(2)(a) to (d) of the Order; or (c) to whom it may otherwise be lawfully distributed (all such persons in (a), (b) and (c) together being referred to as "Relevant Persons").

This presentation must not be acted on or relied on (i) in any EEA Member State, by persons who are not Qualified Investors and (ii) in the UK, by persons who are not Relevant Persons. Any investment or investment activity to which this presentation relates is available only to Qualified Investors in any EEA Member State and Relevant Persons in the UK, and will be engaged in only with such persons. If you are in any doubt as to the matters contained in this presentation (including whether you fall within the definitions of Qualified Investor or Relevant Person), you should consult an authorised person specialising in advising on investments of the kind contained in this presentation.

This presentation and the information contained herein is not intended for publication or distribution in, and does not constitute an offer of securities in, the United States or to any U.S. person (as defined in Regulation S under the U.S. Securities Act of 1933, as amended (the "Securities Act"), Australia, Canada, Japan, the Republic of South Africa or any other jurisdiction where such distribution or offer is unlawful. The Company has not registered and does not intend to register the offering in the United States or to conduct a public offering of any securities in the United States. Securities may not be offered or sold within the United States without registration, except pursuant to an exemption from, or in a transaction not subject to, the registration requirements of the Securities Act. Subject to certain limited exceptions, neither this presentation nor any copy of it may be taken, transmitted or distributed, directly or indirectly, into the United States, its territories or possessions. Any failure to comply with the foregoing restrictions may constitute a violation of U.S. securities laws. The Company has not been, and will not be, registered under the U.S. Investment Company Act of 1940, as amended.

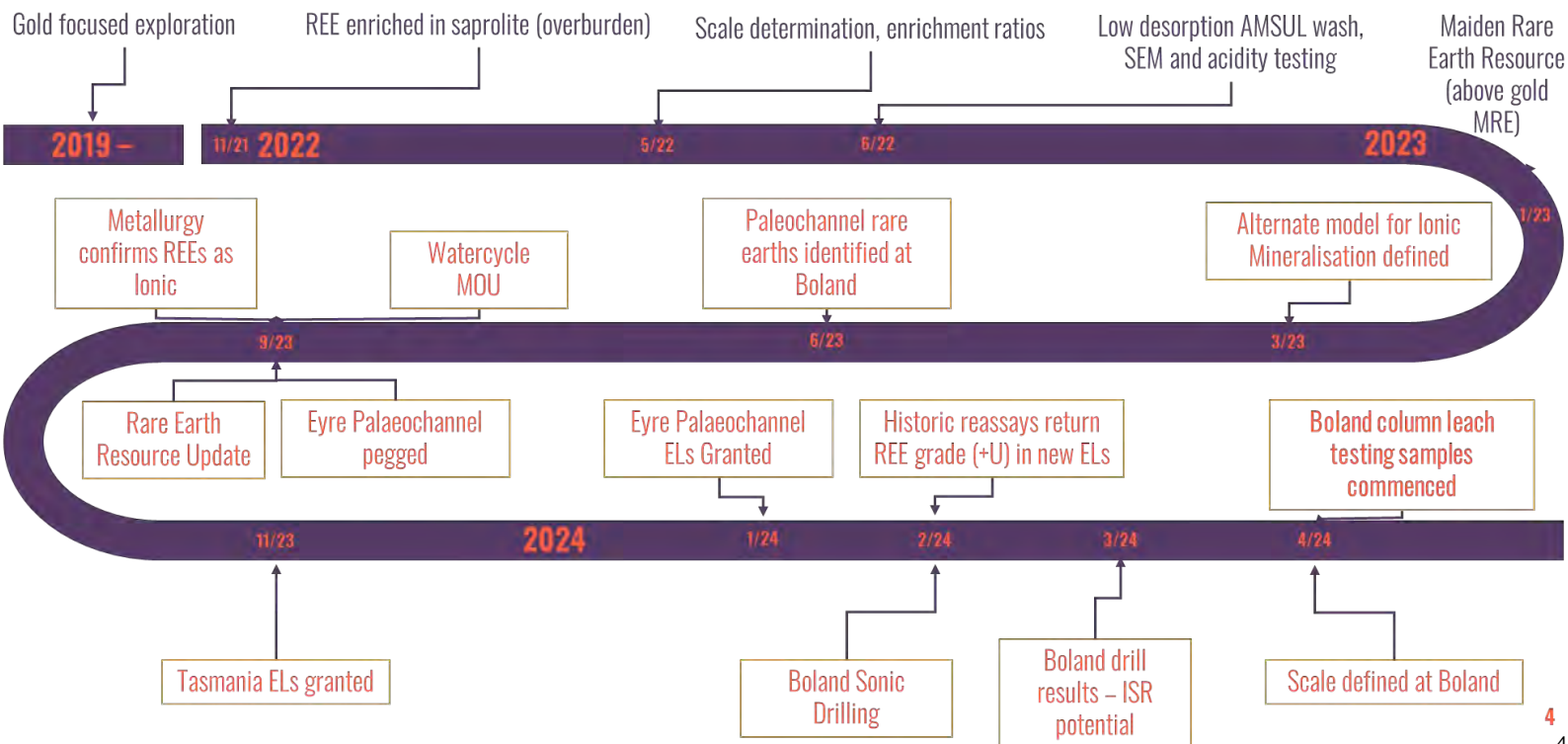
This presentation includes forward-looking statements. The words "expect", "anticipate", "intends", "plan", "estimate", "aim", "forecast", "project" and similar expressions (or their negative) identify certain of these forward-looking statements. These forward-looking statements are statements regarding the Company's intentions, beliefs or current expectations concerning, among other things, the Company's results of operations, financial condition, liquidity, prospects, growth, strategies and the industry in which the Company operates. The forward-looking statements in this presentation are based on numerous assumptions regarding the Company's present and future business strategies and the environment in which the Company will operate in the future. Forward-looking statements involve inherent known and unknown risks, uncertainties and contingencies because they relate to events and depend on circumstances that may or may not occur in the future and may cause the actual results, performance or achievements of the Company to be materially different from those expressed or implied by such forward looking statements. Many of these risks and uncertainties relate to factors that are beyond the Company's ability to control or estimate precisely, such as future market conditions, currency fluctuations, the behaviour of other market participants, the actions of regulators and other factors such as the Company's ability to continue to obtain financing to meet its liquidity needs, changes in the political, social and regulatory framework in which the Company operates or in economic or technological trends or conditions. Past performance should not be taken as an indication or guarantee of future results, and no representation or warranty, express or implied, is made regarding future performance. The Company ~~250/396~~ disclaims any obligation or undertaking to release any updates or revisions to these forward looking statements to reflect any changes in the Company's expectations with respect thereto as any changes in circumstances or assumptions on which any statement is based after the date of this presentation or to keep current any

INDUSTRY DEFINING OPPORTUNITY

Discovered ionic REEs in 2023 within permeable, ISR enabling geology – making Boland globally unique

- Discovery of scalable – rare earth deposit amenable to lowest cost mining process
- Palaeochannel hosted – Ionic mineralisation
- ISR amenable
- Scalable MREC precipitation and gangue element removal
- Low cost CAPEX – Low cost OPEX – Low cost rehabilitation
- Experienced South Australian team
- Financially disciplined and capitalised to execute

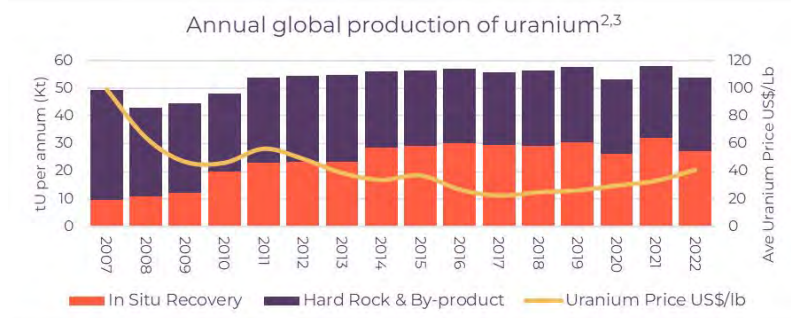
PROJECT HISTORY- RARE EARTHS



IN SITU RECOVERY WHY GRADE IS NOT KING

- Geology & metallurgy are fundamental to recovery cost. ISR and ionic mineralisation provide the opportunity to develop a low-cost and resilient source of rare earths
- ISR CAPEX costs are typically 10-15% of conventional mines¹
- ISR operational costs 30-40% lower than conventional mines¹
- ESG friendly method – temporary ground disturbance, less water consumption, no legacy landforms
- Scalable and resilient to commodity pricing cycles : demonstrated by global

Sources: uranium supply – ~60% of uranium mined by ISR in 2023
 1 Statistics: United States Nuclear Regulatory Commissions www.nrc.gov TradeTech – the nuclear review (October 2016)
 2 [STI/PUB/1697 \(iaea.org\)](https://www.iaea.org/publications/STI/PUB/1697)
 3 [Global price of Uranium \(PUBANUSDM\) | FRB | St. Louis Fed \(stlouisfed.org\)](http://www.frb.org/publications/global/price-of-uranium)

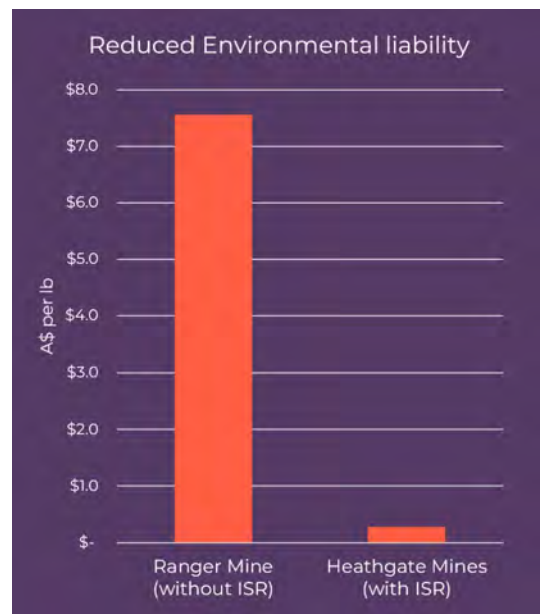


IN SITU RECOVERY LOWERING THE ENVIRONMENTAL COST

“ Rio Tinto told investors the rehabilitation of the Ranger Uranium Mine would “materially exceed” \$2.2 billion - shareholders could face further equity raising. ”

- ISR materially reduces environmental risk and cost
- Rio Tinto has recently confirmed cost blowouts for the Ranger Hard Rock mine to have blown out beyond \$2.2 Billion
- Ranger rehabilitation cost equates to ~\$7.6 per pound mined.
- This is ~28 times higher than the cost of rehabilitation of ISR mines in South Australia

Sources:
 1 Energy Resources Australia announcement dated 26 September 2023
 2 <https://www.world-nuclear.org/information-library/appendices/australia-s-uranium-mines>
 3 <https://web.archive.org/web/20141109104121/http://www.world-nuclear.org/info/Country-Profiles/Countries-A-F/Appendices/Australia-s-Uranium-Mines/>



DERISKING IONIC CLAY PROCESSING

High clay content ores result in metallurgical, productivity and environmental challenges

Ionic clay projects outside of China propose metallurgical flowsheets that include:

PROCESS STEP

- Wet particle size separation
- Wet screen size beneficiation
- Heap leach or tank leaching
- De-sliming and processed ore removal

CHALLENGE

- Water use, bottleneck, cost
- Ore loss, water use, bottleneck
- Bottleneck, environmental risk, cost
- Environmental and geotechnical risk, bottleneck, cost

In-situ recovery removes challenges and infrastructure; decreasing cost and environmental risk

7

REALISING DISCOVERY VALUE

ISR is the key to overcoming capital challenges, increasing future operational profitability and generating an unrivalled environmentally credentialled source of critical rare earths.

In 2024 Cobra has been unlocking investment value by testing three deliverables:



HIGH GRADE

Refined sampling strategy to reflect chemistry boundaries should result in considerable increases of recoverable TREO grades



SCALE

Low-cost approach - over 2,000km² of palaeo-channel

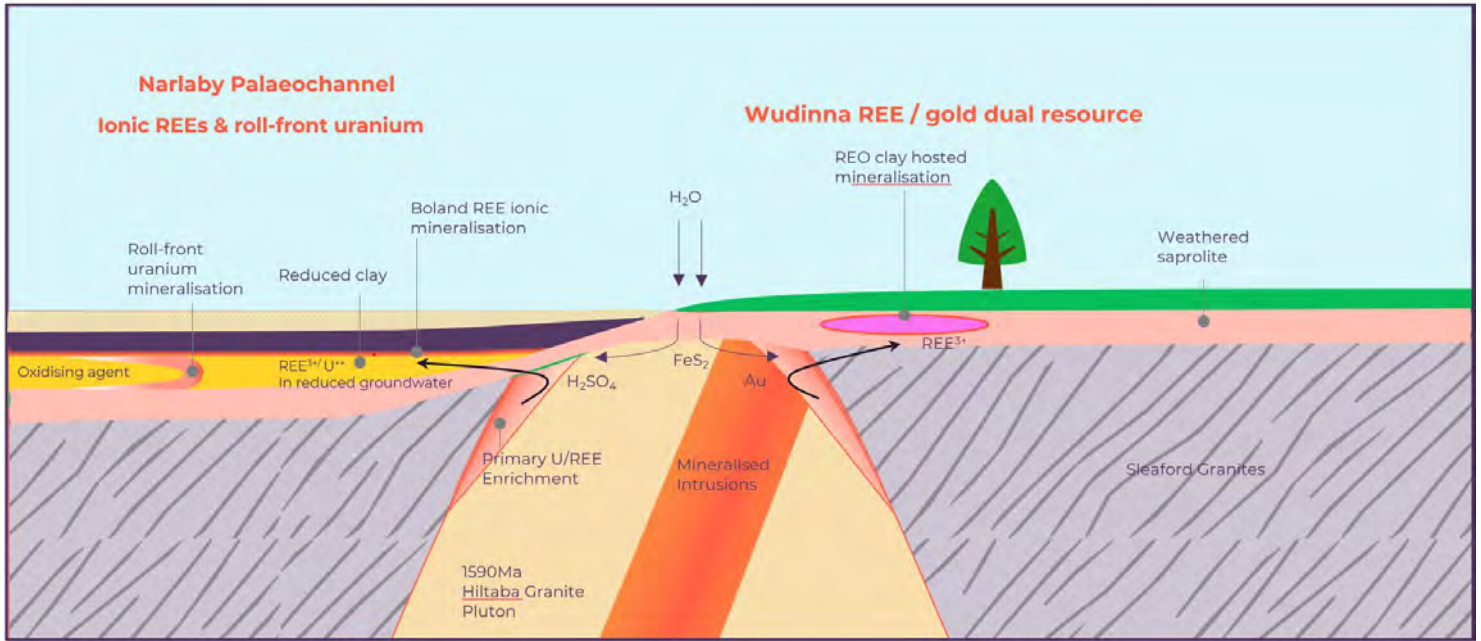


ISR

Drill plan – fast and cost-effective approach to unlocking long-term value

A GEOLOGICAL PROCESS THAT SHORTCUTS MINING & EXTRACTION

Mother Nature has completed the expensive process of hard rock rare earth extraction and mobilised valuable REEs to an accessible storage bank, allowing for a simple and cost-effective withdrawal



9

GROWING A STRATEGIC, SCALABLE LOW-COST IONIC REE PROJECT

Cobra has made a unique ionic REE discovery and has moved to establish a dominant landholding to enable significant scale

Favourable location

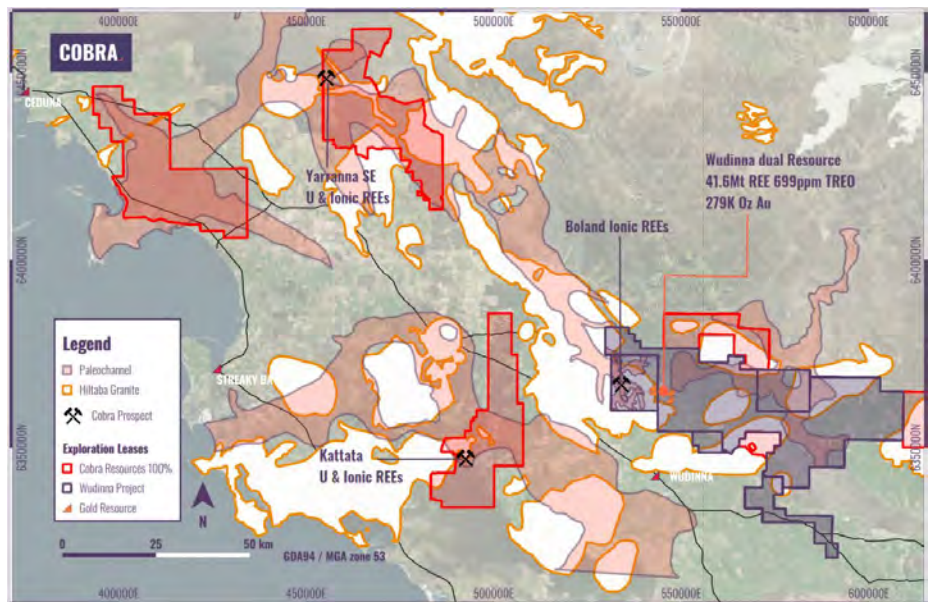
- Multiple ports within 200km
- Nearby infrastructure, including South Australian hydrogen energy hub
- Local sources of sulphuric acid

Geological enrichment and mobility across tenements

- Enriched Hiltaba plutons occur across our land tenure
- Acidic groundwaters demonstrated across palaeosystems (pH as low as 2.2)
- Ionic mineralisation within transgressional marine sequences that are regionally extensive

Geology favourable for REEs

- Enriched source rocks, mobility and ionic adsorption conditions



CONDITIONS FOR IONIC REEs

Enriched source

- ▶ Xenotime, monazite & zircon – primary mineralisation
- ▶ Hiltaba granites contain abundant sulphides – weathering yields acidity

Importance of acidity

- ▶ Saprolite acidities as low as pH2
- ▶ Enrichment/ depletion observed with acidity
- ▶ Groundwater pH conditions at Boland are 6.5-7.5
- ▶ Groundwater in oxidised parts of channel very low – less than pH2
- ▶ Historic assays of 12,000ppb U - 120km down channel

Production points of difference

- ▶ Integration into existing land use - dryland cropping
- ▶ Minimal ground disturbance – no handling of clays
- ▶ Rapid wellfield turnover – desorption characteristics

11

ISR – DEMONSTRATING BOLAND’S ADVANTAGE

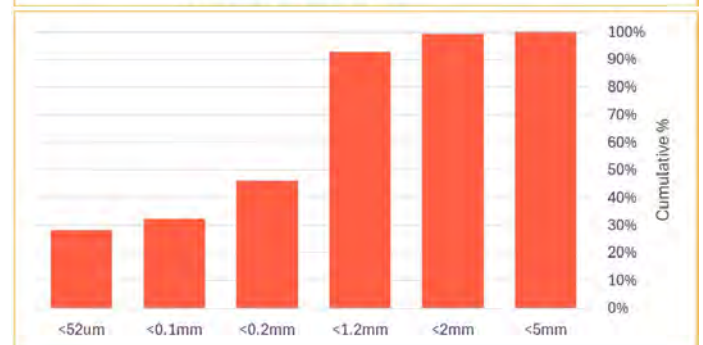
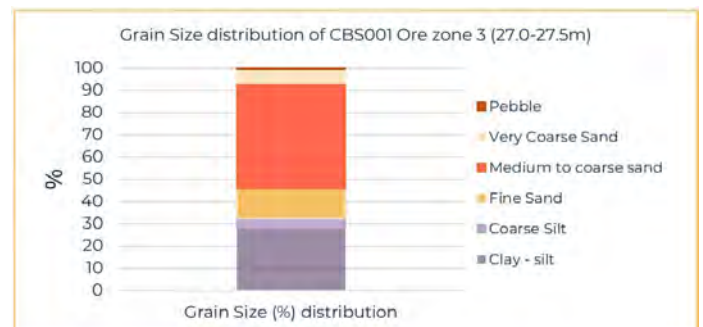
Preliminary results are very favourable for low cost in situ recovery

High permeabilities in Zone 3

- High portion of sand 67% of mineralised interval greater than 0.1mm
- Zone 3 calculated transmissivity of 135 – 275 m/day

Further work planned

- Samples drying for Zones 1 & 2
- Assaying of screened fractions
- Petrology and mineralogy studies
- Pump testing to validate calculations



ADVANCING INSITU RECOVERY & PROVING GRADE

Rare earth mineralisation concentrated within three zones where geology is favourable for in situ recovery

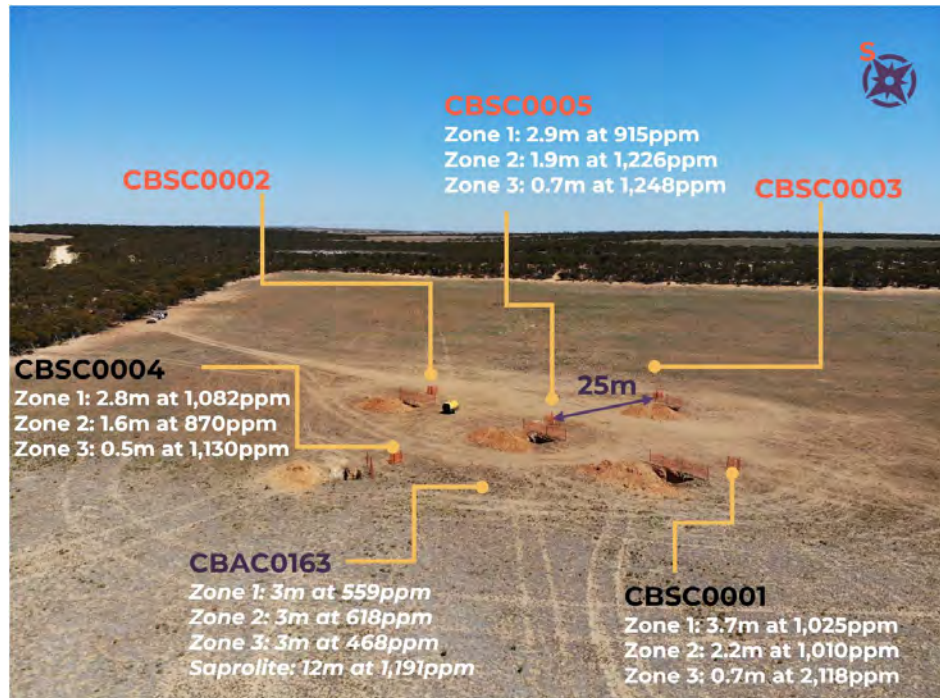
Wellfield installed over defined mineralisation

Intersection weighted averages:

- **180% increase: Zone 1** - 3.1m at 1,007 ppm TREO where Nd_2O_3 + Pr_6O_{11} totals 212 ppm and Dy_2O_3 + Tb_2O_3 totals 23.5 ppm from 15.6m
- **169% increase: Zone 2** - 1.9m at 1,043 ppm TREO, where Nd_2O_3 + Pr_6O_{11} totals 205 ppm and Dy_2O_3 + Tb_2O_3 totals 22 ppm from ~20.5m
- **329% increase: Zone 3** - 0.6m at 1,538 ppm TREO where Nd_2O_3 + Pr_6O_{11} totals 305 ppm and Dy_2O_3 + Tb_2O_3 totals 52 ppm from ~26.6m

Geology favourable for in situ recovery

- Narrow, concentrated zones ideal for ISR
- Confined aquifer, saline and unused
- Permeable sands within mineralised zones



13

RE-ASSAY VALIDATING INTERPRETATION OF SCALE

Low-cost exploration demonstrating scale and de-risking future drilling

11.5 km of mineralisation

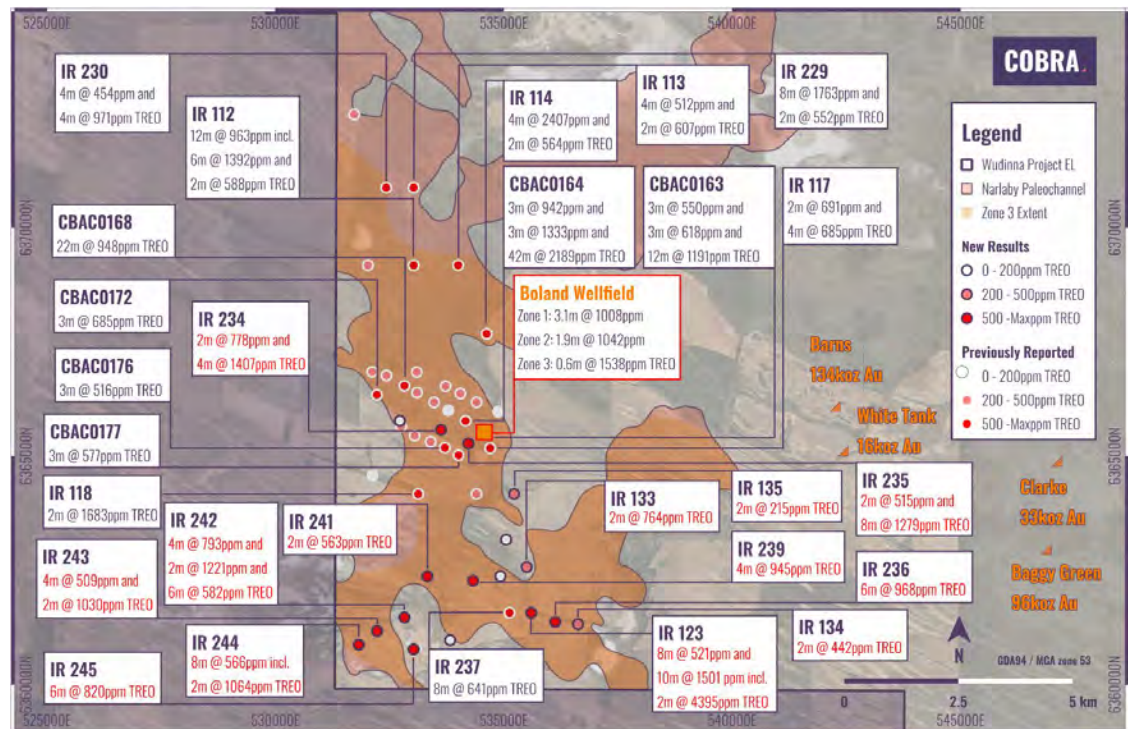
- Re-assay confirms mineralisation in Palaeochannel sediments along 11.5 km

Geological enrichment and mobility across tenements

- Enriched Hiltaba plutons occur across our land tenure
- Acidic groundwaters demonstrated across palaeosystems (pH as low as 2.2)
- Ionic mineralisation within transgressional marine sequences that are regionally extensive

Geology favourable for REEs

- Enriched source rocks, mobility and ionic adsorption conditions



BOLAND IONIC REEs – ENABLING LOW-COST EXTRACTION

Boland heavy rare earth recoveries compare favourably to peers

ANSTO – Metallurgical results confirm exceptional recoveries

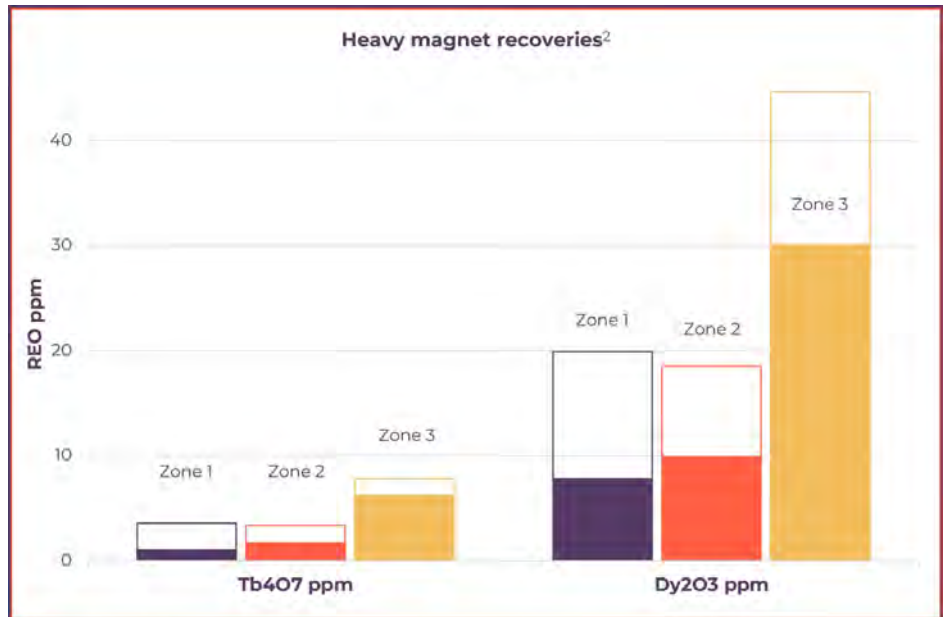
- Rapid recoveries in 30 minutes at pH 3-4
- Further increases in recovery achieved over 6 hrs

Exceptional heavy REE recoveries

- Terbium price USD\$746 per Kg¹
- Dysprosium price USD\$255 per Kg¹
- Boland zone 3 HRE recoveries are highly desirable

Superior ratios

- Magnet REE recoveries up to 58%
- Heavy REE recoveries up to 65%
- Low dissolution of gangue elements – Al, Ca, Fe, U, Th



¹ RE Oxide Pricing: [DPrice of Rare Earth Oxides live | SMM - Metal Market](#)

² Cobra – Average recoveries by mineralised zone

ISR COLUMN LEACH TESTING

Low Cost Low Impact Extraction

- ▶ Column leach trials underway
- ▶ AMSUL extraction
- ▶ Sulfuric acid used to maintain pH 3
- ▶ Run at aquifer pressure and temperature
- ▶ Piloting end to end extraction flow sheet
- ▶ Post test XRD on fresh and spent ore
- ▶ Pregnant solution to be used for MREC trials

MEMBRANE DESORPTION AND FILTRATION

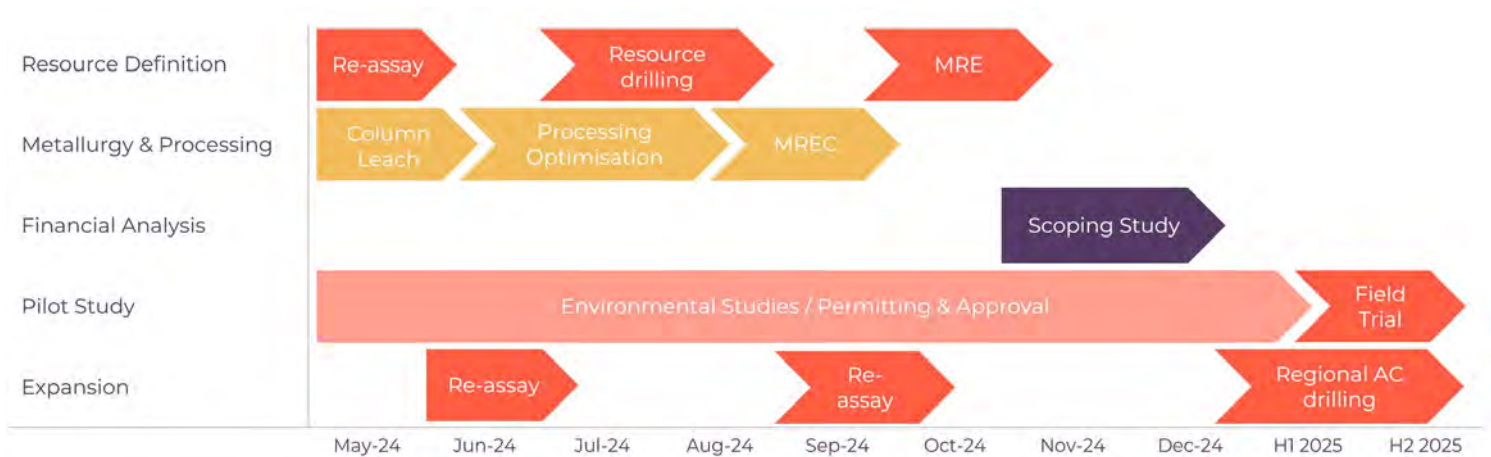
Watercycle Technologies – Low capex, selective and scalable processing

- ▶ Graphene Engineering and Innovation Centre –
Manchester, UK
- ▶ Direct Lithium Extraction and Crystallisation
(DLECT™) technology to process brines
- ▶ Pilot scale production of lithium carbonate
products from brines
- ▶ Piloting end to end extraction systems
- ▶ Chemistry membranes and resins to be tested for
purification, precipitation and potential
separation of REEs

17

PROJECT ROADMAP

Near term news flow to define the value of the opportunity



OUR STRATEGY TO DEMONSTRATE DIFFERENCE



FOCUS

Advance ionic REE ISR
extraction as our core
business



OPTIMISE

Prove In situ recovery,
de-risk commercialisation
pathway



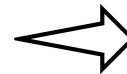
EXECUTE

Define a resource of
significance, develop
metallurgical process



CREATE VALUE

Optimise cost of mining &
production, produce
marketable MREC



IMPLEMENT

Pathway for Cobra to become a
low-cost MREC producer

LITHIUM-ION BATTERY SHEDDING CHALLENGES

By

Andreas Mönch, Adam Christensen & Thomas Rüter

Commonwealth Scientific and Industrial Research Organisation, Australia

Presenter and Corresponding Author

Andreas Mönch
andreas.monch@csiro.au

ABSTRACT

Lithium-ion batteries (LIBs) are increasingly becoming a significant waste stream, presenting substantial challenges for recycling and disposal. Due to their complex design and the variety of materials used, several steps are necessary before they can be reused or recycled. Initially, LIBs are sorted and typically undergo pre-processing, which includes discharge or deactivation, disassembly, and separation. After these steps, they can either be directly recycled or processed using pyrometallurgy, hydrometallurgy, or a combination of these methods.

Each recycling process for lithium-ion batteries has its own advantages and disadvantages. While pyrometallurgy might seem like the simplest option due to its ability to handle a flexible feedstock, it has issues such as relatively low lithium recovery rates and the production of hazardous off-gases and fly ash residues. These challenges have led most recent recycling projects to shift towards hydrometallurgy processing routes.

For safe processing, both pyrometallurgy and hydrometallurgy require the discharge and disassembly of larger battery packs. These packs are commonly used in rapidly growing markets such as Electric Vehicles (EV) and Battery Energy Storage Systems (BESS). Due to competitive manufacturing costs, these sectors are increasingly using battery packs as structural components and employing foam encapsulation for thermal management. This, however, inhibits access to the Battery Management System (BMS) and greatly complicates the discharge and disassembly of the packs.

This manufacturing trend has meant that traditional wet shredding in air is increasingly not viable, due to the inherent inability to guarantee electric discharge, through the lack of access to the BMS, and the volatile organics used in the battery's electrolyte which present significant fire and environmental risks. Current, state-of-the-art employs dry shredding in an inert atmosphere using an airlock, to ensure safer operation. It also allows for the potential recovery of the electrolyte, either through non-aqueous organic washing, direct vacuum distillation, or a combination of both.

While this method theoretically reduces fire and environmental hazards, it is practically impossible to ensure full discharge of LIBs due to inaccessible terminals and inherent voltage rebound. Our tests with a custom designed industrial shredder show that even fully discharged, cells create thermal hotspots and release elevated temperature gases. Battery cells at low charge state will cause electrical arcing during the shredding process, and if oxygen levels cannot be kept below flammability limits, the cell's electrolyte solvents are likely to ignite. Maintaining a near-inert atmosphere in an industrial shredder processing encapsulated EV or BESS packs is impractical due to the battery packs' large geometry and corresponding volume of air trapped within the foam encapsulation, and inevitable process airlock leaks.

This presentation will discuss the magnitude of the challenge and key safety insights from our experimental pilot shredder, which operates in a low oxygen atmosphere when shredding LIB cells at various discharge levels. It will also outline future research directions and suggest potential solutions for upstream manufacturing.

Keywords: Lithium-ion battery, resource recycling, battery shredding, electrolyte recovery.

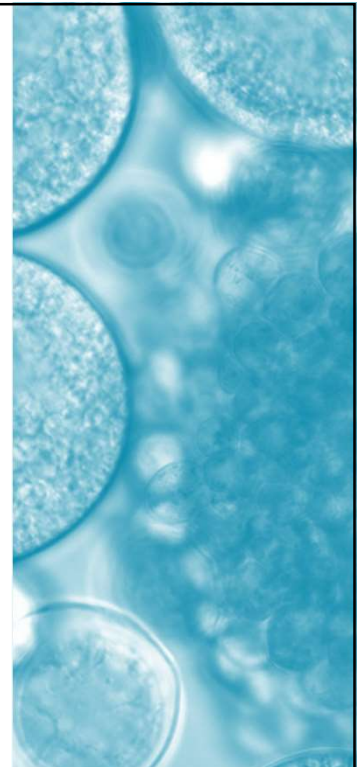
LITHIUM-ION BATTERY SHREDDING CHALLENGES

By

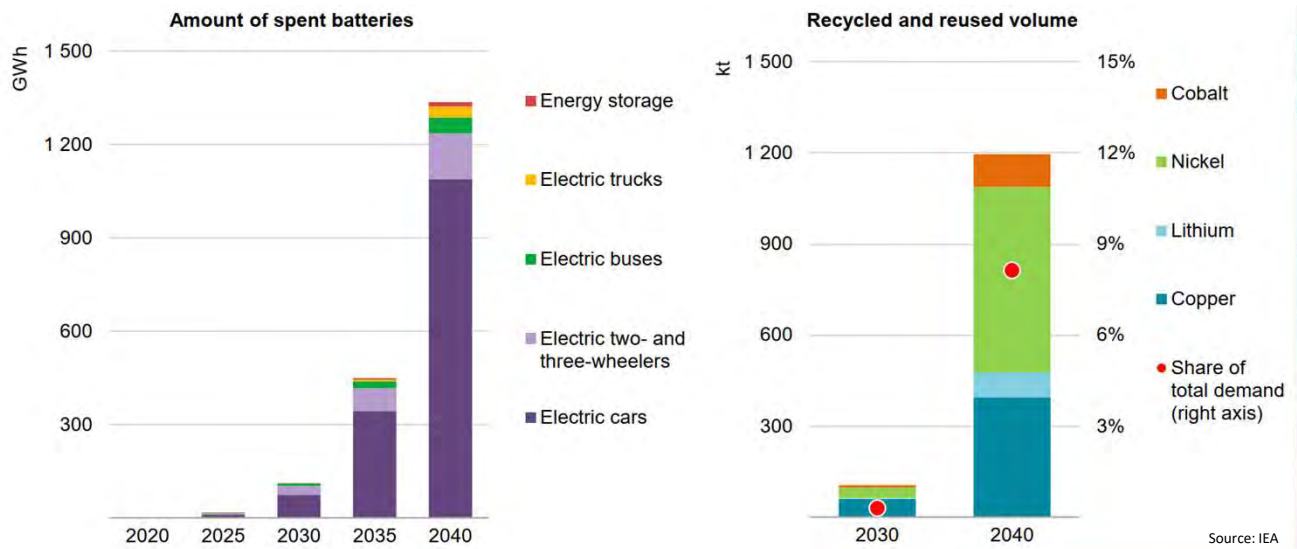
Andreas Mönch, Adam Christensen, Thuy D Huynh & Thomas Rüther
CSIRO, Australia

Presentation Overview

- Front-end of Lithium-ion battery recycling
- Overview of current recycling methods
- Rapidly shifting “state of the art” of recycling
- Our experiences with inert dry shredding
- Changes in battery module manufacture
- Challenges needing to be addressed
- A short video, showing the shredder in action!

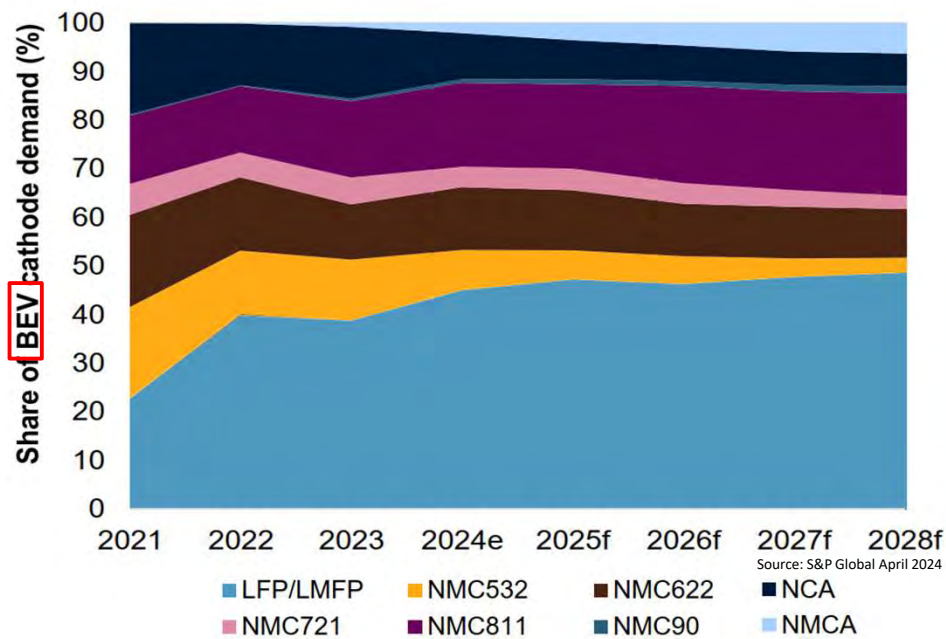


Lithium-ion Battery Waste Steams

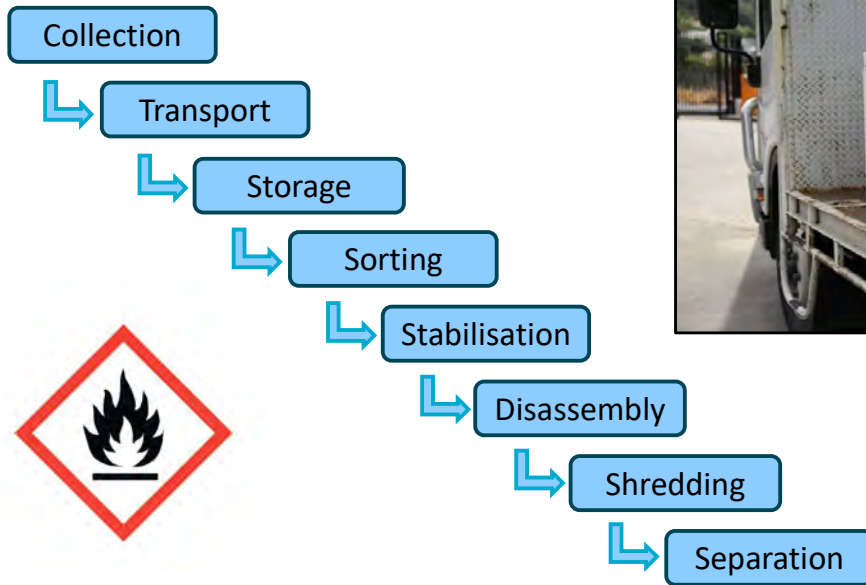


3

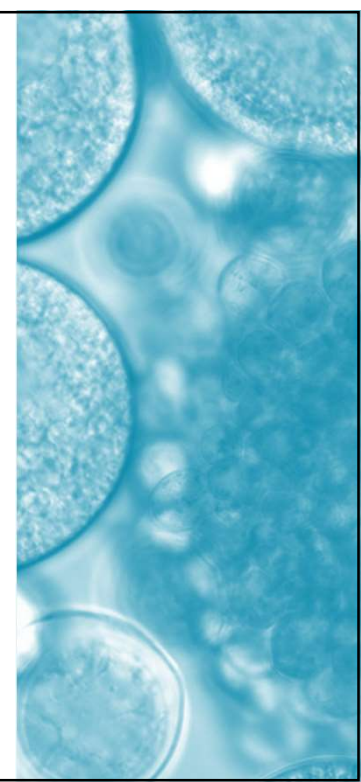
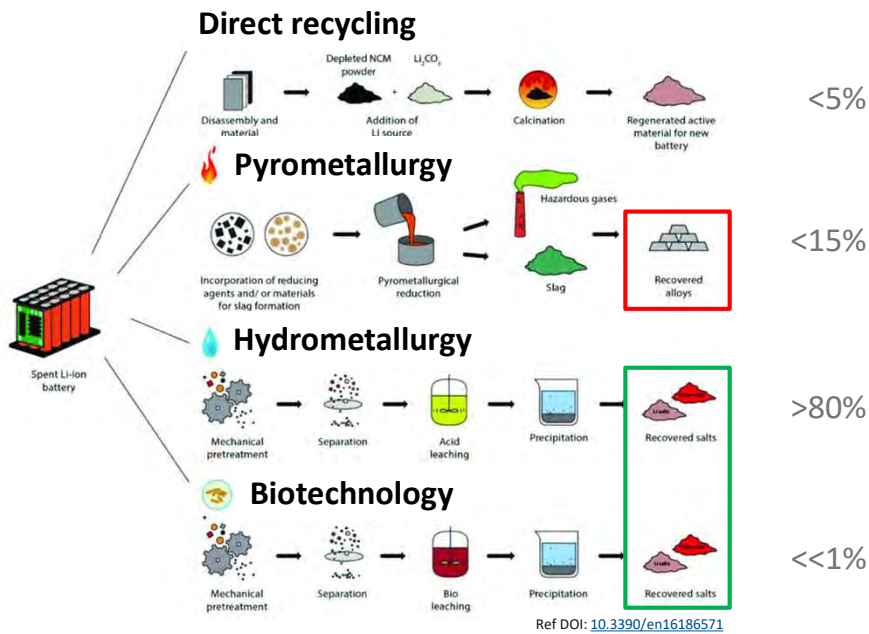
Battery Cathode Chemistry Changes



Pre-Processing Steps



Recycling Methods



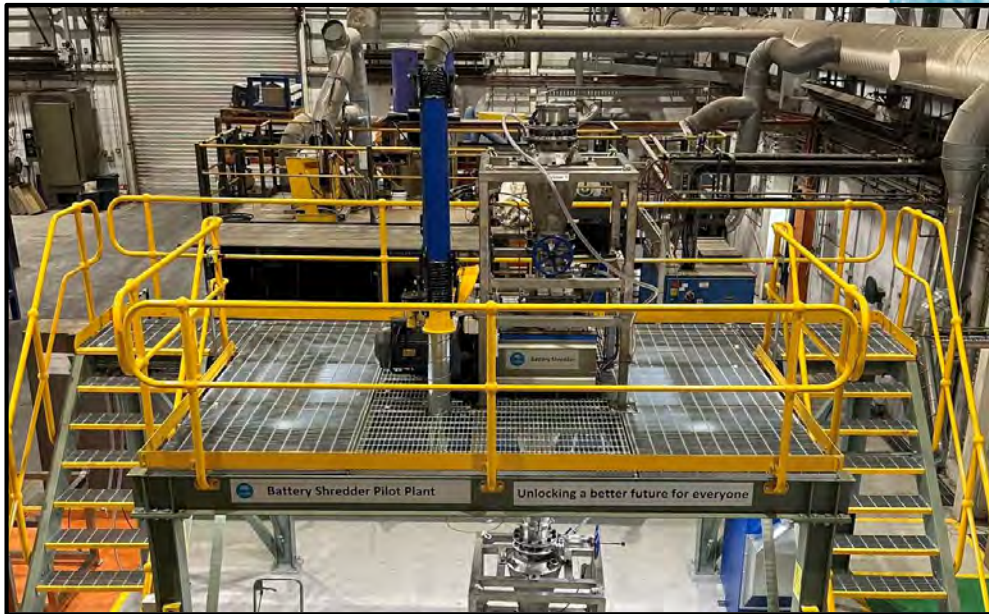
What is State-of-the-Art Shredding?

- Short Answer: It depends...!
- We focused on electrolyte recovery
 - Safety and environmental impacts
 - Ever-changing chemistry mix of feed
 - Use off-the shelf industrial equipment
 - Option of multiple shredding passes
- We decided on building an inert atmosphere shredder for discharged batteries (<0% SoC)

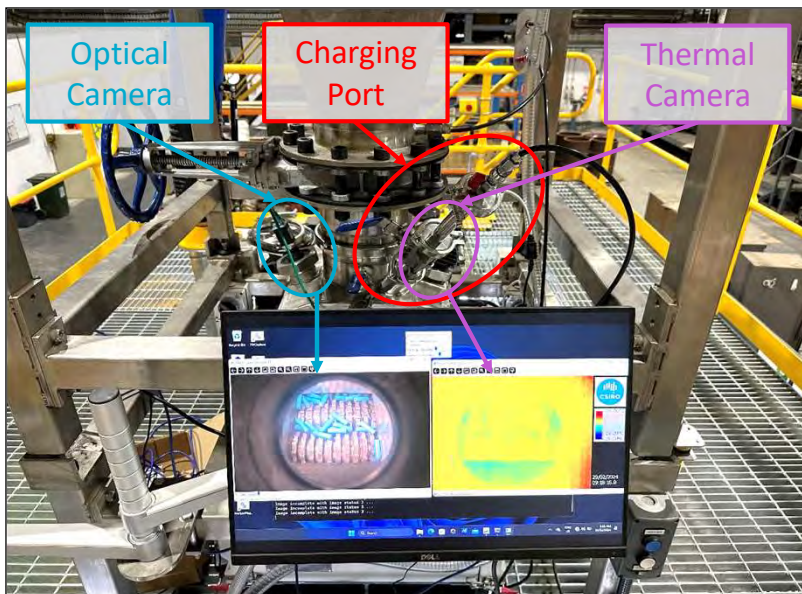
Battery Shredder Pilot Plant



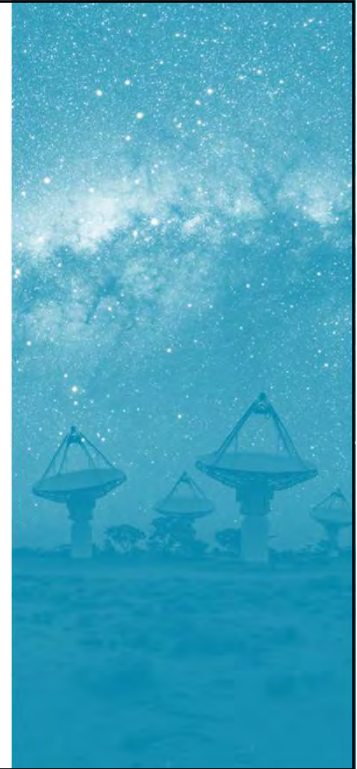
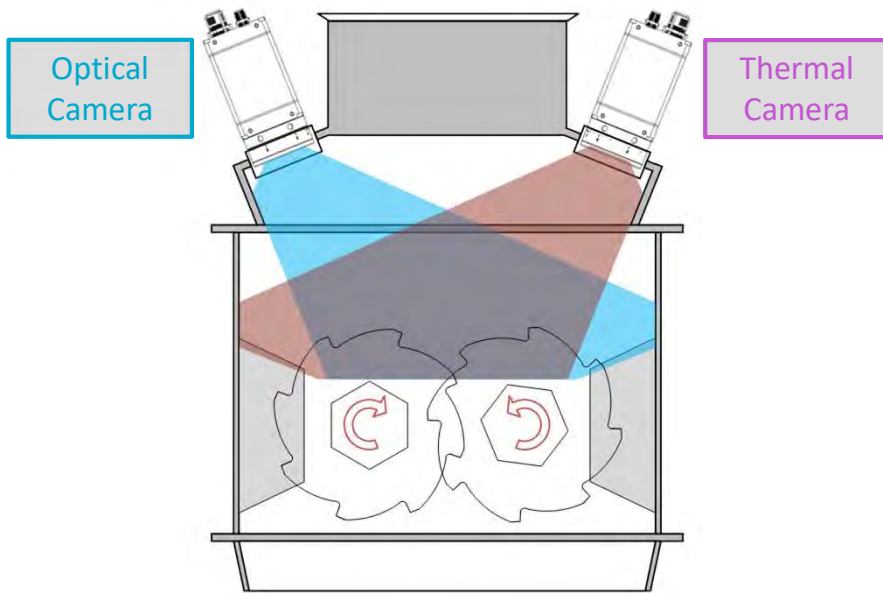
Battery Shredder Pilot Plant



CSIRO's Battery Shredding Facility



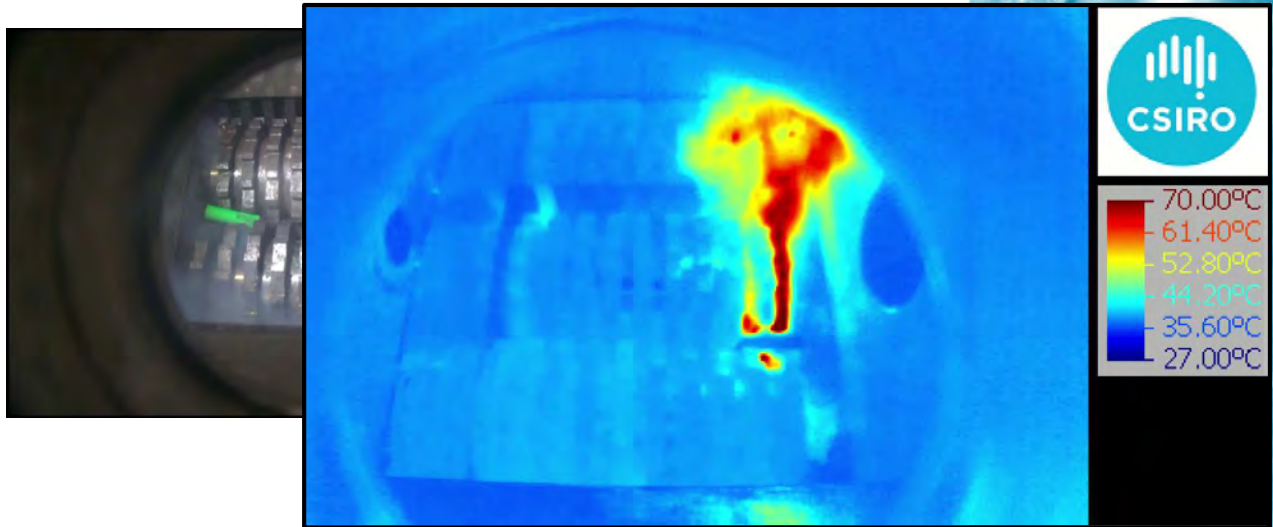
Battery Shredder Head



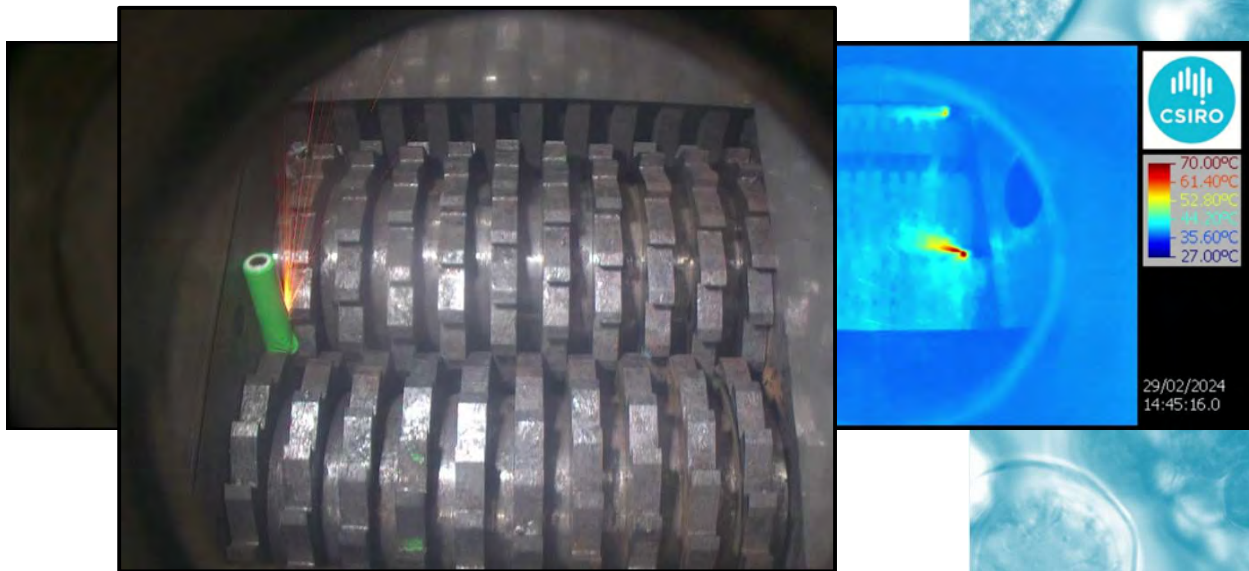
CSIRO's Battery Shredding Facility



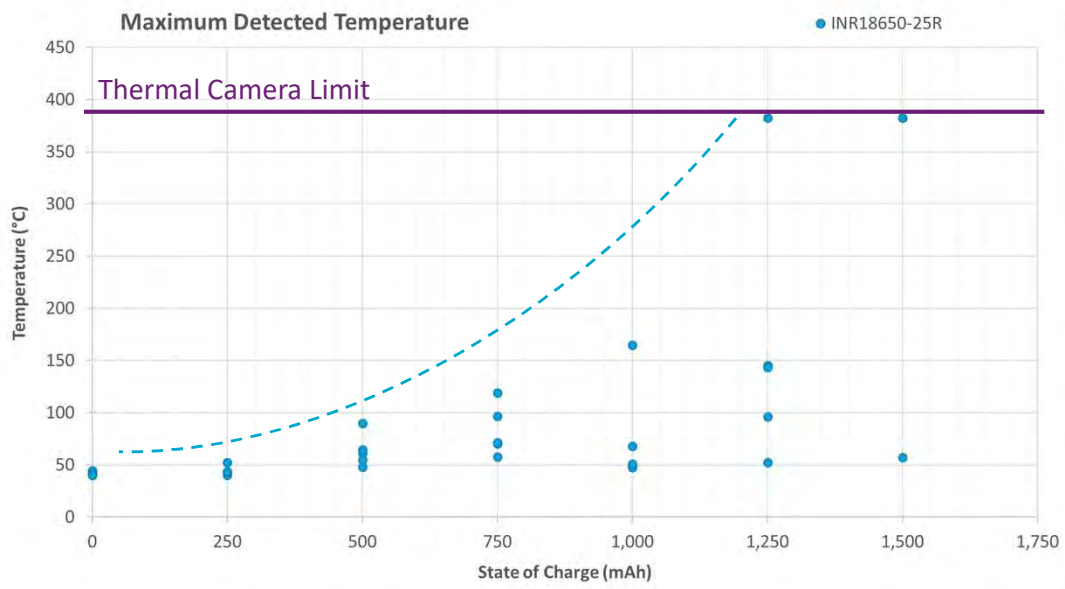
CSIRO's Battery Shredding Facility



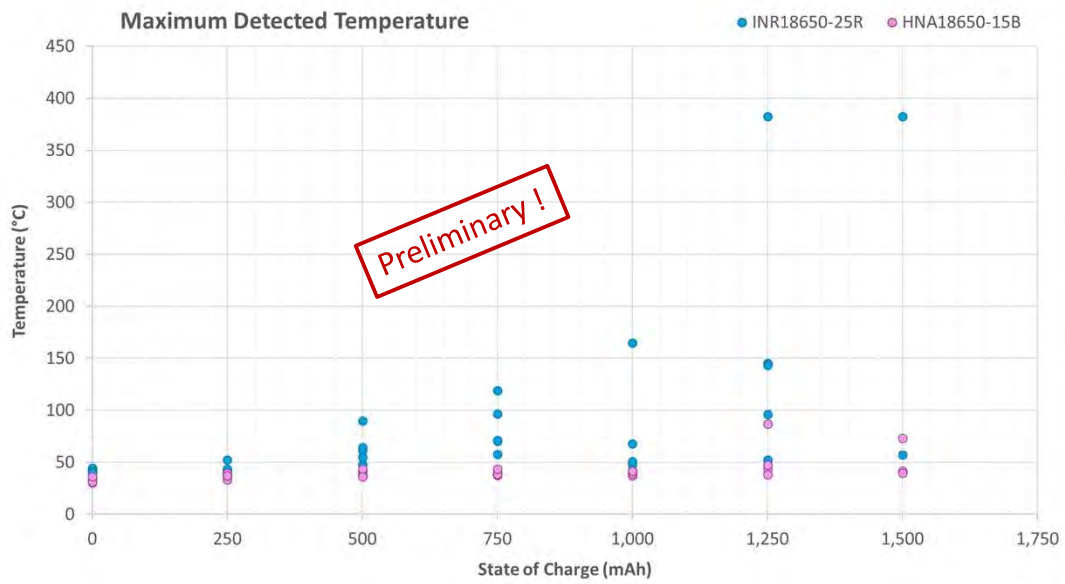
CSIRO's Battery Shredding Facility



Pilot Shredder Results



Pilot Shredder Results



Why look at higher SoCs?



Source: Autoweek VW ID4

Industry moved on very rapidly...

- Module Free Designs



Dischargeable & Repairable



Space Efficient & Stronger

Industry moved on very rapidly...

- Structural Packs



Dischargeable & Repairable



More reliable & Stronger

Brand New Challenges...

- These battery packs now have market dominance
 - Expect EU car manufactures to follow – if allowed!
 - Small scale “wall” battery storage systems are following
 - Will large battery energy storage systems also follow?
 - Consumer goods with Li-ion batteries - were the first!
- CSIROs work serendipitously became even more important and globally relevant
- Recycling industry is already adapting, but at what cost and to whom...?

IMPACT OF ORGANIC IMPURITIES ON ACID LEACHING OF VALUABLE METALS FROM USED LI-ION BATTERIES

By

Mooki Bae, Sookyung Kim, Hongin Kim, Hyun-woo Shim, Jinyoung Je and Hyunju Lee

Korea Institute of Geoscience and Mineral Resources (KIGAM), Republic of Korea

Presenter and Corresponding Author

Mooki Bae
muki.bae@kigam.re.kr

ABSTRACT

As the usage of lithium-ion batteries (Li-ion) increases, the need for efficient recycling methods to recover valuable metals such as lithium, nickel, and cobalt becomes critical. Acid leaching is a commonly used technique for extracting metals from spent Li-ion batteries. However, the presence of organic impurities within the battery materials can significantly impact the leaching process. This study aims to investigate the influence of these organic impurities on the effectiveness of acid leaching processes.

The spent Li-ion batteries underwent thermal treatment to eliminate organic components, including binders and separators, followed by sulfuric acid leaching to extract valuable metals. The thermal treatment was conducted at various temperatures, and the resulting black powder was analyzed to observe changes in metal concentration post-leaching. The impact of organic impurities on the leaching process was assessed by comparing the leaching efficiency of samples with and without thermal treatment.

The thermal treatment procedure involved exposing samples to temperatures of 0°C, 200°C, 400°C, 600°C, and 800°C in ambient air for 2 hours, followed by storage at room temperature for leaching purposes. For LCO-based batteries, primary reactions mostly reached equilibrium within an hour, with additional leaching observed after hydrogen peroxide supplementation. The leaching rate increased with higher thermal treatment temperatures, with differences of up to 20% observed. At 1000°C, the cobalt leaching rate reached 94.6%, while samples treated at 800°C, 600°C, 400°C, and 200°C exhibited cobalt leaching rates of 86.2%, 68.9%, 72.9%, and 72.9%, respectively. Untreated samples displayed a cobalt leaching rate of 77.4%.

The provided NCM-based black powder underwent thermal treatment followed by sulfuric acid leaching. With increasing thermal treatment temperature, the anode material (C, graphite) and organic substances were removed, resulting in concentration changes from Ni 5.27 wt%, Co 1.37 wt%, Mn 0.43 wt%, Li 1.07 wt% to Ni 6.56 wt%, Co 2.82 wt%, Mn 0.63 wt%, Li 1.47 wt%. Although leaching rates remained mostly consistent, higher thermal treatment temperatures led to the extraction of relatively more valuable metals. For instance, samples treated at 800°C for 6 hours exhibited leaching of Ni 1002.4 mg/L, Co 537.6 mg/L, Mn 117.4 mg/L, and Li 274.8 mg/L.

In conclusion, the study underscores the significance of thermal treatment in enhancing the efficiency of acid leaching processes for metal recovery from spent Li-ion batteries. The investigation sheds light on the intricate relationship between thermal treatment temperatures, organic impurities, and leaching efficiency, offering valuable insights for optimizing recycling methodologies in the pursuit of sustainable battery management.

Keywords: Recycling, Li-ion Battery (LIBs), Acid leaching, Thermal treatment, Organic impurities

"ELECTRON-ASSISTED LEACHING OF COBALT AND MAGANESE FROM LIBS USING LFP AS REDUCTANT"

Mooki Bae, Sookyung Kim, Hongin Kim, Hyun-woo Shim, Jinyoung Je, Hyeon-ji JO and Hyunju Lee

Korea Institute of Geoscience and Mineral Resources (KIGAM)

VISION

Leading innovative solution of geo-technology to sustainable Earth

As the only research institute for geological resources in Korea, our mission is to create a brighter future for the Korean peninsula and for the entire world.



MISSION

KIGAM's Geo-research on Land & Ocean, Geo-exploration on Deep Subsurface Resources and Utilization, New Geo-technology on Geo-hazards & Global Climate Change

"Leading Innovative Geo-Science and Technology solutions to create a Sustainable Earth"



Geology Division

Climate Change Response Division

Resources Utilization Division

Marine Geology & Energy Division

Mineral Resources Division

Geologic Hazards Division



Contents

✓ Introduction

Battery Recycling Industry

Project purpose

✓ Results and discussion

Experimental part 1: Acid leaching of spent Li-ion batteries with reductants

Experimental part 2: Mechanism study on REDOX reactions

✓ Conclusions



Battery Recycling Industry

Battery Industry

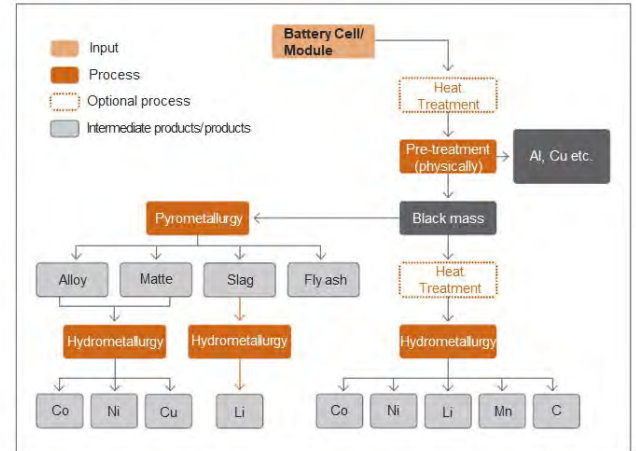
South Korea's Battery Recycling 2024

In 2024, South Korean major companies are actively involved in battery recycling. SK, LG, and Samsung have established partnerships and invested in recycling technologies and facilities. Additionally, POSCO and Doosan are also expanding their efforts in the battery recycling industry.

Key Players Status

1. SK Innovation
 - Developed lithium hydroxide recovery technology.
 - Recycling partnerships with EcoPro and Ascend Elements.
2. LG Energy Solution
 - Invested in Li-Cycle for nickel recycling.
 - Joint venture with Huayou Cobalt in China.
3. Samsung SDI
 - Collaborated with SungEel HiTech for recycling.
 - Established a closed-loop system in global plants.

Battery Recycling

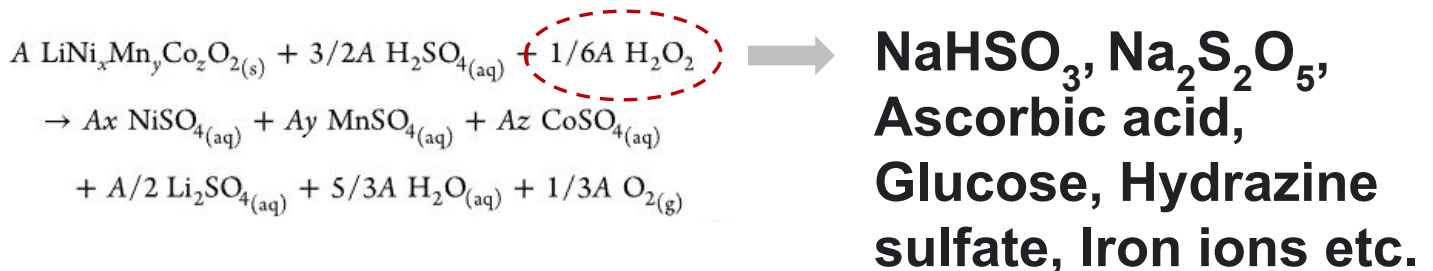


5

Battery Industry

NCM Battery Recycling?: Sulfuric acid Leaching with H_2O_2 as reductant

✓ Sulfuric acid Leaching



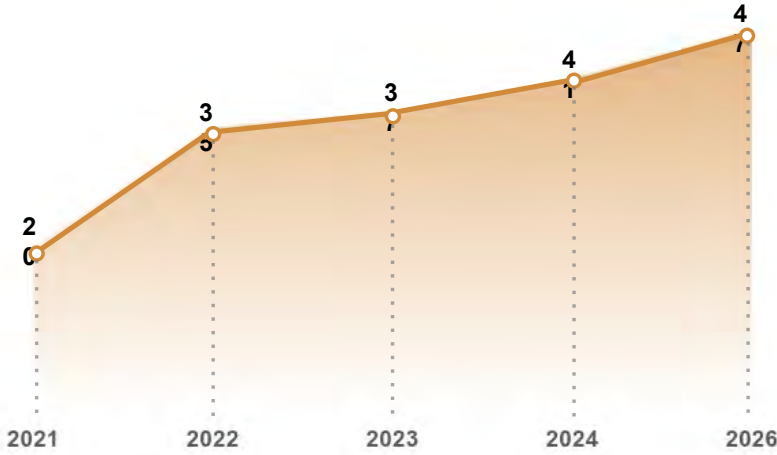
- Reductants are required to enhance the metal solubility especially Co, Mn by transforming from insoluble species Co(III) and Mn(IV) into soluble species Co(II) and Mn(II)
- H_2O_2 is main reducing agents to reduce the transition metals and Among the alternative, Iron ions can be used as reductants

6

Battery Industry

The LFP battery market is growing rapidly, driven by its safety and cost benefits. South Korea battery companies are actively developing and planning mass production to meet increasing global demand.

✓ LFP Battery Market Share (unit: %)



Source: SNE

✓ Development Plans

- LG Energy Solution
- Samsung SDI
- SK On
- POSCO Futurem

Mass-producing batteries for energy storage systems (ESS)

Planning to begin full-scale production in 2026

Development completed; detailed mass production plans undisclosed

Producing 20,000 tons of LFP and other cost-effective cathode materials next year

Battery Industry

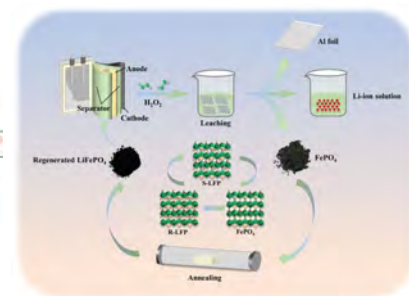
LFP Battery Recycling?: Metal value and Recycling viability

✓ Battery Metal Values

Battery	Values	Viability
NCA (Ni-Co-Al)	\$71 per kWh	High
NCM811 (Ni-Co-Mn)	\$68 per kWh	High
LFP (Li-Fe-P)	\$45 per kWh	Low

Source: KIPOST

✓ Recycling of LFP

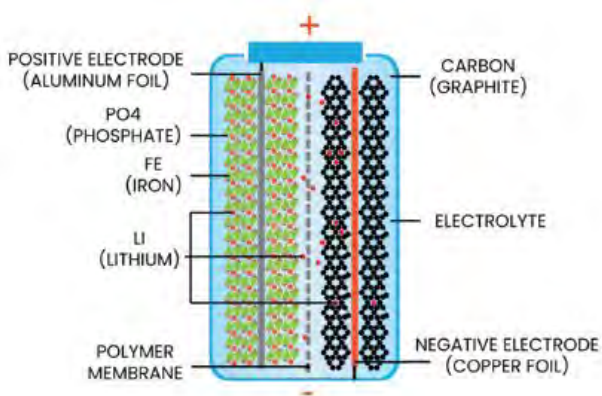


- Economic viability due to high metal prices and Potential decrease in value due to falling Li prices
- Low metal value made recycling uneconomical and lack of incentive for recycling LFP batteries
- For economic reasons, LFP batteries are being recycled through direct recycling or precursor recovery methods.

Battery Industry

LFP Battery Recycling?: LFP made from following materials

✓ Structure of LFP Battery



Positive plate

Al sheet + LiFeYPO_4

Negative plate

Cu sheet + Carbon

Separator

PP + PE Film

Electrolyte

Organic solvent + LiPF_6

Case

PP, Aluminum alloy

9

Results and discussion

Results of Battery Recycling

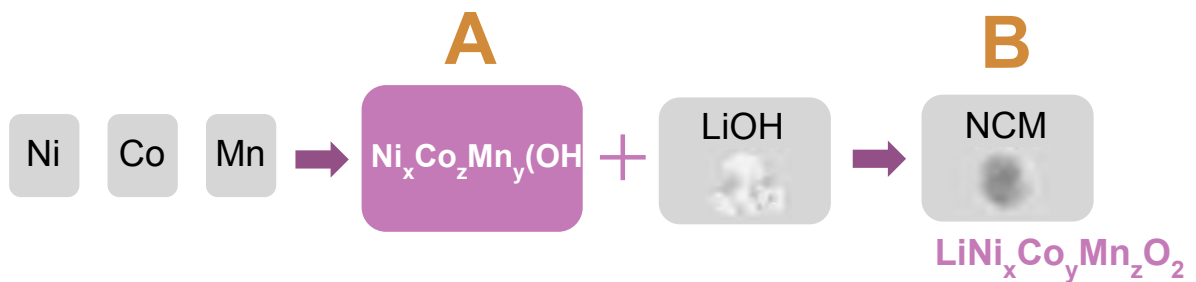
Pretreatment: Physical separation of spent LFP



11

Results of Battery Recycling

Pretreatment: Information of NCM samples



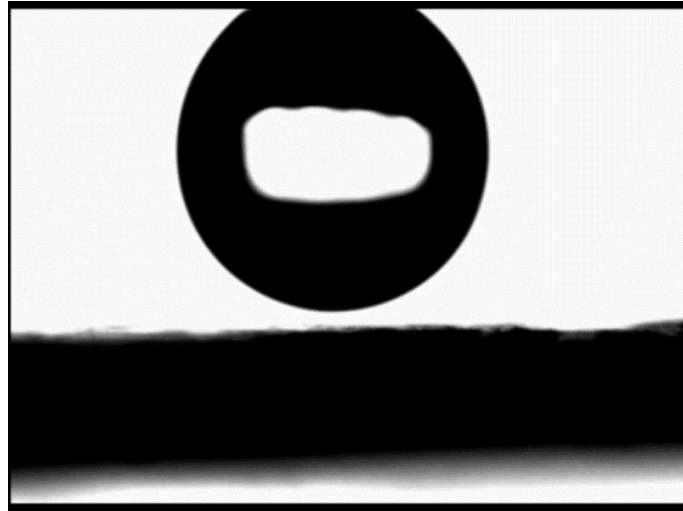
✓ **Composition of NCM samples**

	(unit: wt%)							
	NiO	MnO	Co ₂ O ₃	CuO	Al ₂ O ₃	Fe ₂ O ₃	P ₂ O ₅	SiO ₂
A(S)	26.52	13.95	9.17	7.60	6.05	1.65	0.57	0.25
B(H)	17.86	3.81	6.68	9.41	4.61	1.18	0.30	1.91

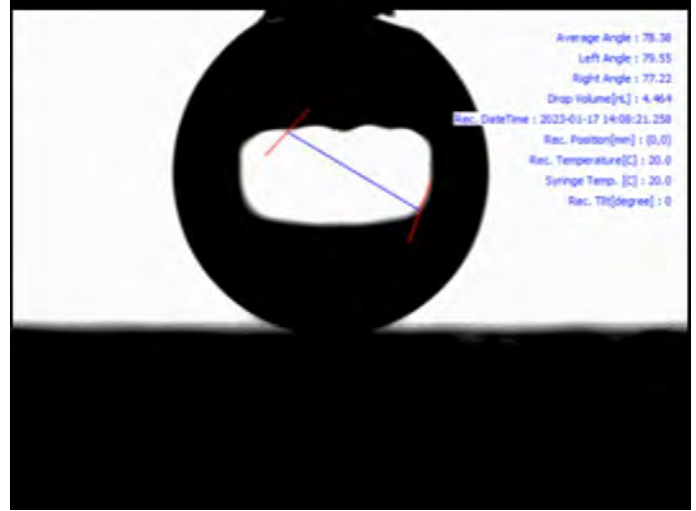
Results of Battery Recycling

Pretreatment: Heat treatment for removing organic and further process

Raw

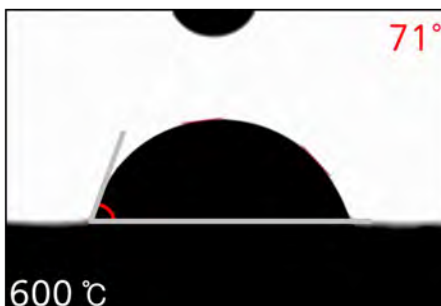
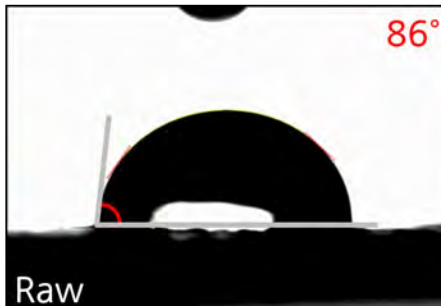


600 °C



Results of Battery Recycling

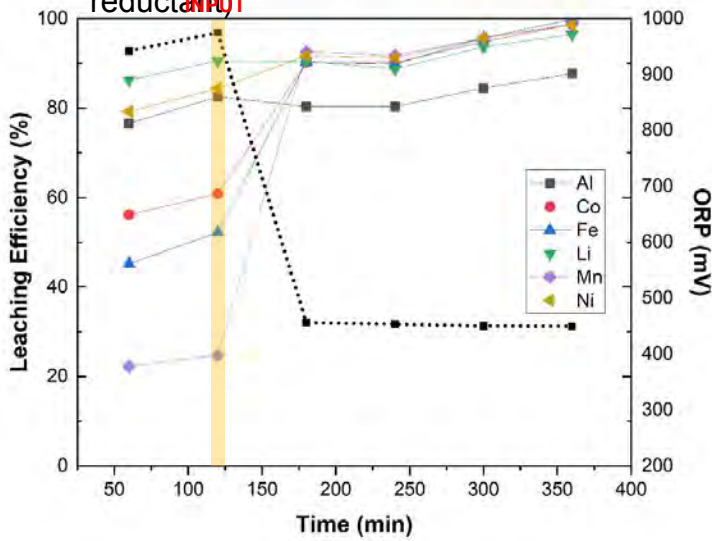
Pretreatment: Heat treatment for removing organic and further process



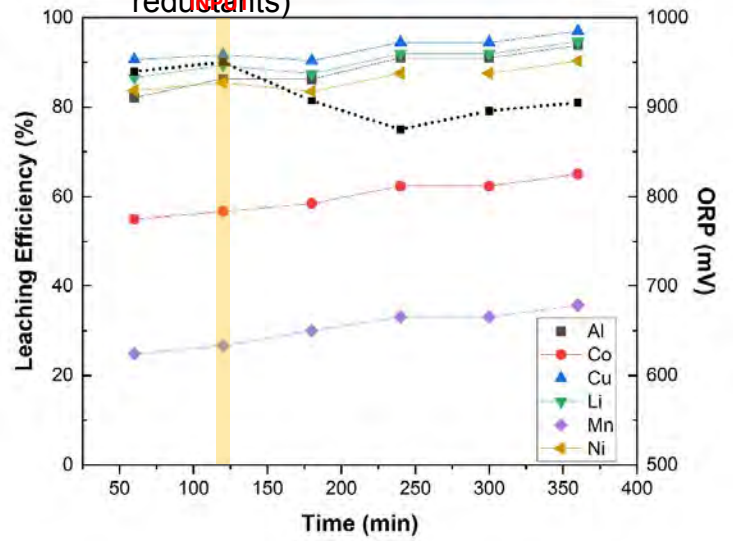
Results of Battery Recycling

Leaching part(i): Effect of Fe and Cu as reductant for sample A(-OH)

✓ Leaching efficiency (Cu as reductant)



✓ Leaching efficiency (Fe as reductant)

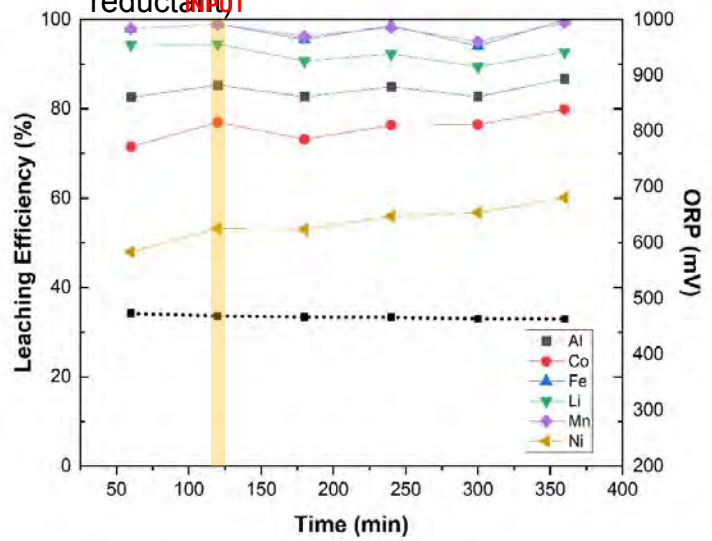


Experimental conditions: Concentration, 2M H₂SO₄; PD, 20%; Reductant(Cu, Fe), 25%/PD; Temp., 80 °C, Time, 6 H

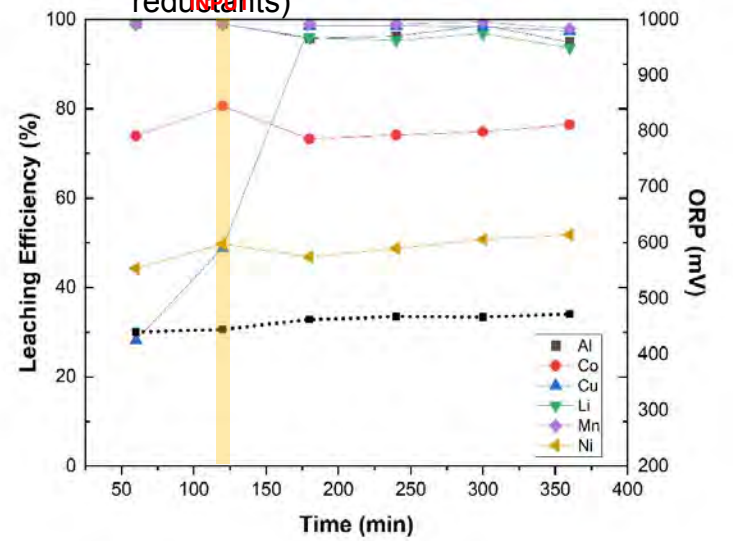
Results of Battery Recycling

Leaching part(ii): Effect of Fe and Cu as reductant for sample B(-O₂)

✓ Leaching efficiency (Cu as reductant)



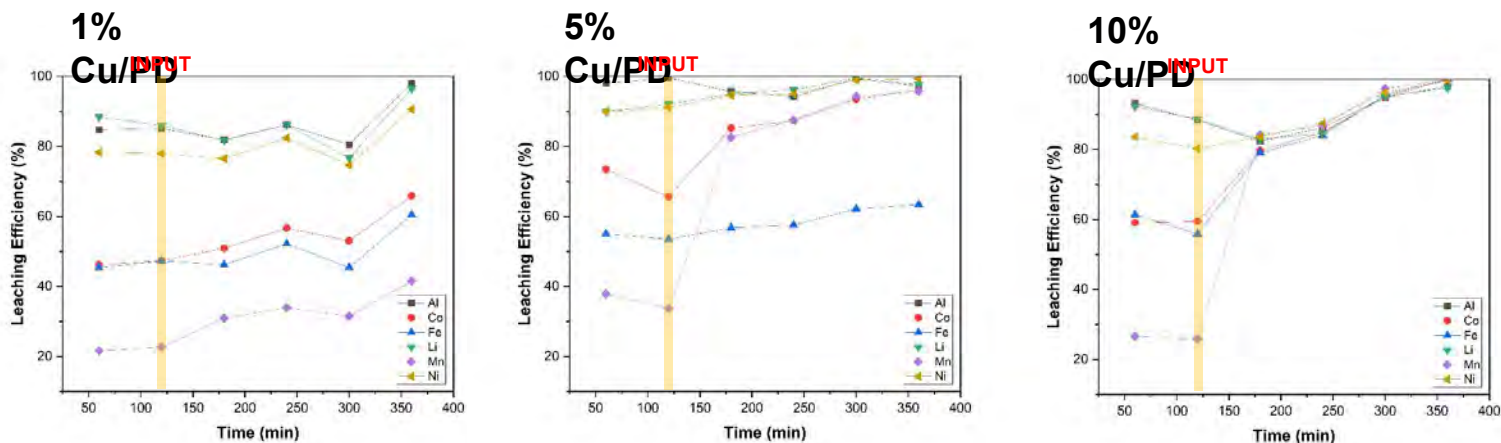
✓ Leaching efficiency (Fe as reductant)



Experimental conditions: Concentration, 2M H₂SO₄; PD, 20%; Reductant(Cu, Fe), 25%/PD; Temp., 80 °C, Time, 6 H

Results of Battery Recycling

Leaching part(i): Effect of Cu dosage on NCM leaching

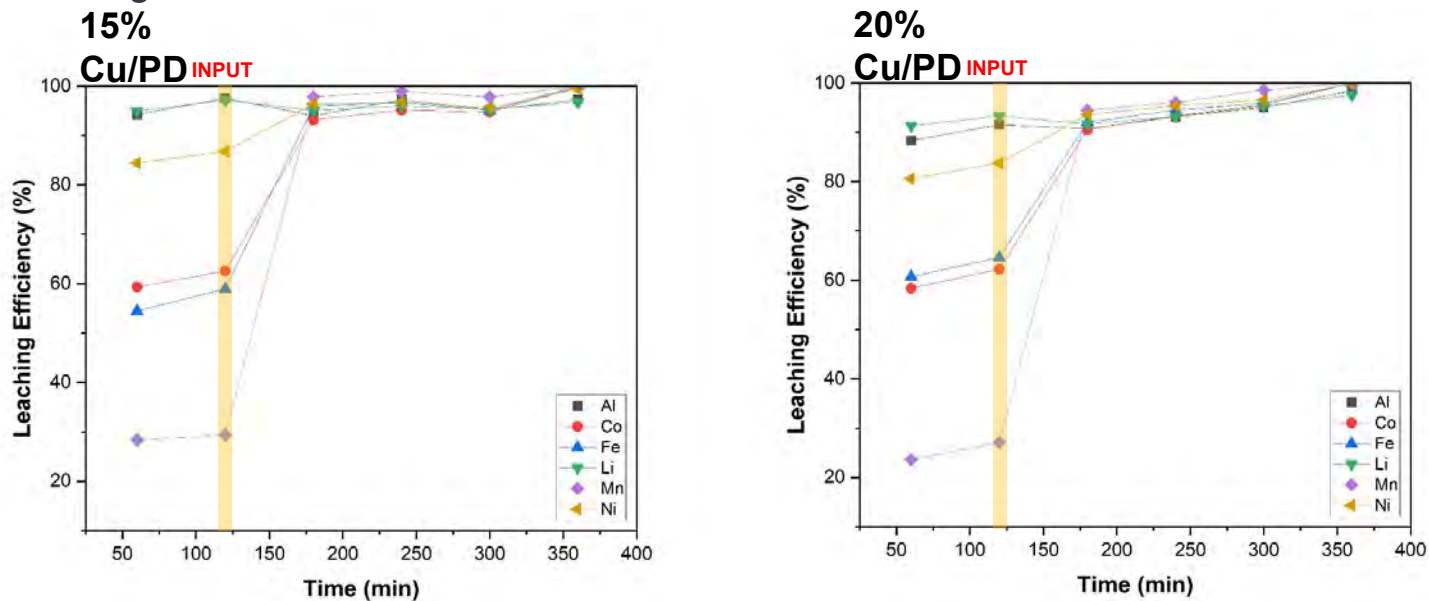


Experimental conditions: Concentration, 2M H₂SO₄; PD, 20%; Reductant(Cu), 1~20%/PD; Temp., 80 °C, Time, 6 H

17

Results of Battery Recycling

Leaching part(i): Effect of Cu dosage on NCM leaching



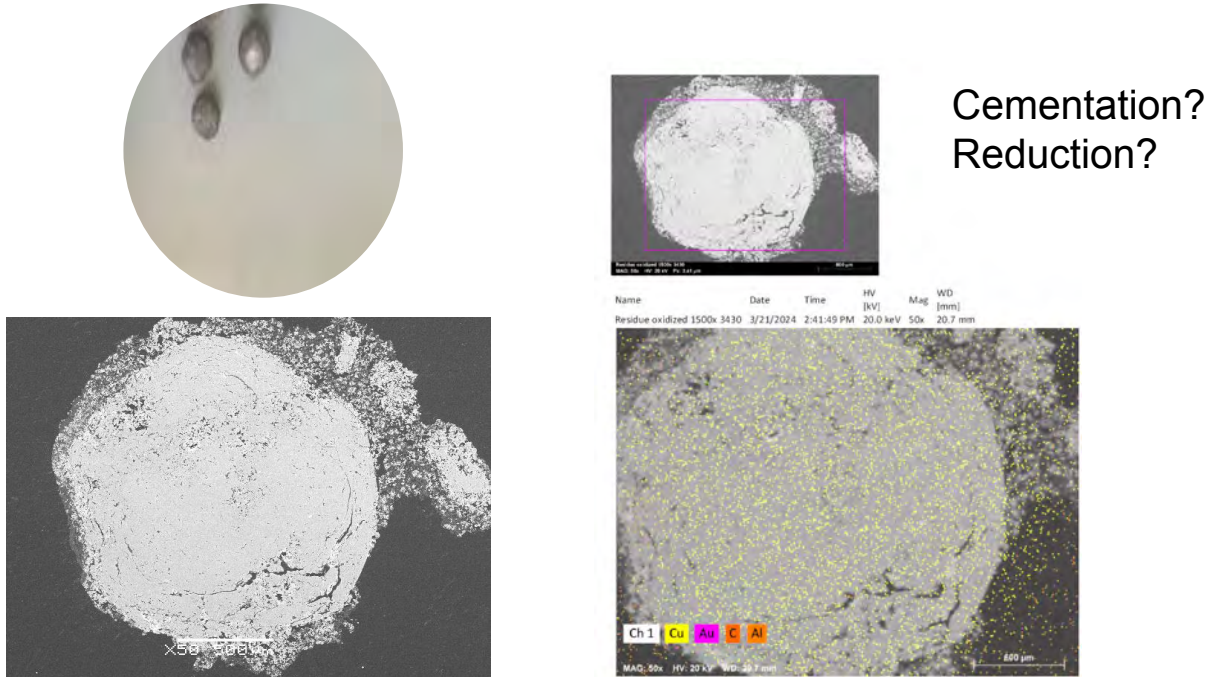
Experimental conditions: Concentration, 2M H₂SO₄; PD, 20%; Reductant(Cu), 1~20%/PD; Temp., 80 °C, Time, 6 H

280/395

18

Results of Battery Recycling

Leaching part(i): Effect of Cu dosage on NCM leaching



19

Results of Battery Recycling

Leaching part(i): Effect of Cu dosage on NCM leaching

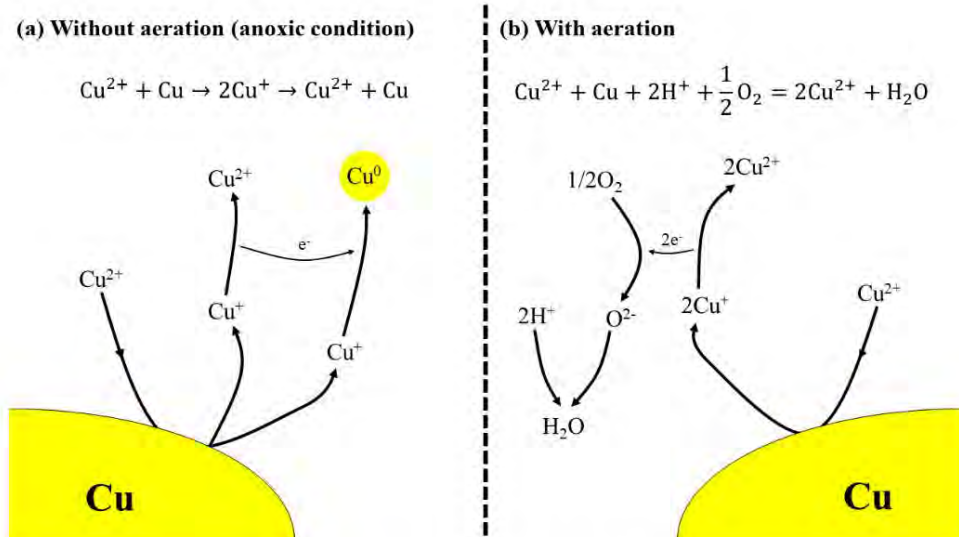


Figure 3. The proposed concept of leaching behavior of copper from Cu metal by Cu^{2+} ions in sulfuric acid leaching: (a) without aeration and (b) with aeration.

Source: Yoo, K., et al. (2020) Improvement of copper metal leaching in sulfuric acid solution by simultaneous use of oxygen and cupric ions. *Metals* 2020, 10, 721

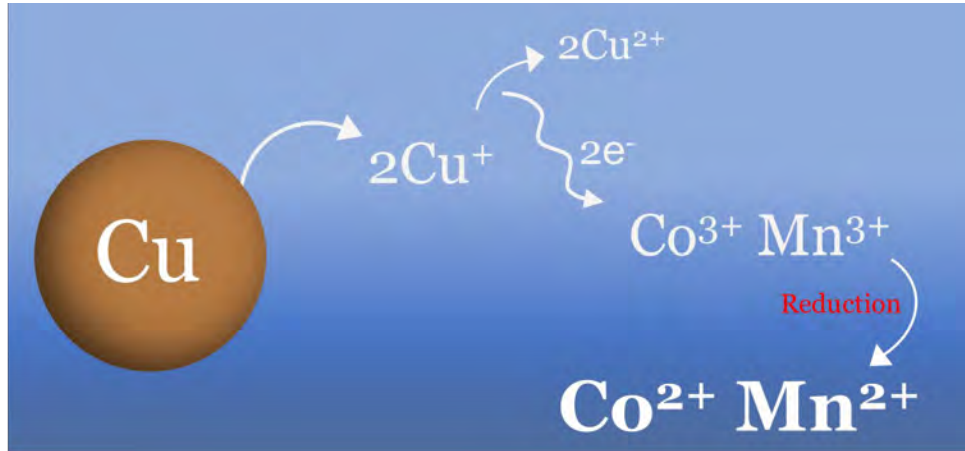
Results of Battery Recycling

Leaching part(i): Effect of Cu dosage on NCM

leaching

Standard reduction potential [V]

+1.82	$\text{Co}^{3+} + \text{e}^- \rightarrow \text{Co}^{2+}$
+1.51	$\text{Mn}^{3+} + \text{e}^- \rightarrow \text{Mn}^{2+}$
+0.34	$\text{Cu}^{2+} + 2\text{e}^- \rightarrow \text{Cu}$
+0.15	$\text{Cu}^{2+} + \text{e}^- \rightarrow \text{Cu}^+$
-0.28	$\text{Co}^{2+} + 2\text{e}^- \rightarrow \text{Co}$
-1.18	$\text{Mn}^{2+} + 2\text{e}^- \rightarrow \text{Mn}$



- Cuprous ions are unstable in sulfuric acid solution, they immediately convert to cupric ions by losing one electron.
- Electron can easily reduce Co^{3+} and Mn^{3+} , which have relatively high redox potentials, making Co and Mn easier to leach.

21

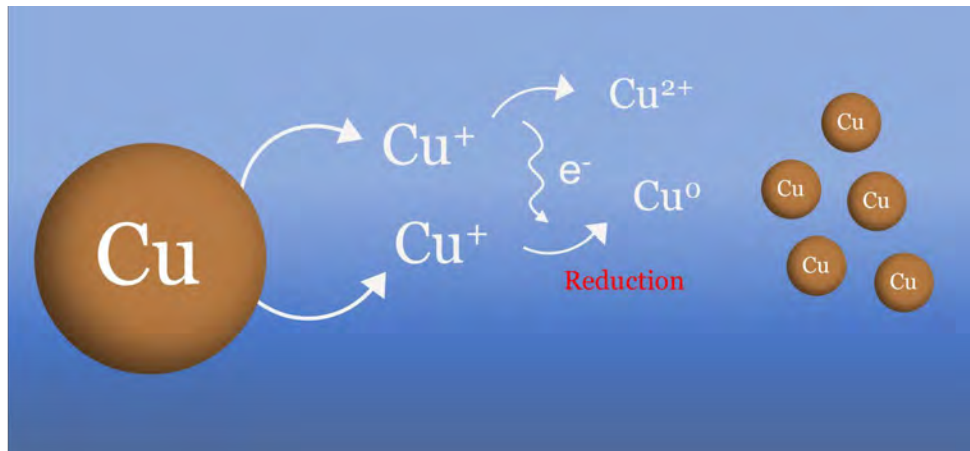
Results of Battery Recycling

Leaching part(i): Effect of Cu dosage on NCM

leaching

Standard reduction potential [V]

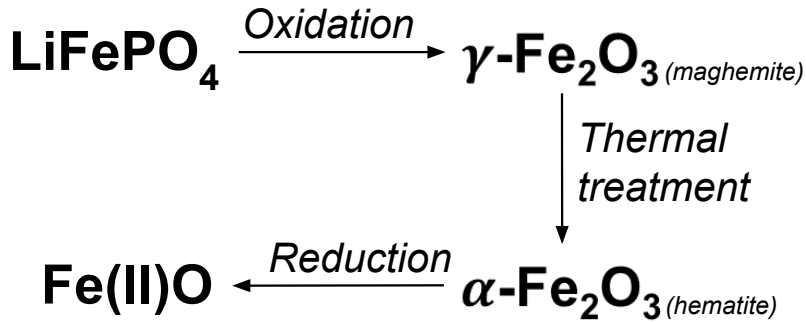
+1.82	$\text{Co}^{3+} + \text{e}^- \rightarrow \text{Co}^{2+}$
+1.51	$\text{Mn}^{3+} + \text{e}^- \rightarrow \text{Mn}^{2+}$
+0.34	$\text{Cu}^{2+} + 2\text{e}^- \rightarrow \text{Cu}$
+0.15	$\text{Cu}^{2+} + \text{e}^- \rightarrow \text{Cu}^+$
-0.28	$\text{Co}^{2+} + 2\text{e}^- \rightarrow \text{Co}$
-1.18	$\text{Mn}^{2+} + 2\text{e}^- \rightarrow \text{Mn}$



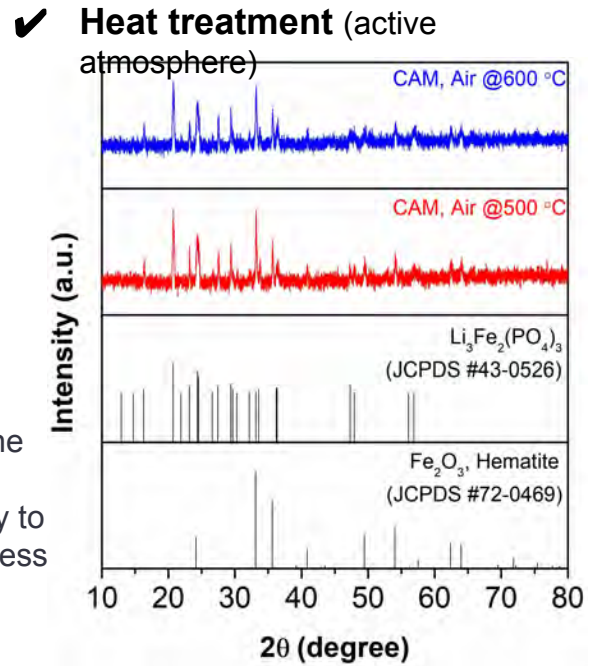
- Most of the cobalt and manganese have been leached, there are no more ions acting as oxidizing agents.
- The electrons released from the oxidation of Cu^+ to Cu^{2+} are received by Cu^+ ions, forming metallic copper precipitates.

Results of Battery Recycling

Leaching parts: Effect of Iron ions on reducing of Co(III), Mn(III) to Co(II), Mn(II)



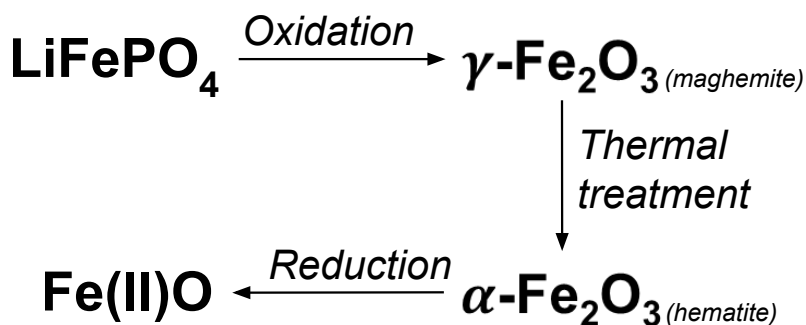
- Heat-treating LFP in an active atmosphere converts it into the Fe_2O_3 phase, incorporating trivalent iron ions (Fe^{3+}).
- To obtain divalent iron ions (Fe^{2+}) from Fe_2O_3 , it is necessary to perform heat treatment in a reducing atmosphere. This process reduces Fe_2O_3 to FeO , providing the desired Fe^{2+} ions.



23

Results of Battery Recycling

Leaching parts: Effect of Iron ions on reducing of Co(III), Mn(III) to Co(II), Mn(II)



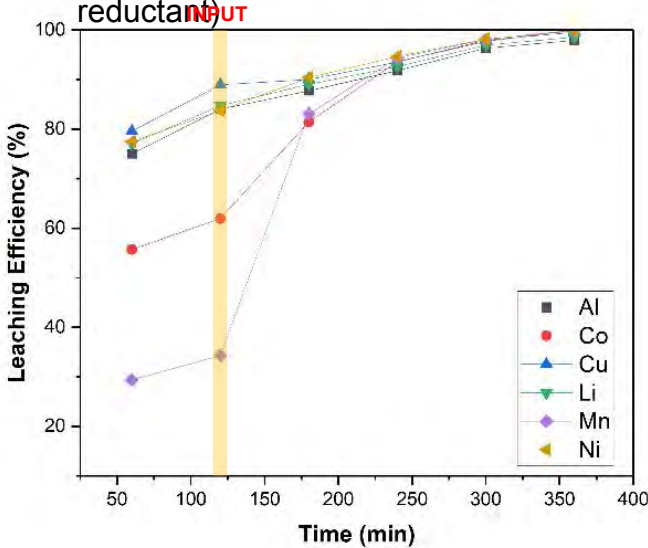
- Heat-treating LFP in an active atmosphere converts it into the Fe_2O_3 phase, incorporating trivalent iron ions (Fe^{3+}).
- To obtain divalent iron ions (Fe^{2+}) from Fe_2O_3 , it is necessary to perform heat treatment in a reducing atmosphere. This process reduces Fe_2O_3 to FeO , providing the desired Fe^{2+} ions.

Standard reduction potential [V]	
+1.82	$\text{Co}^{3+} + \text{e}^- \rightarrow \text{Co}^{2+}$
+1.51	$\text{Mn}^{3+} + \text{e}^- \rightarrow \text{Mn}^{2+}$
+0.77	$\text{Fe}^{3+} + \text{e}^- \rightarrow \text{Fe}^{2+}$
+0.34	$\text{Cu}^{2+} + 2\text{e}^- \rightarrow \text{Cu}$
+0.15	$\text{Cu}^{2+} + \text{e}^- \rightarrow \text{Cu}^+$
-0.28	$\text{Co}^{2+} + 2\text{e}^- \rightarrow \text{Co}$
-0.44	$\text{Fe}^{2+} + 2\text{e}^- \rightarrow \text{Fe}$
-1.18	$\text{Mn}^{2+} + 2\text{e}^- \rightarrow \text{Mn}$

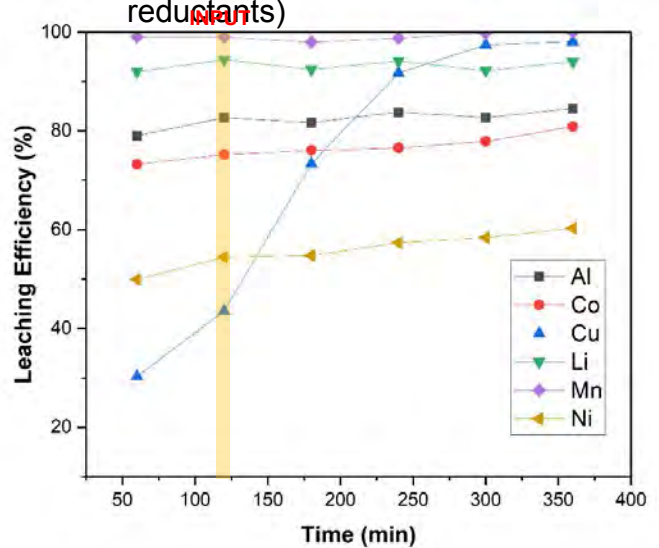
Results of Battery Recycling

Leaching part(iii): Effect of Fe(II)O as reductant for sample A(-OH) and B(-O₂)

✓ (A) Leaching efficiency (FeO as reductant)



✓ (B) Leaching efficiency (FeO as reductants)



Experimental conditions: Concentration, 2M H₂SO₄; PD, 20%; Reductant(FeO), 25%/PD; Temp., 80 °C, Time, 6 H

25

Conclusions

✓ LFP(Fe, Cu) used as reductant for leaching of Co and Mn from LIBs

Co < 99%, Mn < 99%, Ni 99 %, Li 99% at 2M H₂SO₄, 80 °C, 6h, PD 20% with Cu or Fe as reductants

✓ Electron donation aids in Co, Mn leaching during conversion of Fe, Cu ions

Copper ions from monovalent to divalent (Cu⁺ to Cu²⁺)

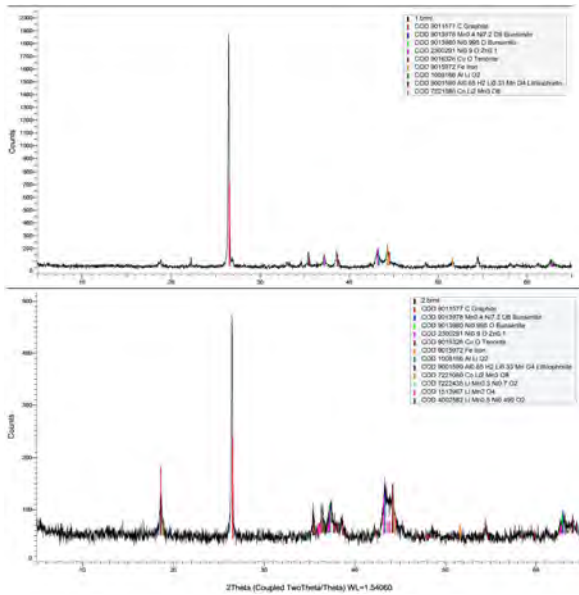
Iron ions should convert to FeO to reduce the ferric ion to ferrous (Fe³⁺ to Fe²⁺)

✓ Phenomena clarified via direct methods (electrochemical analysis)

Investigate whether the electrons generated during the conversion of copper(I) ions to copper(II) ions are utilized in the reduction of cobalt and manganese

LIBs Recycling R&D

Previous Experiment: Efficient Separation Technology for Electrode Active Materials



Results of Battery Recycling

Pretreatment: Heat treatment for removing organic and further process

✓ Composition and potential environmental pollution of LIBs of LIB battery

Part	Composition	Main chemical properties	Potential pollution
Cathode	Al+LiCoO ₂ / LiMn ₂ O ₄ /LiNiO ₂	Strong reaction with H ₂ O/acid/reductants/strong/oxidants, forming toxic oxide	Pollution of heavy metals
Anode	Cu + C(graphite)	Explosion when dust get fire or high temperature	Dust pollution
Electrolyte salts	LiPF ₆ /LiBF ₄ /LiAsF ₆	Strong corrosive, forming HF in H ₂ O	Fluorine
Electrolyte solvents	EC+PC+DC+DEC	Combustible	VOCs
Organic separator	PP/PE	Combustible	VOCs
Binder	PVDF/VDF/EPD	Thermal decomposition produces HF	Fluorine

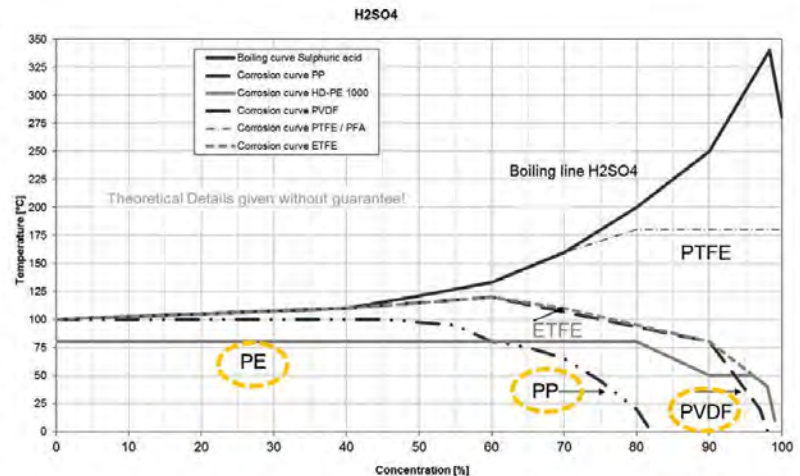


Figure 5: Isocorrosion diagram of some plastic materials in sulphuric acid. The areas below the lines are suitable for these materials.

LEWATIT[®] ION EXCHANGE RESINS FOR THE RECYCLING OF LITHIUM ION BATTERIES

By

Dirk Steinhilber, Stefan Neufeind

LANXESS Deutschland Liquid Purification Technologies, Germany

Presenter and Corresponding Author

Dirk Steinhilber

dirk.steinhilber@lanxess.com

ABSTRACT

The growing demand for high purity battery lithium, nickel, cobalt and copper requires access to new resources. The most economic and environmentally friendly approach is the recycling of end of life batteries. Due the high concentration of battery metals, they can be extracted and recycled with low carbon footprints and a t low cost. Therefore, the European Union established strictly regulated recycling targets and a minimum level of recycled battery metals content for the manufacturing of new batteries. As a result, processes with true circular economy are developed. A lot of cathode off-spec material is already available from cathode producers and more end of life batteries will be available within the next years. Lewatit[®] ion exchange resins are crucial for many process steps in the hydrometallurgical recycling flow sheets. In this paper we describe three of most important applications and the benefits of our resins in the field of battery recycling.

Purification of black mass leachate

Recycling usually starts by discharging, dismantling, and shredding of lithium ion batteries. In hydrometallurgical operations the solid black mass powder is separated by filtration because it contains the valuable metals lithium, nickel, cobalt, manganese. Leaching of the black mass with acid dissolves these valuable metals. However also impurities like Cu, Al, Zn, and Fe are usually contained in the concentrates, because mechanical separation cannot be performed perfectly. These impurities can be efficiently removed with selective chelating resin Lewatit[®] MDS TP 260. We especially developed a new efficient Al regeneration technology with the use of NaOH and elution of the $Al(OH)_4^-$ anionic complex. Thanks to the smaller size of our monodisperse small (MDS) resins and, in turn, shorter diffusion paths, they exhibit faster kinetics during exchange and regeneration. Not only does their high packing density make them ideal for chromatographic separation, but they also have a higher capacity utilization and, in turn, longer service lives with lower requirements for regeneration chemicals.

Purification of individual metal concentrates

Since black mass contains a high concentration of battery metals, separation of the individual metals is usually performed by solvent extraction. The generated metal concentrates are most efficiently purified by our selective chelating resins, e.g. Li with Lewatit[®] MonoPlus TP 207, Ni with Lewatit[®] TP 272, and Co with Lewatit[®] VPOC 1026 and Lewatit[®] MDS TP 220. Our selective chelating resins are especially suited for this separation task because of their high selectivity and loading capacity towards impurities, which ensures efficient removal below the specification limit. At the same time, they show low interaction towards valuable and concentrated battery metals nickel and cobalt, which pass the resin at high yield and recovery.

Waste water treatment

Waste water streams generated by battery metals recycling plants can be efficiently treated by Lewatit[®] MonoPlus TP 207. This resin selectively removes toxic heavy metals in the presence of high concentrations of other constituents of the waste water, e.g., hardness. Valuable battery metals can additionally be recovered and recycled from the resin by selective regeneration.

In conclusion Lewatit[®] ion exchange resins provide benefits including up to two times longer cycle times compared to conventional resins combined with savings on regeneration chemical costs. Excellent exchange kinetics ensures contaminant removal down to trace levels and yields pure battery metal concentrates. Additionally, Lewatit[®] chelating resins possess high resilience towards osmotic and mechanical stress and ensure long resin lifetimes.

Keywords: Lithium ion battery recycling, black mass leachate treatment, selective chelating ion exchange resins



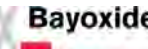



Lewatit® ion exchange resins in the sustainable recycling of lithium ion batteries

Dr. Dirk Steinhilber, Technical Marketing Manager, LANXESS Deutschland GmbH

ALTA 2024 – Perth, May 31, 2024

Versatile specialists – comprehensive product portfolio provides advanced solutions

Products and brands	
 	<ul style="list-style-type: none"> Ion exchange resins, adsorbers, and functional polymers for use in many industries and applications
	<ul style="list-style-type: none"> Granular iron oxide adsorbers for water treatment
	<ul style="list-style-type: none"> Software for designing and optimizing ion exchange resin plants

Customer industries		
 Mining and metallurgy	 Food and beverages	 E-mobility
 Semiconductor	 Household	 Power generation
 Municipal water treatment	 Chemical and petrochemical	 Drinking water
 Paper and pulp	 Pharma and biotech	 Photovoltaic

Strong growth of battery market growth driven by e-mobility & renewables

Key drivers

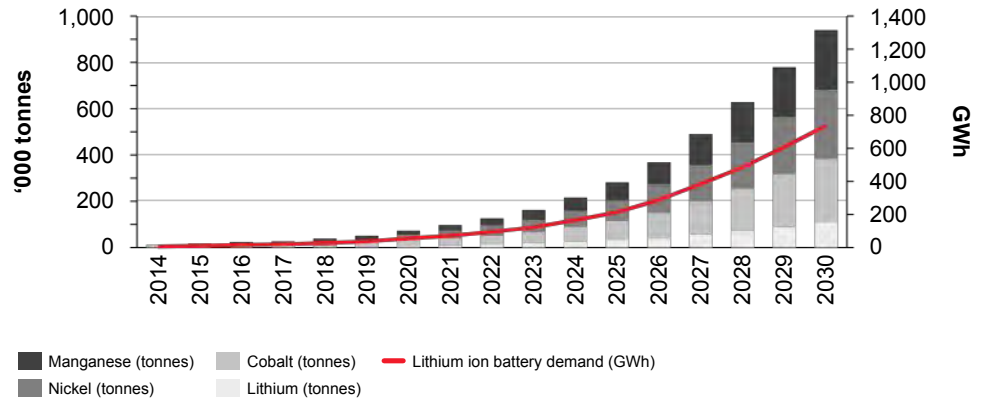
Megatrends driving the battery market

- Global awareness of global warming pushing for adoption of green solutions (CO₂ emissions reduction)
- Widespread introduction of **renewable energies** (stationary storage)
- **Population increase** and **city growth** challenging mobility and energy solutions (e-mobility)

Li-Ion battery is key technology for new concepts of mobility and energy

E-mobility drives demand for battery chemicals

Global lithium-ion and materials demand forecast from EV sales, 2015–2030 (thousand of tonnes, GWh)



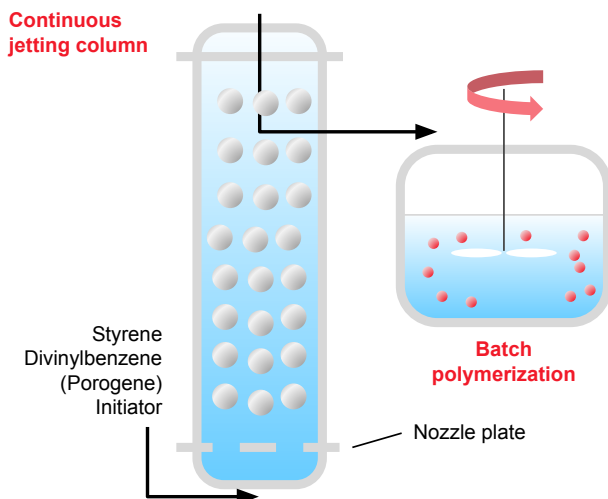
Source: Bloomberg New Energy Finance

31.05.2024

Monodisperse droplet generation by jetting process

Stable scaffolds for demanding metals processing applications!

Formation of monodisperse droplets



Description

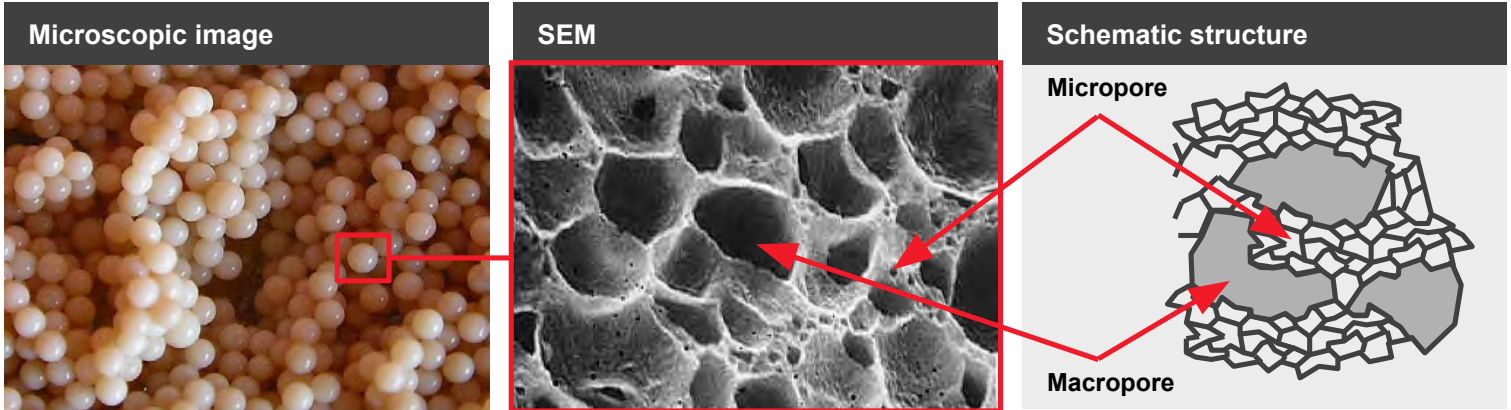
- Continuous process
- Raw materials are fed through a nozzle plate at the bottom of the column
- The resulting monomer jet is chopped into droplets of the same size
- Particle size can be controlled by adjustment of the whole width of the nozzle plate
- The droplets formed at the bottom start to encapsulate as they proceed to the column head
- Polymerization of the monodisperse encapsulated droplets is completed afterwards

31.05.2024

288/395

The structure of macroporous resins

Small opaque beads are actually of a highly permeable sponge-like structure



31.05.2024

Ion exchange groups

A strong portfolio of solutions for critical separation challenges

Solvent impregnated resins	Selective chelating resins		Anion exchange and adsorber
<p>Zn, Cu removal from Ni, Co, Li Lewatit® VP OC 1026</p>	<p>Ca+Mg from Li concentrate Lewatit® MDS TP 208</p>	<p>Ni from Co and Fe(III) Lewatit® MDS TP 220</p>	<p>PFAS from black mass leachate Lewatit® TP 108, Lewatit® MP 62 WS</p>
<p>Co from Ni concentrate Lewatit® TP 272</p>	<p>Al from Li, Bi+Sb from Cu Lewatit® MDS TP 260</p>	<p>Pt group metals from Ni Lewatit® MonoPlus TP 214</p>	<p>Silica from Li and Ni Bayoxide®, FeO(OH)</p>

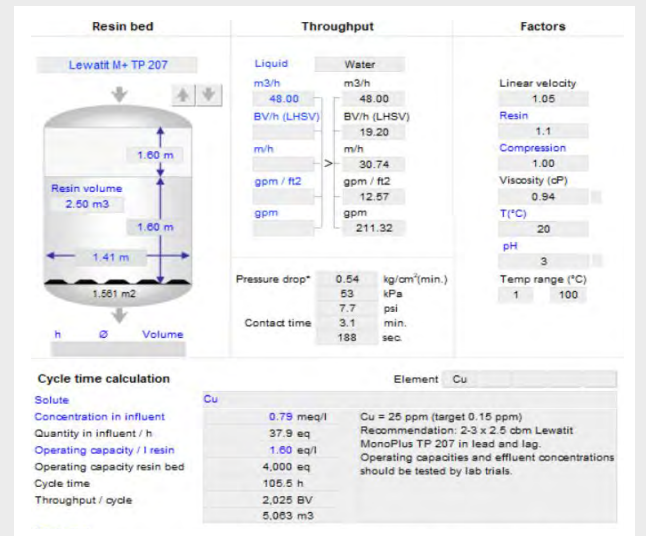
31.05.2024

289/395

Key properties of ion exchange resins

Precise control of resin parameters for critical separation challenges

- Functional group (type of chelating)
- Polymer Matrix (styrenic or acrylic)
- Morphology (gel or macroporous)
- Crosslinking
- Bead size (mono- vs. heterodisperse)
- Kinetics
- Resin swelling



31.05.2024

Lewatit® ion exchange resins in applications for purification and refining of battery metals

A strong portfolio of solutions for the preparation critical battery materials

	Nickel and Cobalt						Copper				Lithium		LiPF ₆
	Recycling	Recovery Fixed Bed	Recovery Resin in Pulp	Concentrate Purification	Separation	Waste Water	Recovery Resin in Pulp	Recovery Fixed Bed	Waste Water	Concentrate Purification	Brine Purification	Recycling	Purification
Lewatit® MonoPlus TP 209 XL		■	■			■	■						
Lewatit® MonoPlus TP 207	■	■		■		■		■	■			■	
Lewatit® VP OC 1026	■			■									
Lewatit® TP 272				■									
Lewatit® MDS TP 220				■	■			■	■				
Lewatit® MDS TP 260	■			■		■		■		■	■	■	
Lewatit® MDS TP 208											■		
Lewatit® MonoPlus TP 214				■									
Lewatit® TP 308											■		
Lewatit® MP 62 WS				■									■
Lewatit® TP 108	■												
Bayoxide® E IN 30				■							■		

31.05.2024

Lithium ion battery material life cycle

Lewatit® is a crucial part in the recycling flow sheet!

- End of the cycle batteries
- Discharge
- Dismantle
- Crush



- Acid Leaching black mass
 - Impurity dissolution
- 100 g/L Ni, Co, Mn, Li
1-10 ppm Zn, Cu, Al, Fe



NMC 622,
NMC 811



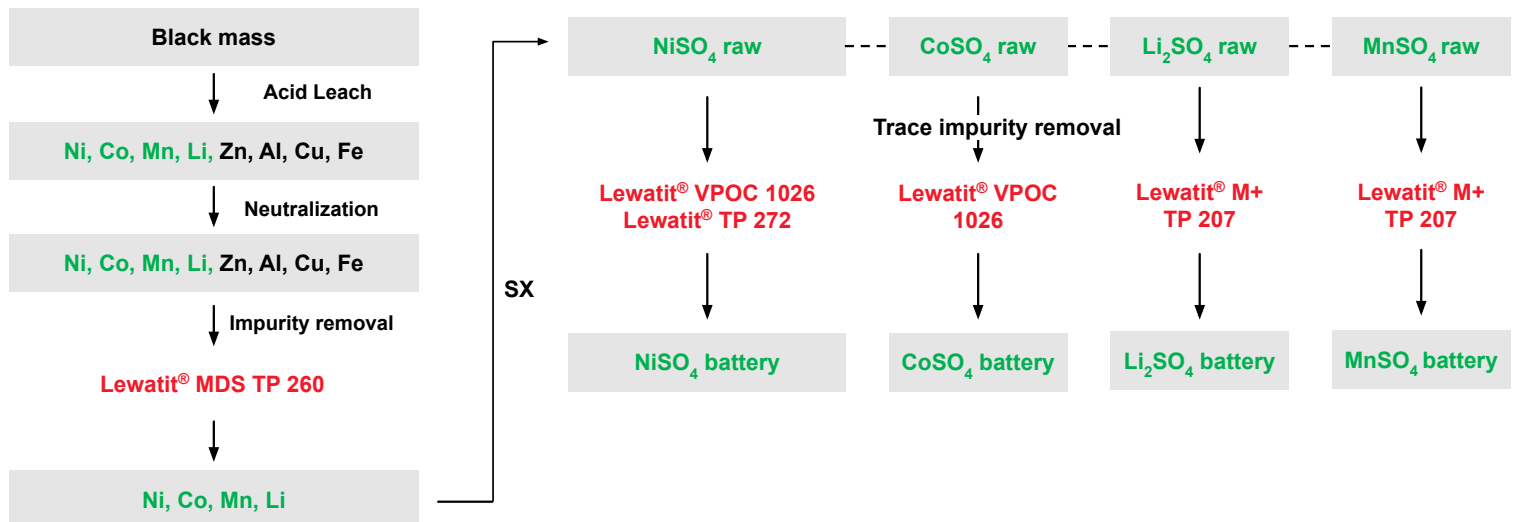
- Lewatit® MDS TP 260 (Zn, Cu, Al, Fe)
 - Lewatit® VPOC 1026 (Zn, Cu, Al, Fe)
 - Lewatit® MonoPlus TP 207 (Cu)
- 100 g/L Ni, Co, Mn, Li



31.05.2024

Process flowsheet refining of black mass leachate

Lewatit® ion exchange resins are required in the most critical streams within the recycling flow sheet

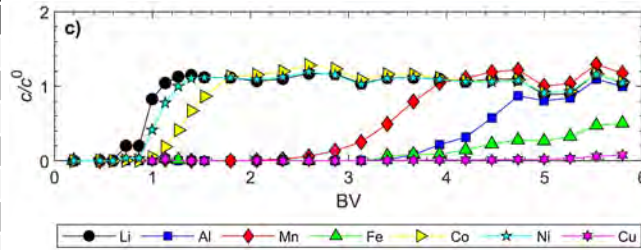


31.05.2024

Polishing black mass leachate Lewatit MDS TP 260

High selectivity of MDS TP 260 for Al, Fe and Cu in presence of Li, Ni, Co, Mn!

Op. Conditions	
Resin in Na form	
Al	1.3 g/L
Fe	0.6 g/L
Cu	1.7 g/L
Co	13.2 g/L
Ni	1.6 g/L
Li	3.9 g/L
Mn	2.0 g/L
SV	2 BV/h
Temp	60°C
pH	3
Breakthrough	0.1 c/c0
Op. Capacity	
Cu	> 0.4 eq. Cu/L
Al	0.4 eq. Al/L
Fe	0.1 eq. Fe/L



Virolainen et al. Hydrometallurgy, 2021, 20, 105602

Benefits

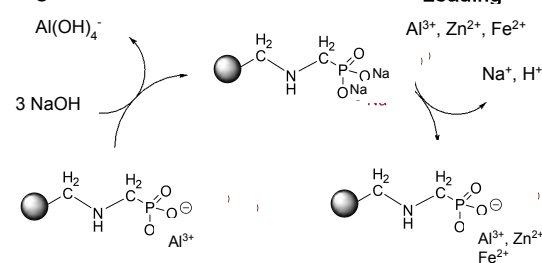
- High selectivity of MDS TP 260 towards contaminants like Al, Zn, Cu, and Fe allow efficient separation
- Savings on CAPEX. Fast exchange kinetics allows small compact filters
- Savings on OPEX, high loading capacities, less frequent regeneration and lower chemical consumption
- Longer lifetime of the resin due to higher stability and less frequent regenerations

31.05.2024

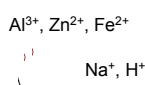
Selective elution of Aluminium and Zinc from Lewatit® MDS TP 260

Efficient and easy elution of Al and Zn by use of NaOH!

Regeneration 2



Loading



Regeneration 1



Benefits

- Al, Zn regeneration efficiency (r.e.) > 99 % by use NaOH
- Conventional acid regeneration yields < 60% r.e.
- Technique by Virolainen et al. yields high r.e. but requires additives (EDTA- and oxalic acid salts)¹
- NaOH is cheap, readily available, renewable NaOH available
- NaOH elutes Al and Zn selectively. Coloaded Ni, Co, Mn recovered by acid elution and feeding upstream

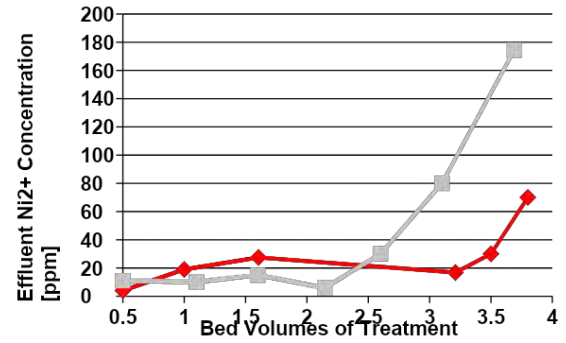
Virolainen et al. Hydrometallurgy, 2021, 20, 105602¹

31.05.2024

Nickel recovery in presence of high concentration of ferric using Lewatit® MDS TP 220

The resin has a high selectivity for nickel over ferric and cobalt!

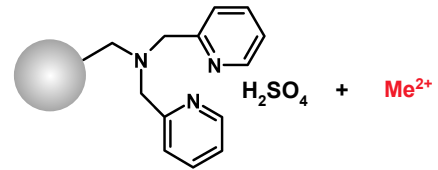
Nickel	2.6 g/L
Ferric	17 g/L
pH	1.8
Temperature	r.T.
Specific velocity	10 BV/h



Other application fields

- Purification of cobalt electrolytes (nickel/cobalt separation)
- Copper recovery at low pH (<2)
- Separation of nickel and copper from chromium (III) and ferric solutions
- Selectivity Series: $\text{Cu}^{2+} > \text{UO}_2^{+} > \text{Pb}^{2+} > \text{Ni}^{2+} > \text{Fe}^{3+} > \text{Zn}^{2+} > \text{Co}^{2+} > \text{Cd}^{2+} > \text{Fe}^{2+} > \text{Cr}^3$

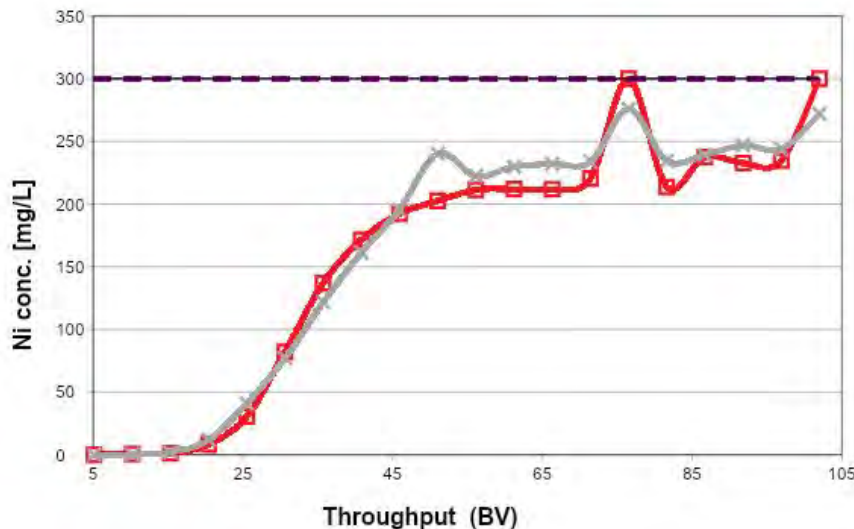
■ Competitor ◆ Lewatit® MDS TP 220



31.05.2024

Removal of nickel from cobalt concentrate

Breakthrough curves of benchmark show higher capacity for Lewatit® MDS TP 220



Operating conditions

Ni²⁺, feed 300 mg/L
Co²⁺, feed 37 g/L
pH 2.0
SV 5 BV/h
Temp 60°C
breakthrough 300 mg/L

Operating capacity

MDS TP 220 14.3 g Ni/Liter
Competitor 13.9 g Ni/Liter

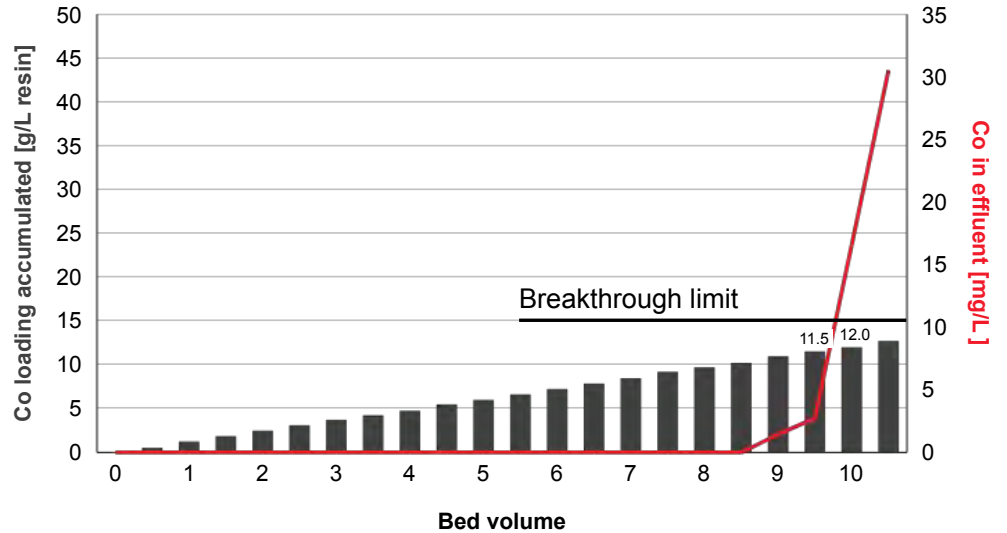
31.05.2024

Lewatit® TP 272 for Ni/Co separation

A selective resin for cobalt over nickel!

Loading

Nickel	≈ 80 g/L
Cobalt	≈ 990 mg/L
(NH ₄) ₂ SO ₄	≈ 50 g/L
pH adjustment	ammonia
pH	≈ 5,0
Temperature	≈ 65°C
Specific velocity	3 BV/h

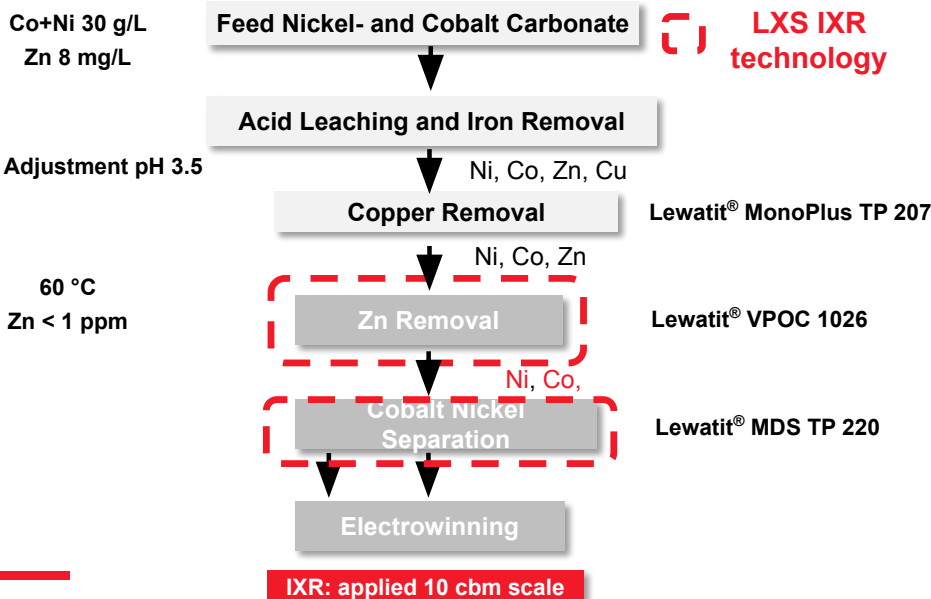


31.05.2024

Ion exchange resins for high purity cobalt refining

Zink and copper removal from cobalt electrolyte

Lewatit® IXR are required in the most critical places within the flow sheet



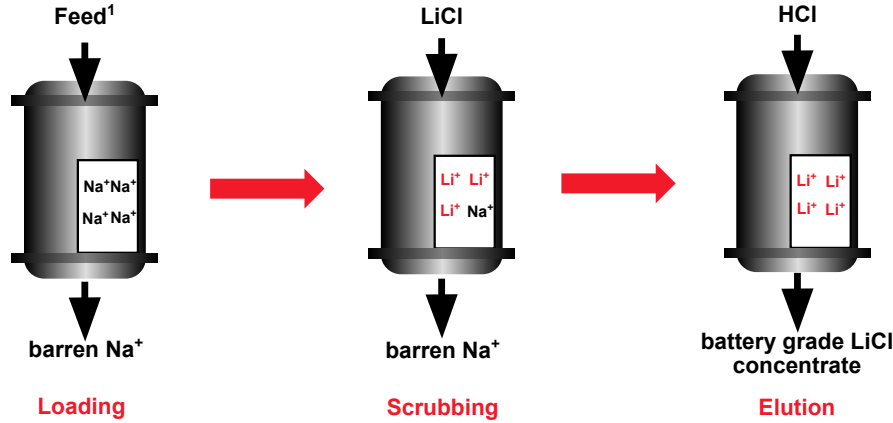
31.05.2024



294/395

Lithium concentration from wastewater by loading and elution and scrubbing cycles

High Li purity in eluate of Lewatit® allows preparation of battery grade LiCl with high yield > 99%!



Benefits

- High Li > 20 g/L concentrations obtained in eluate, recovery as Li₂CO₃
- Pure Li can be obtained by scrubbing off co-loaded Na with Li salt solution
- High Li loading capacities obtained at pH >10 and 60°C
- Empty bed contact times around 12 min. ensure high Li loading
- Process proven on pilot scale and now transferred to industrial scale

¹ Feed: LiCl 1.2 g/L (200 mg Li/L, NaCl 50 g/L, 10 BV/h, 60°C.

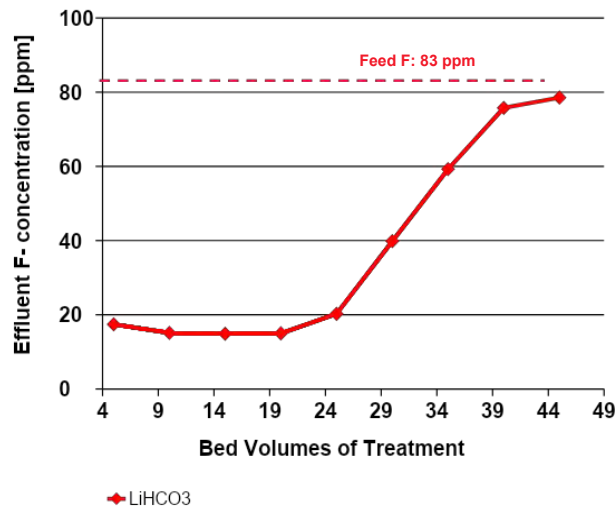
31.05.2024

Selective fluoride removal from lithium concentrates

Aluminium doped MDS TP 260 (Al) shows high fluoride selectivity in bicarbonate and sulphate concentrates!

Selective fluoride removal from lithium concentrates: low fluoride leakage, clean lithium!

Op. Conditions	
Resin in Na form	
Fluoride	83 ppm
LiHCO ₃	75 g/L
pH	8
SV	5 BV/h
Temp	60°C
Breakthrough	30 ppm F
Op. Capacity	
LiHCO ₃	2.1 g F/L



Benefits

- High selectivity of MDS TP 260 (Al) towards F allow efficient separation
- Savings on CAPEX. High exchange kinetics enable the use of small compact filters
- Savings on OPEX, high loading capacities, less frequent regeneration and lower chemical consumption
- Longer resin lifetime due to higher stability and less frequent regenerations
- F removal from Li₂SO₄ removal efficiency to ppb level

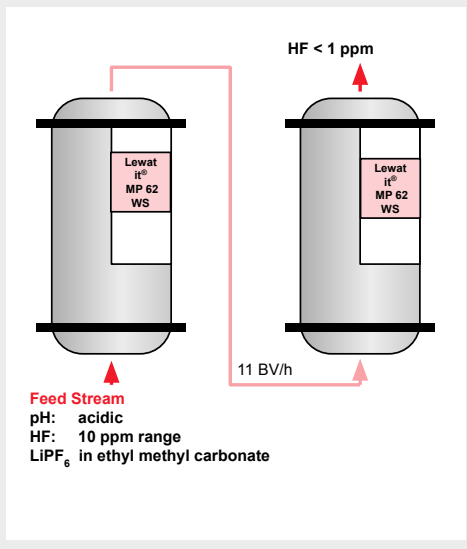
31.05.2024

295/395

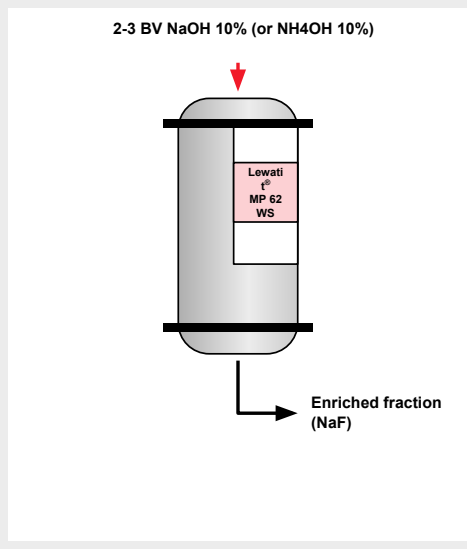
HF removal from LiPF₆ electrolyte

Pure electrolytes free of acid by Lewatit® MP 62 WS

Operation



Regeneration

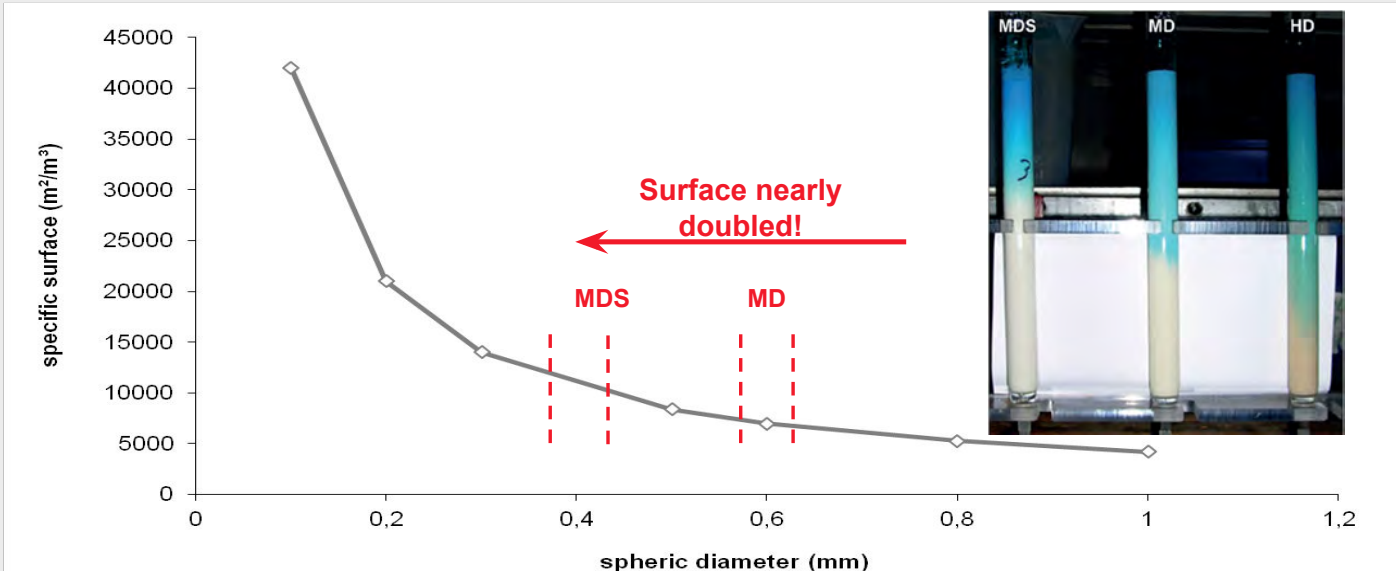


- HF generated by hydrolysis of LiPF₆
- Operating capacities up to 1 eq/L and more possible at high HF feed concentration
- At low feed concentrations operating capacities between 0.5 eq/L and 1 eq/L g/L

31.05.2024

Chromatographic effect in ion exchange

Resins with small and monodisperse bead size for a better utilization of resin capacity



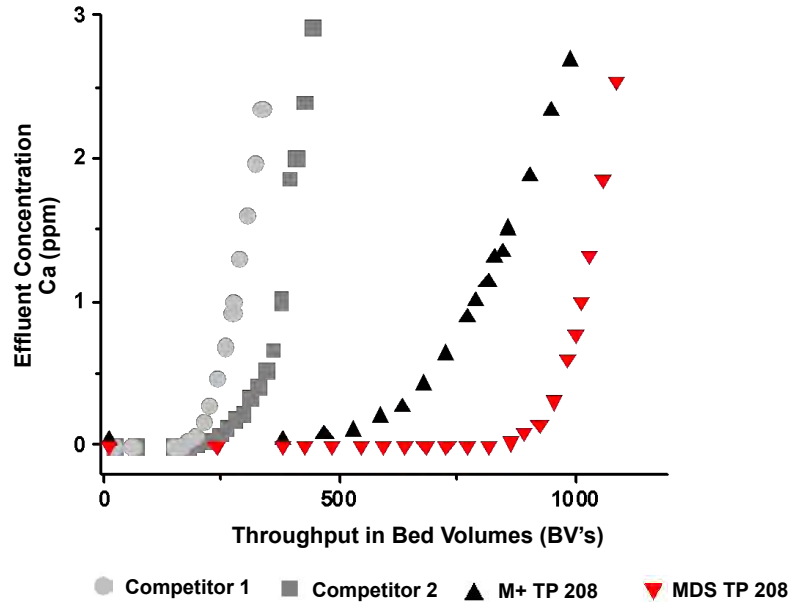
31.05.2024

Calcium capacity from LiCl brines

Lewatit® MDS TP 208 has the highest operating capacity and the lowest leakage!

Softening lithium chloride brine to achieve less than 1 ppm of Ca

Op. Conditions	
Resin in Na form	
CaCl ₂	10 ppm as Ca
LiCl	61.1 g/L (10 g Li/L)
NaCl	60 g/L as NaCl
pH	9
SV	10 BV/h
Temp	60°C
Breakthrough	1 ppm Ca
Op. Capacity	
Competitor 1	2.7 g Ca/L
Competitor 2	3.7 g. Ca/L
Lewatit® M+TP 208	8.3 g Ca/L
Lewatit® MDS TP 208	10.6 g Ca/L



31.05.2024

Calcium Capacity from LiCl Brines

MDS TP 208 can achieve less than 20 ppb hardness in the treated brine

Lewatit® MonoPlus TP 208 vs. MDS TP 208

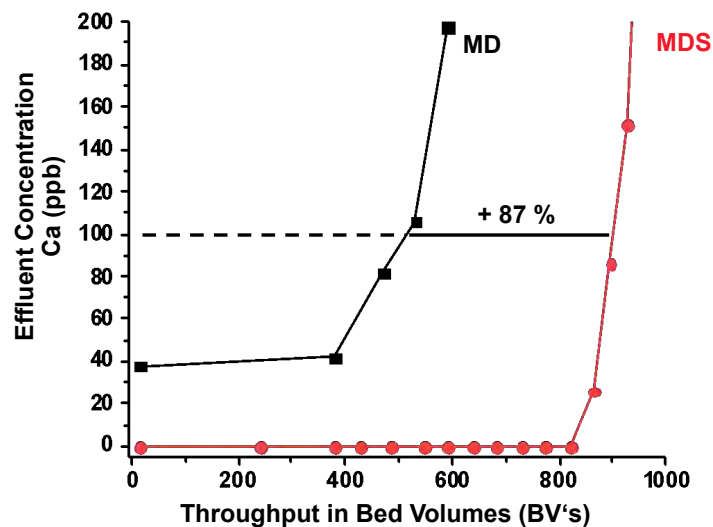
Op. Conditions

Resin in Na form

CaCl ₂ , feed	10 ppm as Ca
LiCl, feed	61.1 g/L (10 g/L as Li)
NaCl, feed	60 g/L as NaCl
pH	9
SV	10 BV/h
Temp	60°C
breakthrough	100 ppb Ca

Op. Capacity

M+ TP208	5,2 g Ca/L
MDS TP 208	9,0 g Ca/L



31.05.2024

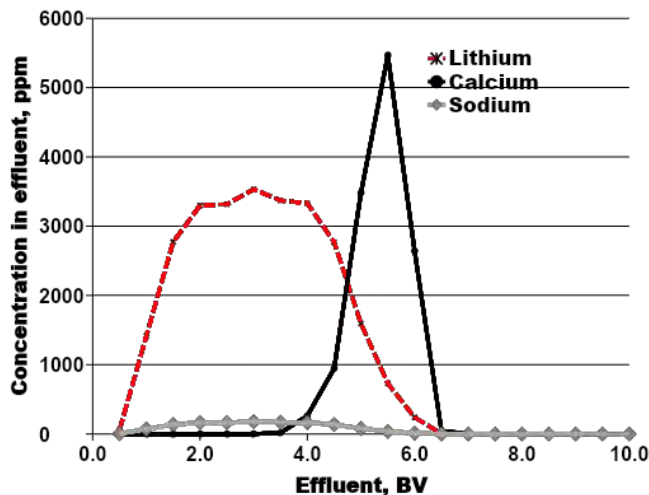
297/395

Lithium recovery by selective regeneration of trial product

Efficient separation between lithium and calcium by split elution, high lithium yield!

More than 70% of co-loaded lithium can be recovered by split elution

Loading conditions	
Resin in Na form	
CaCl ₂ , feed	10 ppm as Ca
LiCl, feed	61.1 g/L (10 g Li/L)
NaCl, feed	60 g/L as NaCl
pH	9
SV	10 BV/h
Temp	60 °C
Regeneration conditions	
HCl	1.5%
SV	1.5 BV/h



31.05.2024

Silica removal from NiSO₄, CoSO₄, LiCl, and LiOH concentrates by use of Bayoxide® E IN 30

Bayoxide® has a low silica leakage in various battery metal concentrates

Nickel sulfate		Co	Fe	Ni	Si
	Feed silicate	970	0	81550	78.9
	Effluent silicate	445	0	65250	2.1
	Removal %	54%	n/a	20%	97%
Lithium chloride		Fe	Li	Si	
	Feed silicate	0	14070	68.8	
	Effluent silicate	0	13535	0.01	
	Removal %	n/a	4%	100%	
Lithium hydroxide		Fe	Li	Si	
	Feed silicate	0	7715	24.8	
	Effluent silicate	0	5145	0.01	
	Removal %	n/a	33%	100%	

10 g of Bayoxide were added to 40 mL of concentrate and shaken for 20 h. After decantation and filtration through 0.4 µm filter, ICP analysis performed. Regeneration procedure is currently optimized.

31.05.2024

298/395

Smart solutions for more efficient use of scarce battery metals – Energized by LANXESS

- One of the leading global solution provider with excellent technical application know-how
- Competence recycling and refining of battery materials
- German standards and certified by international organizations
- Global highly competent sales & technical service team



31.05.2024

LOW-CARBON FOOTPRINT BIO-DILUENTS FOR SOLVENT EXTRACTION IN LITHIUM-ION BATTERY RECYCLING

By

Zubin Arora,

TotalEnergies Fluids, France

Presenter and Corresponding Author

Zubin Arora

zubin.arora@totalenergies.com

ABSTRACT

TotalEnergies Fluids is a leader in the design, production, and sale of high-purity, biodegradable hydrocarbon solvents. Designed as aliphatic diluents dedicated to the solvent extraction (SX) process in hydrometallurgy, the Elixore range offers a choice of perfectly inert, colorless, and odorless solutions for metal extraction in battery recycling.

From the same plant based in the north of France that pioneered the production of Sustainable Aviation Fuel (SAF) at TotalEnergies for the Aviation Industry, TotalEnergies Fluids now produce a range of bio-hydrocarbon solvents, under the name of Biolife range, coming from bio-feedstocks such as Used Cooking Oil (UCO) which offer low carbon footprint solutions to the industry.

These products have been studied in detail over the last year at the Hydrometallurgical lab of CNRS, University of Lorraine, Nancy, France with the aim to design a single Universal Diluent that can be used in the multiple solvent extraction steps of a hydrometallurgical process of Recycling of EV Batteries for extraction of Cu, Al, Mn, Co, Ni, & Li. The results were recently published in a Technical Paper in the prestigious journal Royal Society of Chemistry*.

One such low-carbon bio product commercialized in July 2023 after excellent results is "Elixore Biolife EV 205." This presentation elucidates the distinctive features of this innovative product, emphasizing its remarkably low carbon footprint; a detailed flowsheet illustrating the product's integral role in the hydrometallurgical process of Battery Recycling will be showcased, underscoring its potential to significantly reduce Scope 3 emissions in Battery Recycling plants; and a live industrial project set to use Elixore Biolife EV 205.

Keywords: biodegradable hydrocarbon solvents, low-carbon bio product, biodegradable hydrocarbon solvents, aliphatic diluents, SX, hydrometallurgy, battery recycling

*RSC Advances, 2023, Issue 46, 02 Aug 2023



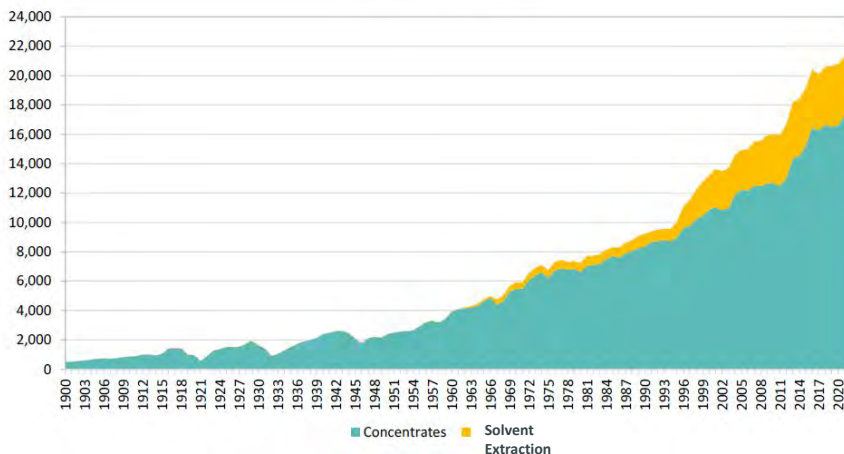
Low-carbon footprint **Bio-diluents** for Solvent Extraction in **Battery Recycling**

Zubin ARORA
 Global Market Manager
 TotalEnergies Fluids
 31st May 2024

The beginning of Solvent Extraction (SX)

COPPER MINE PRODUCTION: WORLD COPPER MINE PRODUCTION, 1900-2022

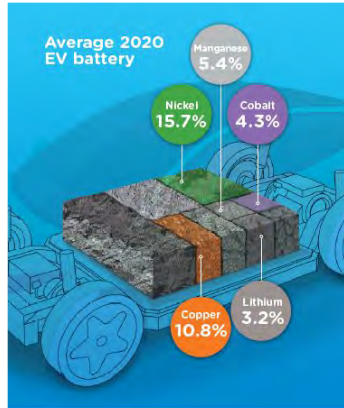
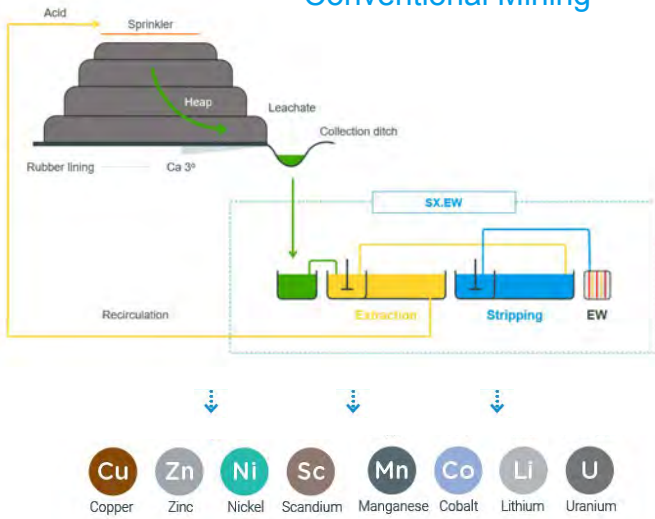
Thousand metric tonnes copper
 Source: ICSG



- SX introduced in 1960s
- Today: ~**20%** of Cu Extraction via SX
- Advantages vs the conventional process:
 - Suitability for low & variable copper ores
 - High Purity: up to 99.99% Cu
 - Improved **HSE**
- Diluent in SX process:
 - **Kerosene**
 - Readily and cheaply available

Today... the applications of Solvent Extraction (SX)

Conventional Mining



Why Solvent Extraction for Li-ion Battery Recycling??

- High Recovery: >90%
- High Purity of metals: >95%
- Cost Effective
- High Material Selectivity
- Low Energy Consumption
- Environmentally Friendly

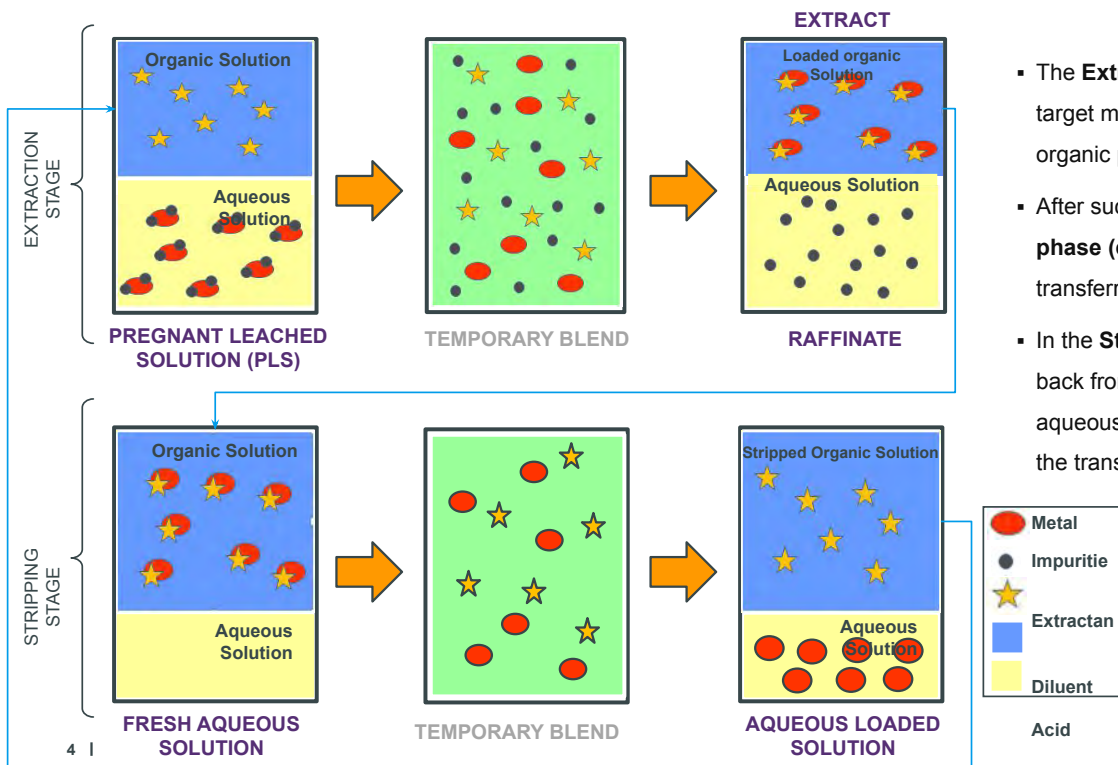


Same metals in Li-ion battery

Today, SX is similarly used for extraction of other metals

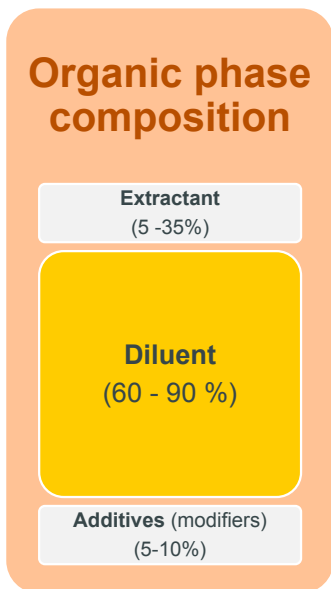
3 | ALTA, Perth, 27-31 May 2024

Solvent Extraction Process



- The **Extraction Stage** involves transferring the target metal from the aqueous phase into the organic phase.
- After successful extraction, the **loaded organic phase (containing the extracted metal)** is transferred to the stripping section.
- In the **Stripping Stage**, the target metal is stripped back from the organic phase using a different aqueous solution by adjusting the pH to promote the transfer back to the aqueous phase.
- The stripped organic phase is then **recycled** back to the extraction stage for further rounds.
- As a result, over an year, **only 10-20%** of the **organic solution / diluent** is used

Organic phase: Composition – Role – Properties



Diluent role

- Primary function is to adjust the extractant concentration
 - Dissolve the extractant and additives
 - Maintain viscosity of organic phase
 - Improve mobility of metal extracts between phases
 - Optimize phase disengagement rate
- Desired characteristics:
 - Minimal solubility in SX aqueous streams to avoid entrainment losses
 - Lower vapor pressure and higher flash point to reduce evaporation losses and fire risk (safety)
 - Minimal amounts of carcinogens such as benzene & PAH (health)

Main Properties

- Solvency power
 - Low viscosity
 - Low flammability
- Appropriate density & hydrocarbon chemistry
 KV40 ~1,5 à 2 mm²/s
 Flash Point > 70°C

3 Diluents Types – Production Routes



Diluent Properties / Characteristics

1 **KEROSENE**

2 **CLEAN FLUIDS**

3 **BIO-DILUENT**

Properties	Method	Units	Kerosene	Elixore 205	Elixore 215	Elixore Biolife EV 205
Density	ASTM	kg/m ³	822	819	819	764
Pensky-Martens Flash Point	ASTM D93	°C	84	75	85	84
Aromatic content	-	-	~20%	< 300 ppm	< 300 ppm	<50 ppm
Initial Boiling Point	ASTM D86	°C	210	198	213	211
Dry Point	ASTM D86	°C	240	234	241	244
Kinematic viscosity at 40°C	ASTM D445	mm ² /s	1.8	1.7	1.9	1.6
Carbon Footprint (LCA)	Cradle to Gate	kgCO ₂ e/ton	+582	+635		-2438

● Type 1 diluents

- Fossil origin
- C9-C20 Aliphatic hydrocarbons
- **2-30% aromatics**
- Kerosene

● Type 2 diluents

- Fossil origin
- C9-C20 Aliphatic hydrocarbons
- **<300 ppm aromatics**
- Clean fluids (Elixore range)

● Type 3 diluents

- **Bio-origin**
- C9-C20 Aliphatic hydrocarbons
- **<50 ppm aromatics**
- Bio-Diluents (Elixore Biolife range)




For the same Flash Point, the bio-diluent gives the lowest aromatics, viscosity and carbon footprint

Comparative Overview

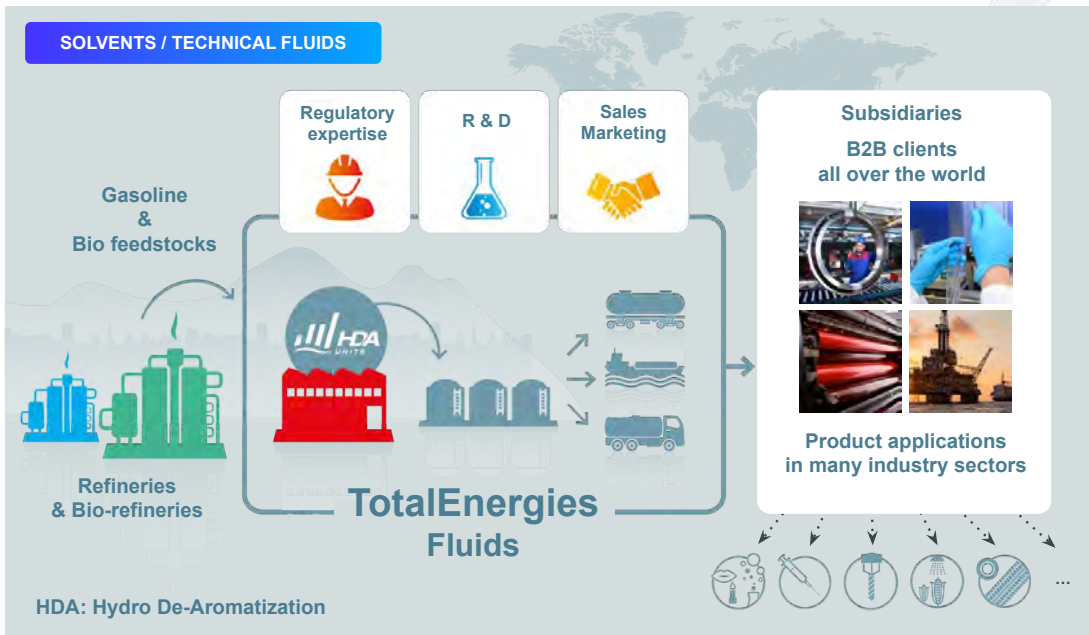
1 **KEROSENE**

2 **CLEAN FLUIDS**

3 **BIO-DILUENT**

	Environmental Impact	1. Carbon Footprint (Cradle to Gate - kgCO ₂ e/ton product)	+582	+635	-2438
		2. VOC Emissions	High	Low	Low
		3. Biodegradability	Partially Biodegradable	Readily Biodegradable	Readily Biodegradable
	Health Impact	1. VOC Emissions (Low volatility improves operator environment)	High	Low	Low
		2. Carcinogenic, Mutagenic & Reprotoxic (CMR)	Classified	Not classified	Not classified
	Safety	1. Flash Point (for same viscosity) (High Flash Point assists in minimizing fire risk)	++	+++	+++
		2. VOC Emissions (Can lead to explosive mixture)	High	Low	Low
	Performance	1. Extraction Efficiency	+++	+++	+++
		2. Average Phase Separation time (Aqueous Continuous / Organic continuous)	+++	+++	+++
	Circuit Stability (Maintenance)	1. Rate of Oxidative Degradation	Standard	Low	Low
		2. Crud Formation	Standard	Low	Low
	Diluent Consumption	1. Organic in Acqueous Entrainment	Standard	Low	Low
		2. Rate of Evaporation	High	Low	Low
	Cost	1. Price	+	++	+++
		2. Diluent consumption	Standard	Low	Low
		3. Savings related to diluent consumption and maintenance (circuit stability)	None	up to 10%	up to 10%
		4. TCO (Total Cost of Ownership)	+++	++	+++

TotalEnergies Fluids... our expertise



OUR FIGURES
Sales: 600 kT / 60% in Europe

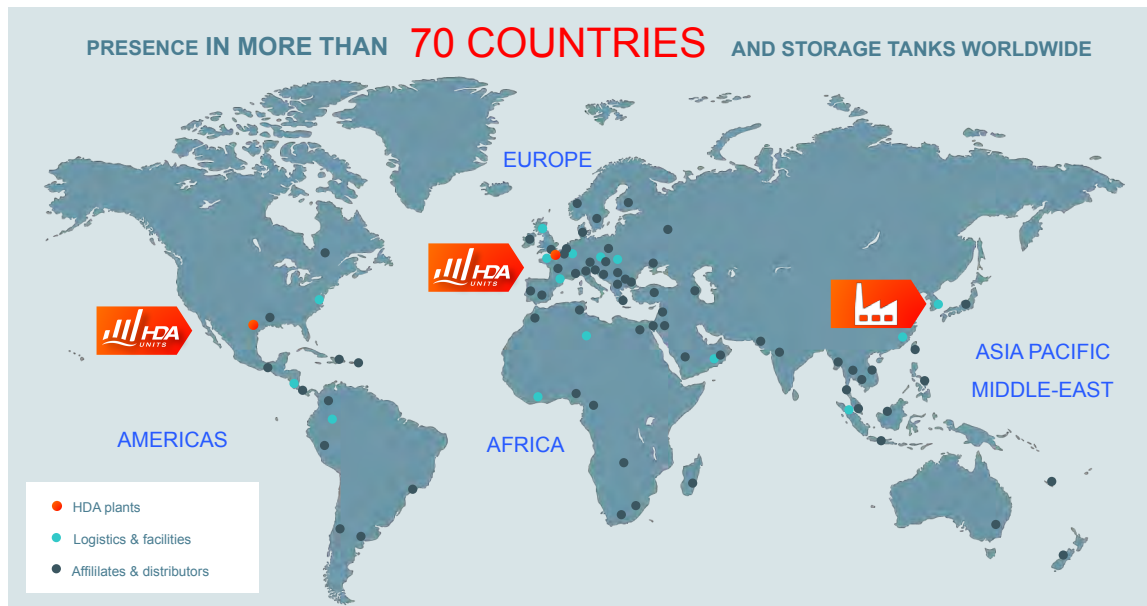
No. 3 in the world, Joint leader in Europe

2,000 customers including 30 key accounts

2 plants: Oudalle (France) and Bayport (USA)

A global network:
50 subsidiaries in more than 70 countries, 250 employees

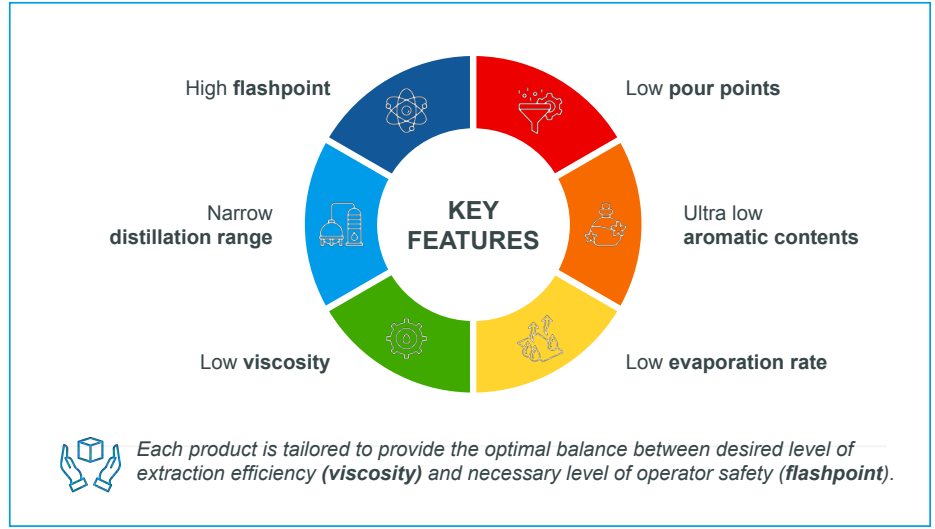
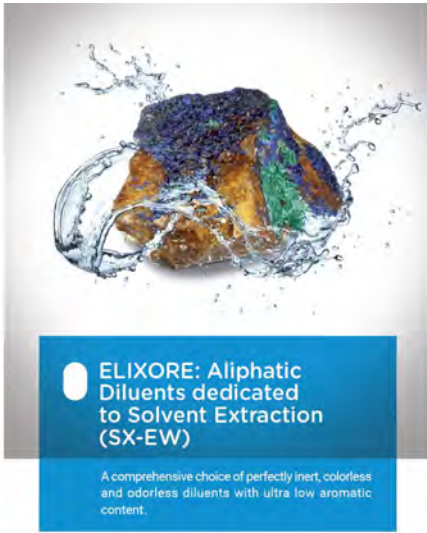
A global partner... a local player



• Diversified logistics facilities

• Proximity to customers all over the world

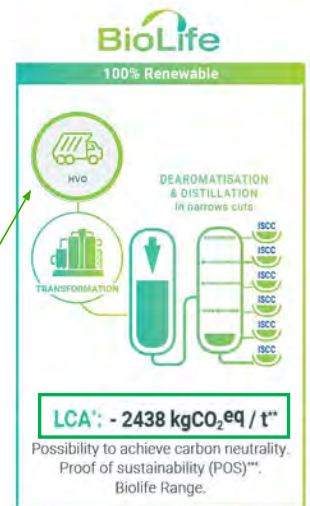
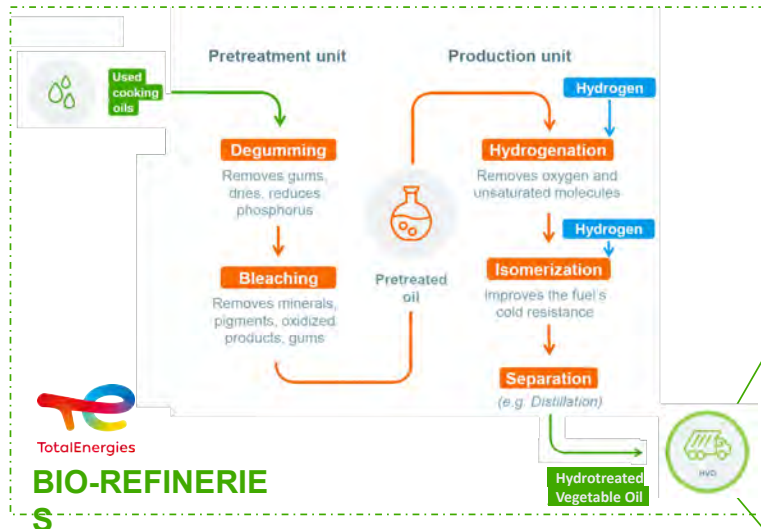
ELIXORE: Aliphatic Diluents for Solvent Extraction



A trusted product in the Mining industry for more than 10 years!

11 | ALTA, Perth, 27-31 May 2024

Transition to Bio-Diluents (Objective 30% by 2030)



- ✓ Life Cycle Assessment carried out per ISO 14040 / 14044 / 14067 standards
- ✓ Calculations are carried out using SIMAPRO modeling & recognized databases
- ✓ The LCA (Cradle to Gate) validated by an external critical review

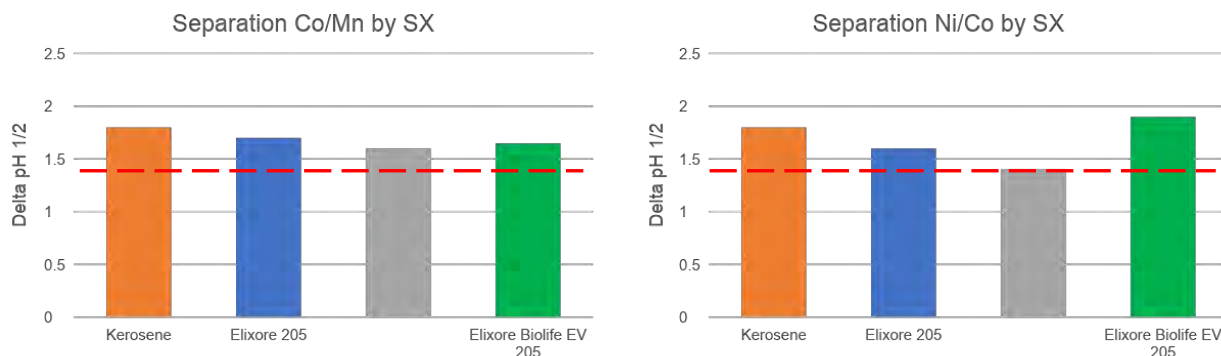
>90% SAF



12 | ALTA, Perth, 27-31 May 2024

Objective: Study the influence of bio-diluents on the extraction of metals using hydrometallurgy in battery recycling

Screening of diluent efficiency



- 4 bio-sourced products were analyzed along with kerosene and Elixore 205
- These products differed in origin, chemical structure, carbon number, viscosity & flash point

Elixore Biolife EV 205 gave the best results – similar to Kerosene & Elixore 205

Elixore Biolife EV 205... Commercialized

RSC Advances

PAPER

View Article Online

Check for updates

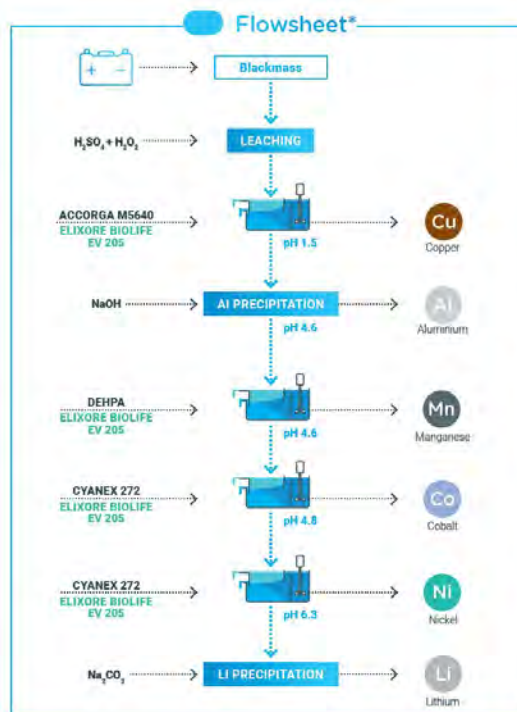
Cite this: RSC Adv., 2025, 13, 23354

Low-carbon footprint diluents in solvent extraction for lithium-ion battery recycling†

Aboudaye M. Ahamed,^a Benjamin Swoboda,^b Zubin Arora,^b Jean Yves Lansot^b and Alexandre Chagnès^{a,*}

This study investigated the influence of the diluent on the extraction properties of three extractants towards cobalt(II), nickel(II), manganese(II), copper(II), and lithium(I), i.e. Cyanex® 272 (bis-(2,4,4-trimethylpentyl) phosphinic acid), DEHPA (bis-(2-ethyl hexyl)phosphoric acid), and Acorga® M5640 (alkylsilylaldéhyde oxime). The diluents used in the formulation of the extraction solvents are (i) low-odour aliphatic kerosene produced from the petroleum industry (ELIXORE 180, ELIXORE 230, ELIXORE 205 and ISANE IP 175) and (ii) bio-sourced aliphatic diluents (DEV 2139, DEV 2139, DEV 1763, DEV 2160, DEV 2161 and DEV 2063). No influence of the diluent and no co-extraction of lithium(II), nickel(II), cobalt(II), manganese(II) and aluminum were observed during copper(II) extraction by Acorga M5640. The nature of the diluent influenced more significantly the extraction properties of manganese(II) by DEHPA as well as cobalt(II) and nickel(II) by Cyanex® 272. Life cycle assessment of the diluents shows that the carbon footprints of the investigated diluents followed the following order: (ELIXORE 180, ELIXORE 230, ELIXORE 205) from petroleum industry > kerosene from petroleum industry > diluent produced from tall oil (DEV 2063) > diluents produced from recycled plastic (DEV 2160, DEV 2161) > diluents produced from used cooking oil (DEV 2138, DEV 2139). By taking into account the physicochemical properties of these diluents (viscosity, flashpoint, aromatic content), the extraction properties of Acorga® M5640, DEHPA, Cyanex® 272 in these diluents and the CO₂ footprint of the diluents, this study showed DEV2063 and DEV2139 were the best diluents. A low-carbon footprint solvent extraction flowsheet using these diluents was proposed to extract selectively cobalt, nickel, manganese, lithium and copper from NMC black mass of spent lithium-ion batteries.

Received 12th July 2023
Accepted 27th July 2023
DOI: 10.1039/d3ra04679f
rsc.li/rsc-advances



- 1 Universal Diluent**
Same diluent in different extraction steps
- 2 Seamless Transition**
1:1 easy replacement for current fossil-based alternatives



Open Access

<https://doi.org/10.1039/D3RA04679f>

E

What's the benefit? ...Choosing Biolife Range



CARBON REDUCTION BENEFIT BY CHOOSING BIO RANGE

A 20 ktpa battery waste treatment plant that will treat 10 ktpa of Blackmass.



Contribute up to 50% of overall emissions

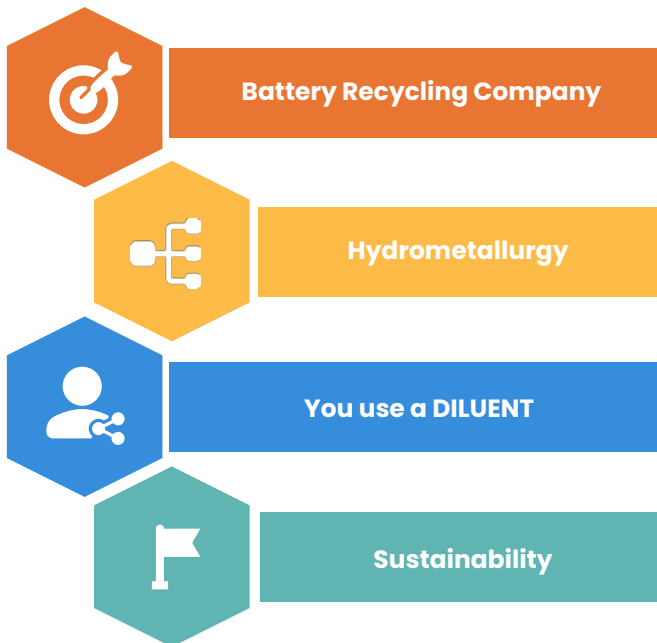
Diluent	Carbon Footprint mtCO ₂ eq./mt)		
	Kerosene	Elixore Biolife EV 205	Carbon Footprint Reduction
1 mt	0.6	-2.4	3
10 mt	6	-24	30
100 mt (Yearly top-up)	60	-240	300
600 mt (First Fill)	360	-1440	1800
1000 mt	600	-2400	3000

20ktpa Battery Waste Input □ 1.8kt Carbon Footprint Reduction

Up to 30% reduction in Scope 3 Emissions

DILUENT COST REPRESENTS <1% OF A BATTERY RECYCLING FACILITY. HOWEVER, A BIO DILUENT CAN SIGNIFICANTLY REDUCE THE CARBON FOOTPRINT OF THE PROCESS.

Key Takeaway



...operating a plant treating **NMC/LCO/NCA Blackmass**

...using **Solvent Extraction**

...potential to use low carbon footprint **Bio-diluent**

...to reduce **Scope 3 emissions** to achieve **CARBON NEUTRALITY**

HYDROMETALLURGICAL PROCESS TO EXTRACT METALS FROM LFP-NMC BLACKMASS IN SPENT LITHIUM-ION BATTERIES

By

^{1,2}Pierric Hubert, ²Laure Clerget, ³Safi Jradi and ¹Alexandre Chagnes

¹Université de Lorraine, GeoRessources, France

²Artemise SA, France

³Université Technologique de Troyes, France

Presenter and Corresponding Author

Alexandre Chagnes
alexandre.chagnes@univ-lorraine.fr

ABSTRACT

Lithium-ion batteries are central to the global shift towards sustainable energy and electric transportation. As we witness the rise of gigafactories and recycling facilities worldwide, catering to the production and reclamation of batteries for electric vehicles, it becomes evident that a similar focus is required for smaller-scale batteries, notably those utilized in electric bicycles, a swiftly expanding market. The processes involved in recycling these batteries may not mirror those of electric vehicle batteries due to disparities in material composition. While electric vehicle batteries predominantly consist of NMC ($\text{LiNi}_x\text{Mn}_y\text{Co}_z\text{O}_2$) or LFP (LiFePO_4) technologies, batteries for electric bicycles encompass a blend of NMC and LFP technologies.

Hence, there arises a necessity to devise adaptable recycling processes capable of handling varying compositions. Moreover, the hydrometallurgical methods employed for treating these materials must effectively recover cobalt, nickel, manganese, and lithium, despite the presence of fluctuating concentrations of iron, a challenge inherent to hydrometallurgy.

This presentation elucidates how leveraging the physicochemistry of transition metals in conjunction with phosphate enables the development of an efficient leaching process. Such a process selectively dissolves cobalt, nickel, manganese, and lithium from mixtures of NMC and LFP batteries, yielding a sufficiently pure leachate conducive to subsequent purification steps via liquid-liquid extraction post-leaching.

Keywords: Hydrometallurgy, Lithium-ion battery, recycling, LFP, NMC, cathode materials.

Hydrometallurgical process to recycle spent Lithium-ion batteries

Metal extraction from LFP-NMC blackmass

P. Hubert^{1,2}, L. Clerget², S. Jradi³ and A. Chagnes¹

¹GeoRessources – Vandoeuvre-lès-Nancy (France)

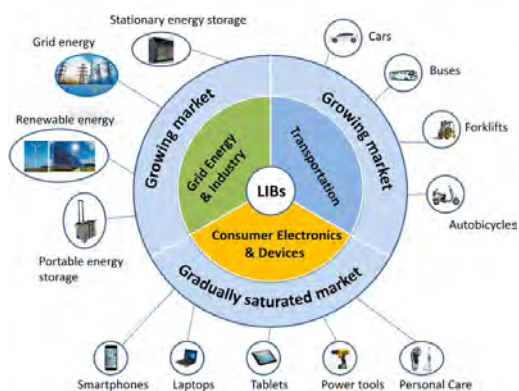
²Artemise SA – Vulaines (France)

³UTT-L2NM – Troyes (France)

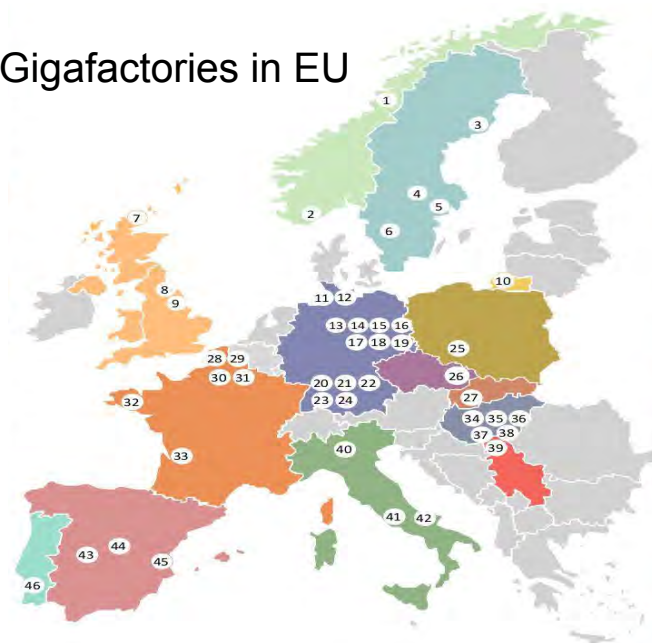
alexandre.chagnes@univ-Lorraine.fr

Page

Li-ion battery is at the center of the energy transition and the electric mobility



Gigafactories in EU



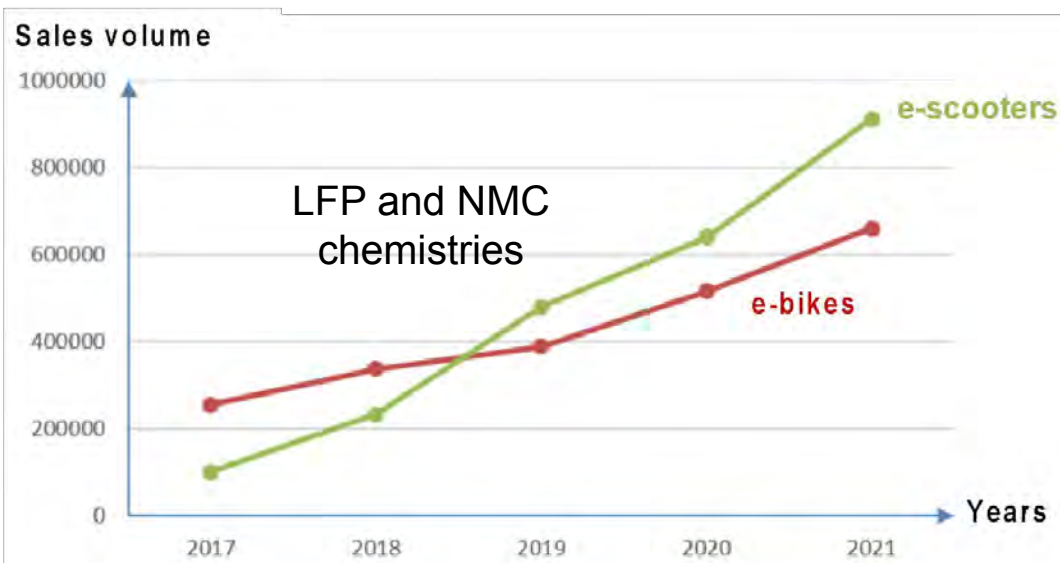
Alexandre CHAGNES - ALTA 2024 - 27-31 May (Perth, Australia)

Battery technologies and applications

	NMC	LFP	NCA
Energy Density (Wh/kg)	150 to 250	150 to 200	200 to 300
Temperature Range (°C)	-20 to 45	-20 to 60	-20 to 55
Life Cycle (#)	2000 to 4000	3000	2500
Charging Efficiency	++	-	++
Best Market Application	Electric vehicles, good power delivery, high range autonomy, require less battery allocation space	Buses and heavy-duty transportation, lower cost, safer, battery space allocation is not a constraint	Electric vehicles, good power delivery, high range autonomy, require less battery allocation space
Company			

Alexandre CHAGNES - ALTA 2024 - 27-31 May (Perth, Australia)

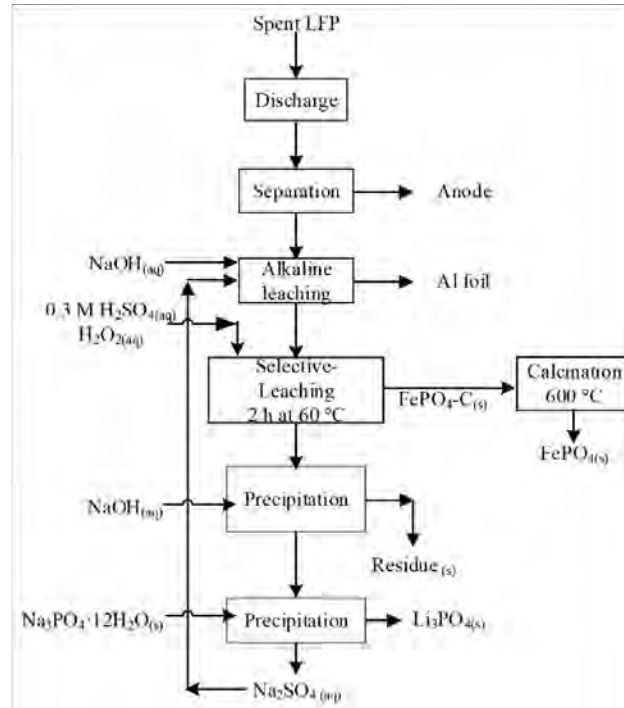
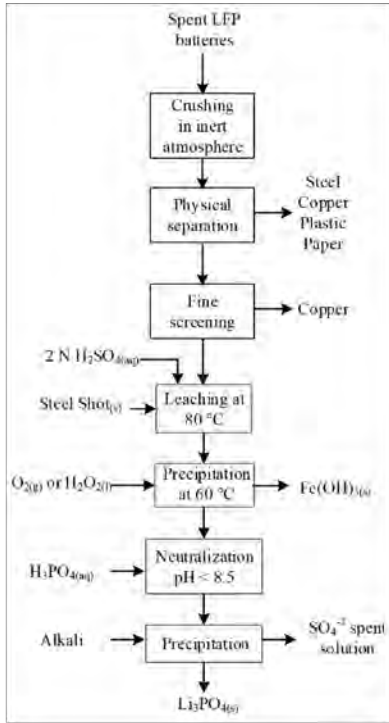
The market of e-bikes, e-scooters is a growing market



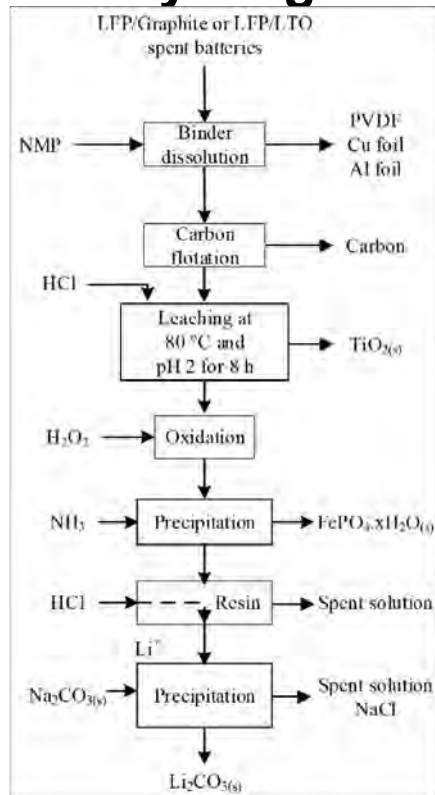
60% increase of e-bike sales between 2017 and 2019 in Europe !

Alexandre CHAGNES - ALTA 2024 - 27-31 May (Perth, Australia)

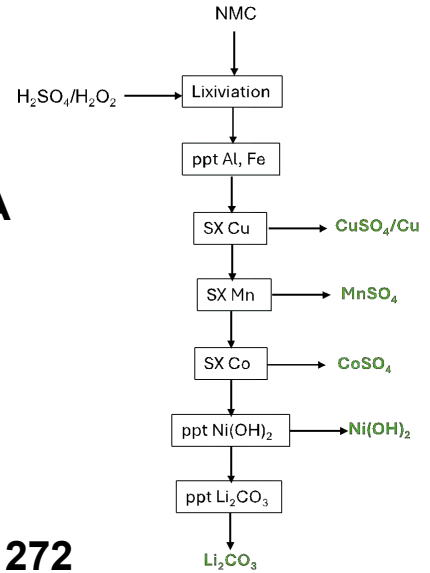
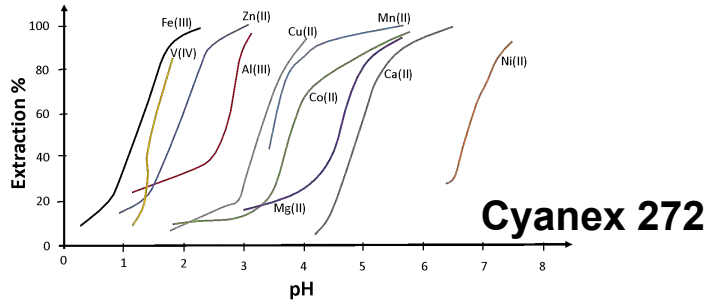
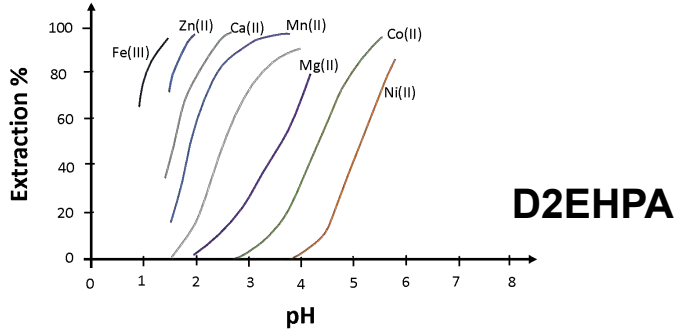
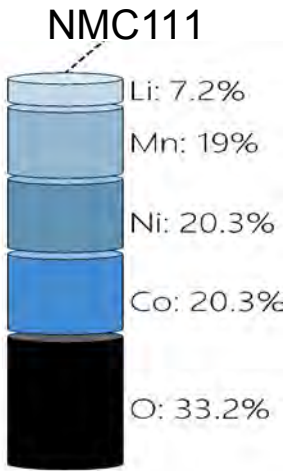
Flowsheets for LFP recycling



Flowsheets for LFP recycling

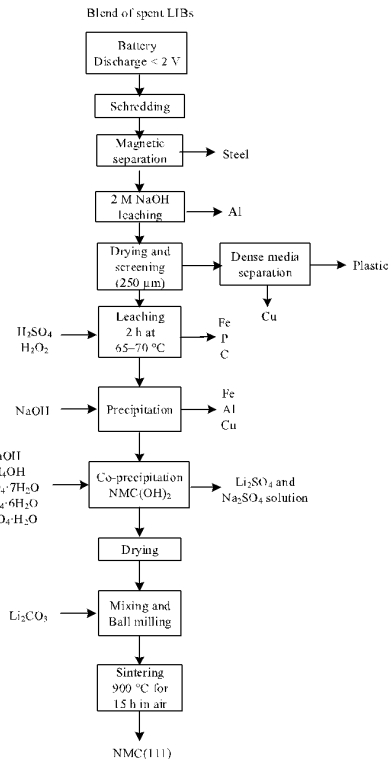


Classical flowsheet for NMC recycling (SX operations)

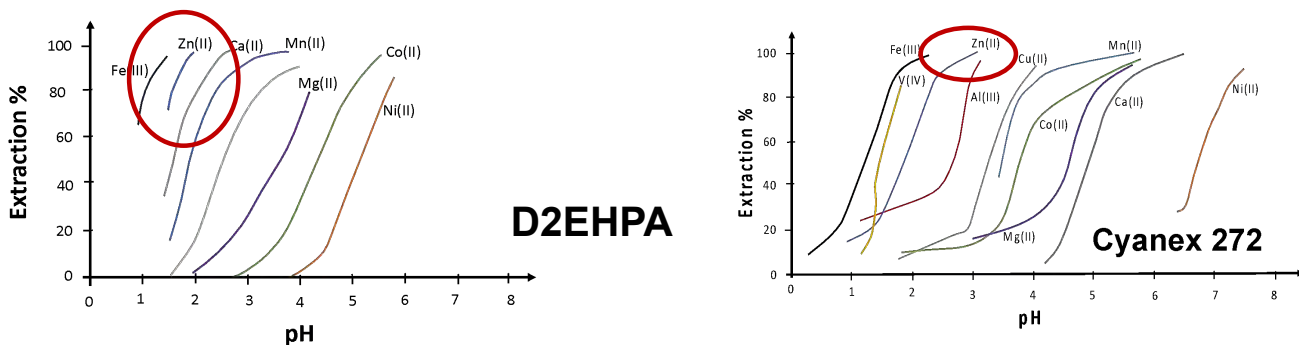


Alexandre CHAGNES - ALTA 2024 - 27-31 May (Perth, Australia)

Flowsheet to recycle blends of NMC and LFP black masses



Alternative flowsheet to recycle blends of NMC and LFP black masses by combining precipitation and SX stages



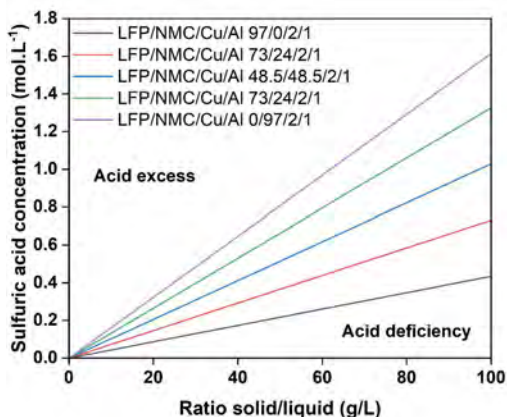
How to manage the presence of iron and what is the impact of the presence of phosphate on the process to recycle mixtures of NMC and LFP in the blackmass?

Alexandre CHAGNES - ALTA 2024 - 27-31 May (Perth, Australia)

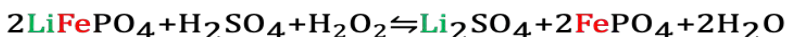
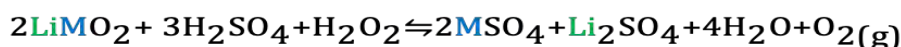
Leaching of NMC-LFP mixtures

Can we play on precipitation-dissolution phenomena to perform selective dissolution of Li, Ni, Mn, Co without iron dissolution ?

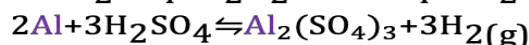
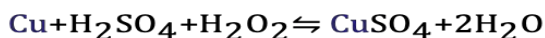
Definition of acid excess and acid deficiency zones as a function of sulfuric acid concentration and solid/liquid ratio.



Cathode dissolution



Impurities dissolution

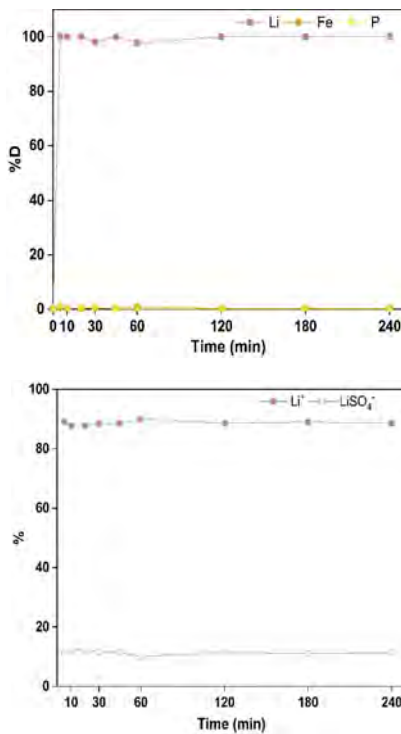


Excess/deficiency frontier

$$C = \frac{S}{L} \left(0.5 \times \frac{\%_{\text{LFP}}}{M_{\text{LFP}}} + 1.5 \times \frac{\%_{\text{NMC}}}{M_{\text{NMC}}} + 1.5 \times \frac{\%_{\text{Al}}}{M_{\text{Al}}} + \frac{\%_{\text{Cu}}}{M_{\text{Cu}}} \right)$$

Alexandre CHAGNES - ALTA 2024 - 27-31 May (Perth, Australia)

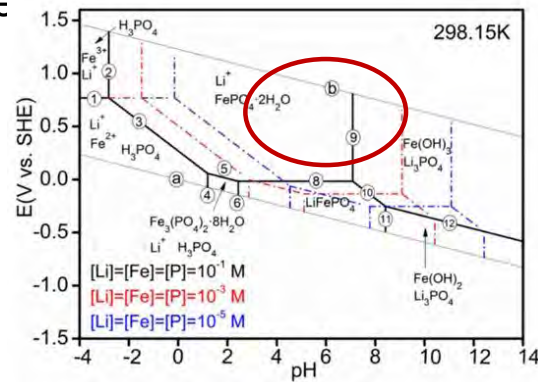
LFP leaching



Acid deficiency leaching conditions

LFP leaching by 0.19 mol L⁻¹ H₂SO₄ + 3% (vol.) H₂O₂ (30 °C and at S/L = 50 g/L).

- 100% Li dissolution
- No Li₃PO₄ precipitation occurred since lithium remained in solution as Li⁺ and LiSO₄⁻ at pH 2



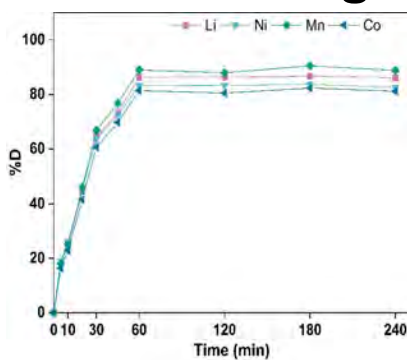
Phreeqc calculations

$$SI(\text{FePO}_4 \cdot 2\text{H}_2\text{O}) = 3.63$$

$$SI(\text{Hematite}) = 1.18$$

$$SI(\text{H-Jarosite}) = 0.96$$

NMC leaching

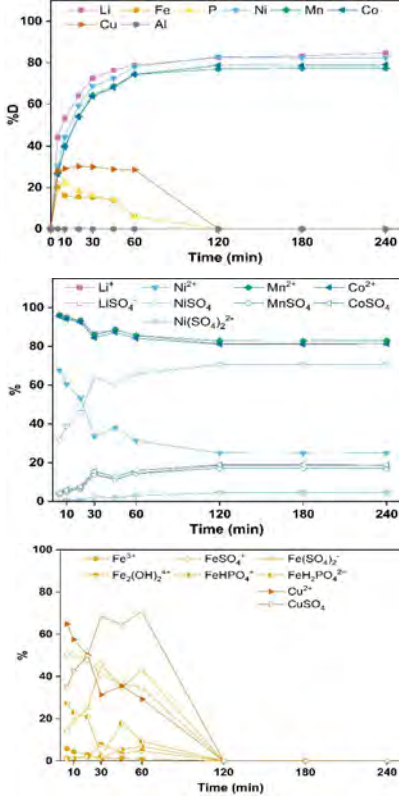


Acid deficiency leaching conditions

NMC leaching by 0.71 mol L⁻¹ H₂SO₄ + 3% (vol.) H₂O₂ (30 °C and at S/L = 50 g/L).

- NMC leaching is slower than LFP leaching
- Same behaviours for Li, Ni, Mn and Co
- Mn(II), Co(II) in solution (583 and 805 mV vs. SHE)
- Predominant species: Li⁺, Mn²⁺ and Co²⁺
- NiSO₄ and Ni(SO₄)₂²⁻ are predominant species

NMC-LFP mixture leaching

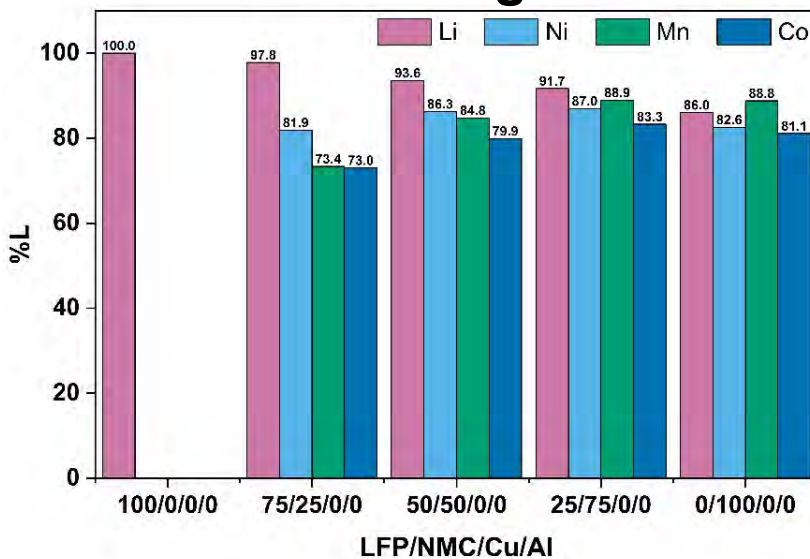


Acid deficiency leaching conditions

LFP/NMC/Cu/Al = 48.5/48.5/1/2 by $0.45 \text{ mol L}^{-1} \text{ H}_2\text{SO}_4 + 3\% \text{ (v/v) H}_2\text{O}_2$ ($30 \text{ }^\circ\text{C}$, S/L = 50 g/L).

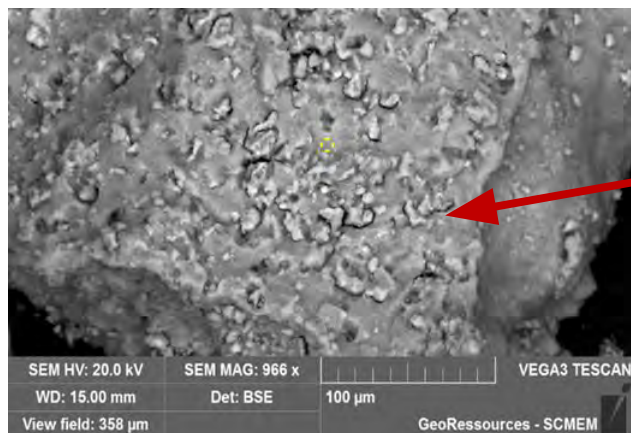
- Same dissolution behaviour of Ni, Co, Mn, Li
- Under these conditions, Mn and Fe exist as Mn(II) and Fe(III)
- No Al dissolution due to AlPO_4 precipitation as confirmed by Phreeqc calculations
- At $t < 30 \text{ min}$, no CuPO_4 , FePO_4 precipitation because $\text{pH} < 1$
- At $t > 120 \text{ min}$, Cu and Fe precipitate totally as $\text{Cu}_3(\text{PO}_4)_2$ and FePO_4 since $\text{pH} > 2$ was reached due to proton consumption
- Under these conditions, no $\text{Co}_3(\text{PO}_4)_2$, $\text{Ni}_3(\text{PO}_4)_2$ or $\text{Mn}_3(\text{PO}_4)_2$ precipitation occurs as confirmed by Phreeqc calculations

NMC-LFP mixture leaching



Dissolution yields of Ni, Mn, Co and Li during the leaching of LFP/NMC mixtures by $\text{H}_2\text{SO}_4 + 3\% \text{ (v/v) H}_2\text{O}_2$ in the absence of copper and aluminium under acid deficiency conditions ($\text{temp} = 30 \text{ }^\circ\text{C}$).

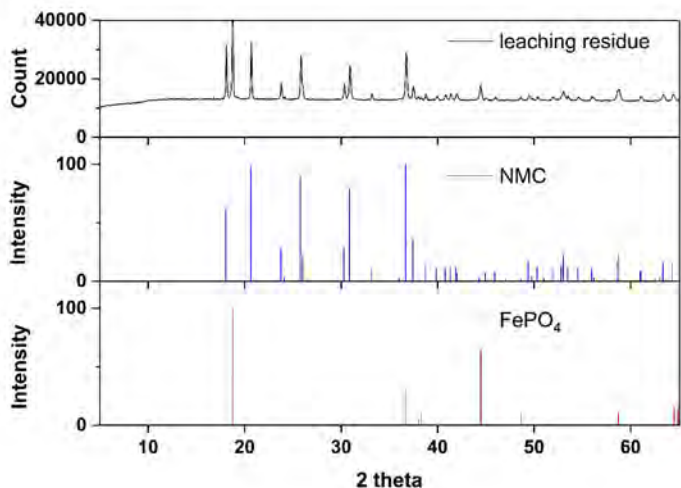
NMC-LFP mixture leaching



Cu cementation on iron particles (confirmed by EDX)

SEM picture of an iron particle remaining in the leaching residue of LFP/NMC/Cu/Al = 48.5/48.5/1/2

Alexandre CHAGNES - ALTA 2024 - 27-31 May (Perth, Australia)



Only FePO_4 and non-dissolved NMC are present in the residue at the end of the leaching in accordance with the Phreeqc calculations

XRD patterns of LFP/NMC = 50/50 leaching residue after 240 min (Leaching reagent: $0.45 \text{ mol L}^{-1} \text{ H}_2\text{SO}_4 + 3\% \text{ (v/v) H}_2\text{O}_2$ (temperature = $30 \text{ }^\circ\text{C}$; S/L = 50 g/L).

Alexandre CHAGNES - ALTA 2024 - 27-31 May (Perth, Australia)

Page 16

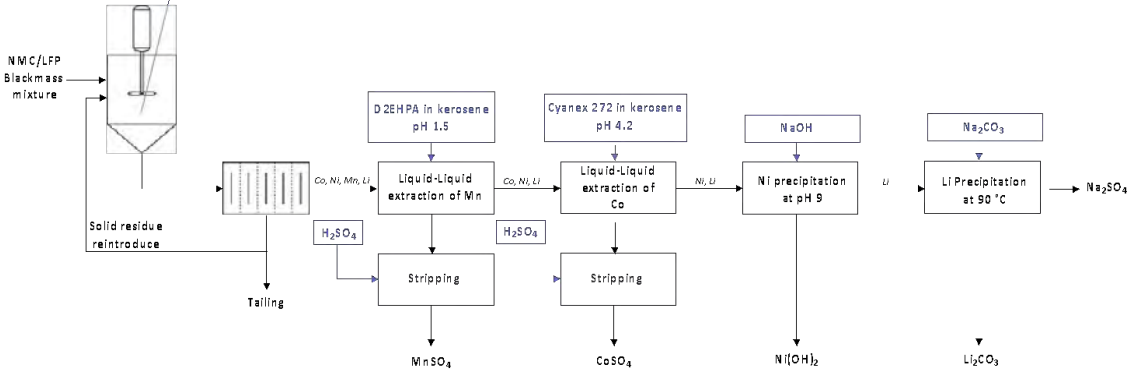
Flexible flowsheet to recover metals from LFP/NMC blackmass mixtures

Acid deficiency conditions

0,5 mol L⁻¹ H₂SO₄
3% H₂O₂
S/L=50 g/L
T=80 °C
240 min

Composition of the leach solution (24% LFP in NMC-LFP-Al-Cu leached by 0,5 mol L⁻¹ de H₂SO₄ + 3 % (vol) H₂O₂).

Élément	Fe	Ni	Mn	Co	Li	P	Cu	Al
Concentration (en g/L)	0	14,85	0,90	2,10	2,79	0	0	0
%L	0	89,07	79,91	84,31	80,52	0	0	0



RECENT TECHNOLOGICAL PROGRESS IN METALS' RECOVERY FROM SPENT NCM BATTERY PROMOTED BY NEW SEPARATION REAGENTS

By

^{1,2} Guiqing Zhang, ^{1,2} Qinggang Li, ^{1,2} Zuoying Cao, ^{1,2} Mingyu Wang, ^{1,2} Wenjuan Guan, ^{1,2} Xinsheng Wu, ^{1,2} Shengxi Wu

¹School of Metallurgy and Environment, Central South University, China

²Laboratory of Metallurgical Separation Science and Engineering, Central South University, China

Presenter and Corresponding Author

Shengxi Wu

csuwushengxi@126.com/shengxiwu@csu.edu.cn

ABSTRACT

Valuable metals recovery from the spent lithium batteries (black mass) is of vital importance, since it eliminates the heavy metal pollution threat and provides an alternative solution for the supply crisis of critical metals (Ni/Co/Mn). However, traditional recovery technologies that consisted of leaching and individual element separation by solvent extraction still faced several challenges: separation difficulties between $\text{Ni}^{2+}(\text{Co}^{2+})/\text{Mg}^{2+}$, $\text{Mn}^{2+}/\text{Ca}^{2+}$, $\text{Li}^+/\text{Ni}^{2+}$, $\text{Li}^+/\text{Na}^+(\text{K}^+)$ and incomplete removal of fluorine due to the limited separation coefficient of previous methods. To solve these issues, a series of solvent including HBL-120 for Ca extraction from Mn, HBL-116 for Ni(Co) extraction from Mg and Li, HBL-121 for Li extraction from Na(K), and HBL-221 for F extraction from Ni(Co&Mn) were designed and synthesised.

- (1) Ca separation from Mn with HBL-120 makes the preferential removal of Ca before impurities extraction with D2EHPA is possible, which eliminates CaSO_4 scaling issue during stripping of impurities extraction with D2EHPA and directly produces pure MnSO_4 product.
- (2) Selective Ni(Co) extraction from Mg containing solutions shortens the Co extraction (HEHEHP) - Ni extraction (HEHEHP) - Mg extraction (Cyanex 272) into Ni(Co) extraction (HBL-116)-Mg precipitation, which saves >50% of labour and land.
- (3) Fluorine originating from the electrolyte and adhesive cannot be completely removed via traditional methods and brought massive Ni(Co) losses in fluorine removal residue. Specific extractant HBL-221 binds fluorine and extracted Me-F complex into organic phase, with <5mg/L F left in raffinate and <0.1 Ni(Co&Mn) loss.
- (4) Li generally reports into a concentrated Na_2SO_4 solution since all the extraction processes for Ni/Co/impurities adopted Na-saponification. However, traditional carbonate precipitation – evaporating concentration process recovered only ~85% of Li (~10% Li loss in Na_2SO_4 crystal) and produced crude Li_2CO_3 entrained considerable Na_2SO_4 . Selective Li extraction from Na(K) concentrated solutions with HBL-121 significantly elevated the Li recovery to >99% and produced Li_2SO_4 solution with $\text{Li}/\text{Na}(\text{K}) > 100$.

So far, all technologies mentioned above have been applied individually or packaged in many hydrometallurgical plants for spent LIBs recycling in China and USA (pilot test). Based on these new extractants, an alternative short process for metal recovery from the leaching solutions of NCM black mass was proposed which includes Ca(Zn) extraction with HBL-120, impurities extraction with D2EHPA, fluorine extraction with HBL-221 (if needed), Co extraction with HEHEHP, Ni extraction with HBL-116 (or Ni/Co co-extraction with HBL-116), Mg precipitation with NaOH, Li extraction with HBL-121. This process owns merits of high metal recovery, reagent saving, short process, and economy.

Keywords: Spent LIBs, recovery, selective extraction, separation, fluorine removal.



Recent Technological Progress in Metals' Recovery from Spent NCM Battery Promoted by New Separation Reagents

Associate Prof. **Shengxi Wu**

E-mail: shengxiwu@hydrometaltech.com/csuwushengxi@126.com

Key Laboratory of Metallurgical Separation Science and Engineering, Chinese Non-Ferrous Industry Association, Institute of Rare Metal Metallurgy research, School of Metallurgy and Environment, Central South University

Recent Technological Progress in Metals' Recovery from Spent NCM Battery Promoted by New Separation Reagents



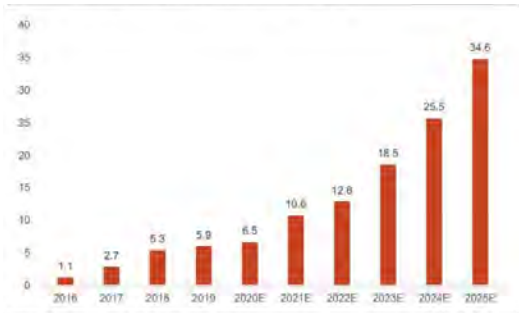
1、Importance of metal recovery from the spent LIBs

2、Key challenges presented in traditional processes

3、Ideal technique solutions for the challenges

4、Perspectives for the recovery of metals from other wastes

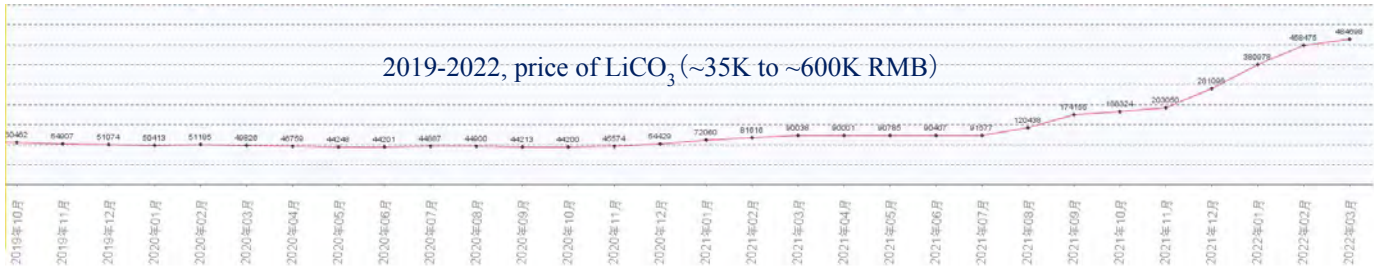
1、Importance of metal recovery from the spent LIBs



Global expansion in NCM materials



Production of LiFePO₄ from 2016-2020 in China

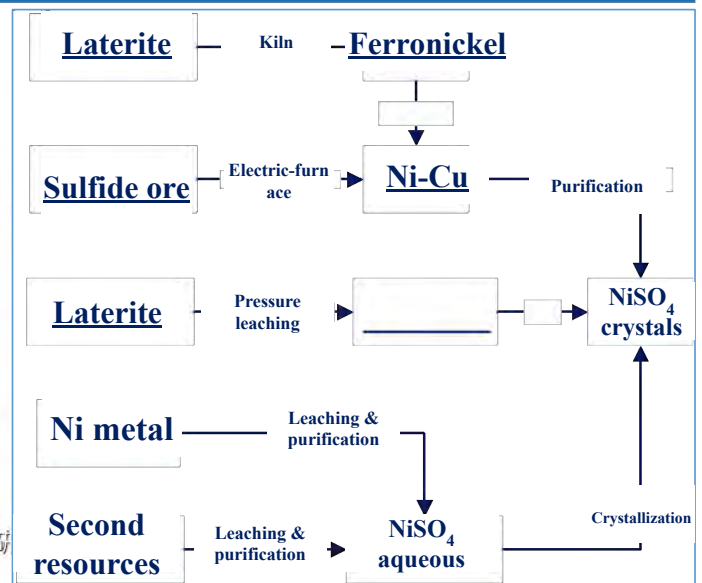
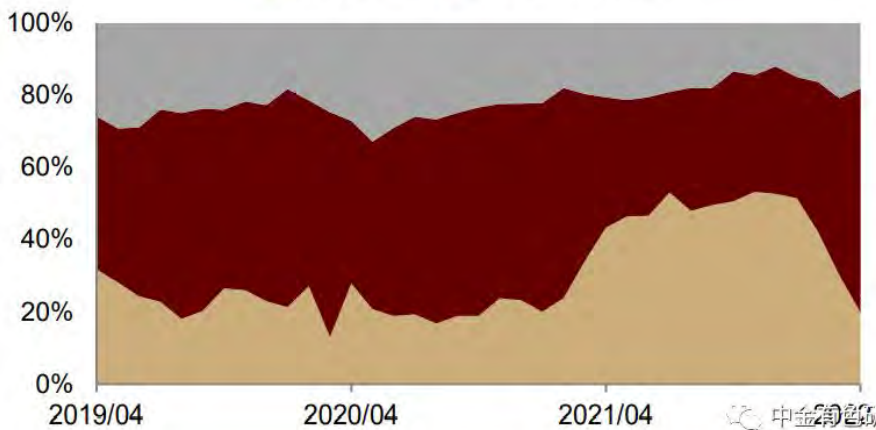


The rapid development of EV/LIBs industry brings huge material demand and rise in price

1、Importance of metal recovery from the spent LIBs.

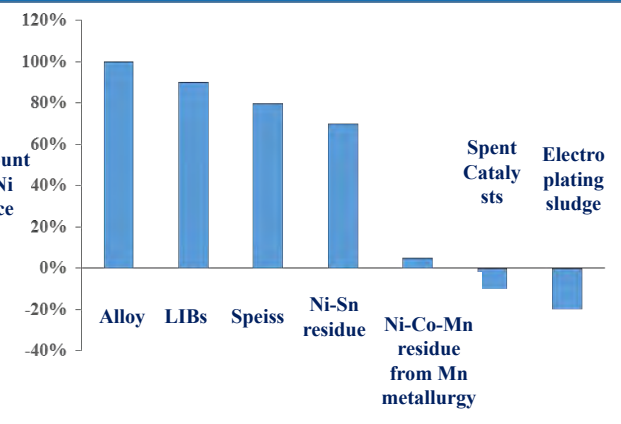
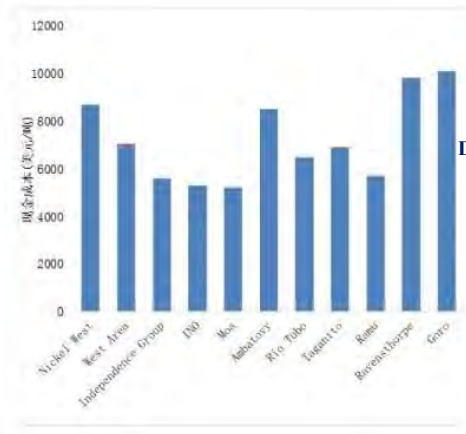
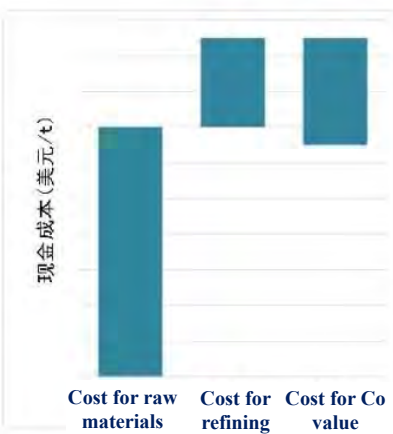
Raw materials for NiSO₄ production

■ Ni metal ■ Minerals ■ Second resources



Processes for NiSO₄ from various sources require an hydrometallurgical purification operation-deeply separation of impurities (Ca/Mg/Fe/Al/Mn/Cu)

1、Importance of metal recovery from the spent LIBs.



Using LIBs / MSB of Ni metal to produce NiSO_4 is a short process, **but with a high raw material cost** (the production cost is about 6000-10000\$/t)

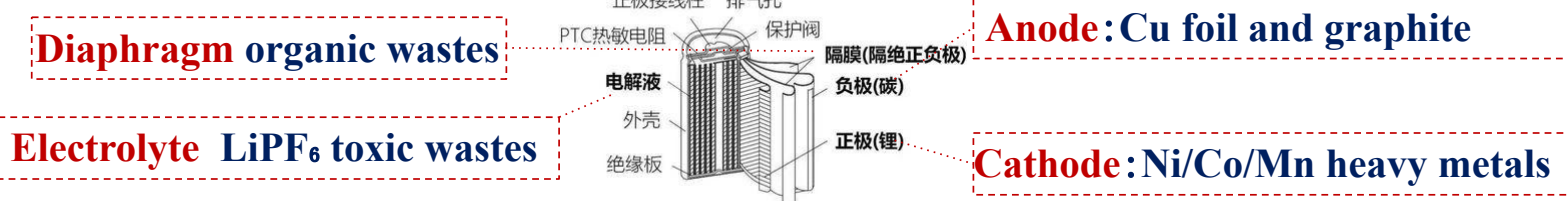
By contrast, recovery Ni from wastes save the material cost but via a complex purification

Ultimate Goal: Green, Efficient, Economic impurity separation technologies

低品位红土镍矿资源开发趋势：“资源+能源+材料”一体化模式
<https://jg.xauat.edu.cn/labs/mse/index.php?r=list/index&lid=1&pageid=1322>

1、Importance of metal recovery from the spent LIBs.

□ Hazardous of spent lithium battery



□ Critical elements presented in spent LIBs

中华人民共和国自然资源部
Ministry of Natural Resources of the People's Republic of China

能源矿产	石油、天然气、页岩气、煤炭、煤层气、铀
金属矿产	铁、铬、铜、铝、金、镍、钨、锡、钼、锑、钴、锂、稀土、锆
非金属矿产	磷、钾盐、晶质石墨、萤石

中国发布24种战略性矿产目录(2016)

Europeiska kommissionen
Critical raw materials

Antimony	Fluorspar	LREEs	Phosphorus
Baryte	Gallium	Magnesium	Scandium
Beryllium	Germanium	graphite	Silicon
Bismuth	Hafnium	rubber	Tantalum
Borate	Helium	Niobium	Tungsten
Cobalt	HREEs	PGMs	Vanadium
Coal	Indium	Phosphate rock	

欧盟发布27种关键矿产清单(2017)

U.S. Department of the Interior
Final List of Critical Minerals 2018

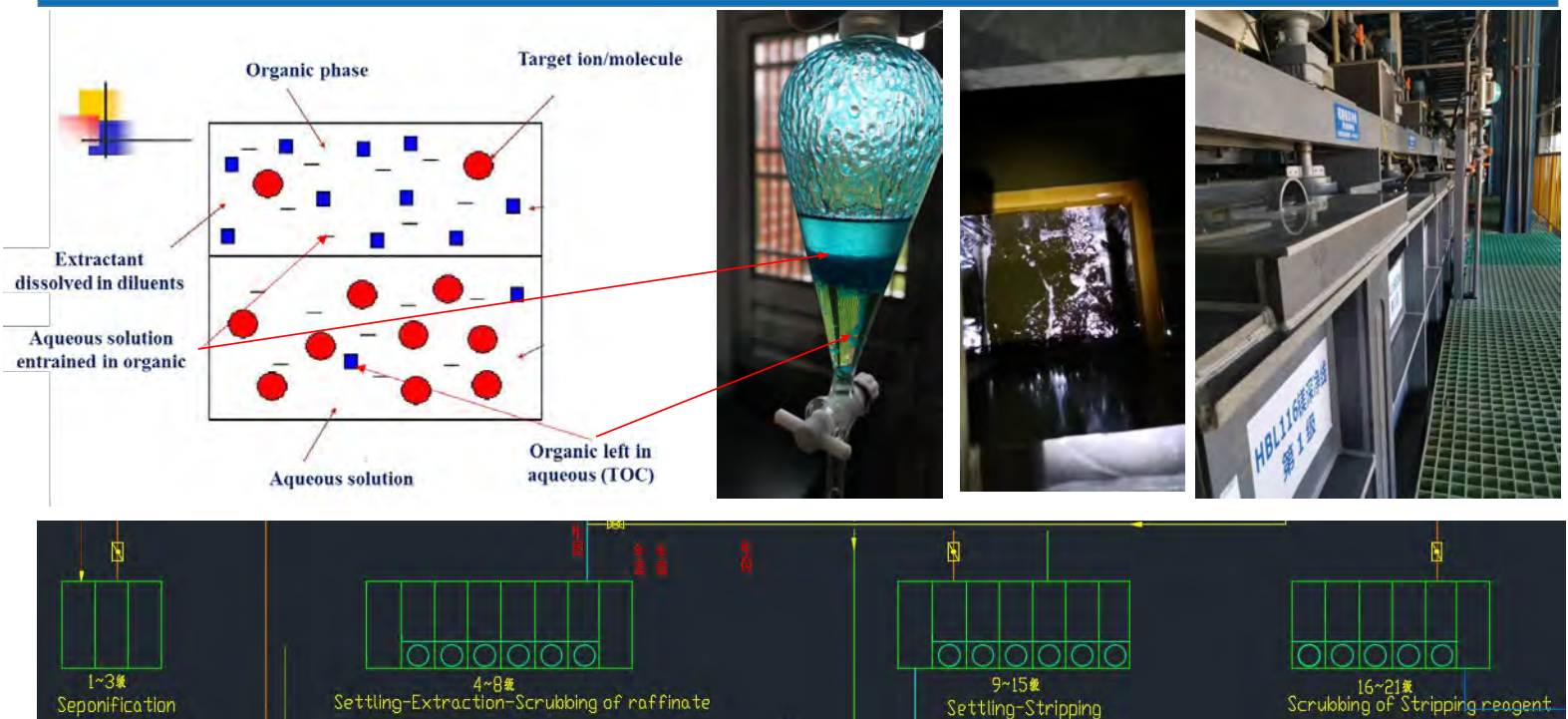
Aluminum (bauxite), antimony, arsenic, barite, beryllium, bismuth, cesium, chromium, cobalt, fluorspar, gallium, germanium, graphite (natural), hafnium, helium, indium, lithium, magnesium, manganese, niobium, platinum group metals, potash, the rare earth elements group, rhenium, rubidium, scandium, strontium, tantalum, tellurium, tin, titanium, tungsten, uranium, vanadium, and zirconium.

美国公布35种关键矿物目录(2018)

1、Importance of metal recovery from the spent LIBs.



1.plus: Basic conceptions and principles in hydrometallurgy



1.plus: Basic conceptions and principles in hydrometallurgy

Reagent Cost Structure for metal recovery from spent LIBs

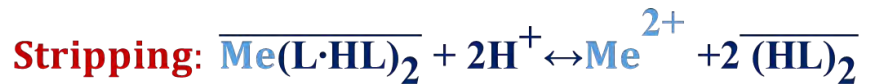
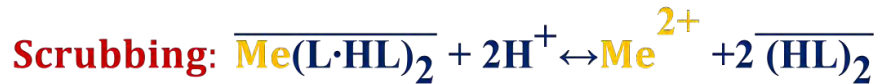
□ Alkali for saponification;

□ Acid for stripping and scrubbing

□ CaO/Na₂S for trace heavy metal and

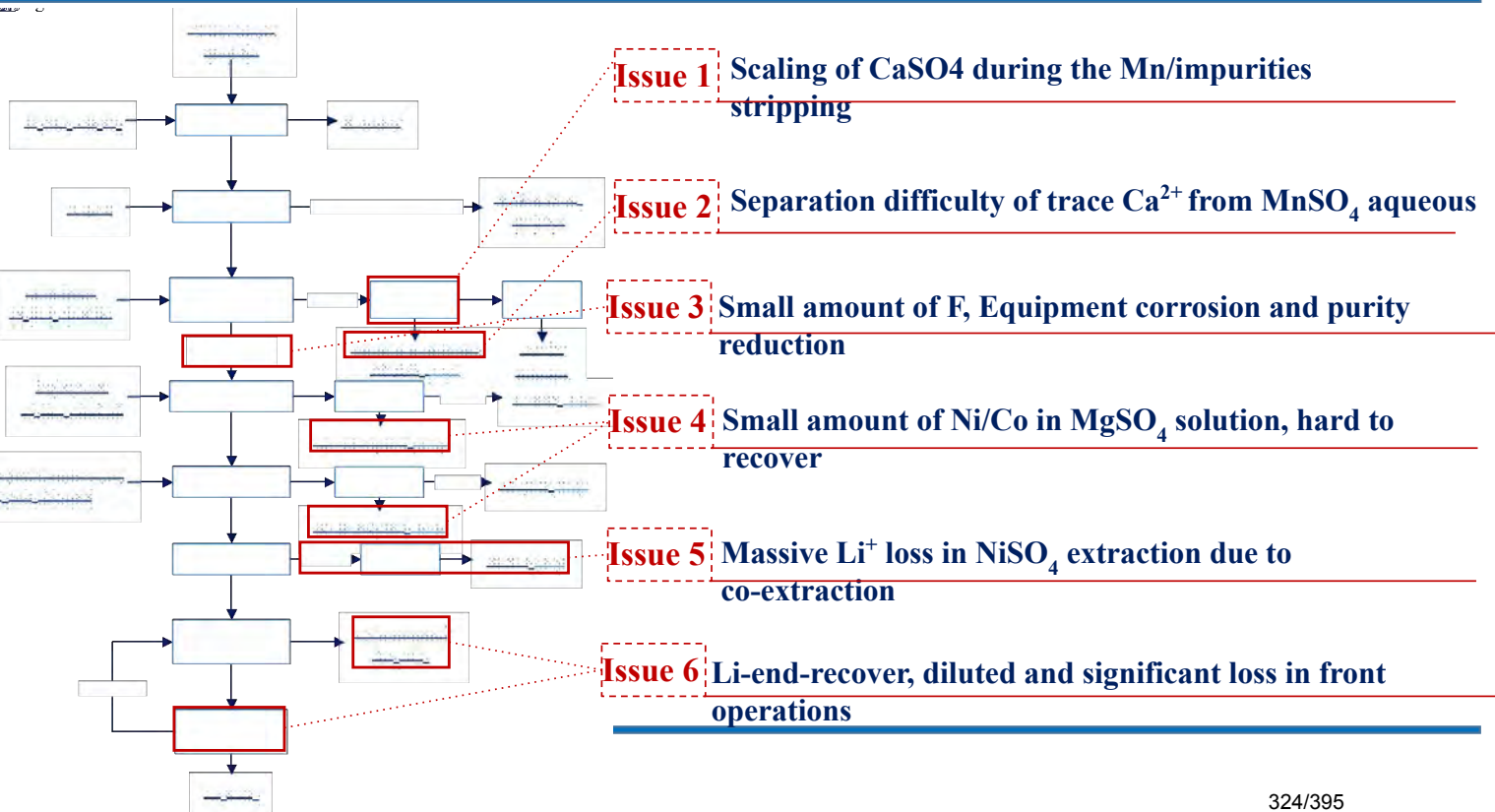
As/P/F precipitation in wastewater

□ NaOH for pH adjusting (neutralization)

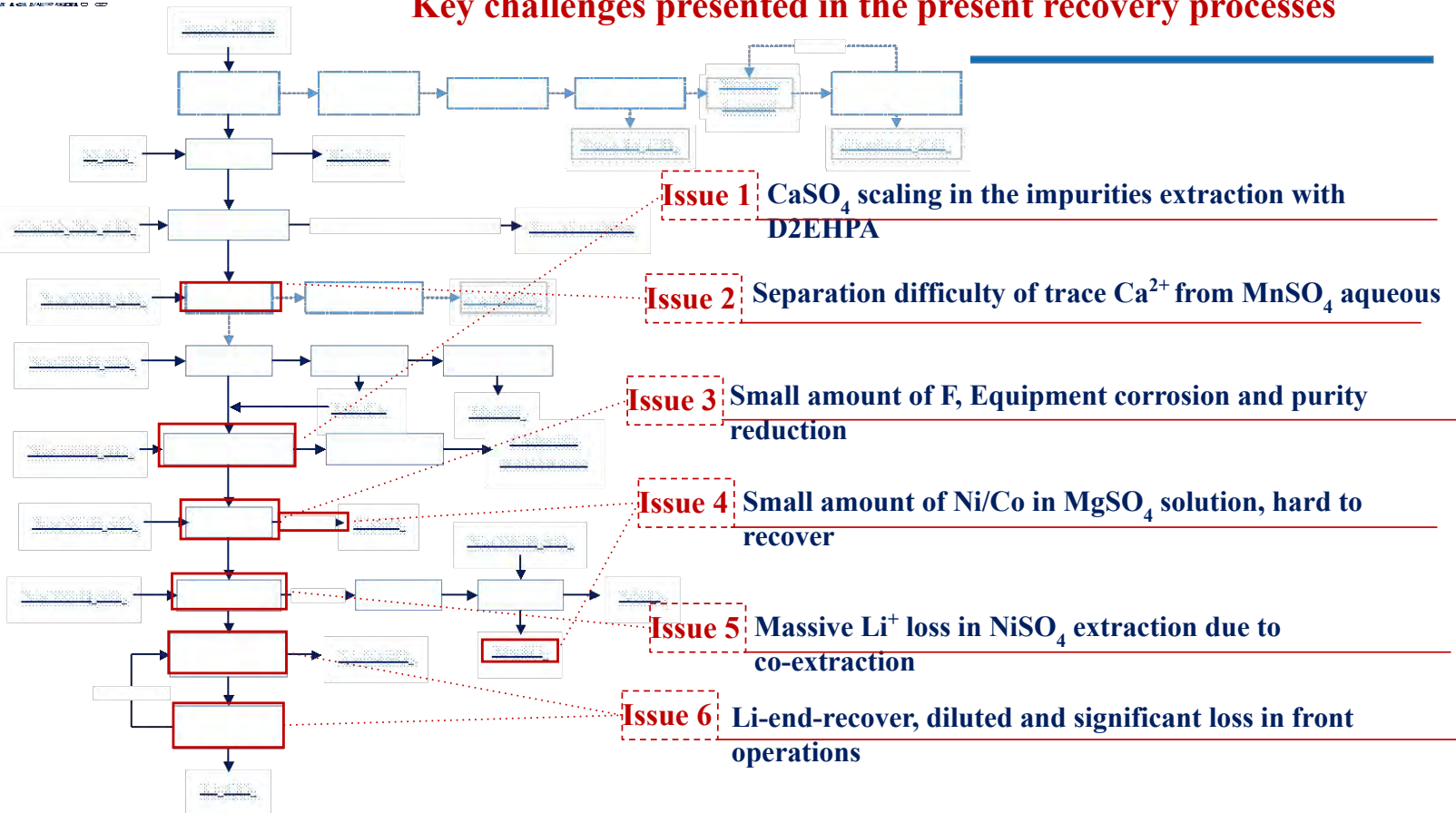


Principle 1st: Extracting small amount of elements from huge body element is economic

Key challenges presented in the present recovery processes



Key challenges presented in the present recovery processes



Key challenges presented in the present recovery processes

Issues faced by preferential Lithium leaching the carbon reduction calcination process

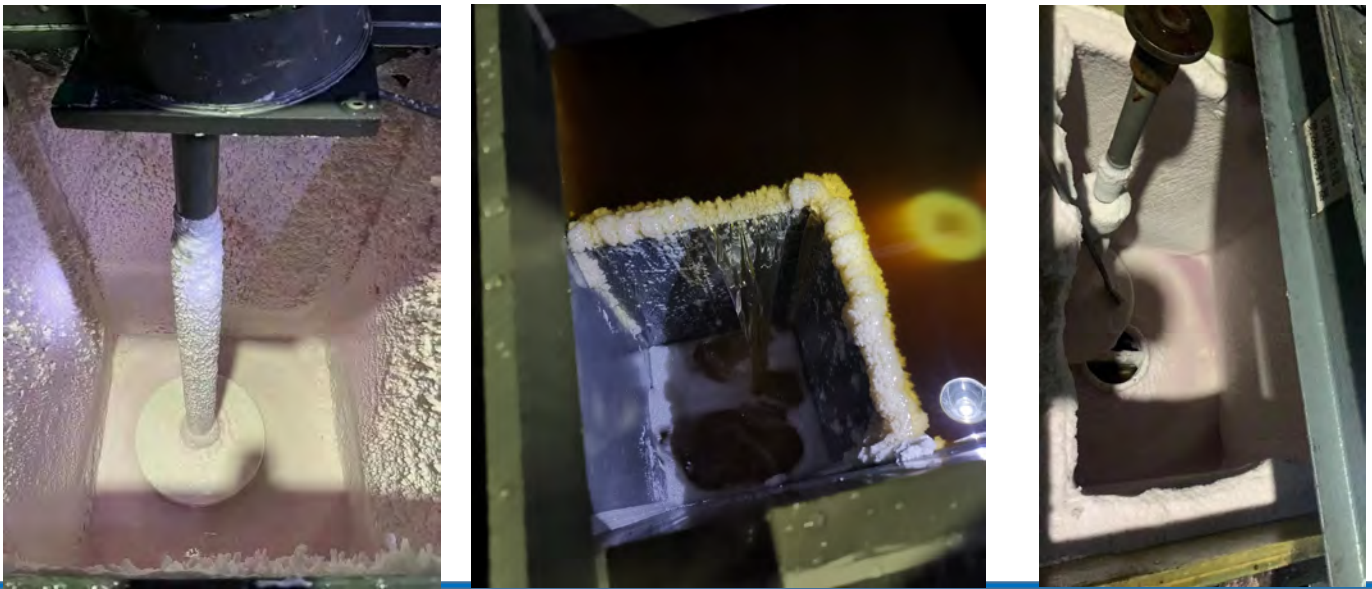
Explosive applications in Chinese Battery recycling plants in 2021~2022 due to the high lithium price

- 7~9% active carbon powder addition;
- 550~700 °C calcination at least for 1h;
- Easy to sinter, Reducing Ni/Co/Mn leaching efficiency
- Over reduction of NCM and form alloys
- Low utilization efficiency of CO_2 (~20%) due to the limited solubility of LiHCO_3 (6~7g/L Li)
- High total cost: about 800~1200 RMB per ton black mass treatment;
- Low recovery of Li only 70~85%, with ~1.0% Li left in leaching residue (NCM);



3.1 Selective extraction of Ca from NCM leaching solution

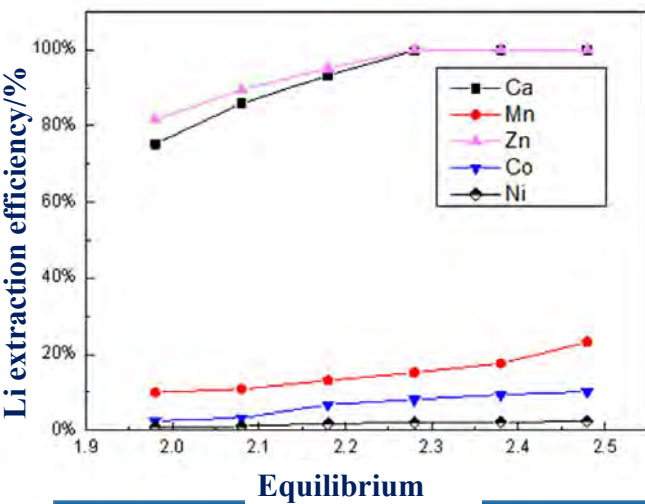
Small amount of 100~500mg/L Ca^{2+} in black mass leaching solution, leading to severe scaling during the scrubbing and stripping section in Mn/Cu/Zn/Al extraction by D2EHPA



Similar cases in Co-medium product recovery

3.1 Selective extraction of Ca from NCM leaching solution

Ca^{2+}/Zn^{2+} can be selectively extracted by HBL-120(HT-040), eliminating the scaling issue during the scrubbing and stripping section in Mn/Cu/Zn/Al extraction by D2EHPA



Five-stage of count-current extraction with HT-019-D-Ca

Row s	Equilibrium pH	Cation in raffinate 离子浓度 (g/L)				Extraction Efficiency/%			
		Ca	Zn	Co	Mn	Ca	Zn	Co	Mn
		Fee	1.15	1.5212	0.0482	1.0674	56.4085	/	/
Row	1.97	0.0463	0.0005	1.0330	55.4325	96.96%	98.96%	3.22%	1.73%
Row	1.98	0.0423	0.0008	1.0337	55.6725	97.22%	98.34%	3.16%	1.30%
Row	1.97	0.0417	0.0003	1.0324	55.6113	97.26%	99.38%	3.28%	1.41%

3.1 Selective extraction of Ca from NCM leaching solution

Ca²⁺/Zn²⁺ can be selectively extracted by HBL-120 (HT-040), eliminating the scaling issue during the scrubbing and stripping section in Mn/Cu/Zn/Al extraction by D2EHPA



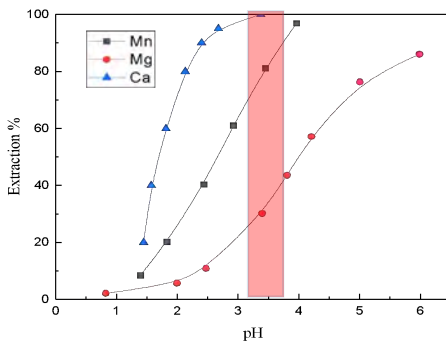
MCC 中冶瑞木新能源科技有限公司
MCC RAMU NEW ENERGY TECHNOLOGY CO.,LTD

Pilot Test Line 1 Selectively extraction of Ca²⁺ from NCM black mass leaching solution

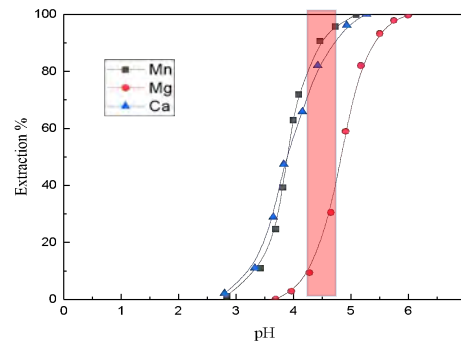
Reagents	NaOH (32%)	H ₂ SO ₄	Solvent Loss	Waste Treatment
Dosage (kg)	0.086	0.18	0.02	0.02

3.2 Deeply removal of trace Ca²⁺ from concentrated MnSO₄ solution

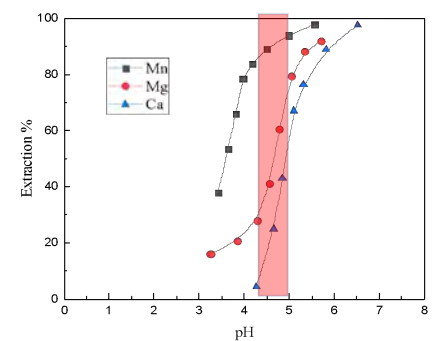
MnSO₄ stripped from loaded D2EHPA contains about 100~200mg/L Ca²⁺, for NCM synthesis, Ca²⁺ should be less than 30mg/L at least



Extraction efficiency of Ca/Mg/Mn vs. pH value by D2EHPA



Extraction efficiency of Ca/Mg/Mn vs. pH value by HEHEHP



Extraction efficiency of Ca/Mg/Mn vs. pH value by Cyanex272

Traditional extractants can hardly separate Ca/Mg from MnSO₄ stripping solutions

3.2 Deeply removal of trace Ca^{2+} from concentrated MnSO_4 solution



Production Line 2 Deeply purification of Ca from MnSO_4 stripping solution in Fangyuan Cycling plant
(Launched in June, 2022)

3.3 Deeply removal of Fluorine from Ni/Co/Mn sulfate solutions

Leaching solutions of spent LIBs contains 100~400mg/L fluorine originated from LiPF_6 and PVDF

And fluorides were introduced to reduce the massive Mg/Ca, left about 3~5g/L of F.

表 1 电池级硫酸钴溶液主要化学成分

项目	指标	
	优等品	一等品
钴 (Co) g/L	110.00~130.00	
钠 (Na) g/L	≤0.0100	≤0.1000
镁 (Mg) g/L	≤0.0050	≤0.0100
铅 (Pb) g/L	≤0.0020	≤0.0050
氟 (F) g/L	≤0.0010	≤0.0100
氯 (Cl) g/L	≤0.050	≤0.080
油分 g/L	≤0.0100	
pH	2.00~6.00	
磁性异物 g/L	≤0.00002	≤0.0001

表 1 电池级硫酸锰溶液主要化学成分

项目	指标	
	优等品	一等品
锰 (Mn) g/L	110.00~130.00	
钠 (Na) g/L	≤0.0500	≤0.1000
镁 (Mg) g/L	≤0.0050	≤0.0100
铅 (Pb) g/L	≤0.0020	≤0.0050
氟 (F) g/L	≤0.0500	≤0.1000
氯 (Cl) g/L	≤0.0500	≤0.1000
油分 g/L	≤0.0100	
pH	1.00~5.00	
磁性异物 g/L	≤0.00002	≤0.00008

表 1 电池级硫酸镍溶液主要化学成分

项目	指标	
	优等品	一等品
镍 (Ni) g/L	115.00~125.00	
钠 (Na) g/L	≤0.5000	≤1.0000
氟 (F) g/L	≤0.0040	≤0.0150
氯 (Cl) g/L	≤0.0100	≤0.1000
油分 g/L	≤0.0050	≤0.0120
pH	2.50~6.00	
磁性异物 g/L	≤0.00002	≤0.00008
水不溶物 %	≤0.0040	≤0.0080

- Latest battery grade standard (1st class product) requires [F] in Ni/Co/Mn solutions less than 10、15、50mg/L
- MVR/MED for Na_2SO_4 evaporation requires the [F] in aqueous less than 50mg/L, generally <10mg/L

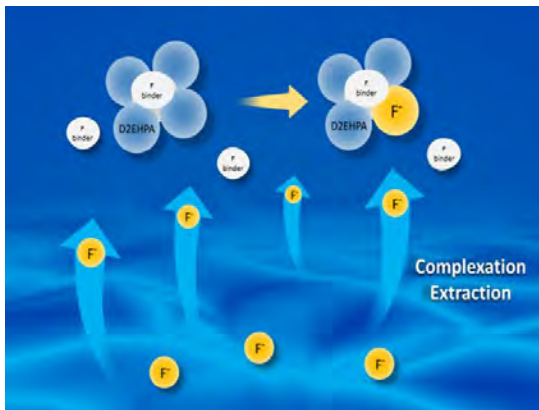
- Industrial wastewater discharge limits the [F] in final less than 6mg/L

3.3 Deeply removal of Fluorine from Ni/Co/Mn sulfate solutions

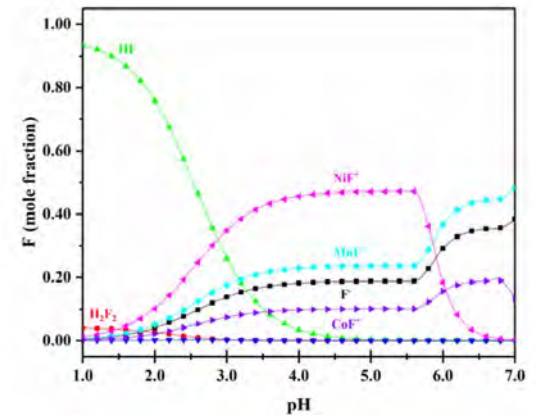
Processes	Reagents	Advantages	Disadvantages
Chemical/Flocculation precipitation	Ca/Al salts: Limestone/Calcium chloride/Calcium carbide slag	Simple operation, Economic	Huge amount of wet residue, slow settle rate, high residual F
Adsorption	Rare earth/Al/Zr... based inorganic adsorbents	Recyclable and easy segregation	Limited cycle times, metal loss, secondary hazardous, impurities introduced
Solvent Extraction	Neutral Extractant	Recyclable and Economic	Only HF can be extracted and limited impurities in aqueous solution
Ion Exchange	Amino phosphate resin, Al-loaded resins	Simple operation and Economic	Strict TOC limit in aqueous, limited loading capacity, large amount of wastewater
Other methods	Electrocoagulation, reverse osmosis, crystallization, etc	Simple operation and no waste generation	Fragile film, High power consumption, high residual F

The existing mature defluorination technologies from Ni/Co/Mn sulfate solutions **limited by economy, impurities introduction and environmental protection**

3.3 Deeply removal of Fluorine from Ni/Co/Mn sulfate solutions



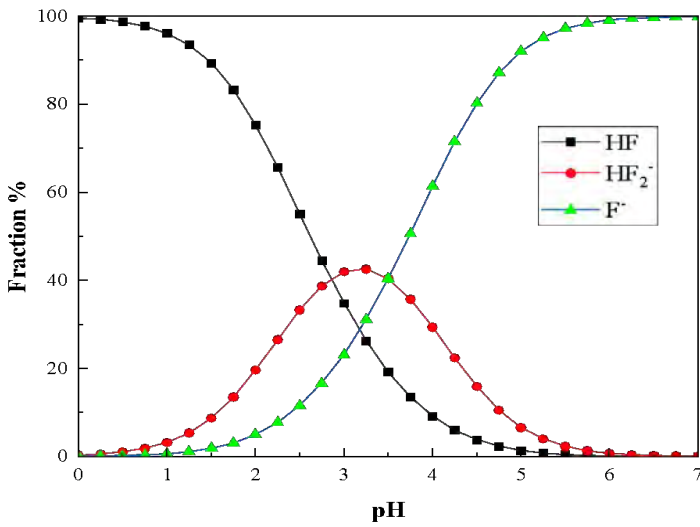
Invention and Purification Technology		申请号	专利
发明人	发明人2	发明人3	发明人4
发明人5	发明人6	发明人7	发明人8
发明人9	发明人10	发明人11	发明人12
发明人13	发明人14	发明人15	发明人16
发明人17	发明人18	发明人19	发明人20
发明人21	发明人22	发明人23	发明人24
发明人25	发明人26	发明人27	发明人28
发明人29	发明人30	发明人31	发明人32
发明人33	发明人34	发明人35	发明人36
发明人37	发明人38	发明人39	发明人40
发明人41	发明人42	发明人43	发明人44
发明人45	发明人46	发明人47	发明人48
发明人49	发明人50	发明人51	发明人52
发明人53	发明人54	发明人55	发明人56
发明人57	发明人58	发明人59	发明人60
发明人61	发明人62	发明人63	发明人64
发明人65	发明人66	发明人67	发明人68
发明人69	发明人70	发明人71	发明人72
发明人73	发明人74	发明人75	发明人76
发明人77	发明人78	发明人79	发明人80
发明人81	发明人82	发明人83	发明人84
发明人85	发明人86	发明人87	发明人88
发明人89	发明人90	发明人91	发明人92
发明人93	发明人94	发明人95	发明人96
发明人97	发明人98	发明人99	发明人100



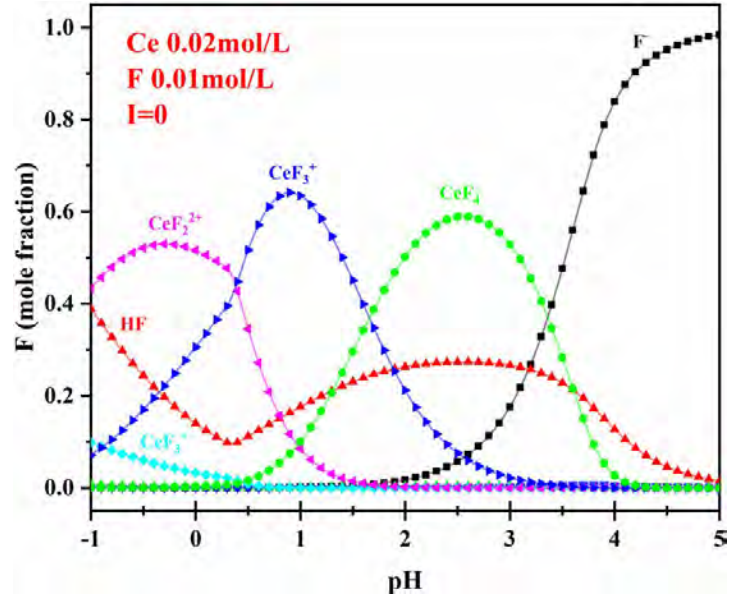
HBL-222 (HT-19-R): Loading F-binder on the carbon chain to complexing F and take the binding complexes into organic phases

HBL-221 (HT-19-D): Extracting HF molecule MeF^+ and F^- by multifunctional group grafting on the carbon chain

3.3 Deeply removal of Fluorine from Ni/Co/Mn sulfate solutions

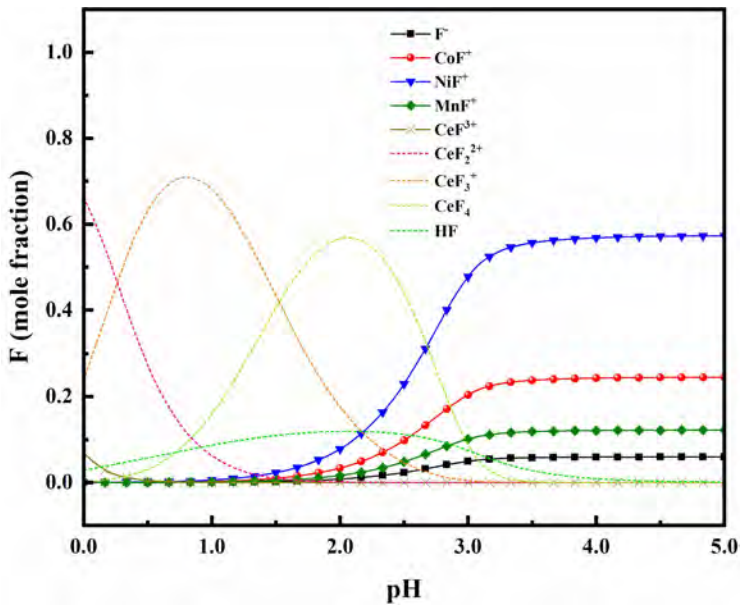


Complexation of fluorine in HF-H₂O aqueous solutions

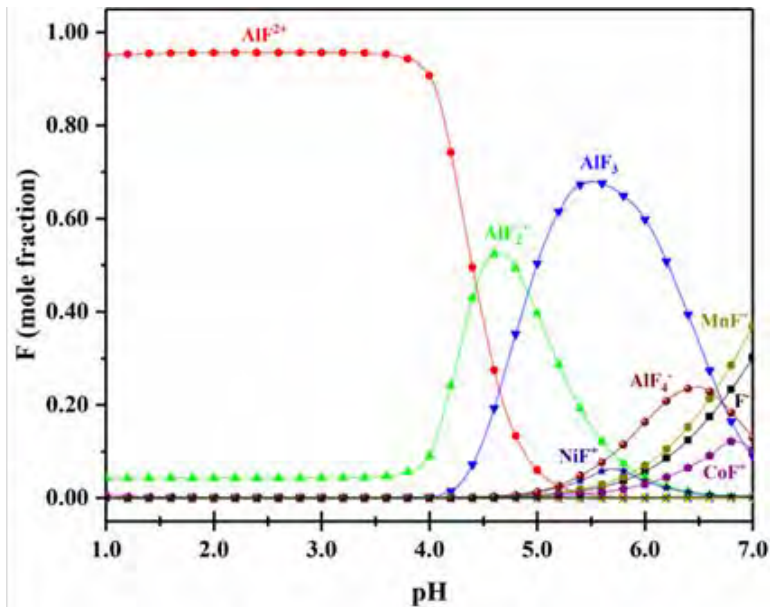


Complexation of fluorine in Ce-F-H₂O aqueous solutions

3.3 Deeply removal of Fluorine from Ni/Co/Mn sulfate solutions

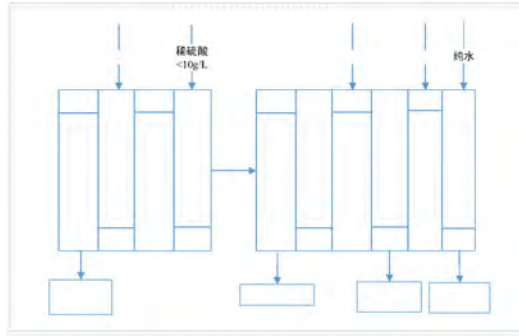
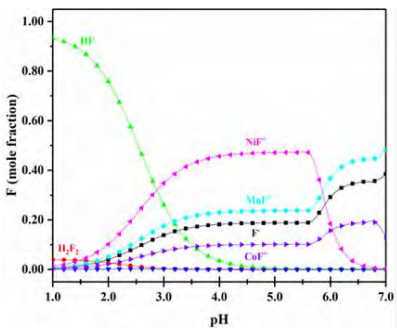


Complexation of fluorine in Ce/Ni/Co/Mn-F-H₂O aqueous solutions



Complexation of fluorine in Al-F-H₂O aqueous solutions

3.3 Deeply removal of Fluorine from Ni/Co/Mn sulfate solutions



Times	pH	[F] _{aq} (mg·L ⁻¹)
1	2.67	106.98
2	2.46	18
...		
7	2.47	12.51
8	2.43	8.09
9	2.41	4.21
10	2.44	3.10

- HBL-121 (HT-19-D) extraction has been used for F removal from Ni/Co/Mn sulfate solutions provided by Guangdong Fangyuan New Materials Group; Hunan Brunp Recycling; Jiangxi Ruida technology and showed an excellent F removal efficiency with only <5mg/L left.
- HBL-121 (HT-19-D) which can also used for Fluorine removal from Li leaching solutions.

3.3 Deeply removal of Fluorine from Ni/Co/Mn sulfate solutions



Pilot Scale Line 2 Deeply removal of F from Ni/Co/MnSO₄ solutions by HBL-222 (HT-019-R) (the left one, 15-stage extraction), HBL-221(HT-019-D) (the right one, 10-stage extraction) for Brunp Recycling (conducted during Oct. 2022)

3.3 Deeply removal of Fluorine from Ni/Co/Mn sulfate solutions

Extraction 7-stage, scrubbing
2-stage, stripping 4-stage, scrubbing
2-stage;



Element	Ni	Co	Mn	Fe	F
Feed	20.21g/L	9.27g/L	5.87g/L	3.2mg/L	3.31g/L
Raffinate	18.90g/L	8.58g/L	5.46g/L		~0.223g/L
Stripping solution	0.004g/L	0.001g/L	0.18g/L	--	~18g/L

Reagents	H ₂ SO ₄	NaOH (10mol/L)	Solvent	Recycled product
Consumption for treating per m ³ solution	22kg	17.8L	~40mg	6.8kg NaF, equal to 52 ¥
Price of reagent	500 ¥/t	1080 ¥/t	<100000 ¥/t	
Cost	10 ¥	19.2 ¥	<4 ¥	

3.3 Deeply removal of Fluorine from Ni/Co/Mn sulfate solutions

Extraction 4-stage, scrubbing
2-stage, stripping 4-stage, scrubbing



Element	pH	Ni	3-stage; Co	Mn	Fe	F
Feed	5.8	31.37g/L	13.87g/L	15.49g/L	3.2mg/L	147mg/L
Raffinate	--	28.95g/L	11.88g/L	14.36g/L		~6.78mg/L
Stripping solution		0.028g/L	0.018g/L	2.29g/L	--	~1.33g/L

Reagents	H ₂ SO ₄	Crude AlSO ₄ (Al 15.6%)	FeSO ₄	Solvent	CaO
Consumption for treating per m ³ solution	2.88kg	2.50kg	0.35kg	~30mg	1.98kg
Price of reagent	500 ¥/t	600 ¥/t	800 ¥/t	<100000/t	600 ¥/t
Cost	1.44 ¥	1.5 ¥	0.28 ¥	<3 ¥	1.18 ¥

3.3 Deeply removal of Fluorine from Ni/Co/Mn sulfate solutions



表 4-1 连续运转实验结果

2021/5/27								
萃取流比 1: 1, 洗涤流比 10: 1, 反萃流比 8: 1, 反洗流比 10: 1 (其中反洗液并入反萃液中)								
时间	料液		萃余液		氟移除率/%	反萃液		
	F(mg/L)	pH	F(mg/L)	pH		F(mg/L)	pH	
流量	37.5ml/min,		41.2ml/min,			4.69ml/min,		
12:00			33.70	2.23	92.62		~1.5	
13:00			21.80	2.10	95.23			
14:00	456.81	5.06	19.98	2.05	95.63			
15:00			9.96	2.13	97.82			
16:00			10.38	2.13	97.73			
17:00			9.11	2.16	98.01	435.98		
18:00			9.11	2.08	98.01	593.11		
19:00	416.80	5.40	3.98	2.13	99.05	593.11		
20:00-21:50 关机, 21:50-00:10 调整反萃、反洗级液面至平衡; 萃余液 Ni 39490mg/L, Co 42920, Mn 6150, Zn 612.8, Si 37.18, Fe 2.								

Pilot Scale Line 3 Deeply removal of F from Ni/Co/MnSO₄ solutions by for Jiangxi Ruida Technology Limit. (conducted during Feb. 2021)

3.3 Deeply removal of Fluorine from Ni/Co/Mn sulfate solutions

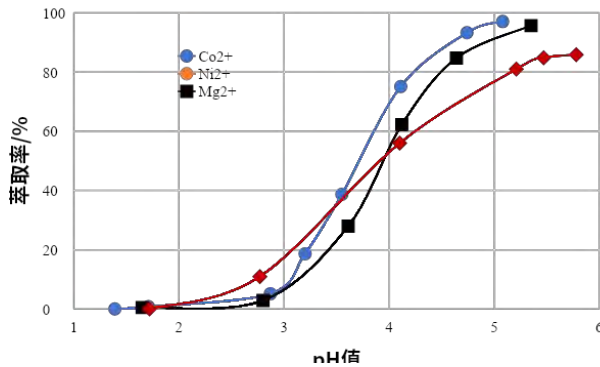


Reagents	Stripping reagent	Scrubbing acid	CaO
Consumption kg/m ³	0.5	1.7	10
Price (RMB/t)	830	500	500
Cost (RMB)	0.42	0.85	5

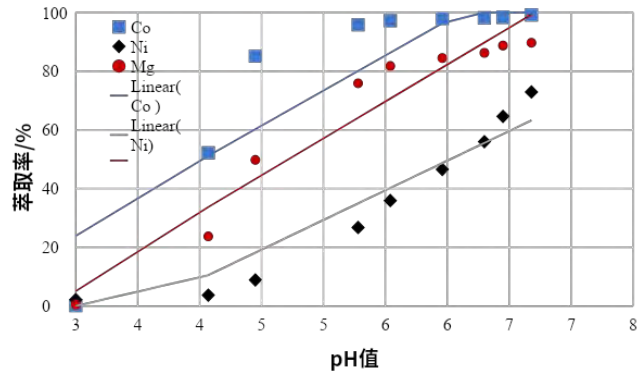
3 Production Lines: Deeply removal of F from Ni/Co/MnSO₄ solutions by for Jiangxi Ruida Technology Limit & Guangdong Fangyuan New Materials Co., LTD (launched in Nov. 2021, June 2022)

3.4 Selectively extraction of Ni/Co from MgSO₄ solutions

Scrubbing aqueous solutions contains Mg:30~60g/L and Ni, Co:1~5g/L. Traditional treatments: Na₂S precipitation at acidic pH (H₂S gas) and produces Ni/CoS solid that is difficult to recover.



Extraction efficiency of Ni/Co/Mg vs. pH by D2EHPA

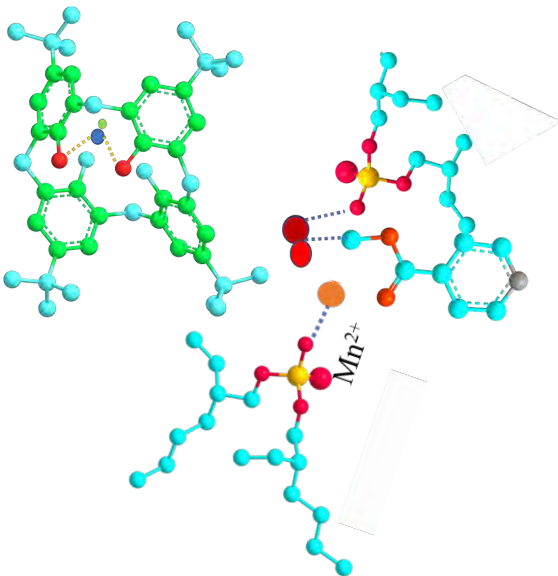


Extraction efficiency of Ni/Co/Mg vs. pH by HEHEHP

Extraction of small amount of Ni/Co from massive Mg is an ideal method.

However, the existing extractants can not achieve this goal.

3.4 Selectively extraction of Ni/Co from MgSO₄ solutions



Synergistic extractants

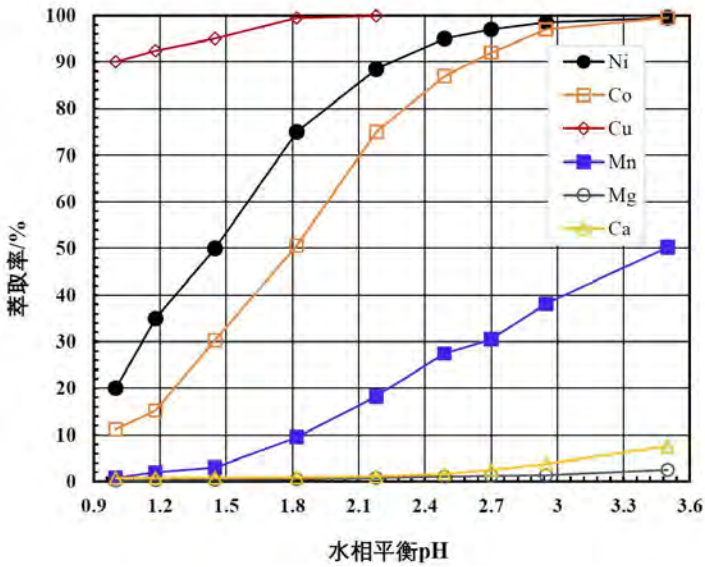
- A represents an acidic organic binder for cation exchange.
- B is a neutral extraction agent, providing coordination atom for target ions

HBL-120/HLB-221/ 222/ 116...

HT-040, HT-19-R/D, 59, 7...

Hydrometaltech, Co, Ltd.

3.4 Selectively extraction of Ni/Co from MgSO₄ solutions

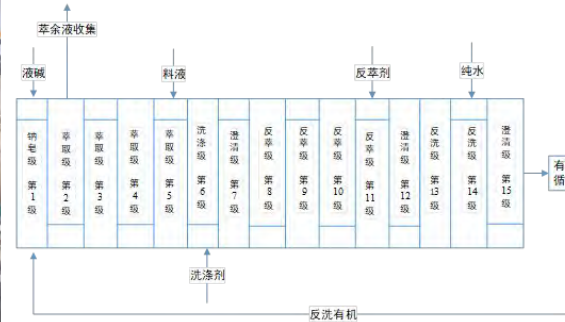


Extraction isothermal of metal cations by HT-059

Excellent separation coefficient between Ni/Co to Mg was achieved by HBL-116 (HT-059)

排数	萃余液含 Ni (g/L)	萃余液含 Co (g/L)	萃余液含 Mg (g/L)	萃余液 pH
1	1.523	2.543	60.22	2.39
2	0.003	0.013	--	3.61
3	0.002	0.013	--	3.63
4	0.003	0.007	--	3.71
5	0.0005	0.003	--	3.80
6	0.0007	0.003	--	3.61
7	0.0008	0.003	--	3.58
8	0.0008	0.007	60.41	3.50
9	0.0006	0.002	60.82	3.53

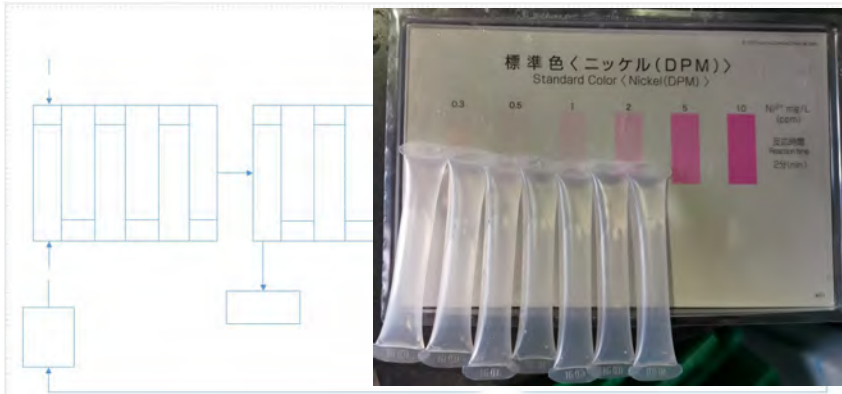
3.4 Selectively extraction of Ni/Co from MgSO₄ solutions



Pilot Scale Line 4: Selectively extraction of Ni/Co from MgSO₄ solutions by HBL-116(HT-059) for Huayou Cobalt Quzhou, Zhejiang. (conducted during June. 2021)

	水相					有机相			水相
	Co	Mg	Ni	pH	NH3-N	Co	Mg	Ni	Fe
萃取一	0.017	15.39	0.0062	4.26	/	0.31	4.66	0.49	/
萃取二	0.13	17.14	0.07	4	/	3.55	1.25	3.56	/
萃取三	1.73	16.08	1.74	3.33	/	2.65	0.14	6.35	/
萃取四	1.43	15.34	3.58	3.15	/	1.07	0.048	8.13	/
萃取五	0.87	14.91	4.66	3.18	/	0.44	0.046	9.83	/
洗涤一	1.51	0.89	10.51	2.82	0.36	0.42	0.0087	8.77	/

3.4 Selectively extraction of Ni/Co from MgSO₄ solutions



Elements	Ni	Co	Mg
Feed (g/L)	0.1~3	1~5	25~60
Stripping (g/L)	1~4.5	10~15	1.07
Raffinate (mg/L)	<1	<1	>32
Extraction efficiency (%)	99.9	99.9	---
Mg removal efficiency (%)	---	---	99.7

Production Lines: Selectively extraction of Ni/Co from MgSO₄ solutions by HBL-116(HT-059). (launched in June 2020)

Raffinate TOC: 8.14-16.06ppm, COD: 59.43-96.68ppm
 Stripping TOC: 4.19-10.97ppm, COD: 28.04-40.67ppm

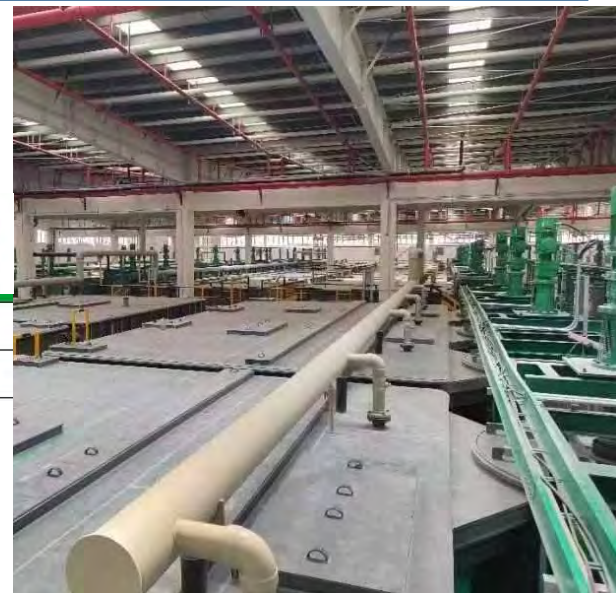
3.4 Selectively extraction of Ni/Co from MgSO₄ solutions

HT-059 extraction production line for Ni selective extraction from Co extraction raffinate produced for the Cu-Co ore, will be launched June 2024, Brunp, Yichang, Hubei, Chine (1462m³/d)



原液成分							
Ni(g/L)	Co(g/L)	Mg(g/L)	NH ₄ ⁺ (g/L)	SO ₄ ²⁻ (g/L)	油分(mg/L)	Cod(g/L)	pH
1.12	0.10	3.38	27.48	93.04	40-60	1.2	5.0-5.5

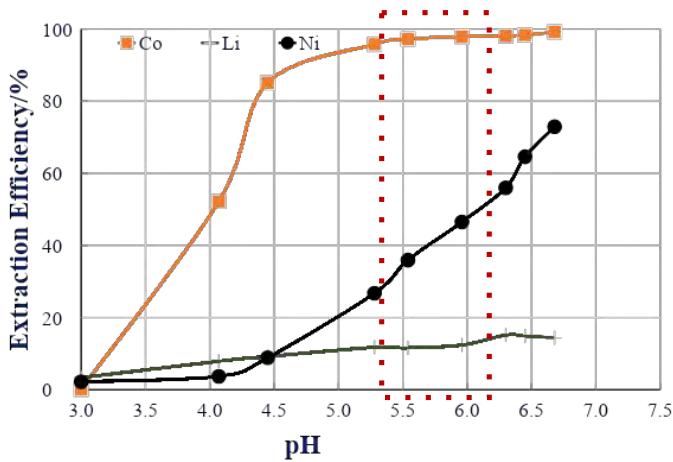
HBL 116 (25%) 萃镍线出口水相金属浓度						
物料 \ 元素	Ni(g/L)	Co(g/L)	Mg(g/L)	油分(mg/L)	Cod(g/L)	pH
萃余液	< 0.005	< 0.005	3.26	40-60	1.20	3.5-4.5
反镍液	40.42	3.61	1.22	50-60	0.60	0.5-1.5



HBL 116 (25%) 萃镍线级数									
萃取功能	铵皂	萃余液澄清	萃取	洗铵镁	有机澄清	反萃	洗酸	有机澄清	总级数
级数	1	2	5	3	1	6	3	1	22
萃取槽混合室规格	φ1.8×2.65m	/	φ1.8×2.65m			/	/	/	/
萃取槽澄清室规格	7*2.1*1.3	7*4.0*1.3	7*4.0*1.3	7*2.1*1.3			7*2.1*1.3	3*7/8*5	/

3.5 Selectively extraction of Ni from Li by HT-059

Extraction of Ni by HEHEHP (PC-88A/P507) leads to ~8% of Li loss

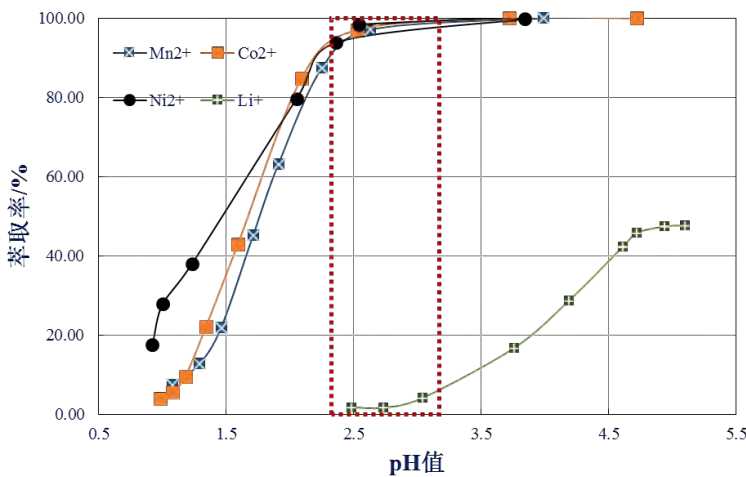


Extraction isothermal of metal cations by P507

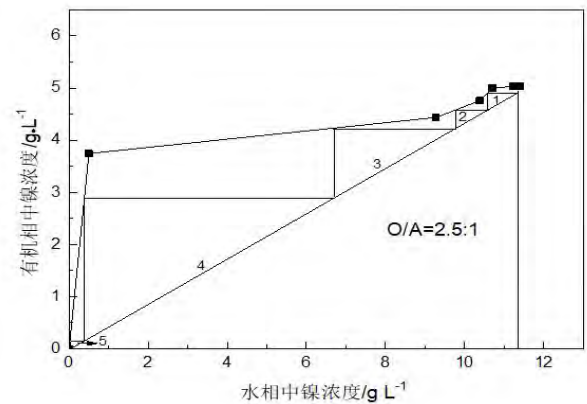
Separation coefficient for Ni to Li by P507 is 10~20

1. Dozens of scrubbing stages, low production efficiency
2. Massive of Ni was co-scrubbed, increasing H^+ / OH^- consumption significantly
3. Uncompleted separation of Li from Ni ($NiSO_4$ contains about 2g/L Li)
4. Huge amount of scrubbing water dilutes the Li in the raffinate

3.5 Selectively extraction of Ni from Li by HT-059



Extraction isothermal of metal cations by HT-059

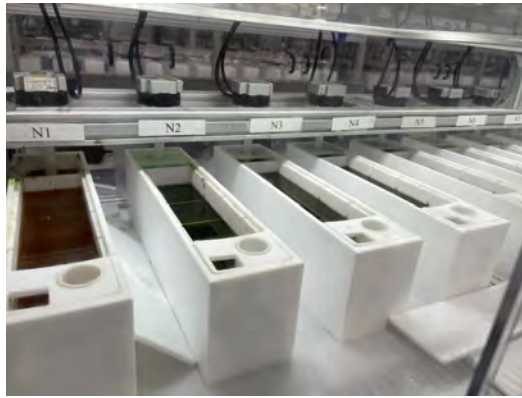


Elements	Concentration/g·L ⁻¹			Efficiency/%
	Feed	Raffinate	Organic	
Ni	10.96	0.0010	4.083	99.98
Li	2.862	2.855	0.0015	<0.1

Using (HBL-116)HT-059 with 5 stages count current extraction could selectively extract Ni from Li

3.5 Selectively extraction of Ni from Li by HT-059

Lanzhou Jintong Energy Storage New Materials Co., LTD., Austin Elements, USA, adopted HT-59 for Ni&Co co-extraction to prepare high-purity sulfate mixed liquor pilot line, Guizhou Dalong Huicheng heavy metal slag acid leaching solution HT-59-1 Ni, Co&Mn co-extraction to prepare battery grade Ni, Co&Mn sulfate mixed aqueous solution production line (2021~2023)

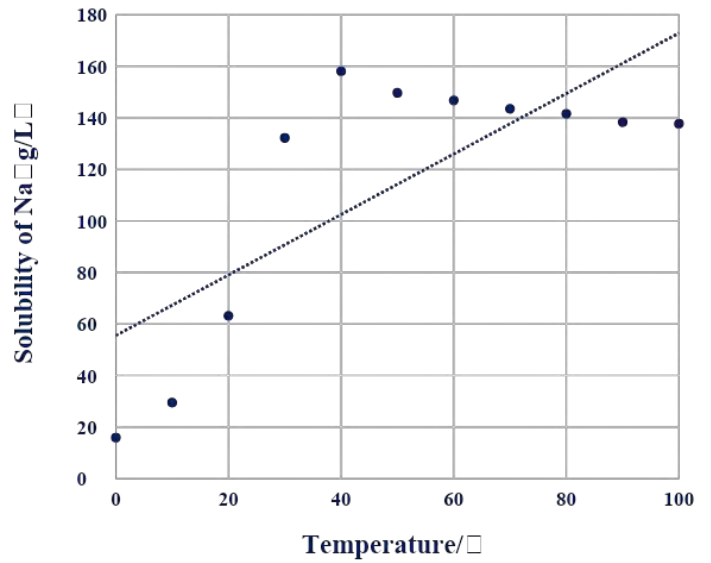
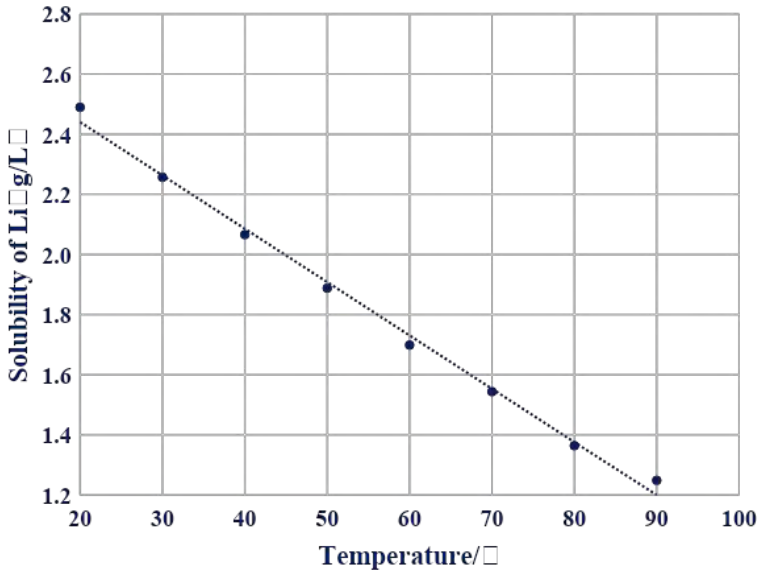


2.6 Separation of Li from the spent LIBs

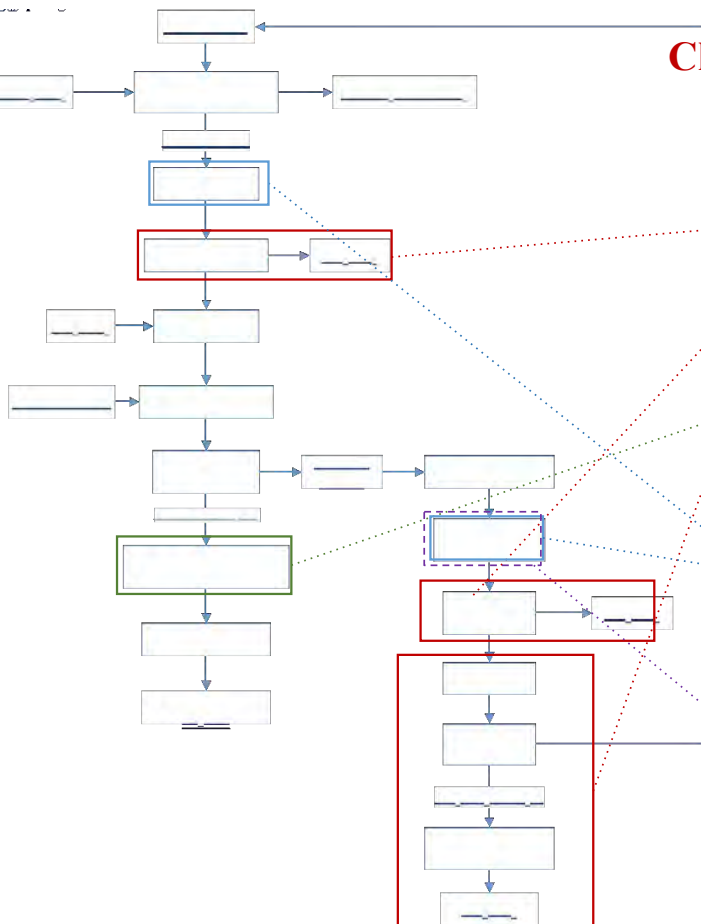
Traditional processes recovery Li at the last step, **loss massive Li in front operations, high energy consumption, high recovery cost**

1. Large amount of scrubbing water from extraction operations of Ni, Co, Mg, Ni, Li concentration in aqueous solution was diluted from **10g/L to 2~3g/L;**
2. **~5% Li** was entrained (isomorphous substitution) in Na_2SO_4 crystals during the evaporation concentration of Li from 2~3g/L to 10g/L;
3. Lower limit of Li is 2g/L for carbonate precipitation, indicating a direct recovery **~80%**, the mother liquor needed a second evaporation and re-precipitation!

2.6 Separation and recovery of Li from the spent LIBs



Traditional separation Na/Li based on the solubility variation **between Na/Li** at high/low temperature



Challenges faced by traditional Li recovery method

- Issue 1** Difficulty in Li separation from High Na/K
Long process, Low recovery, High cost
- Issue 2** Extra Carbonation purification process
High CaPEX & Opex, extra ion exchange
- Issue 3** Repeatedly evaporation-cooling, low [Li]
Energy intensity, expansion of mother liquor
- Issue 4** Circulation of mother liquor for Li recovery
Accumulation of anion impurities, COD

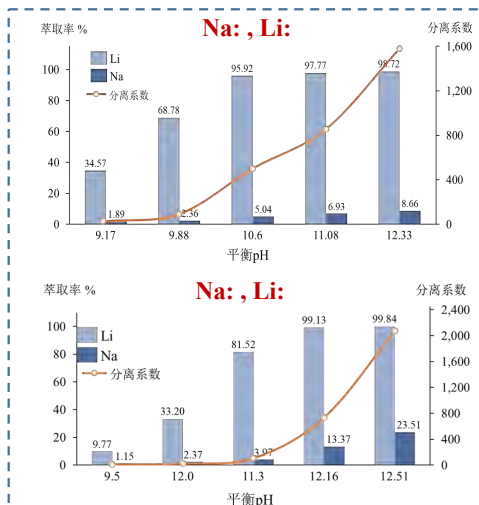
2.6 Separation of Li from the spent LIBs

Li extracted species obtained by different authors.

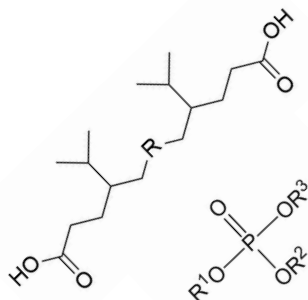
β -diketone	ligand	Extracted species	Reference
LIX 54	Cyanex 923	$\overline{\text{Li(A)(Cyanex 923)}}$	Current study
LIX 54	TOPO	$\overline{\text{Li(A)(TOPO)}_{1.3}}$	Kunugita et al. (1989)
HTTA	TOPO	$\overline{\text{Li(TTA)(TOPO)}_2}$	Healy (1968)
HTTA	TOPO	$\overline{\text{Li(TTA)(TOPO)}_2}$	Kim et al. (2003)
HTTA	PHEN	$\overline{\text{Li(TTA)(PHEN)}}$	Ishimori et al. (2002)
HTTA	DMP	$\overline{\text{Li(TTA)(DMP)}}$	Ishimori and Imura (2002)

- Low loading capacity, <2g/L Li⁺ with >40 vol% of mixed Lix54+Cyanex923/TOPO
- Poor phase segregation performance, >10min of phase separation time
- Easily emulsification generation once pH variation >1.0 or >2.0g/L Li⁺ loaded in organic

2.6 Selectively extraction of Li from Na₂SO₄ by HT-007



- ◆ Excellent Li extraction efficiency and Li to Na separation coefficient (1600-2000) ;



- Selectively extraction of Li from concentrated Na/K salt,
- Li remained in raffinate <5mg/L, Li in stripping aqueous >30g/L

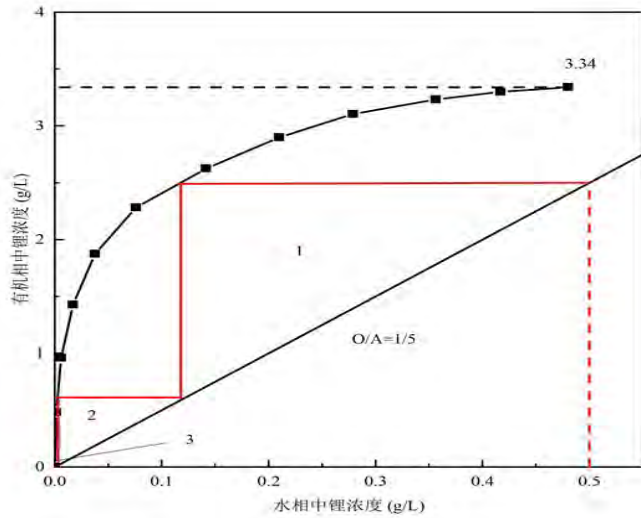


- ◆ Good segregation performance

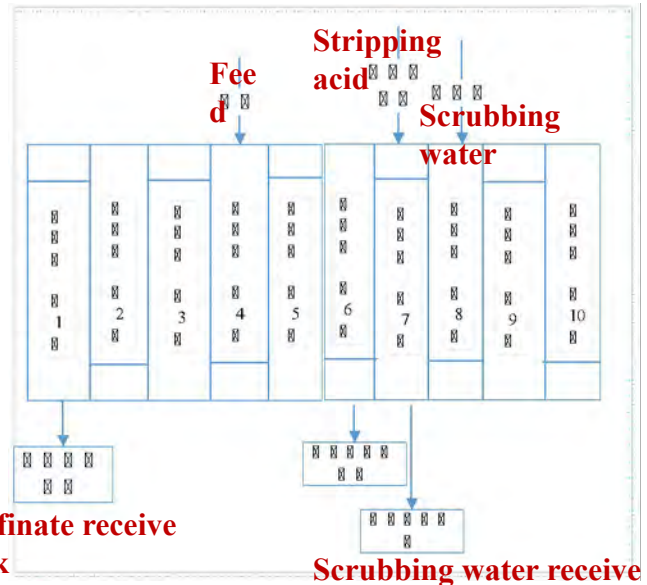
Element	Concentration/g·L ⁻¹			Extraction /%
	Feed	Raffinate	Stripping	
Li	1.5	0.0010	51.2	98.5
Na	52.76	49.48	0.22	<0.1

*Countercurrent extraction, Extraction section 3 stages, Scrubbing 3 stages

2.6 Selectively extraction of Li from Na_2SO_4 by (HBL-121)HT-007



McCabe-Thiele of Li extraction with HT-007



Raffinate receive tank

Scrubbing water receive tank

Solvent of HBL-121 (HT-007) achieved selective extraction of Li from Na in sulfate solutions, $\beta_{\text{Li/Na}}$ is over 1000, Li left in raffinate <5mg/L, Li in stripping solution was over 30g/L.

2.6 Selectively extraction of Li from Na_2SO_4 by HT-007

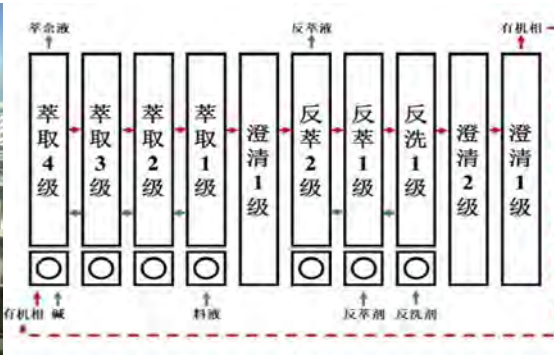


Experimental line and Production Line: Selectively extraction of Li from Na_2SO_4 solutions by HT-007. (launched in Aug. 2023)



廣東芳源新材料集團股份有限公司
Guangdong Fangyuan New Materials Group Co., Ltd.

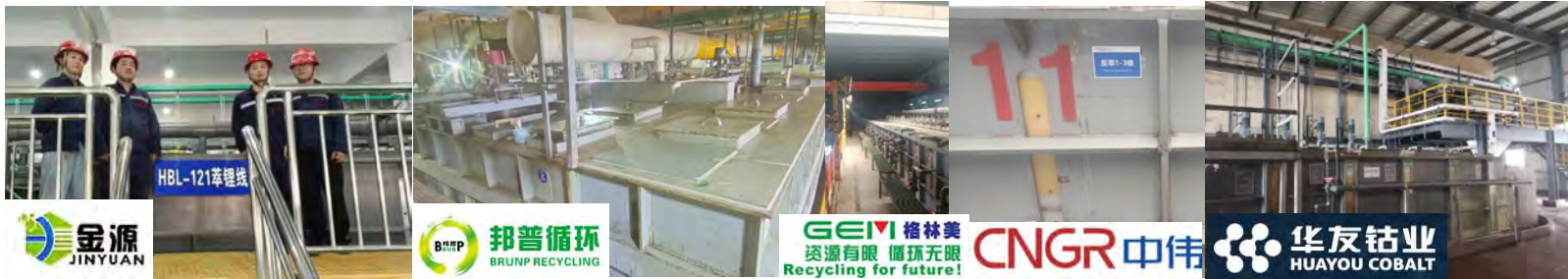
2.6 Selectively extraction of Li from Na_2SO_4 by HT-007



赣州集盛科技有限责任公司 — 技术档案 —									
日期	操作人	设备	物料	试剂	消耗量	回收率	备注	其他	备注
1
2
3
4
5
6
7
8
9
10
11
12
13
14
15
16
17
18
19
20
21
22
23
24
25
26
27
28
29
30

Ganzhou Jisheng Co., LTD, Production Line: **Selectively extraction of Li from Na_2SO_4 solutions by HT-007.** (launched in July. 2023)

2.6 Selectively extraction of Li from Na_2SO_4 by HT-007



Guangdong Weima new materials, Esokai cycle, Hunan Ruisai, Hunan Lisheng New materials, Jiangxi Ruihong... More than ten plants have launched industrial application of HT-007 for Li extraction



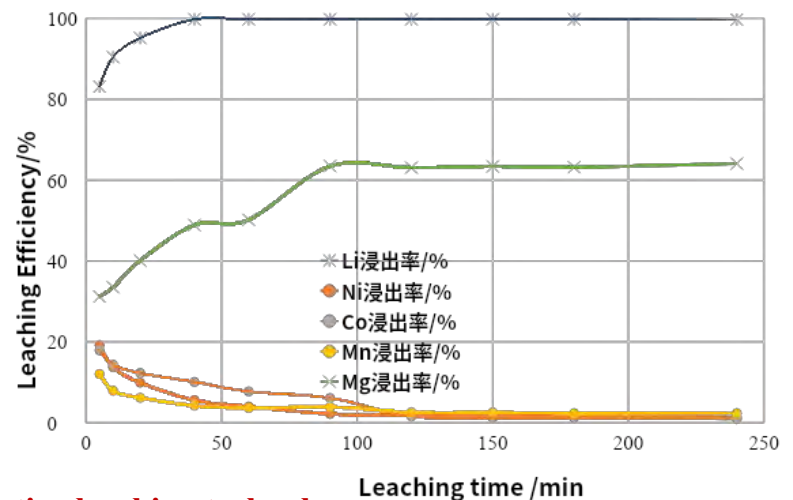
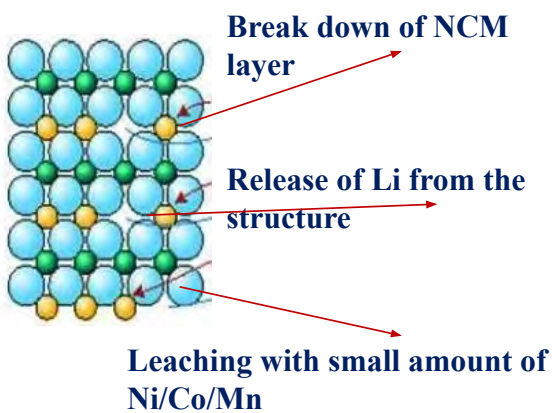
Guangxi Huayou Cobalt, Jiangxi Guoxuan, Pingxiang Tuoyuan, Hubei Libao... 12 enterprises have completed the pilot test and are running the process design

2.6 Selectively extraction of Li from Na_2SO_4 by HT-007



Austin Element from United States, **BASF** from Germany have completed lab-extraction test, and recognized that the extraction process is significantly **better** than the traditional evaporation crystallization

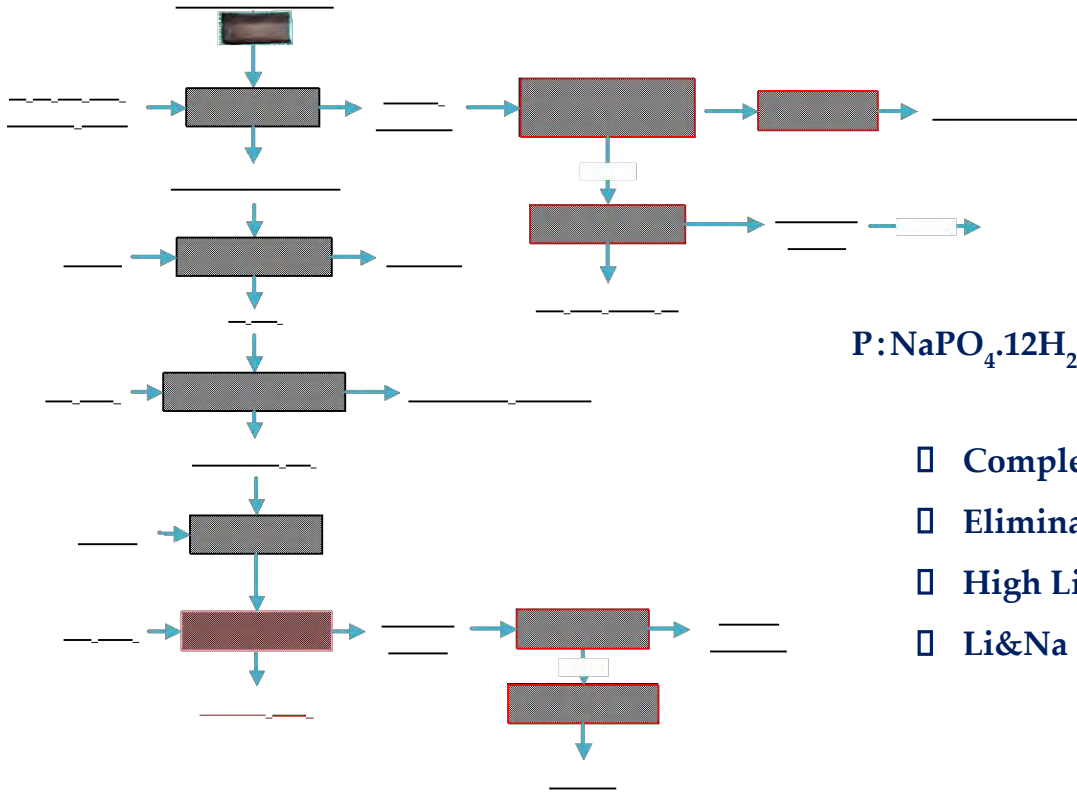
2.7 Firstly separation of Li from the spent LIB cathodes



Reinforced Li selective leaching technology

Li leaching efficiency >98%, Li concentration >20g/L, Ni+Co+Mn leaching efficiency <5%, Mg remained in the NCM solid phase <0.005wt% (no need of Mg removal operation for purification) ;

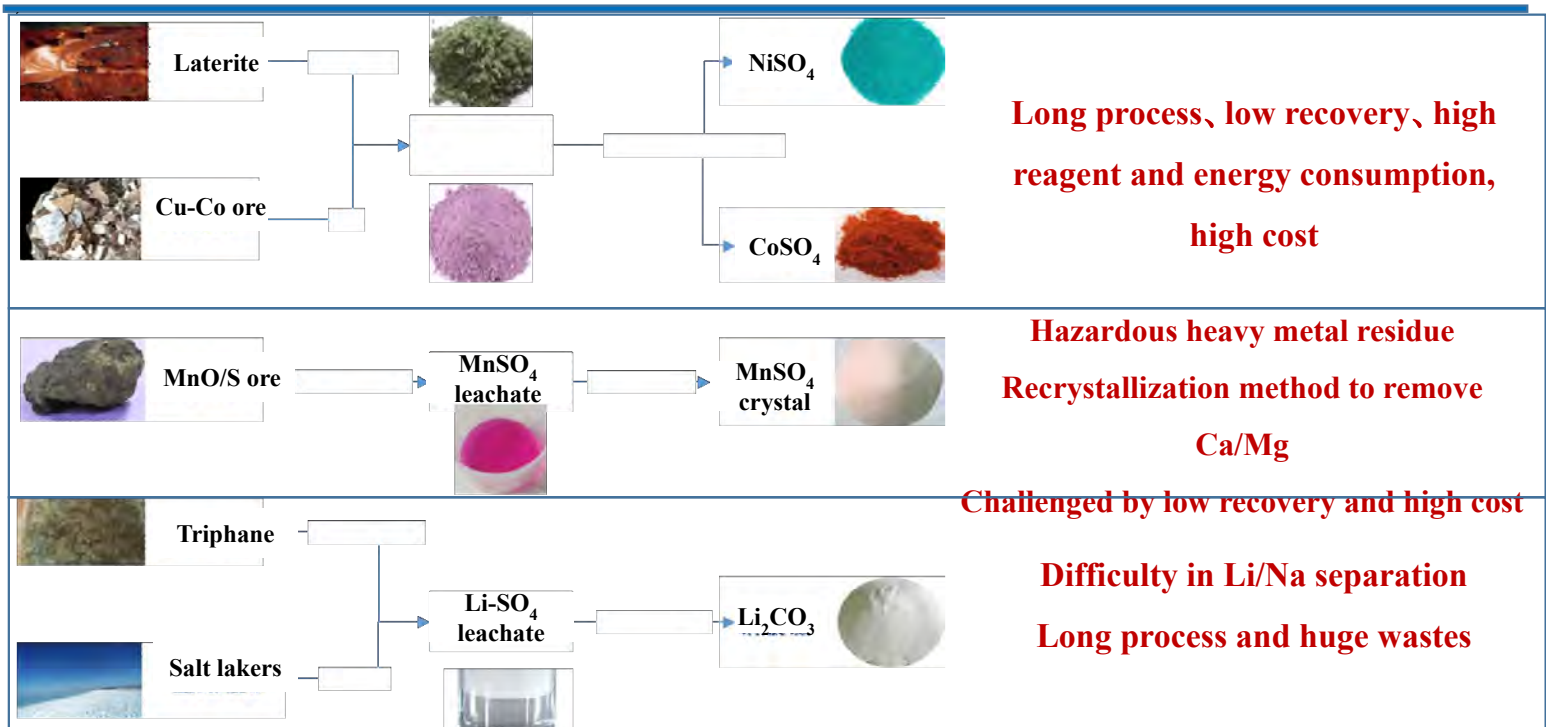
3、 Perspectives for metal recovery from the spent LFP



P: $\text{NaPO}_4 \cdot 12\text{H}_2\text{O}$, Fe: **Crude iron ore**, Li: Li_2CO_3

- Completely recovery of valuable elements
- Eliminate P and iron slag stacking
- High Li recovery
- Li&Na completely separation

3、 Perspectives for the recovery of metals from the spent LIBs



5、Summary- International project solution provider in hydrometallurgy



Hydrometal Tech:

Pioneering Sustainable Solutions provider in Battery Recycling

Hydrometal Tech was founded from a vision to revolutionize the battery recycling technologies in industry. With over 50 years of combined experience in hydrometallurgy, our founders, a group of esteemed professors and engineers, saw the potential to make a substantial impact on the environment and the economy. Our journey began with a commitment to excellence, innovation, and sustainability, which continues to be the bedrock of our operations today.

Website: <https://hydrometaltech.com/>

E-mail: shengxiwu@hydrometaltech.com

OPTIMIZED LITHIUM, COBALT, and NICKEL RECOVERY FROM BATTERY WASTE USING SOLVENT EXTRACTION

By

Leslie Miller, Mohi Bagheri, Peiming Wang, and Sabrina Sequeira

OLI Systems Inc, USA

Presenter and Corresponding Author

Leslie Miller

Leslie.Miller@OLISystems.com

ABSTRACT

This study introduces a database of commercial materials developed for solvent extraction of lithium, cobalt, and nickel: D2EHPA and Cyanex 272. The database contains thermochemical/physical properties, speciation, and activity coefficient parameters for the extractants, their complexes, and the organic solvent. The model predicts the nickel and cobalt extraction performance as a function of the separation pH, temperature, solvent-pregnant liquor (PL) mixing ratio, separation efficiency, extractant concentration in the diluent, and number of stages. The validated model was then used to optimize the operating conditions of the SX units in order to maximize the extraction efficiency while minimizing the co-extraction of impurities.

Next, the developed database was used to simulate a generic hydrometallurgical battery recycling process. The process includes leaching of metals from the spent lithium ion battery, separating metals into a pregnant liquor, extracting Co and Li using D2EHPA and Cyanex 272, and stripping the metals from the organic phase. The model predicted the nickel and cobalt extraction performance as a function of the separation pH, temperature, solvent-PL mixing ratio, separation efficiency, extractant concentration in the diluent, and number of stages. The validated model was then used to optimize the operating conditions of the SX units in order to maximize the extraction efficiency while minimizing the co-extraction of impurities. The simulation results showed that the introduced database can be used to reasonably predict the partitioning of Li, Ni and Co between the water and organic phases. When coupled with a process simulation software, it accurately predicted the heat, mass, and speciation balance among the separation units, and optimized the processes within the constraints of the existing operating conditions.

Keywords: Solvent extraction, D2EHPA, Cyanex 272, Battery recycling, hydrometallurgy, thermodynamic database, process simulation, phase partitioning, process optimization

INTRODUCTION

In the existing literature, there is a lack of a reliable thermodynamic model that could be incorporated into a process simulation tool to design, simulate, and optimize metal recovery during the solvent extraction (SX) process. The increasing demand for batteries, particularly lithium-ion batteries (LIBs) used in electric vehicles (EVs), portable electronics, and renewable energy storage systems, presents a great challenge for the future of critical materials. Battery recycling is needed to meet this demand. Given that battery recycling is required for the continued supply of critical materials, significant scientific advancements in recycling technology are needed for efficient and sustainable operations.

Solvent extraction is an economical option for producing usable, high-value species like lithium and cobalt. As a result, this work focuses on hydrometallurgical processes, like solvent extraction, that can selectively extract critical metals at ambient temperatures.

The development and scaleup of new technologies like SX rely on accurate and versatile modeling and simulation to perform feasibility studies and optimization of process flowsheets. There is presently, however, no reliable thermodynamic model that can be incorporated into a process simulation tool to design and optimize metal recovery during solvent extraction (SX). In this work, a solvent extraction database was developed to model the complex phase and chemical equilibria of liquid-liquid systems. This database, coupled with an MSE electrolyte model (activity model) enables optimization and scale-up of these emerging battery recycling processes.

The SX database was implemented in a process flow simulator to model SX and stripping with acid leaching, pH neutralization, separation, and thermal evaporation. The process model is used to maximize recovery and product purity and minimize chemical use.

THERMODYNAMIC MODELING OF LIQUID-LIQUID EXTRACTION

Thermodynamic modeling of solvent extraction, particularly for the extraction of Co, Ni, or Li, is performed using the MSE model.⁽¹⁻³⁾ Solvent extraction, also referred to as liquid-liquid extraction, is a separation process that involves two phases: an aqueous liquid in equilibrium with an organic liquid phase. Under such a liquid-liquid equilibrium (LLE) condition, the chemical potentials (μ_i^{LA}, μ_i^{LO}) of species i in aqueous A and organic O liquids are determined as

$$\mu_i^{LA} = \mu_i^{LA,0,x}(T, P) + RT \ln x_{A,i} \gamma_{A,i}^{x,*}(T, P, x)$$

$$\mu_i^{LO} = \mu_i^{LO,0,x}(T, P) + RT \ln x_{O,i} \gamma_{O,i}^{x,*}(T, P, x)$$

where $\mu_i^{LA,0,x}(T, P)$ and $\mu_i^{LO,0,x}(T, P)$ represent the standard-state chemical potentials of species i in each phase, estimated from the Helgeson-Kirkham-Flowers (HKF) equation of state.⁽⁴⁾ The parameters $x_{A,i}$ and $x_{O,i}$ are the mole fractions of species i in the aqueous and organic phases, respectively. Lastly, $\gamma_{A,i}^{x,*}$ and $\gamma_{O,i}^{x,*}$ represent the unsymmetrically normalized, mole fraction-based activity coefficients of species i in the aqueous and organic phases, respectively. The MSE activity coefficient model addresses the effect of solution nonideality in the aqueous phase, leveraging the excess Gibbs Energy model to account for long-range electrostatic, short-range intermolecular, and primary ionic midrange interactions.^(5,6) The speciation calculation was made through a computational method that integrates the excess Gibbs Energy model with a formulation for the standard-state properties of each individual species. At equilibrium, the chemical potentials for each component i are equal in the two coexisting organic and aqueous phases, represented mathematically by

$$\mu_i^{LA} = \mu_i^{LO}$$

Due to the requirement of electroneutrality in electrolyte solutions, only the chemical potential of an electrically neutral salt is experimentally accessible, despite cations and anions existing as separate species. Therefore, in an aqueous phase containing a single cation C and a single anion A , the chemical potential of the electrolyte can be obtained as,

$$\mu_{c_{v_c}A_{v_a}} = (v_c\mu_C^0 + v_a\mu_A^0) + vRT \ln(\gamma_{\pm}x_{\pm})$$

where v_c and v_a correspond to the valence charge of the cation and anion, respectively ⁽²⁾, and are calculated by

$$\gamma_{\pm} = (\gamma_C^{v_c} \gamma_A^{v_a})^{\frac{1}{v}}$$

$$x_{\pm} = (x_C^{v_c} x_A^{v_a})^{\frac{1}{v}}$$

and the LLE criterion can be computed according to:⁽²⁾

$$(\gamma_{\pm}x_{\pm})^{L_O} = (\gamma_{\pm}x_{\pm})^{L_A}$$

for which the excess Gibbs Energy model was employed to calculate the activity coefficients in the organic and aqueous liquid phases.⁽²⁾

It is crucial to develop thermodynamic models for metal extraction pH isotherms to predict the distribution ratio, number of required extraction stages, and the overall SX process model. The speciation-based MSE thermodynamic framework computes the pH of mixed-solvent solutions, that can effectively reproduce properties such as solubilities, vapor-liquid equilibria, and solution pH.^[7] Thermodynamic modeling of liquid-liquid systems exhibits greater sensitivity to binary ionic interactions than to vapor-liquid ones.⁽²⁾ Thus, to enhance the accuracy of models in SX liquid-liquid systems without compromising the precision for the VLE calculations, the thermodynamic model includes middle-range interaction terms alongside classical UNIQUAC terms. These additional terms account for interactions between ions and neutral molecules during the SX process, which can enhance the model's predictive capabilities.

The thermodynamic framework in which the database is embedded uses standard-state properties including Gibbs Energy of Formation, entropy, and HKF equation parameters to determine the most thermodynamically favored ion pairs, complexes, LLE, etc. at different system conditions. The chemical potential of each species (equations above) is then obtained by integrating the standard state properties with an activity model that incorporates an ionic-strength-independent virial interaction parameter, UNIQUAC parameters, and temperature- or concentration-dependent middle-range interaction parameters. These interactions govern the behavior between Co/Ni-extractant complexes, the extractant, solvent, modifier, and other chemical components involved in the SX process.

The thermodynamic framework presented herein shows a substantial potential in handling LLE calculations and modeling the chemistry of the SX process involved in Co, Ni, and Li extraction during battery recycling processes. The following section will discuss various considerations regarding thermodynamic modeling of SX chemistry.

SPECIFIC CONSIDERATIONS FOR SOLVENT EXTRACTION DATABASE AND MODELING

There are numerous commercial extractants for hydrometallurgical extraction of Ni, Co, Li and other metals, with D2EHPA (Di(2-ethylhexyl) phosphoric acid) and Cyanex 272 (Bis(2,4,4-trimethylpentyl)phosphinic acid) being among the most commonly utilized. Typically, these extractants are mixed with an organic solvent (diluent), to boost the solubility of the metal-extractant complex in the organic phase. The diluent also serves as an equilibrium modifier, enhancing the selectivity of the extractant. These solvents need to possess specific physical properties, including low solubility in the aqueous phase, mutual miscibility with the extractant, low volatility, high solvency for the extracted metal complex, and a low affinity for interaction with the extractant/modifier.^(8, 9) Although both aromatic and aliphatic solvents, could be used as diluent, their commercial use is often restricted by environmental constraints.

Kerosene is a cost-effective diluent for industrial-scale use. Different classes of commercial kerosene have been synthesized for hydrometallurgical applications, typically consisting of paraffinic, naphthenic, and aromatic hydrocarbons containing between 10 to 16 carbon atoms per molecule. Kerosene exhibits

a wide range of physical properties, including a density of approximately 0.8 g/cm³, a boiling point ranging from 180 to 250°C, and a flash point of 70 to 85°C or higher. In certain cases, commercial sulfonated kerosene is used, resulting in reduced levels of unsaturated impurities, increasing the potential for enhanced metal extraction efficiency.⁽¹⁰⁾ Therefore, it is useful to develop two chemistry models for kerosene, with one representing the lighter end or low-boiling kerosene, and the other representing the heavier end or high-boiling kerosene. These chemistry models offer a reasonable foundation for modeling the SX process, as the exact properties of the diluent may not be as critical as those of the extractants. Alongside the diluent, a phase modifier such as tri-n-butyl phosphate (TBP) or isodecanol may be added as a synergist to SX processes. These additives enhance separation and prevent the formation of a third phase by improving the solubility of the extractant and modifying interfacial properties.⁽¹¹⁾

The SX database currently includes two commercial extractants, D2EHPA and Cyanex 272, four solvent, low- and high-boiling kerosene, iso-octane, toluene, and phase modifiers that are appropriate for separating Ni and Co from battery wastes. Creating the database entailed a detailed analysis of the underlying chemistry. This analysis involves examining the formation and thermodynamic stability of Ni/Co complexes, estimating the thermophysical properties of those complexes, studying extractant dissociation, and considering how these factors could potentially change with SX operating conditions, such as pH, temperature, ionic strength, metal, extractant, or solvent concentrations.

Typically, the quantification of each extraction stage in a SX model involves defining parameters such as the distribution coefficient (D_{Co}, D_{Ni}), percent of metal extracted (E_{Co}, E_{Ni}), and separation factor, which is calculated by the ratio of the Co and Ni distribution coefficients ($\alpha_{Co,Ni}$):⁽¹²⁾

$$D_{Co} = \frac{\text{Concentration of Co in } L_O}{\text{Concentration of Co in } L_A}$$

$$D_{Ni} = \frac{\text{Concentration of Ni in } L_O}{\text{Concentration of Ni in } L_A}$$

$$E_{Co} = \frac{N_{Co,0} - N_{Co}}{N_{Co,0}} \times 100$$

$$E_{Ni} = \frac{N_{Ni,0} - N_{Ni}}{N_{Ni,0}} \times 100$$

$$\alpha_{Co,Ni} = D_{Co}/D_{Ni}$$

where $N_{Co,0}$ and $N_{Ni,0}$ represent the initial moles of Co and Ni in the aqueous phase, and N_{Co} and N_{Ni} are the moles of Co and Ni in aqueous liquid after extraction. To achieve optimal extraction efficiency, it is necessary to adjust the process variables, such as the temperature, solvent-to-feed ratio, aqueous/organic (A/O) volume ratio, extractant and solvent concentrations, pH of the aqueous phase, the type of extractant(s), and the composition of the organic phase. Since commercially available extractants typically consist of large organic molecules, properties for many of these complexes are often unavailable. Thus, it became necessary to use estimation techniques to predict extractant properties.^(13,14) It is also essential to account for phase equilibrium calculations related to the extractants and diluents, particularly their mutual solubility with water, to accurately simulate their separation in the organic liquid from the aqueous phase. For practical applicability, realistic modeling entails parameterizing the model to optimize the concentration of metal-extractant complexes in the organic phase. This involves developing parameters for interactions between Co-/Ni-extractant complexes and interactions among other species in the system.

DATABASE VALIDATION FOR SX PROCESS

The SX database was parameterized using available experimental data. Figure 1 shows comparisons between literature data and model predictions for Co, Ni, and Li extraction using Cyanex 272 and

D2EHPA in kerosene at different temperatures.⁽¹⁵⁻¹⁸⁾ The model predictions demonstrate a reasonable level of consistency in reproducing the SX isotherms for these metals.

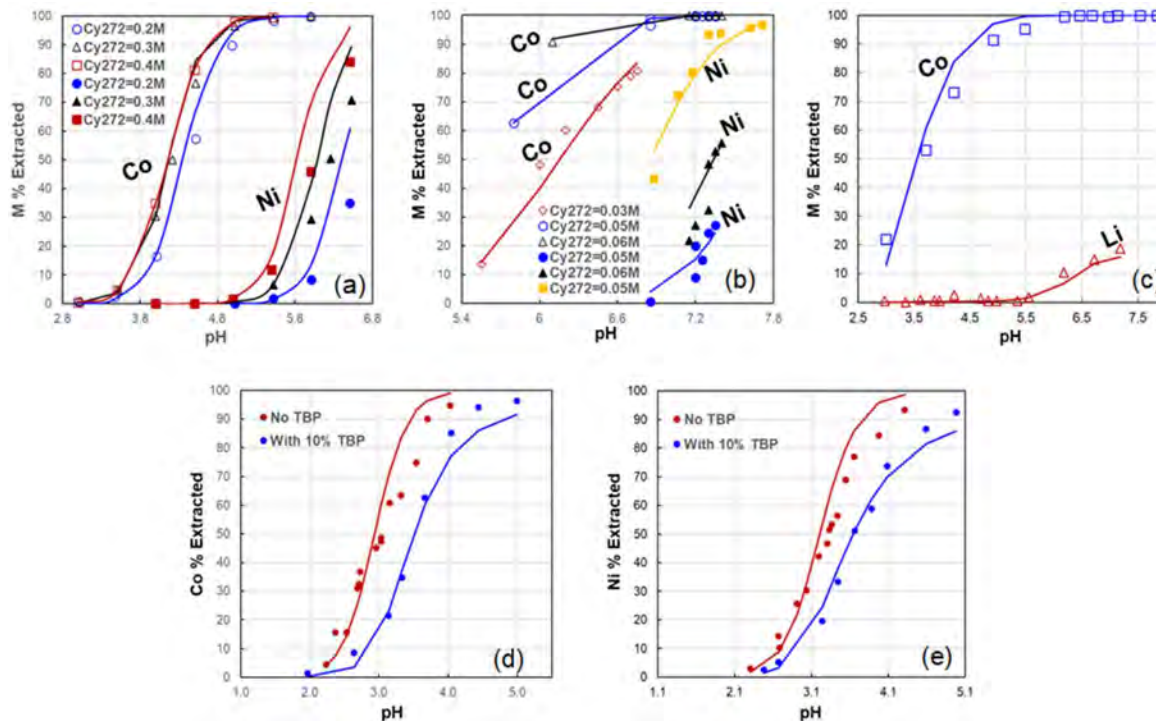


Figure 1. Model predictions (solid lines) vs. literature findings (data points) for percent extraction of metals in (a) 0.017M metal at different concentrations of Cyanex 272 in high-boiling kerosene at 40 °C, (b) 0.01M metal at different concentrations of Cyanex 272 + 0.18 M TBP in low-boiling kerosene at 30 °C, (c) 0.29M Co + 0.25 M Li + 0.64M D2EHPA in high-boiling kerosene at 25 °C, and (d, e) effect of TBP on Co and Ni extraction in solution containing 5 g/L metal + 20% D2EHPA in low-boiling kerosene at 30 °C.

As shown in Figure 1 (a) and (b), Ni extraction typically occurs at a higher pH compared to Co extraction, primarily because the extraction of one Co-Cyanex 272 complex is a dimer, meaning that the metal complexes with two Cyanex 272 molecules, whereas Ni complexes with three. In Figure 1, the percentage of metal extraction is seen to rise with greater concentrations of the extractant and at higher pH levels. This is because the increase in pH leads to changes in speciation by influencing the protonation/deprotonation of the functional groups on the extractant molecules. This process brings more metal ions into their soluble form, facilitating their interaction with the extractant molecule and thereby enhancing overall SX efficiency.^(19,20) When using D2EHPA in high-boiling kerosene (Figure 1(c)), the extraction of Co experiences a rapid increase as the pH rises, particularly in pH levels below 5; complete Co extraction could be obtained when pH is greater than or equal to 6.5. However, Li extraction does not occur when the pH is below 5.5; instead, Li extraction into the organic phase is triggered at pH levels above 5.5. Figures 1 (d) and (e) illustrate the influence of TBP modifier on Co and Ni extraction isotherms, respectively. The presence of TBP modifier can enhance phase separation during metal extraction, as seen in Figures 1 (d) and (e); TBP leads to a shift in the isotherms to higher pH levels. This widening of the Δ pH gap improves the separation of Co from Ni in the subsequent SX steps. The MSE model reasonably captures these process behaviors during SX of Co, Ni, and Li.

BATTERY RECYCLING PROCESSES

The recovery of valuable metals from spent LIBs involves mechanical, thermal, and hydrometallurgical processes. The processes are complex and involve many possible process configurations including shredding, pyrometallurgical, leaching, solvent extraction/stripping, chemical precipitation, and others. The process steps can be combined in different ways, depending on factors like quantity and characteristics of the available materials, and quantity and value of the materials that can be recovered.⁽²⁷⁾

An overview of the battery recycling process pathways is provided in Figure 2. The process can be broken down into a few major steps, including physical separation where batteries are shredded and

separated by size, leading to a pyrometallurgical step to reduce the overall volume of material and leave behind only metals, which can be recovered either through a direct recycling or hydrometallurgical step.

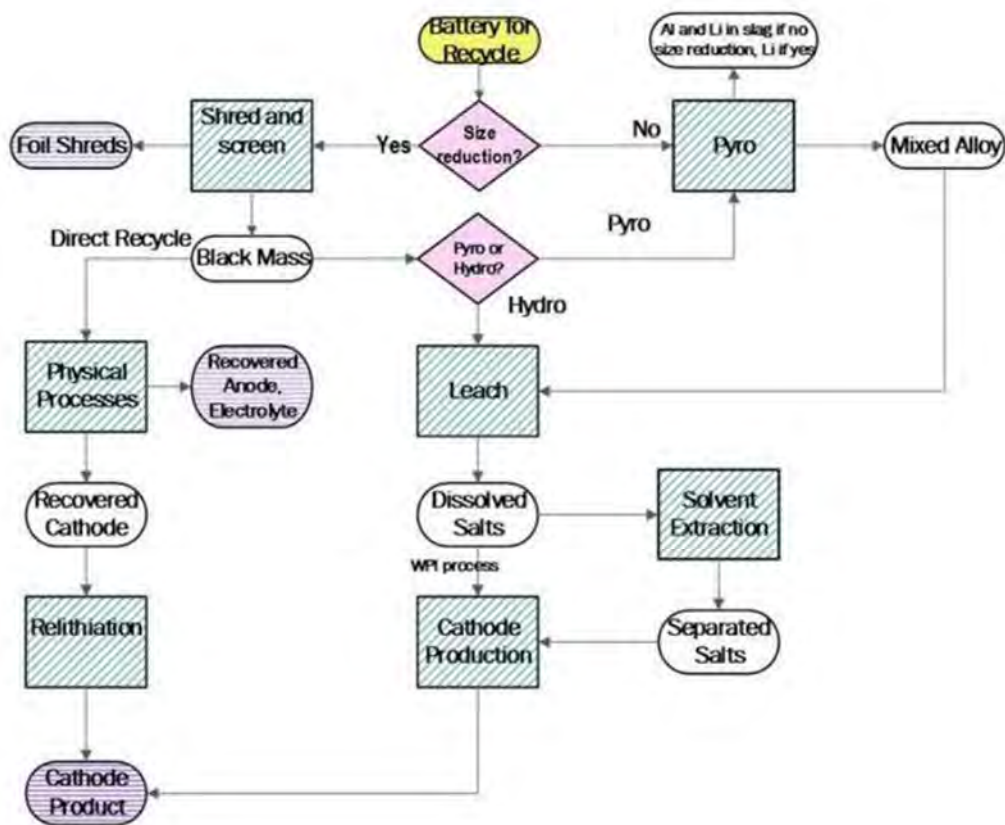


Figure 2. An overview of the possible lithium-ion battery recycling pathways.⁽²⁷⁾

The primary hydrometallurgical processes are acid or alkaline leaching, chemical precipitation, separation, and electrochemical recovery.⁽²¹⁻²⁴⁾ Recently, research has focused on solvent extraction methods as a more environmentally friendly and economical way to recover high purity metals.⁽²⁶⁾ Adding hydrometallurgical processes often combine solvent extraction and stripping with acid leaching, pH neutralization, separation, and thermal evaporation, with the goal of removing impurities and selectively extracting pure battery grade materials. The complexity of the process steps, particularly hydrometallurgical processes that are sensitive to many operating variables (pH, temperature, composition, etc.) highlights the need for computer-assisted battery recycling process models. Some hydrometallurgical unit operations display inherent problems such as slow kinetics, inefficient solid-liquid separation, high cost, and low purity⁽²⁵⁾ which further necessitates the use of mathematical models to predict these non-equilibrium conditions.

THE IMPORTANCE OF MODELING AND SIMULATION

Solvent extraction modeling is challenging for computational models because of the complex chemical behavior in LLE systems, the presence of multiple chemistries and contaminants, and the possible nonideal behavior. Models must account for chemical, physical, and thermodynamic principles in multiphase multicomponent systems, with non-standard feed compositions seen in battery recycling processes. The nonlinear nature of these relationships and the presence of azeotropes or miscibility gaps complicate modeling efforts. Chemical speciation plays a primary role in extraction efficiency, and can be influenced by pH, ionic strength, and the presence of complexing agents. Interfacial phenomena like mass transfer limitations, mixing, emulsions, and kinetics also play a significant role in extraction efficiency, but are beyond the scope of this modeling effort. While modeling these complex behaviors is not a simple task, it highlights the importance of computational methods for process optimization, which analyze the effects of numerous competing variables.

The ability to accurately model the chemical behavior is critical to process design and scale-up. Translating complex processes to industrial scale requires models that can accurately predict performance over a wide range of operating conditions. This involves not just chemical and physical modeling but also considerations of engineering principles, equipment design, safety, and environmental impact.

SIMULATION APPROACH AND ANALYSIS

A process simulation was developed for the extraction of cobalt and lithium from a lithium cobalt oxide (LCO) cathode. The validated SX database was used to test and optimize the operating conditions of a standard hydrometallurgical process. The hydrometallurgical portion of the LCO recycling process is modeled based on feed composition and cobalt extraction steps described in (26) and it is combined with a lithium extraction process described in (28). The feed composition is 24,880 mg/L Co, 3000 mg/L Li, 37.94 mg/L Ni, 159.5 mg/L Fe, 16.06 mg/L Mn, 782.7 mg/L Cu, 1800 mg/L Al, 13 mg/L Ca, 37.6 mg/L Na.

The process model can be split into two sections: cobalt recovery and lithium recovery. The cobalt recovery section is outlined in Figure 3 and consists of impurity removal through pH neutralization with a sodium hydroxide/sodium carbonate mixture. Next, the cobalt-containing stream enters the solvent extraction process with 50% saponified 0.5M Cyanex 272 in kerosene. The solvent is then stripped with 2M H₂SO₄, and the resulting cobalt sulfate product is precipitated via an evaporation/crystallization unit.

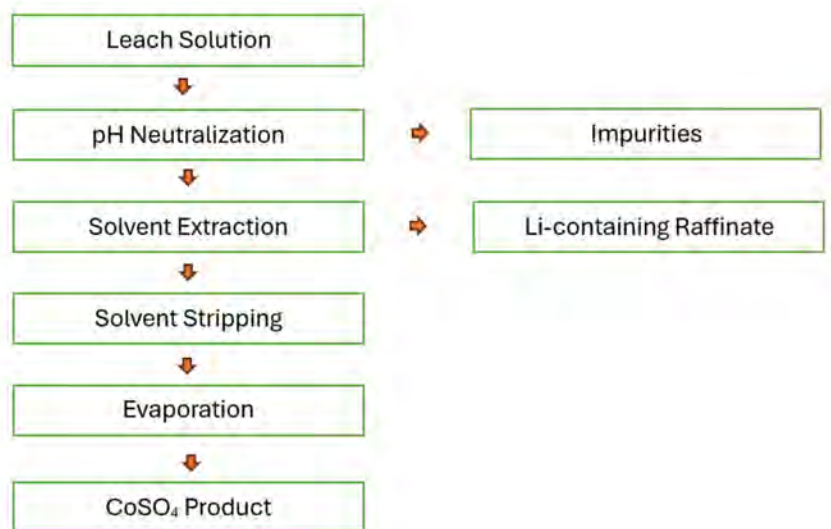


Figure 3. Overview of the hydrometallurgical process modeled for the cobalt extraction step using Cyanex 272.

The lithium extraction section is shown in Figure 4. Using the raffinate from the cobalt extraction process, the lithium-containing stream is acidified with HCl prior to solvent extraction with 0.06M D2EHPA in kerosene. The organic phase is then stripped using 2M H₂SO₄. Finally, a lithium carbonate product is produced via pH neutralization with lime, carbonation with sodium carbonate, and deionized water washing.

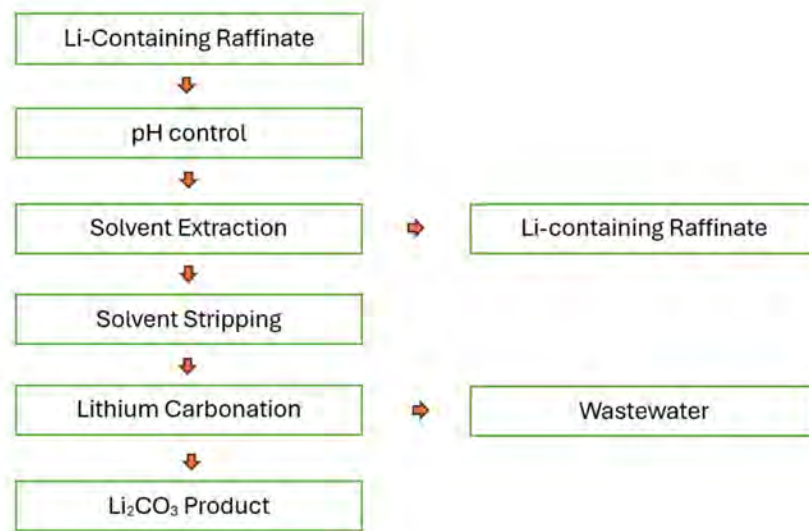


Figure 4. Overview of the hydrometallurgical process modeled for the lithium extraction step using D2EHPA.

The process was modeled using an equilibrium-based steady state flow sheeting software tool where solvent extraction, solvent stripping, and evaporation process units were each modeled as single theoretical equilibrium stages. Figure 5 depicts how the process simulation was designed using a combination of mixers and three- and two-phase separators.

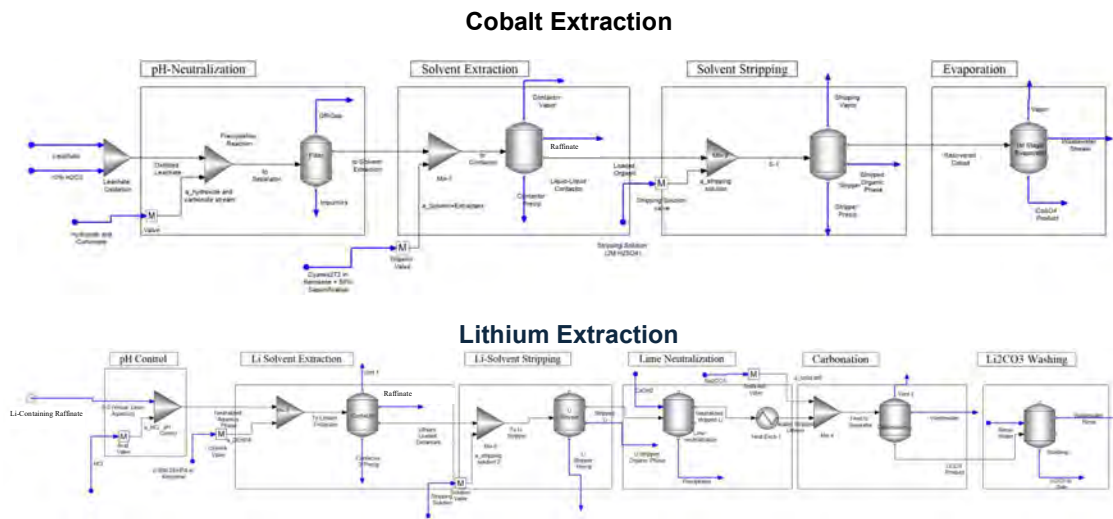


Figure 5. The developed process model for the two solvent extraction steps. The first step uses Cyanex 272 to extract Cobalt from a LCO cathode leach solution, and the second step extracts lithium from cobalt-lean aqueous phase using D2EHPA.

RESULTS

The solvent extraction process units were optimized by adjusting operating pH, solvent-to-feed ratio, and operating temperature. The operating temperature sensitivity was evaluated but it was ultimately determined that the natural rise in process fluid temperature due to heats of reaction at the neutralization step were sufficient for the SX performance while serving the additional purpose of eliminating the need for external heat sources.

Ionic flowrates for the primary process streams in the cobalt extraction and the subsequent lithium extraction processes are reported in Table 1 and 2. The composition results show how cobalt, nickel, lithium, and impurities move through the battery recycling process. The primary contributor to product recovery is solvent extraction and stripping. Product purity is driven by the upstream neutralization and precipitation steps responsible for pH adjustment and impurity removal prior to product precipitation. A benefit to using an advanced electrolyte thermodynamic model like this is the capability to couple pH-driven process units with the solvent extraction steps.

Table 1. Cobalt extraction process with Cyanex 272 showing key ion composition for primary process steps.

	Leachate Liquor	Impurity Precipitation	to Solvent Extraction	After Solvent Extraction	Recovered Cobalt	Li-Containing Raffinate
	mol/hr	mol/hr	mol/hr	mol/hr	mol/hr	mol/hr
Al(+3)	66.71	66.71	0	0	0	0
Ca(+2)	0.32	731.581	19.46	0.96	0.16	5.34
Co(+2)	422.17	0	422.17	415.40	411.08	0.26
Cu(+2)	12.32	12.28	0.03	0	0	0.01
Fe(+2)	2.86	2.84	0.01	0	0	0
Li(+1)	432.22	0	432.22	0	0	432.22
Mn(+2)	0.29	0.15	0.15	0	0	0.03
Ni(+2)	0.65	0	0.65	0.65	0	0

1. Calcium is added to the process as CaCO₃ to induce chemical precipitation of impurities prior to solvent extraction.

Table 2. Lithium extraction process with D2EHPA showing key ion composition for primary process steps.

	Li-Containing Raffinate	Post SX (feed to carbonation)	Precipitation from Lime Softening	Raffinate	Wastewater	LiCO ₃ to Sale
	mol/hr	mol/hr	mol/hr	mol/hr	mol/hr	mol/hr
Al(+3)	0	0	0	0	0	0
Ca(+2)	5.34	4.34	260.51 ¹	0.083	0.027	3.93
Co(+2)	0.26	0.00035	0.26	0.00000	0.000090	0.00018
Cu(+2)	0.0051	0	0	0.0045	0	0.00047
Fe(+2)	0.0021	0.000020	0	0.0021	0.000020	0
Li(+1)	432.22	301.10	0	0.00025	118.50	300.79
Mn(+2)	0.026	0	0.00055	0.025	0	0

1. Calcium is added to the process as Ca(OH)₂ to neutralize the process stream prior to LiCO₃ of impurities prior to solvent extraction.

For the cobalt extraction process, the optimized conditions were a feed stream pH of 6.2, A/O ratio of 1:4, and process operating temperature of 36°C. Together, these conditions generate a final Co recovery of 97.3 % and CoSO₄.1H₂O purity of 99.9%. These results are consistent with the lab experiment findings in (26) although the lower A/O ratio compared to literature indicates opportunity for further model optimization. In the lithium extraction process, the ideal operating conditions were found to be pH 1.5, A/O (molar) ratio of 1:2 and operating temperature of 27°C giving a final recovery of 69.5% and 98.7% purity. Similarly, these operating conditions are consistent with experimental findings on D2EHPA extraction of lithium⁽²⁸⁾. But like with cobalt extraction, the lower A/O ratio in the model compared to literature indicates further opportunity for model optimization like adding additional separation stages and recycling raffinate and extractant streams.

CONCLUSIONS AND FUTURE WORK

A new database for solvent extraction has been introduced and integrated with the MSE thermodynamic framework to effectively model the solvent extraction process for the recovery of Co, Ni, and Li with D2EHPA and Cyanex 272 extractants. The models can be used in a process simulation tool to assist in optimization and scaleup of hydrometallurgical processes found in battery recycling. In the future, the SX database will be expanded to include additional high priority materials like rare earth elements, manganese, copper, and corresponding contaminants. The aim will be to develop a generalized model that encompasses solvent extraction in multicomponent systems representative of battery recycling. Additionally, solvents and diluents will be incorporated as data becomes available.

REFERENCES:

1. P. Wang, A. Anderko, R.D. Young, *A speciation-based model for mixed-solvent electrolyte systems*. Fluid Phase Equilibria 2002. **203**: p. 141-176.
2. P. Wang, A. Anderko, R.D. Springer, R.D. Young, *Modeling phase equilibria and speciation in mixed-solvent electrolyte systems: II. Liquid-liquid equilibria and properties of associating electrolyte solutions*. Journal of Molecular Liquids 2006. **125**: p. 37-44
3. P. Wang, R.D. Springer, A. Anderko, R.D. Young, *Modeling phase equilibria and speciation in mixed-solvent electrolyte systems*. Fluid Phase Equilibria, 2004. **222**: p. 11-17.
4. E.L. Shock, H.C. Helgeson, *Calculation of the thermodynamic and transport properties of aqueous species at high pressures and temperatures: Correlation algorithms for ionic species and equation of state predictions to 5 kb and 1000°C*. Geochimica et Cosmochimica Acta, 1988. **52**: p. 2009-2036.
5. G. Das, M.M. Lencka, A. Eslamimanesh, A. Anderko, R.E. Riman, *Rare-earth elements in aqueous chloride systems: Thermodynamic modeling of binary and multicomponent systems in wide concentration ranges*. Fluid phase Equilibria 2017. **452**: p. 16-57.
6. A. Anderko, P. Wang, , M. Rafal, *Electrolyte solutions: from thermodynamic and transport property models to the simulation of industrial processes*. Fluid Phase Equilibria 2002. **194**: p. 123-142.
7. J.J. Kosinski, P.W., R.D. Springer, A. Anderko, *Modeling acid-base equilibria and phase behavior in mixed-solvent electrolyte systems*. Fluid Phase Equilibria 2007. **256**: p. 34-41.
8. Y. Yang, S. Xu, Y. He, *Lithium recycling and cathode material regeneration from acid leach liquor of spent lithium-ion battery via facile co-extraction and co-precipitation processes*. Waste Management 2017. **64**: p. 219-227.
9. W. Wang, H. Yang, R. Xu, *High-Performance Recovery of Cobalt and Nickel from the Cathode Materials of NMCType Li-Ion Battery by Complexation-Assisted Solvent Extraction*. Minerals 2020. **10**: p. 662.
10. I.M. Ahmed, Z.H. Ismail, M.M. Hamed, *Extraction and separation of Ga(III) from hydrochloric acid solution by Cyanex-921 in sulfonated kerosene*. Journal of Radioanalytical and Nuclear Chemistry, 2018. **317**: p. 969-976.
11. A.K. Jha, M.K. Jha, A. Kumari, S.K. Sahu, B.D. Pandey, *Selective separation and recovery of cobalt from leach liquor of discarded Li-ion batteries using thiophosphinic extractant*. Separation and Purification Technology 2013. **104**: p. 160-166.
12. M.Z. Mubarak, L.I. Hanif, *Cobalt and Nickel Separation in Nitric Acid Solution by Solvent Extraction Using Cyanex 272 and Versatic 10*. Procedia Chemistry 2016. **19**: p. 743-750.
13. X. Shan, W. Qin, Z. Zhou, Y. Dai, *Prediction of pKa values of extractant using novel quantitative structure -Property relationship models*. Journal of Chemical & Engineering Data 2008. **53**: p. 331-334.
14. D.D. Perrin, B. Dempsey, E.P. Serjeant, *pKa prediction for organic acids and bases*. 1981: Chapman & Hall.
15. W. Liu, J. Zang, Z. Xu, J. Liang, Z. Zhu, *Study on the extraction and separation of zinc, cobalt, and nickel using Ionquest 801, Cyanex 272, and their mixtures*. Metals 2021. **11**: p. 401.
16. N.B. Devi, K.C. Nathsarma, V. Chakravorty, *Separation and recovery of cobalt (II) and nickel (II) from sulphate solutions using sodium salts of D2EHPA, PC 88A and Cyanex 272*. Hydrometallurgy 1998. **49**: p. 47-61.
17. D.H. Fatmehsari, D. Darvishi, S. Etemadi, A.R. Eivazi Hollagh, E.K. Alamdari, A.A. Salardini, *Interaction between TBP and D2EHPA during Zn, Cd, Mn, Cu, Co and Ni solvent extraction: A thermodynamic and empirical approach*. Hydrometallurgy 2009. **98**: p. 143-147.
18. P. Zhang, T. Yokoyama, O. Itabashi, T.M. Suzuki, K. Inoue, *Hydrometallurgical process for recovery of metal values from spent lithium-ion secondary batteries*. Hydrometallurgy 1998. **47**: p. 259-271.
19. A.M. Wilson, P.J. Bailey, P.A. Tasker, J.R. Turkington, R.A. Grant, J.B. Love, *Solvent extraction: the coordination chemistry behind extractive metallurgy*. Chemical Society Reviews 2014. **43**: p. 123-134.
20. R. Lommelen, K. Binnemans, *Molecular thermodynamic model for solvent extraction of mineral acids by tri-n-butyl phosphate (TBP)*. Separation and Purification Technology 2023. **313**: p. 123475.
21. M. Contestabile, S. Panero, F. Veglio, *Solvent extraction for the recovery of nickel and cobalt from spent Ni-MH batteries*. Hydrometallurgy, 2021. **62(2)**: p. 163-168.
22. S. Shin, K.K., K. Egawa, J. Park, *Solvent extraction for recycling spent lithium-ion battery*. Journal of Power Sources, 2005. **146(1-2)**: p. 509-513.
23. Y.K. Sohn, D.H. Kim, S.W. Nam, S.H. Shin, *A novel process for recycling spent lithium-ion batteries using solvent extraction*. Journal of Power Sources, 2004. **123(2)**: p. 206-212.

24. T. Zhang, Y. Zhao, A. Li, J. Chen *A novel process for recycling nickel-metal hydride batteries using solvent extraction*. *Journal of Power Sources*, 2001. **99(1-2)**: p. 187-193.
25. B.G. Swainr, D.A. Wheeler, *The hydrometallurgy of nickel and cobalt*. 2004, In: *Mineral Processing for the 21st Century* Springer, Dordrecht. p. 37-51.
26. J. Kang, G. Senanayake, J. Sohn, S. M. Shin, *Recovery of cobalt sulfate from spent lithium-ion batteries by reductive leaching and solvent extraction with Cyanex 272*. *Hydrometallurgy*, 2010. **100(3-4)**: p. 168-171.
27. L. Gaines, *Lithium-ion battery recycling processes: Research towards a sustainable course*. *Resources, Conservation and Recycling* 2018. **135**: p. 102-120.
28. P. Waengwan, T. Eksangsri, *Recovery of Lithium from Simulated Secondary Resources (LiCO₃) through Solvent Extraction*. *Sustainability* 2020. **12(17)**: p. 7179.

INTEGRATED TECHNOLOGIES FOR EFFICIENT RECYCLING OF LITHIUM-ION BATTERIES: SHREDDING, BENEFICIATION, AND SOLVENT EXTRACTION

By

Leonel Yew

Neometals Ltd, Australia

Presenter and Corresponding Author

Leonel Yew

lyew@neometals.com.au

ABSTRACT

Lithium-ion batteries have become essential components in various industries, from consumer electronics to electric vehicles, leading to a surge in demand for efficient recycling processes. This presentation highlights the innovative integrated technologies developed by Neometals/Primobius for the recycling of lithium-ion batteries, emphasizing the critical role of the interplay between the shredding and beneficiation spoke and a Hydrometallurgy hub.

The shredding and beneficiation spoke of our integrated system consists of advanced technology designed to efficiently disassemble and separate battery components, resulting in the generation of "Black Mass" as the output. This Black Mass serves as the high-quality input material for the subsequent processes in our Hydrometallurgy hub.

Our Hydrometallurgy hub incorporates advanced techniques to extract and purify metals from the Black Mass with high efficiency and minimal environmental impact. This hub plays a pivotal role in closing the loop of the lithium-ion battery lifecycle by enabling the reclamation of critical metals for reuse in new battery production.

Through the integration of these technologies, Primobius has established a comprehensive and sustainable approach to lithium-ion battery recycling, addressing the environmental concerns associated with e-waste and contributing to the circular economy. The presentation will showcase the technical aspects and benefits of our integrated system, demonstrating its potential to revolutionize the recycling industry and support the growing demand for clean energy technologies.

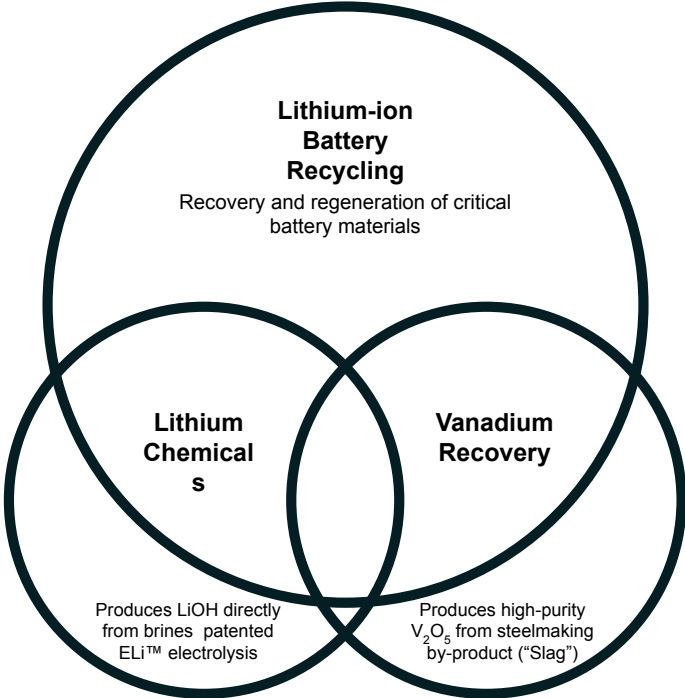
Keywords: Lithium, Shredding, Beneficiation, Solvent Extraction, Li-ion batteries, Recycling,

Integrated Technologies for Efficient Recycling of Lithium-Ion Batteries

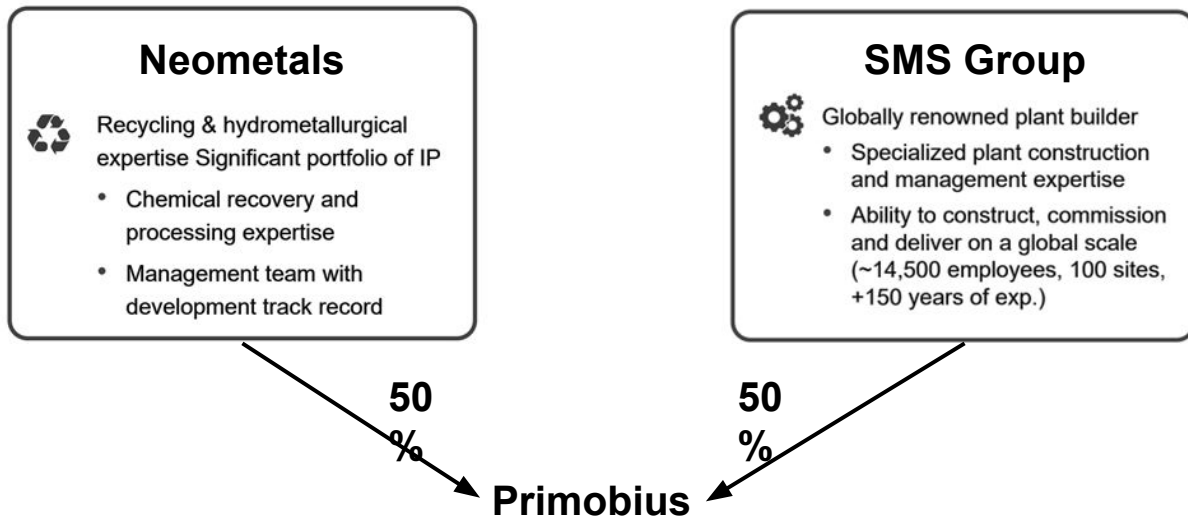
Presented by Leonel Yew

Neometals Presentation | ALTA 2024 Conference | 31 May 2024

Focus



Lithium-ion Battery (LiB) Recycling Project

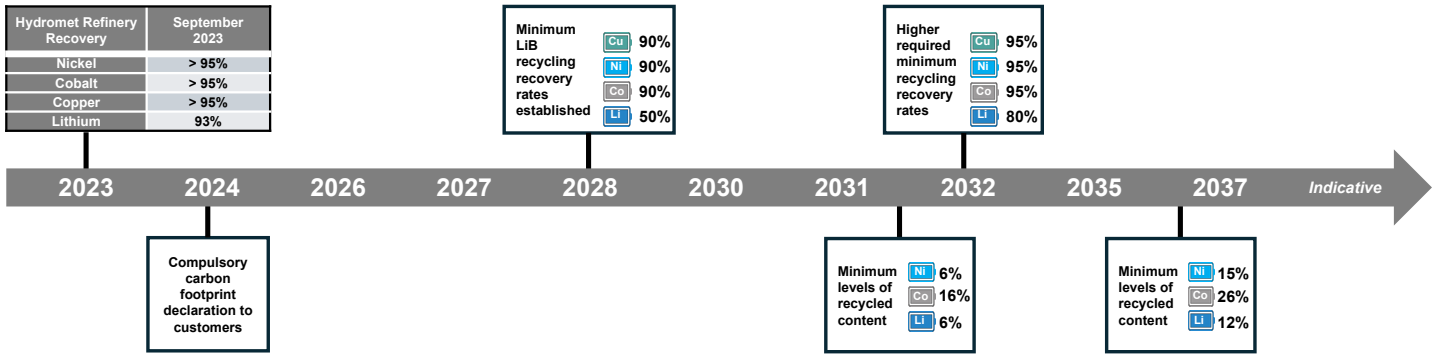


Overview of Presentation

- 1** Background/Challenges of Battery Recycling
- 2** Introduction of our Integrated Battery Recycling Technologies
- 3** Role of Thermodynamic Modelling in Process Development
- 4** Key Milestones – Mercedes Plant

Background/Challenges of Battery Recycling

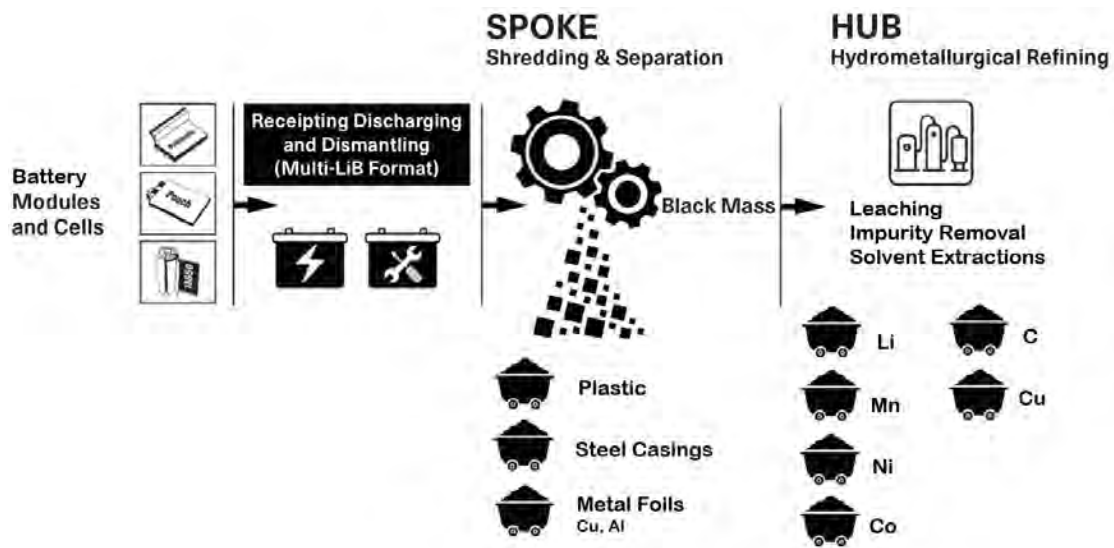
Primobius



 European regulations are pushing the responsibility to “close the loop” to the OEMs

Source: Regulation (EU) 2023/1542 of the European Parliament and of the Council

Integrated Battery Recycling Technologies



Process Development Challenges

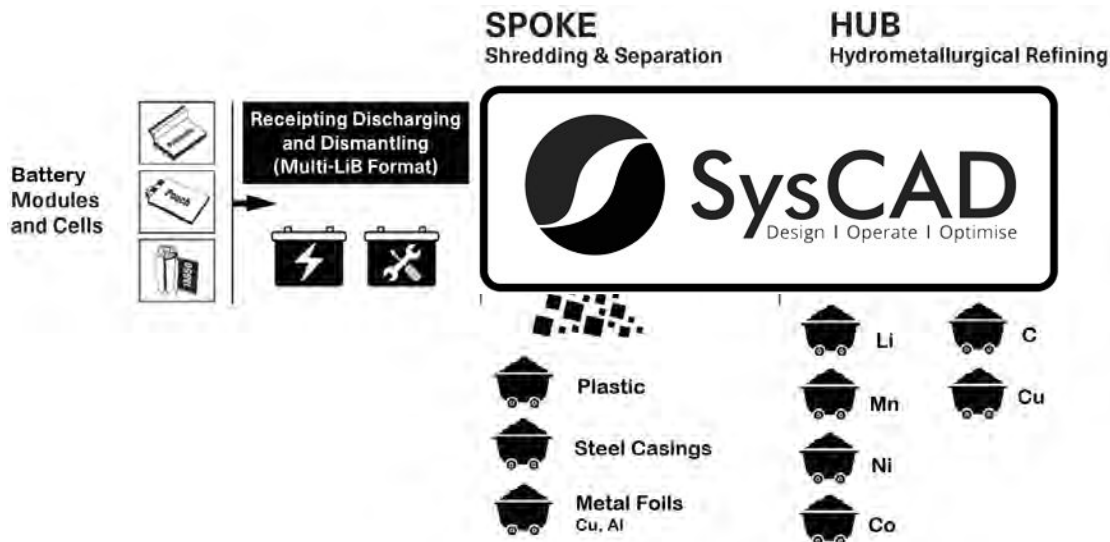
- 1 Inconsistent battery feed composition
- 2 Co-precipitation of battery materials in impurity removal

How do we overcome?



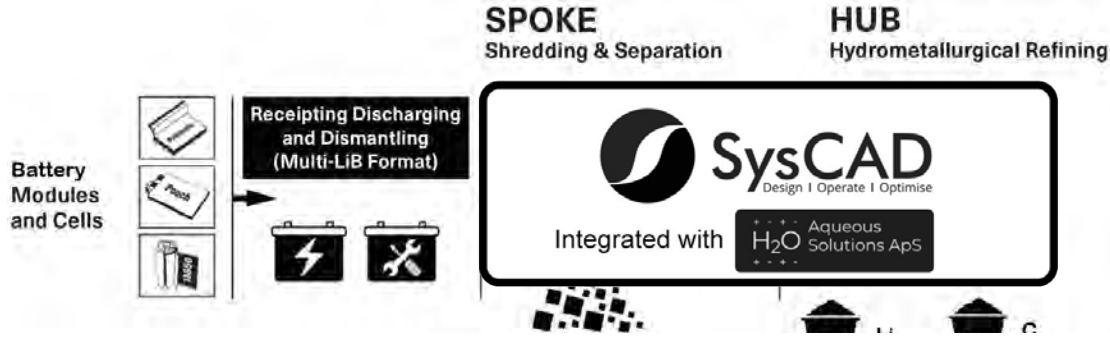
On top of leveraging our demo plant in Hilchenbach for testworks and campaigns, SysCAD simulation and thermodynamic modelling also played a very important role to narrow down the testwork matrix.

SysCAD Simulation



- Inconsistent feed:
- Too many mass balance scenarios
 - Too many testwork matrix

SysCAD Simulation & Thermodynamic Modelling

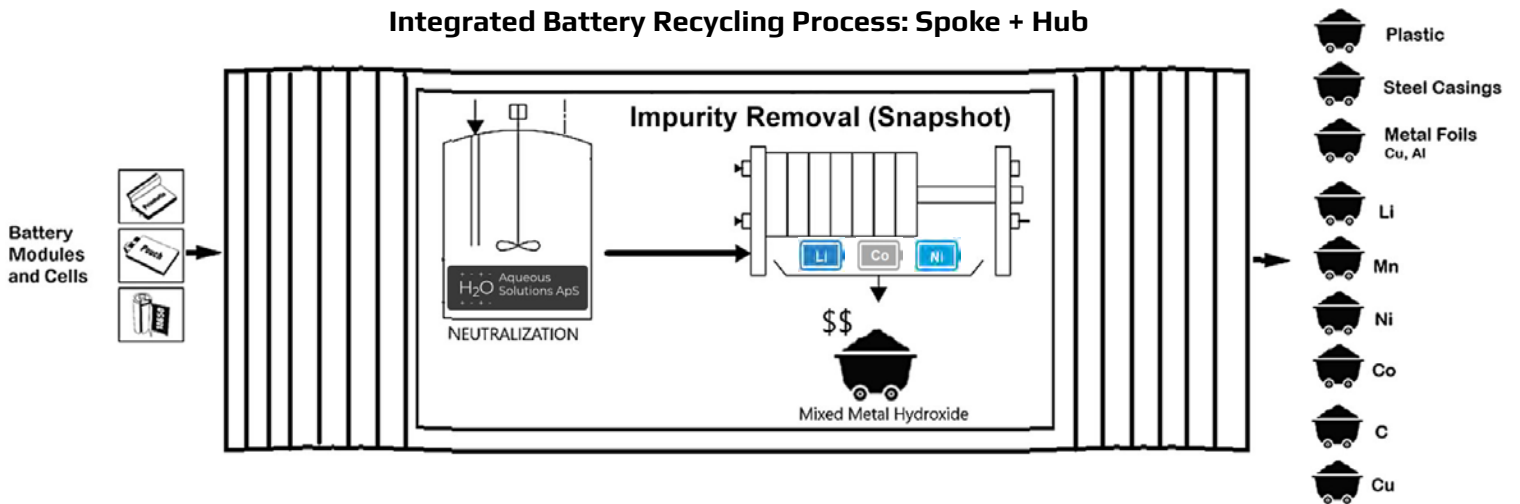


- Quickly simulate different feed composition scenarios
- Significantly narrow down test work matrix
- Provide more insight of the process, help us to understand the process

Example: Impurity Removal

SysCAD Simulation & Thermodynamic Modelling In Impurity Removal

Integrated Battery Recycling Process: Spoke + Hub



Key Milestones

1. Currently operating demonstration plant in Hilchenbach, Germany.
2. Proven to exceed the DEC 2031 EU recovery target.
3. Provide capability to run campaigns.

	Hydromet Refinery Recovery	September 2023
Higher required minimum recycling recovery rates	Cu 95% Ni 95% Co 95% Li 80%	Nickel > 95% Cobalt > 95% Copper > 95% Lithium 93%



Key Milestones

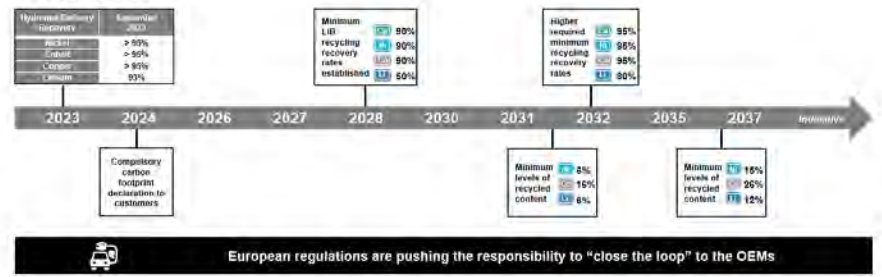
1. Integrated Battery Recycling Plant for Mercedes-Benz under construction.
2. 2500tpa EOL battery feed nameplate.
3. Commissioning start in 2nd half of 2024.



Conclusion

Our integrated technology provide solution to turn spent Li-ion batteries into recycled Li, Co, Ni, Mn, Cu, and Al materials

We have achieved the EU mandated recovery requirement and is confident to stay in business.



We enable customers to:

1. Own their recycling plant.
2. Produce their own recycled battery material.
3. Meet compliance with EU Regulation in 2031 for minimum recycled content in new batteries.

DEVELOPMENT OF AURUBIS' HYDROMETALLURGICAL LI-ION BATTERY RECYCLING PROCESS

By

Andrew Harris, Dr. Leslie Bryson

Aurubis AG, Hamburg Germany

Presenter and Corresponding Author

Andrew Harris
a.harris@aurubis.com

ABSTRACT

Aurubis AG, Europe's largest multi-metal producer and a leading Copper recycler globally, has developed and patented a hydrometallurgical process to recycle both pyrolysed and un-pyrolysed Black Mass (BM) stemming from Li-ion batteries. This purely inorganic process, comprising of leaching, precipitation, and crystallisation processes, was developed by Aurubis' R&D Hydrometallurgy Department and piloted at our Hamburg site successfully since April 2022. Aurubis' process strategy centres on a Lithium-first leach whereby a majority of Lithium is recovered as a sulphate solution which can be purified or converted into intermediates like Lithium Carbonate. Subsequently, a leach process targeting Nickel and Cobalt but including recovery of the remaining Lithium, is relatively straightforward with impurity removal following. From this leach solution, Cobalt, Manganese and Nickel are separated and recovered as intermediate products. The Graphite-rich leach residue from the Pilot plant has been used for flotation flowsheet development where concentrates of > 95% Carbon grade at 85% overall carbon recovery from locked cycle tests have already been recently presented.

We will show the evolution of the Aurubis black mass treatment process by presenting the results from consecutive pilot plant campaigns. Specifically: major value element recoveries, accountabilities and product purities achieved will be presented.

Keywords: Li-ion battery recycling, Black Mass, Critical material recycling

INTRODUCTION

The growing interest in Li-ion battery recycling over the past several years has been driven by many factors e.g., volume of battery production and associated scrap, volume of batteries expected to come to end of life and the value, rarity and criticality of the metals and materials used and finally sustainability concerns. These factors underpin European Union area legislation under Directive 2006/66/EC ^[1] and recently Regulation 2023/1542 ^[2]. Of note in the current Regulation (2023/1542);

- New batteries should contain recycled Co/Li/Ni content of 16%/6%/6%, respectively from 2031, moving to recycled Co/Li/Ni content of 26%/12%/15%, respectively from 2036.
- Collection rate of waste portable batteries from 45% to 63% to 73% starting from 2024, 2027 and 2030, respectively.
- Recycling target of 65% from 2026 for Lithium based batteries by weight, moving to 70% from 2031.
- Recycling targets for materials from waste batteries, from 2028 90% of Co/Ni/Cu and 50% Li and from 2032 95% Co/Ni/Cu and 80% Li should be reached.

Pre-processing of Li-ion battery systems is required before hydrometallurgical recovery of the active battery materials can be attempted. There exist many systems/processes to achieve this but generally, after sorting, dismantling, shredding and physical separation, Li-ion battery waste is usually well separated into copper foils, aluminium foils and a mix of Li-ion battery active anode and cathode material fractions. This active anode and cathode material produced, is known as Black Mass (BM), and is further treated to remove/recover battery electrolyte and other organic material by various methods (pyrolysis, vacuum evaporation/drying, etc);

Aurubis AG started Li-ion battery recycling research and development in 2020. Since then, the R&D Hydrometallurgy team, based in Hamburg Germany, explored the recovery of Li-ion battery active components from BM at Lab and Pilot plant scale. The Lab development culminated in patent applications (e.g., EP4225697 B1) and consecutive Pilot campaigns have resulted in iterative flowsheet changes during which parallel lab exploration and engineering studies have had a large impact on the present flowsheet design.

PILOT PLANT HEALTH AND SAFETY

At Aurubis AG health and safety is our number one priority. BM is a hazardous material with the potential to produce HF, carcinogens, and organic components. Care was taken in the design, construction and operation of the pilot plant to make sure it was safe. The importance of the following items for Pilot Plant design, construction and operation are just as critical as for Industrial Plants.

- HAZOP Study and PLC automation of key safety systems.
- Risk assessments and Commissioning Plan.
- Hazardous gas (HF, SO₂, etc) continuous monitoring detector system.
- OHS exposure measurements and personal bio-monitoring.
- Toolbox safety talks and Work instruction review and improvement.
- Workshops to capture lessons learnt and improvements after successive Pilot campaigns.

Specific measures worth mentioning were; running all reactors under extraction through an off-gas scrubber and HF absorbent and adjusting pH to 3.5 as a minimum for fluoride containing solutions before filtration or handling. The OHS and Plant Operability learnings from the Pilot plant project have proved invaluable for the industrial scale plant design, especially considering BM is a new hazardous feed material to Aurubis.

BM PILOT PLANT FEED

Figure 1 shows the range of element variability across ~20 NMC BM samples received since 2020 at Aurubis. There is a clear variance in a) the valuable base metals Ni/Co/Cu, and b) impurities such as Al, Fe and F. Due to the relative immaturity of the battery recycling industry and the rapidly changing battery technology landscape it is very difficult to predict the future composition of a “typical” black mass. Therefore, developing a flexible process that could handle the main types of BM stemming from NCM Li-ion batteries (or even other types) was viewed as an advantage.

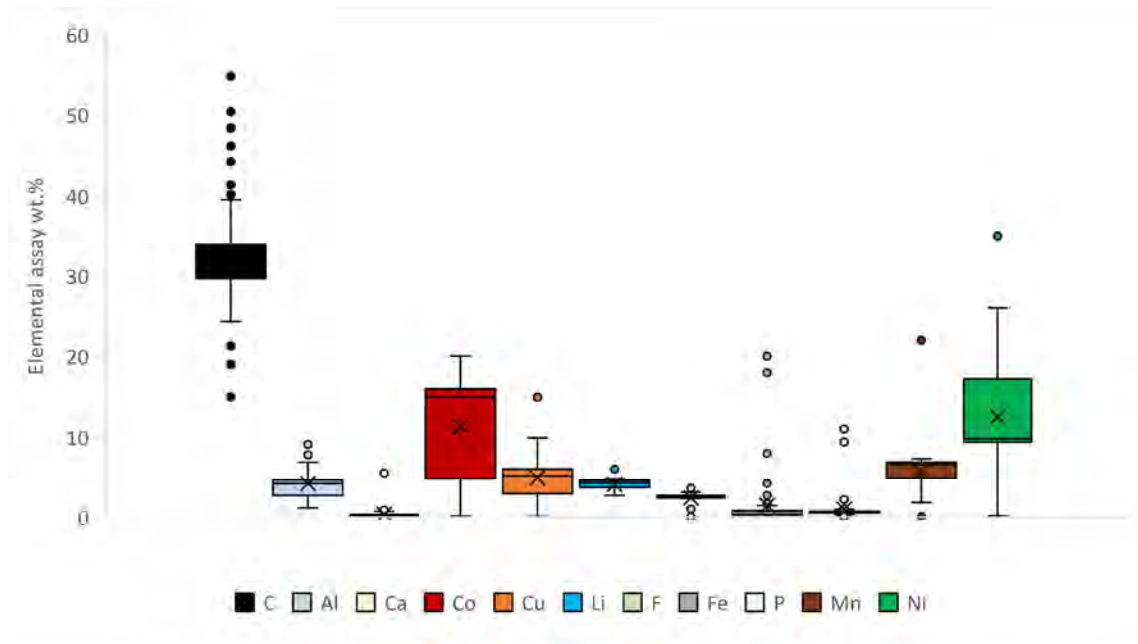


Figure 1 – Variability of Black Mass samples received from 20 suppliers showing box-whisker plots and average value (cross marker). Carbon is analysed by Hot extraction and other elements by microwave digestion-ICP-MS.

BM from two distinct pretreatment routes were elected for plant campaigns. The analytical assays for these two BM types are presented below in Table 1. The pyrolysed BM has significantly higher Co content than the unpyrolysed BM. This material came from an active recycling operation and the high Co is believed to originate from Li-Cobalt-Oxide battery material more common in consumer electronics. The un-pyrolysed material seems to be of the 6:2:2 NMC cathode material origin, more common in EV applications.

Table 1 – Average elemental assay of key elements for the specific BM samples used in the Aurubis Pilot plant.

Pilot Plant BM	C	Al	Ca	Co	Cu	Li	F	P	Mn	Ni
Pyrolysed BM (Campaigns 1-3) Average wt.%	31.03	4.44	0.29	16.03	5.62	4.45	2.66	0.72	6.85	9.55
Un-pyrolysed BM (Campaign - 4) Average wt.%	48.47	1.88	0.013	3.51	1.47	3.46	2.38	0.5	4.35	15.5

PILOT PLANT STAGE 1 COMMISSIONING AND TROUBLESHOOTING

BM lab exploration started with both pyrolysed and un-pyrolysed Nickel-Cobalt-Manganese (NCM) based BM samples. Literature review informed the direction of initial test-work in the realm of oxidative and reductive acidic leaching using Sulphuric acid and various reagents. Aurubis produces of the order ~3500 t Nickel per year as a crude NiSO₄ crystal as an intermediate primarily from the Copper electrorefining tank house bleed solution. Therefore, the first envisaged process for BM thought to produce a similar intermediate that could be blended and sold or further refined as seen fit.

The main challenges encountered in concept flowsheet development were.

- Input material variability
 - Un-pyrolysed BM often resulted in severe foaming behaviour during leaching, especially with gaseous reagents, leading to reactor over frothing. This was believed to result from unpyrolyzed vacuum drying not removing all the organic binders and electrolyte constituents.

- Impurity elements
 - Copper and Aluminium are significant impurities by weight due to their role as current collector foils and they leach to some extent, requiring separation from desired end products.
 - Iron is present usually from the battery casing and components, it also leaches and requires separation from the desired end products.
 - Fluorine and Phosphorous stemming from LiPF_6 electrolyte constituent or similar salts used in the battery electrolyte. Fluorine is a concern when operating in acidic conditions and is not desirable in any product streams.
- Synergism with Aurubis' existing processes (NiSO_4 production)
 - The addition of concentrated sulphuric acid added before Ni-evaporation to promote organic species destruction and depress NiSO_4 solubility for a high yield producing a similar crude $\text{NiSO}_4 \cdot x\text{H}_2\text{O}$ crystal to what Aurubis already produces.
- Reagent selection
 - Oxidant reagents
 - Reductant reagents
 - Neutralising reagents

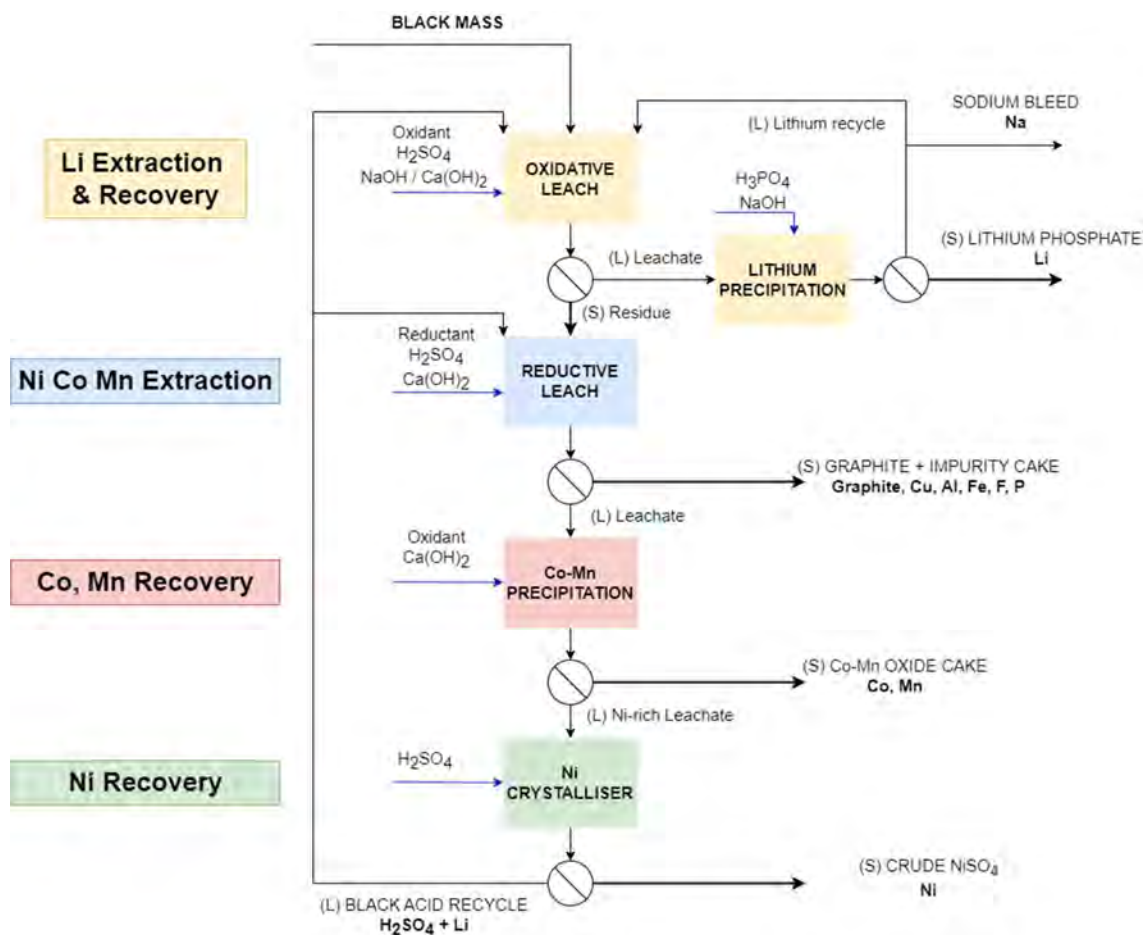


Figure 2 - Flowsheet 1, the Pilot plant was designed based on this flowsheet developed at Laboratory scale.

Figure 2 above, shows the process flowsheet that was the result of Laboratory scale development and the process that the Pilot plant was designed to emulate.

The Pilot plant consists of a mixture of stirred Glass and Metal reactors of 50 – 200 L volume with Filtration equipment (0.1 m² to 0.22 m² Pressure filters, Vacuum filtration).



Figure 3 – Photograph of the Pilot plant showing Reductive leach system and Lithium evaporation system.

The first oxidative leaching step was performed at mildly acidic conditions with a strong oxidising agent to promote de-lithiation of the Cathode-active-material (CAM) Ni-Mn-Co-oxide structure rather than the complete dissolution of that structure. In this way Li was leached to a sulphate solution, which after neutralisation was practically free of other metals. Filter cake wash water was recycled to provide initial suspension water.

The Li solution was then forwarded to an evaporation/precipitation step. The Li-phosphate product was selected due to its low solubility and high potential yield. Phosphoric acid was added with continuous sodium hydroxide addition to maintain alkaline conditions. The filtrate from this step was recycled to the first leaching process to recover the low residual concentration Li with a bleed for Na concentration control.

The residue from the first oxidative leach was re-suspended and forwarded to the reductive leaching step which is more strongly acidic and uses reducing conditions to fully dissolve any remaining metal-oxide structure allowing almost complete recovery of Ni/Co/Mn and remaining Li to solution. Lime was added at the end of this process to partially precipitate impurities (e.g., Al/Cu/Fe/F) and importantly shift pH out of the HF activity zone. Filter cake wash water from this stage was used as re-pulping water for the residue coming from oxidative leaching.

The leachate from the reductive leach process was then re-processed with oxidant to selectively precipitate Co and Mn from solution and therefore produce a Ni-rich sulphate solution. This Ni-leachate was acidified and evaporated to produce the $\text{NiSO}_4 \cdot x\text{H}_2\text{O}$ crystal product and the concentrated "Black acid" leftover after filtering the crystals was used to substitute fresh sulphuric acid in the upstream processes and ultimately recovers the contained Li (~10% of Li is recovered via this manner).

Two Pilot campaigns operated with Flowsheet 1 configuration with the aims listed below. Campaign 1 encountered several equipment breakdown issues and was used for plant commissioning and confirming if optimised conditions from the Lab test work did also hold at Pilot scale. Campaign 2 was a lock-cycle campaign where the main aim was to achieve Black acid recycle and study how impurities built up in each area with consistent recycling of wash waters.

Campaign 1 – Commissioning and Optimisation

- Equipment commissioning through all process steps.
- Developing operating instructions and protocols.
- Temperature, pH and batch duration optimisation confirmation for leaching and precipitation processes.

Campaign 2 – Flowsheet 1 Lock-cycle attempt

- Metal recovery and distributions to close the Mass Balance and underpin a Process model and Process Design Criteria for Engineering Cost Studies.
- Study how and where impurities build up with Cake wash water and NiSO₄ mother liquor recycle streams.
- Measure steady state reagent consumptions for OPEX estimation.
- Produce kg scale product samples and assay product quality for commercial considerations.

Product Quality – Campaign 2

Table 2 shows the Li-phosphate produced contained significant amounts of sodium and fluorine. These are present due to the evaporation stage to increase Li concentration prior to precipitation. The evaporation together with NaOH addition formed Na₂SO₄ at saturation. These impurities should be avoidable with further product washing and re-filtration. The fluorine impurities were assumed to be a LiF precipitate formed during evaporation.

Table 2 - Lithium Phosphate product quality from Pilot Campaign 2.

Li ₃ PO ₄	Li	P	Al	Co	Cu	F	Fe	Mn	Na	Ni
Average (%)	17.6	19.7	0.09	0.01	0.01	2.98	0.01	0.00	2.59	0.01
Min. (%)	15.0	17.0	0.005	0.001	0.001	0.78	0.001	0.001	0.001	0.001
Max. (%)	21.0	22.0	0.23	0.024	0.01	6.3	0.045	0.0062	6.3	0.013

The advantage of Li-phosphate production is a very low solubility limit (~0.3 g/L Li) which enables a very high yield from less concentrated Li-filtrate, for example compared to Li-carbonate (~3-4 g/L Li solubility limit). The disadvantages of this were the high cost of Phosphoric acid and the need for addition Caustic soda as neutralising agent adding to the Na-load of the circuit.

Table 3 Co-Mn Oxide Filter Cake product quality from Pilot Campaign 2.

Co-Mn Cake	Co	Mn	Al	Ca	Cu	F	Fe	Li	Ni	P	H ₂ O
Average (%)	13.06	7.76	0.51	14.43	1.87	0.34	0.49	0.02	0.84	0.03	56.9
Min. (%)	3.60	3.80	0.18	10.00	0.42	0.05	0.05	0.01	0.26	0.01	46.1
Max. (%)	19.00	23.00	1.20	16.00	3.00	0.56	3.10	0.13	2.10	0.15	62.0

The Co-Mn precipitation filter cake contains a high proportion of Gypsum due to Lime addition during the reaction to control pH (as the Co/Mn oxidation reaction produces acid). A portion of Al, Cu, Fe and Ni reported to this Filter cake. Fe likely precipitated as Ferric sulphate due to the oxidative conditions, but Al/Cu/Ni should have remained in solution at this process pH and could have been present due to poor Filter cake washing or localised precipitation due to Lime suspension dosage and mixing conditions. It is undesirable to lose any Ni to this product, however a high recovery of Co and Mn and separation from the remaining Ni filtrate was achieved, which should have effectively removed Co and Mn from the Nickel product.

Table 4 - Acidic NiSO₄.xH₂O crystal product quality from Pilot Campaign 2.

NiSO ₄ .xH ₂ O	Ni	Al	Ca	Co	Cu	F	Fe	H ₂ SO ₄	Li	Mn	P
Average (%)	15.79	0.1	1.68	1.25	3.93	0.09	0.09	19.74	0.18	0.18	0.01
Min. (%)	7.10	0.05	0.03	0.14	1.10	0.01	0.02	12.00	0.04	0.03	0.01
Max. (%)	20.30	0.3	4.40	3.10	5.90	0.30	0.28	31.30	0.29	0.26	0.01

Aurubis currently produces an acidic NiSO₄ intermediate with ~23 wt.% Nickel and ~15 wt.% H₂SO₄ content. However, producing this type of NiSO₄ crystal from BM comes with some additional concerns, with Fluorine being concentrated during evaporation at highly acidic conditions. This means both personal safety concerns due to HF risk and materials of construction are both troublesome. The impurity profile is also very high, with especially Cu crystallising out at this step, not being removed in previous process steps.

Recoveries – Campaign 2

Unfortunately, overall Campaign 2 mass accountability was $< \approx 70\%$ due to several factors. Therefore, overall recoveries were calculated using HSC Sim modelling, with the stage-by-stage elemental distribution from the Pilot plant results. Individual process step accountability was generally $> 90\%$, however the overall mass accountability for the whole Pilot campaign was not acceptable to the R&D team. Improving mass balance accountability was a major focus of the following campaigns described below.

From the HSC Sim modelling, $> 95\%$ recoveries of Li, Co and Mn to their main products were calculated. However, Ni recovery to NiSO_4 product was $< 90\%$, with significant losses in the reductive leaching stage (attributed to poor leaching efficiency, filtration and washing), Co-Mn filter cake (attributed to $\text{Ca}(\text{OH})_2$ mixing, filtration and washing) meaning recovery was only calculated to be 82% .

Table 5 – Pilot Campaign 2 overall elemental recovery to output streams.

Distributes To	Al %	Co %	Cu %	Li %	Mn %	Ni %	F %
Li-Phosphate/Li-Filtrate	0	0	0	<u>96</u>	0	0	47
Graphite-Impurity Cake	<u>78</u>	3	<u>17</u>	1	3	7	<u>27</u>
Co-Mn Oxide Cake	21	<u>96</u>	61	1	<u>96</u>	11	26
Ni-Sulphate	1	1	22	2	1	<u>82</u>	< 1
Overall Mass Accountability	75	67	59	66	70	60	57

PILOT PLANT STAGE 2 . FLOWSHEET EVOLUTION AND FOCUS ON ACCOUNTABILITY

Issues Discovered from Campaign 1 and 2

1. Nickel recovery $< 90\%$.
2. H_3PO_4 cost to produce Li_3PO_4 product.
3. High amount of NaOH addition leading to Na in Li-product and requiring Na-removal or large bleed stream. Cost of NaOH.
4. Fluorine department to products, especially to the Lithium stream.
5. Acidic NiSO_4 purity and Fluorine levels in acidic crystalliser liquid/mother liquid.
6. $< \approx 70\%$ overall accountability due to Pilot plant operation and mass loss meaning a poor level of confidence for mass balancing and PDC.

Solutions

1. Improve Filtration and Cake washing in Reductive leach and Co-Mn Precipitation while improving $\text{Ca}(\text{OH})_2$ addition to minimise unwanted localised precipitation.
2. Change to a Li-carbonate product to remove Phosphoric acid from the process.
3. Substitute a portion of NaOH with $\text{Ca}(\text{OH})_2$ during neutralisation of oxidative leach liquor to prevent F department to the lithium stream.
4. Quantitatively remove Na from the system as Glauber salts and produce Anhydrous Na_2SO_4 as a by-product.
5. Change to conventional $\text{NiSO}_4 \cdot 6\text{H}_2\text{O}$ Crystallisation with pre-evaporation to concentrate impurities before a specific Impurity removal step with Lime before final NiSO_4 crystallisation stage.
6. No NiSO_4 acidification, i.e., no black acid production, Ni-mother liquor recycled completely to Oxidative leaching step for Li recovery.
7. Target $> 90\%$ mass accountability for next campaign
 - a. Process steps were collected under an overall Pilot Plant batch integrity concept.
 - b. All wastewater, sump water and solids reporting to the sump were collected, mass or volume recorded and assayed.
 - c. Sampling plan focussed entirely on elemental mass accounting for each batch and kinetic samples were not taken.
 - d. Start empty and finish empty philosophy, with a planned flush out and clean out of each reactor system was performed after their final batch, end Wash waters were forwarded to next process step for processing, all culminating in filtering the sump contents.

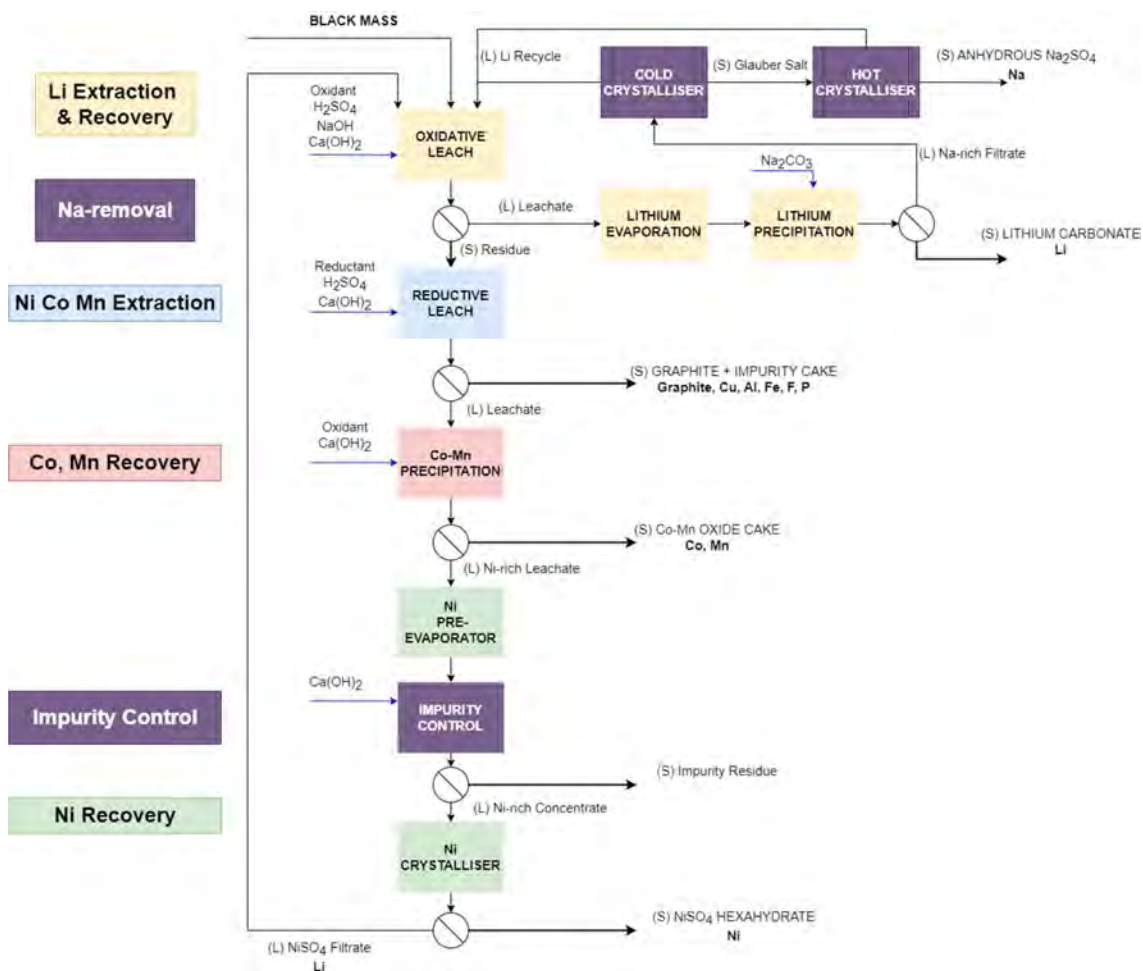


Figure 4 - Flowsheet 2, Campaign 3 flowsheet was updated to solve the problems encountered after Piloting the first flow sheet

The Stage 2 flowsheet shows the changes made after reviewing the problems encountered in Campaign 1 and 2 (Figure 4 above). The Pilot plant was adapted to suit these added process steps with new reactors installed for Li_2CO_3 , Na_2SO_4 , Impurity removal and $NiSO_4$ crystallisation steps. The original Li precipitation reactor was still used for evaporation so as to concentrate the Li filtrate to > 20 g/L [Li] for better yield of Li-carbonate and the original Ni evaporator was used for the bulk pre-evaporation before the smaller volume being transferred to Impurity removal and final crystallisation.

Product Quality – Campaign 3

Li-carbonate produced was a significant improvement in terms of impurities when compared to the earlier Li-phosphate product. Partial $Ca(OH)_2$ addition during Oxidative leach neutralisation stage was found to precipitate fluorine to < 100 ppm in Neutral leach filtrate. Therefore, fluorine levels in the Li product were much lower.

Table 6 – Lithium Carbonate product quality from Campaign 3

	Li_2CO_3	Li	C	Al	Ca	Co	Cu	F	Fe	Mn	Na	Ni
Average (%)	18.64	16.12	0.002	0.14	0.02	0.001	0.165	<0.01	0.002	0.322	0.003	
Min. (%)	18.52	16.02	0.000	0.01	0.00	0.000	0.080	<0.01	0.000	0.240	0.000	
Max. (%)	18.71	16.18	0.003	0.3	0.05	0.002	0.320	<0.01	0.005	0.560	0.007	

Pre-evaporation of the Li filtrate up to the point of Li sulphate solubility allows for a large portion of Calcium to be removed as insoluble $CaSO_4$ and CaF_2 before carbonate precipitation. Li-carbonate precipitation with saturated Na_2CO_3 solution did result in some Na_2SO_4 salting out into the Li-carbonate product but this was effectively washed out of the Li_2CO_3 cake with hot water and could be further

improved by additional washing steps. Further purification by pre-treatment to remove di-valent cations and Fluorine would result in a technical grade Li-carbonate.

Table 7 below shows that Campaign 3 Co-Mn oxide filter cake was relatively similar to Campaign 2, considering no changes were made to the Reductive leach or Co-Mn precipitation stages.

Table 7- Co-Mn Oxide Filter Cake product quality from Pilot Campaign 3

Co-Mn Cake	Co	Mn	Al	Ca	Cu	F	Fe	Li	Ni	P	H ₂ O
Average (%)	12.77	5.86	0.66	14.50	2.33	0.49	0.42	0.01	0.84	0.02	51.83
Min. (%)	12.00	5.00	0.06	13.00	0.38	0.36	0.28	0.00	0.26	0.01	43.90
Max. (%)	13.00	6.50	0.84	15.00	3.60	0.60	0.49	0.03	2.10	0.04	58.37

The Nickel sulphate hexahydrate crystal product produced was acid-free and also with significantly lower amounts of impurities (Al, Cu, F, Mn, Co). Therefore, much more suitable to further refining than the acidic NiSO₄ produced in Campaign 2. Sodium impurities were still present due to the relatively minor amounts of Na making its way via the Oxidative leach residue cake into the rest of the process.

Table 8 – Acid-free Nickel Sulphate hexahydrate crystal product produced from Pilot Campaign 3

NiSO ₄ .6H ₂ O	Ni	Al	Ca	Co	Cu	F	Fe	Na	Li	Mn	P
Average (%)	16.26	0.011	0.18	0.25	0.25	0.05	<0.01	2.61	0.32	0.033	0.10
Min. (%)	14.69	0.002	0.11	0.14	0.05	0.005	<0.01	1.14	0.24	0.006	0.07
Max. (%)	16.95	0.03	0.23	0.98	0.59	0.09	<0.01	4.87	0.38	0.085	0.14

Recoveries – Campaign 3

Campaign 3 recoveries were calculated from measured masses, volumes, densities and elemental assays performed by the Aurubis Analytical Lab in Hamburg. For Li, Co and Mn the overall recovery to products was comparable to Campaign 2 at > 95%, with Ni being the major change dropping to 73% recovery to NiSO₄ product. Ni losses to Graphite cake and Co-Mn product were marginally lower due to filtration and washing improvements, however, the Impurity control process-step resulted in significant Ni recovery losses (although being an effective quantitative removal of Fluorine plus other impurities). The overall mass accountability of Campaign 3 was good with total mass, water and most value elements being accounted for at > 90%. Fluorine accountability remained a problem indicating a potential issue with analysis or unmeasured losses (e.g., Off-gas). Campaign 3 achieved the main goal of producing a result with a sufficient level of confidence to generate a mass balance and process design criteria to underpin a feasibility study.

Table 9 - Pilot Campaign 3 overall elemental recovery to output streams.

Distributes To	Al %	Co %	Cu %	Li %	Mn %	Ni %	F %
Li-Carbonate	0	0	0	<u>95</u>	0	0	<1
Graphite-impurity cake	<u>71</u>	2	<u>24</u>	2	2	5	<u>36</u>
Co-Mn Oxide Cake	17	<u>97</u>	35	< 1	<u>97</u>	10	26
Impurity removal cake	12	< 1	20	2	< 1	12	38
Ni-Sulphate	0	1	21	1	1	<u>73</u>	<1
Mass Accountability	92	90.8	98	98.5	91.6	93.7	70

PILOT PLANT STAGE 3 - UNPYROLIZED BLACK MASS AND FURTHER FLOWSHEET EVOLUTION

Issues discovered in Campaign 3

- Na-removal from the process resulted in voluminous amounts of Glauber salts and scaling this process up is not trivial in terms of CAPEX/OPEX and sale of ensuing volumes of anhydrous Na₂SO₄ (which must be of a high purity).
- Li-carbonate production was straightforward and produced a higher-quality product but still required Na-input like the Li-phosphate product.
- Specific Impurity control step was successful in removing impurities before Ni-crystallisation but resulted in significant Ni losses.
- The Co-Mn oxide product has a high impurity profile and therefore complicates further Co refining.

Solutions

- Full substitution of NaOH with Ca(OH)₂ in the Oxidative leach neutralisation step. This has a downside, increasing the solid residue and consequently the sizing and cost associated with solid-liquid separation step. However, usage of Lime at this stage is important for impurity rejection from the Lithium product stream.
- Produce a Li sulphate concentrate solution or Li₂SO₄.H₂O crystal product to have a Na-free circuit.
- Impurity control precipitation moved upstream of Co-Mn precipitation to reject impurities from the Co and Ni products. Recycling of Impurity residue back to Reductive leach to recover entrained Ni/Co and force impurities out via the Graphite residue.
- Develop further treatment of Co-Mn Oxide product to produce a CoSO₄ intermediate and Mn-residue separately.

Extensions

- Un-pyrolised BM feed material was used and its impact on the process, recoveries and product quality could be studied.
- Included Graphite recovery process via Flotation in process flowsheet and continued sending Reductive leach residue for flotation amenability and flowsheet test-work.

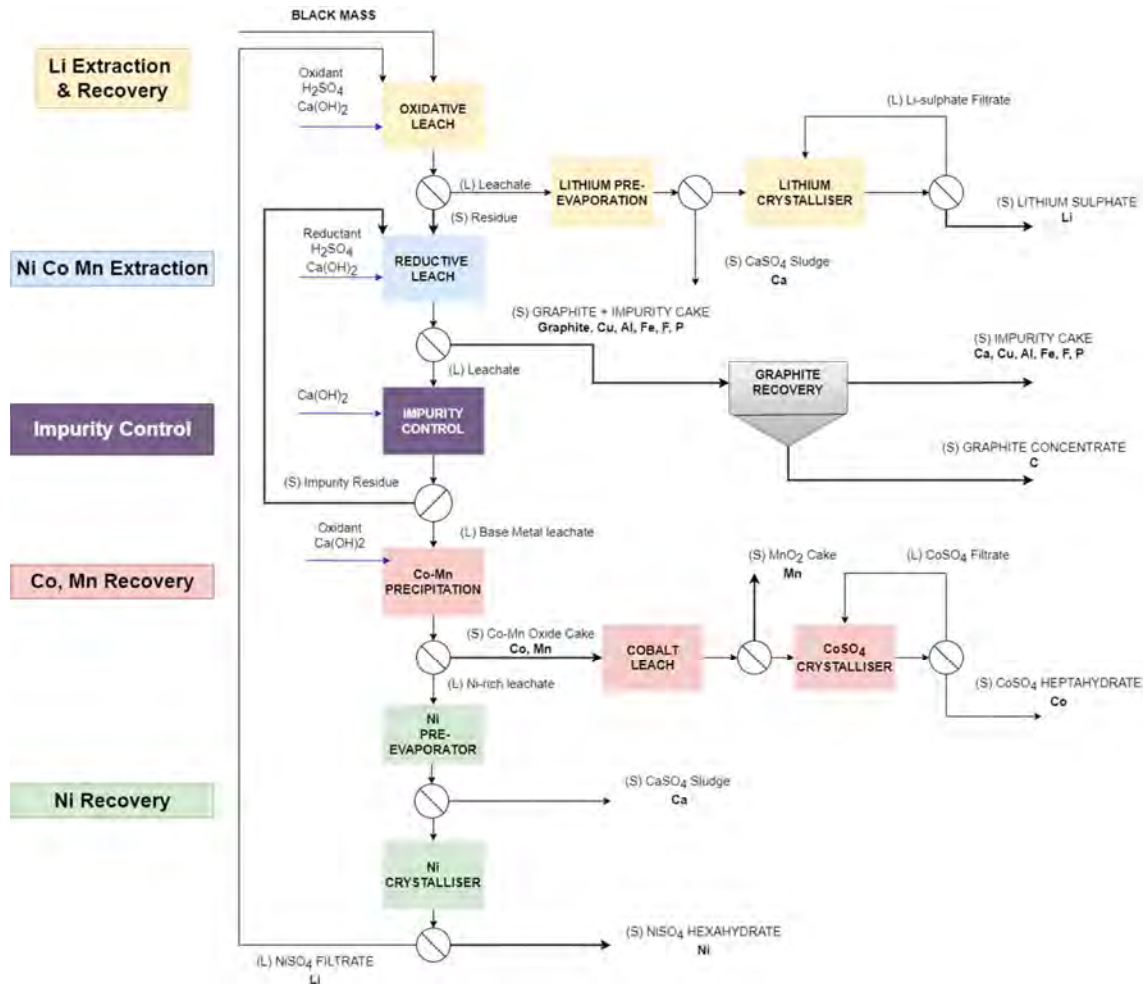


Figure 5 - Flowsheet 3, Pilot Campaign 4 was updated to address problems discovered in Campaign 3 while Graphite and CoSO_4 production are now included in the holistic view.

Figure 5 shows the evolution of the flowsheet to its present form. In the core process there was no longer a need for Na-removal and the Impurity control step was moved before Co-Mn Precipitation to improve product quality. Graphite recovery from the Reductive leach residue has been presented recently and consists of conventional flotation process producing a >95 % Carbon grade concentrate with ~85% carbon recovery [3]. Co was re-dissolved from the Co-Mn precipitate cake selectively over Mn and the resulting Co-rich sulphate liquor was evaporated and crystallised to form a $\text{CoSO}_4 \cdot 7\text{H}_2\text{O}$ crystal.

Product Quality – Campaign 4

Both the Li sulphate solutions and the single batch of crystals produced from Campaign 4 still had very low F content with the benefit of virtually eliminating sodium. Calcium and Fluorine could potentially be further reduced with ion exchange treatment if required. Pre-neutralisation with only lime had the benefit of eliminating most of the F and base metals from the Li stream while negating the need to introduce sodium to the stream.

Table 10 – Lithium sulphate products from Campaign 4, 2 batches of concentrated Lithium solution were produced and a single batch of Lithium sulphate monohydrate crystals were produced.

Li ₂ SO ₄ Concentrate	Li	Al	Ca	Co	Cu	F	Mg	Mn	Na	P
Batch 1 g/L	25	< 0.01	0.37	<0.01	<0.01	0.1	0.02	<0.01	1.3	2.4
Batch 2 g/L	31	< 0.01	0.37	< 0.01	< 0.01	<0.1	0.04	< 0.01	0.54	2.9
Li ₂ SO ₄ .H ₂ O Crystals	Li	Al	Ca	Co	Cu	F	Mg	Mn	Na	P
Single batch wt. %	10.65	<0.005	0.103	<0.005	<0.005	0.76	<0.005	<0.005	0.076	0.18

The main differences in the Co-Mn Oxide cake produced from this stage is explained in terms of the difference in feed BM to Campaign 1 - 3 versus Campaign 4. The pyrolysed BM for campaigns 1-3 had much high Co and lower Ni than the unpyrolyzed BM and as such the Co-Mn oxide filter cake had lower levels of Co and relatively higher content of Ni most probably due to insufficient wash out the high Ni containing filtrate from campaign 4. The lower Al, Cu and Fe values reflect the impurity removal step included before this stage (Figure 5).

Table 11 - Co-Mn Oxide cake produced from Campaign 4

Co-Mn Cake	Co	Mn	Al	Ca	Cu	F	Fe	Li	Ni	P	H ₂ O
Average (%)	9.08	5.86	0.13	15.62	0.645	0.30	0.02	0.01	2.68	0.02	55.98
Min. (%)	7.75	5.00	0.018	15.0	0.17	1.1	0.01	< 0.01	2.05	0.01	44.91
Max. (%)	9.95	6.50	0.52	17.0	2.2	0.1	0.03	0.03	4.15	0.04	66.40

The selective leach of Co from the Co-Mn Oxide cake yielded good results in terms of separating the Co from the Mn improving it for further refining. The next opportunity for optimisation would be the removal of Ni (and also Cu) which would also represent a recovery opportunity for Ni in the overall flowsheet.

Table 12 – Cobalt sulphate crystal product produced at laboratory scale from Pilot plant Co-Mn oxide cake from Campaign 4.

CoSO ₄ .7H ₂ O	Co	Al	Ca	Ni	Cu	F	Fe	Na	Li	Mn
Single batch wt. %	13.96	0.08	0.1	4.67	1.38	0.01	< 0.01	< 0.01	0.005	< 0.01

The Ni-sulphate hexahydrate produced during Campaign 4 had a substantially higher Ni content than Campaign 3 mainly due to the reduction in sodium. The impurity removal stage relocated to before the CoMn precipitation stage still yielded the same benefits in terms of Cu, Al, Fe and F reduction in the final crystal. Reduced levels of Co and Mn as compared to Campaign 3 resulting from improved operation of the Co-Mn precipitation stage also contributed to the crystal quality.

Table 13 – Nickel sulphate hexahydrate crystal product produced from Campaign 4

NiSO ₄ .6H ₂ O	Ni	Al	Ca	Co	Cu	F	Fe	Na	Li	Mn
Single batch wt. %	21.84	0.009	0.41	0.084	0.014	0.078	0	0	0.26	0.017

Graphite Flotation Extension

Table 14 below highlights the quality of Graphite obtainable by conventional flotation of the main Aurubis Hydromet process residue. The Graphite concentrate was produced by lock-cycle flotation flowsheet testing from Campaign 3 Graphite-Impurity Filter cake.

Table 14 – Graphite concentrate produced from lock-cycle flotation test-work using Campaign 3 reductive leach residue as feed material.

Flotation Concentrate	C	Al	Ca	Ni	Cu	Fe	Li	Mn
Washed Lock Cycle Con. wt. %	96.7	1.35	0.48	0.093	0.18	0.175	0.02	0.01

Recoveries – Campaign 4

Table 15 shows that accountabilities > ≈90% were achieved in Campaign 4 with a few exceptions. The Cu accountability of 130% is assumed to be a result sampling inconsistency of Cu content in BM feed material. Cu is usually present in larger particle size distribution and despite sieving and attempted representative sampling it is probable that there was large size Cu segregation in sample containers. Fluorine accountability remains consistently < 70% in all campaigns and more effort will be devoted to analytical techniques for solids and liquids and checking effluents from all parts of the pilot plant. From a recovery perspective, a significant improvement in Ni recovery was made when compared to previous campaigns. This was mostly driven by improved leaching of Ni in the Reductive leach stage but also by successful recycling of the Fluorine-Impurity filter cake. However, Ni distribution to the Co-Mn Oxide cake or CoSO₄ product is a clear opportunity for improving Ni recovery to NiSO₄ product and should be investigated.

Table 15 - Pilot Campaign 4 overall elemental recovery to output streams.

Distributes To	Al %	Co %	Cu %	Li %	Mn %	Ni %	F %
Li-Sulphate	< 1	< 1	< 1	<u>96</u>	< 1	< 1	1
Graphite-Impurity Cake	<u>95</u>	2	<u>84</u>	1	2	1	<u>91</u>
Co-Mn Oxide Cake	3	<u>96</u>	13	<1	<u>97</u>	7	4
Ni-Sulphate	2	2	3	3	1	<u>92</u>	4
Mass Accountability	101	107	130	95	91.6	99	64

CONCLUSIONS AND FUTURE DIRECTION

In this paper the evolution of the Aurubis BM recycling process has been discussed following the progress made through 4 piloting campaigns. There is a vast amount of open domain literature focused on individual unit operations, mostly leaching, required to treat or recycle Li-Ion BM. However, a fully integrated flowsheet is required to do this commercially and there is a paucity of information available in the open domain regarding this. Particularly lacking is process descriptions, impurity management and department, value element recovery and product or intermediate product quality, reagents utilised, and byproducts produced. Most presentations or publications of pilot plant operations typically only present overall claimed recoveries of value elements with very little information on the pilot plant campaign accountability which provides the reader with very little insight into the level of confidence one can expect in these results.

So far, Aurubis R&D has focussed on developing a robust process to maximise recovery of all valuable components as intermediates as opposed to battery grade products. For example, contrary to many Battery recycling processes, Aurubis has developed Graphite recovery, which is undervalued by the industry (particularly Pyrometallurgical processes), as it represents a large mass of Li-ion batteries and is not foreseen to be replaced as the main anode-material^[4].

The process which has been piloted several times with a high level of confidence, has evolved into a robust process with the following distinguishing attributes:

- Processing pyrolysed and un-pyrolysed BM feed types
- Solvent extraction free core separation process
- Li-first recovery
- Graphite recovery
- Sodium free process

The process is continuously being developed along with demo plant scale equipment being commissioned this year for certain unit operations.

AUTHOR ACKNOWLEDGMENTS

The authors wish to acknowledge the contribution of the whole Aurubis R&D department, Hydrometallurgy Lab team, Analytical Laboratories, and support from other teams across the business that make this work possible.

REFERENCES

- [1] EP/EU, *Directive 2006/66/EC of the European Parliament and of the Council of 6 September 2006 on batteries and accumulators and waste batteries and accumulators and repealing Directive 91/157/EEC*, European Parliament, Council of the European Union, 2006.
- [2] EP/EU, "Regulation (EU) 2023/1542 of the European Parliament and of the Council of 12 July 2023 concerning batteries and waste batteries, amending Directive 2008/98/EC and Regulation (EU) 2019/1020 and repealing Directive 2006/66/EC," European Parliament, Council of the European Union, 2023.
- [3] R. Rahbani, A. Harris and L. Bryson, "The introduction of a graphite flotation step in the patent pending Aurubis Hydrometallurgical flowsheet used for recycling of Li ion battery Black Mass," Cape Town, 2023.
- [4] N. Verbaan, "Review of Hydrometallurgical Flowsheets for Processing Black Mass," Detroit, 2023.

MATTE SMELTING AND PURIFICATION PROCESS FOR RECYCLING OF EOL-LiB

By

Joon Sung Choi, Jin Gyun Park, Byong Pil Lee, Jong Ho Kim, Min Seok Seo, So Won Choi
Research Institute of Industrial Science and Technology (RIST), Republic of Korea

Presenter and Corresponding Author

Joon Sung Choi
melts626@rist.re.kr

ABSTRACT

Recently, as the production of electric vehicles has rapidly increased, the production of lithium-ion batteries containing high-purity valuable metals (Ni and Co) is required. According to the amount of End-of-life lithium-ion batteries (EoL-LiB) has rapidly increased, there is a need to improve environmental issues. However, there are limits to process changes for removing impurities and achieving high purity of diversified recycled resources in hydrometallurgical process for recycling of EoL-LiB. Therefore, a transition to hybrid process capable of mass production is required, and the research was conducted on matte smelting and purification process using recycled resources.

Ni and Co contained in various resources were recovered using molten iron in high-temperature smelting process. The recovery behaviour depending on the type of resource by carbon content was compared with the thermodynamic calculations using FactSage 8.2TM. The alloy containing Ni and Co was concentrated through addition of sulphur and oxygen blowing and smelted into matte with improved concentration of Ni and Co. An aqueous solution containing Ni and Co was obtained through a pressure oxidation leaching (POX), and it was confirmed that the Ni and Co recovery rates were closely related to the ORP and pH of the pregnant leaching solution (PLS). The leachate was highly purified into Ni and Co compound through a neutralization process, and the impurity concentration in the Ni and Co compound was maintained below 0.5%. In order to develop the matte smelting and purification process utilizing recycled resources, process condition was established by engineering software (METSIM).

Keywords: EoL-LiB, Recycling, Nickel, Cobalt, matte smelting, matte purification

MATTE SMELTING AND PURIFICATION PROCESS FOR RECYCLING OF EOL-LIB

Joon Sung Choi

Research Institute of Industrial Science and Technology(RIST)

I. Background

I-(1). RIST Introduction

I-(2). Research Objective

I-(1). Introduction (RIST)

RIST is Korea's first private research institute established in 1987 for the purpose of

“Development of national industrial technology and dissemination of achievements”



○ Main research contents and facilities

[Nickel extraction process]

[LIB recycling process]

[RKEF & PS. Converting process]

- Rotary kiln simulator**
 - Specifications
 - Indirect heating, temperature Max. 900°C.
 - Capacity Max. 2kg/hr.
 - Hydrogen/nitrogen atmosphere
 - Field of use: raw material drying/sintering/reduction
- Submerged arc furnace (SAF)**
 - Specifications
 - DC single phase 280kW(70V, 4000A).
 - Capacity Max. 150~200kg
 - Continuous operation
 - Field of use: ferrous alloys reduction smelting
- Mix-settler for Solvent Extraction**
 - Specifications
 - 20 stages: mixing zone 2L, settling zone 4L
 - Mixed saponification/pH control
 - Field of use: Purification of LIB BP, Matte, MHP/MSP

I-(1). Introduction (RIST)

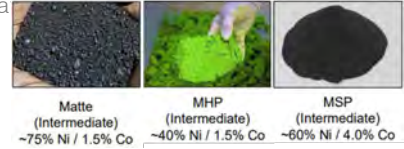


I-(1). Introduction (RIST)

Different smelting processes are required depending on the type of ore.

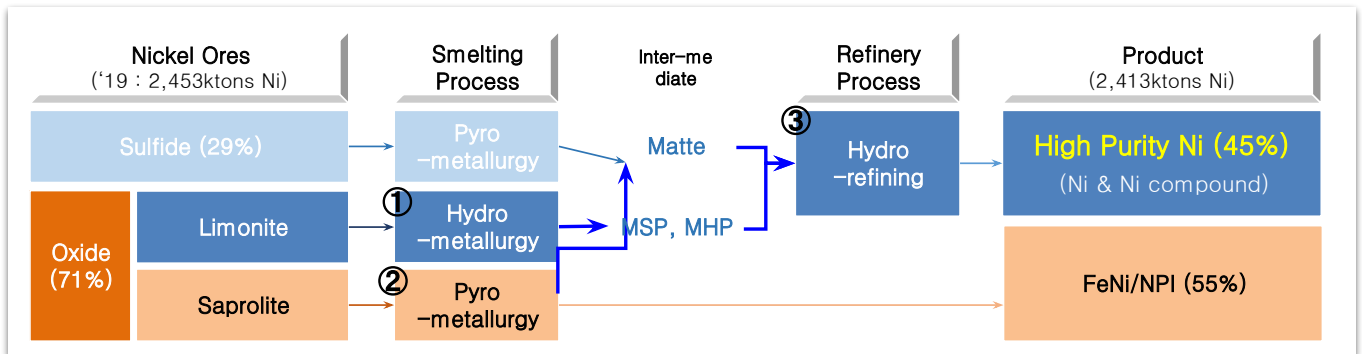
○ **High purity Nickel** is manufactured through refinery process from **Nickel intermediate**

- Nickel Sulfide : Classical method (smelting+converting) to Matte intermediate
- Limonite (Oxide) : Hydrometallurgy to MHP, MSP intermediate
- Saprolite (Oxide) : Pyrometallurgy to Matte intermediate
(RKEF ‡ to FeNi, NPI → using in STS) ‡ Rotary Kiln, Electric Furnace



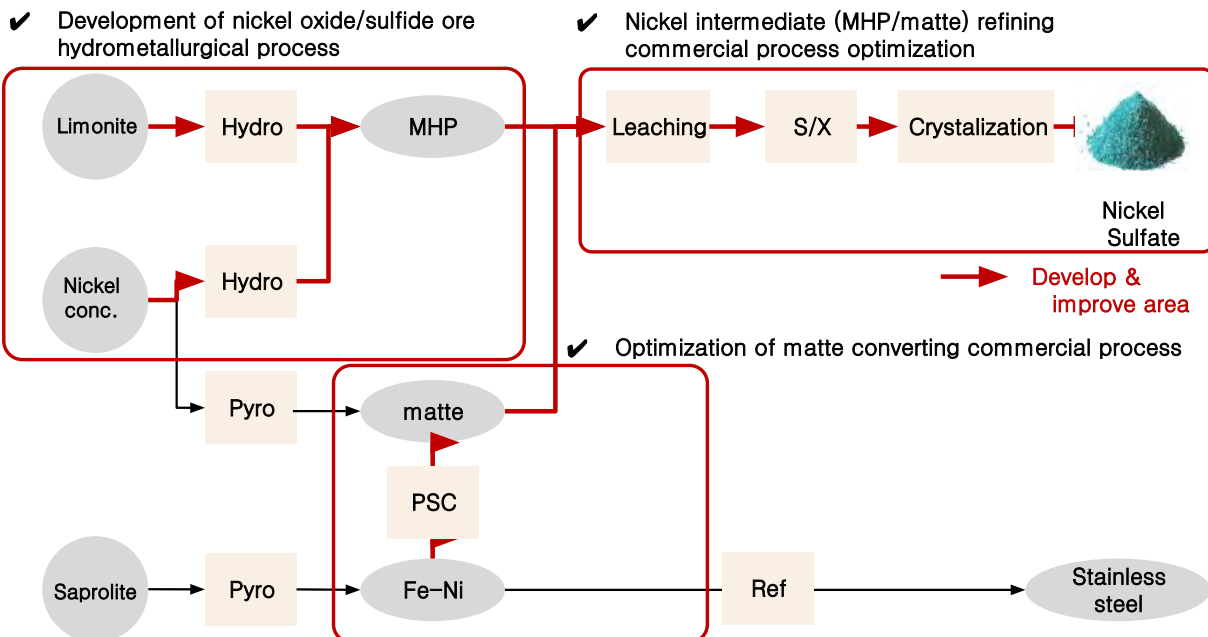
○ **Nickel intermediate**

- **Matte** : High grade Nickel sulfide (Ni_3S_2), Nickel content around 75% (Ni matte : Ni 72%)
- **MHP**(Mixed Hydroxide Precipitate) : Ni, Co mixed hydroxide ($Ni(OH)_2$), Nickel content around 40% (MHP : Ni 42%)
- **MSP**(Mixed Sulfide Precipitate) : Ni, Co mixed sulfide (Ni_3S_2), Nickel content around 60%



I-(1). Introduction (RIST)

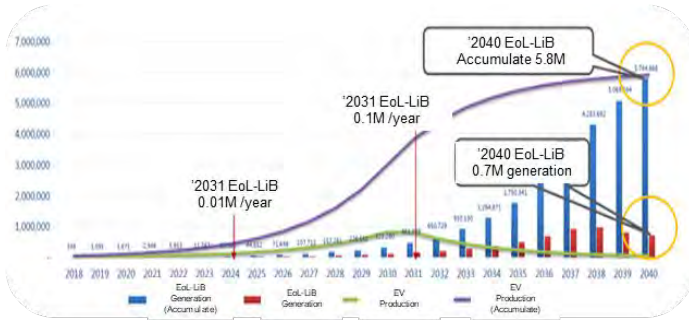
Development of eco-friendly nickel smelting technology and optimization of commercial smelting/refining process



I-(2). Research Objective

Current status of low-quality circulating resources

○ **EoL-LiB market outlook** :As demand for lithium ion batteries (LiB) such as EV and ESS increases, the amount of **EoL-LiB generated increases rapidly**.

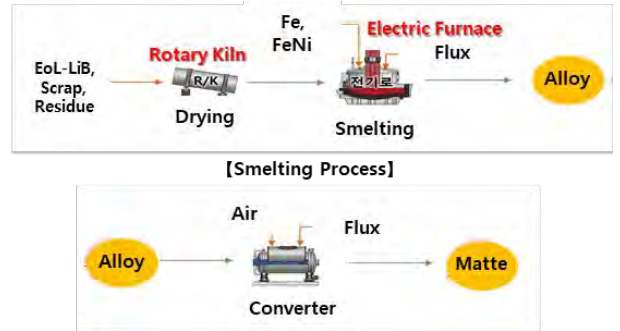


[EoL-LiB Market Outlook]

- As the amount of EoL-LiB is rapidly increasing, the recycling process is also changing from a hydrometallurgy to a pyrometallurgy that can solve **environmental problems and mass production**, or to a **hybrid metallurgy process (pyro & hydro)**. (Umicore, Sumitomo, etc.)

Development of smelting process for recycled resources

○ **Recovery of rare metals** :Aims to develop an economical and eco-friendly process through high-temperature concentration of rare metals (Ni, Co, etc.) utilizing collected metals (Fe, FeNi, etc.)



[Smelting Process]

[Converting Process]

- Optimization of process conditions (**temperature, flux additive, captured metal ratio**) is required through thermodynamic review and experiment of smelting-converter-purification process

I-(2). Research Objective

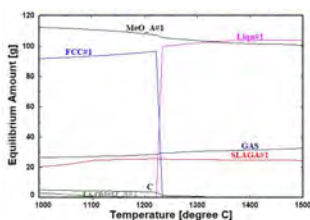
Recycling of EoL-LiB through hybrid metallurgy (Smelting-Convertion-Purification)

○ **Objective** : Technology that collects valuable metals such as Ni and Co from recycled resources in the molten state by using low-cost Fe capture metals and then selectively oxidizes and separates iron using air (oxygen) to concentrate valuable metals.

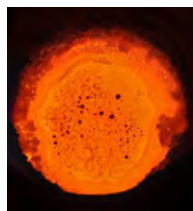


○ **Research** :

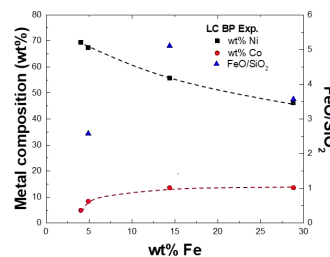
- **Smelting Process** :Recovery of metal using hot metal (Fe, FeNi)
- **Converting Process** :Concentration of metal using Air and sulfur (+ slag recycling)
- **Purification Process** :Purification of metal using autoclave with H_2SO_4 and oxygen



[Thermodynamic Consideration]



[Smelting Process]



[Converting Process]

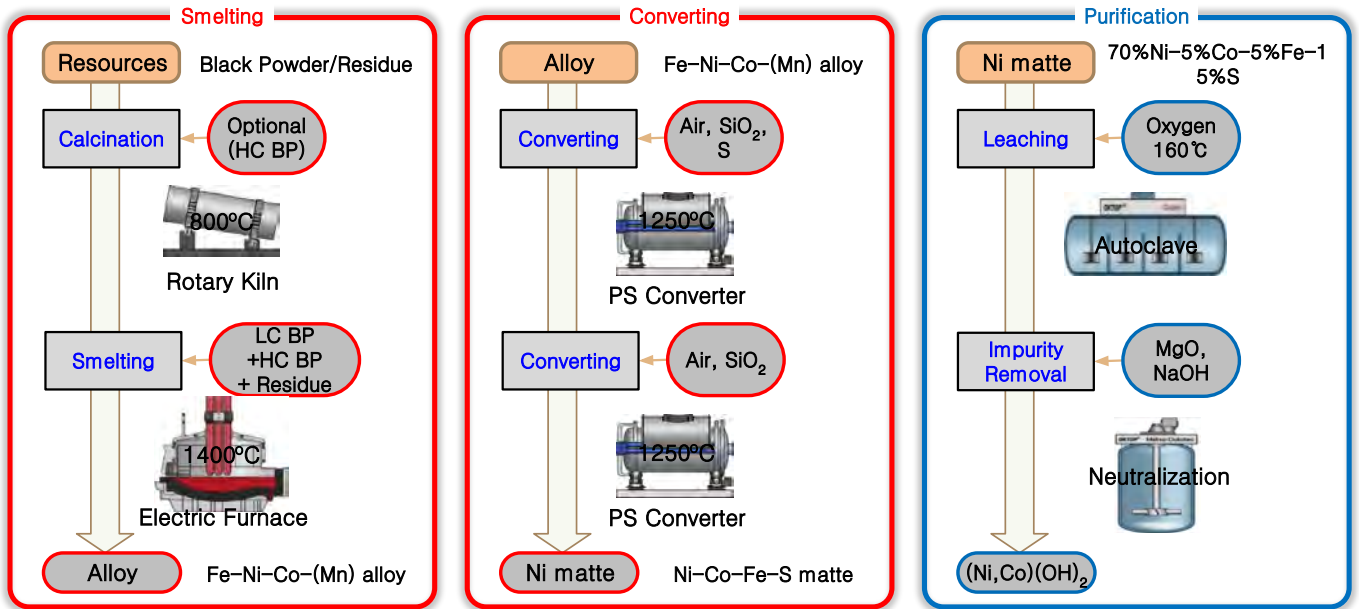


[Purification Process]
384/395

I-(2). Research Objective

■ Recycling of EoL-LiB through hybrid metallurgy (Smelting-Convertng-Purification)

○ **Objective** : Technology that collects valuable metals such as Ni and Co from recycled resources in the molten state by using low-cost Fe capture metals and then selectively oxidizes and separates iron using air (oxygen) to concentrate valuable metals.

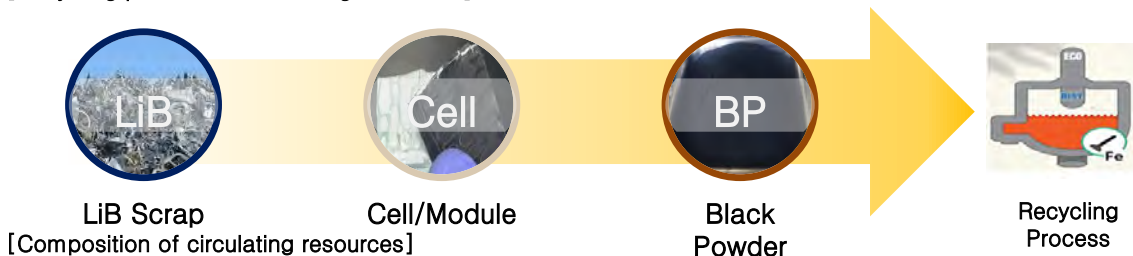


I-(2). Research Objective

■ Circulating resources

- ① Low Carbon Black Power (LC BP)
- ② High Carbon Black Power (HC BP)
- ③ Residue (Petroleum catalyst residue)

[Recycling process of circulating resources]



	Oxide (wt%)						
	Li ₂ O	NiO	CoO	MnO ₂	Al ₂ O ₃	C	sum
LC BP	15wt%	40wt%	10wt%	10wt%	-	2wt%	-
HC BP	10wt%	20wt%	10wt%	10wt%	5wt%	30wt%	-
Residue	-	8wt%	1wt%	-	80wt%	-	-

[Research Method]

- ① Thermodynamic Calculation (FactSage™)
- ② Smelting & Converting process (Pyro-Lab test)
- ③ Purification process (Hydro-Lab test)
- ④ Process Simulation (METSIM & HSC chemistry)

II. Research

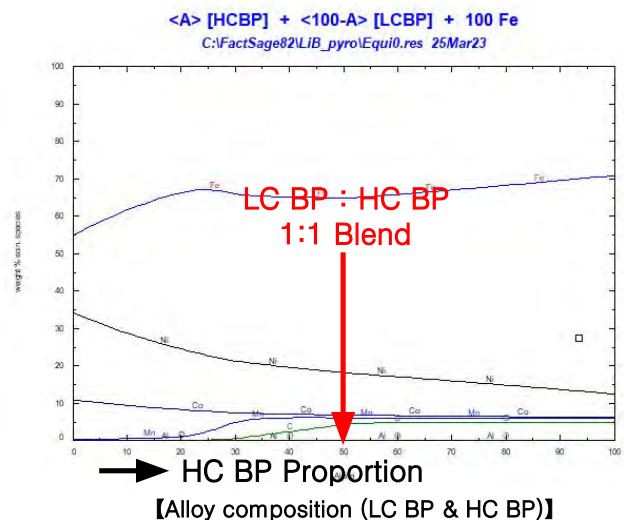
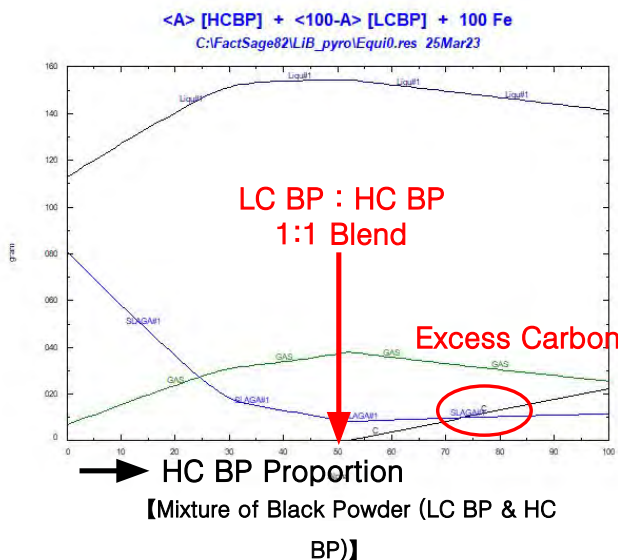
- II-(1). Smelting Process of EoL-LiB
- II-(2). Converting Process of EoL-LiB
- II-(3). Purification Process of EoL-LiB
- II-(4). Process Design using Simulation

II-(1). Smelting Process of EoL-LiB

■ Smelting Process of EoL-LiB

○ Thermodynamic Calculation (FactSage™) : <A>g LC BP & <100-A>g HC BP +Fe 100g

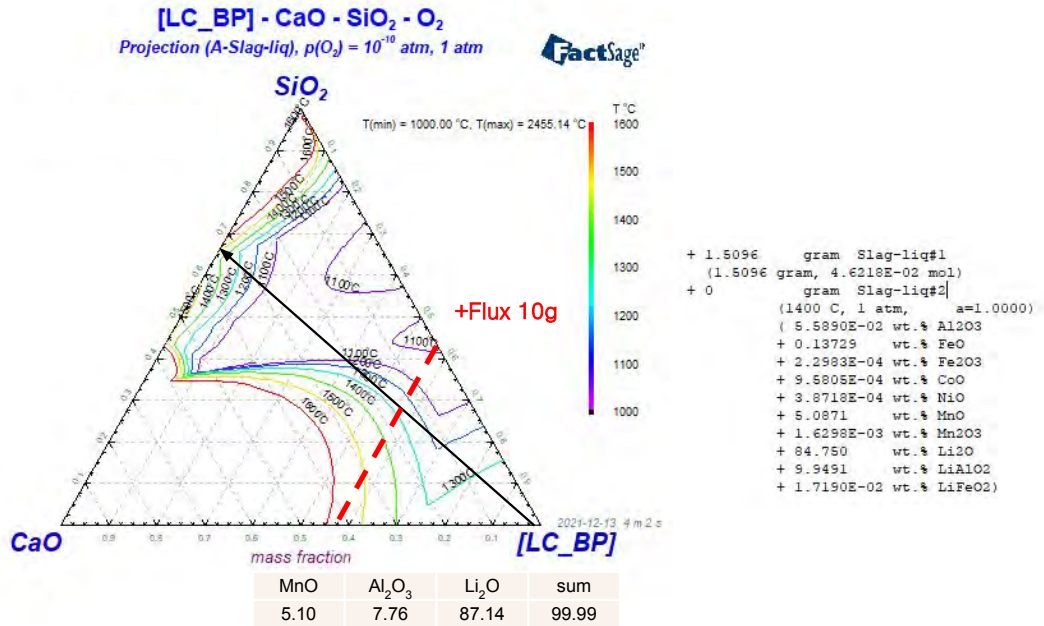
- LC BP : HC BP = 1:1 Blending □ Recovery of metal (Ni, Co, Mn) in Fe (65%Fe-18%Ni-7%Co-6%Mn-3%C)
- Carbon saturated iron due to the high carbon content in HC BP



II-(1). Smelting Process of EoL-LiB

■ Smelting Process of EoL-LiB

○ Thermodynamic Calculation (FactSage™)



II-(1). Smelting Process of EoL-LiB

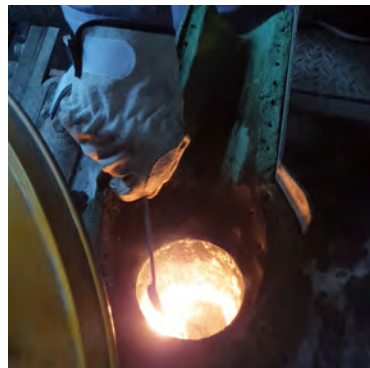
■ Smelting Process of EoL-LiB

○ Experimental Condition

- Input : Fe 2.5kg, LC BP 1.25kg, HC BP 1.25kg, flux SiO₂250g
- Apparatus : 10kg induction melting furnace
- Temperature : 1500~1600°C
- Procedure : Fe melting → Input LC BP + HC BP + Flux (SiO₂) → ... → Alloy production



【Furnace】



【Input B.P & flux】



【Smelting of B.P in Fe】



【Alloy production】

II-(2). Converting Process of EoL-LiB

■ Converting Process of EoL-LiB

○ Experimental Condition

- Input : Ni-Co alloy, Sulfur, Air, flux SiO₂
- Apparatus : 10kg induction melting furnace
- Temperature : 1300~1400°C
- Procedure : Alloy melting → Input Sulfur → Air blowing + Flux (SiO₂) → ... → Ni matte production



【Furnace】



【Input sulfur】



【Air blowing】



【Matte production】

II-(2). Converting Process of EoL-LiB

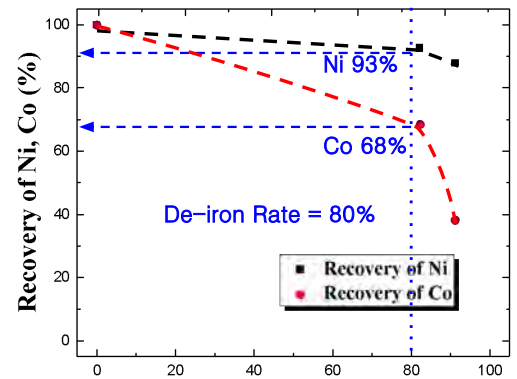
■ Converting Process of EoL-LiB

○ Experimental Condition

- (smelting test) Recovery of metal in B.P blending using Fe hot metal
 - (Ni+Co)>20% Alloy (Fe-Ni-Co)
 - Li₂O-SiO₂ Slag (100% Li recovery in slag)
- (smelting test) Recovery of metal in B.P using Fe and FeNi hot metal
 - (Ni+Co)>70% Alloy (Fe-Ni-Co)
 - Li₂O-FeO-MnO-SiO₂ Slag (100% Li, 100% Mn recovery in slag)
- (converting test) Removal of Fe and concentration of metal using Air (O₂)
 - (Ni+Co)> 75% Matte (Ni-Co-S)
 - As decreased the Fe content, the recovery of Co decreases

- Recovery Rate

$$= \frac{\text{Metal weight in alloy}}{(\text{Metal weight in alloy}) + (\text{Metal weight in slag})}$$



【Concentration of Ni, Co in Converting Process】

Recovery [%]	Ni	Co	(Ni+Co)	Mn	(Li) (slag)	Metal Composition	Slag composition
LC BP & HC BP Smelting	99.7	99.90	99.76	93.28	100	66%Fe-16%Ni-7%Co-5%Mn	Li ₂ O-(FeO-MnO)-SiO ₂ -(MgO)
LC BP Smelting	97.53	91.20	96.03	0.44	78.49	50%Fe-38%Ni-11%Co	Li ₂ O-FeO-MnO-SiO ₂ -MgO
LC BP Smelting (FeNi)	97.5	88.44	95.9	0.79	100	28%Fe-60%Ni-11%Co	Li ₂ O-FeO-MnO-SiO ₂ -(MgO)
LC BP & HC BP Converting	96.73	87.91	94.32	-	-	33%Fe-34%Ni-12%Co-S	FeO-SiO ₂ -MnO-(MgO)
LC BP Converting	89.69	25.92	76.48	-	-	5%Fe-68%Ni-5%Co-S	FeO-SiO ₂ -MgO
LC BP Converting (FeNi)	89.03	41.60	80.75	-	-	2%Fe-70%Ni-5%Co-S	FeO-SiO ₂ -MgO

II-(2). Converting Process of EoL-LiB

■ Converting Process of EoL-LiB



[Final slag (High Ni)]

Slag Composition (wt.%)							FeO/SiO ₂ ratio
FeOx	NiO	CoO	MgO	SiO ₂	Al ₂ O ₃	S	
41.8	10.96	11.52	7.69	22.04	2.40	0.19	1.90

① Process (1) : step converting

○ Experimental condition

- Sample : FeNi matte(Fe 40%) 2kg+ Final slag 200g
- Temperature : 1400 °C, 30min, N₂ gas bubbling(3L/min)

[Step converting : Recovery rate]

	Ni	Co	(Ni+Co)
Ni, Co recovery (%)	72.72	96.13	84.72
Total Recovery	96.11	97.44	96.82

② Process (2) : smelting & slag recycling

○ Experimental condition

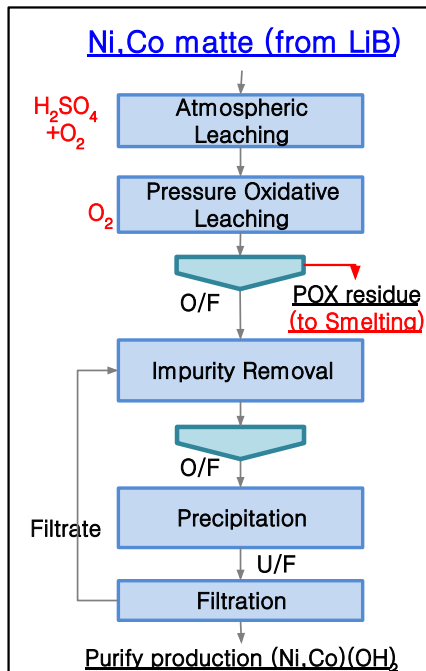
- Sample : Fe 2kg+ Final slag 200g
+ LC BP 200g + SiO₂ 200g (flux)
- Temperature : 1400 °C

[Smelting & slag recycling : Recovery rate]

	Ni	Co	(Ni+Co)
Ni, Co recovery (%)	78.47	80.46	79.49
Total Recovery	98.41	93.84	97.81

II-(3). Purification Process of EoL-LiB

■ Purification Process of EoL-LiB



○ Leaching Condition (Ni 99%, Co 99% recovery & Si 97%, Fe 90% removal)

- POX Leachate (PLS) : 84g/L Ni - 4.6g/L Co - 0.3g/L Fe
- POX residue (waste) : Fe₂O₃-SiO₂-NiS compound (6% Ni-7%Si-41%Fe)

[Leaching Condition]

	Temperature	Atmosphere	H ₂ SO ₄	pH	ORP	Time
Atmospheric Leaching	90°C	Air + O ₂	60g/L	0.4~1.3	-200mV	Total 8h
Pressure Oxidative Leaching	160°C	O ₂ 10~15bar	-	1.3~1.9	500mV	Total 7h

○ Neutralization Condition (47% Ni-3.2%Co precipitate)

- Neutralization solution (Impurity removal) : 81.5g/L Ni - 4.5g/L Co - 1.4g/L Na
- Purify production : (Ni,Co)(OH)₂ (Purity > 99.5%)

[Neutralization Condition]

	Temperature	Neutralization reagent	Amount of reagent	pH	ORP	Time
Impurity Removal	25°C	1M NaOH	Leachate 1.3%	1.8~5.5	496 □202mV	Total 3h
Precipitation	25°C	1M NaOH	Leachate 126%	5.5~7.7	202 □167mV	Total 3h

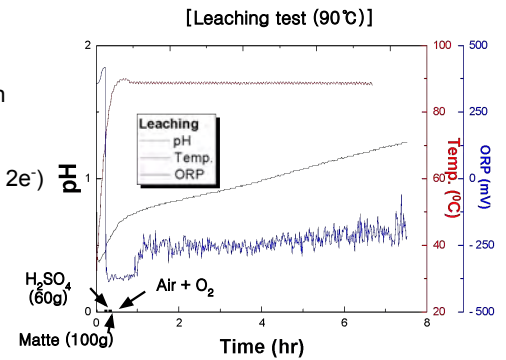
II-(3). Purification Process of EoL-LiB

■ Purification Process of EoL-LiB

○ Leaching test (90 °C)

- pH : pH 0.5 reached then increased the pH 1.3 due to the leaching reaction
- ORP : decreased the ORP at initial reaction (300mV □ -370mV) (H_2SO_4)
increased the ORP at final reaction (-370mV □ -200mV) ($Ni^0 = Ni^{2+} + 2e^-$)
- Leaching the metals (Ni, Co, Fe) in matte (from LiB)

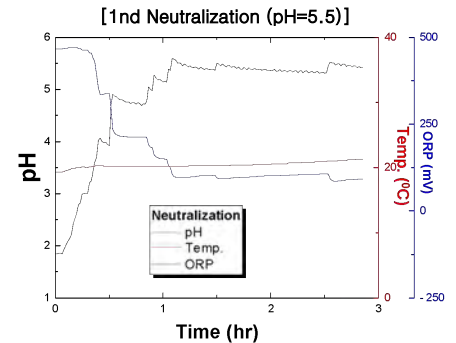
Atmospheric Leaching	pH	H_2SO_4	Sol./Liq.
Condition	0.5~2.0	60g/L	1:8



○ Neutralization test (25 °C)

- pH : 1st Neut. (pH 5.5), 2nd Neut. (pH 7.5) <Reagent : NaOH>
- ORP : decreased the ORP as the neutralization reaction (~90mV) ($Ni^{2+} + 2e^- = Ni^0$)

	pH	ORP	1M NaOH	Residue weight
1 st Neutralization	5.5	202mV	4.63g	66.77g
2 nd Neutralization	7.5	167mV	458.4g	29.76g



II-(3). Purification Process of EoL-LiB

Need to develop **neutralization process**

(Leaching recovery ~99% & Precipitation recovery ~70%)

■ Purification Process of EoL-LiB

○ Recovery of Purification process

(#1) (POX : 160°C, 15bar) (Neutralization ~ Precipitation)

POX leaching (pH 1.9, ORP 500mV)	Ni	Co	Fe
Recovery (%; Solution)	106.9%	71.2%	7%
Recovery (%; Solid)	99.5%	99.8%	34%
Recovery (%)	99.6%	99.8%	10%

Neutralization (pH 5.5)	Ni	Co	Fe
Recovery (%; Solution)	99.2%	99.6%	0%

Precipitation (pH 7.5)	Ni	Co
Recovery (%; Solution)	68%	83%
Recovery (%; Solid)	56%	71%
Recovery (%)	64%	81%

(#2) (POX : 160°C, 12bar) (Neutralization ~ Precipitation)

POX leaching (pH 1.9, ORP 500mV)	Ni	Co	Fe
Recovery (%; Solution)	104.8%	71.9%	5.7%
Recovery (%; Solid)	99.6%	99.9%	45.8%
Recovery (%)	99.6%	99.8%	9.5%

Neutralization (pH 5.5)	Ni	Co	Fe
Recovery (%; Solution)	99.8%	100.2%	0.0%

Precipitation (pH 7.5)	Ni	Co
Recovery (%; Solution)	72%	85%
Recovery (%; Solid)	64%	75%
Recovery (%)	70%	83%

(#3) (POX : 160°C, 10bar) (Neutralization ~ Precipitation)

POX leaching (pH 1.9, ORP 500mV)	Ni	Co	Fe
Recovery (%; Solution)	99.5%	65.9%	0.9%
Recovery (%; Solid)	99.3%	99.3%	17.5%
Recovery (%)	99.3%	98.9%	1.1%

Neutralization (pH 5.5)	Ni	Co	Fe
Recovery (%; Solution)	99.1%	103.3%	0.0%

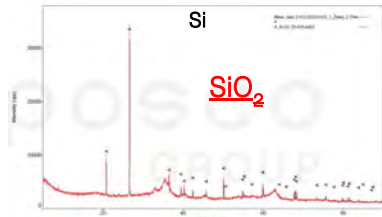
Precipitation (pH 7.5)	Ni	Co
Recovery (%; Solution)	71%	85%
Recovery (%; Solid)	61%	70%
Recovery (%)	68%	82%

II-(3). Purification Process of EoL-LiB

■ Purification Process of EoL-LiB

- Precipitation production (Purify = 99.5%)

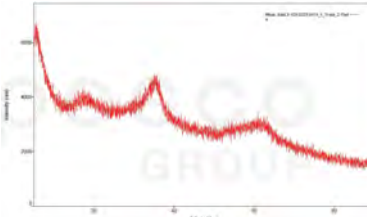
6.62%Ni-0.2%Co-41.8%Fe-7.57%



[POX residue]

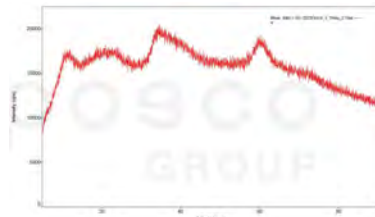


[POX residue]

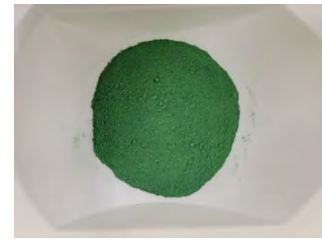


[1st Neut. residue]

47%Ni-3.3%Co



[2nd Neut. precipitate]



[2nd Neut. precipitate]

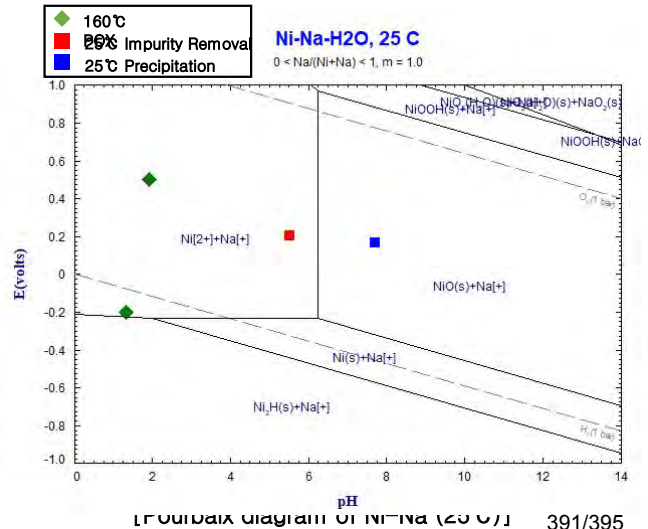
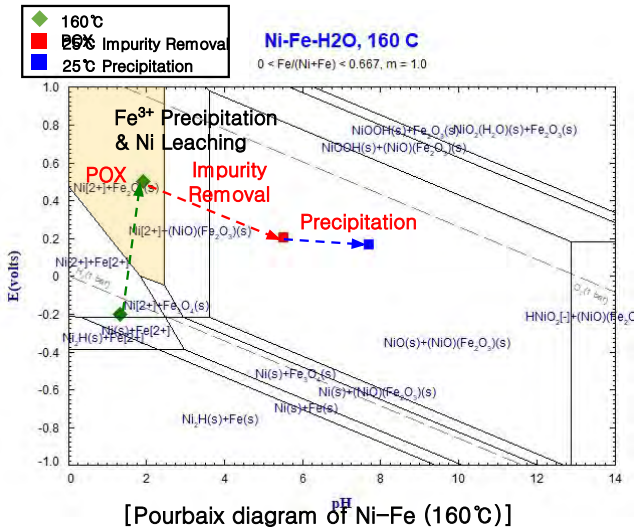
	Composition (wt%)												
	Ni	Co	Mn	Al	Mg	Si	Ca	Fe	Na	P	Li	C	S
Production	47.1	3.23	0.01	0.011	<0.01	0.255	0.016	<0.01	0.039	0.01	0.01	0.065	5.17

II-(3). Purification Process of EoL-LiB

■ Purification Process of EoL-LiB <FactSage™>

- Pourbaix Diagram (E-pH)

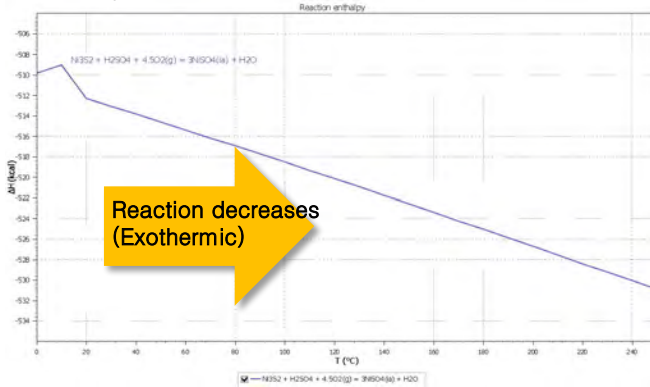
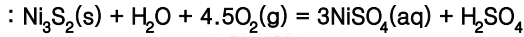
- POX : pH 1.3~1.9 & ORP 500mV □ Fe₂O₃ (hematite) precipitate & Ni Leaching
- Impurity Removal : pH 1.9~5.5 Neutralization □ Fe³⁺, Al (pH 2.0), Si (pH 4.5) remove & Ni loss
- Precipitation : pH 5.5~7.7 Neutralization □ Ni precipitation & Na, Si co-precipitation



II-(3). Purification Process of EoL-LiB

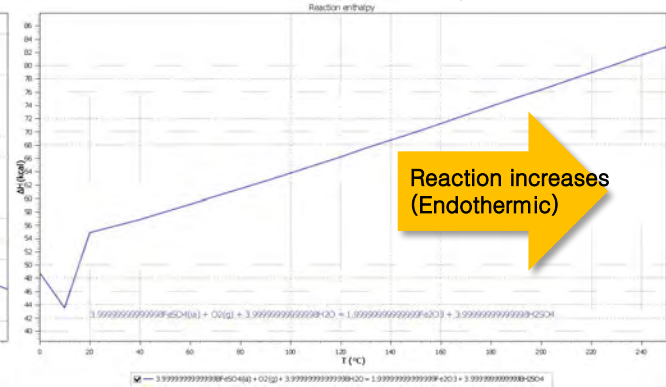
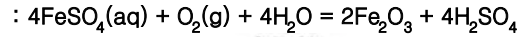
■ Purification Process of EoL-LiB <HSC chemistry>

○ Sulfide Leaching Reaction (POX)



Reaction Equation					
$\text{Ni}_3\text{S}_2 + \text{H}_2\text{SO}_4 + 4.5\text{O}_2(\text{g}) = 3\text{NiSO}_4(\text{ia}) + \text{H}_2\text{O}$					
Reaction Data					
T °C	ΔH kcal	ΔS cal/K	ΔG kcal	K	Log K
150.000	-522.56 5	-378.91 0	-362.22 9	1.262E+187	187.101

○ Fe Precipitation (HPAL)



Reaction Equation					
$4\text{FeSO}_4(\text{ia}) + \text{O}_2(\text{g}) + 4\text{H}_2\text{O} = 2\text{Fe}_2\text{O}_3 + 4\text{H}_2\text{SO}_4$					
Reaction Data					
T °C	ΔH kcal	ΔS cal/K	ΔG kcal	K	Log K
160.000	71.241	232.051	-29.272	5.898E+014	14.771

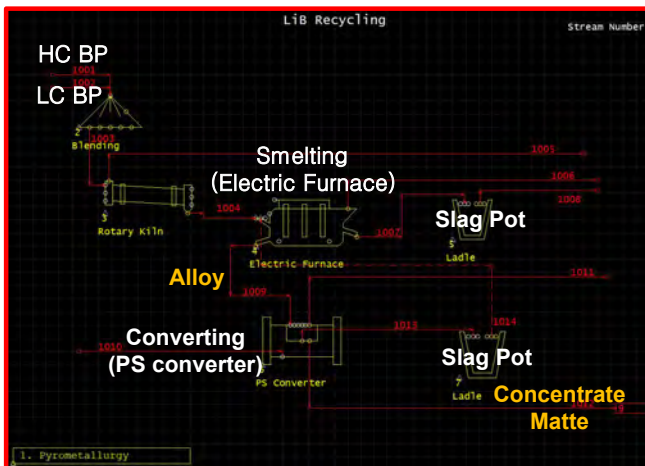
II-(4). Process Design using Simulation

■ Process Design (METSIM)

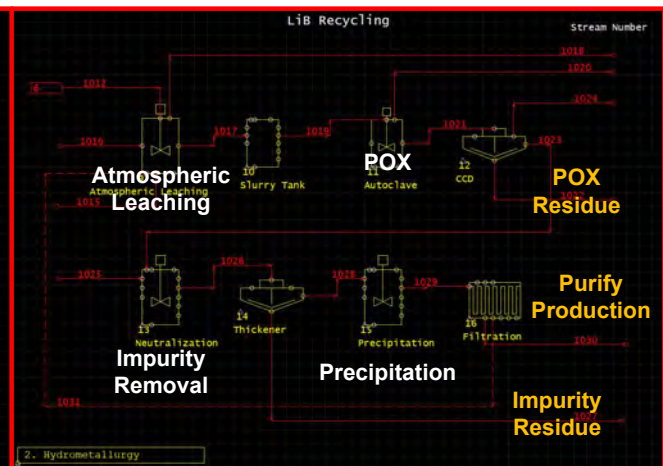
○ METSIM simulation

- Pyro-smelting process : LC BP & HC BP blending □ Calcination (Rotary Kiln) □ Smelting (Electric Furnace)
- Pyro-converting process : Converting (PS Converter) □ Slag recycling (Ladle)
- Hydro-purification process : Atmospheric Leaching □ Pressure Oxidative Leaching □ Precipitation ($\text{Ni}(\text{OH})_2$)
- Process simulation based on the experimental database.

[Pyrometallurgy Process]



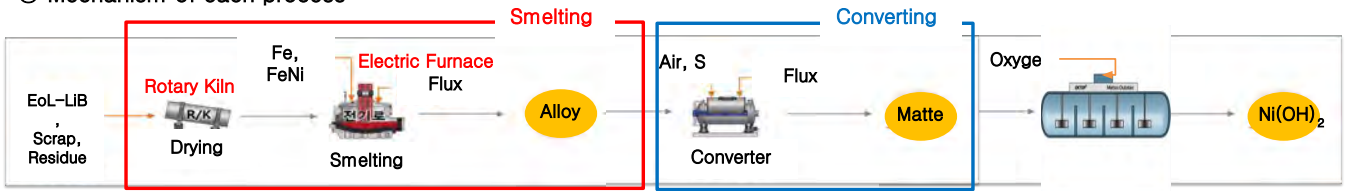
[Hydrometallurgy Process]



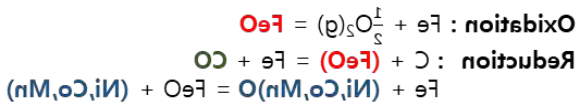
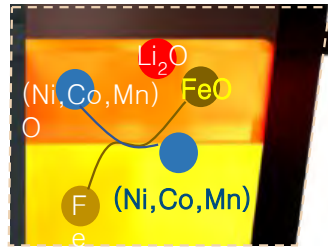
III-(1). Concluding Remarks

Conclusion : Process Design for recycling of EoL-LiB

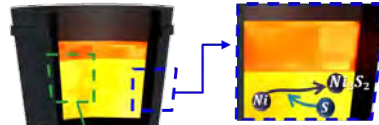
○ Mechanism of each process



Smelting Process



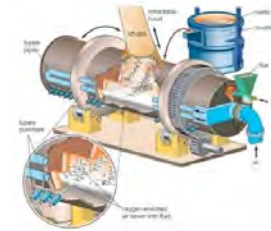
Converting Process



Sulfidation (Step 1)



Oxidation (Step 2)

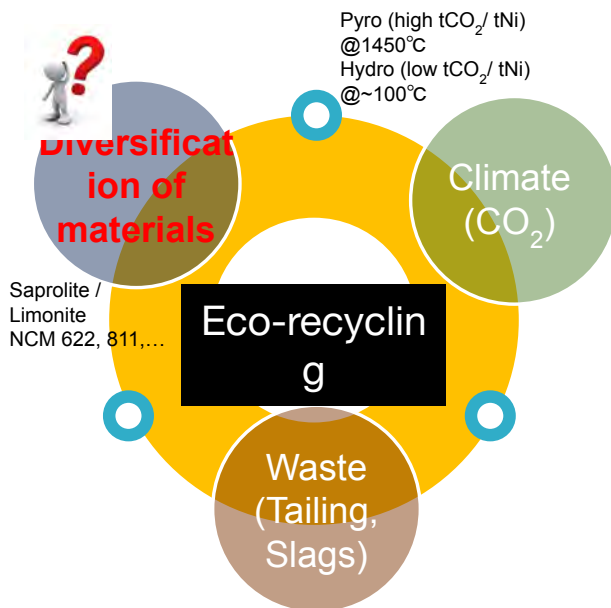


[PS Converter]

III-(1). Concluding Remarks

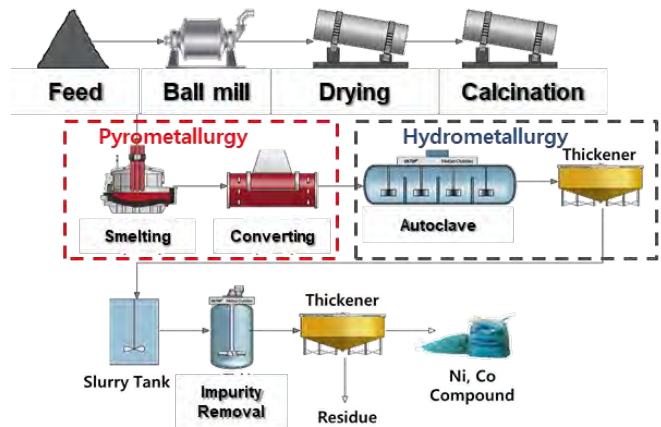
Conclusion : Process Design for recycling of EoL-LiB

○ Eco-friendly process for recycling of EoL-LiB



Pyro (high tCO_2/tNi)
 @ 1450°C
 Hydro (low tCO_2/tNi)
 @ ~100°C

○ Process Design (hybrid process : pyro- & hydro-)



※ Hybrid process for recycling of EoL-LiB

→ Development of **high-capacity & raw material diversification** process utilizing existing **facilities**

III-(2). Future Works

■ Conclusion & Future works

1. Smelting & Converting Process for recycling of EoL-LiB

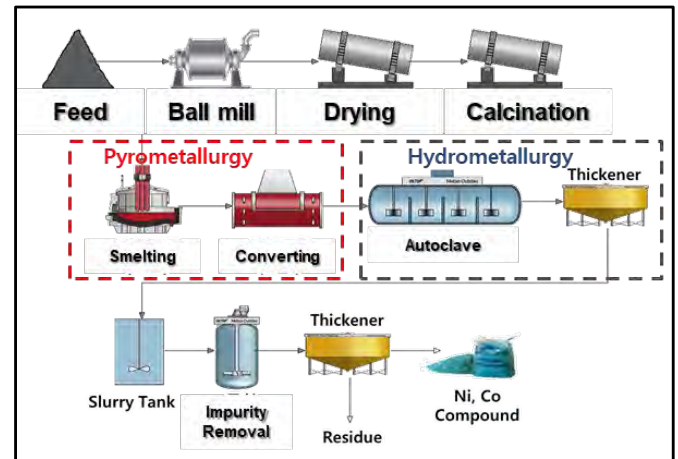
- (smelting) Recovery of metal in B.P using Fe and FeNi hot metal
 - (Ni+Co)>70% Alloy (Fe-Ni-Co)
 - $\text{Li}_2\text{O-FeO-MnO-SiO}_2$ Slag (100% Li, 100% Mn recovery in slag)
- (converting) Removal of Fe and concentration of metal using Air (O_2)
 - (Ni+Co)> 75% Matte (Ni-Co-S)
 - As decreased the Fe content, the recovery of Co decreases
- (slag recycling) Recovery of Ni, Co for slag recycling
 - Smelting : (Ni+Co)>96.8% / Step converting : (Ni+Co)>97.8%

2. Purification Process for recycling of EoL-LiB

- (Purification) POX-Neutralization to purify Ni, Co
 - Purify production (Ni,Co(OH)_2) (Purity>99.5%)

3. Future works

- Process design (Concept, Mass balance, Basic Flow design)
 - Engineering D/B through the process cycle design & simulation
 - Process design criteria through the experimental database



[Process Design for recycling of circulating resources]

Acknowledgements

This work was supported by the Ministry of Trade, Industry and Energy under Project No. 20217510100080.
(저품질 고상 복합자원의 자원순환 오픈 플랫폼 구축을 위한 희소금속 농축회수(200kg/일) 원천기술개발)